U.PORTO

DOUTORAMENTO

CIÊNCIAS BIOMÉDICAS

Bioactive Secondary Metabolites from Marine-Derived Fungi Collected from Thai Waters

Decha Kumla

D

2019

U.PORTO

Decha Kumla. Bioactive Secondary Metabolites from Marine-Derived Fungi Collected from Thai Waters

Bioactive Secondary Metabolites from Marine-Derived Fungi Collected from Thai Waterss

Decha Kumla

D.ICBAS **2019**

INSTITUTO DE CIÊNCIAS BIOMÉDICAS ABEL SALAZAR

DECHA KUMLA

Bioactive Secondary Metabolites from Marine-Derived Fungi Collected from Thai Waters

Thesis submitted to Instituto de Ciências Biomédicas Abel Salazar, Universidade do Porto to obtain the degree of Doctor in Biomedical Sciences

Adviser - Dr. Anake Kijjoa
Category - Full Professor
Affiliation - Instituto de Ciências Biomédicas Abel Salazar da Universidade do Porto

Co-adviser - Dr. José Augusto Caldeira Pereira
Category - Assistant Professor
Affiliation - Instituto de Ciências Biomédicas Abel Salazar da Universidade do Porto

Co-adviser - Dr. Tida Dethoup
Category - Associate Professor
Affiliation - Department of Plant Pathology, Faculty of Agriculture, Kasetsart University, Bangkok, Thailand

Experimental work of this thesis have been carried out in the Departamento de Química, Instituto de Ciências Biomédicas Abel Salazar (ICBAS) da Universidade do Porto. The candidate performed this work, supported by Erasmus Mundus ALFABET project under the Erasmus Mundus Action 2 Mobility project, for a PhD's scholarship. This work was partially supported through national funds provided by FCT/MCTES-Foundation for Science and Technology from the Minister of Science, Technology and Higher Education (PIDDAC) and European Regional Development Fund (ERDF) through the COMPETE-Programa Operacional Factores de Competitividade (POFC) programme, under the project PTDC/MAR-BIO/4694/2014 (reference POCI-01-0145-FEDER-016790; Project 3599-Promover a Produção Científica e Desenvolvimento Tecnológico e a Constituição de Redes Temáticas (3599-PPCDT) in the framework of the programme PT2020, the project INNOVMAR-Innovation and Sustainability in the Management and Exploitation of Marine Resources (reference NORTE-01-0145-FEDER-000035, within Research Line NOVELMAR), supported by North Portugal Regional Operational Programme (NORTE 2020), under the PORTUGAL 2020 Partnership Agreement, through the European Regional Development Fund (ERDF), as well as by POCI-01-0145-FEDER-028736 and UID/Multi/04423/2019.

STATUS THESIS

The results of the work of this thesis have been published, as original articles, in the following journals.

LIST OF PUBLICATIONS

1. **Kumla D**., Aung T.S., Buttachon S., Dethoup T., Gales L., Pereira J.A., Inácio A., Costa P.M., Lee M., Sekeroglu N., Silva A.M.S, Pinto M.M.M. and Kijjoa A. (**2017**). A New Dihydrochromone Dimer and Other Secondary Metabolites from Cultures of the Marine Sponge-Associated Fungi *Neosartorya fennelliae* KUFA 0811 and *Neosartorya tsunodae* KUFC 9213. *Mar. Drugs 15* (12), 375, doi: 10.3390/md15120375.

2. **Kumla D**., Pereira J.A., Dethoup T., Gales L., Silva J.F., Lee M., Costa P.M., Silva A.M.S., Sekeroglu N., Pinto M.M.M. and Kijjoa A. (**2018**). Chromone Derivatives and Other Constituents from Cultures of the Marine Sponge-Associated Fungus *Penicillium erubescens* KUFA0220 and Their Antibacterial Activity. *Mar. Drugs 16* (8), 289, doi: 10.3390/md16080289.

3. **Kumla D**., Dethoup T., Gales L., Pereira J.A., Silva J.F., Costa P.M., Silva A.M.S., Pinto M.M.M. and Kijjoa A. (**2019**). Erubescensoic Acid, a New Polyketide and a Xanthonopyrone SPF-3059-26 from the Culture of the Marine Sponge-Associated Fungus *Penicillium erubescens* KUFA 0220 and Antibacterial Activity Evaluation of Some of Its Constituents. *Molecules 24* (1), 208, doi: 10.3390/molecules24010208.

COMMUNICATIONS

Oral presentations

1. **Kumla D**., Pereira J. A., Dethoup T., Silva J.F., Gales L., Lee M., Costa P.M., Silva A.M.S., Sekeroglu N., Pinto M.M.M. and Kijjoa A. Secondary Metabolites from the Culture of the Marine Sponge-Associated Fungus *Penicillium erubescens* KUFA0220 and Their Antibacterial Activity. The 5th International Symposium on Pharmaceutical and Biomedical Sciences, 26-28 April 2019, Cappadocia, Turkey.

2. **Kumla D**., Pereira J.A., Dethoup T. and Kijjoa A. 2019. Secondary Metabolites from Cultures of the Marine Sponge-Associated Fungus *Penicillium erubescens* KUFA0220 and Their Antibacterial Activity**.** International Summer School on Natural Products (ISSNP2019) at the University Centre CESTEV, 1-5 July 2019, Naples, Italy.

Posters presentations

1. **Kumla D.**, Dethoup T., Buttachon S., Pereira J. A. and Kijjoa A. Secondary Metabolites from the Culture of Marine Sponge- Associated Fungus *Neosartorya tsunodae* KUFC 9213. Poster Presentation in the 2nd International Conference on Marine Fungal Natural Products (MaFNaP-2017), 27-29 June 2017, at Wissenschaftszentrum, Kiel, Germany.

2. **Kumla D.**, Dethoup T., Pereira J. A. and Kijjoa A. Secondary Metabolites from the Culture of Marine Sponge- Associated Fungus *Neosartorya tsunodae* (KUFC 9213). Poster Presentation in the First Meeting PhD Biomedical Sciences, 7th May 2018, at Instituto de Ciências Biomédicas Abel Salazar, University of Porto, Porto, Portugal.

Declaração

Declaro que a presente tese é de minha autoria e não foi utilizada previamente noutro curso ou unidade curricular, desta ou de outra Instituição. As referências a outros autores (afirmações, ideias, pensamentos) respeitam escrupulosamente as regras da atribuição, e encontram-se devidamente indicadas no texto e nas referências bibliográficas, de acordo com as normas de referenciação. Tenho consciência de que a prática de plágio e auto-plágio constitui um ilícito académico.

Em relação aos artigos publicados em anexo, declaro que:

1. A minha participação nos três artigos citados na tese corresponde à obtenção dos extratos brutos de culturas dos fungos marinhos, fracionamento dos extratos, isolamento e purificação dos compostos por técnicas de cromatografia, determinação de pontos de fusão, espectros no infravermelho, medição de rotação ótica, medição dos espectros de dicroísmo circular eletrónica, interpretação dos espectros de Ressonância Magnética Nuclear (RMN) uni- (^{1}H, ^{13}C, DEPT) e bidimensionais (COSY, HSQC, HMBC, NOESY), interpretação dos espectros de massa da alta resolução, e elucidação estrutural dos compostos isolados.
2. Uma parte do artigo "**Kumla, D.,** Aung T.S., Buttachon S., Dethoup T., Gales L., Pereira J.A., Inácio A., Costa P.M., Lee M., Sekeroglu N., Silva A.M.S, Pinto M.M.M. and Kijjoa A. 2017. A New Dihydrochromone Dimer and Other Secondary Metabolites from Cultures of the Marine Sponge-Associated Fungi *Neosartorya fennelliae* KUFA 0811 and *Neosartorya tsunodae* KUFC 9213. *Mar. Drugs* 2017, 15 (12), 375. doi:10.3390/md15120375" que descreveu o isolamento e elucidação estrutural dos compostos isolados do fungo marinho *Neosartorya fennelliae* KUFA 0811 pertence à tese do Mestrado em Ciências do Mar-Recursos Marinhos de Tin Shine Aung (Título da tese: Bioactive Secondary Metabolites from the Culture of the Marine Sponge-Associated Fungus *Neosartorya fennelliae* KUFA 0811). Contudo, esta parte não foi incluída nesta tese.
3. Não há uma reprodução do artigo de uma forma integral.
4. Como todos os artigos indicados em anexo são publicados em revistas de "Open Access", são automaticamente autorizados para integração na tese.

Decha Kumla

_____

Decha Kumla

Porto, 8 Novembro 2019.

INDEX

FIGURES INDEX

TABLES INDEX

ACKNOWLEDGEMENT

I would like to express my deep gratitude and sincere appreciation to my supervisor, Professor Dr. Anake Kijjoa of the Instituto de Ciências Biomédicas Abel Salazar (ICBAS), Universidade do Porto, who gave me the precious opportunity to carry out my PhD study. I wish to thank him for his continuous support, encouragement, motivation, recommendation, as well as for his patience. Without his guidance, I surely could not succeed in doing my research and writing this thesis. I am really proud to be a PhD's student under his supervision.

My sincere thanks go to my co-supervisors, Associate Professor Dr. Tida Dethoup of the Department of Plant Pathology, Kasetsart University, Bangkok, Thailand, and Professor Dr. José Augusto Caldeira Pereira, of ICBAS, for their assistance and constant support during the execution of this thesis.

I also wish to thank the ALFABET project of the Erasmus Mundus Action 2 program for granting me a PhD's scholarship to study in the University of Porto, Portugal.

I am thankful to Mrs. Bárbara Costa, Director of the International Relations office of the University of Porto for her interest and engagement in building the Alfabet Project of the Erasmus Program, which gave many foreign students a precious opportunity to apply for scholarships to study in the University of Porto.

I am deeply grateful to Ms. Ana Castro Paiva of the International Relations Office of the University of Porto, who played a decisive role for me to earn the scholarship of the Alfabet Project of the Erasmus Mundus Action 2 to pursue my doctoral study at ICBAS. My sincere thanks also go to Ms. Ana Sofia Ferreira, also of the International Relations Office of the University of Porto, for her kind assistance in all aspects which makes my stay in Porto a very pleasant experience.

I am deeply indebted to Professor Dr. Artur Manuel Soares Silva of the Departamento de Quimica, Universidade de Aveiro, for providing all the 1D and 2D NMR spectra, to Professor Dr. Luís Gales of ICBAS and I3S for the X-ray

crystallography analysis, and also to Dr. Michael Lee of the Department of Chemistry, Leicester University, UK, for providing high resolution mass spectra.

Also, my thankful word goes to Prof. Dr. Paulo Costa of ICBAS, for being in charge of antibacterial assays of the compounds isolated from the marine-derived fungi in this thesis.

I would like to express my gratitude also to Prof. Dr. Madalena Maria de Magalhães Pinto of the Faculty of Pharmacy, University of Porto, for her kindness and support, also to Prof. Dr. Poonpipope Kasemsap, Director of the Horticulture Innovation Lab Regional Center at Kasetsart University, Bangkok, Thailand, for support and encouragement for me to study in this prestigious university.

I would like to thank Prof. Dr. Vitor Vasconcelos, Director of the Interdisciplinary Centre of Marine and Environmental Research (CIIMAR) for his constant support, encouragement and for accepting me to be part of this presigious research center.

I am thankful to Prof. Dr. Eduardo Rocha, Director of the Doctoral Program in Biomedical Sciences of ICBAS for his assistance and encouragement as well as for being ready to solve all the inherent problems concerning my doctoral study.

I would like to express my sincere thanks to Mrs. Júlia Bessa, Ms. Sonia Pereira Santos and Mrs. Isabel Silva not only for their technical assistance, but also for giving me a mental support, valuable advices and unconditional friendship.

I wish to thank Ms. Sara Cravo of the Laboratório de Química Orgânica e Farmacêutica da Faculdade de Farmácia, Universidade do Porto, for her technical assistance and friendship during my doctoral study.

My special thanks also go to Dr. Suradet Buttachon, Assistant researcher of CIIMAR for all his helps, supports and companionship during these years. I also appreciate all of my lab mates for their encouragement, understanding and for taking over parts of my work during the time of completion of this thesis as well as the nice working atmosphere.

My specially thanks also go to Ms. Ana Paula Pereira, secretary of the Doutoral Program in Biomedical Sciences of ICBAS for being so forthcoming and helpful with my PhD's process.

I also appreciate the friendship and good environment provided by all the staff members of the Department of Chemistry of ICBAS.

Last but not the least, I would like to express my deep gratitude to my grandparents, Mr. Somchai Kumla and Mrs. Thongma Phawakhang and to my mother Mrs Bubpha Amornsirichokchai and to my sisters and brother for their love, patience, encouragement and continuing support throughout the period of this work.

ABSTRACT

The main goal of this thesis was to isolate, purify and elucidate the structures of secondary metabolites produced by cultures of the marine-derived fungi as well as to evaluate their *in vitro* potential biological activities. For this propose, two marine sponge-associated fungi, namely *Neosartorya tsunodae* KUFC 9213 and *Penicillium erubescens* KUFA 0220 were selected to study.

From the ethyl acetate extract of the culture of *N. tsunodae* KUFC 9213, isolated from the marine sponge *Aka coralliphaga*, which was collected at the coral reef of Similan Islands, Phang Nga Provice, Thailand, nine previously reported compounds, including (1*R*, 8*S*, 9*R*)-1,9-dihydroxy-8-(2-hydroxypropan-2-yl)-4-methoxy-5-methyl-1,7,8,9-tetrahydro-3*H*-furo[3,4-f]chromen-3-one (chromanol) (**NT 1**), (3β,5α,22*E*)-3,5-dihydroxyergosta-7,22-dien-6-one (**NT 2**), byssochlamic acid (**NT 3**), hopan-3β,22-diol (**NT 4**), chevalone C (**NT 5**), sartorypyrone B (**NT 6**), helvolic acid (**NT 7**), lumichrome (**NT 8**) and harmane (**NT 9**), were isolated.

The ethyl acetate extract of the culture of *P. erubescens* KUFA 0220, isolated from the marine sponge *Neopetrosia* sp., which was collected from the coral reef at Samaesan Island, Chonburi province, Thailand, furnished six previously unreported secondary metabolites, including a chromene derivative, 1-hydroxy-12-methoxycitromycin (**PE 5**), a polyketide, erubescensoic acid (**PE 13**), and four chromone derivatives, penialidin G (**PE 10**), erubescenschromone A (**PE 14**), 7-hydroxy-6-methoxy-4-oxo-3-[(1*E*)-3-oxobut-1-en-1-yl]-4*H*-chromene-5-carboxylic acid (**PE 15**) and erubescenschromone B (**PE 16**), along with fourteen previously reported metabolites, sitostenone (**PE 1**), ergosterol 5,8-endoperoxide (**PE 2**), citromycin (**PE 3**), 12-methoxycitromycin (**PE 4**), myxotrichin D (**PE 6**), 12-methoxycitromycetin (**PE 7**), anhydrofulvic acid (**PE 8**), myxotrichin C (**PE 9**),

penialidin D (**PE 11**), penialidin F (**PE 12**), SPF-3059-30 (**PE 17**), SPF-3059-26 (**PE 18**), GKK1032B (**PE 19**) and secalonic acid A (**PE 20**).

The structures of the isolated compounds were established based on extensive analysis of 1D and 2D NMR and HRMS spectral data. In the case of the previously reported metabolites, their ^{1}H and ^{13}C NMR data and other physical data were compared with those reported in the literature. The absolute stereochemistry of (1*R*, 8*S*, 9*R*)-1,9-dihydroxy-8-(2-hydroxypropan-2-yl)-4-methoxy-5-methyl-1,7,8,9-tetrahydro-3*H*-furo[3,4-f]chromen-3-one (**NT 1**), erubescensoic acid (**PE 13**), erubescenschromone A (**PE 14**) and 7-hydroxy-6-methoxy-4-oxo-3-[(1*E*)-3-oxobut-1-en-1-yl]-4*H*-chromene-5-carboxylic acid (**PE 15**) were established by X-ray analysis, while the absolute configurations of the stereogenic carbons of (3β,5α,22*E*)-3,5-dihydroxyergosta-7,22-dien-6-one (**NT 2**), penialidin F (**PE 12**) and erubescenschromone B (**PE 16**) were determined by comparison of experimental and calculated electronic circular dichroism (ECD) spectra.

NT 1, **NT 2**, **NT 4**, **NT 8**, **NT 9**, isolated from *N. tsunodae* KUFC 9213, and **PE 1**, **PE 3**-**PE 8**, **PE 11-PE 13**, **PE 14-PE 20**, isolated from *P. erubescens* KUFA 0220, were evaluated for their antibacterial activity against Gram-positive bacteria, including three reference strains: *Staphylococcus aureus* ATCC 29213, *Enterococcus faecalis* ATCC 29212, *E. faecium* ATCC 19434, a clinical isolate *S. aureus* 40/61/24, a methicillin-resistant (MRSA) *S. aureus* 66/1, three strains of vancomycin-resistant enterococci (VRE), *E. faecium* 1/6/63, *E. faecalis* A5/102 and *E. faecalis* B3/101, as well as Gram-negative bacteria, including two reference strains *Escherichia coli* ATCC 25922 and *Pseudomonas aeruginosa* ATCC 27853, and the clinical isolate *E. coli* SA/2, an extended-spectrum β-lactamase producer (ESBL). The results showed that only GKK1032B (**PE 19**) displayed an *in vitro* growth inhibition of Gram-positive bacteria, *E. faecalis* ATCC 29212, vancomycin-resistant *E. faecalis* (VRE) B3/101, *E. faecium* ATCC 19434, *E. faecium* 1/6/63 (VRE) and *S. aureus* ATCC 29213 with minimal inhibitory concentration (MIC) values of 8, 8, 16, 32 and 32 mg/mL,

respectively, while secalonic acid A (**PE 20**) exhibited growth inhibition of methicillin-resistant *S. aureus* (MRSA) with MIC value >64 mg/mL. The screening of a potential synergy with antibiotics revealed that SPF-3059-26 (**PE 18**) was able to reduce the MIC of cefotaxime (CTX) of *E. coli* SA/2 (ESBL) for four-fold while it increased the MIC of oxacillin (OXA) of MRSA *S. aureus* 66/1 by two-fold with a MIC value of 128 mg/mL. None of the tested compounds were active against Gram-negative bacteria tested.

Keywords: *Neosartorya tsunodae* KUFC 9213; *Penicillium erubescens* KUFA 0220; marine sponge-associated fungi; chromanol derivative; polyketides, chromone derivatives; GKK 1032B; pyranochromone; spirofuranochromone; erubescensoic acid; SPF-3059-26; antibacterial activity.

RESUMO

O principal objetivo desta tese foi isolar, purificar e elucidar as estruturas de metabolitos secundários produzidos por culturas de fungos marinhos, bem como avaliar as suas potenciais atividades biológicas *in vitro*. Assim, foram selecionados dois fungos marinhos associados a esponjas, a saber, *Neosartorya tsunodae* KUFC 9213 e *Penicillium erubescens* KUFA 0220.

A partir do extrato de acetato de etilo da cultura de *N. tsunodae* KUFC 9213, isolado da esponja marinha *Aka coralliphaga*, coletada no recife de coral das Ilhas Similan, Província de Phang Nga, Tailândia, foram isolados nove compostos já publicados anteriormente, incluindo (1*R*, 8*S*, 9*R*) -1,9-di-hidroxi-8- (2-hidroxipropan-2-il)-4-metoxi-5-metil-1,7,8,9-tetra-hidro-3*H*-furo[3,4-*f*]cromen-3-ona (cromanol) (**NT 1**), (3β, 5α, 22*E*)-3,5-di-hidroxiergosta-7,22-dien-6-ona (**NT 2**), ácido byssochlamico (**NT 3**), hopan-3β,22-diol (**NT 4**), chevalona C (**NT 5**), sartorypyrona B (**NT 6**), ácido helvólico (**NT 7**), lumicromo (**NT 8**) e harmane (**NT 9**).

O extrato de acetato de etilo da cultura de *P. erubescens* KUFA 0220, isolado da esponja marinha *Neopetrosia* sp., que foi coletada no recife de coral da Ilha de Samaesan, província de Chonburi, Tailândia, forneceu seis metabolitos secundários não descritos anteriormente, incluindo um derivado de cromeno, 1-hidroxi-12-metoxicitromicina (**PE 5**), um policetídeo, ácido erubescensoíco (**PE 13**) e quatro derivados de cromona, penialidina G (**PE 10**), erubescenscromona A (**PE 14**), 7-hidroxi-6-metoxi-4-oxo-3-[(1*E*)-3-oxobut-1-en-1-il]-4H-cromeno-5-ácido carboxílico (**PE 15**) e erubescenscromona B (**PE 16**), juntamente com catorze metabolitos relatados anteriormente: sitostenona (**PE 1**), ergosterol 5,8-endoperóxido (**PE 2**), citromicina (**PE 3**), 12-metoxicitromicina (**PE 4**), mixotriquina D (**PE 6**), 12-metoxicitromicetina (**PE 7**), ácido anidrofulvico (**PE 8**), mixotriquina C (**PE 9**),

penialidina D (**PE 11**), penialidina F (**PE 12**), SPF-3059-30 (**PE 17**), SPF-3059-26 (**PE 18**), GKK1032B (**PE 19**) e ácido secalónico A (**PE 20**).

As estruturas dos compostos isolados foram estabelecidas com base na análise de dados espectrais de RMN 1D e 2D bem como dos espectros da massa da alta resolução. No caso dos metabolitos anteriormente descritos, os seus dados de ^{1}H e ^{13}C RMN e outros dados físicos foram comparados com os relatados na literatura. A estereoquímica absoluta de (1*R*, 8*S*, 9*R*) -1,9-di-hidroxi-8-(2-hidroxipropan-2-il)-4-metoxi-5-metil-1,7,8,9-tetra-hidro-3*H*-furo [3,4-*f*] cromen-3-ona (**NT 1**), ácido erubescensoíco (**PE 13**), erubescenscromona A (**PE 14**) e 7-hidroxi-6-metoxi-4-oxo-3-[(1*E*)-3-oxobut-1-en-1-il]-4H-cromeno-5-ácido carboxílico (**PE 15**) foi estabelecido por análise cristalografia de raios X, enquanto as configurações absolutas dos carbonos estereogénicos de (3β, 5α, 22*E*) -3,5 -di-hidroxiergosta-7,22-dien-6-ona (**NT 2**), penialidina F (**PE 12**) e erubescenscromona B (**PE 16**) foram determinados por comparação de espectros experimentais e calculados de dicroísmo circular eletrônico (ECD).

Os compostos **NT 1**, **NT 2**, **NT 4, NT 8**, **NT 9**, isolados de *N. tsunodae* KUFC 9213, e **PE 1**, **PE 3-PE 8**, **PE 11-PE 13**, **PE 14-PE 20**, isolados de *P. erubescens* KUFA 0220, foram avaliados quanto à sua atividade antibacteriana contra bactérias de Gram-positivo, incluindo três cepas de referência: *Staphyllococus aureus* ATCC 29213, *Enterococcus faecalis* ATCC 29212, *E. faecium* ATCC 19434, isolado clínico *S. aureus* 40/61/24, resistente a meticilina (MRSA) *S. aureus* 66/1, três cepas de enterococos resistentes à vancomicina (VRE), *E. faecium* 1/6/63, *E. faecalis* A5/ 102 e *E. faecalis* B3/101, além de bactérias de Gram-negativo, incluindo duas referências, as estirpes *Escherichia coli* ATCC 25922 e *Pseudomonas aeruginosa* ATCC 27853 e também o isolado clínico *E. coli* SA/2, um produtor de β-lactamase de largo espectro (ESBL). Os resultados mostraram que apenas GKK1032B (**PE 19**) apresentou inibição do crescimento *in vitro* de bactérias de Gram positivo, *E. faecalis* ATCC 29212, *E. faecalis* resistente a vancomicina (VRE) B3/101, *E. faecium* ATCC 19434,

E. faecium 1/6/63 (VRE) e *S. aureus* ATCC 29213 com valores de concentração inibitória mínima (CIM) de 8, 8, 16, 32 e 32 mg/mL, respetivamente, enquanto o ácido secalónico A (**PE 20**) exibiu inibição do crescimento *S. aureus* (MRSA) resistente à meticilina, com valor de CIM >64 mg/mL. A triagem de uma sinergia potencial com antibióticos revelou que o SPF-3059-26 (**PE 18**) foi capaz de reduzir o CIM de cefotaxima (CTX) na *E. coli* SA/2 (ESBL) por quatro vezes, enquanto aumentou o CIM de oxacilina (OXA) de MRSA no *S. aureus* 66/1 por duas vezes, com um valor de CIM de 128 mg/mL. Nenhum dos compostos testados foi ativo contra bactérias de Gram negativo testadas.

Palavras-chave: *Neosartorya tsunodae* KUFC 9213; *Penicillium erubescens* KUFA 0220; fungos marinhos associados a esponjas; derivado de cromanol; policetídeos; cromona; GKK 1032B; piranocromona; espirofuranocromona; ácido erubescensoíco; SPF-3059-26; atividade antibacteriana.

LIST OF ABBREVIATIONS AND SYMBOLS

ACE	Angiotensin Converting Enzyme Inhibitor
ASM	Astemizole
A375-C5	Melanoma
A549	Non-small cell lung cancer cell line
BCNPs	Biochemical natural products
BEL-7404	Hepatic cancer cell line
BIU-87	Bladder cancer cell line
brs	Broad singlet
B16F10	Melanoma cancer cell line
B16	Murine melanoma cancer cell line
c	Concentration
Ca^{2+}	Calcium ion
CC	Column chromatography
CLSI	The Clinical and Laboratory Standards Institute
cm	Centimeter
COSY	Proton-Proton Correlation spectroscopy
COX-2	Cyclooxygenase-2
CPE	Cytopathic effect
CTX	Cefotaxime
CZA	Czapek's agar

CYA	Czapek Yeast Autolysate Agar
d	Doublet
dd	Double doublet
ddd	Double double doublet
DEPT	Distortionless Enhancement by Polarization Transfer
DES	Diethyl Sulphate
DFT	Density Functional Theory
DMSO	Dimethylsulfoxide
DMSO-d_6	Deuterated Dimethylsulfoxide
DNA	Deoxyribonucleic acid
DPPH	2,2-Diphenylpicrylhydrazyl
Du145	Human prostate carcinoma cell line
ECA-109	Esophageal cancer cell line
EC_{50}	Half maximal effective concentration
ECD	Electronic circular dichroism
ED_{50}	Median effective dose
EtOAc	Ethyl acetate
EtOH	Ethanol
FDA	Food and Drug Administration
FIC	Fractional inhibitory concentration
g	Gram
GI_{50}	Half maximal growth inhibitory concentration

GluPY	Glucose-peptone-yeast extract
GlyPY	Glycerol-peptone-yeast extract
H1N1	Influenza A virus
H1299	Lung carcinoma cell line
HCT-116	Human colon carcinoma cell line
HeLa	Human cervical carcinoma cell line
HepG2	Human liver hepatocellular cell line
HEP3B	Hepatic cancer cell line
HL-60	Human leukemia cell line
HLE	Human leukocyte elastase
HMBC	Heteronuclear Multiple Bond Correlation
HRESIMS	High Resolution Electrospray Ionization Mass Spectrometry
HRMS	High Resolution Mass Spectrometry
HSQC	Heteronuclear Single Quantum Coherence
Hs683	Oligodendroglioma cell line
Huh7	Human hepatocarcinoma cell line
Hz	Hertz
IC_{50}	Half maximal inhibitory concentration
iNOS	Inducible nitric oxide synthase
IR	Infrared
IR%	Inhibition rates
ITS	Internal Transcribed Spacer

J	Coupling constant in Hz
KB	Human epidermoid carcinoma cell line
Ki	The inhibitor constant
K562	Human myelogenous leukemia cell line
L	Liter
L02	Human hepatic L02 cell line
L5178Y	Murine lymphoma cell line
LC_{50}	Lethal Concentration 50
LD_{50}	Median lethal dose
LM3	Murine LM3 breast cancer cell line
LPS	Lipopolysaccharide
m	Multiplet
m/z	Mass-to-charge ratio
MA	Mouse Leydig tumor cell line
mAb	Monoclonal antibodies
MBC	Minimal Bactericidal Concentration
MCF-7	Breast adenocarcinoma cell line
MDA-MB-231	Human Breast Adenocarcinoma cell line
Me	Methyl
MEA	Malt Extract Agar
MeOH	Methanol
mg	Milligram

MHz	Mega hertz
MIC	Minimum Inhibitory Concentration
mL	Milliliter
mm	Millimeter
mM	Millimolar
mp	Melting point in °C
MPLC	Medium pressure liquid chromatography
mRNA	Messenger RNA
MRSA	Methicillin-resistant *Staphylococcus aureus*
MS	Mass spectrometry
NCEs	New chemical entities
NCI-H187	Human small-cell lung cancer cell line
NCI-H226	Non-small cell lung cancer cell line
NCI-H446	Human small-cell lung carcinoma cell line
NCI-H460	Non-small cell lung cancer cell line
NCM 460	Normal colonic epithelial cell line
nm	Nanometer
NMEs	New molecular entities
NMNPs	Non-mammalian natural products
NMR	Nuclear Magnetic Resonance
NO	Nitric Oxide
NOESY	Nuclear Overhauser Effect Spectroscopy

OAc	Acetoxy
OD	Optical Density
ODc	Optical Density cut-off value
OE21	Esophageal cancer cell line
OMe	Methoxy
ORTEP	Oak Ridge Thermal Ellipsoid Plot
OSMAC	One Strain Many Compounds
OXA	Oxacillin
PANC-1	Human pancreatic cell line
PCR	Polymerase chain reaction
PDA	Potato Dextrose Agar
PDB	Potato Dextrose Broth
PHVD	Prevention of heart and vascular disease
PN/NT	Protection of neurons/neurotoxicity
QS	Quorum Sensing
RD	Human rhabdomyosarcoma cell line
ROS	Reactive oxygen species
s	Singlet
SD	Standard Deviation
SEM	Scanning Electron Microscope
SGC-7901	Human gastric cancer cell line
SK-MEL 2	Human melanoma cell line

sp.	Species (singular)
spp.	Species (plural)
Src-KDR	Protein Tyrosine Kinases
STS	Soft tissue sarcoma
SW1990	Human pancreatic cancer cell line
SW480	Human colon carcinoma cancer cell line
t	Triplet
TDDFT	Time-dependent Density Functional Theory
TLC	Thin Layer Chromatography
TMV	Tobacco mosaic virus
UV	Ultraviolet
U251	Human glioma cell line
U373	Glioblastoma cell line
U-373 MG	Human astrocytoma cell line
VAN	Vancomycin
VRE	Vancomycin-resistant enterococci
VREF	Vancomycin-resistant *Enterococcus faecium*
WHO	World Health Organization
δ	Chemical shift value in ppm
µg	Microgram
µL	Microliter
µM	Micromolar

ε	Molar absorptivity (molar extinction coefficient)
^{13}C NMR	Carbon-13 Nuclear Magnetic Resonance
^{1}H NMR	Proton Nuclear Magnetic Resonance
[^{3}H]EBOB	[^{3}H] Ethynylbicycloorthobenzoate
$[M+H]^{+}$	Pseudo-molecular ion (Positive ion mode)
$[\alpha]^{20}_{D}$	Specific optical rotation at 20 °C for D (sodium) line
®	Register or Trademark
°C	Celsius degrees
Å	Angstrom

CHAPTER I

INTRODUCTION

1. GENERAL INTRODUCTION

1.1. Natural Products Discovery

Natural products are the organic compounds that are produced from primary and/or secondary metabolism of living organisms such as plants, animals and microorganisms. Natural products represent one of the most important sources for drug discovery and drug design. Extracts from plants were widely used to obtain natural compounds for various purposes (Füllbeck *et al*., 2006). Example of these is morphine (**1**), which was first isolated from the dried latex of the unripe poppy (*Papaver somniferum*) seed capsule between (1803 and 1805) by Friedrich Sertürner (Schmitz, 1985). Morphine was used for decreasing the feeling of pain as well as to reduce the symptom of shortness of breath (Krishnamurti and Rao, 2016). Another important plant natural product is artemisinin (**2**), a novel class of antimalarial drug, which was isolated from *Artemisia annua*, a plant used in traditional Chinese medicine (Klayman, 1985). Later, microbial secondary metabolites came into focus in the drug discovery field. Penicillin (**3**), isolated from the fungus *Penicillium notatum* in 1929 (Fleming, 1929), was the first antibiotic, whose discovery not only revolutionized the pharmaceutical industry but also inspired scientists to search for new drugs from microorganisms (Demain and Sanchez, 2009). Another important fungal metabolite is mycophenolic acid (**4**), produced by *Penicillium brevicompactum*, was first used as antibiotic, and later as an immunosuppressant in kidney, heart, and liver transplantation (Bentley, 2000).

Therefore, natural products have played, and still continue to play, a main key role in drug discovery and development. Moreover, many of drugs available in the market today were discovered from natural sources (Koparde *et al*., 2019).

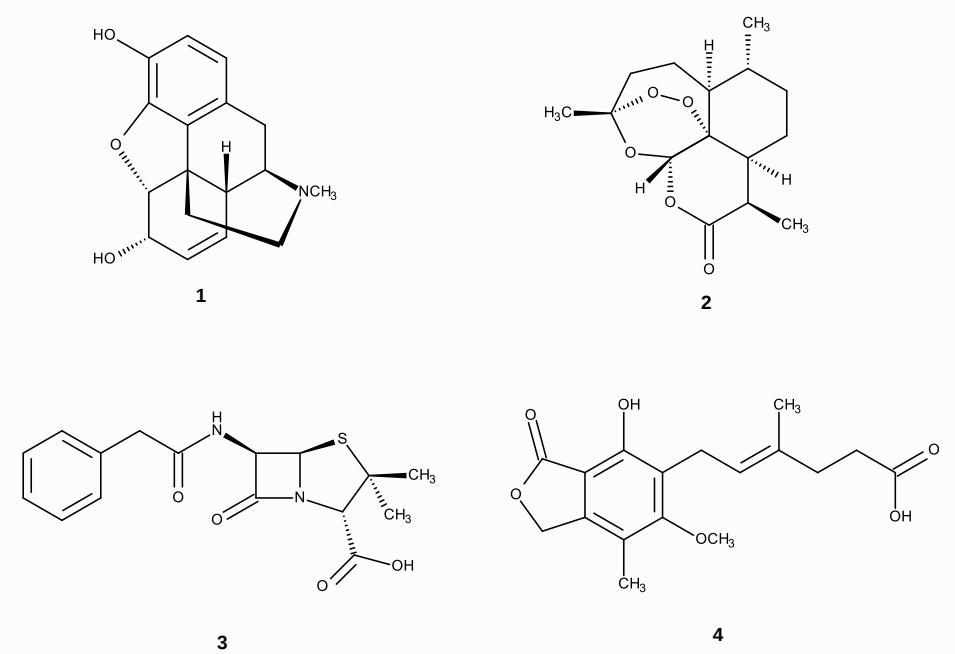

Figure 1. Structures of morphine (1), artemisinin (2), penicillin (3) and mycophenolic acid (4)

According to Patridge *et al*. (2016), plants are still the most abundant sources of natural products (47%), followed by bacteria (30%), fungi (23%) and others (5 %) of (Figure 2).

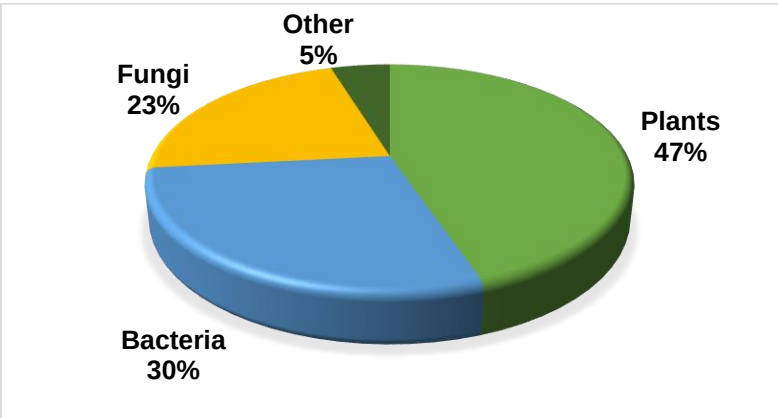

Figure 2. The percentage of natural product new molecular entities (NMEs), separated by environmental source (Patridge *et al*., 2016)

Despite a sharp decline in the numbers of natural products for the FDA-approved drugs, Newman and Cragg argued that approximately half of all new drugs during the past reports are of natural product origin or designed based on natural product structures.

Although natural products have contributed significantly to the landscape of new molecular entities (NMEs); an analysis of all the United States Food and Drug Administration (FDA)-approved NMEs revealed that natural products and their derivative represent more than one-third of all the NMEs. However, since the 1930s, the total number of natural products has decreased continuously whereas the synthetic and semisynthetic derivatives have increased. The decline of interest in natural products in recent years has greatly affected the pipeline of NMEs. Several reports analyzing the influence of natural products on the FDA-approved drugs have been published. Patridge *et al*. (2016), in their analysis of the FDA-approved NMEs from 1931-2013, reported that 547 of natural products and their derivatives had been approved by the FDA. These derivatives also included non-mammalian natural products (NMNPs) and biochemical natural products (BCNPs), which represented more than one-third (38%) of all FDA-approved NMEs. From this analysis, it was clear that the numbers of natural products-based NMEs began to decline since the 1970s, and stayed around 24% until 2013. On the other hand, Newman and Cragg reported that, during the year 1981 to 2014, more than 50% of all the approved small-molecule drugs had originated from natural products.

In 2018, 59 new drugs were approved by the FDA. These include 42 new chemical entities (NCEs) and 17 biologics. Among the biologics, there are 12 monoclonal antibodies (mAb), three pegylated enzymes, one protein, and one fusion protein (Table 1). Interestingly, 2018 has seen the valorization of natural products in drug discovery as 10 drugs inspired by natural products were approved.

Table 1. Biologics approved by the food and drug administration (FDA) in 2018

Class	Active Ingredient	Trade Name	Disease
Monolclonal antibody	Burosumab	Crysvita™	X-linked dominant hypophosphatemic rickets
	Cemiplimab	Libtayo™	Cutaneous squamous cell carcinoma
	Emapalumab	Gamifant™	Hemophagocytic lymphohistiocytosis
	Erenumab	Aimovig™	Migraine prevention
	Fremanezumab	Ajovy™	Migraine prevention
	Galcanezumab	Emgality™	Migraine prevention
	Ibalizumab	Trogarzo™	Multidrug-resistant HIV-1
	Lanadelumab	Takhzyro™	Hereditary angioedema attacks
	Mogamulizumab	Poteligeo™	Relapsed or refractory mycosis fungoides and Sézary disease
	Moxetumomab pasudotox	Lumoxiti™	Relapsed or refractory hairy cell leukemia
	Ravulizumab	Ultomiris™	Paroxysmal nocturnal hemoglobinuria and atypical hemolytic uremic syndrome
	Tildrakizumab	Ilumya™	Moderate-to-severe plaque psoriasis
Pegylated enzymes	Calaspargase pegol	Asparlas™	Acute lymphoblastic leukemia
	Elapegademase	Revcovi™	Adenosine deaminase severe combined immunodeficiency
	Pegvaliase	Palynziq™	Phenylketonuria
Protein	Cenegermin	Oxervate™	Neurotrophic keratitis
Fusion protein	Tagraxofusp-erzs	Elzonris™	Blastic plasmacytoid dendritic cell neoplasm

Source; Torre B.G. and Albericio F., (2019)

1.1.1. Plant Sources of Natural Products in Drug Discovery

Plant kingdom is the oldest source of drug discovery which provides about 25% of the drugs used today. Although there are approximated by 250,000 species of plant in the world, about 10% of them have been evaluated for biological activity (Verpoorte, 1998). Interestingly, among 252 drugs considered by the World Health Organization (WHO) as basic and essential, 11% are exclusively of plant origin, and a significant number of the synthetic drugs are obtained based on natural products (Rates, 2001). Natural products from plants have provided many effective drugs with antioxidant, anti-inflammatory, antitumor, antimutagenic, anti-carcinogenic, antibacterial, or antiviral activities (Maridass and Britto, 2008). Examples of important drugs obtained from plants are shown in table 2.

Table 2. Significant plant-derived pharmaceutical products

Drug	Source plant	Indication	References
Atropine	*Atropa belladonna*	anticholinergic pupil dilation	Berdai *et al*., 2012
Digoxin	*Digitalis lanata*	cardiotonic	Chauhan *et al*.,2012
Nitisinone	*Callistemon citrinus*	hereditary tyrosinaemia type 1 (HT-1) (genetic disease)	Mitchell *et al*., 2001
(L)-dopa	*Mucuna deeringiana*	antiparkinsonism	Katzenschlager *et al*., 2004
Diosgenin	*Dioscorea deltoidea*	antifertility	Shah, 2010
Morphine, Codeine	*Papaver somniferum*	analgesic antitussive	Benyhe, 1994
Apomorphine hydrochloride	*Papaver somniferum*	antiparkinsonism	Deleu *et al*., 2004
Colchicine	*Colchicum autumnale*	antitumour antigout	Schlesinger *et al*., 2006
Quinine	*Cinchona ledgeriana*	antimalarial	Kremsner *et al*.,1994
Chloroquine, Mefloquine	*Artemisia annua* (Quinhaosu)	antimalarial	Buss and Waigh, 1995
Vincristine, Vinblastine	*Catharanthus roseus*	antitumour	Banskota *et al*., 2002

1.1.2. Microbial Sources of Natural Products in Drug Discovery

Microorganisms are an important and prolific source of bioactive compounds that have yielded some of the most important products for new drugs and lead compounds suitable for further modification during drug development in the pharmaceutical industry (Gordon and David, 2013). Microorganisms have been exceptionally rich sources of drugs, including antibiotics, immunosuppressants, anticancer, antihypertensive and anti-inflammatory (Dewick, 2002; Li *et al*., 2014). Following the discovery of penicillin (**3**), a myriad of antibiotics have been discovered from microorganisms. Examples of these are tetracycline (**5**) (Duggar,1948), chloramphenicol (**6**) (Mildred *et al*., 1949), erythromycin (**7**) (McGuire *et al*., 1952), tobramycin (**8**) (Koch and Rhoades, 1970) and vancomycin (**9**) (Hiramatsu *et al*., 1997).

Another interesting example is althiomycin (**10**). Althiomycin (**10**) is a thiazole antibiotic which was first described by Yamaguchi *et al.*, (1957) and was later isolated from cultures of *Streptomyces althioticus*, *Myxococcus virescens*, *M. xanthus*, and *Cystobacter fuscus* (Kunze *et al*., 1982). This compound exhibits antibacterial activity against both Gram-positive and Gram-negative bacteria.

Besides antibiotics, microorganisms are also an important source of drugs for other therapeutic areas. For example, the antiparasitic drug ivermectin (**11**) which was isolated from *Streptomyces* sp. (Buss and Waigh, 1995). Doxorubicin (**12**) (Adriamycin®), a drug used for treatment of acute leukaemia, lung cancer, thyroid cancer and both Hodgkins and non-Hodgkins lymphomas. (Dewick, 2002; Butler, 2004), was isolated from *Streptomyces peucetius*.

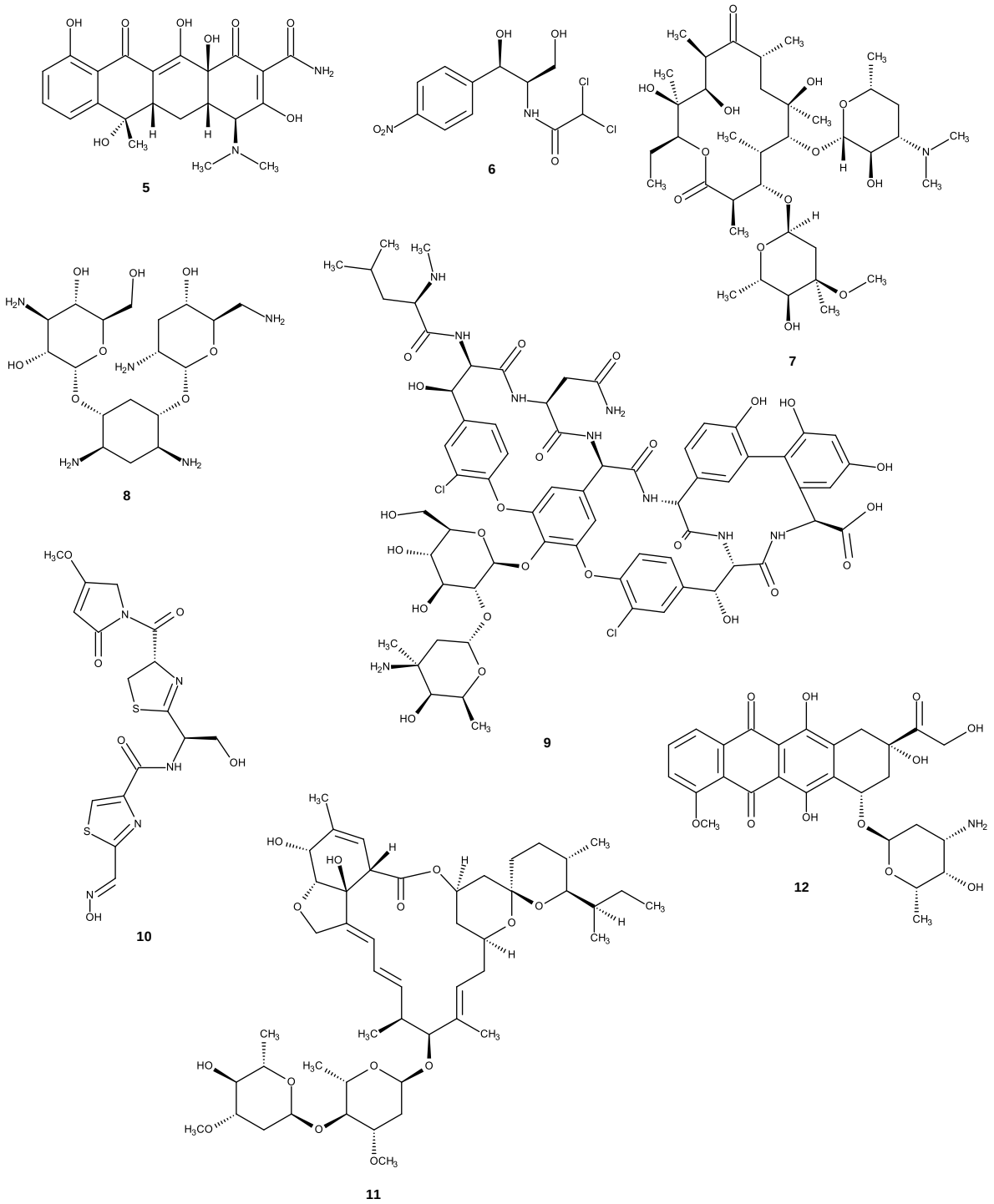

Figure 3. Structures of tetracycline (**5**) chloramphenicol (**6**) erythromycin (**7**), tobramycin (**8**) and vancomycin (**9**), althiomycin (**10**), ivermectin (**11**) and doxorubicin (**12**)

1.1.3. Other Sources of Natural Products in Drug Discovery

Besides plants and microorganisms, other organisms have been also interesting sources of drugs. For example, teprotide (**13**), an angiotensin converting enzyme inhibitor (ACE inhibitor), which was first isolated from the viper snake *Bothrops jararaca*. Although teprotide (**13**) is an effective antihyperension, its use was hampered by a lack of oral activity and a high cost of production. However, due to its long-lasting *in vivo* activity, teprotide (**13**) was chosen as a lead compound to obtain the antihypertension drug captopril (**14**) (Buss and Waigh, 1995).

Epibatidine (**15**), a chlorinated alkaloid secreted from the frog *Epipedobates tricolor*. This compound was used as a model for the development for the novel class of potential painkillers (Daly *et al*., 2005, Salehi *et al*., 2019). DMXBA or GTS-21 (**16**), a 3-benzylidene adduct of anabaseine, was isolated from the marine worm *Amphiporus lactifloreus*. This compound is a mixed nicotinic receptor agonist/antagonista and its synthetic version has completed phase II trials in Alzheimer disease. (Kem *et al*., 2006). Ziconotide (**17**) is a synthetic version of *N*-type calcium channel blocker ω-conotoxin MVIIA (ω-MVIIA), a peptide found in the venom of the fish-eating marine snail, *Conus magus*. It was approved by the FDA in December 2004 and by EU in February 2005, for the treatment of patients suffering from chronic pain. Ziconotide (**17**) is marketed by Elan Pharmaceuticals as Prialt® (Givern, 2007).

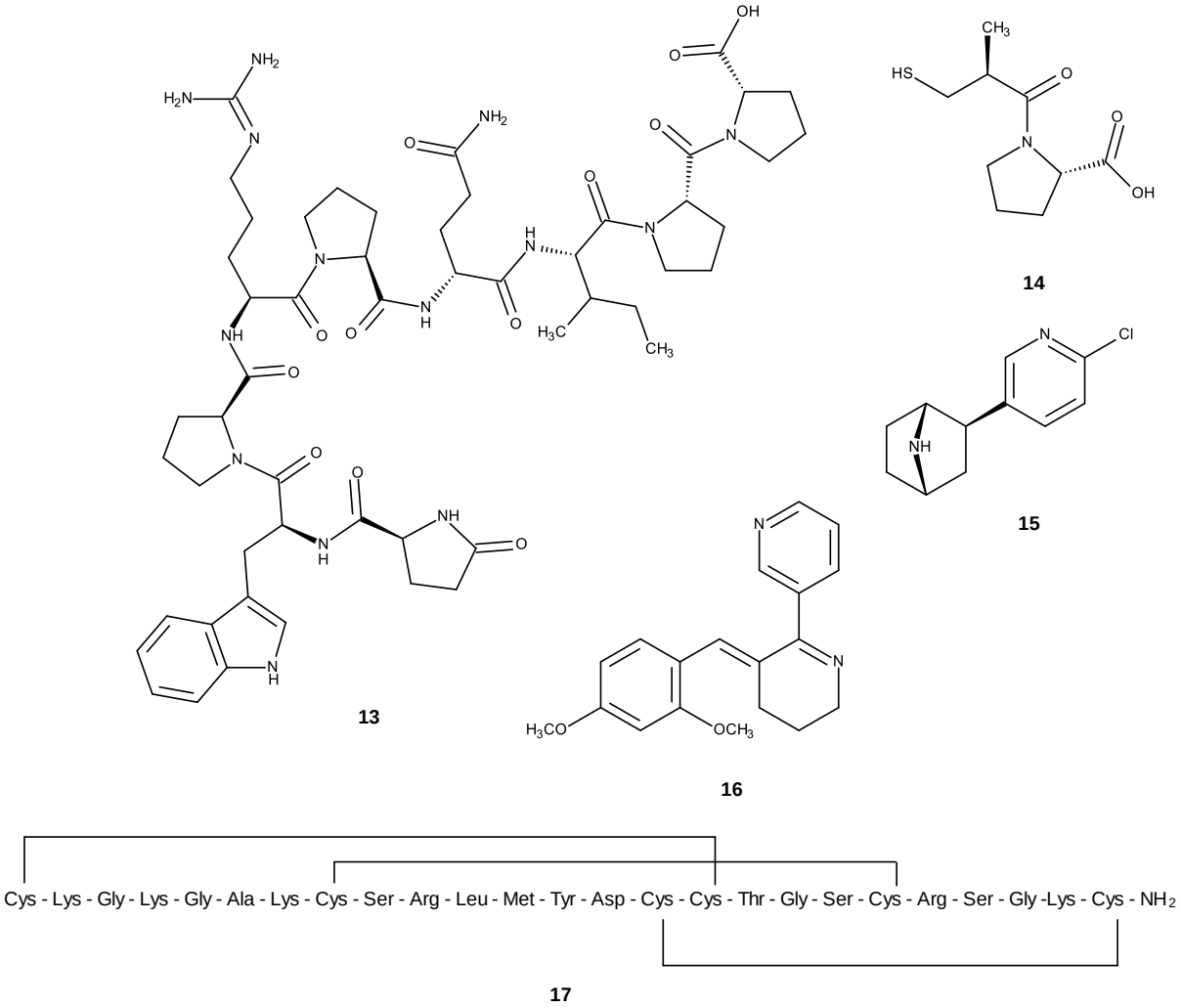

Figure 4. Structures of teprotide (**13**), captopril (**14**), epibatidine (**15**), GTS-21 (**16**) and ziconotide (**17**)

1.2. Drugs Discovery from Marine Sources

The oceans, which cover more than 70% of the earth's surface and more than 95% of the earth's biosphere, are the habitat of marine organisms (Fouillaud *et al.*, 2016; Jin *et al.*, 2016). The biodiversity from the oceans, which is estimated between 250,000 and one million of marine species, could contribute a large resource to the discovery of NCEs, serving as unprecedented novel bioactive structures and scaffolds with a great potential for medical treatments or templates for new therapeutics (Montaser and Luesch, 2011). Among marine organisms, macroorganisms such as

algae, sponges, corals, and other marine invertebrates are not only the richest source of bioactive metabolites with potential for the development of new medicines and agrochemicals but also the major hosts of symbiotic microorganisms such as actinomyces, bacteria and fungi. In particular, microbial symbionts like bacteria are important producers of marine natural products (Gulder and Moore, 2009). Marine natural products usually exhibit a wide range of biological and pharmacological activities, such as antitumor, antibacterial, anticoagulant, anti-inflammatory, antifungal, anthelmintic, antiplatelet, antiprotozoal and antiviral activities. They can also affect the cardiovascular, endocrine, immune, and nervous systems (Glaser and Mayer, 2009). Hu *et al.*, (2015) have reported the number of bioactive compounds from marine organisms during the year 1985 to 2012. Among the reported 4,196 bioactive marine natural products, 2,225 (56%) showed anticancer activity and 521 (13%) showed antibacterial activity. The rest of the compounds possessed antifungal (5%), pest resistance (insect/vermin) (3%), antivirus (3%), prevention of heart and vascular disease (PHVD) (1%), and protection of neurons/neurotoxicity (PN/NT) (1%), whereas 755 compounds (18%) did not fit in the above-mentioned bioactivity groups (Figure 5).

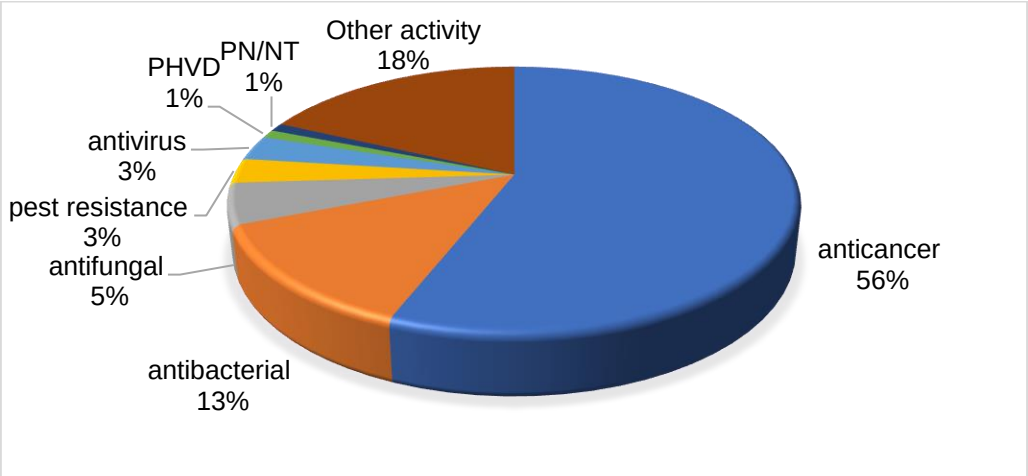

Figure 5. Bioactivities of new marine natural products (Hu *et al.*, 2015)

In addition, Mayer and Gustafson reviewed 72 natural compounds as potential new anticancer agents, which discovered from marine organisms during the year from 2003 to 2006, mostly isolated from sponges (36 compounds), tunicates (13 compounds), mollusks (7 compounds), algae (3 compounds), bacterium (3 compounds), soft coral, worm, bryozoan and fungi were isolated for two compounds from each species, as well as one compound from sea hare and sea cucumber.

Marine natural products have become a hot topic of research in the field of drug discovery around the world because the FDA and the European Medicine Agency have approved some of the marine-derived compounds and their derivatives. For examples, the anticancer drug, cytarabine (**18**) (Cytosar-U®, Depocyt®), and the antiviral drug, vidarabine (**19**) (Vira-A®), were developed from pyrimidine ribosides spongothymidine and spongouridine, originally isolated from the Caribbean sponge *Tethya crypta*. Ziconotide (**17**) (Prialt®), a cyclic peptide isolated from the marine snail *Conus magus,* is used for a pain management. Finally, trabectedin or ET-743 (**20**) (Yondelis®; Pharmamar), a tetrahydroisoquinoline alkaloid first isolated from a colonial tunicate *Ecteinascidia turbinata*, was approved by European Commission for treatment of soft tissue sarcoma (STS) in 2007, and won a final European approval for treatment of ovarian cancer in 2009. However, the current supply is based on a semisynthetic process from cyanosafracin B, an antibiotic obtained by fermentation of bacterium *Pseudomonas fluorescens*. Interestingly, it was later proved that this alkaloid was biosynthesized by the bacterial symbiont *Candidatus Endoecteinascidia frumentensis.*

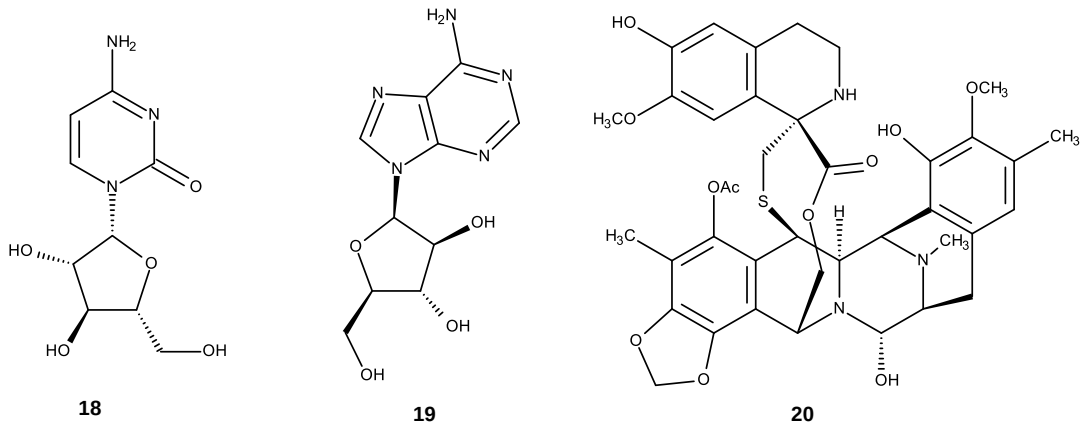

Figure 6. Structures of cytarabine (**18**), vidarabine (**19**) and trabectedin (**20**)

1.2.1. Marine Invertebrates as Sources of Marine Natural Products

The investigation on marine natural products started in the early 1950s when Bergmann and Feeney isolated two pyrimidine ribosides**,** spongouridine (**21**) and spongothymidine (**22**) from the marine sponge *Cryptotethya crypta*. Since then natural products and new compounds have been continuously isolated from marine invertebrates, many of which displayed interesting biological and pharmacological activities. Examples of these are cyclic peptides discodermins B-D (**23**-**25**), isolated from the marine sponge, *Discodermia kiiensis*/Lithistida, which showed antibacterial activity against *Bacillus subtilis* at 3 µg/mL (Matsunaga *et al*., 1985). In 1999, Urban and his group reported the isolation of four imidazo-azolo-imidazole alkaloids, axinellamines A-D (**26**-**29**), from an Australian marine sponge, *Axinella* sp.; however, only axinellamines B-D (**27**-**29**) displayed bactericidal activity against *Helicobacter pylori* with MIC of 16.7 µg/mL. Arenosclerins A-C (**30-32**), tetracyclic alkylpiperidine alkaloids isolated from the marine sponge *Arenosclera brasiliensis* exhibited antibacterial activity against *Staphylococcus aureus*, *Pseudomonas aeruginosa*, *Mycobacterium tuberculosis*, with MIC between 16 µg/mL and 30 µg/mL (Torres *et al*., 2002). Isoaaptamine (**33**), a 1*H*-benzo[de][1,6]-naphthyridine alkaloid isolated from the marine sponge, *Aaaptos aaptos*. This compound exhibited inhibitory activity against sortase A (SrtA), an enzyme that plays a key role in cell wall protein anchoring and virulence in *S. aureus* with an IC_{50} value of 3.7 µg/mL.

Some compounds isolated from marine invertebrates also have antiviral activity. Papuamides A-D (**34**-**37**), cyclic depsipeptides were isolated from the marine sponge *Theonella mirabilis* and *T. swinhoei*. However, only papuamides A and B showed inhibition of the *in vitro* infection of human T-lymphoblastoid cells by HIV-1_{RF} with an EC_{50} of *ca*. 4 ng/mL. Haplosamates A and B (**38** and **39**), sulfamated steroids isolated from the marine sponge *Xestospongia* sp. were found to inhibit HIV-1 integrase with IC_{50} of 50 µg/mL and 15µg/mL, respectively (Qureshi and Faulkner, 1999). A bromoindole alkaloid, named dragmacidin F (**40**), isolated from the marine sponge *Halicortex* sp, showed an *in vitro* antiviral activity against HSV-1 with EC_{50} of 95.8 µM, and HIV-1 with EC_{50} of 0.91 µM (Cutignano *et al*., 2000). The cyclic depsipeptides, mirabamides A-D (**41**-**44**), were isolated from the marine sponge

Siliquariaspongia mirabilis. Mirabamides A (**41**), C (**43**) and D (**44**) inhibited HIV-1 in neutralization and fusion assays, indicating that these compounds acted at early stage of the HIV-1 entry (Plaza *et al*., 2007).

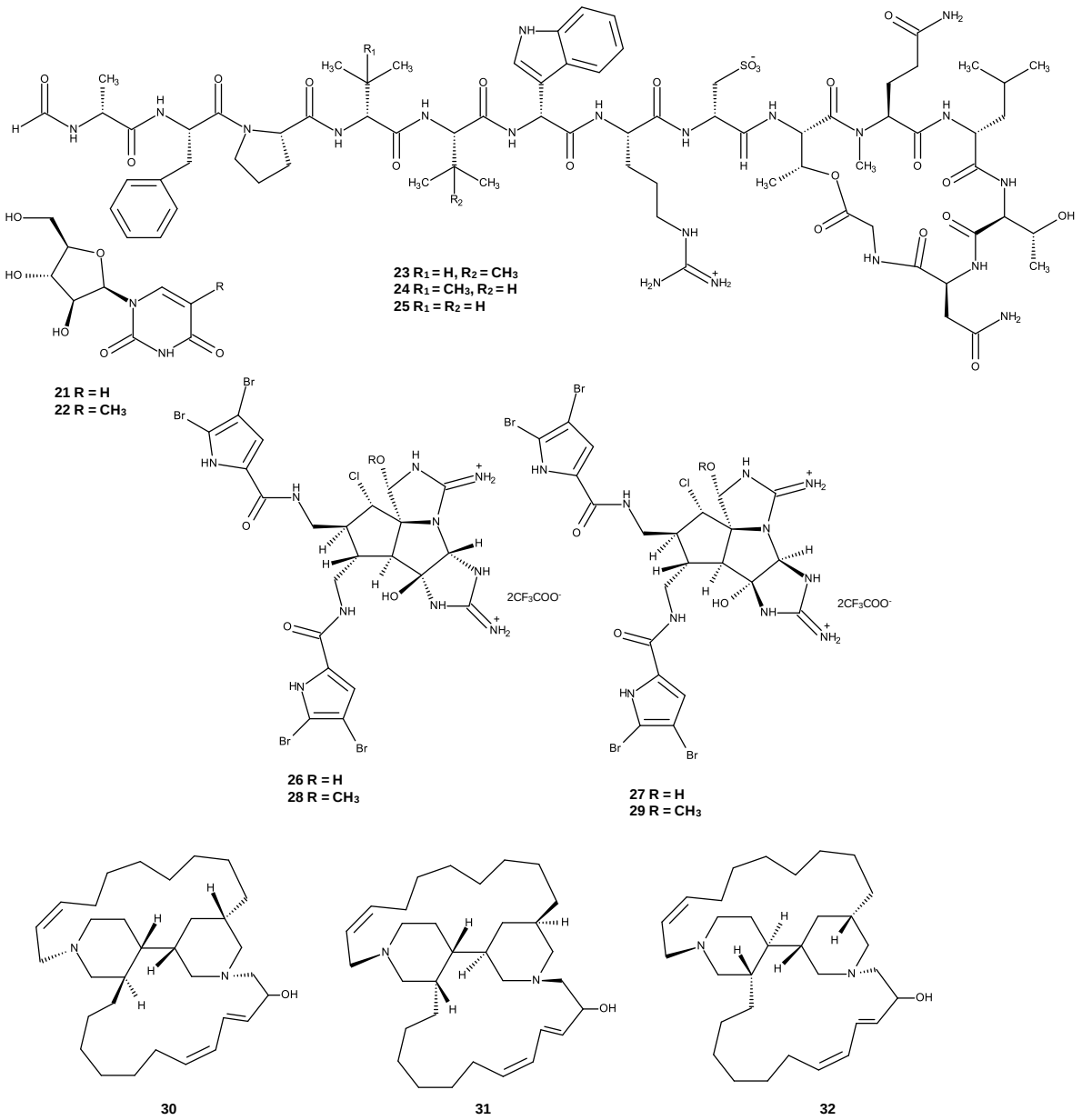

Figure 7. Structures of spongouridine (**21**), spongothymidine (**22**), discodermins B (**23**), C (**24**), D (**25**), axinellamines A (**26**), B (**27**), C (**28**), D (**29**), Arenosclerins A (**30**), B (**31**) and C (**32**)

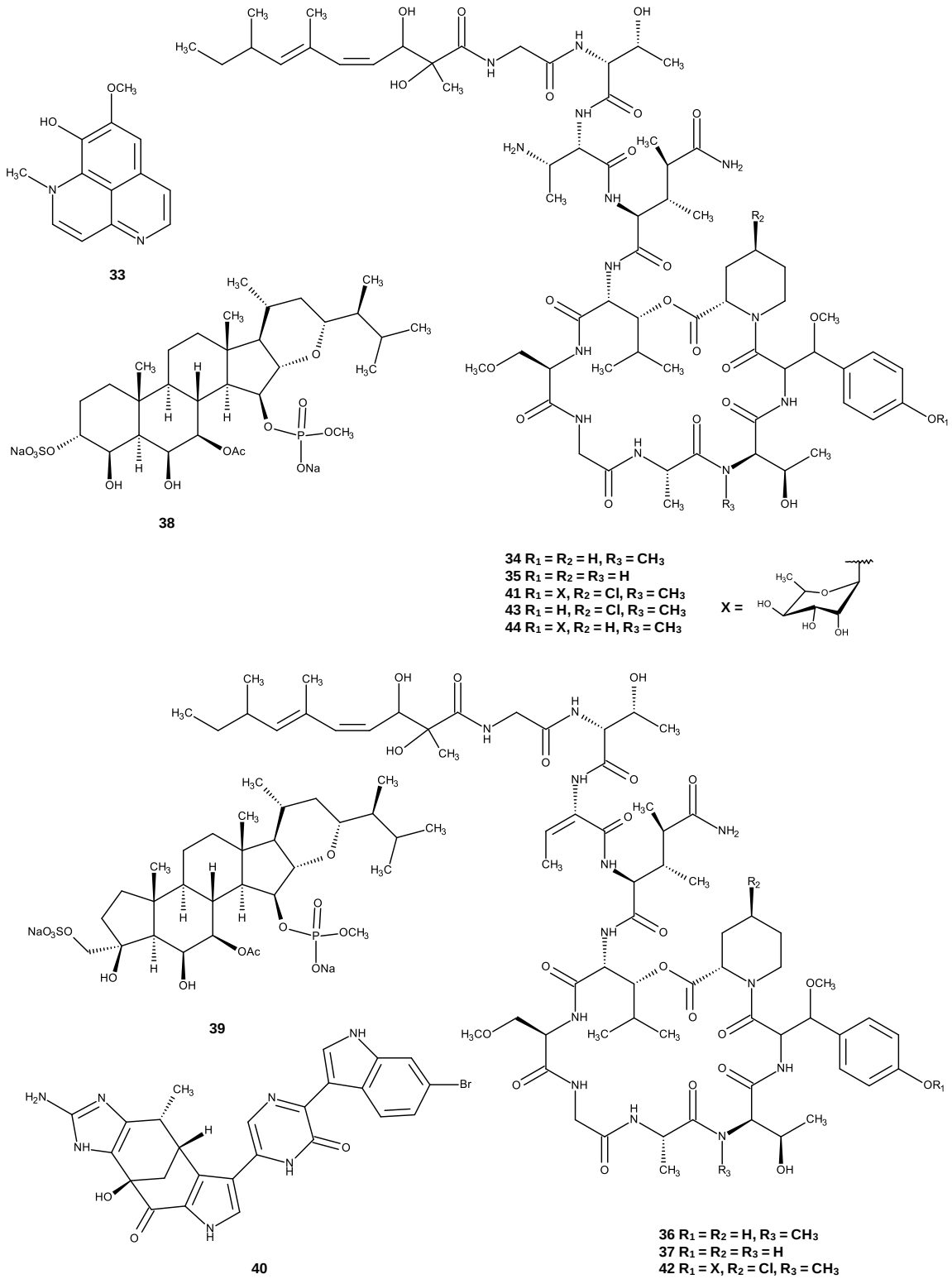

Figure 8. Structures of isoaaptamine (**33**), papuamides A (**34**), B (**35**), C (**36**), D (**37**), haplosamates A (**38**), B (**39**), dragmacidin F (**40**), mirabamides A (**41**), B (**42**), C (**43**) and D (**44**)

1.2.2. Marine Bacteria as Sources of Marine Natural Products

Marine bacteria are an important source of marine natural products, many of which constitute novel lead structures for drug discovery. There are several reviews on bioactive compounds from marine-derived bacteria. However, only some examples of interesting bioactive secondary metabolites of bacteria, especially actinomycetes, which are relevant in drug discovery are discussed herein. Salinosporamide A (NPI-0052; **45**) was isolated from an Actinomycete bacterium, *Salinospora* strain CNB-392, which was isolated from the heate-treated marine sediment sample. This compound exhibited potent *in vitro* cytotoxicity against HCT-116 (human colon carcinoma) cell line with an IC_{50} value of 11 ng/ mL, and even greater potency (LC_{50} values less than 10 nM) against NCI-H226 (non-small cell lung cancer), SF-539 (CNS cancer), SK-MEL-28 (melanoma), and MDA-MB-435 /breast cancer) cell lines. Salinosporamide A (**45**) was found to inhibit proteasomal chymotrypsin-like proteolytic activity with an IC_{50} value of 1.3 nM (Feling *et al*., 2003). Salinosporamide A (NPI-0052; **45**) is currently in clinical trials for the treatment of various cancers. Later on, Williams *et al.*, (2007) described isolation of saliniketals A and B (**46** and **47**), bicyclic polyketides, from the marine actinomycete *S. arenicola.* Compounds **46** and **47** were found to inhibit ornithine decarboxylase induction, an important target for the chemoprevention of cancer, with IC_{50} values of 1.95 ± 0.37 and 7.83 ± 1.2 µg/mL, respectively.

Kwon *et al*., (2006) reported isolation of marinomycins A-D (**48**-**51**), unusual macrodiolides from the saline culture of *Marinispora* strain CNQ-140, a member of a new group of actinomycetes, which was isolated from a marine sediment. Compounds **48**-**51** showed significant antibiotic activities, with MIC values at 0.1−0.6 µM, against vancomycin-resistant *Enterococcus faceium* (VREF) and methicillin-resistant *S. aureus* (MRSA). These compounds also inhibited proliferation against the NCI's 60 cancer cell line panel, with average LC_{50} values of 0.2−2.7 µM.

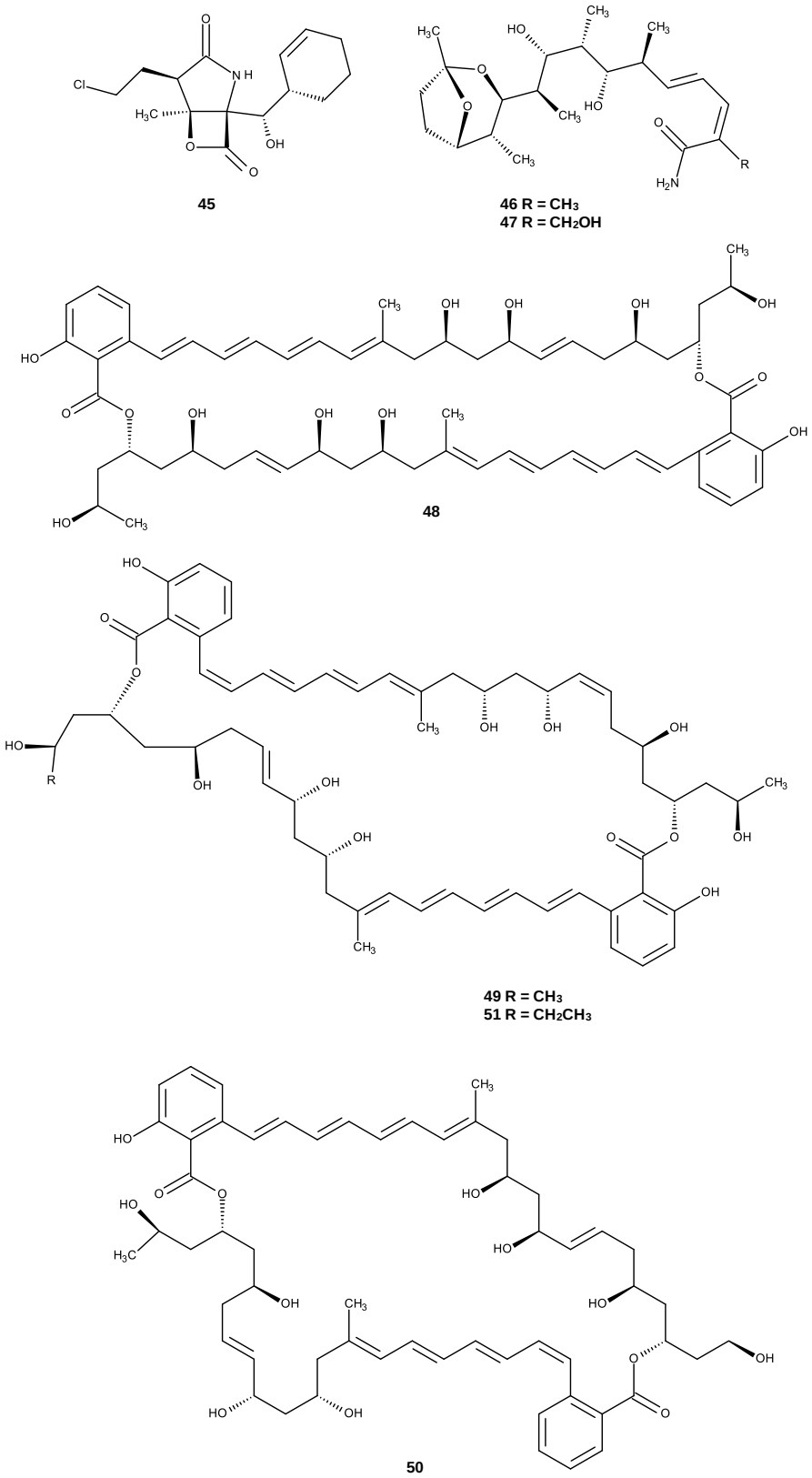

Figure 9. Structures of salinosporamide A (**45**), saliniketals A (**46**), B (**47**), marinomycins A (**48**), B (**49**), C (**50**) and D (**51**)

1.2.3. Marine Fungi as Sources of Marine Natural Products

Fungi are among the most diverse and important organisms in the world, and around 70,000 fungal species have already been described worldwide. Among these, about 1,500 species are marine-derived, primarily from coastal ecosystems (Fouillaud *et al*., 2016). Marine-derived fungi are often associated with marine organisms and substrata such as sponges, corals, sea anemone, tunicates, higher algae, sea grasses, mangroves, starfish, sea urchin, molluscs, woody substrates, driftwoods and sediments (Abad *et al*., 2011; Devarajan *et al*., 2002; Jin *et al*., 2016). In recent years, marine fungi have gained a growing interest from the scientific community as sources of bioactive compounds for biotechnological application. This interest is due to the fact that fungi produce secondary metabolites with potential pharmacological and biological activities (Imhoff, 2016; Rateb and Ebel, 2011). Marine-derived fungi are important sources for novel bioactive secondary metabolites such as alkaloids, glycosides, lipids, polyketides, peptides, proteins, terpenoids, many of which displayed antiviral, antitumor, antibacterial and antifungal properties (Arasu *et al*., 2013; Bugni and Ireland, 2004; Gomes *et al*., 2014; Jin *et al.*, 2016; Manimegalai *et al*., 2013; Rateb and Ebel, 2011; Rowley *et al*., 2003; Shen *et al*., 2009 and Wang *et al*., 2015).

In 2016, Jin *et al*. reported new compounds isolated from marine-derived fungi, during the period of 2014 and 2015, based on their sources: marine animals 30.1%, mangrove 25.5%, sediment 22.9%, alga 14.4%, sea water 4.6% and other 2.6% (Figure 10). Additionally, overview of new chemical structures isolated from marine-derived fungi revealed that alkaloids (27%) and polyketides (25.7%) constituted the main chemical classes, followed peptides (13.8%) and terpenes (9.9%), and in lesser extent lactones (3.9%) and steroids (3.3%) (Figure 11). Among the biological activities majority of the compounds exhibited cytotoxicity (37.5%) and antimicrobial activity (33.5%, i. e. antibacterial 18.9%, antifungal 7.9% and antiviral 7.2%), followed by antioxidant (5.3%), lipid-lowering (5.3%) and other activities (18.4%) (Figure 12).

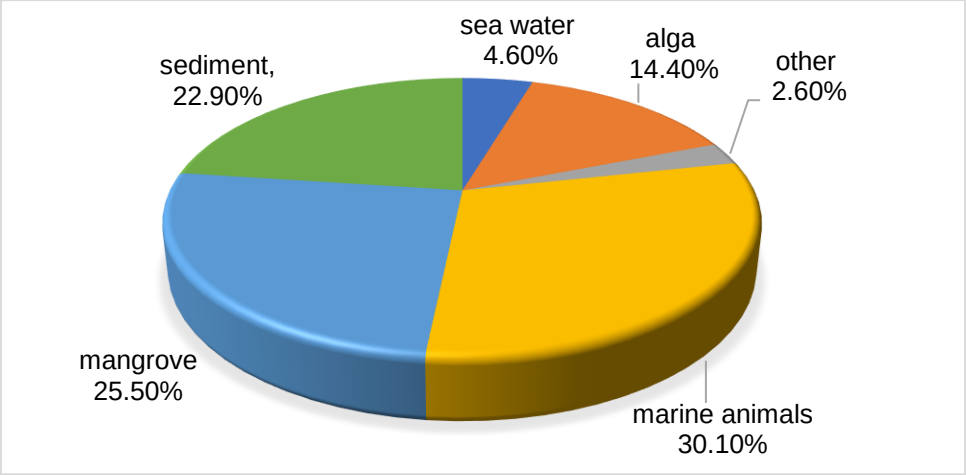

Figure 10. New compounds from marine-derived fungi, in the period of 2014-2015, according to sources of the fungal strains (Jin *et al*., 2016)

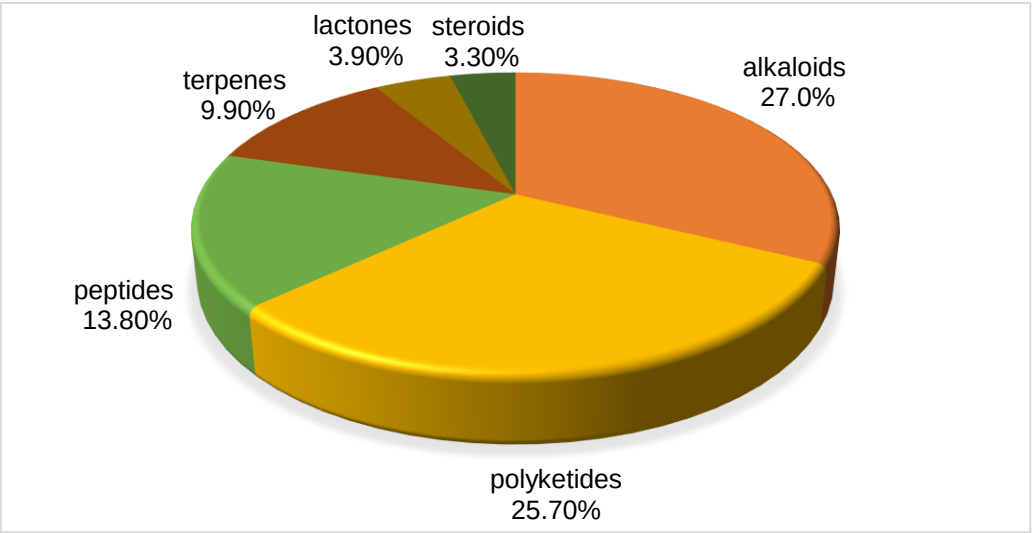

Figure 11. New compounds from marine-derived fungi, in the period of 2014-2015, according to their structural types (Jin *et al*., 2016)

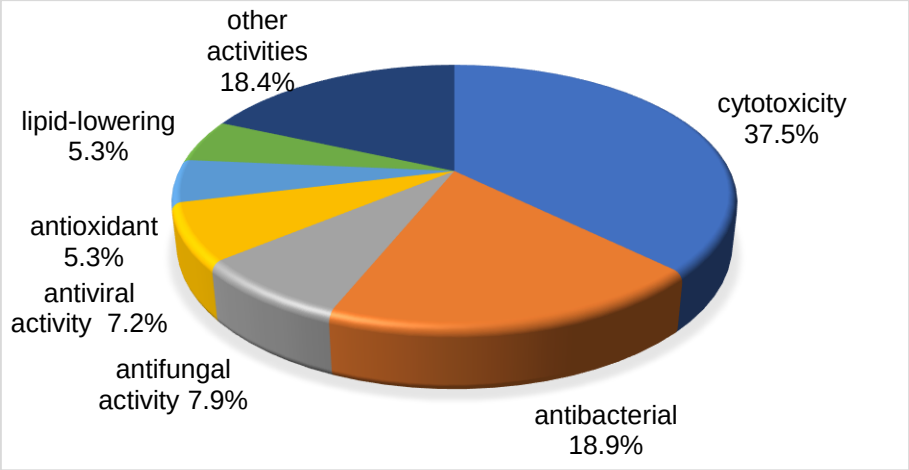

Figure 12. Bioactive categories of new compounds from marine-derived fungi, in the period of 2014-2015 (Jin *et al*., 2016)

Currently, there is a huge increase in the number of reported secondary metabolites isolated from marine-derived fungi, with many new bioactive compounds being described each year. For examples, a new antimicrobial anthraquinone, monodictyquinone A (**52**) was isolated from the EtOAc extract of a marine-derived fungus *Monodictys* sp., which was isolated from the sea urchin *Anthocidaris crassispina*, collected at Toyama Bay in the Sea of Japan. This compound showed antibacterial activity against *Bacillus subtilis*, *Escherichia coli*, and *Candida albicans*, with 2.5 µg/disk (El-Beih *et al*., 2007). Spartinoxide (**53**), isolated from the culture of the algicolous fungus *Phaeosphaeria spartinae* which was isolated from the marine alga *Ceramium* sp., collected in the North Sea, Germany, showed potent inhibitory activity against human leukocyte elastase (HLE), with IC_{50} values of 1.71-0.30 µg/mL. (Elsebai *et al*., 2010). Anhydrofusarubin (**54**), an anthraquinone derivative isolated from the marine endophytic fungus *Fusarium* sp. strain No. b77, showed a significant inhibition of the growth of HEp2 and HepG2 cells, with IC_{50} values of 8.67 and 3.47 µM, respectively (Shao *et al*., 2010). Two new bianthraquinone derivatives, alterporriols K (**55)** and L (**56**), were isolated from the mangrove endophytic fungus *Alternaria* sp. ZJ9-6B, which was isolated from the mangrove *Aegiceras corniculatum*, collected in the South China Sea. Compounds **55** and **56** were moderately active

against MDA-MB-435 and MCF-7 human breast cancer cell lines with IC_{50} values of 13.1-29.1 μM (Huang *et al*., 2011). Four new norsesquiterpene peroxides, talaperoxides A-D (**57**-**60**) together with one known analogue, steperoxide B (**61**) produced from the mangrove endophytic fungus, *Talaromyces flavus,* which was isolated from the leaves of a mangrove plant, *Sonneratia apetala*, collected on the coastal saltmarsh of the South China Sea. Compounds **58** and **60** displayed cytotoxicity against human breast cancer cell lines (MCF-7 and MDA-MB-435), human hepatoma cell line (HepG2), human cervical cancer cell line (HeLa), and human prostatic cancer cell line (PC-3) with IC_{50} values between 0.70 and 2.78 μg/mL (Li *et al*., 2011).

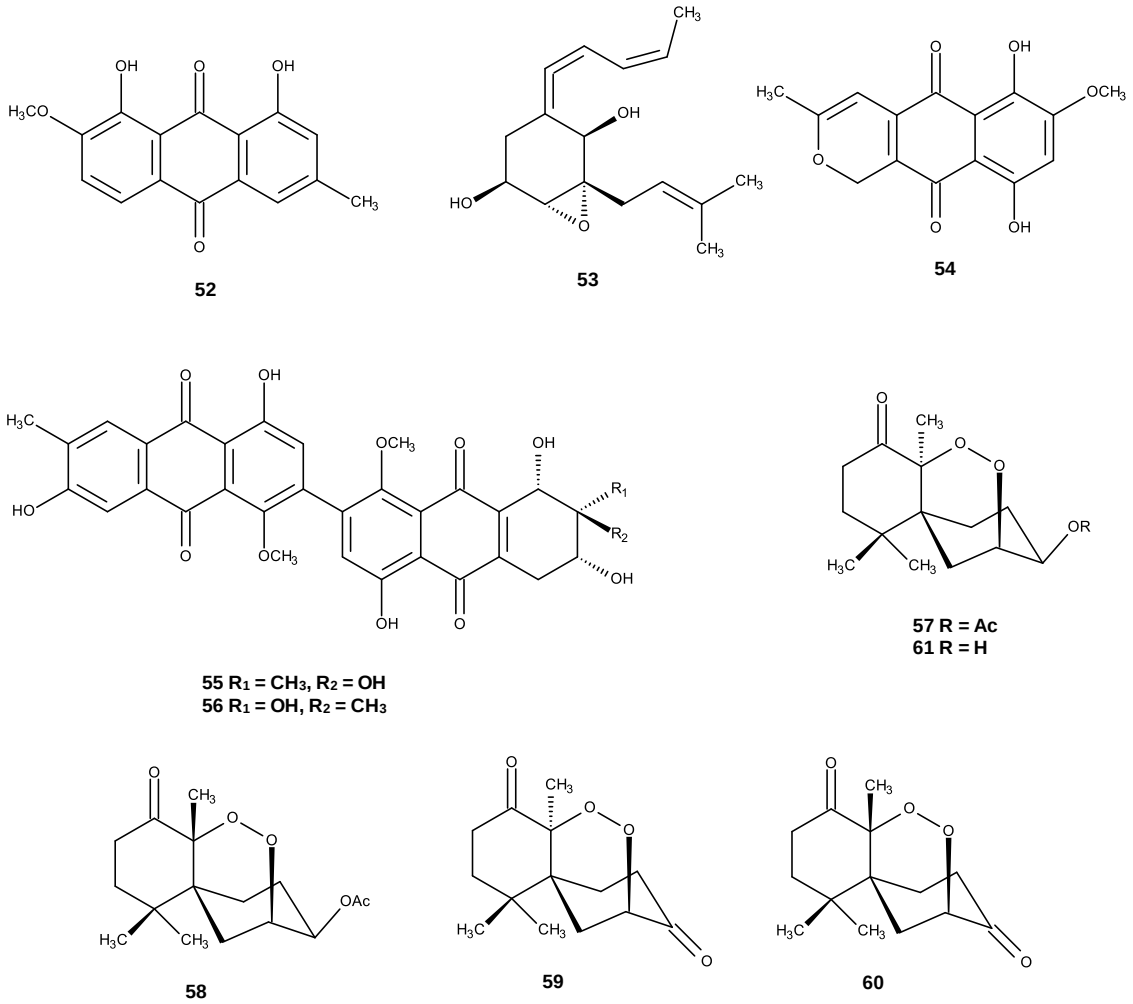

Figure 13. Structures of monodictyquinone A (**52**), spartinoxide (**53**), anhydrofusarubin (**54**), alterporriols K (**55)**, L (**56**), talaperoxides A (**57**), B (**58**), C (**59**), D (**60**) and steperoxide B (**61**)

A new chlorinated anthraquinone, 6-*O*-methyl-7-chloroaverantin (**62**), isolated from the marine-derived fungus *Aspergillus* sp. SCSIO F063, which was isolated from a marine sediment sample collected in the South China Sea, displayed significant inhibition against SF-268, MCF-7 and NCI-H460 tumor cell lines, with IC_{50} values of 7.11, 6.64, and 7.42 µM, respectively (Huang *et al*., 2012). Two new cadinane-type sesquiterpenoids hypocreaterpenes A (**63**) and B (**64**) were isolated from the fungus *Hypocreales* sp. HLS-104, which was isolated from the marine sponge *Gelliodes carnosa*. These compounds showed moderate inhibitory effects on the nitric oxide (NO) production in lipopolysaccharide (LPS)-treated RAW264.7 cells (Zhu *et al*., 2013). A new sesterterpene ophiobolin K (**65**) was isolated from a deep-sea marine-derived fungus *Emericella variecolor* strain GF-10 which was collected from a sediment at 70 m depth at Gokasyo Gulf, Japan. The compound inhibited biofilm formation in *Mycobacterium smegmatis* with MIC 4.1 µM (Arai *et al*., 2013). Two new antibiotics, trichodin A (**66**) and pyridoxatin (**67**) were identified from the marine-derived fungus, *Trichoderma* sp. strain MF106 which was obtained from the Greenland Seas. Compounds **66** and **67** showed moderate antibiotic activity against the Gram-positive *Bacillus subtilis*, *Staphylococcus epidermidis* (MRSA), and yeast, *Candida albicans,* with IC_{50} values of 24 µM. (Wu *et al*., 2014). Rubrumazine B (**68**), an indolediketopiperazine, was isolated from the algicolous fungus *Eurotium cristatum* EN-220, which was isolated from the marine alga *Sargassum thunbergii*, collected at the coast of Qingdao, China. This compound exhibited moderate activity against plant-pathogenic fungus *Magnaporthe grisea* with MIC 64 µg/mL (Du *et al*., 2017).

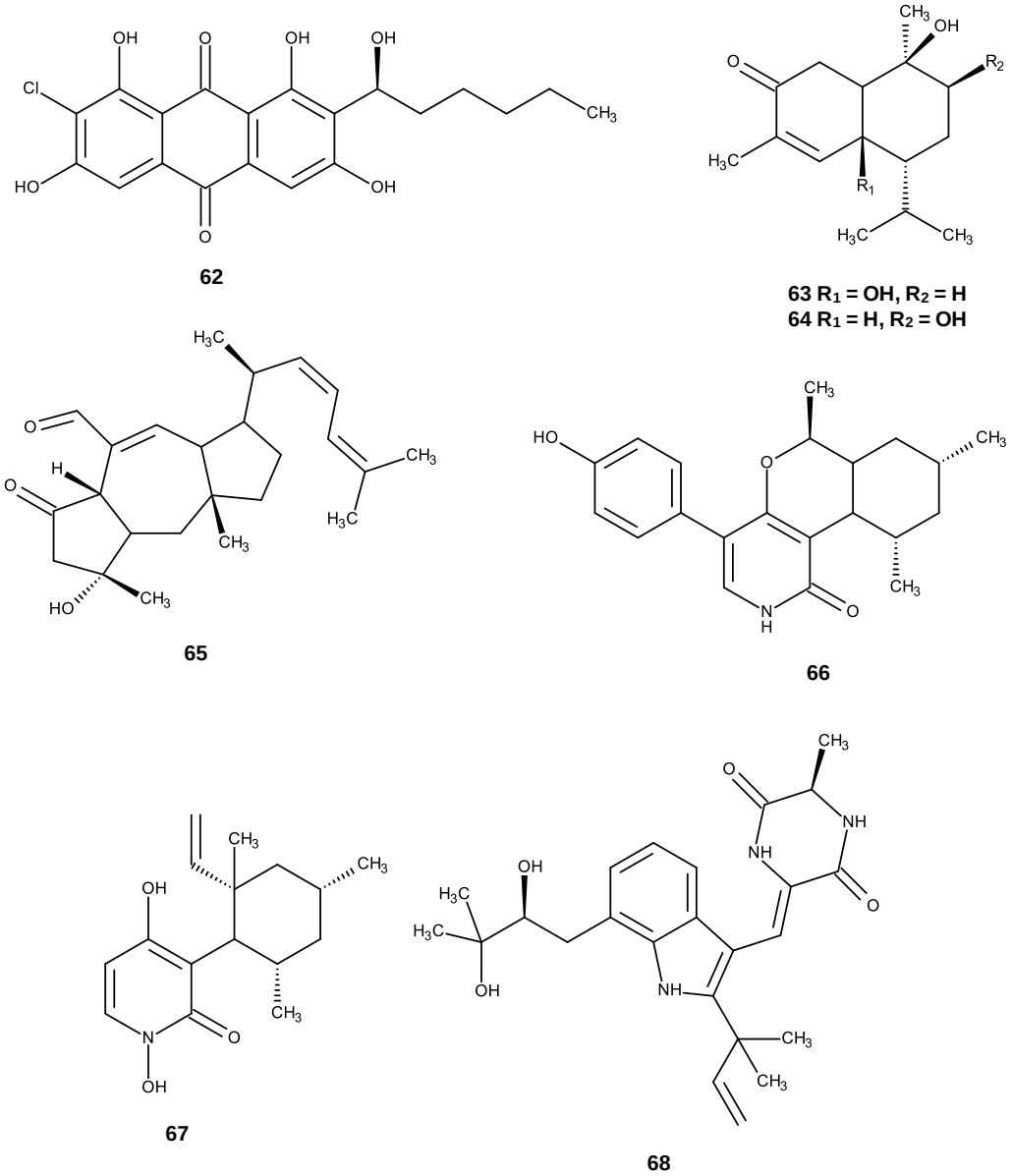

Figure 14. Structures of 6-*O*-methyl-7-chloroaverantin (**62**), hypocreaterpenes A (**63**), B (**64**), ophiobolin K (**65**), trichodin A (**66**), pyridoxatin (**67**) and rubrumazine B (**68**)

1.3. Scope of the Present Study

The main goal of the present investigation was to isolate and identify bioactive secondary metabolites produced by cultures of the marine sponges-associated fungi for evaluation of their antibacterial activity against multidrug-resistant bacteria. For this purpose, two fungal strains belonging to the genera *Neosartorya* and *Penicillium,* which were isolated from marine sponges, collected from Thai waters, were taxonomically identified and cultured in the laboratory by using solid medium (cooked rice) to produce the secondary metabolites. This work is divided into three main parts:

1.3.1. Isolation and Identification of Marine Sponges-Associated Fungi

The samples marine sponges were collected from different locations (Similan Islands in Phang Nga Province, Southern Thailand, and Samaesan island in the Gulf of Thailand, Chonburi province, Thailand) by scuba diving.

The fungal identification was based on morphological characteristics as observed under a light microscope. Moreover, the ornamentation of ascospores was conducted using the scanning electron microscopy (SEM). The identity of the fungi was also confirmed by molecular techniques, using ITS primers.

1.3.2. Isolation and Identification of Secondary Metabolites

For the isolation and purification of the secondary metabolites from the crude extracts of the marine sponge-associated fungi, various chromatographic techniques such as column chromatography (CC), medium pressure liquid chromatography (MPLC), and preparative thin layer chromatography (TLC) were employed. The structure elucidation of the isolated compounds were based on spectroscopic methods namely 1D (^{1}H and ^{13}C NMR, DEPTs) and 2D NMR (COSY, HSQC, HMBC and NOESY) techniques and High Resolution Mass Spectrometry (HRMS). For chiral compounds, which exist in suitable crystalline form, their absolute stereochemistry was established by X-ray crystallography. On the other hand, comparison of calculated

and experimental electronic circular dichroism was used when the compounds exist in non-crystalline form.

1.3.3. Biological Activity Evaluation of the Secondary Metabolites

Some of the isolated secondary metabolites were evaluation for their antibacterial activity against reference and multidrug-resistant strains of Gram-positive and Gram-negative bacteria, as well as for their synergetic effect with antibiotics currently used. The capacity of the active compounds to inhibit biofilm formation was also studied.

CHAPTER II

CHEMISTRY OF THE FUNGI GENERA

NEOSARTORYA AND *PENICILLIUM*

2.1. Secondary Metabolites from *Neosartorya* Species

The genus *Neosartorya* (Family Trichocomaceae) is a teleomorph (sexual state) of the genus *Aspergillus* section *Fumigati* (Samson *et al*., 2007). Unlike *Aspergillus* and *Penicillium* species, the fungi of the genus *Neosartorya* have not been widely investigated for their secondary metabolites However, literature search reveals that some members of this genus produce many interesting secondary metabolite, including xanthones, alkaloids, γ-lactones derivatives, pyripyropenes, polyketides and meroterpeneoids, many of which exhibited interesting biological activities such as antibacterial, antimalarial and cytotoxic activities (Rajachan *et al*., 2016). Given the importance of the investigation of the secondary metabolites from the marine fungi of this genus, chemical classes and biological activities of the secondary metabolites produced by the fungi of this genus are highlighted. For this purpose, the secondary metabolites isolated and identified are listed for each investigated species.

2.1.1. *Neosartorya fennelliae*

New dihydrochromone dimer, paecilin E (**69**), together with eleven known compounds, dankasterone A (**70**), *β*-sitostenone (**71**), ergosta-4,6,8 (14), 22-tetraen-3-one (**72**), cyathisterone (**73**), byssochlamic acid (**74**), dehydromevalonic acid lactone (**75**), chevalone B (**76**), aszonalenin (**77**), helvolic acid (**78**), secalonic acid A (**79**) and fellutanine A (**80**) (Figure 15) were isolated from the culture of the marine sponge-associated fungus *N. fennelliae* KUFA 0811, isolated from the marine sponge *Clathria reinwardtii*, which was collected from Samaesan Island in the Gulf of Thailand. Paecilin E (**69**) exhibited inhibitory effect against *Staphylococcus aureus* ATCC 29213 and *Enterococcus faecalis* ATCC 29212 with MIC values of 32 and 16 µg/mL, respectively, while dankasterone A (**70**) was effective against *Enterococcus faecalis* ATCC 29212 and *Enterococcus faecalis* A5/102 (VRE), with MIC of 32 and 64 µg/mL, respectively (Kumla *et al*., 2017).

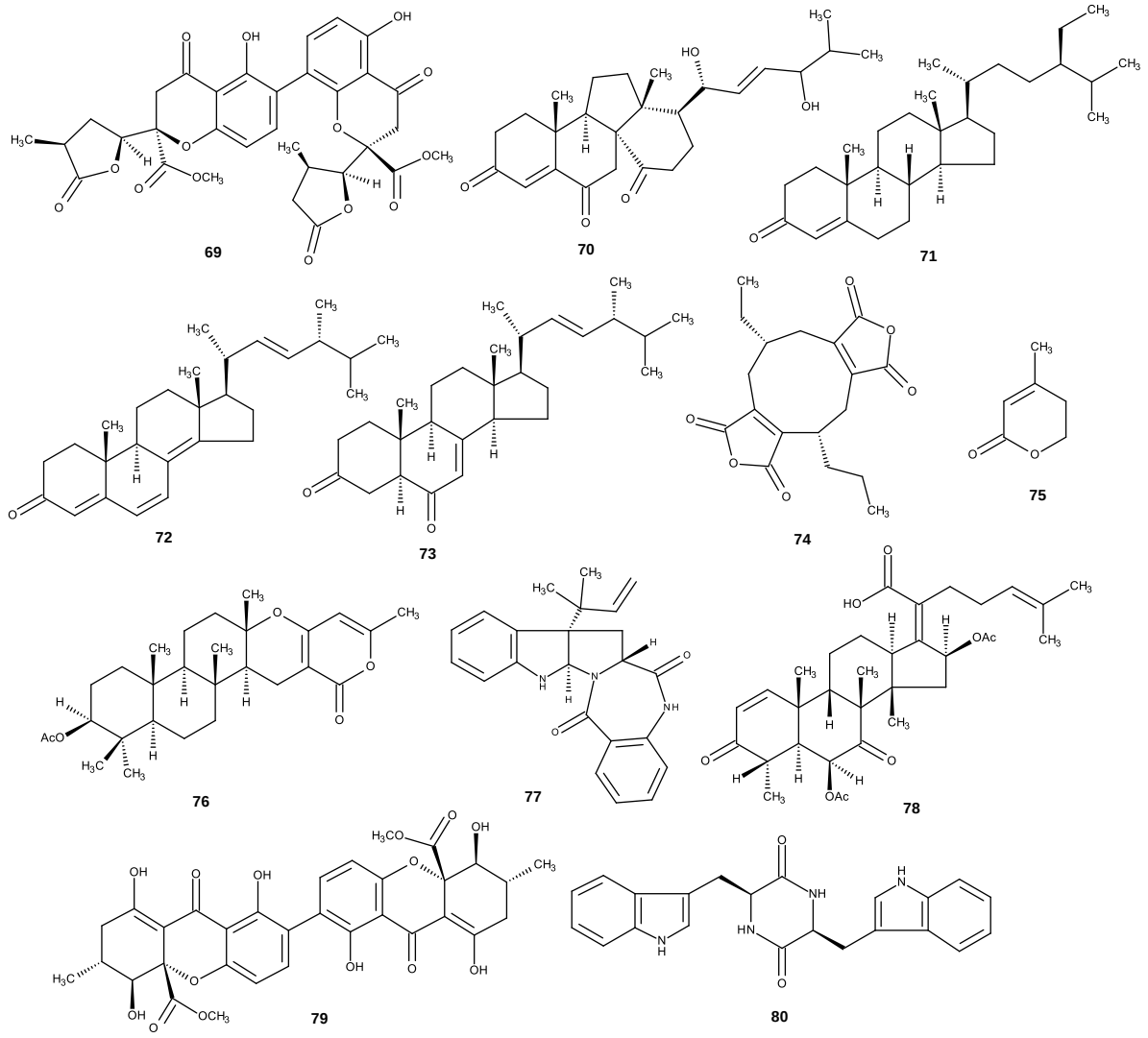

Figure 15. Structures of paecilin E (**69**), dankasterone A (**70**), *β*-sitostenone (**71**), ergosta-4,6,8 (14), 22-tetraen-3-one (**72**), cyathisterone (**73**), byssochlamic acid (**74**), dehydromevalonic acid lactone (**75**), chevalone B (**76**), aszonalenin (**77**), helvolic acid (**78**), secalonic acid A (**79**) and fellutanine A (**80**)

2.1.2. *Neosartorya fischeri*

Wong *et al*., (1993) reported isolation of fiscalins A-C (**81-83**) and tryptoquivaline (**84**) (Figure 16), from the culture of *N. fischeri,* isolated from plant rhizosphere collected in Taiwan. Compounds **81-83** exhibited the binding inhibition of

substance P ligand to the neurokinin (NK-1) receptor of U-373 MG (human astrocytoma) cell with *Ki* values of 57, 174 and 68 µM, respectively. Neosartorin (**85**) and eumitrin A1 (**86**) (Figure 16) was isolated from a soil fungus, *N. fischeri*, which was collected from the river Vah sediment in Slovakia (Proksa *et al*., 1998). Later**,** Wakana *et al*. (2006) isolated the cyclopentenone derivatives, isoterrein (**87**) and terrein (**88**), together with nortryptoquivalone (**89**) (Figure 16) and aszonalenin (**77**) (Figure 15), from cultures of *N. fischeri* stain IFM52672.

Two new compounds, named fischeacid (**90**) and fischexanthone (**91**), together with AGI-B4 (**92**), chrysophanol (**93**), emodin (**94**), 5'-deoxy-5'methylamino-adenosine (**95**), adenosine (**96**), 3,4-dihydroxybenzoic acid (**97**), sydowinin A (**98**) and sydowinin B (**99**) (Figure 16), were isolated from the marine-derived fungus *N. fischeri* strain $1008F_1$. AGI-B4 (**92**) exhibited a potent inhibition of the proliferation of human gastric cancer (SGC-7901) and hepatic cancer (BEL-7404) cell lines, with IC_{50} values of 0.29 ± 0.005 and 0.31 ± 0.004 mmol/L^{-1}, respectively. In addition, AGI-B4 (**92**) and 3,4-dihydroxybenzoic acid (**97**) exhibited replication inhibitory activity of TMV with IC_{50} values of 0.26 ± 0.006 and 0.63 ± 0.008 mmol/L^{-1}, respectively (Tan *et al*., 2012).

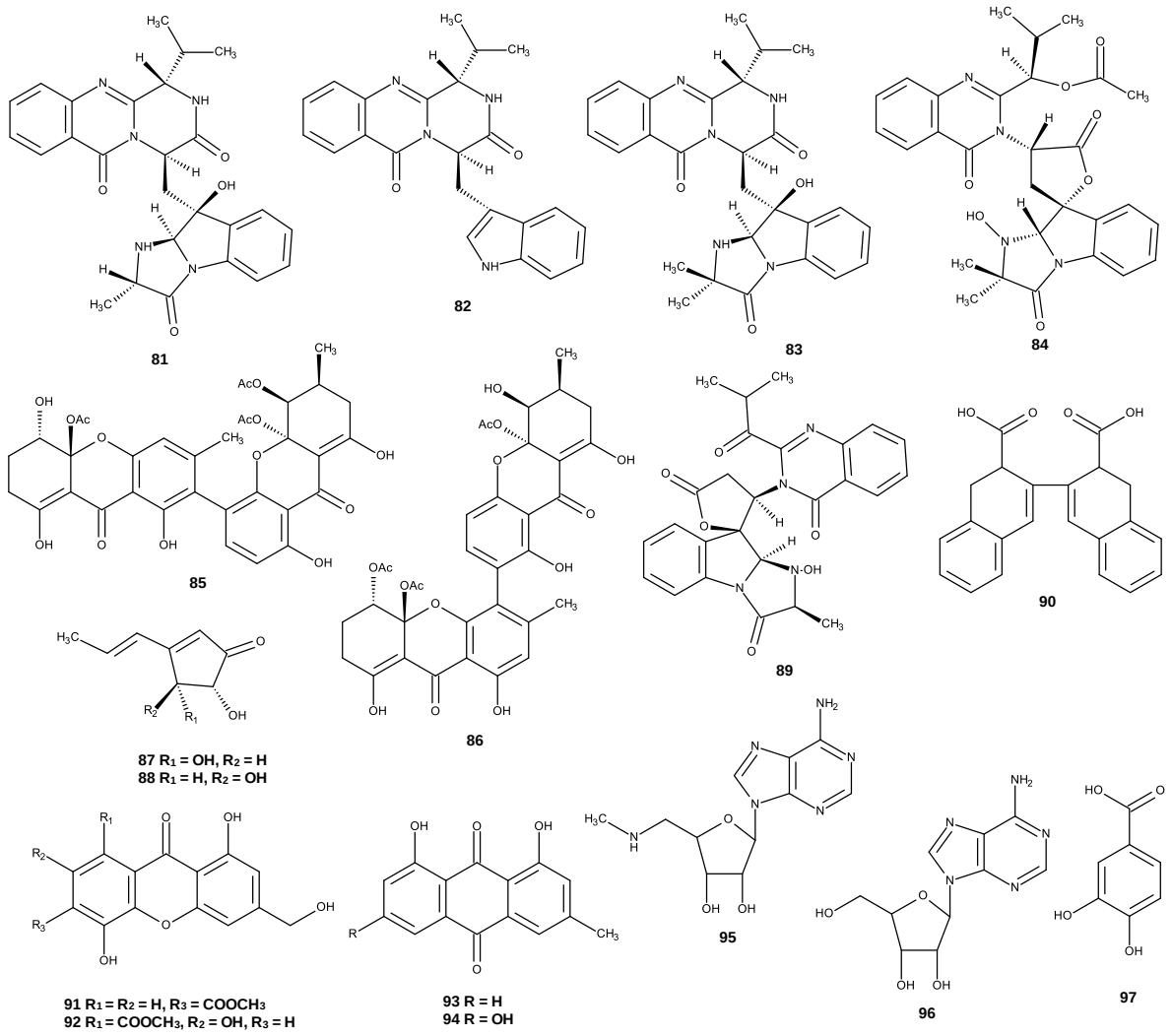

Figure 16. Structures of fiscalins A (**81**), B (**82**), C (**83**), tryptoquivaline (**84**), Neosartorin (**85**), eumitrin A1 (**86**), isoterrein (**87**), terrein (**88**), nortryptoquivalone (**89**), fischeacid (**90**), fischexanthone (**91**), AGI-B4 (**92**), chrysophanol (**93**), emodin (**94**), 5'-deoxy-5'methylamino-adenosine (**95**), adenosine (**96**), 3,4-dihydroxybenzoic acid (**97**), sydowinin A (**98**) and sydowinin B (**99**)

A new secondary metabolite named neosartoricin (**100**) (Figure 17) was isolated from a transformant *N. fischeri* T2, which integrated *nsc*R-overexpression cassette. Compound **100** did not exhibit significant inhibitory activity against either

Gram-positive or Gram-negative bacteria, nor the yeasts *Saccharomyces cerevisiae* and *Candida albicans* > 64 µg/mL (Chooi *et al*., 2013).

Eamvijarn *et al.*, (2013) reported the isolation of two new compounds, sartorypyrone A (**101**) and 1-formyl-5-hydroxyaszonalenin (**102**) (Figure 17), together with aszonalenin (**77**) (Figure 15), helvolic acid (**78**) (Figure 15), acetylaszonalenin (**103**), 13-oxofumitremorgin B (**104**) and aszonapyrone A (**105**) (Figure 17), from the soil fungus *N. fischeri* stain KUFC 6344. Compound **101** exhibited significant cytotoxic activity against MCF-7 (breast adenocarcinoma), NCI-H460 (non-small cell lung cancer) and A375-C5 (melanoma) human cell lines with GI_{50} values of 13.6 ± 0.9 µM, 11.6 ± 1.5 µM and 10.2 ± 1.2 µM, respectively.

Zheng *et al*., (2014) reported the isolation of three new and together with six previously reported prenylated diketopiperazine alkaloids from the culture of fungus *N. fischeri* stain CGMCC 3.5378. The structures of the new metabolites, neofipiperazines A-C (**106**-**108**) (Figure 17), were elucidated by HRMS and NMR analysis. Moreover, the absolute configurations of **106** and **107** were established by X-ray analysis. Shan *et al*., (2014) isolated a new aszonalenin analogue, 6-hydroxyaszonalenin (**109**) (Figure 17) together with the previously reported metabolites: aszonalenin (**77**) (Figure 15), acetylaszonalenin (**103**), aszonapyrone A (**105**), fumitremorgin B (**110**), verruculogen (**111**) and andaszonapyrone B (**112**) (Figure 17). while Chen *at al.* (2014) isolated another new prenylated diketopiperazine, neofipiperazine D (**113**) and three previously described metabolites: fumitremorgin C (**114**), ergosterol (**115**) and ergosterol peroxide (**116**) (Figure 17), from the culture of same fungus. Compound **113** was evaluated for its *in vitro* cytotoxicity against MCF-7 (breast carcinoma), H1299 (lung carcinoma), HUVEC (human umbilical vein endothelial cells), MDA-MB-231 (breast carcinoma) cell lines, however, no activity was detected at concentration of 20 µM.

Kaifuchi *et al*., (2015) isolated a new meroditerpene, sartorypyrone D (**117**) (Figure 17), together with the previously reported derivatives, sartorypyrone A (**101**), and aszonapyrones A (**105**) and B (**112**) (Figure 17), from the culture of the soil fungus *N. fischeri* FO-5897, which was collected at Funabashi city, Chiba, Japan. Compounds **117** and **101** potently inhibited NADH-fumarate reductase (NFRD), while compounds

105 and **112**, exhibited moderate NFRD inhibitions. Moreover, compounds **117**, **101** and **105** showed antibacterial activity against Gram-positive bacteria, *B. subtilis*, *Kocuria rhizopila* and *Mycobacterium smegmatis* with IC_{50} values of 8.0, 9.0 and 10.0 µg/mL, respectively whereas compound **112** showed antibacterial activity against only *M. smegmatis*.

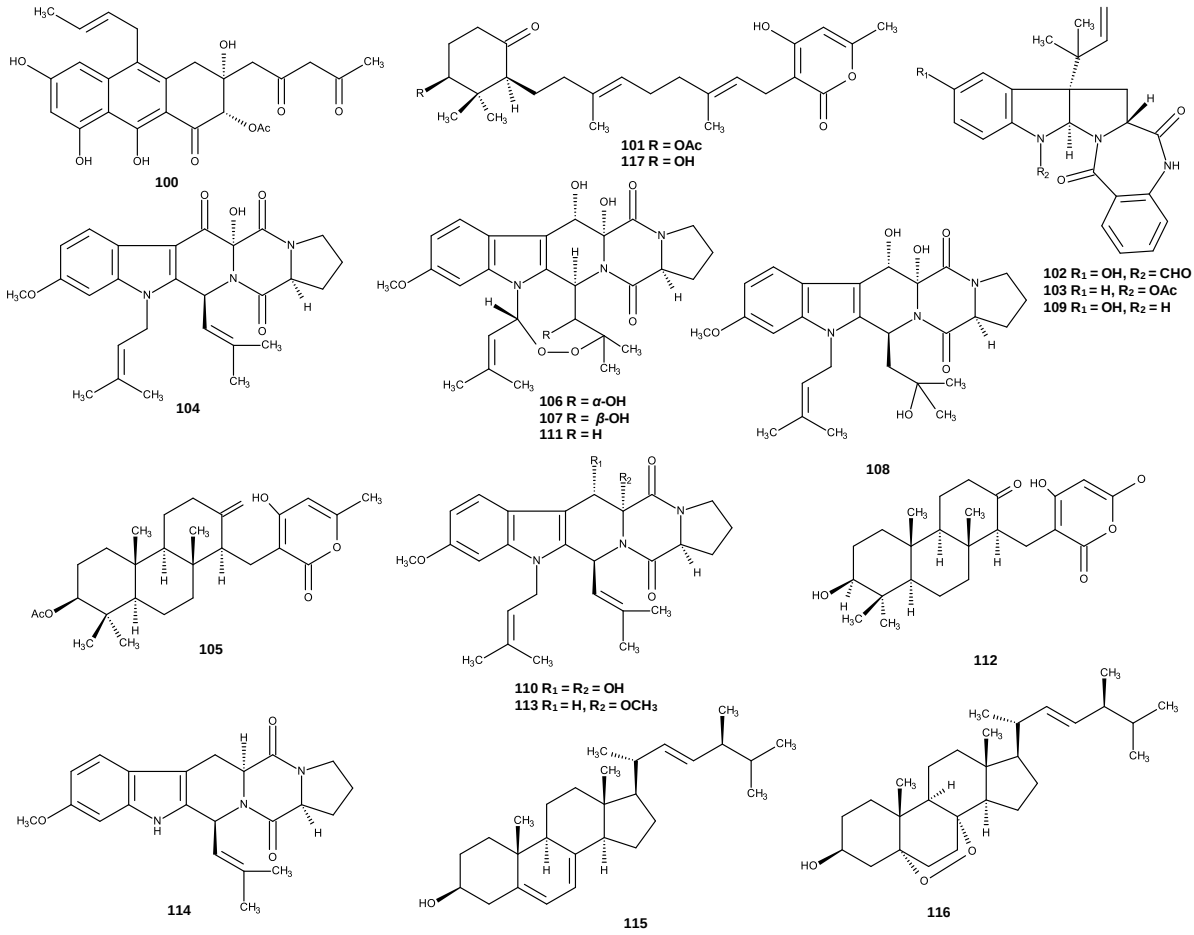

Figure 17. Structures of neosartoricin (**100**), sartorypyrone A (**101**), 1-formyl-5-hydroxyaszonalenin (**102**), acetylaszonalenin (**103**), 13-oxofumitremorgin B (**104**), aszonapyrone A (**105**), neofipiperazines A (**106**), B (**107**), C (**108**), 6-hydroxyaszonalenin (**109**), fumitremorgin B (**110**), verruculogen (**111**), andaszonapyrone B (**112**), neofipiperazine D (**113**), fumitremorgin C (**114**), ergosterol (**115**), ergosterol peroxide (**116**) and sartorypyrone D (**117**)

Wu *et al*., (2015) described the isolation of two new tryptoquivaline analogs tryptoquivaline T (**118**) and tryptoquivaline U (**119**) (Figure 18) together with the previously reported fiscalin B (**82**) (Figure 16), from marine fungus, *N. fischeri* which was isolated from marine mud in the intertidal zone of Hainan Province of China., Compounds **82**, **118** and **119** showed cytotoxic activity against HL-60 (human leukemia) cell lines with IC_{50} values at 88.8, 82.3 and 90.0 μM, respectively.

By using One Strain Many Compounds (OSMAC) method, Ying *et al*., (2018) were able to isolate four pyropenes, including two new, 1,7,11-trideacetylpyripyropene A (**120**) and 1,11-dideacetyl pyripyropene A (**121**) (Figure 18) and two previously reported pyripyropene A (**122**) and 7-deacetyl pyripyropene A (**123**) (Figure 18), eight previously reported steroids dankasterone A (**70**) (Figure 15), ergosterol (**115**) (Figure 17), 22*E*,24*R*-ergosta-7,22-diene-3*β*,5*α*,6*β*,9*α*-tetraol (**124**), 22*E*,24*R*-ergosta-7,22-diene-3*β*,5*α*,6*β*-triol (**125**), 3*β*,5*α*,9*α*-trihydroxy-(22*E*,24*R*)-ergosta-7, 22-dien-6-one (**126**), 3*β*,5*α*-dihydroxy-(22*E*,24*R*)-ergosta-7,22-dien-6-one (**127**), (14*α*,22*E*)-14hydroxyergosta-7,22-diene-3,6-dione (**128**) (Figure 18) and four prenylated indole alkaloids [acetylaszonalenin (**103**) (Figure 17), verruculogen (**111**) (Figure 17), 12*β*-hydroxyverruculogen TR-2 (**129**) and fumitremorgin A (**130**) (Figure 18). The four isolated pyripyropenes were tested for their cytotoxicity against MDA-MB-231 cell line (breast cancer), but none of them showed activity as compared with the positive control taxol (Ying *et al*., 2018).

A new meroditerpenoid, sartorypyrone E (**131**) (Figure 18) and eight previously reported metabolites, including aszonalenin (**77**) (Figure 15), sartorypyrone A (**101**) (Figure 17), acetylaszonalenin (**103**) (Figure 17), fumitremorgin B (**110**) (Figure 17), pyripyropene A (**122**), fumitremorgin A (**130**), cyclotryprostatin B (**132**) and fischerin (**133**) (Figure 18) were isolated from extracts of cultured endophytic fungus, *N. fischeri* stain JS0553, which was isolated from the plant *Glehnia littoralis* (Umbelliferae) which was collected in a swamp area in Suncheon, South Korea. Compound **133** exhibited significant neuroprotective activity on glutamate-mediated HT22 cell death through inhibition of ROS, Ca2+ influx, and phosphorylation of mitogen-activated protein kinase, including c-Jun *N*-terminal kinase, extracellular signal-regulated kinase and p38 (Bang *et al*., 2019).

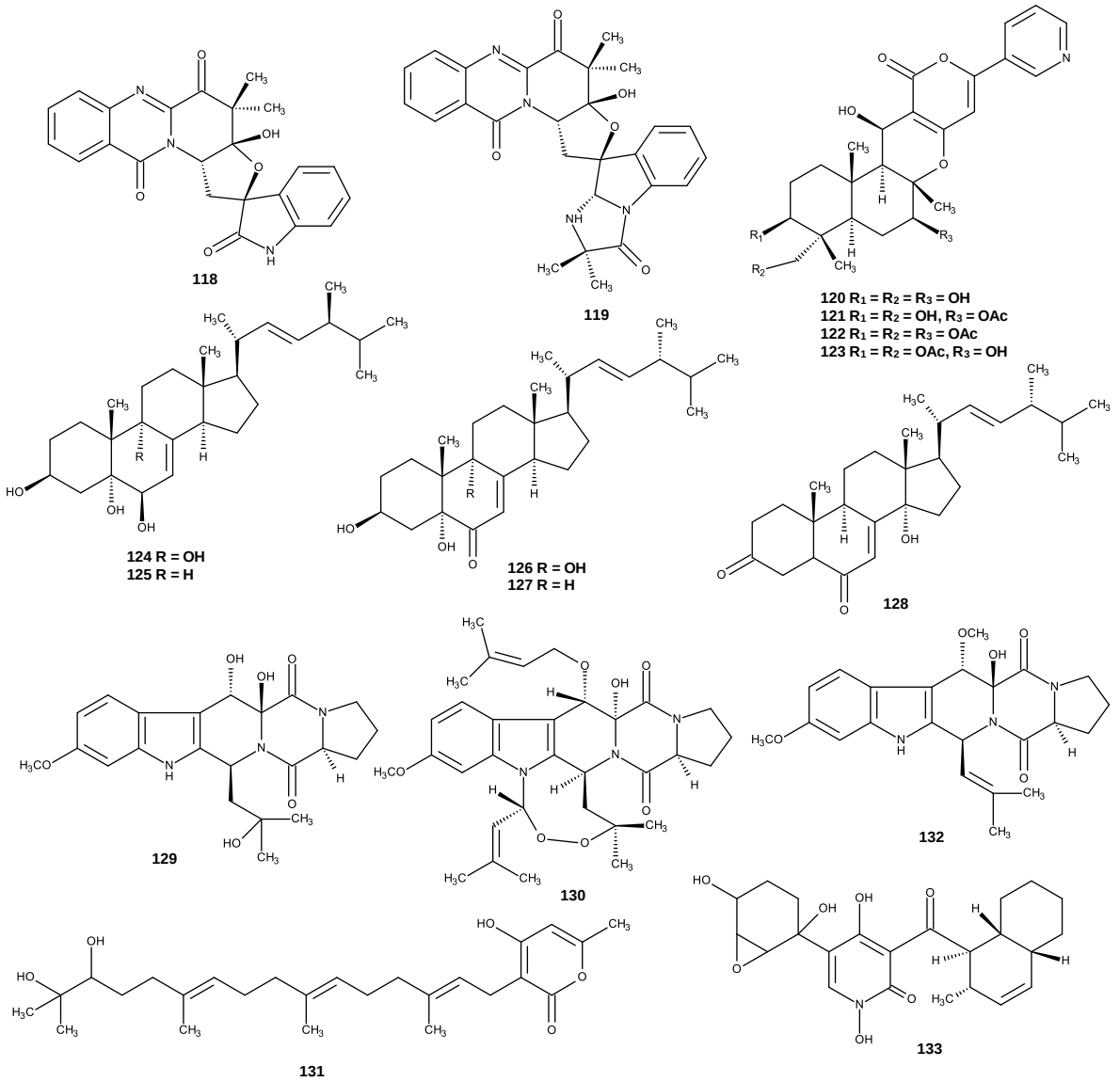

Figure 18. Structures of tryptoquivaline T (**118**), tryptoquivaline U (**119**), 1,7,11-trideacetylpyripyropene A (**120**), 1,11-dideacetyl pyripyropene A (**121**), pyripyropene A (**122**), 7-deacetyl pyripyropene A (**123**), 22*E*,24*R*-ergosta-7,22-diene-3*β*,5*α*,6*β*,9*α*-tetraol (**124**), 22*E*,24*R*-ergosta-7,22-diene-3*β*,5*α*,6*β*-triol (**125**), 3*β*,5*α*,9*α*-trihydroxy-(22*E*,24*R*)-ergosta-7, 22-dien-6-one (**126**), 3*β*,5*α*-dihydroxy-(22*E*,24*R*)-ergosta-7,22-dien-6-one (**127**), (14*α*,22*E*)-14hydroxyergosta-7,22-diene-3,6-dione (**128**), 12*β*-hydroxyverruculogen TR-2 (**129**), fumitremorgin A (**130**), sartorypyrone E (**131**), cyclotryprostatin B (**132**) and fischerin (**133**)

2.1.3. *Neosartorya glabra*

Bicyclic lactones, glabramycins A-C (**134**-**136**) (Figure 19) were isolated from the culture of the strain of *N. glabra* which was isolated from hot water-pasteurized soil collected at Candamia, near Valdefresno province of León, Spain. Glabramycin C (**136**) displayed strong antibiotic activity against *Streptococcus pneumoniae* with MIC value at 2 µg/mL, and modest antibiotic activity against *S. aureus* with MIC value at 16 µg/mL (Jayasuriya *et al*., 2009).

Three new reversed prenylated indole derivatives, sartoryglabins A-C (**137**-**139**) (Figure 19), were isolated from the soil fungus *N. glabra* KUFC 6311, Compound **137**-**139** were evaluated for their capacity to inhibit the *in vitro* growth of MCF-7 (breast adenocarcinoma), NCI-H460 (non-small cell lung cancer) and A375-C5 (melanoma) cell lines. Compound **137** exhibited strong growth inhibitory activity against the MCF-7 cell line with GI_{50} value of 27.0±0.57 µM, whereas **138** and **139** showed moderate growth inhibitory activity against MCF-7 cell line with GI_{50} values of 53.0 ± 4.7 and 44.0± 7.2 µM, respectively (Kijjoa *et al*., 2011).

Liu *et al.*, (2015) reported the isolation of two new polyketides, named neosarphenols A (**140**) and B (**141**) (Figure 19) were isolated, together with six previously reported polyketides methoxyvermistatin (**142**), 6-demethylvermistatin (**143**), vermistatin (**144**), penicillide (**145**), purpactin A (**146**), phialophoriol (**147**) and two previously described meroterpenoids [chrodrimanin A (**148**) and chrodrimanin B (**149**) (Figure 19) from *N. glabra* stain CGMCC 32286. All the isolated compounds were evaluated for their cytotoxic activity against human breast cancer (MCF-7 and MDA-MB-231) and a human pancreatic cancer cell (PANC-1) cell lines, however, only **140** and **145** displayed moderate cytotoxic activity against PANC-1 cell line with IC_{50} values of 14.38 and 10.93 µM while the IC_{50} of the positive control, paclitaxel, was 0.45 µM.

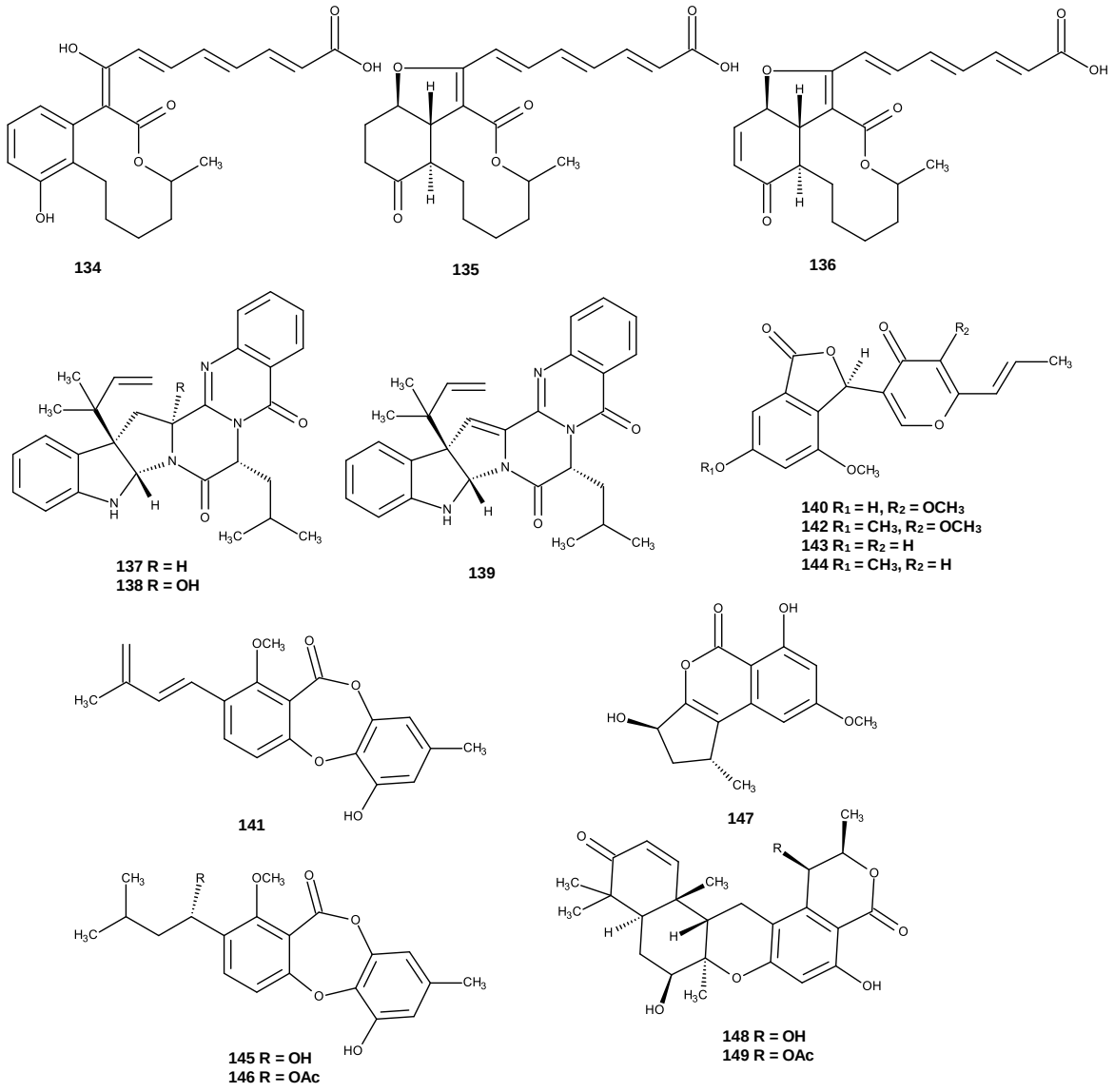

Figure 19. Structures of glabramycins A (**134**), B (**135**), C (**136**), sartoryglabins A (**137**), B (**138**), C (**139**), neosarphenols A (**140**), B (**141**), methoxyvermistatin (**142**), 6-demethylvermistatin (**143**), vermistatin (**144**), penicillide (**145**), purpactin A (**146**), phialophoriol (**147**), chrodrimanin A (**148**) and chrodrimanin B (**149**)

Two new cyclotetrapeptides, sartoryglabramides A (**150**) and B (**151**) and a new analog of fellutanine A epoxide (**152**) (Figure 20) were together with six known compounds including ergosta-4, 6, 8 (14), 22-tetraen-3-one (**72**) (Figure 15), aszonalenin (**77**) (Figure 15), helvolic acid (**78)** (Figure 15), fellutanine A (**80**) (Figure

15), ergosterol peroxide (**116)** (Figure 17), (3*R*)-3-(1*H*-indol-3-ylmethyl)-3,4-dihydro-1*H*-1,4-benzodiazepine-2,5-dione (**153**), takakiamide (**154**) and (11a*R*)-2,3-dihydro-1*H*-pyrrolo[2,1-*c*][1,4]benzodiazepine-5,11(10*H*,11a*H*)-dione (**155**) (Figure 20), from the culture of the marine sponge-associated fungus *Neosartorya glabra* KUFA 0702, which was isolated from the marine sponge *Mycale* sp., collected from the coral reef at Samaesarn Island, Thailand. The isolated compounds were tested for their antibacterial activity against Gram-positive (*Escherichia coli* ATCC 25922) and Gram-negative (*S. aureus* ATCC 25923) bacteria, as well as for their antifungal activity against filamentous (*Aspergillus fumigatus* ATCC 46645), dermatophyte (*Trichophyton rubrum* ATCC FF5) and yeast (*Candida albicans* ATCC 10231); however, none of the tested compound exhibited either antibacterial or antifungal activities (Zin *et al*., 2016).

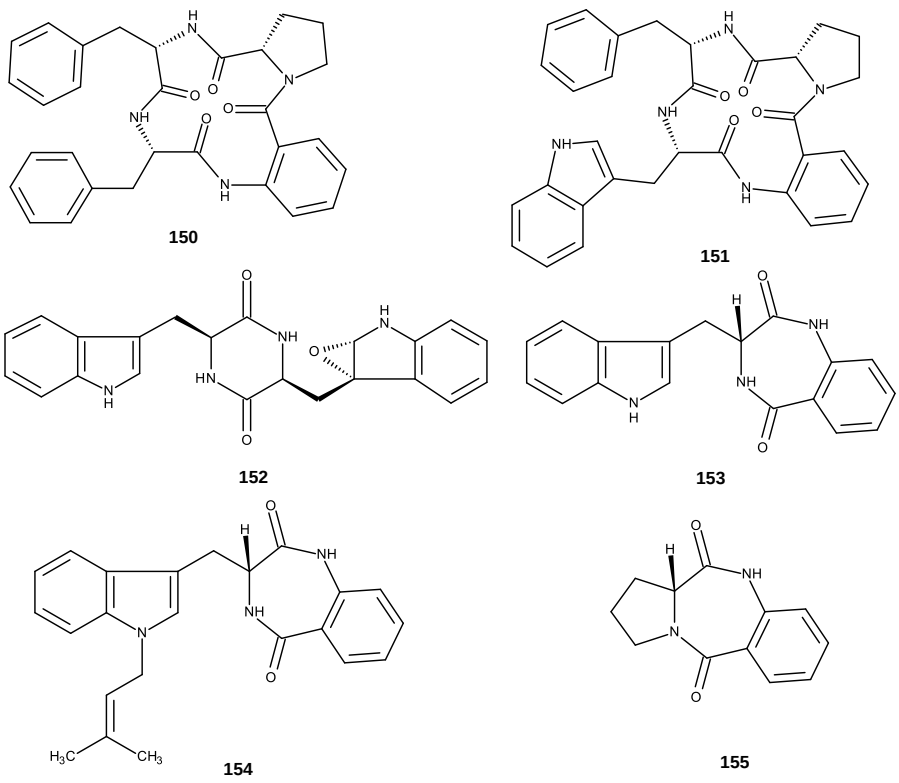

Figure 20. Structures of sartoryglabramides A (**150**), B (**151**), fellutanine A epoxide (**152**), 3*R*)-3-(1*H*-indol-3-ylmethyl)-3,4-dihydro-1*H*-1,4-benzodiazepine-2,5-dione (**153**), takakiamide (**154**) and (11a*R*)-2,3-dihydro-1*H*-pyrrolo[2,1-*c*][1,4]benzodiazepine-5,11(10*H*,11a*H*)-dione (**155**)

2.1.4. *Neosartorya laciniosa*

Aszonapyrone A (**105**) (Figure 17), aszonapyrone B (**112**) (Figure 17), tryptoquivaline L (**156**) and 3'-(4-oxoquinazolin-3-yl) spiro[1*H*-indole-3,5'-oxolane]-2,2'-dione (**157**) (Figure 21) were isolated from the marine-derived fungus *N. laciniosa* KUFC 7896 which was isolated from the diseased coral *Porites lutea,* collected in the Gulf of Thailand. Compounds **105** and **112**, were evaluated for their *in vitro* growth inhibitory activity against MCF-7, NCI-H460 and A375-C5 cell lines. Only **105** displayed growth inhibitory activity against MCF-7, NCI-H460 and A375-C5 cell lines, with GI_{50} values of 17.8±7.4 mM, 20.5± 2.4 mM and 25.0± 4.4 mM, respectively (Eamvijarn *et al*., 2013). Later on, tryptoquivaline T (**118**) (Figure 18), a new tryptoquivaline derivative, was isolated from the unexamined fractions of the extract of this fungus. Compound **118** did not show any antibacterial activity against four reference strains *(S. aureus, B. subtilis, E. coli, and P. aeruginosa*), as well as the environmental multidrug-resistant isolates (Gomes *et al*., 2014).

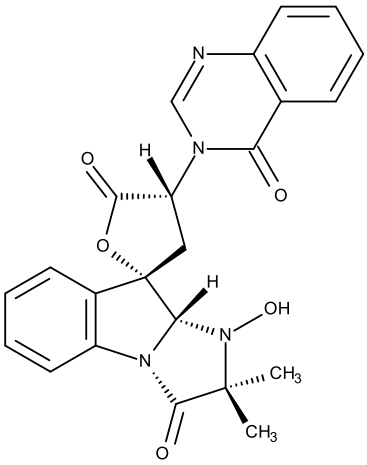

156

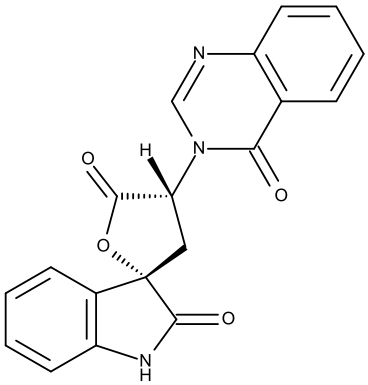

157

Figure 21. Structures of tryptoquivaline L (**156**) and 3'-(4-oxoquinazolin-3-yl) spiro[1*H*-indole-3,5'-oxolane]-2,2'-dione (**157**)

2.1.5. *Neosartorya paulistensis*

A new meroditerpene, sartorypyrone C (**158**) (Figure 22), was isolated together with the previously described tryptoquivaline L (**156**) (Figure 21), 3′-(4-oxoquinazolin-3-yl) spiro [1H-indole-3,5′-oxolane]-2,2′-dione (**157**) (Figure 21), tryptoquivaline H (**159**), tryptoquivaline F (**160**) and 4(3*H*)-quinazolinone (**161**) (Figure 22), from the culture of the marine sponge-associated fungus *N. paulistensis* KUFC 7897, which was isolated from the marine sponge *Chondrilla australiensis*, collected from the Gulf of Thailand. The isolated compounds were evaluated for their antibacterial activity against with four reference strains, *S. aureus* ATCC 25923, *B. subtilis* ATCC 6633, *E. coli* ATCC 25922 and *P. aeruginosa* ATCC 27853 (Gomes *et al.,* 2014).

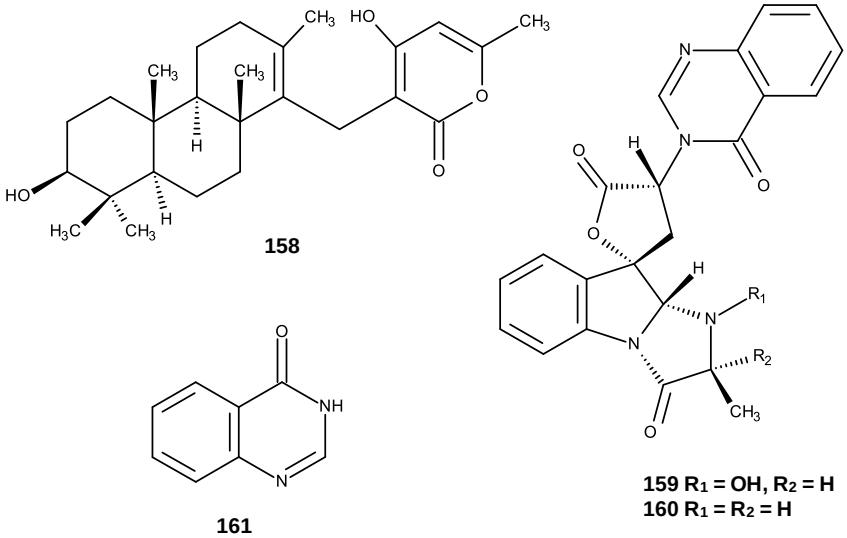

Figure 22. Structure of sartorypyrone C (**158**), tryptoquivaline H (**159**), tryptoquivaline F (**160**) and 4(3*H*)-quinazolinone (**161**)

2.1.6. *Neosartorya pseudofischeri*

Three new secondary metabolites: 3,8-diacetyl-4-(3-methoxy-4,5-methylene-dioxy) benzyl-6-oxa-3,8-diazebicyclo [3.2.1] octane (**162a, b**), pseudofischerine (**163**)

and 3-hydroxy-5-methylphenyl-2,4-dihydroxy-6-methylbenzoate (**164**) (Figure 23) were isolated together with the previously reported pyripyropene A (**122**) (Figure 18), sesquiterpene (**165**), eurochevalierine (**166**) and brasiliamide B (**167**) (Figure 23) form the culture of the soil-derived fungus *N. pseudofisheri* S.W. Petterson, Compounds **165** and **166** were evaluated for their *in vitro* growth inhibitory activities on the human U373 and Hs683, A549, MCF-7, SKMEL-28 and OE21 cell lines. Compound **166** was found to display the *in vitro* anticancer activity in the range displayed by etoposide and carboplatin while **165** exhibited less activity than **166** and similar activity to carboplatin. By using the computer-assisted phase contrast microscopy, it was found that 50 µM of **166** reduced the growth of U373 GBM cells by 65% and reduced the growth of A549 NSCLC by 50% over a 72h period of observation. Therefore, the authors concluded that **166** is cytostatic and not cytotoxic (Eamvijarn *et al*., 2012).

Later on, fischerindoline (**168**) (Figure 23) another pyrroloindole terpenoid, was isolated together with pyripyropenes A (**122**) (Figure 18), cadinene sesquiterpene (**165**), eurochevalierine (**166**), pyripyropene E (**169**), gliotoxin (**170**) and *bis*(dethio)*bis*(methylthio)gliotoxin (**171**) (Figure 23), from the solid and liquid cultures of fungus *N. pseudofischeri* strain CBS 404.67 which was purchased from Centraalbureau voor Schimmelcultures of Baan (The Netherlands). Compound **168** exhibited the *in vitro* growth inhibitory activity against A549, Hs683, MCF-7, SKMEL28, U373 and a mouse B16F10 cell lines with IC_{50} values of 29, 32, 25, 32, 37 and 27 µM, respectively (Masi *et al*., 2013).

The marine fungus, *N. pseudofischeri*, which was isolated from the inner tissue of starfish *Acanthaster planci* and cultured in glycerol-peptone-yeast extract (GlyPY), produced two new diketopiperazines, neosartins A (**172**) and B (**173**), and six know known diketopiperazines, 1,2,3,4-tetrahydro-2, 3-dimethyl-1,4-dioxopyrazino[1,2-a]indole (**174**), 1,2,3,4-tetrahydro-2-methyl-3-methylen e-1,4-dioxopyrazino[1,2-a]indole (**175**), 1,2,3,4-tetrahydro-2-methyl-1,3,4-trioxopyrazino[1,2-a] indole (**176**), 6-acetylbis(methylthio)gliotoxin (**177**), bisdethiobis(methylthio)gliotoxin (**178**), didehydrobisdethiobis(methylthio)gliotoxin (**179**) and *N*-methyl-1*H*-indole-2-carboxamide (**180**). However, when cultured in glucose-peptone-yeast extract (GluPY) medium, the fungus produce neosartin C (**181**)

(Figure 24), tetracyclic-fused alkaloid, together with pyripyropene A (**122**) (Figure 17), gliotoxin (**170**) (Figure 23) and five known gliotoxin analogues, 6-acetylbis-(methylthio)-gliotoxin (**177**), bisdethiobis-(methylthio) gliotoxin (**178**), acetylgliotoxin (**182**), reduced gliotoxin (**183**) and bis-*N*-norgliovictin (**184**) (Figure 24). Compounds **170, 173-184** were evaluated for their antibacterial activity against *S. aureus* (ATCC29213) and MRA *S. aureus* (R3708) and *E. coli* (ATCC25922) by a broth dilution method. While compounds **170** and **183** exhibited inhibitory activity against all the three bacteria, with MIC values ranging from 1.52 to 97.56 μM, **175** and **182** inhibited the growth of *S. aureus* ATCC29213 and R3708 with MIC values of 283.11, 70.70 μM and 86.91, 21.73 μM, respectively. Moreover, **170**, **175**, **178** and **183** exhibited potent cytotoxicity against the human embryonic kidney (HEK) 293 cell line and human colon cancer cell lines, HCT-116 and RKO (a poorly differentiated colon carcinoma cell line) (Liang *et al*., 2014).

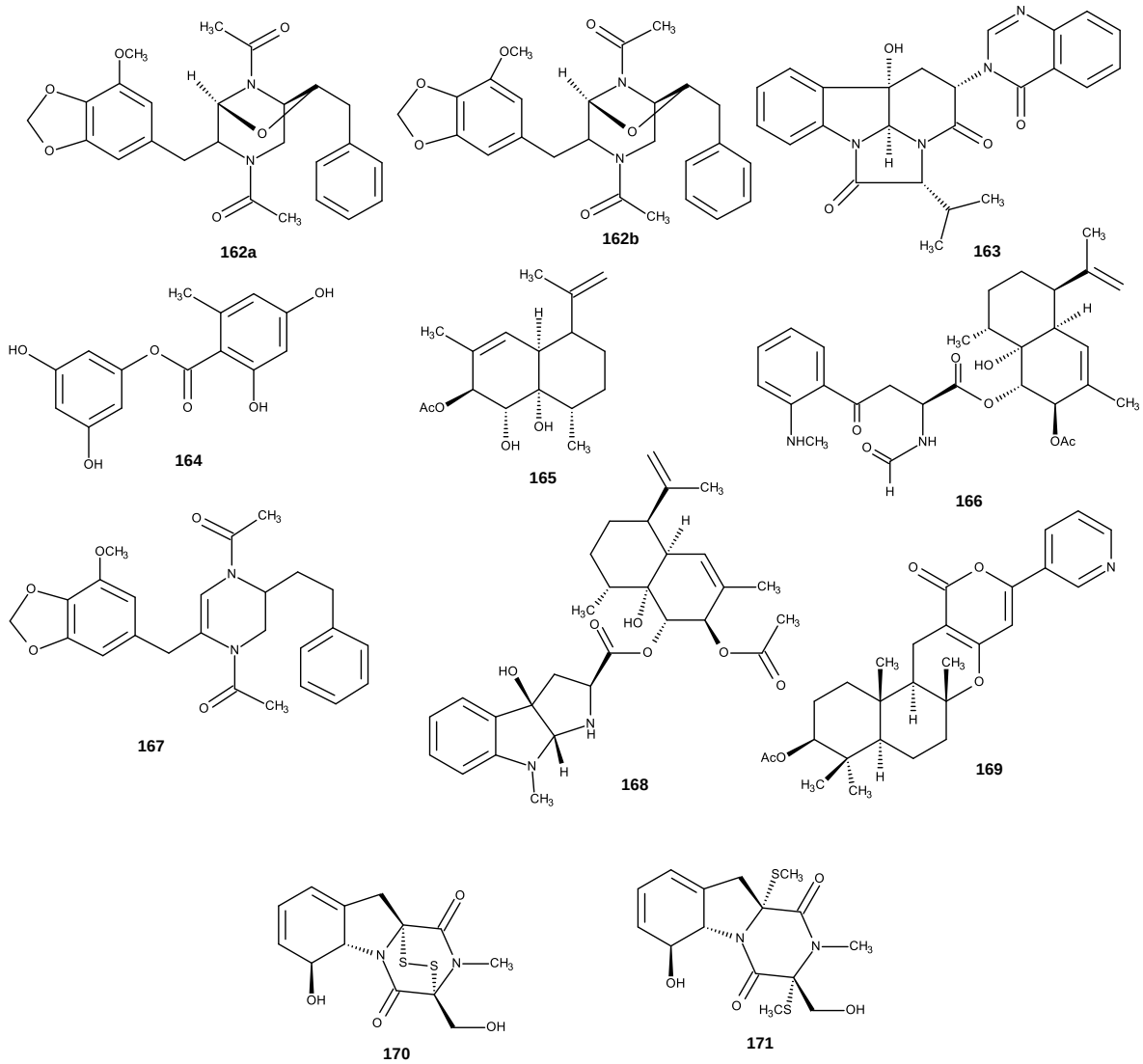

Figure 23. Structures of 3,8-diacetyl-4-(3-methoxy-4,5-methylene-dioxy) benzyl-6-oxa-3,8-diazebicyclo [3.2.1] octane (**162a, b**), pseudofischerine (**163**), 3-hydroxy-5-methylphenyl-2,4-dihydroxy-6-methylbenzoate (**164**), sesquiterpene (**165**), eurochevalierine (**166**), brasiliamide B (**167**), fischerindoline (**168**), pyripyropene E (**169**), gliotoxin (**170**) and *bis*(dethio)*bis*(methylthio)gliotoxin (**171**)

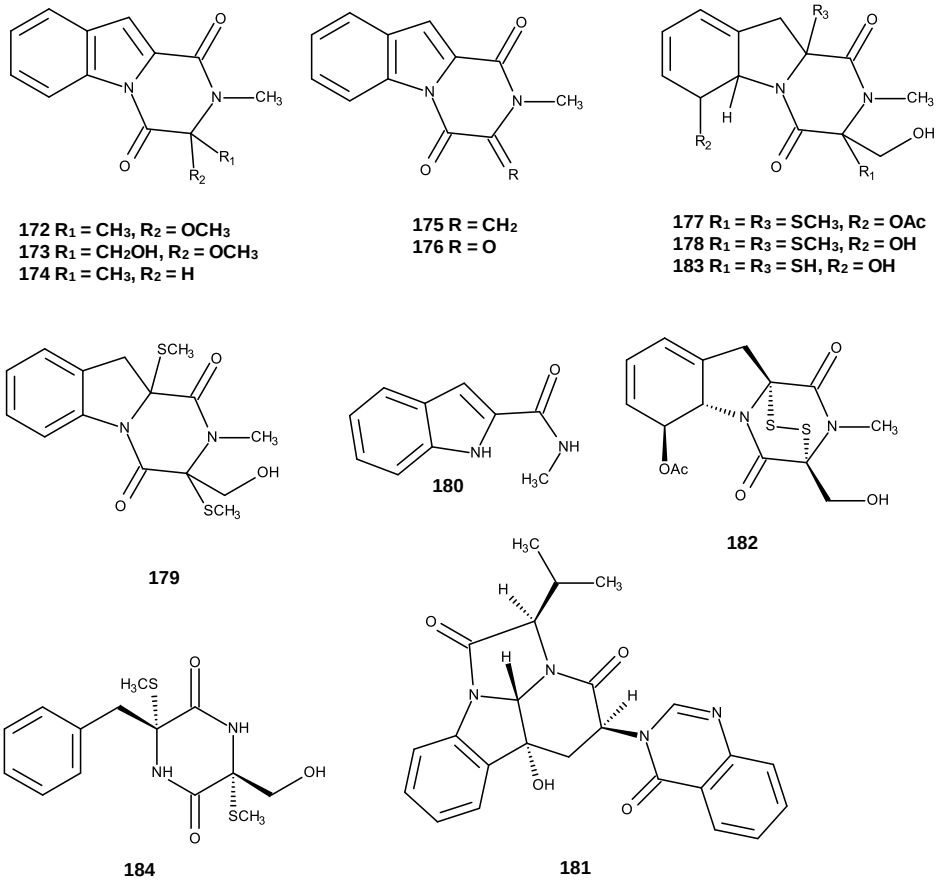

Figure 24. Structures of neosartins A (**172**), B (**173**), 1,2,3,4-tetrahydro-2, 3-dimethyl-1,4-dioxopyrazino[1,2-a]indole (**174**), 1,2,3,4-tetrahydro-2-methyl-3-methylen e-1,4-dioxopyrazino[1,2-a]indole (**175**), 1,2,3,4-tetrahydro-2-methyl-1,3,4-trioxopyrazino[1,2-a] indole (**176**), 6-acetylbis(methylthio)gliotoxin (**177**), bisdethiobis(methylthio)gliotoxin (**178**), didehydrobisdethiobis(methylthio)gliotoxin (**179**), N-methyl-1*H*-indole-2-carboxamide (**180**), neosartin C (**181**), acetylgliotoxin (**182**), reduced gliotoxin (**183**) and bis-*N*-norgliovictin (**184**)

Later on, Lan *et al*., (2016) by using the insecticidal activity against the fall armyworm *Spodoptera frugiperda*-guided screening, isolated five new metabolites, including 5-olefin phenylpyropene A (**185**), 13-dehydroxylpyripyropene A (**186**), deacetylsesquiterpene (**187**), 5-formyl-6-hydroxy-8-isopropyl-2-naphthoic acid (**188**) and 6,8-dihydroxy-3-((1*E*,3*E*)-penta-1,3-dien-1-yl) isochroman-1-one (**189**) (Figure

25) and eleven previously described metabolites, phenylpyropenes A (**190**) and C (**191**), pyripyropene A (**122**) (Figure 18), 7-deacetyl pyripyropene A (**123**) (Figure 18), (1*S*,2*R*,4a*R*,5*R*,8*R*,8a*R*)-1,8a-dihydroxy-2-acetoxy-3,8-dimethyl-5-(prop-1-en-2-yl) 1,2,4a,5,6,7,8,8aoctahydronaphthalene (**192**), isochaetominine C (**193**), trichodermamide A (**194**), indolyl-3-acetic acid methyl ester (**195**), 1-acetyl-*β*-carboline (**196**), 1,2,3,4-tetrahydro-6-hydroxyl-2-methyl-l,3,4trioxopyrazino[l,2-a]-indole (**197**) and fumiquinazoline F (**198**) (Figure 25), from the methanol extract of the mycelia of the same fungus, culture in GluPY. Compounds **185**, **193** and **197** exhibited significant cytotoxicity against the Sf9 cells from *S. frugiperda*.

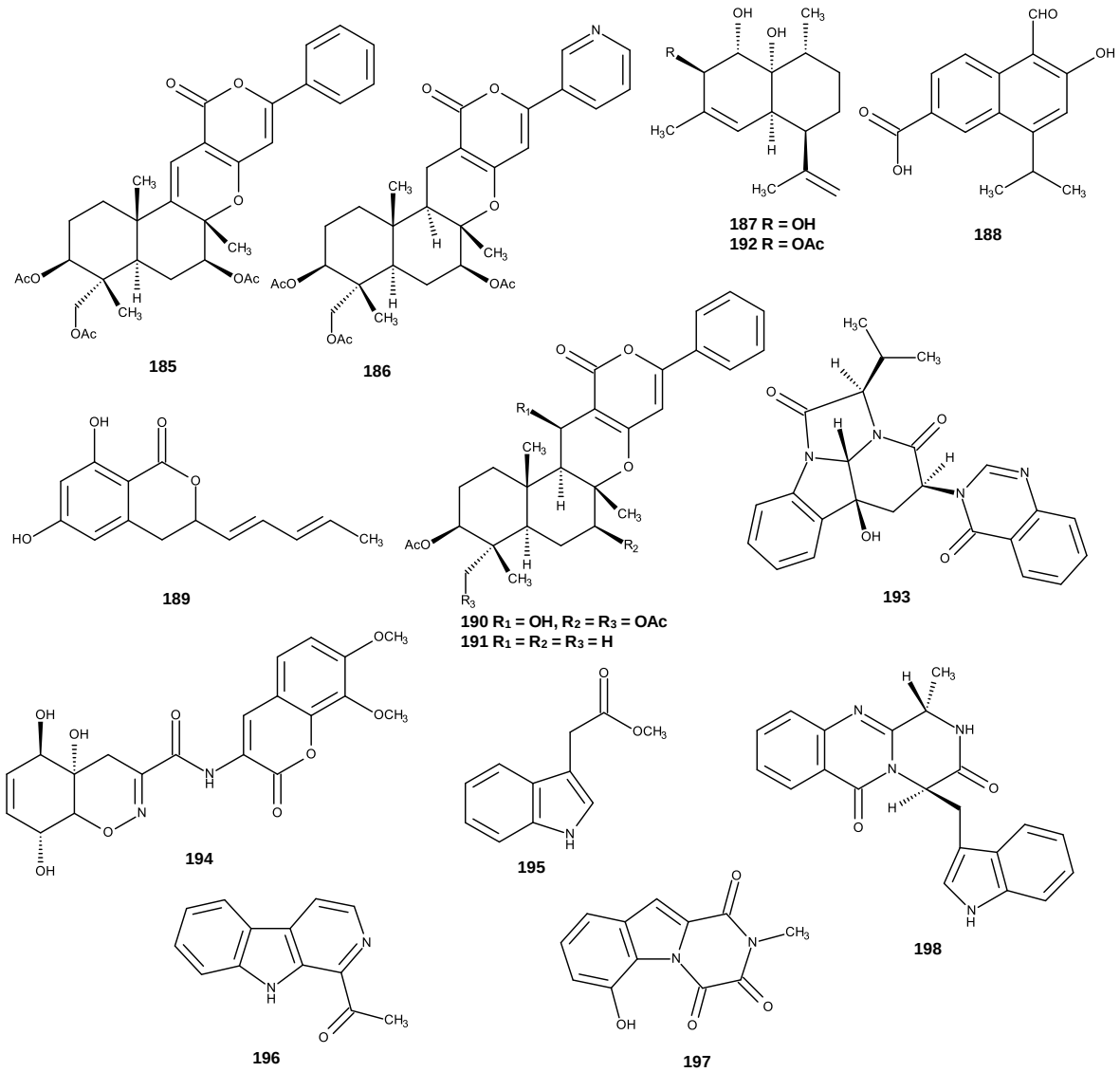

Figure 25. Structures of 5-olefin phenylpyropene A (**185**), 13-dehydroxylpyripyropene A (**186**), deacetylsesquiterpene (**187**), 5-formyl-6-hydroxy-8-isopropyl-2-naphthoic acid (**188**), 6,8-dihydroxy-3-((1*E*,3*E*)-penta-1,3-dien-1-yl) isochroman-1-one (**189**), phenylpyropenes A (**190**), C (**191**), (1*S*,2*R*,4a*R*,5*R*,8*R*,8a*R*)-1,8a-dihydroxy-2-acetoxy-3,8-dimethyl-5-(prop-1-en-2-yl) 1,2,4a,5,6,7,8,8 aoctahydro naphthalene (**192**), isochaetominine C (**193**), trichodermamide A (**194**), indolyl-3-acetic acid methyl ester (**195**), 1-acetyl-*β*-carboline (**196**), 1,2,3,4-tetrahydro-6-hydroxyl-2-methyl-l,3,4trioxopyrazino[l,2-a]-indole (**197**) and fumiquinazoline F (**198**)

2.1.7. *Neosartorya quadricincta*

Ozoe *et al*., (2004) reported the isolation of a new prenylated dihydroisocoumarin derivative, PF1223 (**199**) (Figure 26) from the culture of *N. quadricincta* strain PF1223. PF1223 (**199**), at 2.2 μM, inhibited the specific binding of the noncompetitive antagonist, [^{3}H] ethynylbicycloorthobenzoate (EBOB), to housefly head membranes by 65%.

Seven new benzoic acid derivatives, including quadricinctapyrans A (**200**) and B (**201**) quadricinctoxepine (**202**), quadricinctone B (**203**), quadricinctafurans A and B (**204** and **205**) and quadricinctone D (**206**) and two new polyketide derivatives, quadricinctones A (**207**) and C (**208**) (Figure 26), were isolated, together with the previously reported 2,3-dihydro-6-hydroxy-2,2-dimethyl-4H-1-benzopyran-4-one (**209**) (Figure 26), from the ethyl acetate extract of the culture of the marine sponge-associated fungus *N. quadricincta* KUFA 0081 which was isolated from the marine sponge *Clathria reinwardti*, collected from the coral reef in the Gulf of Thailand. Compounds **201-209** were tested for their antibacterial activity against Gram-positive and Gram-negative bacteria, as well as multidrug-resistant isolates from the environment and for their antifungal activity against yeast (*Candida albicans* ATCC 10231), filamentous fungus (*Aspergillus fumigatus* ATCC 46645) and dermatophyte (*Trichophyton rubrum* FF5). Additionally, these compounds were evaluated for their *in vitro* growth inhibitory activity against three cell lines, including MCF-7 (breast adenocarcinoma), NCI-H460 (non-small cell lung cancer) and A375-C5 (melanoma). However, none of the tested compounds showed activities in these assays (Prompanya *et al*., 2016).

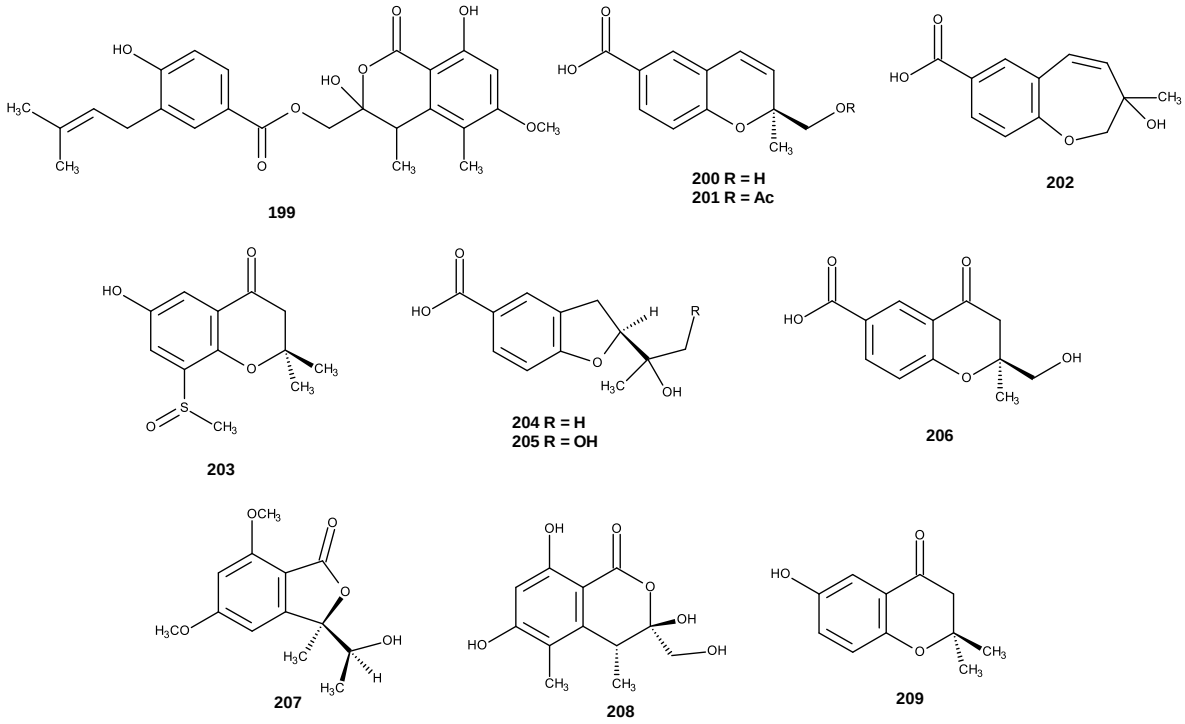

Figure 26. Structures of PF1223 (**199**), quadricinctapyrans A (**200**), B (**201**) quadricinctoxepine (**202**), quadricinctone B (**203**), quadricinctafurans A (**204**), B (**205**), quadricinctones D (**206**), A (**207**), C (**208**) and 2,3-dihydro-6-hydroxy-2,2-dimethyl-4H-1-benzopyran-4-one (**209**)

2.1.8. *Neosartorya siamensis*

Buttachon *et al*., (2012) reported the isolation of seven new indole alkaloids including sartorymensin (**210**), tryptoquivaline O (**211**), 3'-(4-oxoquinazolin-3-yl)spiro[1H-indole-3,5'-oxolane]-2,2'-dione (**212**), neofiscalin A (**213**), *epi*-neofiscalin A (**214**) *epi*-fiscalin A (**215**) and *epi*-fiscalin C (**216**) (Figure 27), together with 2,4-dihydroxy-3-methylacetophenone (**217**) (Figure 27), fiscalins A (**81**) (Figure 16) and C (**83**) (Figure 16), tryptoquivaline (**84**) (Figure 16), tryptoquivalines L (**156**) (Figure 21), H (**159**) (Figure 22) and F (**160**) (Figure 22), from the soil-derived fungus *N. siamensis* strain KUFC 6349, which was isolated from forest soil at Sameasarn Island, Thailand. All the compounds were tested for their *in vitro* growth inhibitory activity on the human

U373, Hs683 (glioblastoma), A549 (non-small cell lung cancer), MCF-7 (breast cancer) and the SKMEL-28 (melanoma) cell lines. Only sartorymensin (**210**) showed moderate *in vitro* growth inhibitory activity against the human U373 and Hs683 (glioblastoma), A549 (non-small cell lung cancer), MCF-7 (breast cancer) and SKMEL-28 (melanoma) cancer cell lines with IC_{50} values of 44, 50, 39, 43 and 73 μM, respectively.

Later on, fiscalins A (**81**) (Figure 16), C (**83**) (Figure 16), tryptoquivaline (**84**) (Figure 16), tryptoquivaline L (**156**) (Figure 21), H (**159**) (Figure 22), F (**160**) (Figure 22), 3'-(4-oxoquinazolin-3-yl)spiro[1H-indole-3,5'-oxolane]-2,2'-dione (**212**), neofiscalin A (**213**) , *epi*-neofiscalin A (**214**), *epi*-fiscalin A (**215**), *epi*-fiscalin C (**216**), 2,4-dihydroxy-3-methylacetophenon (**217**), chevalone C (**218**) and nortryptoquivaline (**219**) (Figure 27) were isolated from the strain KUFA 0017 of this fungus which was isolated from the sea fan *Rumphella* sp. Compounds **81**, **159**-**160** and **214**-**219** were evaluated for their anticancer activity against three human cancer cell lines, i. e. malignant melanoma (A375), hepatocellular carcinoma (HepG2) and colon carcinoma (HCT116). Compounds **81**, **214**-**216** and **218**-**219** exhibited growth inhibitory activity against the three cell lines with IC_{50} values ranging from 24 to 153 μM. Compounds **81**, **218** and **219** induced HCT116 cell death while compounds **81**, **214**, **215** and **219** induced significant HepG2 cell death (Prata-Sena *et al*., 2016).

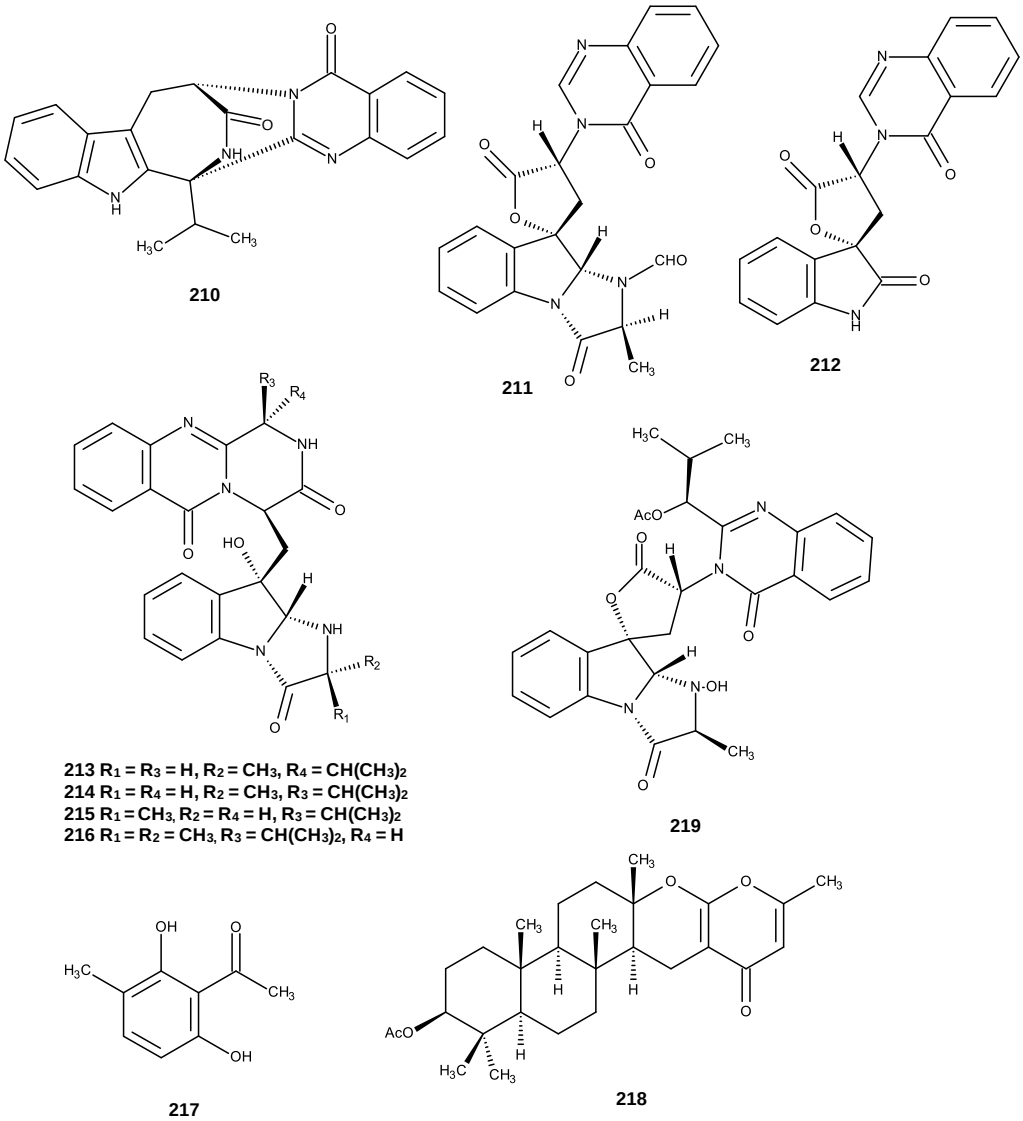

Figure 27. Structures of sartorymensin (**210**), tryptoquivaline O (**211**), 3'-(4-oxoquinazolin-3-yl)spiro[1H-indole-3,5'-oxolane]-2,2'-dione (**212**), neofiscalin A (**213**), *epi*-neofiscalin A (**214**) *epi*-fiscalin A (**215**), epi-fiscalin C (**216**), 2,4-dihydroxy-3-methylacetophenon (**217**), chevalone C (**218**) and nortryptoquivaline (**219**)

2.1.9. *Neosartorya spinosa*

Six new metabolites, including two ester epimers, 2*S*,4*S*-spinosate (**220**) and 2*S*,4*R*-spinosate (**221**), four meroterpenoids, named 1-hydroxychevalone C (**222**), 1-

acetoxychevalone C (**223**), 1,11-dihydroxychevalone C (**224**), and 11-hydroxychevalone C (**225**) (Figure 28) and the previously described chevalone B (**76**) (Figure 15), tryptoquivaline (**84**) (Figure 16), tryptoquivalines L (**156**) (Figure 21), chevalone C (**218**) (Figure 27), nortryptoquivaline (**219**) (Figure 27), chevalone E (**226**) and quinadoline A (**227**) (Figure 28) were isolated from the soil-derived fungus, *N. spinosa* strain KKU-1NK1, Compound **222** showed antimycobacterial activity against *Mycobacterium tuberculosis* with a MIC value of 26.4 μM. While **223** exhibited antimalarial activity against *Plasmodium falciparum* (K1, multidrug-resistant strain) with IC_{50} value of 6.67 μM. Additionally, compounds **222**-**224** exhibited cytotoxicity against human epidermoid carcinoma (KB) and NCI-H187 cancer cell lines with IC_{50} values in the range of 32.7-103.3 μM (Rajachan *et al*., 2016).

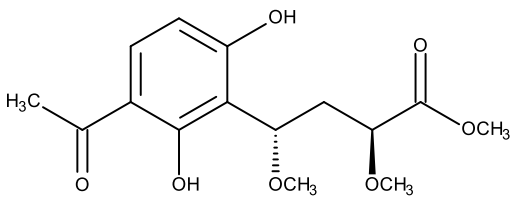

220

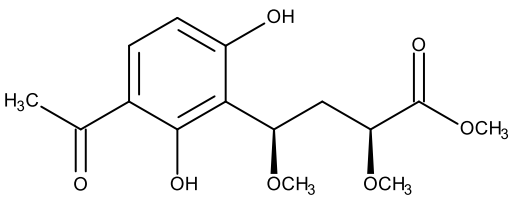

221

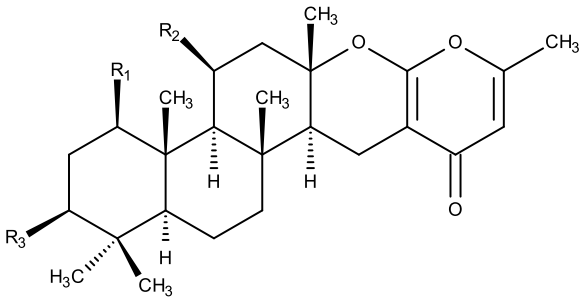

222 R_1 = OH, R_2 = H, R_3 = OAc
223 R_1 = OAc, R_2 = H, R_3 = OAc
224 R_1 = OH, R_2 = OH, R_3 = OAc
225 R_1 = H, R_2 = OH, R_3 = OAc
226 R_1 = R_2 = H, R_3 = OH

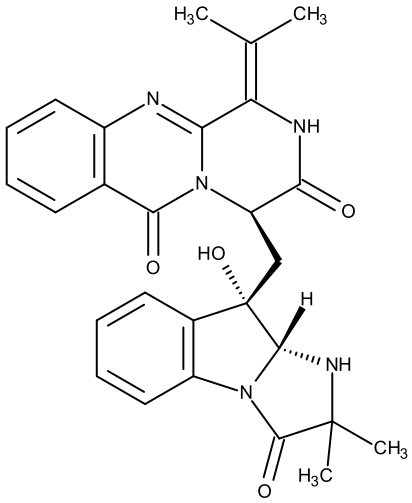

227

Figure 28. Structures of 2*S*,4*S*-spinosate (**220**), 2*S*,4*R*-spinosate (**221**), 1-hydroxychevalone C (**222**), 1-acetoxychevalone C (**223**), 1,11-dihydroxychevalone C (**224**), 11-hydroxychevalone C (**225**), chevalone E (**226**) and quinadoline A (**227**)

2.1.10. *Neosartorya takakii*

Zin *et al*., (2015) reported the isolation of three new compounds including a meroditerpene sartorenol (**228**), a prenylated indole alkaloid takakiamide (**229**) and tryptoquivaline U (**230**) (Figure 29) as well as the previously described, chevalone B (**76**) (Figure 15), aszonalenin (**77**) (Figure 15), acetylaszonalenin (**103**) (Figure 17), aszonapyrone A (**105**) (Figure 17), tryptoquivaline L (**156**) (Figure 21), 3′-(4-oxoquinazolin-3-yl) spiro[1H-indole-3,5′-oxolane]-2,2′-dione (**157**) (Figure 21), tryptoquivaline H (**159**) (Figure 22), tryptoquivaline F (**160**) (Figure 22) and 6-hydroxymellein (**231**) (Figure 29) from the culture of the algicolous fungus, *N. takakii* strain KUFC 7898, which was isolated from the alga *Amphiroa* sp. Compounds **228**-**230** were tested for their antibacterial activity against Gram-positive (*S. aureus* ATCC 25923 and *B. subtilis* ATCC 6633) and Gram-negative (*E. coli* ATCC 25922 and *P. aeruginosa* ATCC 27853) bacteria as well as methicillin-resistant S*. aureus* (MRSA) and vancomycin-resistant Enterococci (VRE) from the environment but none of them exhibited activity.

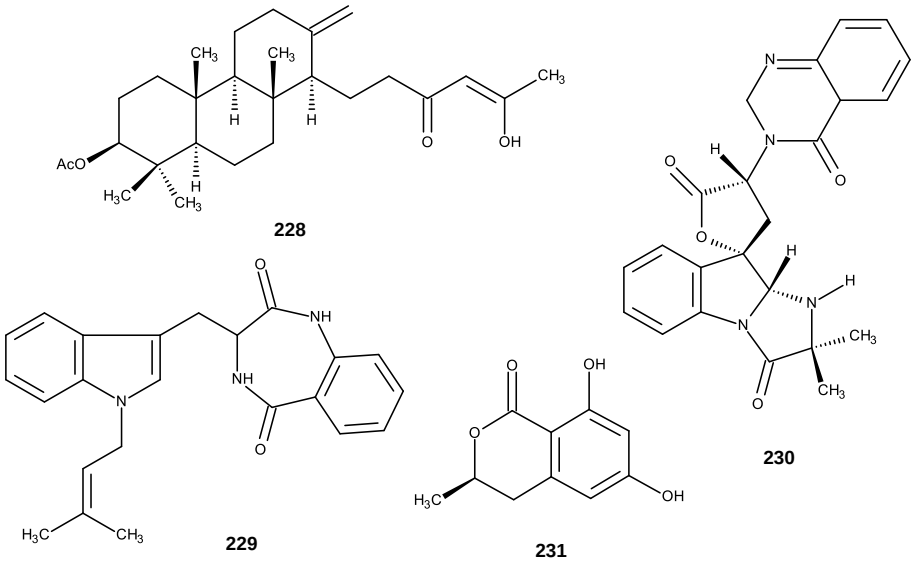

Figure 29. Structures of sartorenol (**228**), takakiamide (**229**), tryptoquivaline U (**230**) and 6-hydroxymellein (**231**)

2.1.11. *Neosartorya tatenoi*

A new meroditerpene tatenoic acid (**232**) (Figure 30) was isolated together with the previously described aszonalenin (**77**) (Figure 15), aszonapyrone A (**105**) (Figure 17), aszonapyrone B (**112**) (Figure 17), ergosterol (**115**) (Figure 17) and D-mannitol (**233**) (Figure 30) from the soil fungus *N. tatenoi* KKU-2NK23 Aszonapyrone A (**105**) was found to exhibit antimalarial activity against *Plasmodium falciparum,* with IC_{50} value of 1.34 mg/mL, and cytotoxicity against NCI-H187 and KB, with IC_{50} values of 4.62 and 48.18 mg/mL, respectively (Yim *et al*., 2014).

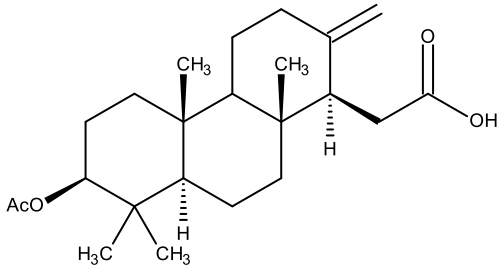

232

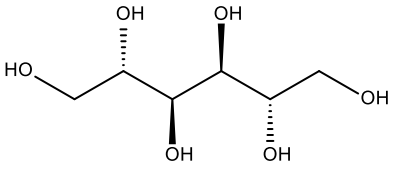

233

Figure 30. Structure of tatenoic acid (**232**) and D-mannitol (**233**)

2.1.12. *Neosartorya udagawae*

Yu *et al*., (2016) reported the isolation of four new quinazoline-containing indole alkaloids, neosartoryadins A (**234**) and B (**235**) and fiscalins E (**236**) and F (**237**) (Figure 31) and fiscalin C (**83**) (Figure 16) from the culture of an endophytic fungus *N. udagawae* HDN13-313, which was isolated from the root of the mangrove plant *Aricennia marina*. All isolated compounds were tested cytotoxicity against the HL-60 cancer cell line and against influenza A virus (H1N1). None of the isolated compound showed cytotoxicity against the HL-60 cancer cell line (IC_{50} > 50 μM). Compounds **234** and **235** showed inhibitory effects against influenza A virus (H1N1), in the cytopathic effect (CPE) inhibition assay, with IC_{50} values of 66 and 58 μM, respectively.

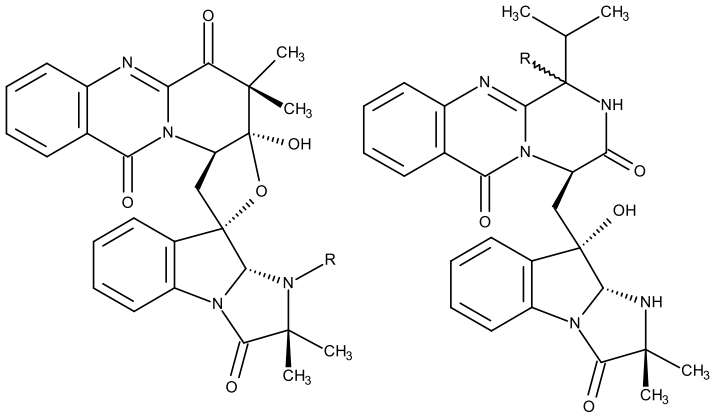

234 R = H
235 R = OH

236 R = OCH_3, 3*R*
237 R = OCH_3, 3*S*

Figure 31. Structures of neosartoryadins A (**234**), B (**235**), fiscalins E (**236**) and F (**237**)

2.1.13. *Neosartorya* species

Two previously unreported tryptoquivalines P (**238**) and Q (**239**) were isolated from the culture of *Neosartorya* sp.HN-M-3, which was isolated from marine mud in the intertidal zone of Hainan Province, China (Figure 32) (Sun *et al*., 2012).

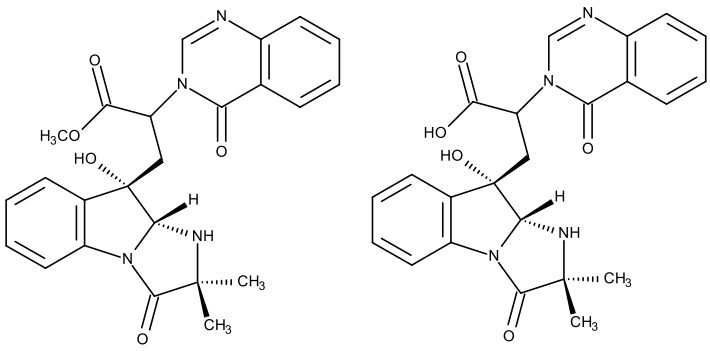

238 **239**

Figure 32. Structures of tryptoquivalines P (**238**) and Q (**239**)

2.2. Secondary Metabolites from *Penicillium* Species

Penicillium is one of the largest fungal genera of the Phylum Ascomycota, and more than 250 species of *Penicillium* have been identified up to now (Abastabar *et al*., 2016). *Penicillium* species are the most common fungi found in a diverse range of habitats, from soil to plants as well as to the air. Although many *Penicillium* species are common soil inhabitants, they also can be found from the marine environments. Many of secondary metabolites for examples sterols, alkaloids, diketopiperazines, quinolines, quinazolines, polyketides, camazulene and azetidine were produced by *Penicillium* (Jyoti and Singh, 2016). Fungi of the genus *Penicillium* are of commercial and industrial importance due to their capacity to produce antibacterial, antifungal, anti-insecticidal, antiviral, immune suppressants, cholesterol-lowering agents and mycotoxins (Ghanbari *et al*., 2014; Abastabar *et al*., 2016). Consequently, fungi of the genus *Penicillium* have been explored for the new leads and opportunities for drug discovery.

Herein, we describe the secondary metabolites, isolated from various species of *Penicillium*, and their associated biological activities.

2.2.1. *Penicillium adametzioides*

Two previously undescribed bisthiodiketopiperazine derivatives, adametizines A (**240**) and B (**241**) and two new acorane sesquiterpenes, adametacorenols A (**242**) and B (**243**) (Figure 33) were isolated from a liquid potato dextrose broth (PDB) culture medium and a rice solid culture medium of *P. adametzioides* AS-53 which was isolated from an unidentified marine sponge, collected at Hainan Island, China. Compound **242** exhibited antibacterial activity against *S. aureus*, *Aeromonas hydrophilia*, *Vibrio harveyi* and *V. parahaemolyticus* with minimum inhibitory concentration (MIC) values of 8, 8, 32 and 8 μg/mL, respectively, and antifungal activity against plant-pathogenic fungi, *Gaeumannomyces graminis* (MIC value of 16 μg/mL), while **243** showed growth inhibitory activity against *S. aureus* with the MIC value of 64 μg/mL (Liu *et al*., 2015). Moreover, neither of them displayed significant cytotoxic activity (IC_{50} > 10μM) against A549 (human lung adenocarcinoma), Du145 (human prostate carcinoma), HeLa

(human cervical carcinoma), HepG2 (human liver hepatocellular), Huh7 (human hepatocarcinoma), L02 (human hepatic L02), LM3 (murine LM3 breast), MA (mouse Leydig tumor), MCF-7 (human breast carcinoma), NCI-H446 (human small-cell lung carcinoma), SGC7901 (human gastric carcinoma), SW1990 (human pancreatic cancer), SW480 (human colon carcinoma cancer), and U251 (human glioma) cell lines.

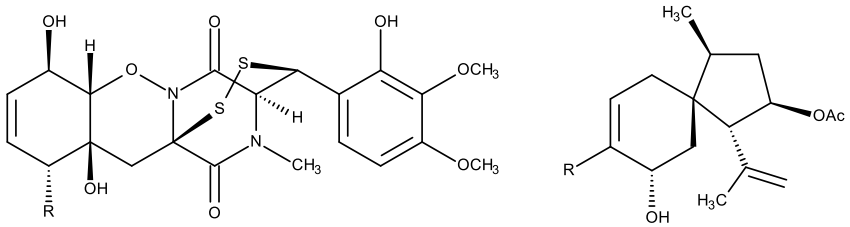

240 R = Cl
241 R = OH

242 R = CH_3
243 R = CH_2OH

Figure 33. Structures of adametizines A (**240**), B (**241**), adametacorenols A (**242**) and B (**243**)

2.2.2. *Penicillium aurantiogriseum*

Yu *et al*., (2010) reported the isolation of two previously undescribed polyketides, verrucosidinol (**244**) and verrucosidinol acetate (**245**), together with the previously reported verrucosidin (**246**), norverrucosidin (**247**) and a mixture of *cis*- and *trans*-terrestric acids (**248** and **249**), (Figure 34) from the marine-derived fungus *P. aurantiogriseum*, isolated from marine mud of the Bohai Sea. Compounds **244** and **245** did not show significant activity against *S. aureus*, *P. aeruginosa*, *C. albicans* SC5314 (MIC value ≥ 64 μg/mL).

Later on, the same group has isolated three previously unreported quinazolin-4-one containing alkaloids, auranomides A (**250**), B (**251**) and C (**252**) and the previously reported auranthine (**253**) and aurantiomides C (**254**) (Figure 34) from the culture of the same fungus. Compounds **250**-**252** were tested for their cytotoxicity

against Human myelogenous leukemia (K562), human renal cell carcinoma (ACHN), human hepatocellular liver carcinoma (HEPG2) and human lung adenocarcinoma (A549) cell lines, however, only auranomide B (**251**) showed moderate inhibitory effect against HEPG2 cell line, with IC_{50} value of 0.097 µm/mL. Moreover, the three compounds also did not exhibit antimicrobial activity against *S. aureus* (MRSA) and *C. albicans* (Song *et al*., 2012).

Ma *et al.*, (2015) described isolation of six previously undescribed polyketides containing decalin ring system, peaurantiogriseols A-F (**255**-**260**), together with two previously reported aspermytin A (**261**) and 1-propanone,3-hydroxy-1(1,2,4a,5,6,7,8,8a-octahydro-2,5-dihydroxy-1,2,6-trimethyl-1-naphthalenyl) (**262**), from the mangrove endophytic fungus *P. aurantiogriseum* strain 328# which was isolated from the bark of the mangrove plant *Hibiscus tiliaceus*. All the isolated compounds, at a concentration of 50 mM, displayed low inhibitory activity against human aldose reductase. Moreover, all the compounds tested showed exhibited neither activity of inducing neurite outgrowth (PC-12) nor antimicrobial activity against *E. coli* ATCC 25922, *S. aureus* ATCC 25923, *C. albicans* ATCC 60193 (Ma *et al*., 2015).

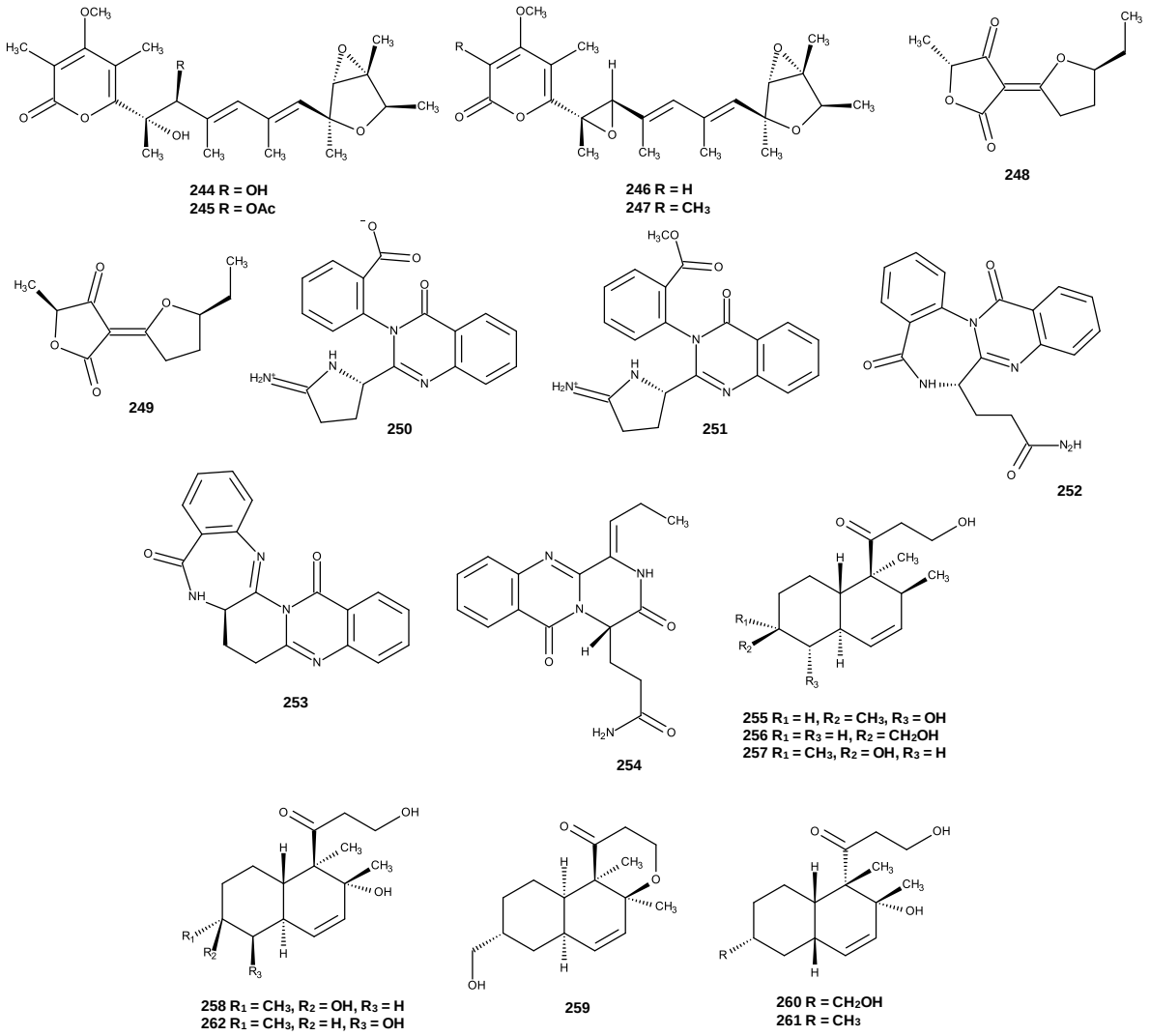

Figure 34. Structures of verrucosidinol (**244**), verrucosidinol acetate (**245**), verrucosidin (**246**), norverrucosidin (**247**), *cis*-terrestric acids (**248**), *trans*-terrestric acids (**249**), auranomides A (**250**), B (**251**), C (**252**), auranthine (**253**), aurantiomides C (**254**), peaurantiogriseols A (**255**), B (**256**), C (**257**), D (**258**), E (**259**), (**260**), aspermytin A (**261**) and 1-propanone,3-hydroxy-1(1,2,4a,5,6,7,8,8a-octahydro-2,5-dihydroxy-1,2,6-trimethyl-1-naphthalenyl) (**262**)

2.2.3. *Penicillium brefeldianum*

Three previously unreported indolediketopiperazine peroxides, 24-hydroxyverruculogen (**263**), 26-hydroxyverruculogen (**264**) and 13-*O*-prenyl-26-hydroxyverruculogen (**265**) (Figure 35) were isolated, together with four previously reported homologues: verruculogen (**111**) (Figure 17), fumitremorgin A (**130**) (Figure 18), cyclotryprostatin A (**266**) and TR-2 (**267**) (Figure 35) from culture extracts of *P. brefeldianum* SD-273, which was isolated from a sediment collected from the estuary of the Pearl River in South China Sea. All the isolated compounds were tested for the antibacterial activity against *E. coli* and *S. aureus* as well as the cytotoxicity against B16 (murine melanoma), HuH-7 (hepatocarcinoma), SW-1990 (human pancreatic adenocarcinoma), Hela (human epithelial carcinoma), Du145 (human prostate carcinoma), H460 (non-small cell lung cancer), MCF-7 (human breast adenocarcinoma) and SGC-7901 (human gastric cancer) cell lines. However, none of the compounds exhibited either antibacterial or cytotoxicity (An *et al*., 2014).

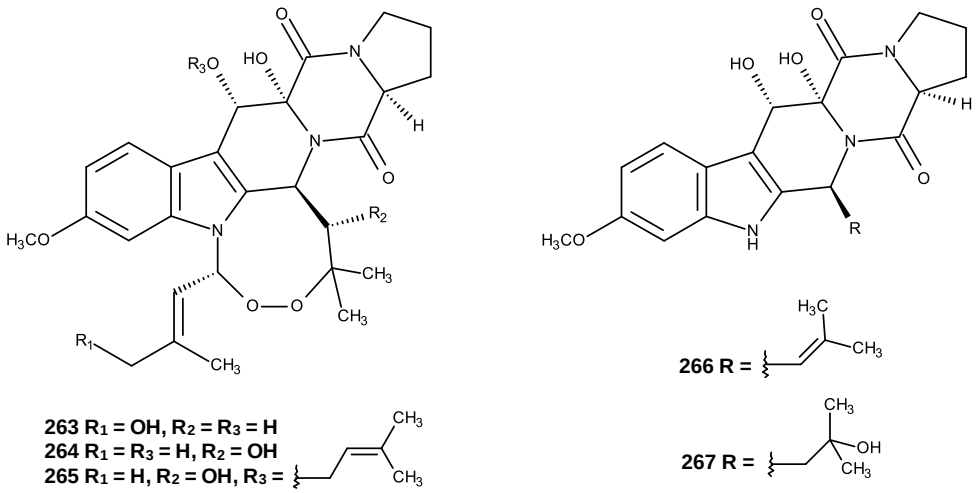

Figure 35. Structures of 24-hydroxyverruculogen (**263**), 26-hydroxyverruculogen (**264**), 13-O-prenyl-26-hydroxyverruculogen (**265**), cyclotryprostatin A (**266**) and TR-2 (**267**)

2.2.4. *Penicillium brevicompactum*

The culture extract of *P. brevicompactum* strain DFFSCS025 was isolated from a deep-sea sediment sample collected at the South China Sea. Four previously undescribed metabolites including brevianamide X (**268**), brevianamide Y (**269**) and two mycochromenic acid derivatives: 6-(Methyl 3-methylbutanoate)-7-hydroxy-5-methoxy-4-methylphthalan-1-one (**270**) and (3′*S*)-(*E*)-7-Hydroxy-5-methoxy-4-methyl-6-(2-(2-methyl-5-oxotetrahydrofuran-2-yl)vinyl)isobenzofuran-1(3*H*)-one (**271**), together with the previously reported 6-(3-carboxybutyl)-7-hydroxy-5-methoxy-4-methylphthalan-1-one (**272**), 7-hydroxy-6-[2-hydroxy-2-(2-methyl-5-oxotetrahydro-2-furyl)ethyl]-5-methoxy-4-methyl-1-phthalonone (**273**), 5-hydroxy-7-methoxy-4-methylphthalide (**274**), mycochromenic acid (**275**), (-)-brevianamide C (**276**) and (+)-brevianamide A (**277**) (Figure 36), were isolated from the culture extract of *P. brevicompactum* strain DFFSCS025 which was isolated from a deep-sea sediment sample collected at the South China Sea.

All the isolated compounds were assayed for their cytotoxicity against HCT 166 (human colon cancer) cell line. However, only **276** exhibited moderate cytotoxicity with IC_{50} value of 15.6 µM.

Compounds **268, 270, 272** and **275** were tested for their antifouling activity using the settlement inhibition assays with *Bugula neritina* larvae Only **270** and **272** exhibited antifouling activity with EC_{50} values of 13.7 and 22.6 µM, respectively (Xu *et al*., 2017).

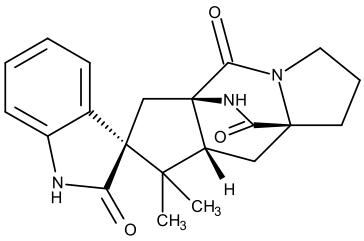

268

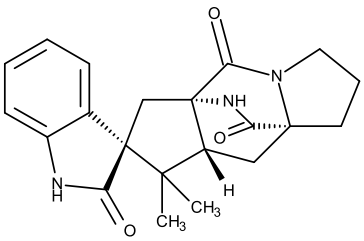

269

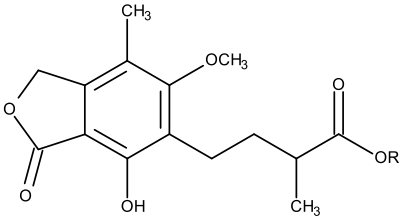

270 R = CH$_3$
272 R = H

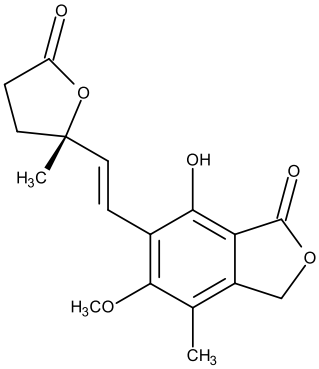

271

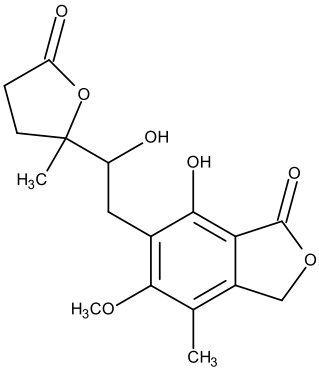

273

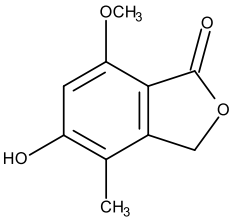

274

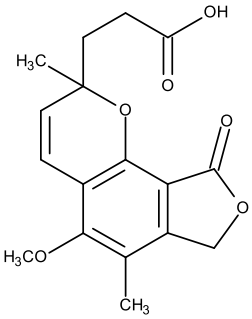

275

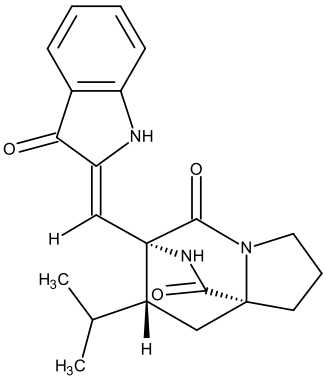

276

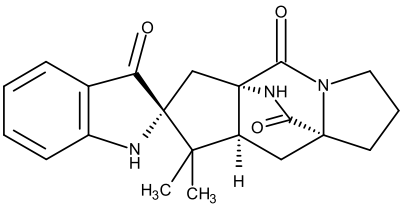

277

Figure 36. Structures of brevianamide X (**268**), brevianamide Y (**269**), 6-(Methyl 3-methylbutanoate)-7-hydroxy-5-methoxy-4-methylphthalan-1-one (**270**), (3′*S*)-(*E*)-7-Hydroxy-5-methoxy-4-methyl-6- (2- (2-methyl-5-oxotetrahydrofuran-2-yl) vinyl) isobenzofuran-1 (3*H*)-one (**271**), 6-(3-carboxybutyl)-7-hydroxy-5-methoxy-4-methylphthalan-1-one (**272**), 7-hydroxy-6-[2-hydroxy-2- (2-methyl-5-oxotetrahydro-2-furyl) ethyl]-5-methoxy-4-methyl-1-phthalonone (**273**), 5-hydroxy-7-methoxy-4-methylphthalide (**274**), mycochromenic acid (**275**), (-)-brevianamide C (**276**) and (+)-brevianamide A (**277**)

2.2.5. *Penicillium brocae*

Meng and coworkers (2014) described the isolation of six previously unreported disulfide-bridged diketopiperazines, brocazines A-F (**278-283**) and the previously reported analogue, epicorazine A (**284**) (Figure 37) from the culture of the endophytic fungus *Penicillium brocae* strain MA-231, which was isolated from the fresh tissue of the marine mangrove plant *Avicennia marina*. Compounds **278, 279, 282** and **283** exhibited cytotoxic activity against Du145 (human carcinoma of prostate), HeLa (human cervix carcinoma), HepG2 (human liver hepatocellular), MCF-7 (human breast carcinoma), NCI-H460 (human large cell lung carcinoma), SGC-7901 (human gastric carcinoma), SW1990 (human pancreatic cancer), SW480 (human colon carcinoma) and U251 (human glioma) cell lines, with IC_{50} values ranging from 0.89 to 9.0 μM.

Later on, the same group (Meng *et al*., 2015) has isolated five new sulfide diketopiperazines, penicibrocazines A-E (**285-289**) as well as the previously described phomazine B (**290**) (Figure 37), from the culture of the same fungus. Compounds **285-290** were assayed for their antimicrobial activity against several human-, aqua-, and plant-pathogenic microbes. Compounds **286-288** and **290** exhibited antimicrobial activity against *S. aureus*, with MIC values of 32.0, 0.25, 8.0, and 0.25 μg/mL, respectively, while **286, 288, 289** and **290** displayed growth inhibitory activity against the plant pathogen *Gaeumannomyces graminis,* with MIC values of 0.25, 8.0, 0.25, and 64.0 μg/mL, respectively. On the other hand, **287** showed a growth inhibitory activity against *Micrococcus luteus* with MIC value of 0.25 μg/mL. Compounds **285-290** were also evaluated for cytotoxicity against Du145, HeLa, HepG2, MCF-7, NCI-H460, SGC-7901, SW1990 and U251 cell lines, however, none of them exhibited significant activity (IC_{50} > 10 μM). In continuation of the work on this fungus, the same group has later isolated four previously unreported diketopiperazine derivatives, including spirobrocazines A−C (**291-293**) and a new bisthiodiketopiperazine derivative, brocazine G (**294**) (Figure 37). Compounds **291-294** were evaluated for anticancer activity against the sensitive and cisplatin-resistant human ovarian cancer cell lines A2780 and A2780 CisR. While **293** exhibited moderate activity against A2780 cells (IC_{50} = 59 μM), **293** displayed strong activity against both A2780 and A2780 CisR cells, with IC_{50} values of 664 and 661 nM, respectively (IC_{50} values of the positive

control cisplatin were 1.67 and 12.63 μM, respectively). Compounds **291-294** were also assayed for antibacterial activity. Compound **294** exhibited strong and selective activity against *S. aureus* with MIC value of 0.25 μg/mL (MIC value of the positive control, chloromycetin was 0.5 μg/mL), while **291** displayed moderate activity against *E. coli, S. aureus* and *V. harveyi*, with MIC values of 32.0, 16.0, and 64.0 μg/mL, respectively (the positive control chloromycetin has MIC values of 2.0, 0.5, and 2.0 μg/mL, respectively). Compound **291** showed antibacterial activity against *E. coli, Aeromonas hydrophilia*, and *V. harveyi*, with a MIC value of 32.0 μg/mL (Meng *et al*., 2016).

Another strain of this fungus*, Penicillium brocae* MA-192, also isolated from the fresh leaves of the marine mangrove plant *A. marina*. The EtOAc extract of the mycelium and broth of this fungus furnished three previously alkaloids, brocaeloids A-C (**295-297**) (Figure 37). Compound **296** exhibited brine shrimp (*Artemia salina*) lethality with the LD_{50} value of 36.7 μm (Zhang *et al*., 2014).

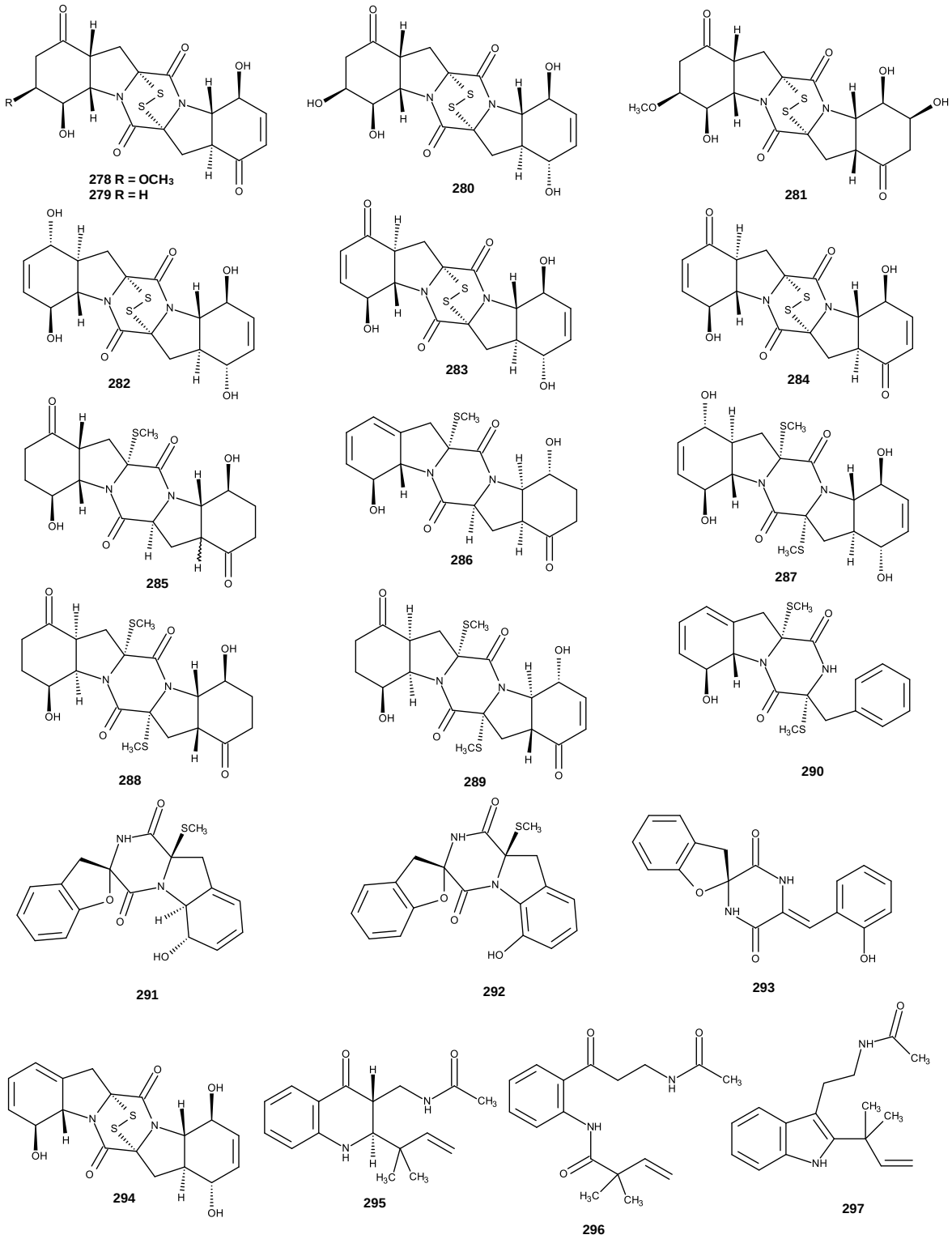

Figure 37. Structures of brocazines A (**278**), B (**279**), C (**280**), D (**281**), E (**282**), F (**283**), epicorazine A (**284**), penicibrocazines A (**285**), B (**286**), C (**287**), D (**288**), E (**289**), phomazine B (**290**), spirobrocazines A (**291**), B (**292**), C (**293**), brocazine G (**294**), brocaeloids A (**295**), B (**296**) and C (**297**)

2.2.6. *Penicillium citrinum*

Tsuda's group (Tsuda *et al*., 2005) isolated three new pyrrolidine alkaloids, scalusamides A-C (**298-300**), together with the previously reported pyrrolo [2,1-*b*]oxazine derivatives, 2-heptyl-3-methyl-4-oxo-6,7,8,8a-tetrahydro-4*H*-pyrrolo[2,1-*b*]-1,3-oxazine (**301**) and 2-[(*E*)-hept-5-enyl]-3-methyl-6,7,8,8a-tetrahydropyrrolo[2,1-*b*][1,3]oxazin-4-one (**302**) (Figure 38) from the culture of *P. citrinum* strain N055, which was isolated from the gastrointestine of an Okinawan parrot fish (*Scalus ovifrons*). Compound **298** (scalusamide A) exhibited antifungal activity against *Cryptococcus neoformans* with MIC = 16.7 µg/mL), and antibacterial activity against *Micrococcus luteus* with MIC = 33.3 µg/mL).

Later on, the same group has isolated a previously undescribed tetracyclic alkaloid, perinadine A (**303**) (Figure 38) from the same fungus. Compound **303** exhibited weak antibacterial activity against *M. luteus* and *B. subtilis* with MIC of 33.3 and 66.7 µg/mL, respectively, as well as weak cytotoxicity against murine leukemia L1210 cells with IC_{50} of 20 µg/mL (Sasaki *et al*., 2005).

Zheng *et al.*, (2016) described the isolation of a new benzopyran derivative, (2*R**,4*R**)-3,4-dihydro-5-methoxy-2-methyl-2H-1-benzopyran-4-ol (**304**), together with the previously described (*2R**,*4R**)-3,4-dihydro-4-methoxy-2-methyl-2H-1-benzopyran4-ol (**305**), (4*S*)-3,4-dihydro-4,8-dihydroxy-l(2H)-naphthalenoe (**306**), 5,7-dihydroxy-2-propylchromone (**307**), (*R*)-6-hydroxymellein (**308**), 1-(2,6-dihydroxyphenyl)butan-1-one (**309**) (Figure 38), from the culture of the endophytic fungus *P. citrinum* HL-5126 which was obtained from the leaves of mangrove plant *Brguiera sexangula* var. *rhynchopetala*. Compound **309** exhibited antibacterial activity against *B. subtilis*, *B. cereus* and *M. tetragenus* with the same MIC values of 6.94 µM. Later on, the same group (Huang *et al*., 2016) has isolated three previously undescribed dihydroisocoumarin which were named penicimarins G-I (**310-312**) together with the previously reported aspergillumarin A (**313**) and three meroterpenoids dehydroaustin (**314**), 11*β*-acetoxyisoaustinone (**315**) and austinol (**316**) (Figure 38) from the same fungus. Compounds **310** and **311** showed a broad spectrum of antibacterial activity against *S. epidermidis, S. aureus, E. coli, B. cereus, and V. alginolyticus* while **312** and **316** showed moderate activity against *S.*

epidermidis and *S. aureus* (MIC = 10 µM). All the isolated compounds did not exhibit cytotoxicity against HeLa, MCF-7and A549 cells (IC_{50} > 50 µM).

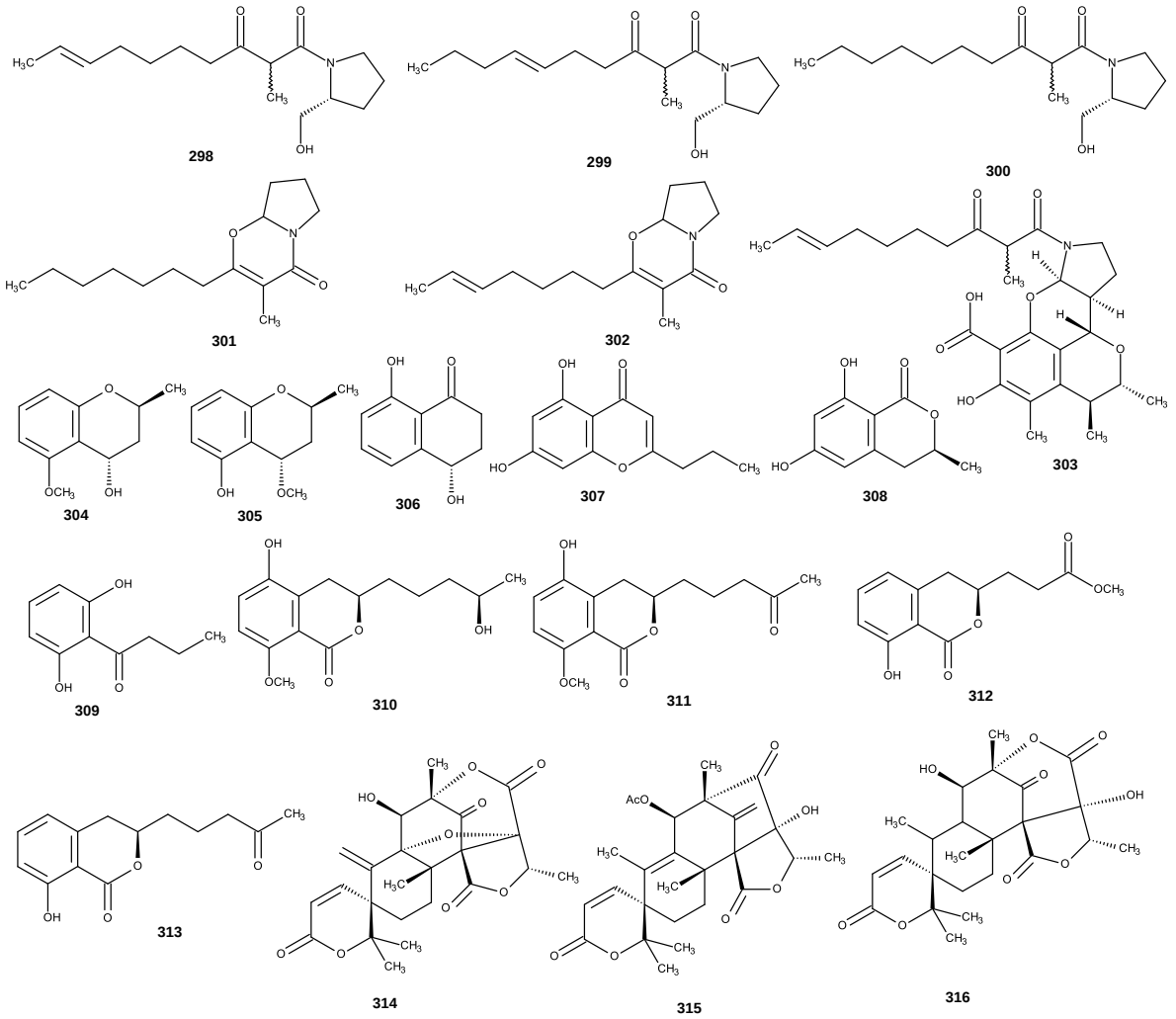

Figure 38. Structures of scalusamides A (**298**), B (**299**), C (**300**), 2-heptyl-3-methyl-4-oxo-6,7,8,8a-tetrahydro-4*H*-pyrrolo[2,1-*b*]-1,3-oxazine (**301**), 2-[(*E*)-hept-5-enyl]-3-methyl-6,7,8,8a-tetrahydropyrrolo[2,1-*b*][1,3]oxazin-4-one (**302**), perinadine A (**303**), (2*R**,4*R**)-3,4-dihydro-5-methoxy-2-methyl-2H-1-benzopyran-4-ol (**304**), (*2R**,*4R**)-3,4-dihydro-4-methoxy-2-methyl-2H-1-benzopyran4-ol (**305**), (4*S*)-3,4-dihydro-4,8-dihydroxy-l(2H)-naphthalenoe (**306**), 5,7-dihydroxy-2-propylchromone (**307**), (*R*)-6-hydroxymellein (**308**), 1-(2,6-dihydroxyphenyl)butan-1-one (**309**), penicimarins G (**310**), H (**311**), I (**312**), aspergillumarin A (**313**), dehydroaustin (**314**), 11*β*-acetoxyisoaustinone (**315**) and austinol (**316**)

Liu *et al*., (2015) isolated a previously unreported alkaloid penicitrinine A (**317**) (Figure 39) from the culture of *P. citrinum* which was isolated from the marine sediment in Fujian, China. Compound **317** was evaluated in a panel of twenty-three cancer cell lines derived from ten different types of tumors; however, the most sensitive cell lines were malignant melanoma cell line A-375, lung cancer cell line SPC-A1 and stomach cancer cell line HGC-27 with IC_{50} values of 20.12 μM, 28.67 μM and 29.49 μM, respectively. Compound **317** significantly induced A-375 cell apoptosis by decreasing the expression of Bcl-2 and increasing the expression of Bax. It was found also that **317** significantly suppressed metastatic activity of A-375 cells by regulating the expression of MMP-9 and its specific inhibitor TIMP-1.

Two previously unreported citrinin dimer derivatives, penicitol D (**318**) and 1-*epi*-citrinin H1 (**319**) as well as the previously reported citrinin H1 (**320**), penicitrinol A (**321**), (3*S*,4*S*)-sclerotinin A (**322**), stoloniferol B (**323**), (3*R*)-6-methoxymellein (**324**), (3*R*)-6-methoxy-7-chloromellein (**325**), phenol A (**326**), citrinin H2 (**327**), (3*S*)-hydroxy-4-epi-isosclerone (**328**), (3*R*,4*S*)-6,8-dihydroxy-1,1-dimethyl-3,4,5-trimethylisochroman (**329**) and (3*S*)-(3',5'-dihydroxy-2'-methylphenyl)-2-butanone (**330**) (Figure 39) were isolated from a deep sea-derived fungus *P. citrinum* strain NLG-S01-P1, was isolated the seawater sample at a depth of 4650 m in the West Pacific Ocean. All the isolated compounds were evaluated for antibacterial activity against methicillin-resistant *S.aureus* (MRSA) (ATCC 43300, CGMCC 1.12409), *Vibrio vulnificus* MCCC E1758, *V. campbellii* MCCC E333, *V. rotiferianus* MCCC E385, as well as cytotoxicity against A549 and HeLa cell lines. Compound **318** exhibited cytotoxic activity against HeLa cells, with the IC_{50} value of 4.1 μM. Compounds **318** and **319** displayed antibacterial activity against methicillin-resistant *S. aureus* (MRSA) (ATCC 43300, CGMCC 1.12409) with MIC values ranging from 7 to 8 μg/mL, while **322** and **327** were active against *V. vulnificus* and *V. campbellii*, with MIC values ranging from 15 to 17 μg/mL (Wang *et al*., 2019).

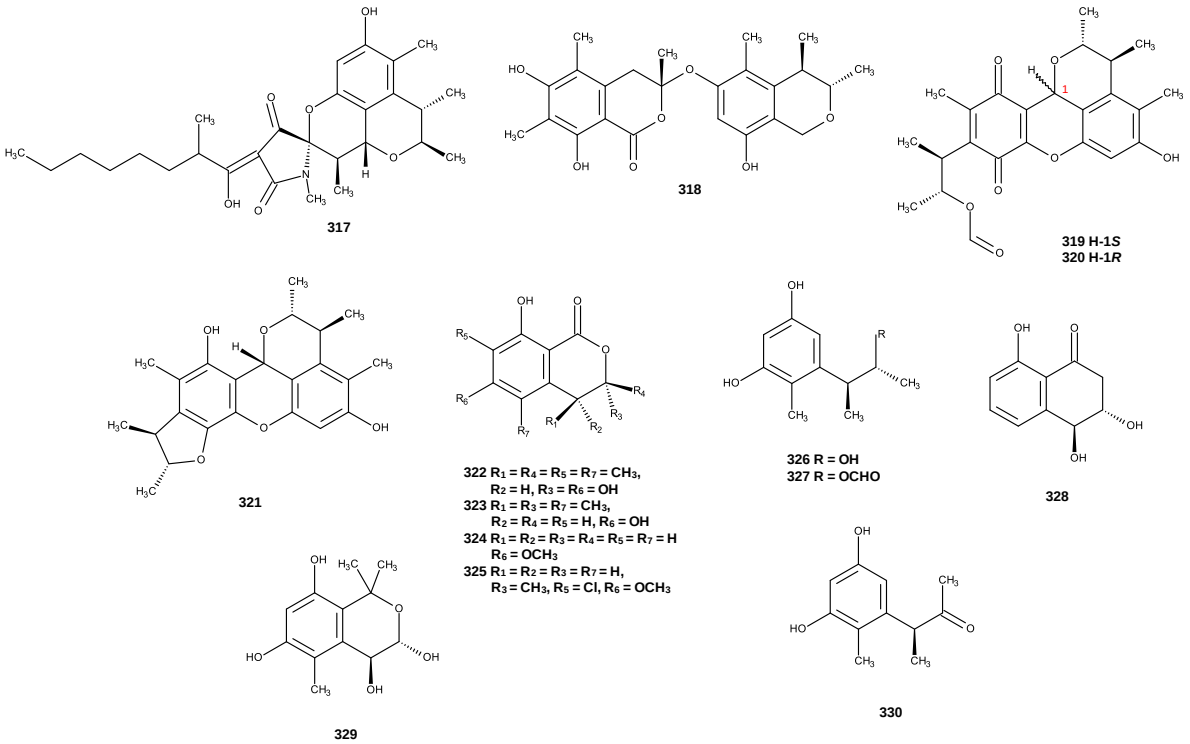

Figure 39. Structures of penicitrinine A (**317**), penicitol D (**318**), 1-*epi*-citrinin H1 (**319**), citrinin H1 (**320**), penicitrinol A (**321**), (3*S*,4*S*)-sclerotinin A (**322**), stoloniferol B (**323**), (3*R*)-6-methoxymellein (**324**), (3*R*)-6-methoxy-7-chloromellein (**325**), phenol A (**326**), citrinin H2 (**327**), (3*S*)-hydroxy-4-epi-isosclerone (**328**), (3*R*,4*S*)-6,8-dihydroxy-1,1-dimethyl-3,4,5-trimethylisochroman (**329**) and (3*S*)-(3',5'-dihydroxy-2'-methylphenyl)-2-butanone (**330**)

2.2.7. *Penicillium commune*

A previously unreported 1-*O*-(2,4dihydroxy-6-methylbenzoyl)-glycerol (**331**) (Figure 40) was isolated together with thirteen previously described compounds: ergosterol (**115**) (Figure 17), ergosta-7,22-dien-3*β*,5*α*,6*β*-triol (**125**) (Figure 18), 3-indolylacetic acid methyl ester (**195**) (Figure 25), 1-*O*-acetylglycerol (**332**), *N*-acetyltryptophan (**333**), 1(2,4-dihydroxy-3,5-dimethylphenyl)ethanone (**334**), 2-(2,5-dihydroxyphenyl)acetic acid (**335**), (4*R*,5*S*)-5-hydroxyhexan-4-olide (**336**), thymidine (**337**), uracil (**338**), thymine (**339**), *β*-sitosterol (**340**) and *β*-daucosterol (**341**) (Figure 40) from the extract of a solid culture (cooked rice) of the endophytic fungus *P.*

commune strain G2M, which was isolated from a mangrove plant *Hibiscus tiliaceus* Linn (Yan *et al*., 2010).

Gao *et al*., (2011) reported the isolation of six, previously unreported azaphilone derivatives, named the extracts of the mycelia and culture broth of comazaphilones A-F (**342-347**) (Figure 40) from *P. commune* QSD-17 which was isolated from a marine sediment, collected from the southern China Sea. All isolated compounds were tested for their antimicrobial activity and cytotoxicity, which compound **344** exhibited activity against methicillin-resistant *S. aureus* (MRSA), *P. fluorescens*, and *B. subtilis*, with MICs values of 16, 64, and 32 µg/mL, respectively, while **345** showed activity against *S. aureus* (MRSA) and *P. fluorescens* with MICs values of 32 and 16 µg/mL, respectively; **345** showed activity at MICs values of 32 and 16 µg/mL against *P. fluorescens* and *B. subtilis*, respectively. In addition, **345**, **346** and **347** displayed potent cytotoxic activity against SW1990 cell line with IC_{50} values of 51, 26 and 53 µM, respectively.

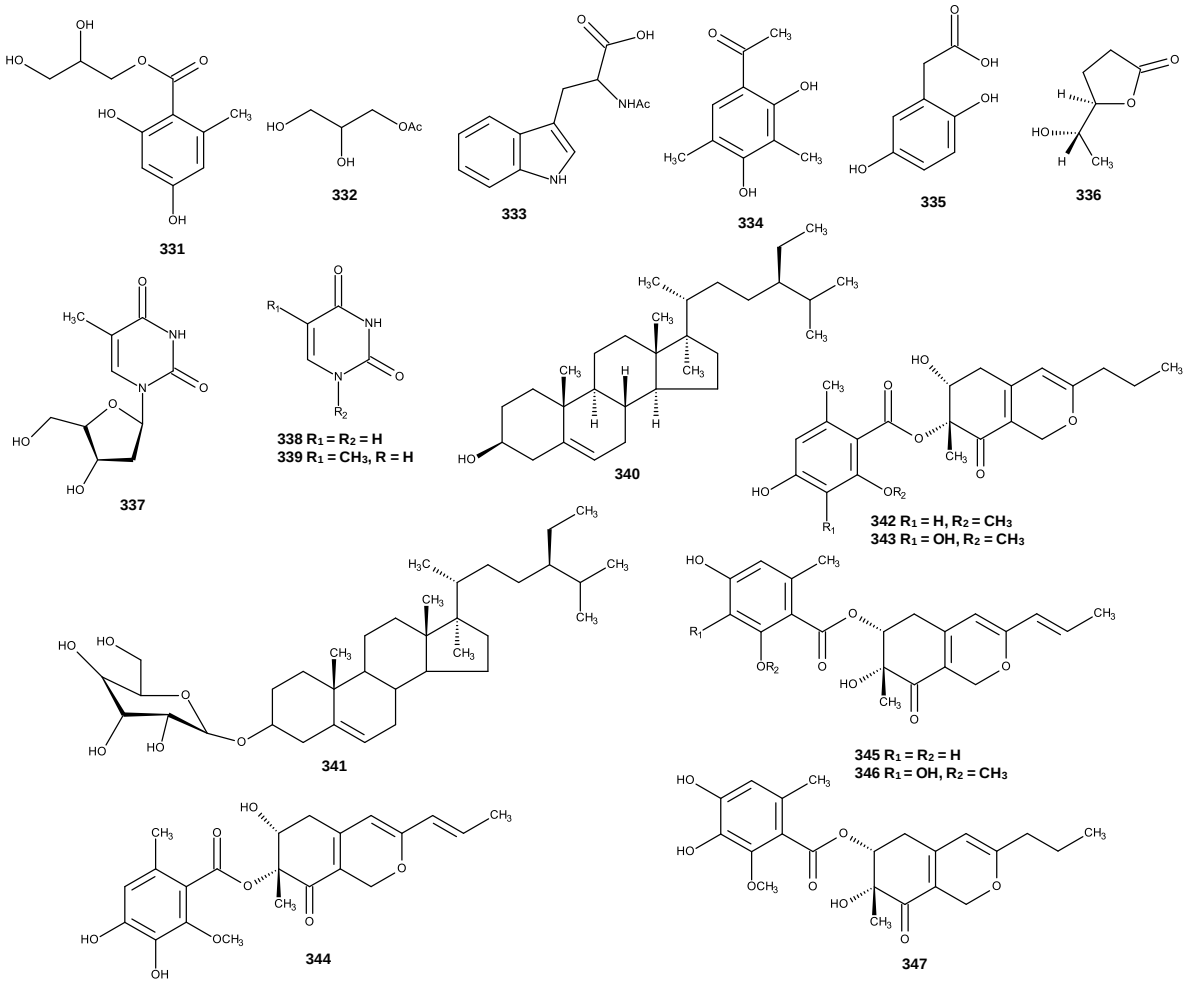

Figure 40. Structures of 1-*O*-(2,4dihydroxy-6-methylbenzoyl)-glycerol (**331**) 1-*O*-acetylglycerol (**332**), *N*-acetyltryptophan (**333**), 1(2,4-dihydroxy-3,5-dimethylphenyl)ethanone (**334**), 2-(2,5-dihydroxyphenyl)acetic acid (**335**), (4*R*,5*S*)-5-hydroxyhexan-4-olide (**336**), thymidine (**337**), uracil (**338**), thymine (**339**), *β*-sitosterol (**340**), *β*-daucosterol (**341**), comazaphilones A (**342**), B (**343**), C (**344**), D (**345**), (**346**) and F (**347**)

2.2.8. *Penicillium dipodomyis*

The mutant of the fungus *P. dipodomyis* YJ-11 which was collected from the marine sediment, obtained by overexpression the global regulator LaeA, was found to

produce several sorbicillinoids, including the previously unreported 10,11-dihydrobislongiquinolide (**348**) and 10,11,16,17-tetrahydrobislongiquinolide (**349**) and the previously described bislongiquinolide (**350**),16,17-dihydrobislongiquinolide (**351**), sohirnone A (**352**) and 20,30-dihydrosorbicillin (**353**) (Figure 41). Compounds **348-352** showed neither cytotoxicity against HL-60, K562, BEL-7402, HCT-116, A549, Hela, L-02, MGC-803, SH-SY5Y, PC-3, H446, U87, MDA-MB-231, HO8910, ASPC-1 and MCF-7 cell lines (with concentration tested at 30 µM) nor antimicrobial activity (Yu *et al*., 2019).

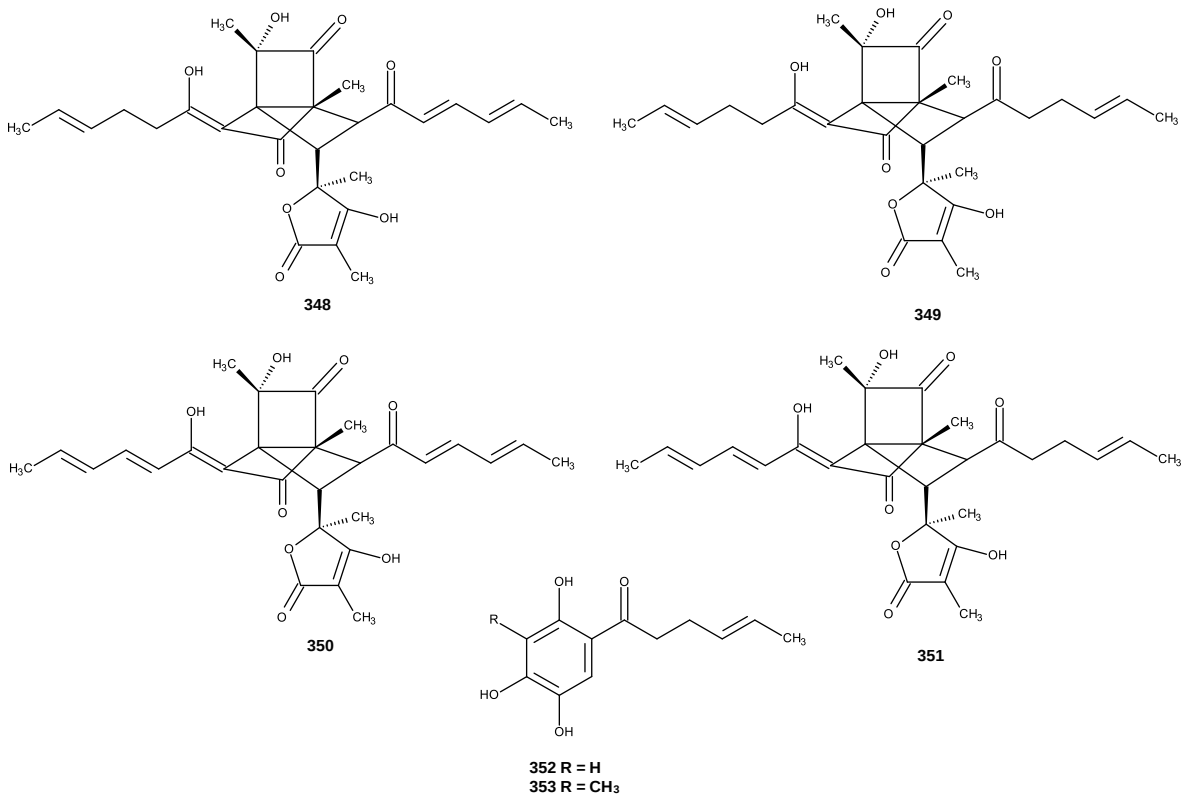

Figure 41. Structures of 10,11-dihydrobislongiquinolide (**348**), 10,11,16,17-tetrahydrobislongiquinolide (**349**), bislongiquinolide (**350**), 16,17-dihydrobislongiquinolide (**351**), sohirnone A (**352**) and 20,30-dihydrosorbicillin (**353**)

2.2.9. *Penicillium expansum*

Four previously unreported bisabolane sesquiterpenoid derivatives, expansols A (**354**) and B (**355**), (*S*)-(+)-11-dehydrosydonic acid (**356**) and (7*S*,11*S*)-(+)- 12-acetoxysydonic acid (**357**) were isolated, together with the previously reported (*S*)-(+)-sydonic acid (**358**) and diorcinol (**359**) (Figure 42), from the culture extract of the mangrove endophytic fungus *P. expansum* 091006, which was isolated from the surface-sterilized roots of the mangrove plant *Excoecaria agallocha,* collected in Hainan Province, China. Compound **354** displayed moderate cytotoxicity against HL-60 cell line with an IC_{50} value of 15.7 μM, while **355** showed cytotoxicity against A549 and HL-60 cell lines with IC_{50} values of 1.9 and 5.4 μM, respectively (Lu *et al*., 2010).

Fan *et al*., (2015) described isolation of three previously unreported alkaloids, communesin I (**360**), fumiquinazoline Q (**361**) and protuboxepin E (**362**), along with nine previously reported analogues communesins A (**363**) and B (**364**), cottoquinazoline A (**365**), prelapatin B (**366**), glyantrypine (**367**), protuboxepins A (**368**) and B (**369**), chaetoglobosin C (**370**) and penochalasin E (**371**) (Figure 42) from the culture extract of *P. expansum* Y32, collected from a seawater sample collected from a depth of about 30 m in the Indian Ocean. All the isolated compounds were evaluated for cardiovascular effects using zebrafish embryos. Compounds **360-371** showed a significant mitigative effect on bradycardia caused by astemizole (ASM) at different concentrations. Compounds **361-362**, **365-366** and **368-371** at concentrations of 20 μg/mL, 50 μg/mL and 100 μg/mL, exhibited potent vasculogenetic activity while **360**, **363** and **367** displayed moderate effects and **364** showed no effect.

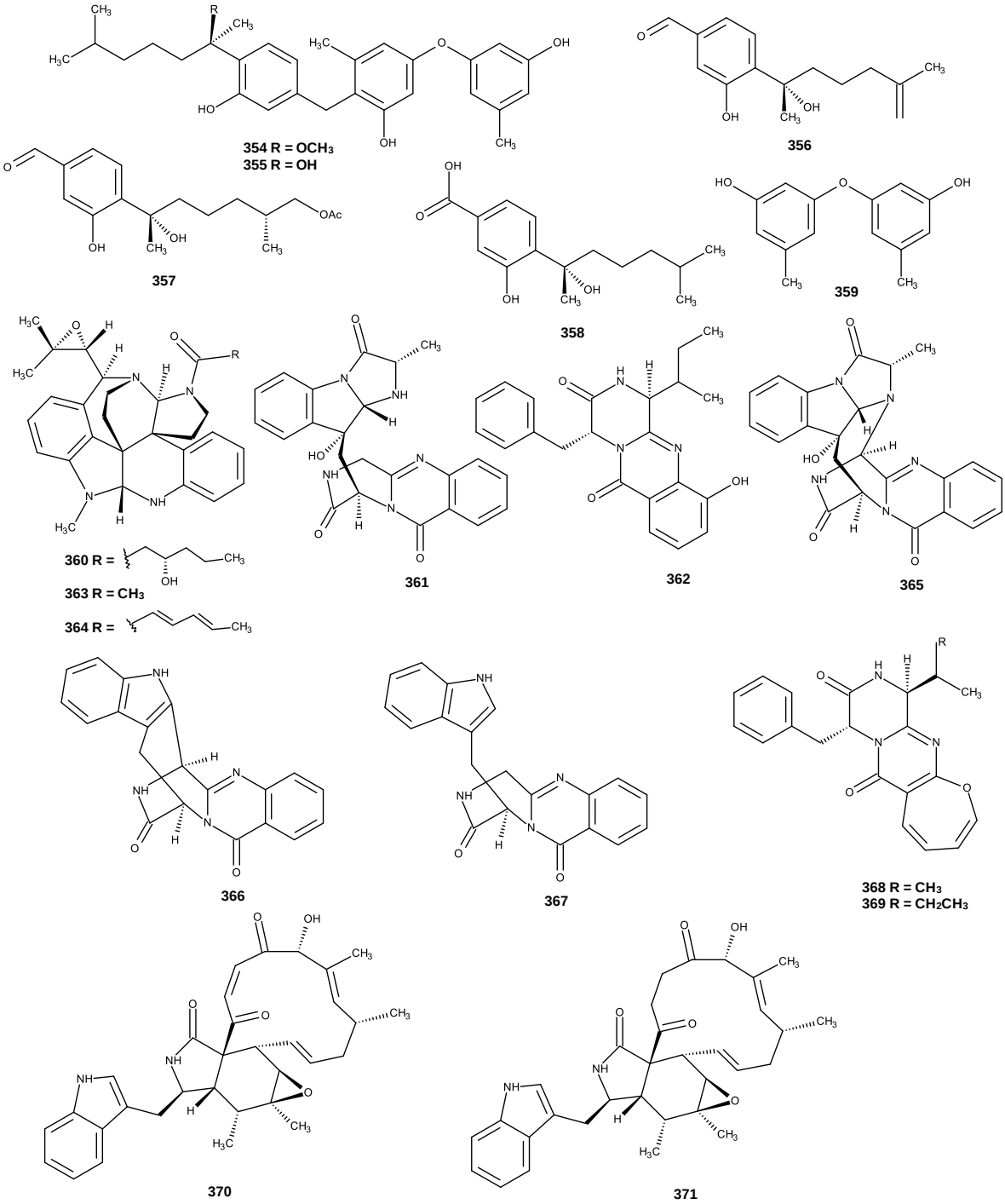

Figure 42. Structures of expansols A (**354**), B (**355**), (*S*)-(+)-11-dehydrosydonic acid (**356**), (7*S*,11*S*)-(+)- 12-acetoxysydonic acid (**357**), (S)-(+)-sydonic acid (**358**), diorcinol (**359**), communesin I (**360**), fumiquinazoline Q (**361**), protuboxepin E (**362**), communesins A (**363**), B (**364**), cottoquinazoline A (**365**), prelapatin B (**366**), glyantrypine (**367**), protuboxepins A (**368**), B (**369**), chaetoglobosin C (**370**) and penochalasin E (**371**)

2.2.10. *Penicillium granulatum*

Five new ergostanes, penicisteroids D-H (**372-376**) and 27 previously described compounds: penicisteroid A (**377**), penicisteroid C (**378**) (Figure 43), anicequol, ergosta-7,22-diene-3*β*,5*α*,6*β*,9*α*-tetraol, ergosterol peroxide, ergosterol, (22*E*,24*R*)-3*β*,5*α*-trihydroxy- ergost-7,22-dien-6-one, (3*β*,5*α*,6*β*,22*E*)-ergosta-7,22-diene-3,5,6-triol, (3*β*,5*α*,*6β,22E*)-6-methoxyergosta7,22-diene-3,5-diol,5*α*,6*α*,8*α*,9*α*-diepoxy-(22*E*,24*R*)-ergoxt-22-ene-3*β*,7*β*-diol, (24*S*)-24-ethylcholesta-3*β*,5*α*-diol6-one, (24*S*)-24-ethylcholesta-3*β*,5*α*,6*α*-triol, topsentisterol D3, incisterol A2, conidiogenones B, conidiogenone G, conidiogenone D, conidiogenone C, conidiogenones I, meleagrin, roquefortine C, roquefortine, (5*S*)-5-(1*H*-indol-3-ylmethyl)-2,4-imidazolidione, sorbicillin, 20,30-dihydrosorbicillin, trichodimerol and dihydrotrichodimerol, were obtained from the deep-sea-derived fungus *P. granulatum* MCCC 3A00475. All the isolated compounds were tested for cytotoxic activity against human glioma cell line (SHG-44), liver cancer cell lines (HepG2 and 7402), non-small cell lung cancer cell line (A549), bladder cancer cell line (BIU-87), esophageal cancer cell line (ECA-109), cervix cancer cell line (Hela-S3), pancreatic cancer cell line (PANC-1), colon carcinoma cell lines (SW620 and HcT116), breast cancer cell lines (MCF-7 and MB-231). All the tested compounds showed selectively cytotoxicity against A549, BIU-87, BEL-7402, ECA-109, Hela-S3, and PANC-1 cells. However, none exhibited antiproliferative effect against SW620, HcT116, MCF-7 and MB-231 cancer cell lines. For cytometry and the Western blotting indicated **373** and **375-378** were able to induce apoptosis in A549 cells. Additionally, **373** and **377** could also inhibit cell proliferation by cell cycle arresting at G0/G1 phase (Xie *et al*., 2019).

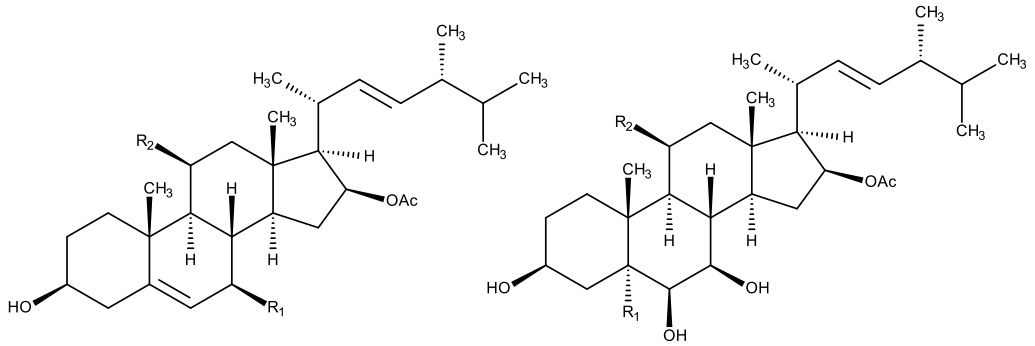

372 $R_1 = R_2 = H$
373 $R_1 = R_2 = OH$
378 $R_1 = OH, R_2 = H$

374 $R_1 = R_2 = OH$
375 $R_1 = OH, R_2 = H$
376 $R_1 = R_2 = H$
377 $R_1 = H, R_2 = OH$

Figure 43. Structures of penicisteroids D (**372**), E (**373**), F (**374**), G (**375**), H (**376**) penicisteroid A (**377**) and penicisteroid C (**378**)

2.2.11. *Penicillium janczewskii*

Two new diastereomeric quinolinone alkaloids, 3*S**,4*R**-dihydroxy-4-(4‘-methoxyphenyl)-3,4-dihydro-2(1*H*)-quinolinone (**379**) and 3*R**,4*R**-dihydroxy-4-(4‘-methoxyphenyl)-3,4-dihydro-2(1*H*)-quinolinone (**380**) were isolated together with the known analogs, peniprequinolone (**381**) and 3-methoxy-4-hydroxy-4-(4′methoxyphenyl)-3,4-dihydro-2(1*H*)-quinolinone (**382**) (Figure 44), from *P. janczewskii* strain H-TW5/869, isolated from surface water collected from North Sea. Compounds **379** and **380** showed a low to moderate general toxicity against MDA-MB 231 (human breast adenocarcinoma), DU-145 (human prostate carcinoma), HT-29 (human colon carcinoma), A549 (human non-small cell lung carcinoma), CAKI-1 (human kidney carcinoma), SK-MEL 2 (human melanoma) and K562 (human myeloid leukemia) cells, with **380** being slightly more potent. Compounds **380** showed strong cytotoxicity against SKOV-3 (He *et al*., 2005).

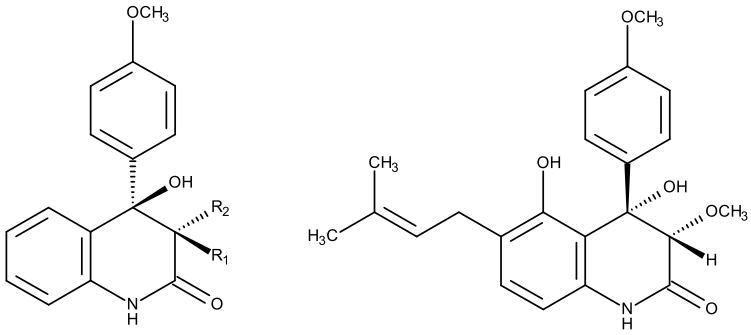

379 R_1 = H, R_2 = OH
380 R_1 = OH, R_2 = H
382 R_1 = OCH_3, R_2 = H

381

Figure 44. Structures of 3*S**,4*R**-dihydroxy-4-(4‘-methoxyphenyl)-3,4-dihydro-2(1*H*)-quinolinone (**379**), 3*R**,4*R**-dihydroxy-4-(4‘-methoxyphenyl)-3,4-dihydro-2(1*H*)-quinolinone (**380**), peniprequinolone (**381**) and 3-methoxy-4-hydroxy-4-(4′methoxyphenyl)-3,4-dihydro-2(1*H*)-quinolinone (**382**)

2.2.12. *Penicillium lividum*

Zhuravleva *et al*., (2014a) reported the isolation of nine previously unreported australide meroterpenoids, qustalide H acid (**383**), austalide P acid butyl ester (**384**), austalide P acid (**385**), austalide Q acid (**386**), 13-deoxyaustalide Q acid (**387**), 17-*O*-demethylaustalide B (**388**), 13-*O*-Deacetylaustalide I (**389**), 13-deacetoxyaustalide I (**390**) and 17*S*-dihydroaustalide K (**391**) (Figure 45), from the culture extract of the algicolous fungus *P. lividum* KMM 4663, isolated from superficial mycobiota of the brown alga *Sargassum miyabei*, collected from the Sea of Japan. Compounds **383**, **387**, **389** and **390** were assayed for their cytotoxic activity against MDA-MB-231 and JB6 Cl41 cell lines, however, of the compounds exhibited cytotoxicity (IC_{50} < 10 μM). Moreover, these compounds were also evaluated for their effect on the basal AP-1 dependent transcriptional activity was also studied using JB6 Cl41 cells stably expressing a luciferase reporter gene controlled by an AP-1-DNA binding sequence, however, only **383**, **389** and **390** are able to inhibit the transcriptional activity of the oncogenic nuclear factor AP-1 at non-cytotoxic concentrations after 12 h of treatment. Additionally, **383**-**386**, **389** and **390** were found to exhibit strong inhibitory activities

against the enzyme endo-1,3-*β*-D-glucanase from a crystalline stalk of the marine mollusk *Pseudocardium sachalinensis.*

Further investigation of the culture extract of *P. lividum* KMM 4663, by the same group, led to the isolation of previously undescribed meroterpenoids sargassopenillines B-G (**392**-**397**) (Figure 45). Compounds **392**, **393** and **397** did not exhibit *in vitro* cytotoxic activity against MDA-MB-231 and JB6 Cl41 cell lines, (IC_{50} < 100 μM). Compound **396** also exhibited cytotoxicity against splenocytes with IC_{50} value 38 μM. Moreover **394** and **396**, at a non-toxic concentration (10 μM) were found to inhibit the adhesion of macrophages (30%-40% of inhibition). Compound **393** was found to inhibit the transcriptional activity of the oncogenic nuclear factor AP-1 with IC_{50} value of 15 μM after 12 h of treatment (Zhuravleva *et al*., 2014b).

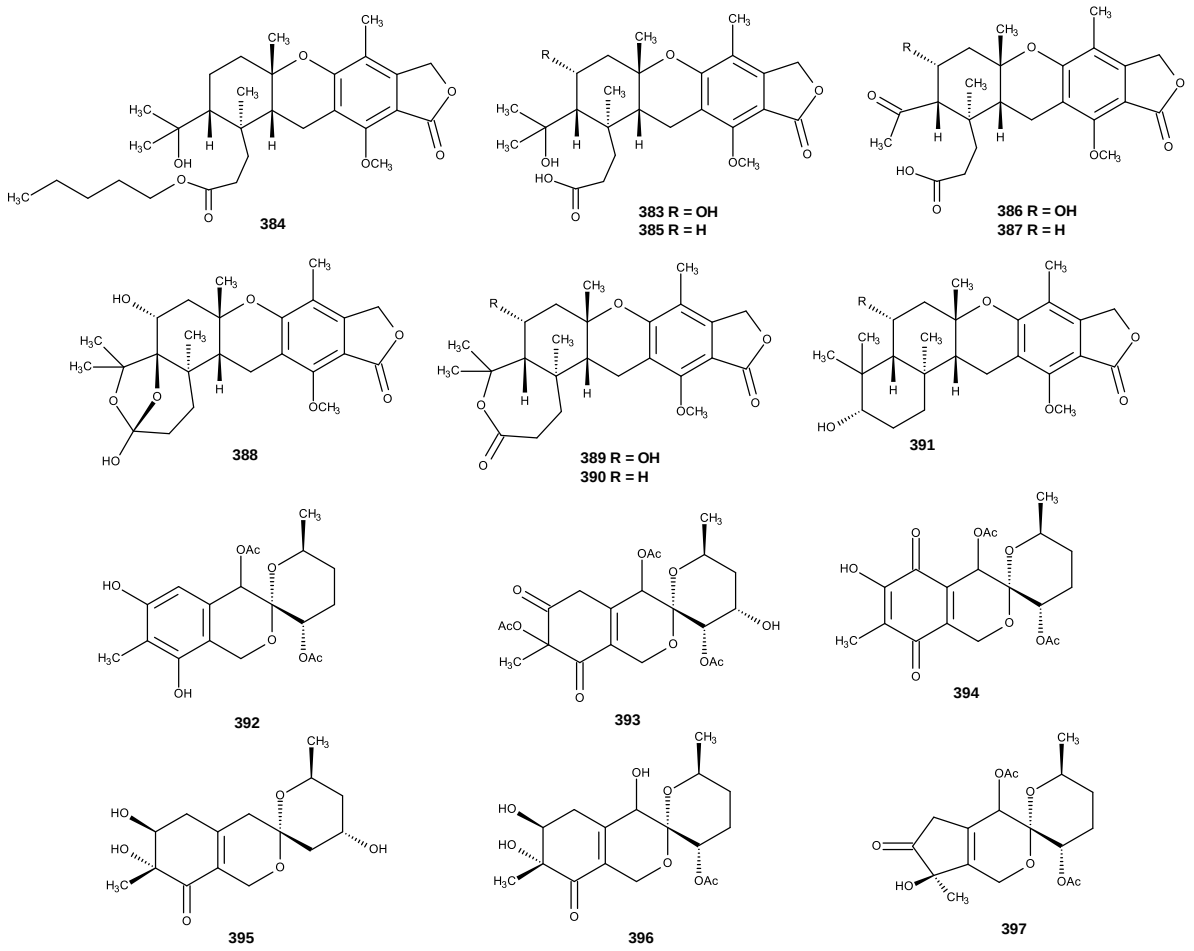

Figure 45. Structures of qustalide H acid (**383**), austalide P acid butyl ester (**384**), austalide P acid (**385**), austalide Q acid (**386**), 13-deoxyaustalide Q acid (**387**), 17-*O*-demethylaustalide B (**388**), 13-*O*-Deacetylaustalide I (**389**), 13-deacetoxyaustalide I (**390**), 17*S*-dihydroaustalide K (**391**), sargassopenillines B (**392**), C (**393**), D (**394**), E (**395**), F (**396**) and G (**397**)

2.2.13. *Penicillium notatum*

The previously reported isocoumarin derivative, dihydrocitrinone (**398**) (Figure 46) was isolated from the culture extract of *P. notatum* B-52, isolated marine sediment collected in Qinghai Lake, Qinghai, China. Compound **398** was inactive against the P388, BEL-7402, A-549 and HL-60 cell lines (Xin *et al*., 2007).

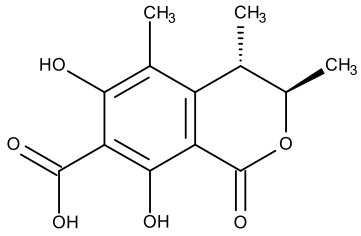

398

Figure 46. Structure of dihydrocitrinone (**398**)

2.2.14. *Penicillium oxalicum*

Shen *et al.*, (2013) isolated the previously unreported 2-(4-hydroxybenzoyl) quinazolin-4(3*H*)-one (**399**), together with the previously described 2-(4-hydroxybenzyl) quinazolin-4(3*H*)-one (**400**), rubinaphthin A (**401**), citreorosein (**402**) and methyl 4-hydroxyphenylacetate (**403**) (Figure 47) from the culture extract of the marine-derived fungus *P. oxalicum* 0312F$_1$. Compounds **400** and **403** exhibited higher inhibitory activity of the replication of TMV, with EC$_{50}$ values 100.80 mg/mL and 137.78 mg/mL, respectively, while **399** and **400** showed moderate inhibitory activity. Moreover, **399** displayed moderate inhibitory activity of the proliferation of human gastric cancer cell SGC-7901.

Bao *et al*., (2013) described the isolation of two previously undescribed polyketides, 6,8,5’,6’-tetrahydroxy-3’-methylflavone (**404**) and paecilin C (**405**) (Figure 47), together with six previously reported metabolites including emodin (**94**) (Figure 16), citreorosein (**402**), secalonic acid D (**406**), secalonic acid B (**407**), penicillixanthone A (**408**) and isorhodoptilometrin (**409**) (Figure 47) from a culture broth of a gorgonian coral-associated fungus *Penicillium* sp. SCSGAF 0023 (*P. oxalicum*), isolated from gorgonian coral *Dichotella gemmacea* which was collected from the South China Sea, Sanya, Hainan, China. Compounds **94, 402, 404** and **409** showed significant antifouling activity against *Balanus amphitrite* larvae settlement with EC$_{50}$ values of 6.7, 6.1, 17.9 and 13.7 µg/mL, respectively. Compound **406-408** showed moderate antibacterial activity against four tested bacterial strains, i. e. *B. subtilis*, *E. coli* JVC1228, *M. luteus* UST950701006, *P. nigrifaciens* UST010620-005.

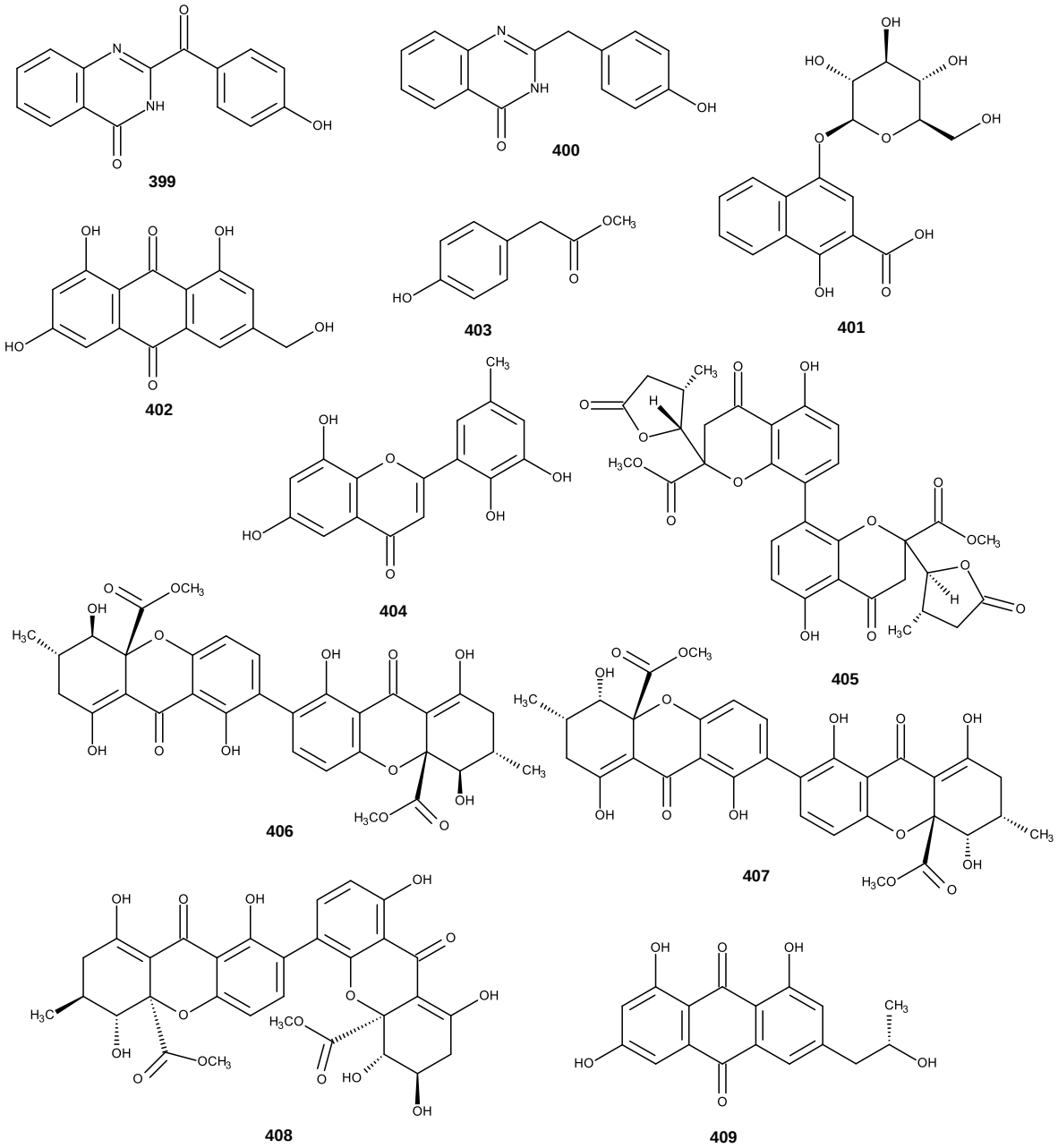

Figure 47. Structures of 2-(4-hydroxybenzoyl) quinazolin-4(3*H*)-one (**399**), 2-(4-hydroxybenzyl) quinazolin-4(3*H*)-one (**400**), rubinaphthin A (**401**), citreorosein (**402**), methyl 4-hydroxyphenylacetate (**403**), 6,8,5',6'-tetrahydroxy-3'-methylflavone (**404**), paecilin C (**405**), secalonic acid D (**406**), secalonic acid B (**407**), penicillixanthone A (**408**) and isorhodoptilometrin (**409**)

Sun *et al*., (2013) has isolated two previously unreported dihydrothiophene-condensed chromones, oxalicumones A (**410**) and B (**411**) and a new natural product oxalicumones C (**412**) (Figure 48) from the culture extract of *P. oxalicum* SCSGAF 0023, which was isolated from the gorgonian *Muricella flexuosa* which was collected from the South China Sea. Compound **410** exhibited cytotoxicity against A 375 and SW-620 cell lines with IC_{50} of 11.7 and 22.6 µM, respectively.

A larger scale fermentation of *P. oxalicum* SCSGAF 0023, by the same research group, led to the isolation of two new analogues dihydrothiophene-condensed chromones, oxalicumones D and E (**413** and **414**), together with the previously reported oxalicumones A-C (**410-412**), coniochaetones A and B (**415** and **416**), *α*-diversonolic ester (**417**) and *β*-diversonolic ester (**418**) (Figure 48). All the isolated compounds were tested for their cytotoxicity against eight human tumor cell lines, H1975, U937, K562, BGC823, MOLT-4, MCF-7, HL60 and Huh-7 cell lines, by MTT method. Compounds **414** and **410** showed significant cytotoxicity against the eight tested cell lines with $IC_{50} \leq 50$ µM while **411** exhibited strong activity against U937, MOLT-4 and HL60, with $IC_{50} \leq 10$ µM (Bao *et al*., 2014).

Mangrove-derived endophytic fungus *P. oxalicum* EN-201, isolated from fresh leaves of the marine mangrove plant *Rhizophora stylosa* which collected from Hainan Island, China, produced two new alkaloids, penioxamide A (**419**) and 18-hydroxydecaturin B (**420**) (Figure 48). Compounds **419** and **420** showed brine shrimp (*Artemia salina*) lethality, with LD_{50} values of 5.6 and 2.3 µM, respectively (Zhang *et al*., 2015).

Li *et al*., (2015) reported the isolation of a new phenolic enamide, methyl (*Z*)-3-(3,4-dihydroxyphenyl)-2-formamidoacrylate (**421**) and a new meroterpenoid, 15-hydroxydecaturin A (**422**), together with WF-5239 (**423**) and seven other meroterpenoids including decaturin A (**424**), decaturin B (**425**), decaturin D (**426**), decaturin E (**427**), decaturin F (**428**), oxalicine A (**429**) and oxalicine B (**430**) (Figure 48) from the fermentation broth of marine alga-derived endophytic fungus *P. oxalicum* EN-290 which was isolated from the green alga *Codium fragile*, collected from Qingdao Coastline, China. All the isolated compounds were tested for antimicrobial activities against two pathogenic microbes: *S. aureus* and *V. parahaemolyticus*, and

anti-HAB activity against HAB causative species *Nitzschia closterium*. However, only **421** displayed activities against *S. aureus* and *V. parahaemolyticus*, with MIC values of 2.0 and 16.0 µg/mL, respectively as well as strong activities against HAB causative species *Nitzschia closterium* with inhibition zones of 20, 16, and 10 mm at concentrations of 20, 10 and 5 mg/mL, respectively.

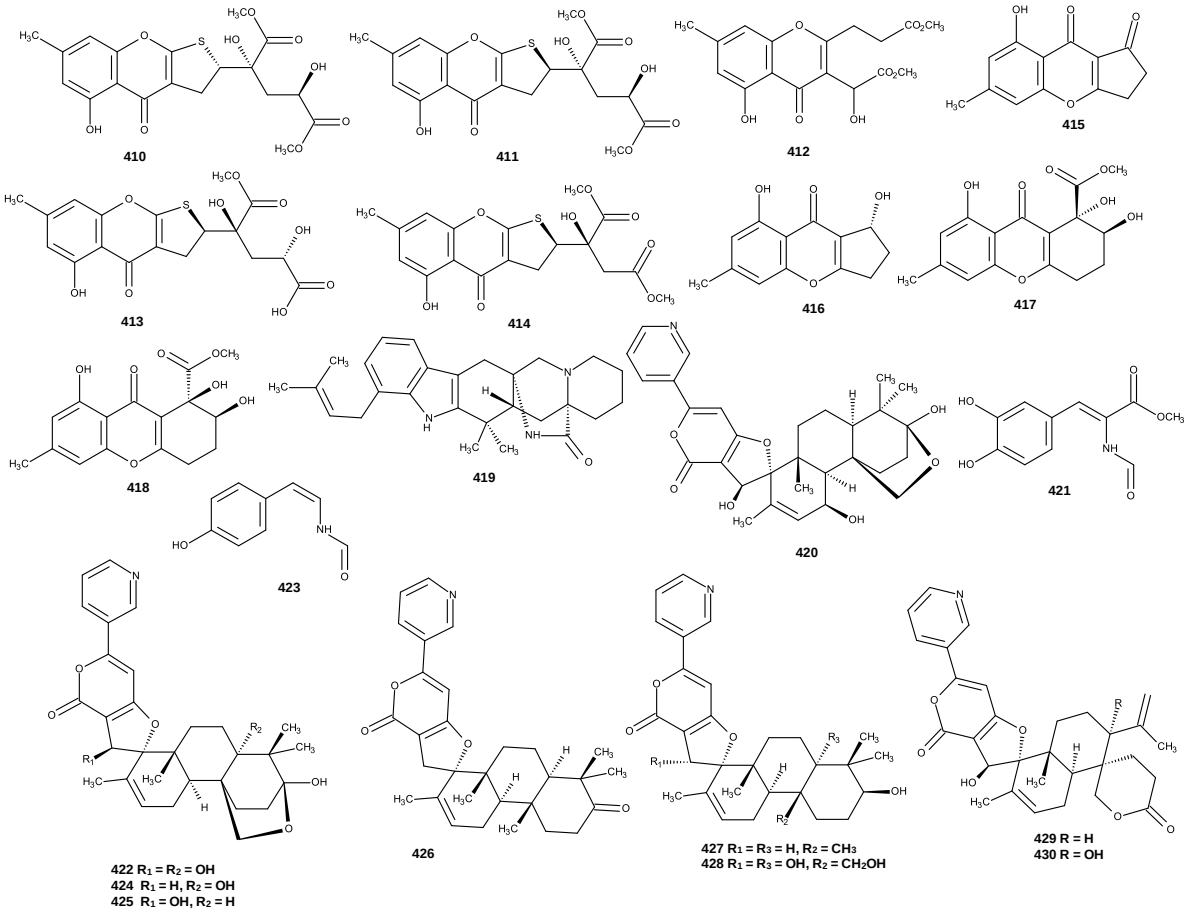

Figure 48. Structures of oxalicumones A (**410**), B (**411**), oxalicumones C (**412**), oxalicumones D (**413**), E (**414**), coniochaetones A (**415**), B (**416**), *α*-diversonolic ester (**417**), *β*-diversonolic ester (**418**), penioxamide A (**419**),18-hydroxydecaturin B (**420**), methyl (*Z*)-3-(3,4-dihydroxyphenyl)-2-formamidoacrylate (**421**), 15-hydroxydecaturin A (**422**), WF-5239 (**423**), decaturin A (**424**), decaturin B (**425**), decaturin D (**426**), decaturin E (**427**), decaturin F (**428**), oxalicine A (**429**) and oxalicine B (**430**)

2.2.15. *Penicillium paneum*

Li *et al.*, (2011) reported the isolation of a previously unreported triazole carboxylic acid, penipanoid A (**431**), two new quinazolinone alkaloids, penipanoids B (**432**) and C (**433**), as well as the previously reported quinazolinone derivative, 2-(4-hydroxybenzyl)quinazolin-4(3*H*)-one (**434**) from the extract of the solid- cultured *P. paneum* SD-44, which was isolated from marine sediment, collected from South China Sea (Figure 49). Compound **431** exhibited activity against the SMMC-7721 cell line with an IC_{50} value of 54.2 μM, while **434** displayed significant cytotoxic activity against the A-549 and BEL-7402 cell lines with IC_{50} values of 17.5 and 19.8 μM, respectively. Compounds **431-434** were tested for the antimicrobial activity against two bacteria (*S. aureus* and *E. coli*) and five plant-pathogenic fungi (*Alternaria brassicae*, *Fusarium oxysporium* f. sp. *vasinfectum*, *Coniella diplodiella*, *Physalospora piricola*, and *Aspergillus niger*) but none displayed significant activity.

Later on, the same research group has reexamined the culture extract of the same fungus and isolated three imperviously described anthranilic acid derivatives, penipacids A-E (**435-439**) and the known synthetic analog, LH^2 (**440**) (Figure 49). Compounds **435-440** were evaluated for the cytotoxicity against Hela and RKO cell lines; however, only **435** and **439** exhibited inhibitory activity against RKO cell line with an IC_{50} value of 8.4 and 9.7 μM, respectively, while **440** displayed cytotoxic activity against Hela cell line with the IC_{50} value of 6.6 μM. All the isolated compounds were also assayed for their antimicrobial activity against two bacteria (*S. aureus* and *E. coli*) and three plant-pathogenic fungi (*Alternaria brassicae*, *Fusarium graminearum*, and *Rhizoctonia cerealis*) but none exhibited significant activity (Li *et al*., 2013).

The same fungus was also examined by the same research group. The extract of the liquid culture of this fungus furnished three new prenylated indole alkaloids, including two *β*-carbolines, penipalines A (**441**) and B (**442**) and an indole carbaldehyde derivative, penipaline C (**443**), along with two previously described analogs, (-)-(3*S*)-2,3,4,9-tetrahydro-1,1dimethyl-1*H*-*β*-carboline-3-carboxylic acid (**444**) and 1,7-dihydro-7,7-dimethylpyrano[2,3-g]indole-3-carbaldehyde (**445**) (Figure 49). Compounds **441-443** were tested for their cytotoxic activity against A-549 and

HCT-116 cell lines, however, only **442-443** displayed cytotoxicity against A-549 cell line, with IC_{50} of 20.44 and 21.54 µM, respectively (Li *et al*., 2014).

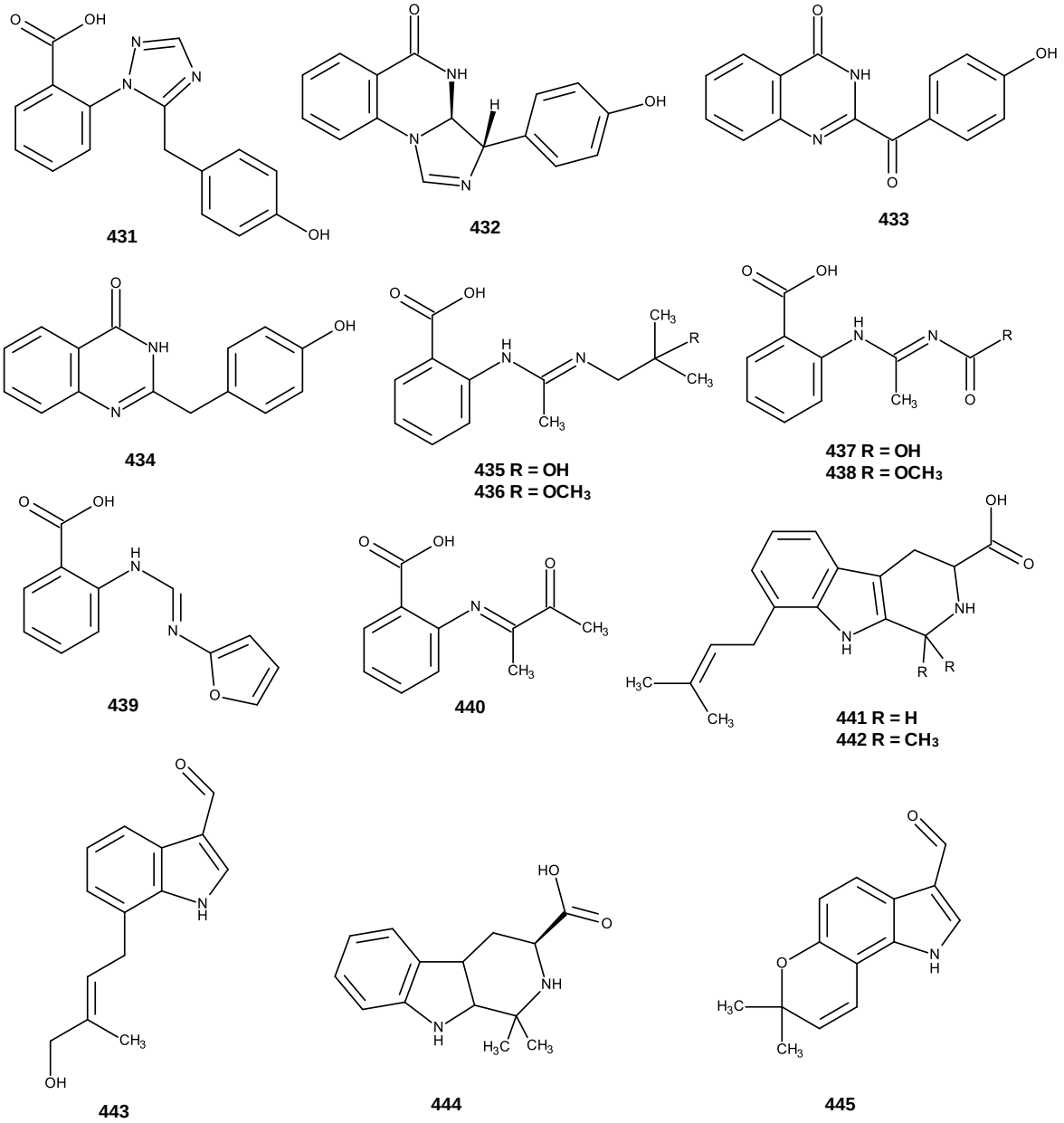

Figure 49. Structures of penipanoids A (**431**), B (**432**), C (**433**), 2-(4-hydroxybenzyl)quinazolin-4(3*H*)-one (**434**), penipacids A (**435**), B (**436**), C (**437**), D (**438**), E (**439**), LH^2 (**440**), penipalines A (**441**), B (**442**), penipaline C (**443**), (-)-(3*S*)-2,3,4,9-tetrahydro-1,1dimethyl-1*H*-*β*-carboline-3-carboxylic acid (**444**) and 1,7-dihydro-7,7-dimethylpyrano[2,3-g]indole-3-carbaldehyde (**445**)

2.2.16. *Penicillium pinophilum*

A previously unreported diketopiperazine derivative, pinodiketopiperazine A (**446**) and a new phthalide derivative, 6,7-dihydroxy-3-methoxy-3-methylphthalide (**447**) were isolated together with the previously reported alternariol 2,4-dimethyl ether (**448**), L-5-oxoproline methyl ester (**449**), *N*-methylphenyldehydroalanyl-L-prolin-anhydrid (**450**), cyclo-trans-4-OH-(D)-Pro-(D)-Phe (**451**), cyclo(D)-Pro-(D)-Val (**452**), rubralide C (**453**), 5′-epialtenuene (**454**) and altenuene (**455**) (Figure 50) from the culture of *P. pinophilum* SD-272, isolated from sediment samples, which was collected from the Pearl River in South China Sea. Compound **447** displayed potent brine shrimp (*Artemia salina*) lethality with LD_{50} 11.2 μM. Compounds **446**, **448**, **450-453** at 20 μg/disk, exhibited antibacterial activity against *E. coli* with inhibition zones of 10.0, 9.0, 8.0, 8.0, 7.0 and 10.0 mm (the inhibition zone of the positive control chloromycetin is 15.0 mm) (Wang *et al*., 2013).

Three previously undescrbed azaphilone derivatives, pinophilins D-F(**456-458**), and a new diphenyl ether derivative, hydroxypenicillide (**459**), were isolated together with six previously reported metabolites, including azaphilone derivatives, Sch 1385568 (**460**), pinophilin B (**461**), Sch 725680 (**462**), (−)-mitorubrin (**463**), (−)-mitorubrinol (**464**) and (−)-mitorubrinic acid (**465**) (Figure 50) and three diphenyl ether derivatives, penicillide (**145**) (Figure 19), purpactin A (**146**) (Figure 19) and isopenicillide (**466**) (Figure 50), from the culture extract of *P. pinophilum* strain XS20090E18 which was isolated from the inner part of an unidentified Gorgonian (XS-200909), collected from the coral reef in the South China Sea. Compounds **145**, **146**, **459** and **466** exhibited inhibitory activity against the larval settlement of the barnacle *Balanus amphitrite* with EC_{50} values of 6.0, 2.6, 20, and 10 μg/mL (LC_{50}/EC_{50} > 50), respectively. Moreover, **459** exhibited cytotoxic activity against the human cervical carcinoma (HeLa) cell line with an IC_{50} value of 6.1 μM, while **145** displayed cytotoxicity against the human laryngeal carcinoma (Hep-2) cells and human rhabdomyosarcoma (RD) cells with IC_{50} values of 6.7 and 7.8 μM, respectively (Zhao *et al*., 2015).

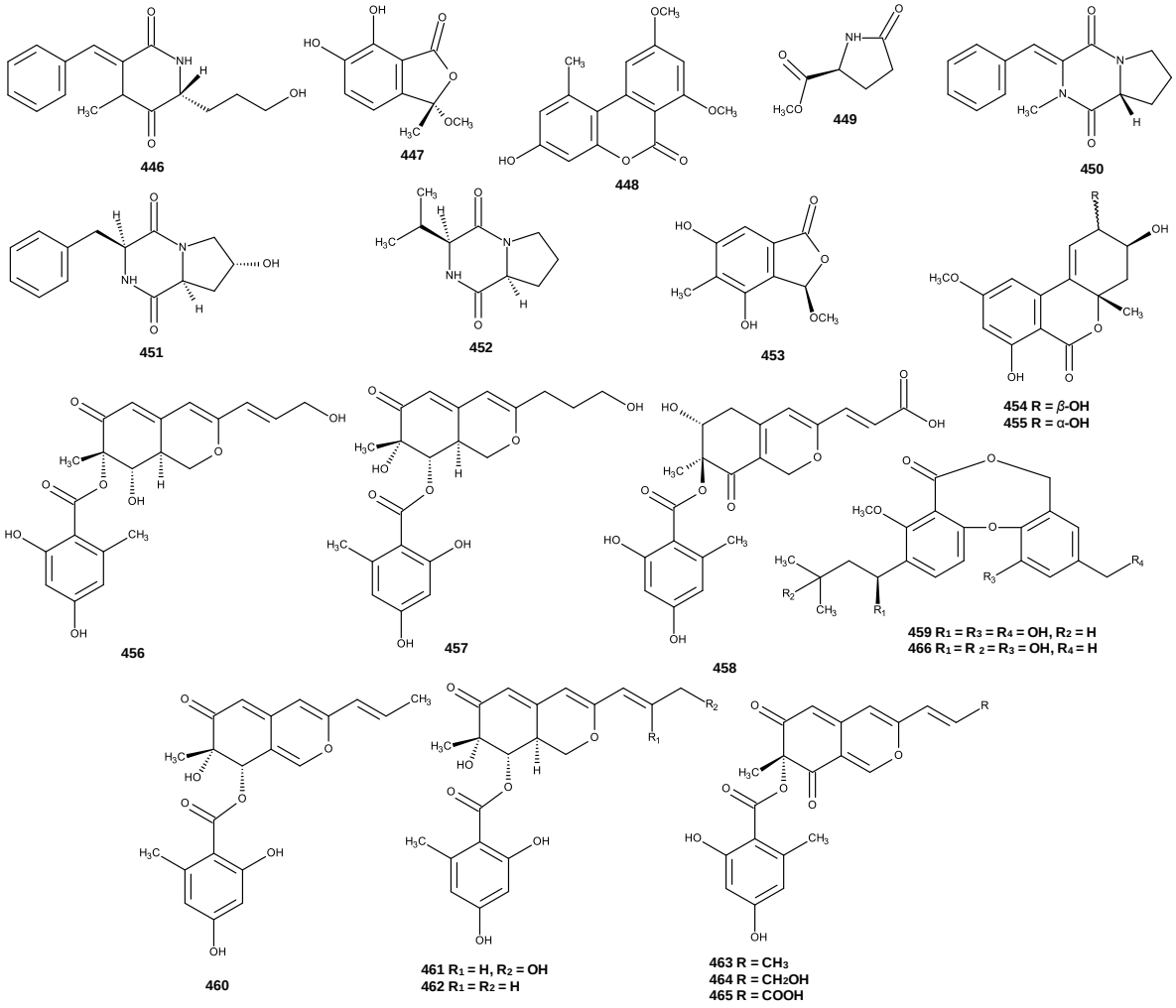

Figure 50. Structures of pinodiketopiperazine A (**446**), 6,7-dihydroxy-3-methoxy-3-methylphthalide (**447**), alternariol 2,4-dimethyl ether (**448**), L-5-oxoproline methyl ester (**449**), *N*-methylphenyldehydroalanyl-L-prolin-anhydrid (**450**), cyclo-trans-4-OH-(D)-Pro-(D)-Phe (**451**), cyclo(D)-Pro-(D)-Val (**452**), rubralide C (**453**), 5′-epialtenuene (**454**), altenuene (**455**), pinophilins D (**456**), E (**457**), F (**458**), hydroxypenicillide (**459**), Sch 1385568 (**460**), pinophilin B (**461**), Sch 725680 (**462**), (−)-mitorubrin (**463**), (−)-mitorubrinol (**464**), (−)-mitorubrinic acid (**465**) and isopenicillide (**466**)

2.2.17. *Penicillium purpurogenum*

Six previously unreported metabolites including, purpurquinones A-C (**467-469**), purpuresters A (**470**) and B (**471**) and 2,6,7-trihydroxy-3-methylnaphthalene-1,4-dione (**472**), were isolated together with the previously reported TAN-931 (**473**) (Figure 51), (-)-mitorubrin (**463**) (Figure 50) and orsellinic acid, from the extract of the culture (at pH 2) of an acid-tolerant fungus, *P. purpurogenum* strain JS03-21, which was isolated from the local red soil collected from Yunnan, China. Using the CPE inhibition assay, **468**, **469**, **470** and **473** exhibited stronger anti-H1N1 activity than ribavirin (positive control) with IC_{50} values of 61.3, 64.0, 85.3, 58.6, and 100.8 μM, respectively (Wang *et al*., 2011).

Chai *et al.*, (2013) described isolation of janthinone (**474**), fructigenine A (**475**), aspterric acid methyl ester (**476**) and citrinin (**477**) (Figure 51), from the 5-1-4 mutant of the marine-derived fungus *P. purpurogenum* strain G59, by treating the spores of the wild type G59 with high concentration of gentamycin in aqueous DMSO. Compounds **474-477** inhibited the proliferation of K562 cells with inhibition rates of 34.6% (**474**), 60.8% (**475**), 31.7% (**476**) and 67.1% (**477**) at 100 μg/mL, respectively (Chai *et al*., 2012).

Simultaneously, Fang *et al.*, (2012) described isolation of three merosesquiterpenes, including the previously unreported purpurogemutantin (**478**) and purpurogemutantidin (**479**) and the previously reported macrophorin A (**480**) (Figure 51), from the mutant BD-1-6 obtained by random diethyl sulfate (DES) mutagenesis of a marine-derived *P. purpurogenum* G59. Compounds **478** and **479** inhibited the growth of K562, HL-60, HeLa, BGC-823 and MCF-7 cell lines, with the inhibition rates (IR%) ranging from 62.8%-88.0% at 100 μg/mL. Compound **480** inhibited the growth of K562 and HL-60 cell lines with IC_{50} values of 1.48 and 0.85 μM, respectively.

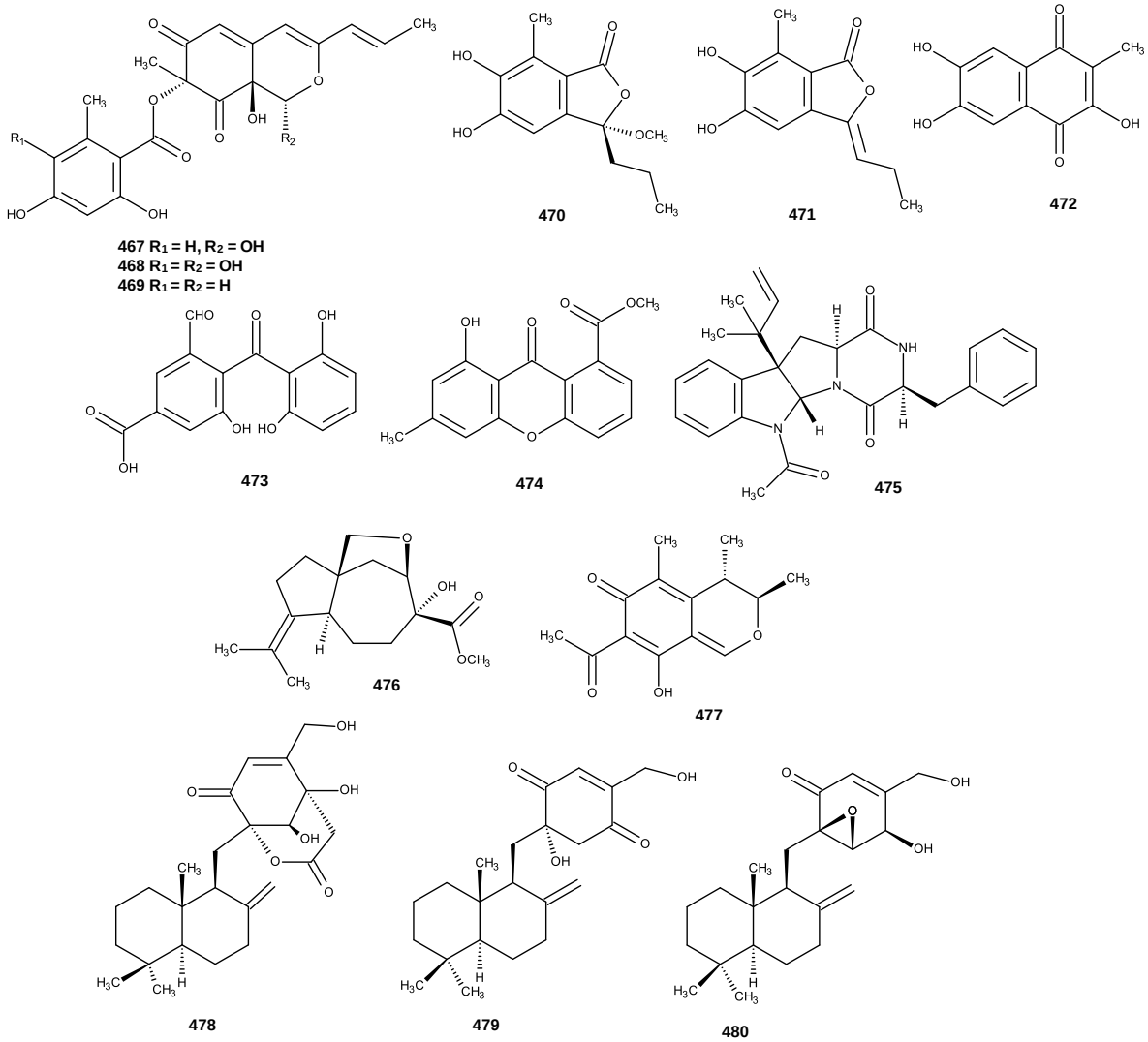

Figure 51. Structures of purpurquinones A (**467**), B (**468**), C (**469**), purpuresters A (**470**), B (**471**), 2,6,7-trihydroxy-3-methylnaphthalene-1,4-dione (**472**), TAN-931 (**473**), janthinone (**474**), fructigenine A (**475**), aspterric acid methyl ester (**476**), citrinin (**477**), purpurogemutantin (**478**), purpurogemutantidin (**479**) and macrophorin A (**480**)

Wu *et al*., (2014) obtained the mutant AD-2-1 of the marine-derived *P. purpurogenum* strain G59 by using diethyl sulfate mutagenesis. The culture extract of the mutant AD-2-1 produced besides nine lipopeptides, including seven previously unreported penicimutalides A-G (**481-487**) and two previously reported fellutamides B

(**488**) and C (**489**), the previously described polyketides 1′-*O*-methylaverantin (**490**), averantin (**491**), averufin (**492**), nidurufin (**493**) and sterigmatocystin (**494**) (Figure 52).

Later on, the same group (Wu *et al.*, 2015) has described isolation of curvularin (**495**), penicitrinone A (**496**), erythro-23-*O*-methylneocyclocitrinol (**497**), 22*E*-7α-methoxy-5α, 6α-epoxyergosta-8(14),22-dien-3*β*-ol (**498**) (Figure 52) and citrinin (**477**) (Figure 51), from the a mutant 4-30, obtained by treatment of the spores of *P. purpurogenum* strain G59 with neomycin. The authors have found that these compounds were newly synthesized by this mutant and not found in the extract of the wild-type.

Xia *et al.*, (2015) have also isolated three new chromones, epiremisporine B (**499**), epiremisporine B1 (**500**) and isoconiochaetone C (**501**), together with the previously described remisporine B (**502**), and methyl 8-hydroxy-6-methyl-9-oxo-9*H*-xanthene-1-carboxylate (**503**) (Figure 52), coniochaetone A (**415**) (Figure 48), from the mutant AD-1-2 obtained from the DES mutagenesis of a marine-derived fungus, *P. purpurogenum* G59. Compounds **415**, **499-503** were assayed (by MTT method) for their inhibitory effects on four human cancer cell lines, i. e. K562, HL-60, HeLa and BGC-823. Compounds **415**, **499-503** showed growth inhibition of the tested cancer cell lines at variable inhibition rates (IR%) at 100 µg/mL. Compound **502** showed IC_{50} values of 144.3 µM for K562 and 130.7 µM for HL-60. **499** showed IC_{50} values of 119.8 µM for K562 and 109.2 µM for HL-60; **500** showed IC_{50} values of 90.0 µM for K562 and 92.7 µM for HL-60.

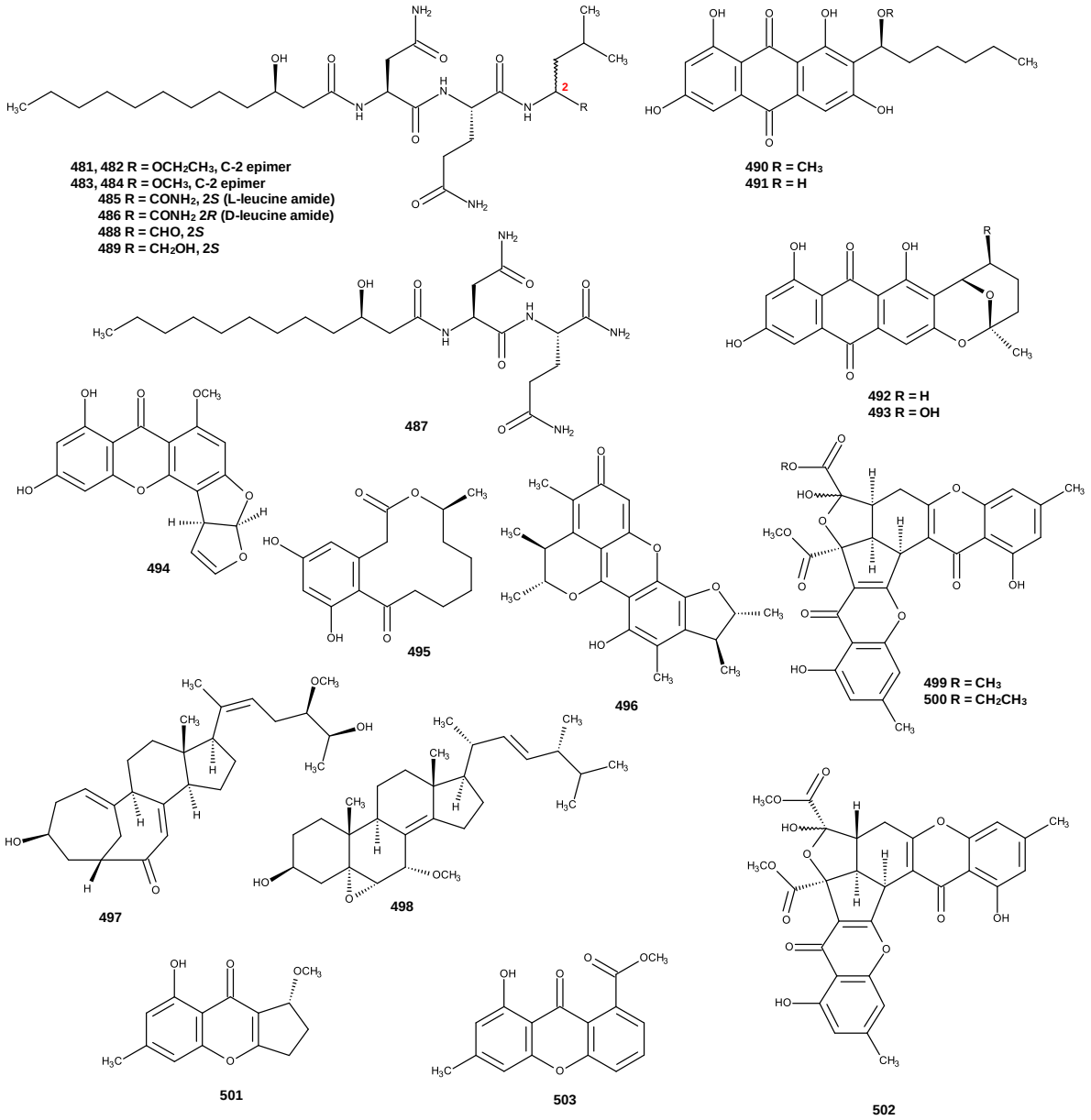

Figure 52. Structures of penicimutalides A (**481**), B (**482**), C (**483**), D (**484**), E (**485**), F (**486**), G (**487**), fellutamides B (**488**), C (**489**), 1′-*O*-methylaverantin (**490**), averantin (**491**), averufin (**492**), nidurufin (**493**), sterigmatocystin (**494**), curvularin (**495**), penicitrinone A (**496**), erythro-23-*O*-methylneocyclocitrinol (**497**), 22*E*-7α-methoxy-5α, 6α-epoxyergosta-8(14),22-dien-3*β*-ol (**498**), epiremisporine B (**499**), epiremisporine B1 (**500**), isoconiochaetone C (**501**), remisporine B (**502**), and methyl 8-hydroxy-6-methyl-9-oxo-9*H*-xanthene-1-carboxylate (**503**)

2.2.18. *Penicillium raistrickii*

Ma *et al*., (2016) reported isolation of five new pyran rings containing polyketides, penicipyrans A-E (**504**-**508**) (Figure 53), from the culture extract of the saline soil-derived *P. raistrickii*, which was isolated from the saline soil, collected from the coast of Bohai Bay in Zhanhua, Shandong Province of China. Compound **508** presented cytotoxicity against K562 and HL-60 cell lines with IC_{50} values of 8.5 and 4.4 µM, respectively.

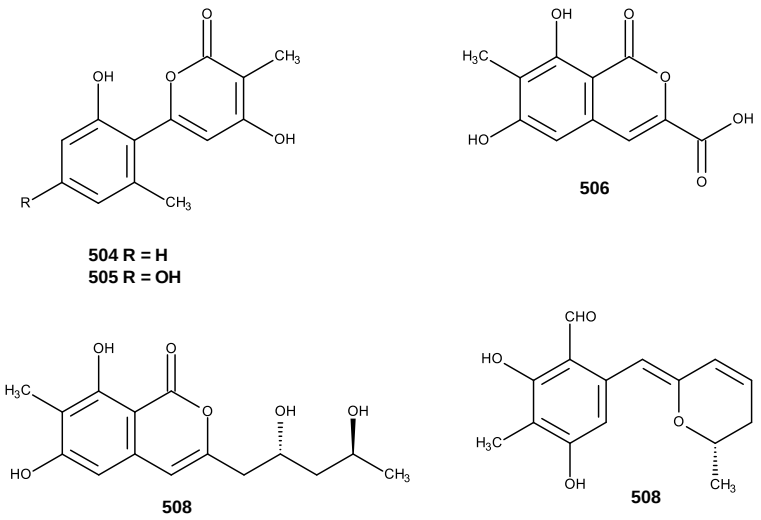

Figure 53. Structures of penicipyrans A (**504**), B (**505**), C (**506**), D (**507**) and E (**508**)

2.2.19. *Penicillium sacculum*

A new polyketide, penicillolide (**509**) (Figure 54) was isolated from the EtOAc extract of the fermentation broth of *P. sacculum* GT-308, which was collected from the halophyte *Atriplex* sp. in the mesolittoral zone of Dongying City, Shandong Province, China (Liu *et al*., 2016).

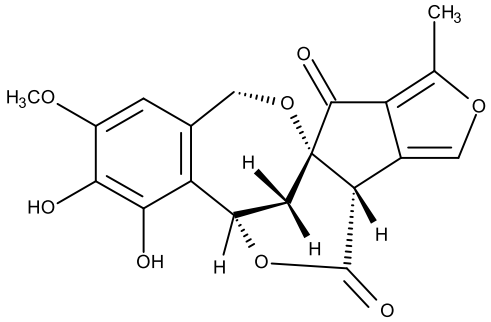

509

Figure 54. Structure of penicillolide (**509**)

2.2.20. *Penicillium sclerotiorum*

Jia *et al*., (2019) reported the isolation of four new azaphilones, sclerotiorins A-D (**510-513**), together with the previously reported metabolites, including sclerotiorin E (**514**), geumsanol G (**515**), (+) sclerotiorin (**516**), isochromophilones I (**517**), IV (**518**), VI (**519**), VIII (**520**), and IX (**521**), TL-1-monoactate (**522**), ochrephilone (**523**), 8-acetyldechloroisochromophilone III (**524**) and scleratioramine (**525**) (Figure 55), from the fermentation broth of the marine-sponge associated fungus *P. sclerotiorum* OUCMDZ-3839, which was isolated from a marine sponge *Paratetilla* sp. Compounds **510-525** were examined for the anti-H1N1-virus activity in the MDCK cell line by the CPE (cytopathic effect) + MTT method; however, compounds **514, 516, 521-525** showed stronger inhibitory activity on H1N1 than the ribavirin (positive control), with IC_{50} values ranging from 78.6 to 156.8 µM. Moreover, compounds **517** and **525** displayed significant inhibitory activity against α-glycosidase, with IC_{50} values of 17.3 and 166.1 µM, respectively.

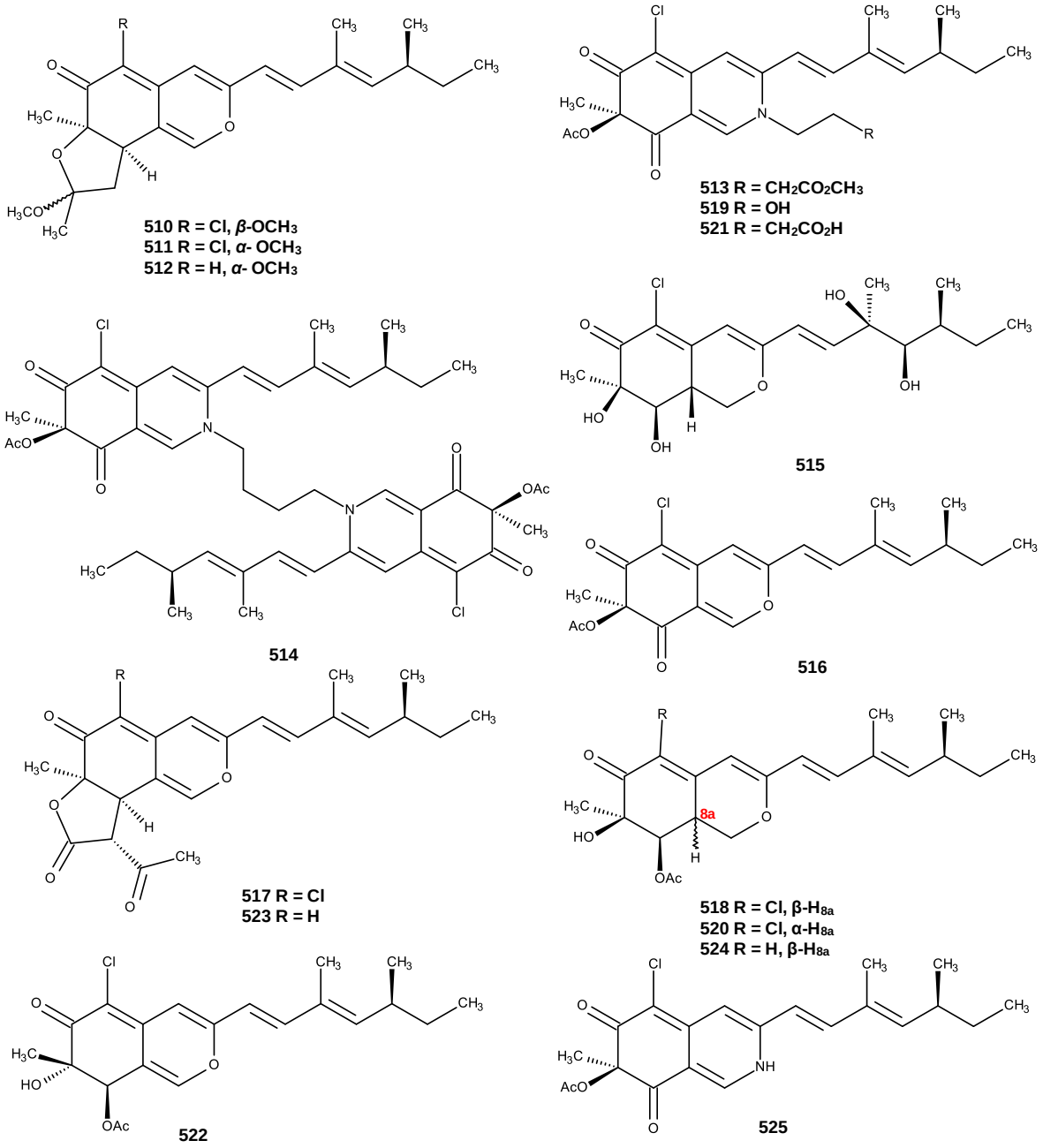

Figure 55. Structures of sclerotiorins A (**510**), B (**511**), C (**512**), D (**513**), sclerotiorin E (**514**), geumsanol G (**515**), (+) sclerotiorin (**516**), isochromophilones I (**517**), IV (**518**), VI (**519**), VIII (**520**), IX (**521**), TL-1-monoactate (**522**), ochrephilone (**523**), 8-acetyldechloroisochromophilone III (**524**) and sclerationamine (**525**)

2.2.21. *Penicillium steckii*

A previously unreported polyketide, tanzawaic acid Q (**526**), (Figure 56) was isolated, together with four previously reported, tanzawaic acids A (**527**), C (**528**), D (**529**) and K (**530**) from the culture filtrates of the fungus *P. steckii* strain 108YD142, which was isolated from an unidentified marine sponge sample collected at Wangdolcho, East Sea, Korea. Compound **526** showed inhibition of the lipopolysaccharide (LPS)-induced inducible nitric oxide synthase (iNOS) and cyclooxygenase-2 (COX-2) proteins and mRNA expressions in RAW 264.7 macrophages. Moreover, **526** was also able to reduce mRNA levels of inflammatory cytokines (Shin *et al*., 2016).

Later on, Yu *et al.*, (2016) reported the isolation of additional previously unreported tanzawaic acid derivative, named tanzawaic acids R-X (**531-537**), together the previously described tanzawaic acids A (**527**) , B (**538**), C (**528**), D (**529**), E (**539**), M (**540**) and arohynapene B (**541**) (Figure 56), from the culture extract of an endophytic fungus *P. steckii* HDN13-279, which was isolated from the leaf of a mangrove plant *Sonneratia caseolaris*, collected from mangrove conservation area of Hainan, China. Compounds **532**, **533**, **536**, **539** and **541** significantly decreased the oleic acid (OA)-elicited lipid accumulation in HepG2 liver cells at the concentration of 10 µM. All the isolated compounds were tested for their cytotoxicity activity against HL-60, HCT-116, K562, Hela and A549 cell lines, but none was active cytotoxic effect at the concentration of 30 µM (Yu *et al*., 2018).

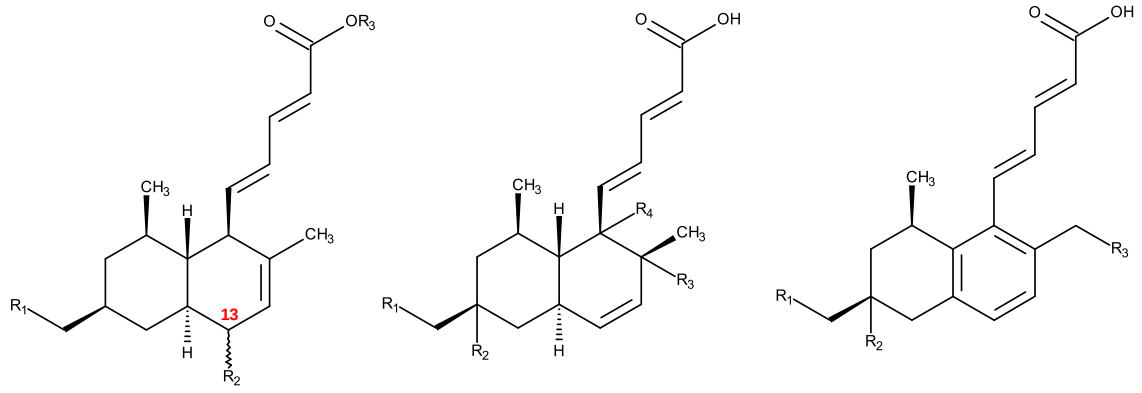

526 $R_1 = R_3 = H$, $R_2 = OH$; 13*S*
531 $R_1 = R_2 = OH$, $R_3 = H$; 13*S*
532 $R_1 = OH$, $R_2 = OCH_3$, $R_3 = H$; 13*S*
533 $R_1 = R_3 = H$, $R_2 = OCH_3$; 13*R*
534 $R_1 = R_3 = H$, $R_2 = OCH_3$; 13*S*

528 $R_1 = R_2 = R_3 = H$, $R_4 = OH$
530 $R_1 = R_2 = R_4 = H$, $R_3 = OH$
535 $R_1 = R_3 = H$, $R_2 = R_4 = OH$
536 $R_1 = R_2 = H$, $R_3 = R_4 = OH$
538 $R_1 = R_2 = R_3 = R_4 = H$
539 $R_1 = R_3 = R_4 = H$, $R_2 = OH$
540 $R_1 = OH$, $R_2 = R_3 = R_4 = H$

527 $R_1 = R_2 = R_3 = H$
529 $R_1 = R_3 = H$, $R_2 = OH$
537 $R_1 = OH$, $R_2 = R_3 = H$
541 $R_1 = R_2 = H$, $R_3 = OH$

Figure 56. Structures of tanzawaic acid Q (**526**), tanzawaic acids A (**527**), C (**528**), D (**529**), K (**530**), tanzawaic acids R (**531**), S (**532**), T (**533**), U (**534**), V (**535**), W (**536**), X (**537**), tanzawaic acids B (**538**), E (**539**), M (**540**) and arohynapene B (**541**)

2.2.22. *Penicillium stoloniferum*

Two new isocoumarin derivatives, stoloniferol A (**542**) (Figure 57) and stoloniferol B (**323**) (Figure 39) and the previously reported 5*α*, 8*α*-epidioxy-23-methyl-(22*E*, 24*R*)-ergosta-6, 22-dien-3*β*-ol (**543**) (Figure 57), were isolated from the ethyl acetate extract of the culture of a sea squirt-derived fungus, *P. stoloniferum* QY2-10, which was collected at Jiaozhou Bay, Qingdao, China. Compounds **323, 542-543** were evaluated against P388, BEL-7402, A-549 and HL-60 cell lines, however only (**543**) showed selective cytotoxic activity against the P388 cell line, with an IC_{50} value of 4.07 µM, while **323** and **542** were inactive (IC_{50} > 100 µM) (Xin *et al*., 2007).

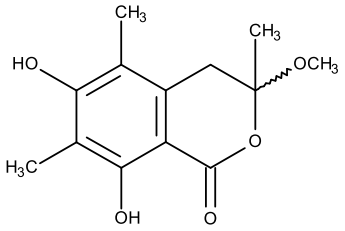

542

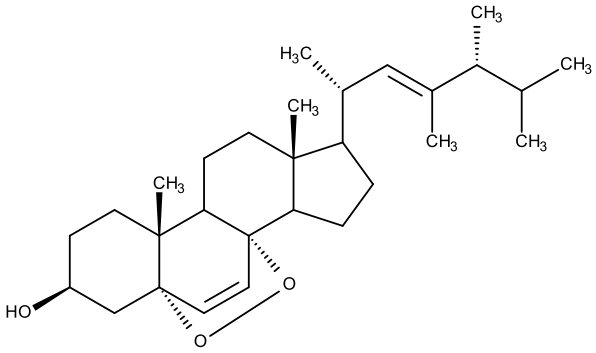

543

Figure 57. Structures of stoloniferol A (**542**) and 5*α*, 8*α*-epidioxy-23-methyl-(22*E*, 24*R*)-ergosta-6, 22-dien-3*β*-ol (**543**)

2.2.23. *Penicillium terrestre*

Liu *et al.*, (2005a) described the isolation four previously undescribed metabolites 2-(2', 3'-dihydrosorbyl)-3,6-dimethyl-5-hydroxy-1,4-benzoquinone (**544**), 3-acetonyl-2,6-dimethyl-5-hydroxy-1,4- benzoquinone (**545**), dihydrobisvertinolone (**546**), tetrahydrobisvertinolone (**547**) (Figure 58) from the culture extract of a marine-derived fungus *P. terrestre*, isolated from marine sediments, collected in Jiaozhou Bay in China. Compounds **546** and **547** exhibited *in vitro* cytotoxicity against P388 and A-449 cell lines. Simultaneously, the same group (Liu *et al*., 2005b) also isolated two previously unreported polyketide, polyketides, penicillones A (**548**) and B (**549**) (Figure 58), from the culture extract of the same fungus. Compound **548** exhibited weak cytotoxicity against P388 and A-449 cell lines. While **549** was inactive against P388.

Further study by the same research group on *P. terrestre* led to the isolation of two previously unreported bisorbicillinoids dihydrotrichodimerol (**550**) and tetrahydrotrichodimerol (**551**), and the previously reported trichodimerol (**552**) (Figure 58) (Liu *et al*., 2005c).

Later on, Chen *et al*., (2008) isolated new metabolites, terrestrols A-H (**553-560**), and a monomer (**561**), were isolated together with previously reported analogues **562, 563, 564** and **565** (Figure 58) from the culture extract of the same fungus. All of isolated compounds were evaluated for their cytotoxic activity against HL-60, MOLT-

4, BEL-7402 and A-549 cell lines, protein tyrosine kinases (Src, KDR) and DPPH, the results showed that compounds (**553-561**) displayed cytotoxic effects on HL-60, MOLT-4, BEL-7402 and A-549 cell lines with IC_{50} values in the ranging 5-65 µM (Chen *et al*., 2008).

In continuation of this work, Li *et al*., (2011) described isolation of two new chlorinated sorbicillinoids, chloctanspirones A (**566**) and B (**567**), together with terrestrols K (**568**) and L (**569**) (Figure 58) from the culture extract of the same fungus. All the isolated compounds were assayed for their cytotoxicity against HL-60 and A-549 human cancer cell lines. However, **566** was active against both cell lines with IC_{50} value of 9.2 and 39.7 µM, respectively, while **567** was less active against HL-60 with IC_{50} value of 37.8 µM.

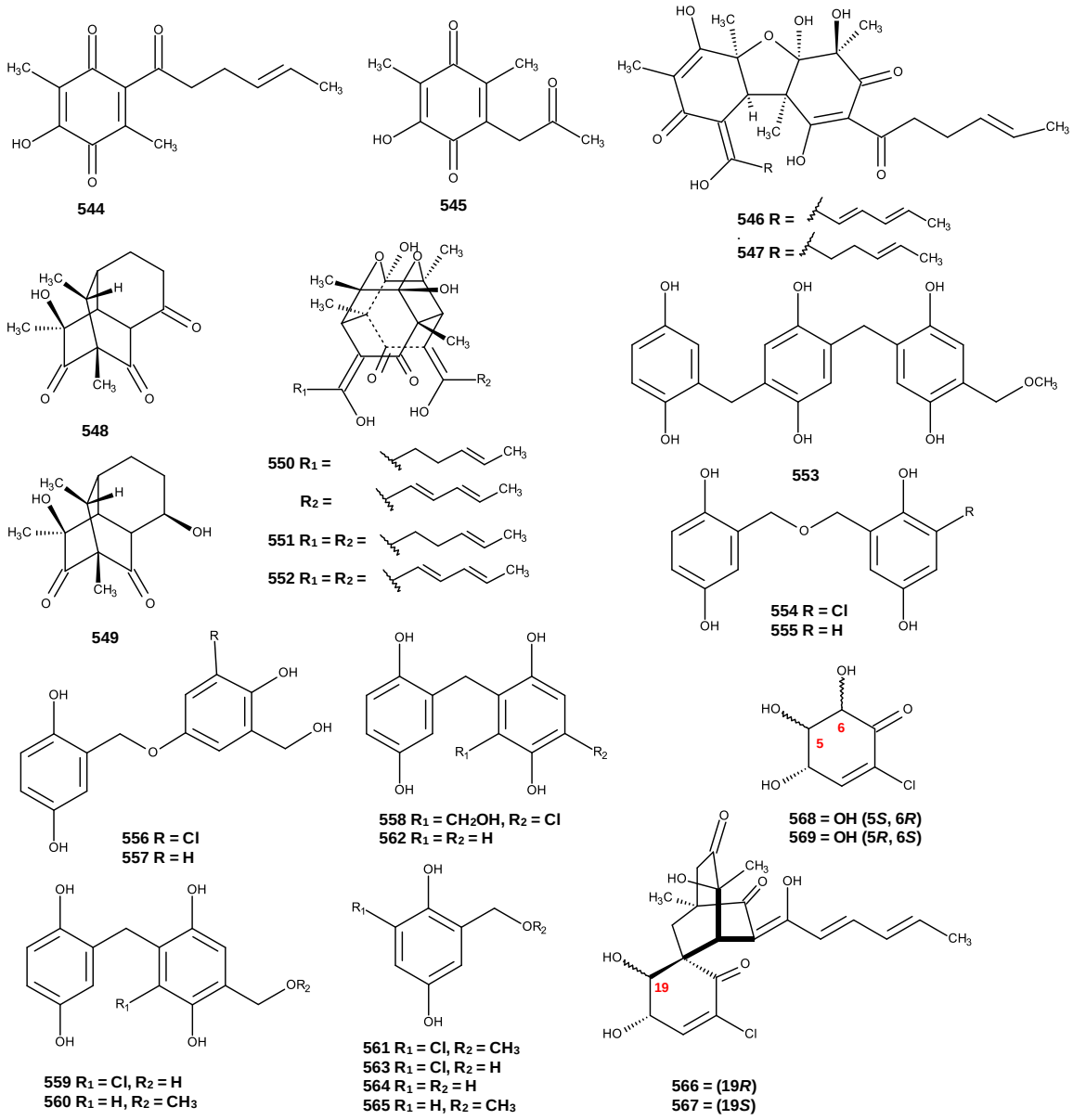

Figure 58. Structures of 2-(2', 3'-dihydrosorbyl)-3,6-dimethyl-5-hydroxy-1,4-benzoquinone (**544**), 3-acetonyl-2,6-dimethyl-5-hydroxy-1,4- benzoquinone (**545**), dihydrobisvertinolone (**546**), tetrahydrobisvertinolone (**547**), penicillones A (**548**), B (**549**), dihydrotrichodimerol (**550**), tetrahydrotrichodimerol (**551**), trichodimerol (**552**), terrestrols A (**553**), B (**554**), C (**555**), D (**556**), E (**557**), F (**558**), G (**559**), H (**560**), monomer (**561**), **562**, **563**, **564**, **565**, chloctanspirones A (**566**), B (**567**), terrestrols K (**568**) and L (**569**)

2.2.24. *Penicillium thomii*

The culture extract of the strains *Penicillium thomii* KMM 4645, isolated from superficial mycobiota of the brown alga *Sargassum miyabei* , collected from the Sea of Japan, furnished previously unreported austalide meroterpenoid austalide H acid butyl ester (**570**), qustalide H acid (**571**), austalide P acid butyl ester (**572**) (Figure 59), austalide P acid (**385**), austalide Q acid (**386**), 13-*O*-Deacetylaustalide I (**389**), 13-deacetoxyaustalide I (**390**) (Figure 45) (Zhuravleva *et al.,* 2014a). Further investigation of the same fungus, yield another unpreviously described meroterpenoids sargassopenillines A (**573**) and E (**574**) (Figure 59) (Zhuravleva *et al*., 2014b).

Afiyatullov *et al*., (2015) isolated four new eudesmane-type sesquiterpenes, thomimarines A-D (**575-578**) (Figure 59) from the culture extract of *P. thomii* KMM 4667, which was isolated from superficial of mycobiota of the rhizome sea grass *Zostera marina*, which was collected in Sea of Japan. Compounds **575-576** and **578**, at concentration of 10 µM, were found to induce a down-regulation of NO production in microphages stimulated with LPS.

Later on, the same research group (Afiyatullov *et al*., 2017) reported the isolation of twelve new polyketides, zosteropenillines A-L (**579-590**), together with the previously described pallidopenilline A (**591**) (Figure 59), from the same fungus. At non-cytotoxic concentration (10.0 µM), **580**, **586** and **588** induced a moderate down-regulation of NO production in LPS-stimulated macrophages, being **580** the most active. Compounds **579-581, 585-586, 588** and **589** were found to be able to inhibit autophagy in the human drug-resistant prostate cancer cells PC3.

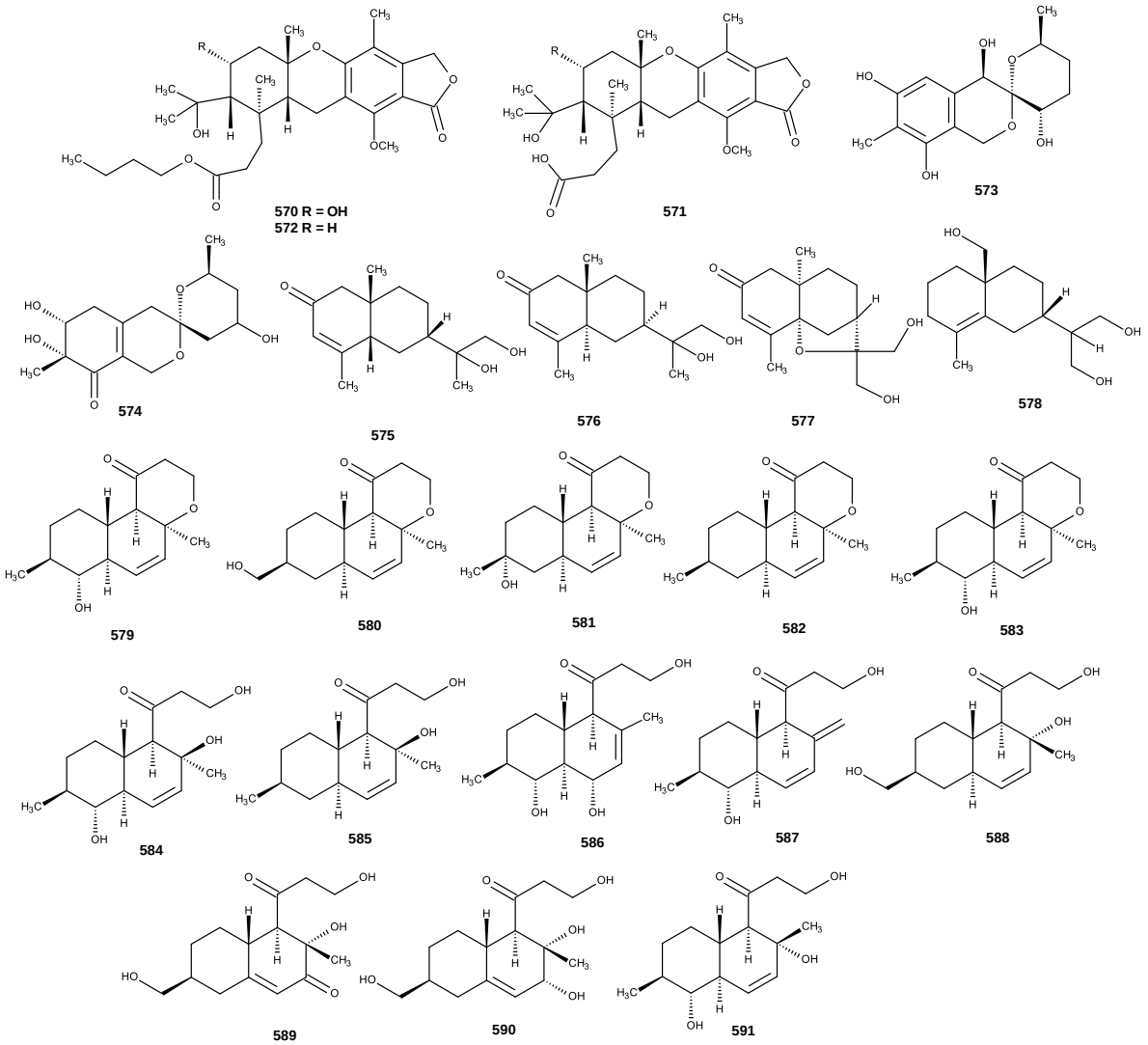

Figure 59. Structures of austalide H acid butyl ester (**570**), qustalide H acid (**571**), austalide P acid butyl ester (**572**), sargassopenillines A (**573**), E (**574**), thomimarines A (**575**), B (**576**), C (**577**), D (**578**), zosteropenillines A (**579**), B (**580**), C (**581**), D (**582**), E (**583**), F (**584**), G (**585**), H (**586**), I (**587**), J (**588**), K (**589**), L (**590**) and pallidopenilline A (**591**)

2.2.25. *Penicillium tropicum*

A new cyclohexapeptide, penitropeptide (**592**) and a new polyketide, penitropone (**593**), together with the previously reported 6-hydroxy-8-methoxy-3*S*, 5-

dimethyl-3,4-isocoumarin (**594**) (Figure 60) and adametizine B (**241**) (Figure 33) were isolated from the ethyl acetate extract of the culture of an endophytic fungus *P. tropicum*, isolated from leaves of *Sapium ellipticum*. The isolated compounds were evaluated for their cytotoxicity against the human ovarian cell line (A2780), but none of them were active at the concentration of 10.0 µM. None of the isolated compounds showed inhibitory activity against *Staphylococcus aureus* ATCC 25923 and *Acinetobacter baumannii* ATCC BAA1605 whit highest test concentration at 64 µg/mL (Zeng *et al*., 2016).

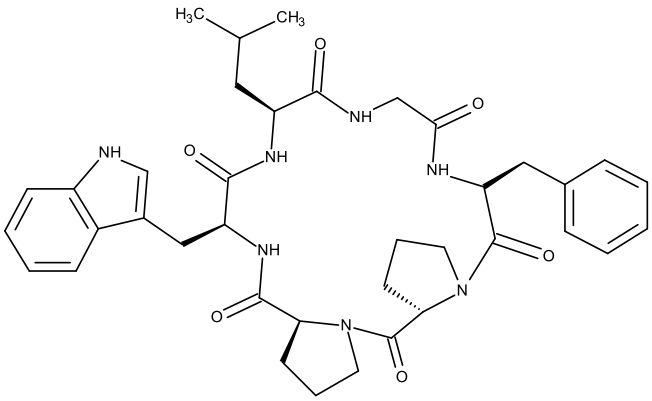

592

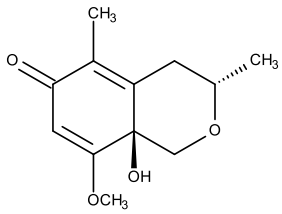

593

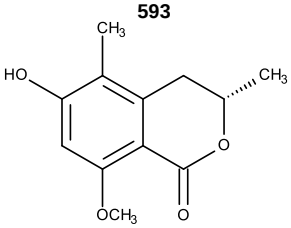

594

Figure 60. Structures of penitropeptide (**592**), penitropone (**593**) and 6-hydroxy-8-methoxy-3*S*, 5-dimethyl-3,4-isocoumarin (**594**)

2.2.26. *Penicillium vinaceum*

A previously unreported diketopiperazine alkaloid, penicillivinacine (**595**) was isolated together with previously described metabolites, including indole-3-carbaldehyde (**596**), *α*-cyclopiazonic acid (**597**), terretrione A (**598**), brevianamide F (**599**), cyclo-D-Tro-L-Pro (**600**) and citreoisocoumarin (**601**) (Figure 61), were isolated from the culture extract of a marine sponge-associated fungus *P. vinaceum*, which was isolated from the marine sponge *Hyrtios erectus.* Compounds **595** and **598** exhibited strong antimigratory activities against the highly metastatic triple negative

human breast cancer cells (MDA-MB-231) with IC_{50} value of 18.4 and 17.7 µM, respectively (Asiri *et al*., 2015).

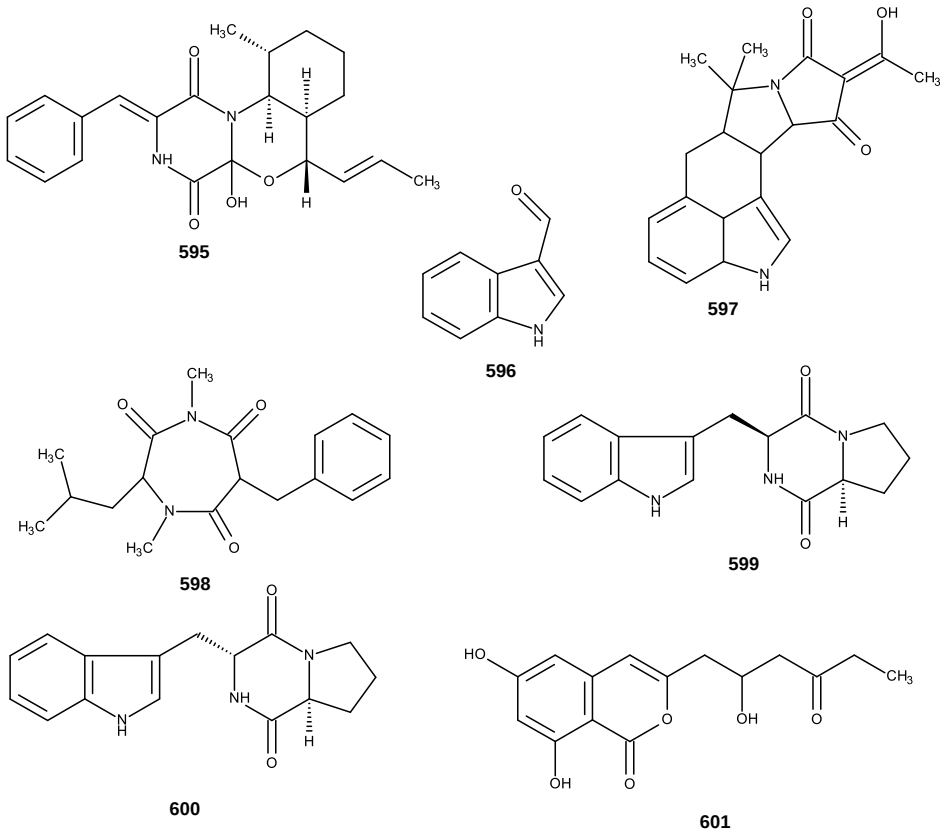

Figure 61. Structures of penicillivinacine (**595**), indole-3-carbaldehyde (**596**), *α*-cyclopiazonic acid (**597**), terretrione A (**598**), brevianamide F (**599**), cyclo-D-Tro-L-Pro (**600**) and citreoisocoumarin (**601**)

2.2.27. *Penicillium species*

A penicillide derivative, prenpenicillide (**602**), and a new xanthone derivative, prenxanthone (**603**) were isolated, together with the previously described metabolites, NG-011 (**604**), NG-012 (**605**), 15G256 *β* (**606**), 15G256*α*-2 (**607**), and bioxanthracene 2 (**608**) (Figure 62), penicillide (**145**) (Figure 19), from the ethyl acetate extract of the culture of the fungus *Penicillium* sp. strain ZLN29, which was isolated from the sediments, collected in the Jiaozhou Bay of China. All the isolated compounds were

evaluated for their cytotoxicities against HepG2, HL-60, BEL-7402 and K562 cell lines; however, only **145** and **602** exhibited weak cytotoxicities against HepG2 cell line with IC_{50} values of 9.7 and 9.9 mm, respectively. None of the compounds exhibited any cytotoxicity against BEL-7402 and K562 cell lines (Gao *et al*., 2013).

A previously unreported fusarielin I (**609**) was isolated, together with the previously reported griseofulvin (**610**) and dechlorogriseofulvin (**611**) (Figure 62) from the culture of a marine-derived fungus *Penicillium* sp. strain IO1, which was isolated from the marine sponge *Ircinia oros.* Another strain, *Penicillium* sp. lO2, also isolated from the same sponge, furnished the previously reported metabolites curvularin (**495**) (Figure 52), trichodimerol (**552**) (Figure 55) and dehydrocurvularin (**612**) (Figure 62). Co-cultivation of both strains produced the known norlichexanthone (**613**) and monocerin (**614**) (Figure 62). Compounds **612** and **614** displayed cytotoxicity against murine lymphoma (L5178Y) cell line with IC_{50} values of 4.7 and 8.4 mM, respectively (Chen *et al*., 2015).

Liu *et al.*, (2016) described the isolation of two new benzophenone derivatives, peniphenone (**615**) and methyl peniphenone (**616**) (Figure 63), along with the previously described metabolites sydowinin A (**98**) (Figure 16), sydowinin B (**99**) (Figure 16), remisporine B (**502**) (Figure 52), methyl 8-hydroxy-6-methyl-9-oxo-9H-xanthene-1-carboxylate (**503**) (Figure 52), conioxanthone A (**617**), pinselin (**618**), andepiremisporine B (**619**) (Figure 63) from the culture extract of an endophytic fungus *Penicillium* sp. ZJ-SY2, which was isolated from the leaves a mangrove plant *Sonneratia apetala.* Compounds **98**, **615**, **617** and **618** exhibited potent immunosuppressive activity with IC_{50} values ranging from 5.9 to 9.3 µg/mL.

Penicillatides A (**620**) and B (**621**), were isolated, together with the previously reported cyclo (*R*-Pro–*S*-Phe) (**622**) and cyclo(*R*-Pro–*R*-Phe) (**623**) (Figure 63) from the organic extract of the culture of a marine-derived fungus *Penicillium* sp, isolated from the Red Sea tunicate *Didemnum* sp. Compounds **621-623** were evaluated for their cytotoxic and antiproliferative activities against colorectal carcinoma (HCT 116), hepatocellular carcinoma (HepG2, and breast cancer (MCF-7) cell lines. Compounds **621** and **622** exhibited significant activity against HCT-116, with IC_{50} of 23.0 and 38.9 µM, respectively, while **623** was weakly active against this cell line. None of the

compounds showed activity against HepG2 (≥50 µM). Moreover, **621** and **623** showed significant activity against *V. anguillarum*, and moderate activity against both *S. aureus* and *C. albicans* (Youssef and Alahdal, 2018).

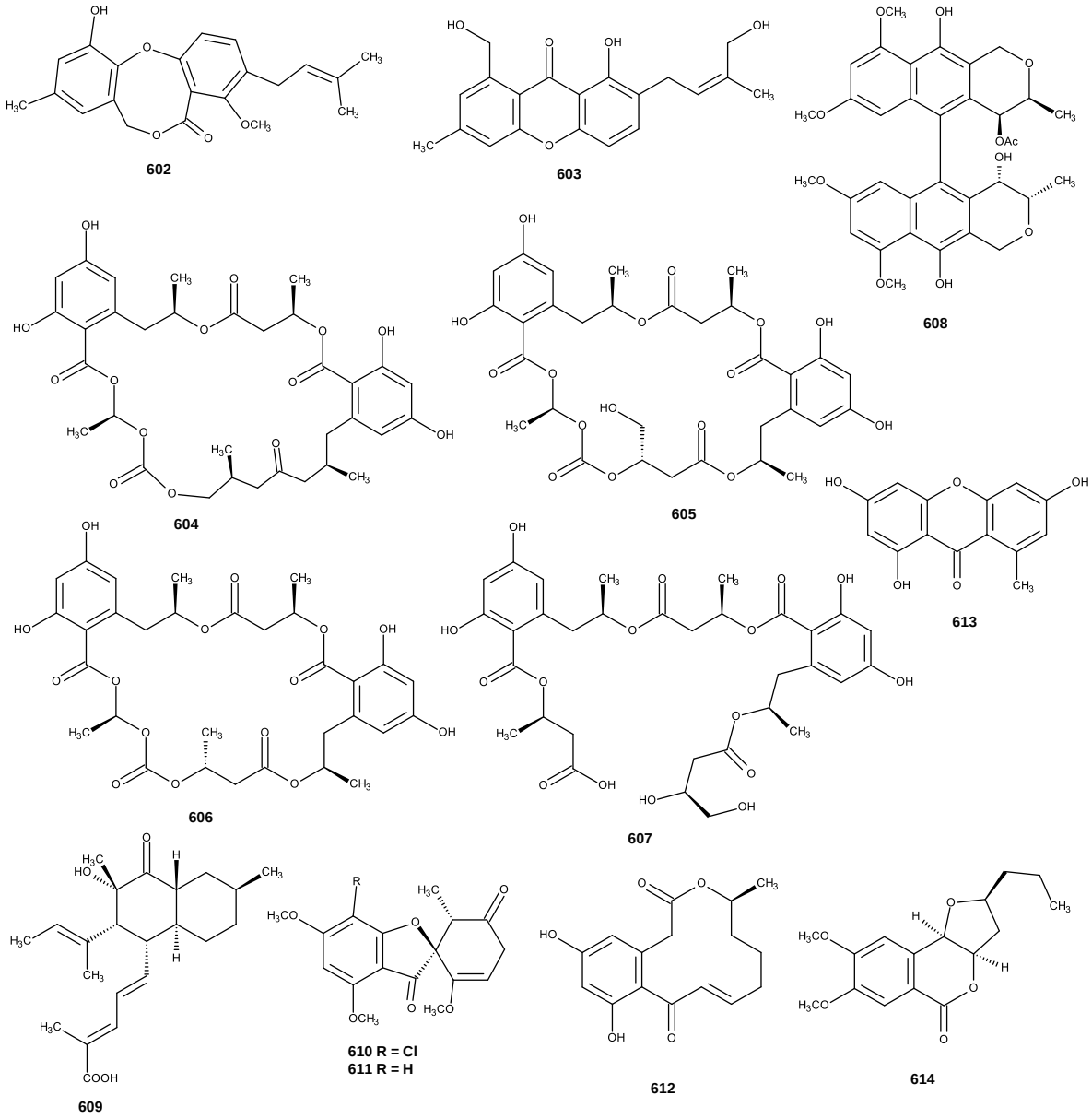

Figure 62. Structures of prenpenicillide (**602**), prenxanthone (**603**), NG-011 (**604**), NG-012 (**605**), 15G256 *β* (**606**), 15G256*α*-2 (**607**), bioxanthracene 2 (**608**), fusarielin I (**609**) griseofulvin (**610**), dechlorogriseofulvin (**611**), norlichexanthone (**613**) and monocerin (**614**)

Yang *et al.*, (2018) described the isolation of a new spiroditerpenoid, brevione O (**624**), together with the known breviones I (**625**), J (**626**) and H (**627**) and a previously reported diketopiperazine alkaloid brevicompanine G (**628**) (Figure 63) from the ethyl acetate extract of a solid-rice culture of a marine coral-derived fungal strain *Penicillium* sp. TJ403-1, which was isolated from inner tissues of a fresh soft coral of the genus *Alcyonium*, collected from the Sanya Bay, Hainan Island, China. All the isolated compounds were evaluated for cytotoxic activity against HL-60 (acute leukemia), MM231 (breast cancer), A-549 (lung cancer), HEP3B (hepatic cancer), SW-480 (colon cancer) and one normal colonic epithelial cell (NCM460) cell lines, however, only **625** showed significant inhibitory activities against HL-60, A-549, and HEP3B tumor cell lines with IC_{50} values of 4.92 ± 0.65, 8.60 ± 1.36 and 5.50 ± 0.67 µM, respectively (Yang *et al*., 2018).

The ethyl acetate extract of cultures of the endophytic fungus *Penicillium* sp strain TGM112, which was isolated from the mangrove plant *Bruguiera sexangula* var. *rhynchopetala*, from the South China Sea, furnished three new lactones penicilactones A-C (**629-631**) (Figure 63). Compound **629** displayed antibacterial activity against *S. aureus* with an MIC value of 6.25 µg/mL. Moreover, **630** also exhibited insecticidal activity against newly hatched larvae of *Culex quinquefasciatus* with LC_{50} value of 78.5 µg/mL (Bai *et al*., 2019).

Pang *et al.*, (2019) described isolation of two previously unreported alkaloids, (*S*)-methyl 2-acetamido-4-(2-(methylamino) phenyl)-4-oxobutanoate (**632**) and quinolactacin E (**633**) and one new pyrone derivative, germicidin O (**634**) (Figure 64), together with previously described compounds including sydowinin A (**98**) (Figure 16), phenol A (**326**) (Figure 39), dihydrocitrinone (**398**) (Figure 46), *β*-diversonolic ester (**418**) (Figure 48), penicitrinone A (**496**) (Figure 52), stoloniferol A (**542**) (Figure 57), pinselin (**618**) (Figure 63), quinolactacin B (**635**), quinolonimide (**636**), quinolonic acid (**637**), 4-hydroxy-3-methyl-2(1*H*)-quinolinone (**638**), coniochaetone J (**639**), 6,8-dihydroxy-3,4,5-trimethylisochroman (**640**), moniliphenone (**641**), frangula-emodin (**642**), methyl-2-(2-acetyl-3,5-dihydroxy-4,6-dimethylphenyl) acetate (**643**), latifolicinin C (**644**) and 22-acetylisocyclocitrinol A (**645**) (Figure 64) from the ethyl acetate extract of the solid-rice culture of the sponge-derived fungus *Penicillium* sp. strain

SCSIO41015, which was isolated from the marine sponge a *Callyspongia* sp., collected from the Guangdong Province of China. Compound **642** exhibited selective cytotoxic activity against the human gastric cancer cells MGC803, with IC_{50} value of 5.19 µM, and potent antibacterial activity against *S. aureus* with an MIC value of 3.75 µg/mL, while **618** and **326** displayed weak antibacterial activity against *S. aureus* and *Acinetobacter baumannii,* respectively, both with MIC values of 57 µg/mL (Pang *et al*., 2019).

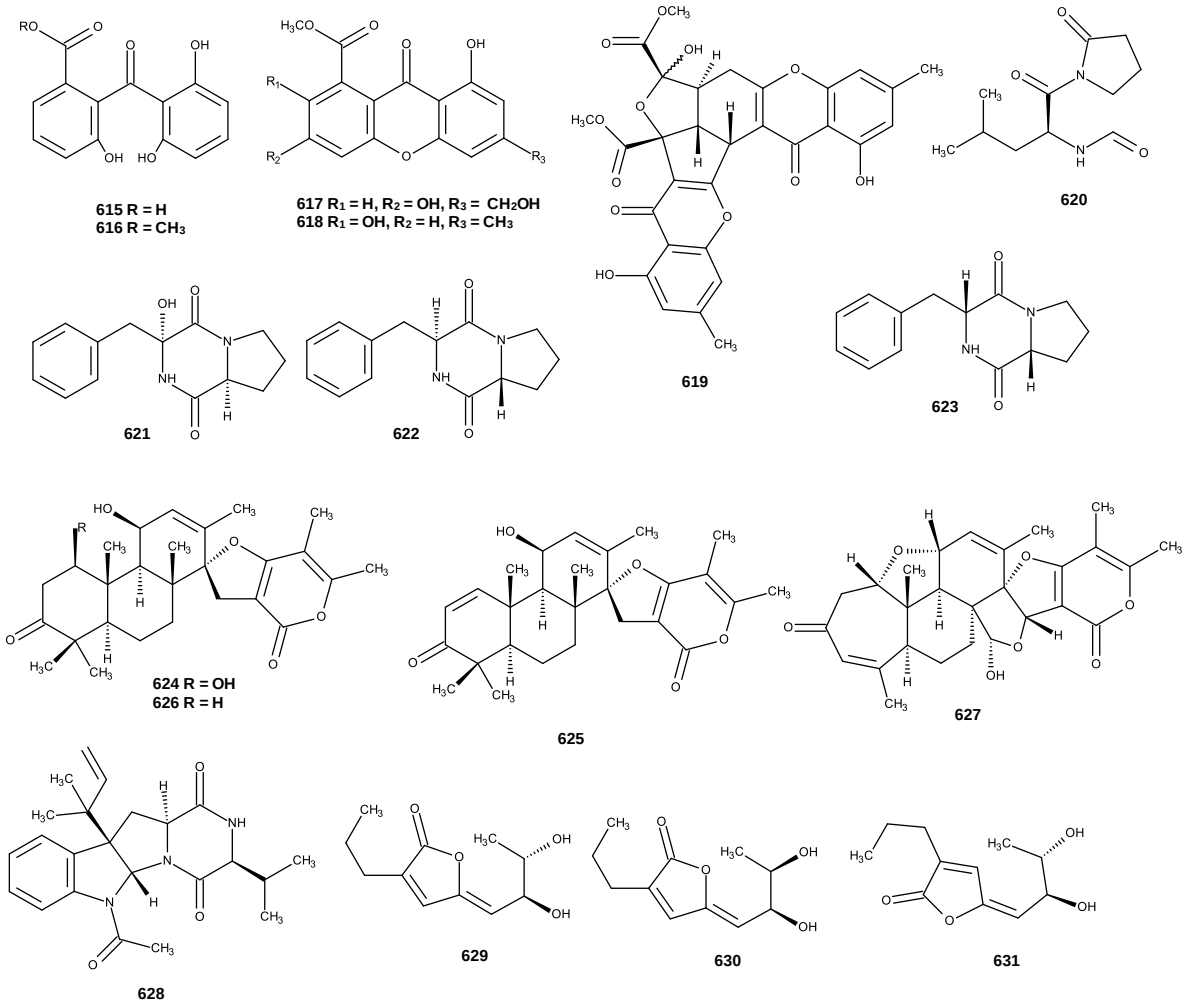

Figure 63. Structures of peniphenone (**615**), peniphenone (**616**), conioxanthone A (**617**), pinselin (**618**), andepiremisporine B (**619**), Penicillatides A (**620**), B (**621**), cyclo (*R*-Pro–*S*-Phe) (**622**), cyclo (*R*-Pro–*R*-Phe) (**623**), brevione O (**624**), breviones I (**625**), J (**626**), H (**627**), brevicompanine G (**628**), penicilactones A (**629**), B (**630**) and C (**631**)

Zhang *et al.*, (2019) isolated four new metabolites, including peniquinone A (**646**) and peniquinone B (**647**), penizofuran A (**648**) and quinadoline D (**649**) (Figure 64), together with previously reported metabolites, i. e. quinadoline A (**227**) (Figure 28), griseofulvin (**610**) (Figure 62), dechlorogriseofulvin (**611**) (Figure 62), 3,4-dimethoxy-5-methylphenol (**650**), orcinol (**651**), 1,3,5,6-tetrahydroxy-8-methylxanthone (**652**), mucorisocoumarin A (**653**), penicillic acid (**654**), dihydropenicillic acid (**655**), isogriseofulvin (**656**), dehydrogriseofulvin (**657**), *trans*-capsaicin (**658**) and dihydrocapsaicin (**659**) (Figure 64) from the culture extract of *Penicillium* sp. L129, which was isolated from the rhizosphere-soil of *Limonium sinense* (Girald) Kuntze, collected in Yangkou Beach in Qingdao, China. Compound **646** displayed cytotoxicity against MCF-7, U87 and PC3 cell lines with IC_{50} values of 12.39 9.01 and 14.59 µM, respectively, while **647** exhibited cytotoxicity against MCF-7, U87 and PC3 cell lines with IC_{50} values of 25.32, 13.45 and 19.93 µM, respectively (Zhang *et al*., 2019).

The previously undescribed monomeric naphtho-γ-pyrones, peninaphones A-C (**660-662**), along with two previously reported bis-naphtho-γ-pyrones **(663** and **664**) (Figure 65), were isolated from the culture extract of *Penicillium* sp. Strain HK1-22, which was isolated from the mangrove rhizosphere soil, collected from the Dongzhaigang mangrove natural reserve in Hainan Island, China. Compounds **660-662** exhibited antibacterial activity against *S. aureus* (ATCC43300, 33591, 29213 and 25923) with MIC values in the range of 12.5-50 µg/mL. Compound **662** also exhibited significant activity against the rice sheath blight pathogen *Rhizoctonia solani* (Zheng *et al.*, 2019).

Song *et al*., (2019) described isolation of the previously unreported pyrrospirones C-I (**665-671**), penicipyrrodiether A (**672**), penicipyrroether A (**673**) and pyrrospirone J (**674**) (Figure 65), together with the previously reported metabolites: ergosterol (**115**) (Figure 17), stoloniferol B (**323**) (Figure 39), pinselin (**618**) (Figure 63), 2,4,5 trimethylresorcinol (**675**), coniochaetone E (**676**) and quinolactacin A1 (**677**) (Figure 65) from the ethyl acetate extract from a liquid culture of *Penicillium* sp. ZZ380, which was isolated from marine crab *Pachygrapsus crassipes.* Compounds **673** and **674** were evaluated for their antiproliferative activity against human glioma U87MG

and U251 cells by sulforhodamine B assays. Both of the compounds showed different activities toward different glioma cells. While the IC_{50} values of **673** the IC_{50} values of 1.64-5.50 µM against U87MG and U251 cells, those of **674** were 10.52-17.92 µM, respectively. Moreover, **673** displayed good antibacterial activity against MRSA and *E. coli*, with MIC values of 1.7 µg/mL and 3.0 µg/mL, respectively, while **674** was inactive at a concentration of 50 µg/mL.

Park *et al.*, (2019) described the isolation of six previously unreported phenalenone derivatives, including *ent*-peniciherqueinone (**678**), 12-hydroxynorherqueinone (**679**), *ent*-isoherqueinone (**680**), oxopropylisoherqueinone A (**681**), oxopropylisoherqueinone B (**682**), 4-hydroxysclerodin (**683**), along with five previously described triketone (**684**), herqueinone (**685**), isoherqueinone (**686**), sclerodin (**687**) and scleroderolide (**688**) (Figure 66), from the culture extract of a *Penicillium* sp. which was isolated from marine sediments collected from Gagudo, Korea.

All the isolated compounds were inactive against the K562 (human chronic myeloid leukemia) and A549 (adenocarcinomic human alveolar basal epithelial) cancer cell lines (IC_{50} > 10 µM). Moreover, **684** was found to moderately inhibit NO production in RAW 264.7 cells with an IC_{50} value of 3.2 µM, while the rest of the isolated compounds were inactive (IC_{50} > 20 µM). In the angiogenesis assay, **683** exhibited tube formation in HUVECs with an IC_{50} of 20.9 µM.

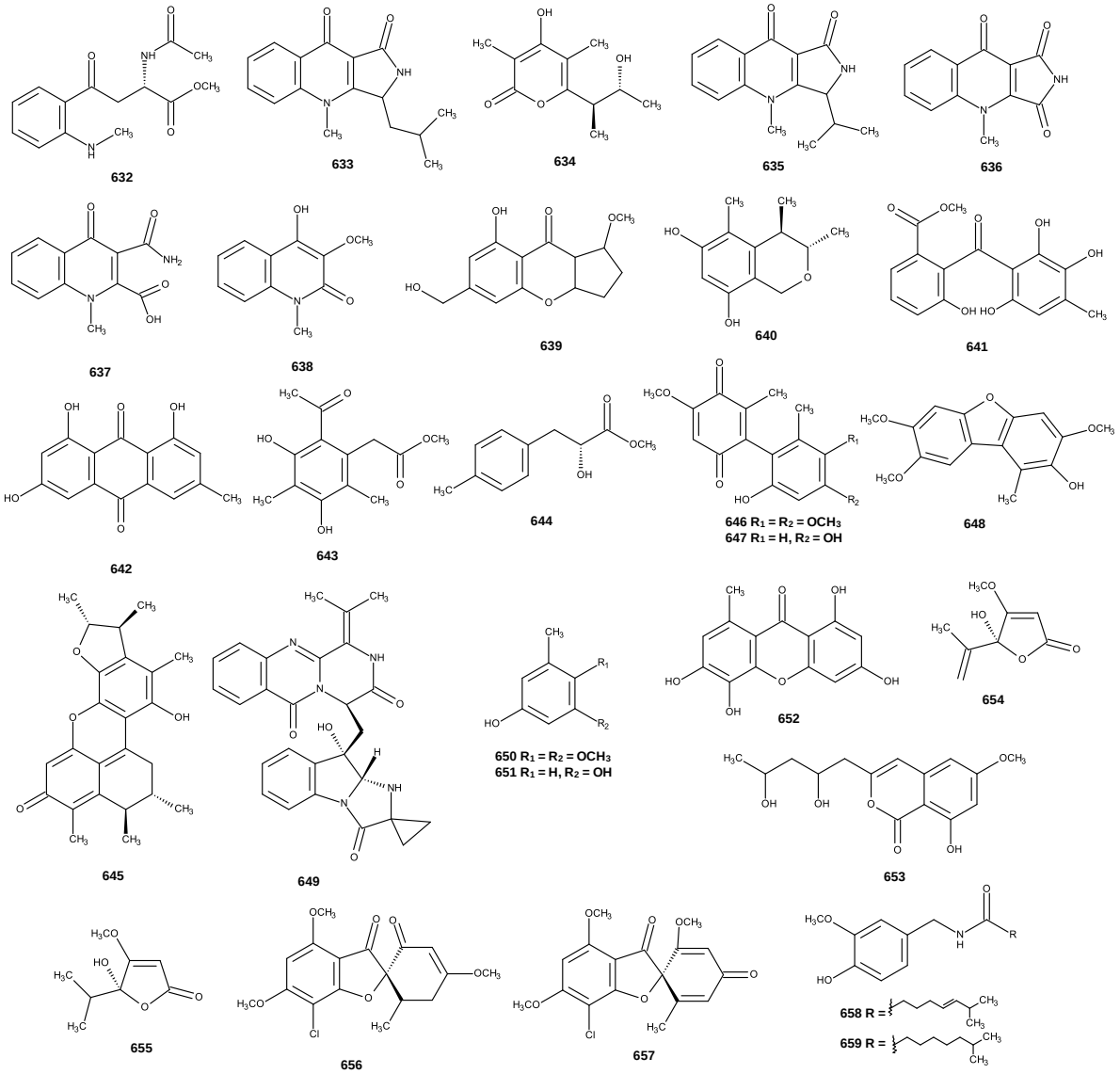

Figure 64. Structures of (*S*)-methyl 2-acetamido-4-(2-(methylamino) phenyl)-4-oxobutanoate (**632**), quinolactacin E (**633**), germicidin O (**634**), quinolactacin B (**635**), quinolonimide (**636**), quinolonic acid (**637**), 4-hydroxy-3-methyl-2(1*H*)-quinolinone (**638**), coniochaetone J (**639**), 6,8-dihydroxy-3,4,5-trimethylisochroman (**640**), moniliphenone (**641**), frangula-emodin (**642**), methyl-2-(2-acetyl-3,5-dihydroxy-4,6-dimethylphenyl) acetate (**643**), latifolicinin C (**644**), 22-acetylisocyclocitrinol A (**645**), peniquinone A (**646**), peniquinone B (**647**), penizofuran A (**648**), quinadoline D (**649**), 3,4-dimethoxy-5-methylphenol (**650**), orcinol (**651**), 1,3,5,6-tetrahydroxy-8-methylxanthone (**652**), mucorisocoumarin A (**653**), penicillic acid (**654**), dihydropenicillic acid (**655**), isogriseofulvin (**656**), dehydrogriseofulvin (**657**), *trans*-capsaicin (**658**) and dihydrocapsaicin (**659**)

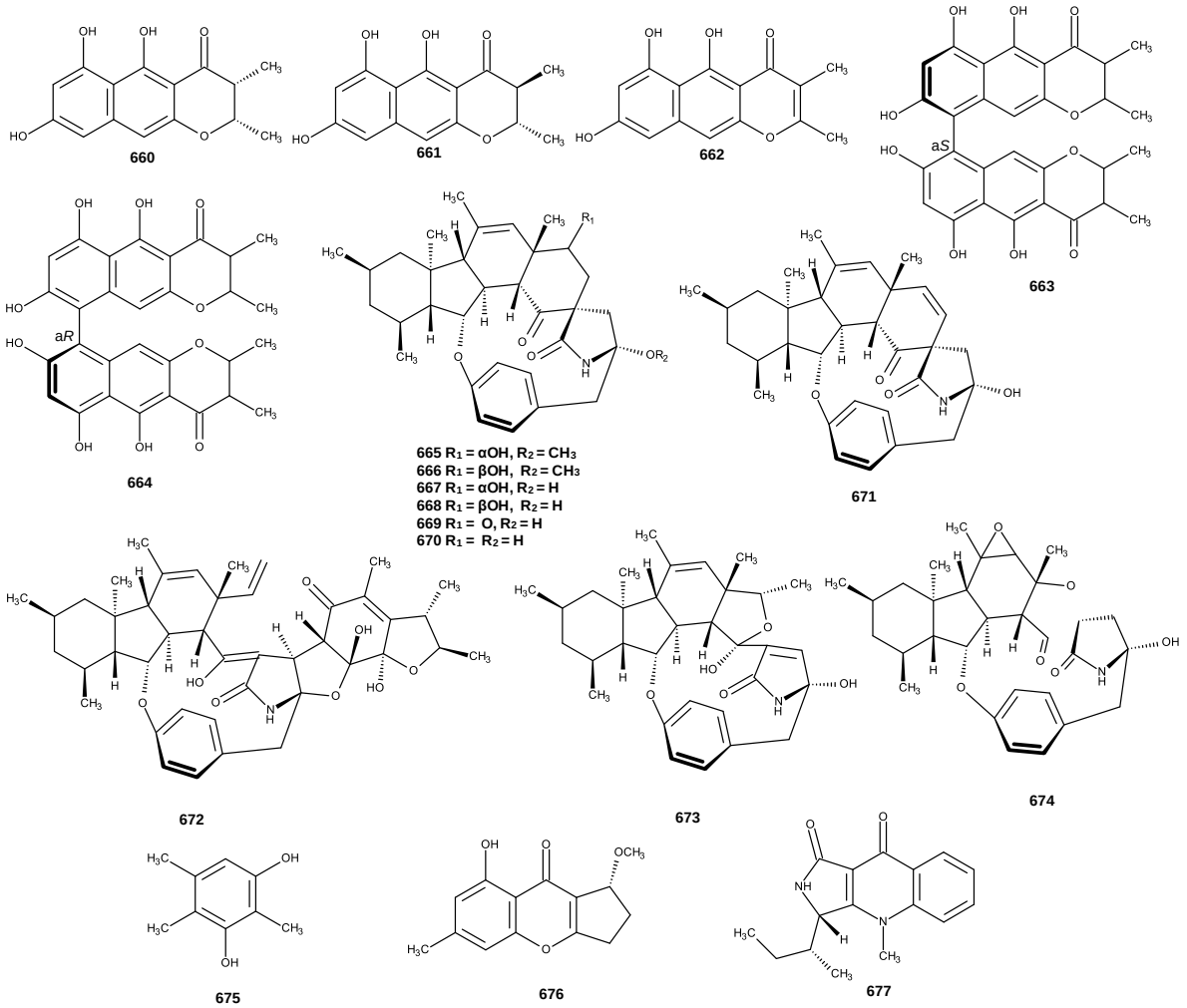

Figure 65. Structures of peninaphones A (**660**), B (**661**), C (**662**), bis-naphtho-γ-pyrones **(663**), (**664**), pyrrospirones C (**665**), D (**666**), E (**667**), F (**668**), G (**669**), H (**670**), I (**671**), penicipyrrodiether A (**672**), penicipyrroether A (**673**), pyrrospirone J (**674**), 2,4,5 trimethylresorcinol (**675**), coniochaetone E (**676**) and quinolactacin A1 (**677**)

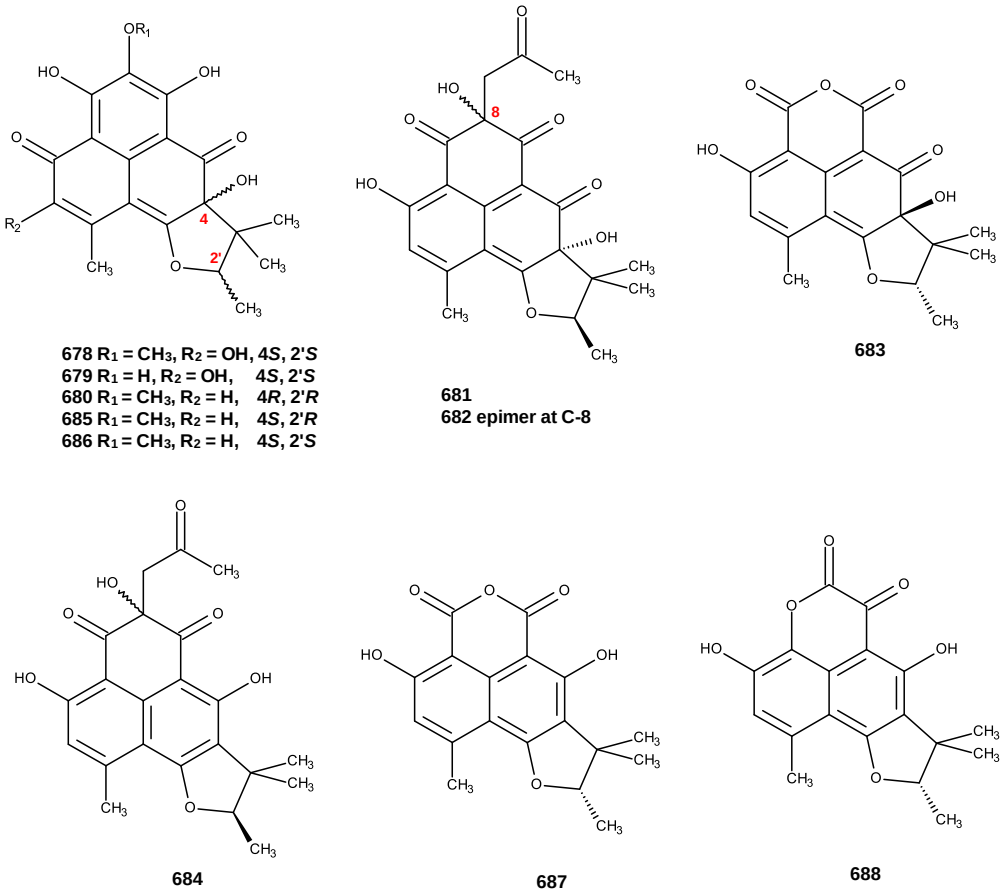

Figure 66. Structures of *ent*-peniciherqueinone (**678**), 12-hydroxynorherqueinone (**679**), *ent*-isoherqueinone (**680**), oxopropylisoherqueinone A (**681**), oxopropylisoherqueinone B (**682**), 4-hydroxysclerodin (**683**), triketone (**684**), herqueinone (**685**), isoherqueinone (**686**), sclerodin (**687**) and scleroderolide (**688**)

CHAPTER III

RESULTS AND DISCUSSIONS

3.1. Chemical Investigation of Secondary Metabolites from the Culture Extracts of Marine-derived Fungi

3.1.1. Secondary Metabolites Isolated from the Marine-Derived *Neosartorya tsunodae* KUFC 9213

Chromatographic fractionation and purification of the ethyl acetate extract of the culture of the marine-derived fungus, *Neosartorya tsunodae* KUFC 9213, resulted in the isolation of nine previously reported metabolites (1*R*, 8*S*, 9*R*)-1,9-dihydroxy-8-(2-hydroxypropan-2-yl)-4-methoxy-5-methyl-1,7,8,9-tetrahydro-3*H*-furo[3,4-f]chromen-3-one (chromanol) **(NT 1)**, (3β,5α,22*E*), 3,5-dihydroxyergosta-7,22-dien-6-one **(NT 2)**, byssochlamic acid **(NT 3)**, hopan-3β,22-diol **(NT 4)**, chevalone C **(NT 5)**, sartorypyrone B **(NT 6)**, helvolic acid **(NT 7)**, lumichrome **(NT 8)** and harmane **(NT 9)** (Figure 67).

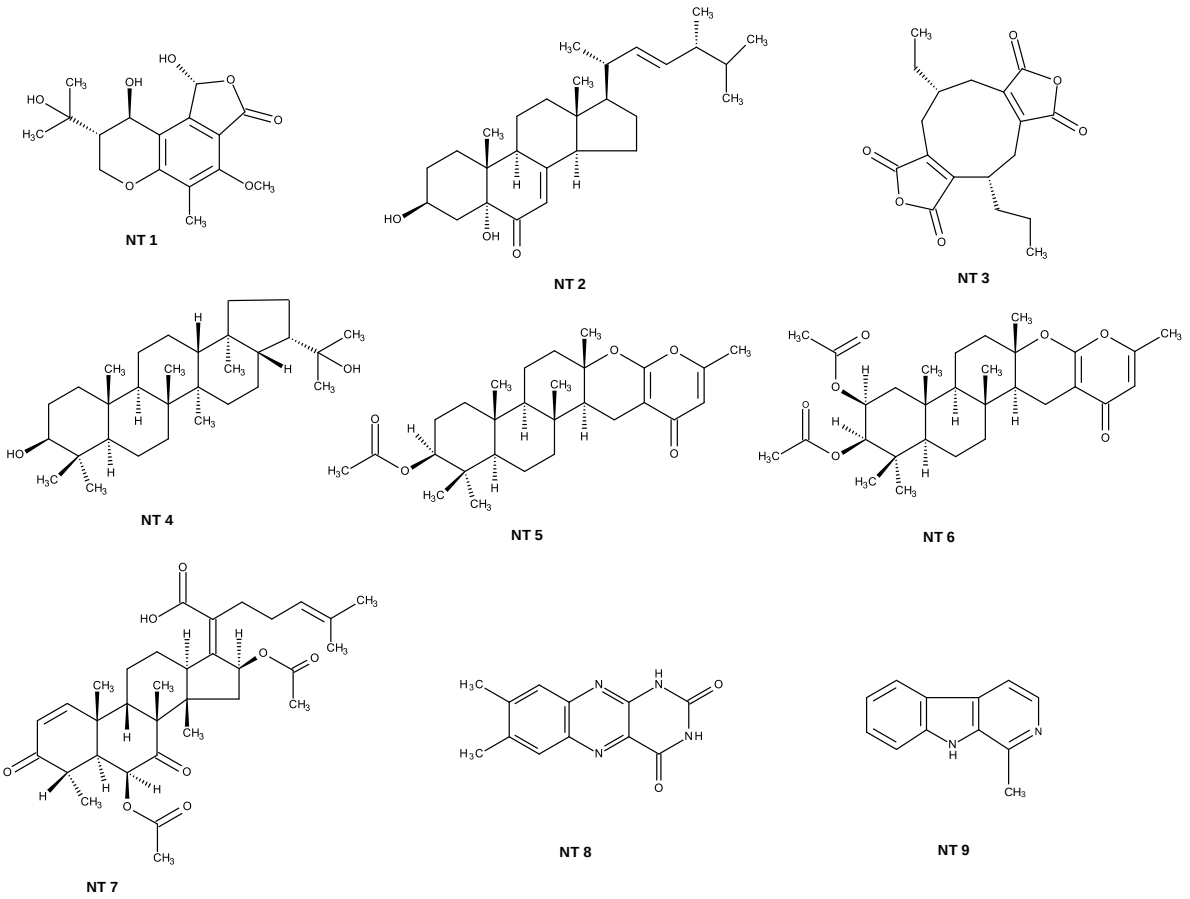

Figure 67. Secondary metabolites isolated from *Neosartorya tsunodae* KUFC 9213

3.1.1.1 Chromanol (NT 1)

Compound **NT 1** was isolated as white crystals (mp, 223-224 ºC), and its molecular formula $C_{16}H_{20}O_7$ was established on the basis of the (+)-HRESIMS *m/z* 347.1111 $[M+Na]^+$, indicating seven degrees of unsaturation. The IR spectrum showed absorption bands for hydroxyl (3467, 3434 cm^{-1}), ester carbonyl (1743 cm^{-1}) and aromatic (1597, 1541 cm^{-1}). The ^{13}C NMR spectrum, in combination with DEPTs and HSQC spectra (Table 3), revealed the presence of one conjugated carbonyl (δ_C 166.1), six non-protonated sp^2 (δ_C 158.4, 155.9, 146.8, 120.0, 117.4, 109.4), one hemi-acetal (δ_C 95.6), one oxyquaternary sp^3 (δ_C 69.9), one oxymethylene sp^3 (δ_C 63.9), one methoxyl (δ_C 61.6), two methine sp^3 (δ_C 57.8, 46.6), and three methyl (δ_C 28.4, 27.7, 8.6) carbons. The ^1H NMR spectrum, in conjunction with the HSQC spectrum (Table 3), displayed three quaternary methyl singlets at δ_H 1.24 (δ_C 27.7), 1.27 (δ_C 28.4) and 2.05 (δ_C 8.6), one methoxyl singlet at δ_H 3.67 (δ_C 61.1), one double triplet at δ_H 1.79 (*J* = 11.9, 2.8 Hz; δ_C 46.6), a broad signal of the oxymethine proton at δ_H 5.16 (δ_C 57.8), a singlet at δ_H 6.64 (δ_C 95.6), a broad signal of the hydroxyl group at δ_H 4.51, and two double doublets of mutually coupled methylene protons at δ_H 4.29 (*J* = 12.0, 10.6 Hz) and 4.53 (*J* = 12.0, 2.4 Hz).

That **NT 1** is a derivative of 7-methoxy-8-methyl-3,4-dihydro-2*H*-chromene was substantiated by the COSY (Table 3) correlation from the double doublet at δ_H 4.29 (*J* = 12.0, 10.6 Hz, H-7α) to the double triplet at δ_H 1.79 (*J* = 11.9, 2.8 Hz, H-8), and by strong HMBC correlations (Table 3) from the methyl singlet at δ_H 2.05 (Me-10, δ_C 8.6) to quaternary sp^2 carbons at δ_C 155.9 (C-4), δ_C 120.0 (C-5), δ_C 158.4 (C-5a), and weak correlations to the non-protonated sp^2 carbons at δ_C 109.4 (C-3a) and δ_C 146.8 (C-9a), from the methoxyl singlet at δ_H 3.67 (δ_C 61.1) to C-4, and from the double doublet of methylene protons at δ_H 4.29 (*J* = 12.0, 10.6 Hz, H-7a) and δ_H 4.53 (*J* = 12.0, 2.4 Hz, H-7b) to C-5a, C-8 (δ_C 46.6) and C-9 (δ_C 57.8). That the substituent on C-8 was a 2-hydroxypropan-2-yl was corroborated by the HMBC correlations from Me-13 (δ_H 1.27, *s*) to C-14 (δ_C 27.7), C-12 (δ_C 69.9) and C-8, from Me-14 (δ_H 1.24, *s*) to C-13 (δ_C 28.4), C-12 and C-8 as well as from OH-12 (δ_H 4.51, *brs*) to C-13, C-12 and C-14. Finally, the 5-hydroxydihydrofuran-2(3*H*)-one was fused to the benzene ring of the 3, 4-dihydro-2*H*-chromene ring system at C-3 and C-11 was confirmed by the

HMBC correlation from the singlet at δ_H 6.64 (H-1; δ_C 95.6) to the conjugated carbonyl carbon at δ_C 166.1 (C-3) (Figure 68).

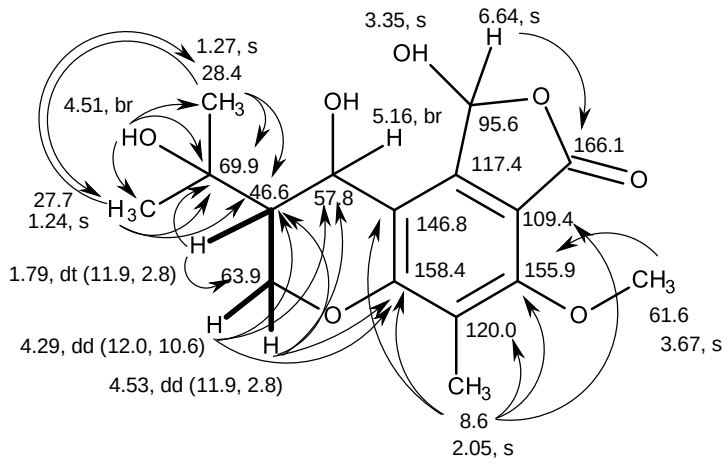

Figure 68. Key COSY (▬) and HMBC (⟶) correlations in **NT 1**

The NOESY spectrum (Table 3) supported the proposed structure by displaying correlations from H-1 to OH-1 (δ_H 3.35, *s*) and H-9 (δ_H 5.16, *br*), from H-7α (δ_H 4.29, *dd, J* = 12.0, 10.6 Hz) to H-7β (δ_H 4.53, *dd*, *J* = 12.0, 2.4 Hz), from H-8 (δ_H 1.79, *dd*, *J* = 11.9, 2.8 Hz) to H-7β, Me-1' (δ_H 1.27, *s*) and Me-3' (δ_H 1.24, *s*), from Me-1' to H-8, Me-3' and OH-2' (δ_H 4.51, *br*), Me-3' to H-8, Me-1' and OH-2', and from Me-10 (δ_H 2.05, *s*) to OMe-4 (Figure 69).

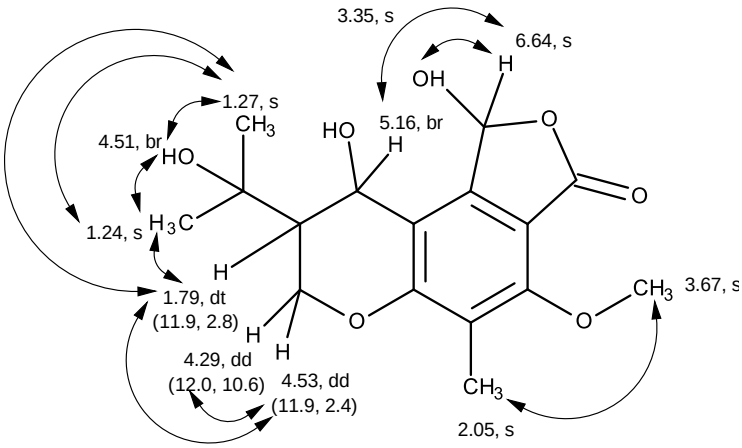

Figure 69. Key NOESY (⟷) correlations in **NT 1**

Literature search revealed that the planar structure of **NT 1**, was the same as that of one of the highly substituted chromanols (compound **4** in Achenbach *et al*., 1982), isolated from cultures of *Aspergillus duricaulis* (Achenbach *et al*., 1982). However, there were no details of the ^{1}H and ^{13}C NMR data of the isolated compounds. The authors have proposed that, due to the comparatively broad ^{1}H signals, which appeared as two sharp signals each, when the ^{1}H NMR was run in completely acid-free solvent, the compound was a mixture of two diastereoisomers, differing in the absolute configurations at C-1, due to a ring-chain tautomerism of the hydroxyphthalide. Moreover, the authors have found that this compound did not show any optical rotation or a Cotton effect (Achenbach *et al*., 1982), and there was no indication of the determination of the absolute configurations of any stereogenic carbons of the isolated chromanol derivatives.

Later on, the same group (Achenbach *et al*., 1985) has described the same compound (compound **6** in the literature) as colorless oil which contained a mixture of the epimers (**6a** and **6b** in the literature) and reported two sets of ^{1}H and ^{13}C NMR data (in deuterated acetone) of both epimers in the mixture but without assignment of the stereochemistry of C-1. On the contrary, **NT 1** is optically active (levorotatory), with, $[\alpha]_{D}^{25}$ - 80 (*c* 0.05, $CHCl_3$), and exhibited only one set of the ^{1}H and ^{13}C NMR data (Table 3). Therefore, we concluded that **NT 1** was a pure compound and not a mixture of the epimers as described by Archenbach *et al*., 1982 and 1985.

This prompted us to investigate the absolute configurations of the stereogenic carbons in **NT 1**. Since **NT 1** could be obtained in a suitable crystal (mp 223-224 ºC), its X-ray analysis was carried out and the ORTEP view is shown in figure 70. Therefore, **NT 1** was identified as (1*R*, 8*S*, 9*R*)-1, 9-dihydroxy-8-(2-hydroxypropan-2-yl)-4-methoxy-5-methyl-1, 7, 8, 9-tetrahydro-3*H*-furo[3,4-f]chromen-3-one. (Figure 71).

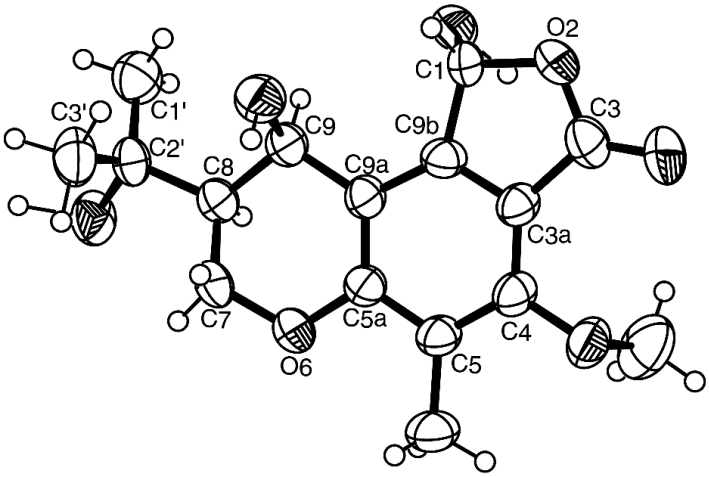

Figure 70. ORTEP view of **NT 1**

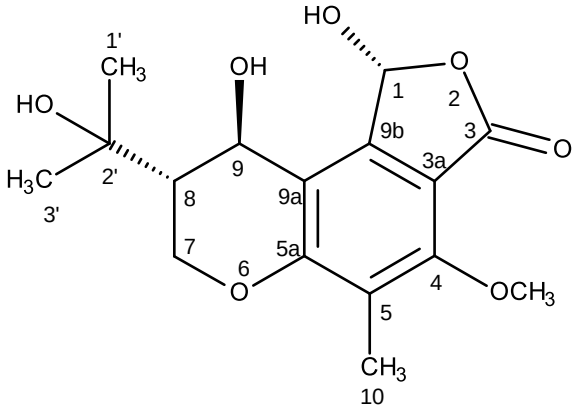

Figure 71. Structure of chromanol **(NT 1)**

Table 3. ^{1}H and ^{13}C NMR (300 MHz and 75 MHz, DMSO-d_6) and HMBC assignment for **NT 1**

Position	δ_C, type	δ_H, (*J* in Hz)	COSY	HMBC	NOESY
1	95.6 CH	6.64, *s*	-	C-3	OH-1, H-9
3	166.1 C	-	-	-	-
3a	109.4 C	-	-	-	-
4	155.9 C	-	-	-	-
5	120.0 C	-	-	-	-
5a	158.4 C	-	-	-	-
7α	63.9 CH_2	4.29, *dd* (12.0, 10.6)	H-7β, 8	C-5a, 8, 9	-
β		4.53, *dd* (11.6, 2.4)	H-7α	C-5a, 8, 9	H-7β
8	46.6 CH	1.79, *dt* (11.9, 2.8)	H-7α	C-2', 7	H-8, Me-1', 3'
9	57.8 CH	5.16, *br*	-	-	-
9a	146.8 C	-	-	-	-
9b	117.4 C				
10	8.6 CH_3	2.05, *s*	-	C-3a, 4, 5, 5a, 9a	OMe-4
1'	28.4 CH_3	1.27, *s*	-	C-2', 3', 8	H-8, OH-2', Me-3'
2'	69.9 C				
3'	27.7 CH_3	1.24, *s*	-	C-1', 2', 8	H-8, OH-2', Me-1'
OMe-4	61.6 CH_3	3.67, *s*	-	C-4	-
	-OH	4.51, *br*	-	C-1', 2', 3'	-

3.1.1.2. (3*β*, 5*α*, 22*E*), 3,5-Dihydroxyergosta-7,22-diene-6-one (NT 2)

Compound **NT 2** was isolated as a white solid (mp 190-191 ^{o}C). Based on the (+)-HRESIMS *m/z* 429.3388 $[M+H]^+$ (calculated 429.3369 for $C_{28}H_{45}O_3$), the molecular formula $C_{28}H_{44}O_3$ was attributed to **NT 2**, indicating seven degrees of unsaturation. The ^{13}C NMR spectrum displayed 28 carbon signals which, in combination with DEPT and HSQC spectra, can be classified as one conjugated ketone carbonyl (δ_C 198.7), one non-protonated sp^2 (δ_C165.5), three methine sp^2 (δ_C135.0,132.5 and 119.7), one

oxyquaternary sp^3 (δ_C77.7), two quaternary sp^3 (δ_C 44.8 and 40.5), one oxymethine sp^3 (δ_C67.5), six methine sp^3 (δ_C 56.1, 55.8, 43.9, 42.8, 40.2 and 33.1), seven methylene sp^3 (δ_C 38.9, 36.4, 30.4, 30.2, 27.8, 22.5 and 21.9) and six methyl (δ_C 21.1, 19.9, 19.6, 17.6, 16.4 and 12.7) carbons.

The ^{1}H NMR spectrum (Table 4), in combination with the HSQC spectrum, showed signals of a broad singlet of an olefinic proton at δ_H 5.63 (δ_C 119.7), two double doublets of the olefinic protons at δ_H 5.24 (*J* = 15.3, 7.6 Hz; δ_C 132.5) and δ_H 5.16 (*J* = 15.3, 7.6 Hz; δ_C 135.0), a multiplet of the oxymethine proton at δ_H 4.04 (δ_C 67.5), a double-double doublet of another methylene proton at δ_H 2.53 (*J* = 11.8, 7.0, 2.2 Hz; δ_C 43.9) and various overlapped proton signals at δ_H 1.2-2.2, in addition to four methyl doublets at δ_H 1.03 (*J* = 6.6 Hz; δ_C 21.1), δ_H 0.92 (*J* = 6.8 Hz; δ_C 17.6), δ_H 0.84 (*J* = 6.9 Hz; δ_C 19.9), δ_H 0.82 (*J* = 6.9 Hz; δ_C 19.6) and two methyl singlets at δ_H 0.94 (δ_C 16.4) and δ_H 0.60 (δ_C 12.7), respectively. The COSY spectrum (Table 4) exhibited correlations from the double doublet of the olefinic proton at δ_H 5.24 (H-23; δ_C 132.5) to the double doublet at δ_H 5.16 (H-22; δ_C 135.0) and a multiplet at δ_H 1.85 (H-24; δ_C 42.8), H-22 to H-23 and a multiplet at δ_H 2.03 (H-20; δ_C 40.2), a methyl doublet at δ_H 1.03 (Me-21; δ_C 21.1) to H-20 and a methyl doublet at δ_H 0.92 (H-26; δ_C 21.1) to H-24. These COSY correlations suggested the presence of the following coupling system:

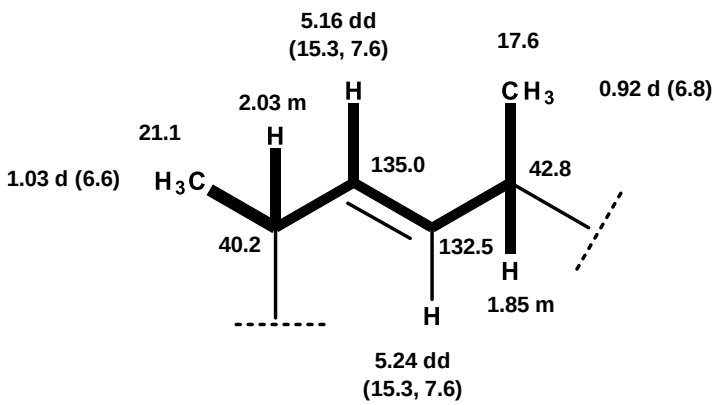

The HMBC spectrum (Table 4) not only confirmed this 3-hexene skeleton by showing correlations from H-23 to C-20, 26 and 24, H-22 to C-20, 21, 24, H_3-21 to C-

20, 22, H_3-26 to C-23 and 24, but also from H_3-26 to the methine sp^3 carbon at δ_C 33.1 (C-25), from the methyl doublet at δ_H 0.82 (H_3-28) to C-24, C-25 and the methyl carbon at 19.9 (C-27), the methyl doublet at δ_H 0.84 (H_3-29) to C-24,C- 25 and the methyl carbon at 19.6 (C-28), thus confirming the presence of the (3*E*)-5,6-dimethylhept-3-en-2-yl moiety.

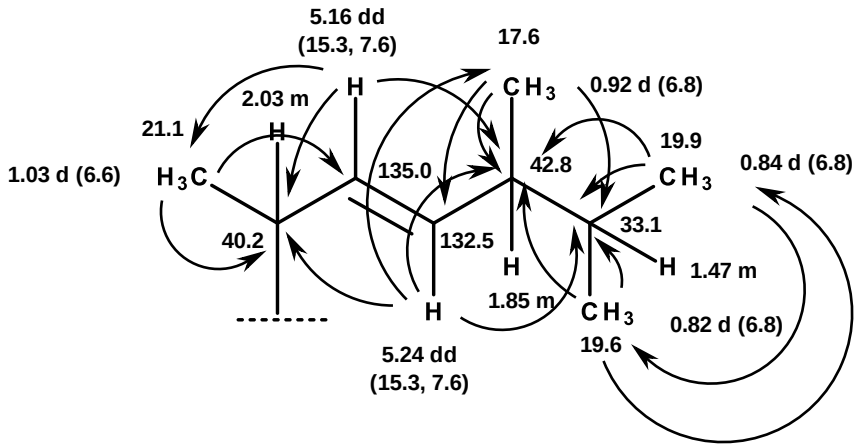

Since the (3*E*)-5,6-dimethylhept-3-en-2-yl moiety, together with the two sp^2 carbons at δ_C 165.5 (C = 8) and 119.7 (CH = 7), constitutes two degrees of unsaturation, consequently, **NT 2** must have a tetracyclic skeleton.

The COSY spectrum (Table 4) showed correlations from the multiplet of the oxymethine proton at δ_H 4.04 (H-3) to the methylene multiplets at δ_H 1.6 and 2.1 (H_2-4; δ_C 36.4) and at δ_H 1.4 and 1.6 (H_2-2; δ_C 30.4). The HMBC spectrum exhibited correlations from H_2-2 to the oxymethine carbon at δ_C 67.5 (C-3; δ_H 4.04), from H-4 to C-3 and the oxyquaternary carbon at δ_C 77.7 (C-5), from the methyl singlet at δ_H 0.94 (Me-19; δ_C 16.4) to the methylene carbons at δ_C 27.8 (C-1), 30.4 (C-2), the quaternary carbon at δ_C 40.5 (C-10) and C-5. Moreover, the COSY spectrum (Table 4) also showed cross peaks from the singlet of the olefinic proton at δ_H 5.63 (H-7; δ_C 119.7) to the *ddd* at 2.53 (H-9; δ_C 43.9), while H-9 exhibited correlations to C-7, C-8, C-10, C-19 and the carbonyl carbon at δ_C 198.7. Moreover, one of H_2-4 (δ_H 2.1, *m*) also showed correlation to the carbonyl carbon at δ_C 198.7. Therefore, this carbonyl carbon was placed at C-6. Taking together the COSY and HMBC correlations, as well as the number of quaternary, methine, methylene, methyl carbons and the molecular formula,

the partial structure of **NT 2** consists of 7,8a-dihydroxy-4a-methyl-4a,5,6,7,8,8a-hexahydronaphthalen-1(4*H*)-one.

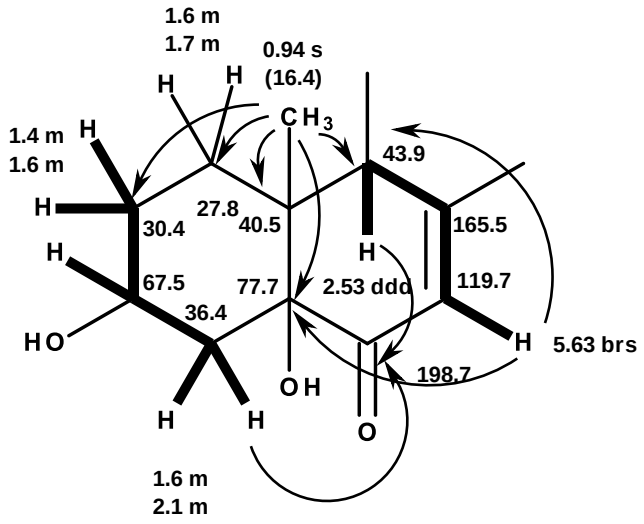

Another bicyclic portion consists of a 3a-methyloctahydro-1*H*-indene moiety, which is fused with the hexahydronaphthalen-1(4*H*)-one moiety, through C-13 and C-14. This was evidenced by HMBC correlations from the methyl singlet at δ_H 0.60 (δ_C 12.7, Me-18) to the methylene sp^3 carbon at δ_C 38.9 (C-12), the quaternary sp^3 carbon at δ_C 44.8 (C-13) and the methine sp^3 carbons at δ_C 55.8 (C-14, δ_H 2.13, *m*) and 56.1 (C-17, δ_H 1.35, *m*), H-14 (δ_H 2.13, *m*) to C-18, the methylene sp^3 carbons at δ_C 22.5 (C-15), 30.2 (C-16), 38.9 (C-12), C-13 and C-7, as well as H-7 to C-14.

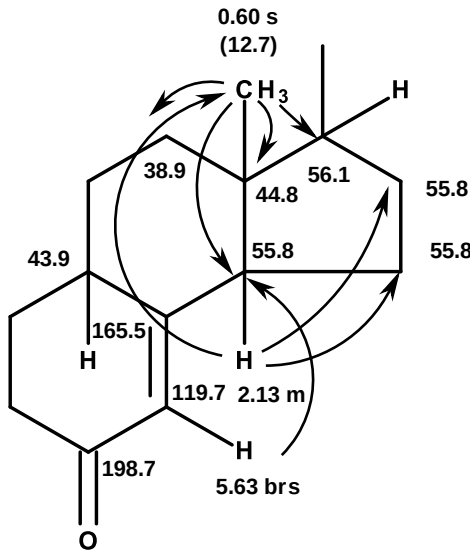

Since H_3-21 showed HMBC correlation to C-17, the (3*E*)-5,6-dimethylhept-3-en-2-yl is connected to the cyclopentane ring through C-17. Therefore, **NT 2** is an ergostane sterol with the planar structure as shown below:

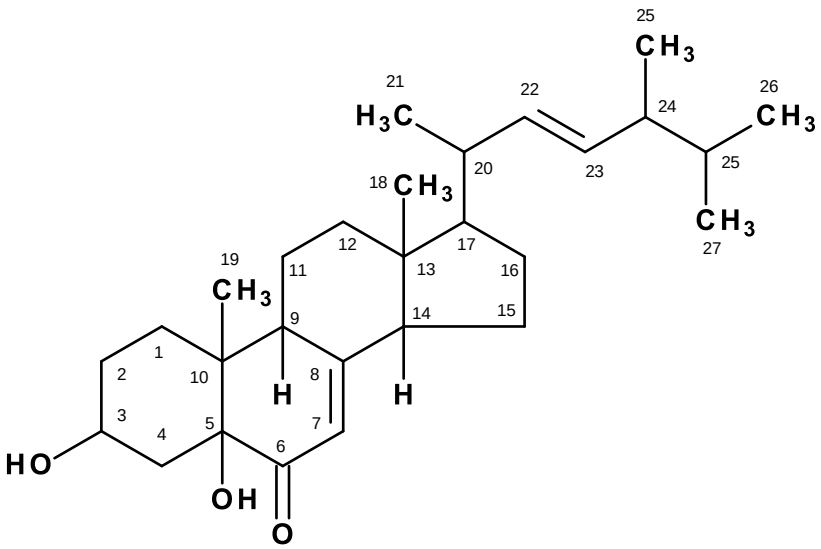

The ^{1}H and ^{13}C chemical shift values of **NT 2** are compatible with those of (3*β*, 22*E*)-3,5-dihydroxyergosta-7,22-dien-6-one; however, the absolute configuration of C-5 still needed to be unequivocally established.

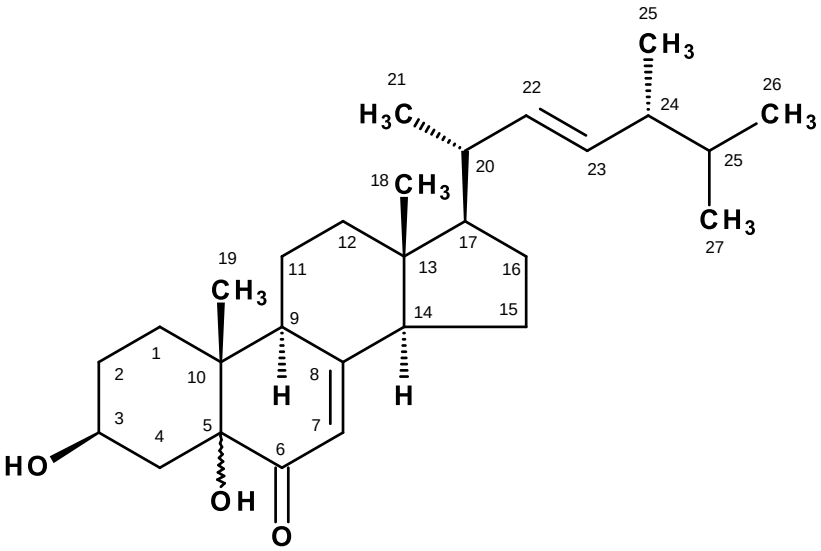

However, the information obtained from an extensive literature search could not provide an unambiguous conclusion of the stereochemistry of the hydroxyl group at C-5. Aiello *et al*. (1991), first described the isolation of five new 5α-hydroxy-6-keto-Δ^7sterols, including 24-methylcholesta-7, 22*E*-dien-3β, 5α-diol-6-one. Although they reported the ^{1}H NMR data of all the new compounds, the ^{13}C NMR data of only colesta-7-en-3*β*, 5*α*-diol-6-one (compound **1** in the reference) were presented. Interestingly, the authors suggested that, due to the low field chemical shift of H-3 (δ_H 4.03, *m*), the hydroxyl group on C-5 was in the α position. However, no rotation of this compound was reported. Later on, Ishizuka *et al*., (1997) reported the isolation of various sterols, including 3β, 5α-dihydroxy (22*E*, 24*R*)-ergosta-7, 22-dien-6-one (compound **6** in the reference) from the fruit bodies of an edible mushroom *Grifola frondosa* (Fr.) S.F. Gray (Polyporaceae). Although there were only ^{1}H NMR data for some key protons, the chemical shift values were similar to those of **NT 2**. Interestingly, the rotation of this compound was reported as dextrorotatory, $[\alpha]_D^{25}$ + 9.1 ($CHCl_3$, *c* = 0.1). Finally, the authors confirmed the structure of this compound by chemical transformation of ergosterol acetate by treatment with $Na_2Cr_2O_7$, followed by deprotection of 3-acetoxy group. Recently, Fangkratok *et al*., (2013) reported the isolation of (3β, 5α 22*E*)-3, 5-dihydroxyergosta-7, 22-dien-6-one from the extract of the mycelia of *Lentinus polychrous*, a Thai local edible mushroom. The ^{1}H and ^{13}C NMR data of this compound were very similar to those of **NT 2** except for the chemical shift value of C-10 which differs *ca.* 3.5 ppm [δ_C 36.6 in (3*β*, 5*α* 22*E*)-3,5-dihydroxyergosta-7,22-dien-6-one and

δ_C 40.5 in **NT 2**]. Furthermore, the sign of the rotation reported by Fangkratok *et al*., (2013) was levorotatory, $[\alpha]_D^{20}$ - 4.37 (EtOH, *c* = 0.01), which is opposite to that of **NT 2**, i. e. $[\alpha]_D^{20}$ + 60 ($CHCl_3$, *c* = 0.05). Moreover, the reference cited by Fangkratok *et al*., (2013) for (3β, 5α 22*E*)-3,5-dihydroxyergosta-7,22-dien-6-one (Zhao *et al*., 2010) did not present the structure of this compound.

In order to clarify the controversy related to the structure of (3*β*, 5*α* 22*E*)-3,5-dihydroxyergosta-7,22-dien-6-one, and to determine unequivocally the stereochemistry of the hydroxyl group at C-5 of **NT 2**, the absolute configuration of C-5 was determined by comparison of the experimental electronic circular dichroism (ECD) spectrum with the calculated ECD spectra. Conformational analysis of the C-5*S* and C-5*R* diastereoisomers of **NT 2**, by molecular mechanics (MMFF95 force field), resulted in similar lowest energy conformations for both compounds, with rings A and C having a chair conformation (Figure 72).

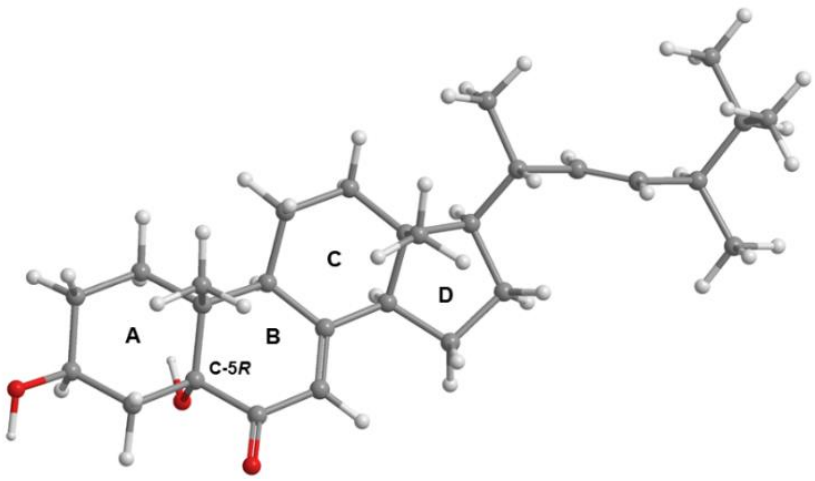

Figure 72. Most stable conformation of **NT 2** (C-5*R*). Rings A and C have a chair conformation

However, both model's conformational energies were further minimized by a DFT (density functional theory) method starting with ring A in chair conformation and also in boat conformation. This was considered necessary because rings A and B

house the main low energy UV and ECD chromophore groups, which may engage in intramolecular hydrogen bonds, depending on the particular conformation of ring A. The DFT minimization showed that the amount of energy released by the formation of intramolecular hydrogen bonds is not enough to stabilize the boat conformations. The chair conformations are more stable than its boat counterparts in excess of 2 kcal/mol (Gibbs energy in methanol), making it overwhelmingly predominant. As such, ECD spectra were calculated for the A-chair C-5*S* and C-5*R* diastereoisomers of **NT 2**, using a TD-DFT method. Figure 73 compares these spectra and shows how the calculated spectrum for the C-5*R* isomer fits the experimental data much better, providing enough evidence to conclude that **NT 2** is the C-5*R* diastereoisomer, rather than the C-5*S*.

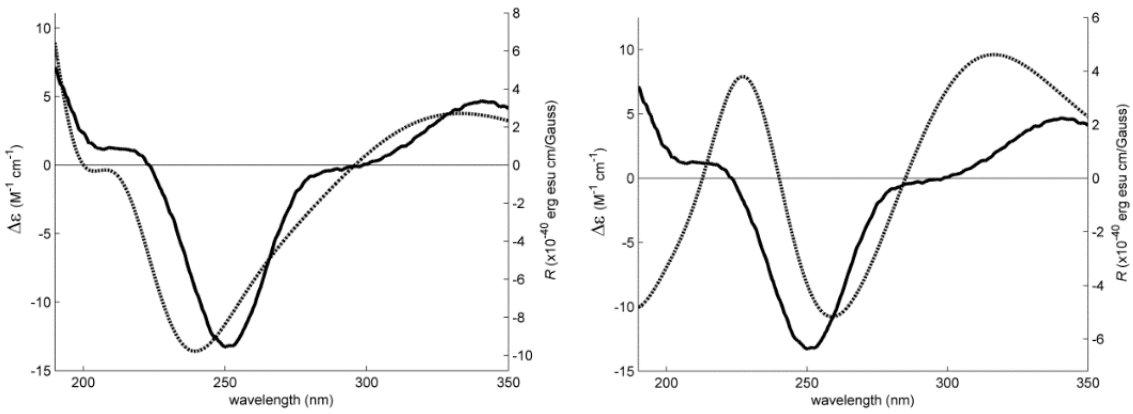

Figure 73. Experimental ECD spectrum (solid lines, left axes) of **NT 2** in methanol (equal on both sides). Simulated ECD spectra (dotted lines, right

Therefore, the structure of **NT 2** was unequivocally elucidated as (3*β*, 5*α*, 22*E*), 3,5-dihydroxyergosta-7,22-diene-6-one (Figure 74).

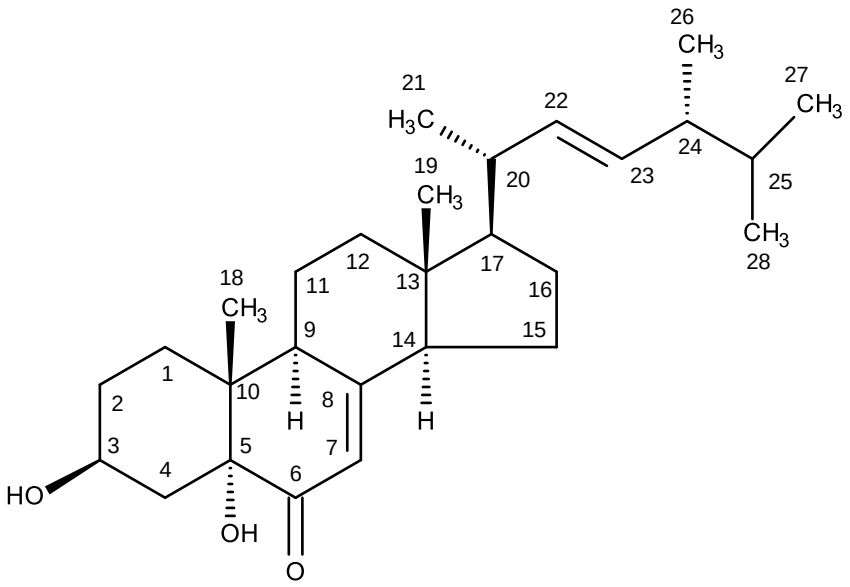

Figure 74. Structure of (3*β*, 5*α*, 22*E*), 3,5-dihydroxyergosta-7,22-diene-6-one **(NT 2)**

Table 4. ^{1}H and ^{13}C NMR (500 MHz and 125 MHz, $CDCl_3$,) and HMBC assignment for **NT 2**

Position	δ_C, type	δ_H, (*J* in Hz)	COSY	HMBC
1_α.	27.8 CH_2	1.70, *m*		
$_\beta$.		1.60 *m*		
2_α.	30.4 CH_2	1.60, *m*		
$_\beta$.		1.40, *m*		C-3
3.	67.5 CH	4.04, *m*	H-$2_{\alpha,\beta}$, $4_{\alpha,\beta}$	
4_α.	36.4 CH_2	2.10, *m*		C-3, 5, 6
$_\beta$.		1.60, *m*		C-3
5.	77.7 C			
6.	198.7 C			
7.	119.7 CH	5.63, *s*	H-5	C-5, 9, 14
8.	165.5 C			
9.	43.9 CH	2.53, *ddd* (11.8, 7.0, 2.2)	H-9, $11_{\alpha,\beta}$	C-6, 7, 8, 10, 19
10.	40.5 C			
11_α.	21.9 CH_2	1.72, *m*		
$_\beta$.		1.61, *m*		
12_α.	38.9 CH_2	2.10, *m*		
$_\beta$.		1.43, *m*		
13.	44.8 C			
14.	55.8 CH	2.13, *m*		C-7, 12, 13, 16, 18
15_α.	22.5 CH_2	1.35, *m*		
$_\beta$.		1.77, *m*		
16_α.	30.2 CH_2	1.87, *m*		
$_\beta$.		1.42, *m*		
17.	56.1 CH	1.35, *m*		
18.	12.7 CH_3	0.60, *s*		C-12, 13, 14, 17
19.	16.4 CH_3	0.94, *s*		C-1, 2, 5, 10
20.	40.2 CH	2.03, *m*		
21.	21.1 CH_3	1.03, *d* (6.6)	H-20, 21	C-17, 20
22.	135.0 CH	5.16, *dd* (15.3, 7.6)	H-20	C-17, 20, 21, 24
23.	132.5 CH	5.24, *dd* (15.3, 7.6)	H-22, 24	C-20, 24, 25, 26
24.	42.8 CH	1.85, *m*		
25.	33.1 CH	1.47, *m*		
26.	17.6 CH_3	0.92, *d* (6.8)	H-24	C-23, 24, 25
27.	19.9 CH_3	0.84, *d* (6.9)	H-25, 28	C-24, 25, 28
28.	19.6 CH_3	0.82, *d* (6.9)	H-25, 27	C-24, 25, 27

3.1.1.3. Byssochlamic acid (NT 3)

Compound **NT 3** was isolated as a white solid (mp, 171-172 ^{o}C) and its molecular formula $C_{18}H_{20}O_6$ was established on the basis of the (+)-HRESIMS *m/z* 333.1326 $[M+H]^+$ (calculated 333.1338 for $C_{18}H_{21}O_6$), indicating nine degrees of unsaturation. The ^{13}C NMR spectra displayed 18 carbon signals which, in combination with DEPTs and HSQC spectra (Table 5), revealed the presence of four conjugated ketone carbonyls (δ_C 165.4 C, 165.3 C, 164.9 C and 164.1 C), four non-protonated sp^2 (δ_C 146.2, 146.1, 145.0 and 144.2), two methine sp^3 (δ_C 47.9 and 40.8), six methylene sp^3 (δ_C 31.5, 27.9, 23.4, 22.0, 21.7 and 21.4) and two methyl (δ_C 13.9 and 12.9) carbons.

The ^{1}H NMR spectrum (Table 5), in conjunction with the HSQC spectrum, exhibited, besides three double doublets at δ_H 3.14 (*J* = 10.7, 2.4 Hz; δ_C 21.4), δ_H 2.90 (*J* = 13.0, 2.9 Hz; δ_C 27.9) and δ_H 2.27 (*J* =10.7, 2.9 Hz; δ_C 21.7), three triplets at δ_H 1.80 (*J* = 12.5 Hz; δ_C 27.9), δ_H 1.09 (*J* = 6.9 Hz; δ_C 12.9) and δ_H 0.86 (*J* = 7.3 Hz; δ_C 13.9), and multiplets at δ_H 2.50 (δ_C 40.8), H-5'a 2.15 (δ_C 31.5), 2.12 (δ_C 47.9), 2.11 (δ_C 23.4), 1.53 (δ_C 31.5), 1.15 (δ_C 22.0) and 1.04 (δ_C 23.4).

The COSY spectrum (Table 5) exhibited correlation from the methyl triplet at δ_H 0.86 (*J* = 7.3, Me-3'/δ_C 13.9) to the multiplet at δ_H 1.15 (H_2-4'/δ_C 22.0), the multiplet at δ_H 1.53 (H-5'b/δ_C 31.5) to H_2-4' and the multiplet at δ_H 2.15 (H-5'a/δ_C 31.5), the multiplet at δ_H 2.50 (H-7/δ_C 40.8) also gave cross peaks to H-5'a. The HMBC spectrum (Table 5) showed correlations from Me-3' to the carbon signals at δ_C 22.0 (C-4') and δ_C 31.5 (C-5'), H_2-4' to C-5' and C-7 (δ_C 40.8) while H-7 gave HMBC cross peaks to C-4', C-5' and the carbon signal at δ_C 164.1 (C-11). In addition, the double doublets at δ_H 2.90 (*J* = 13.0, 2.9 Hz, H-1a/ δ_C 27.9) exhibited HMBC correlations to the carbon signals at δ_C 145.0 (C-8) and 164.9 (C-10) while the triplet at δ_H 1.80 (*J* = 12.5 Hz, H-1b/ δ_C 27.9) displayed the HMBC correlations to the quaternary carbon at δ_C 144.2 (C-9), C-8 and C-10. Combination of the data obtained from the COSY and HMBC correlations led to the construction of a partial structure (fragment A) as shown in figure 75.

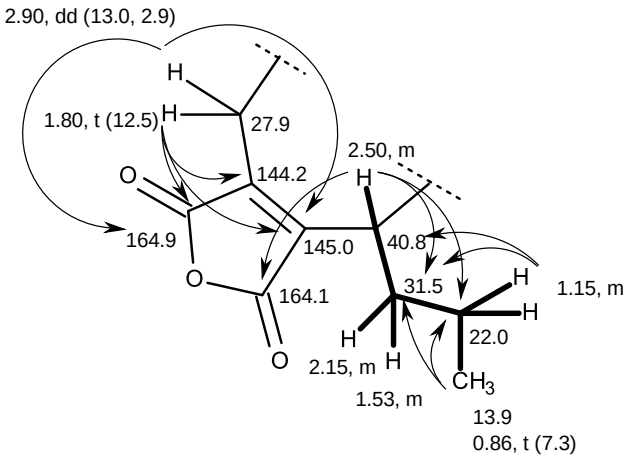

Figure 75. COSY (▬) and HMBC (⟶) correlations of fragment A

The COSY spectrum also showed correlations from the methyl triplet at δ_H 1.09 (*J* = 6.9 Hz, Me-1'/ δ_C 12.9) to the multiplets at δ_H 2.11 (H-2'a) and 1.04 (H-2'b/δ_C 23.4), and from H-2'b to the multiplet at δ_H 2.12 (H-2/δ_C 47.9), while the HMBC spectrum showed correlations from Me-1' to the carbon signals at δ_C 23.4 (C-2') and 47.9 (C-2). Moreover, the double doublet at δ_H 3.14 (*J* = 10.7, 2.4 Hz, H-3a/δ_C 21.4) displayed HMBC correlations to the carbon signals at δ_C 146.1 (C-5), δ_C 146.2 (C-4) and the carbonyl at δ_C 165.3 (C-12), while H-2 showed the HMBC correlation to C-4. In addition, the double doublet at δ_H 2.27 (*J* =10.7, 2.9 Hz, H_2-6/δ_C 21.7) showed HMBC correlations to C-4 and C-5 and the carbonyl carbon at δ_C 165.4 (C-13), respectively. The aforementioned COSY and HMBC correlations led to construction of another partial structure (fragment B) as shown in figure 76.

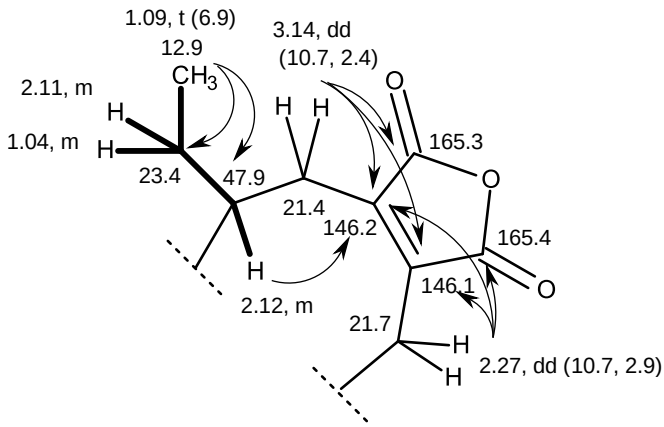

Figure 76. COSY (▬) and HMBC (⟶) correlations of fragment B

The HMBC correlations from H-1a of fragment A to C-2 and C-2' of fragment B, from H-7 of fragment A to C-5 and C-6 of fragment B, from H_2-6 of fragment B to C-8 of fragment A and the multiplet at δ_H 2.11 (δ_C 23.4), from H-2'a of fragment B to the methylene sp^3 δ_C 27.9 (C-1) of fragment A, corroborated the linkage of the two fragments through C-1 to C-2, and C-7 to C-8, thus completing the structure of **NT 3** (Figure 77).

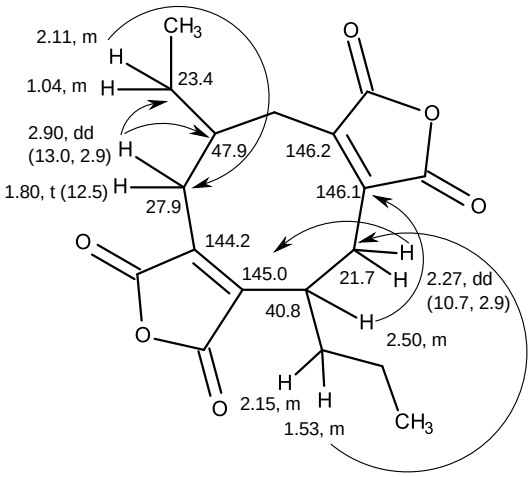

Figure 77. Key HMBC (⟶) correlations of fragment A and fragment B

From the above evidence, the structure of **NT 3** was elucidated as byssochlamic acid (Figure 78).

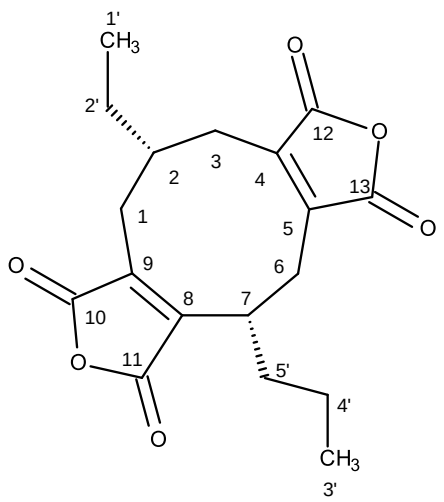

Figure 78. Structure of byssochlamic acid (**NT 3**)

Table 5. ^{1}H and ^{13}C NMR (300 MHz and 75 MHz, $CDCl_3$) and HMBC assignment for **NT 3**

Position	δ_C, type	δ_H, (*J* in Hz)	COSY	HMBC
1a	27.9 CH_2	2.90, *dd* (13.0, 2.9)	H-1b	C-2, 2', 8, 10
b		1.80, *t* (12.5)	H-1a	C-2, 7, 8, 9, 10
2	47.9 CH	2.12, *m*		C-4
3a	21.4 CH_2	3.14, *dd* (10.7, 2.4)	H-3b	C-4, 5, 12
b		2.26, *m*	H-3a	
4	146.2 C	-		
5	146.1 C	-		
6	21.7 CH_2	2.27, *dd* (10.7, 2.9)		C-4, 5, 8, 13
7	40.8 CH	2.50, *m*	H-5'a	C-4', 5, 5', 6, 11
8	145.0 C	-		
9	144.2 C	-		
10	164.9 C	-		
11	164.1 C	-		
12	165.3 C	-		
13	165.4 C	-		
1'	12.9 CH_3	1.09, *t* (6.9)		C-2, 2'
2'a	23.4 CH_2	2.11, *m*		C-1, 1', 4
b		1.04, *m*	H-2, 1', 2'a	C-1'
3'	13.9 CH_3	0.86, *t* (7.3)	H-4'	C-4', 5'
4'	22.0 CH_2	1.15, *m*		C-5', 7
5'a	31.5 CH_2	2.15, *m*		C-8
b		1.53, *m*	H-4', 5'a	C-6

This compound is a member of the nonadride family, which was first isolated from the fungus *Byssochlamys fulva* (Raistrick and Smith, 1933). In 2006, Li *et al*., reported the isolation of byssochlamic acid from an unidentified mangrove-derived

fungus (strain No. k38) from the South China Sea coast. This compound has been recently isolated from the marine sponge-associated fungus *Neosartorya fennelliae* strain KUFA 0811, which was collected from Samaesan Island, Amphur Sattahip, Chonburi Province, Thailand (Aung, 2017).

3.1.1.4. Hopane 3*β*,22-diol (NT 4)

Compound **NT 4** was isolated as white crystals (mp, 176-177°C). The ^{13}C NMR spectrum (Table 6) exhibited 30 carbon signals which, in combination with DEPT and HSQC spectra, can be categorized as one oxyquaternary sp^3 (δ_C 71.6), five quaternary sp^3 (δ_C 43.7, 41.4, 41.2, 38.5 and 36.6), one oxymethine sp^3 (δ_C 78.6), five methine sp^3 (δ_C 54.7, 53.8, 50.4, 49.8 and 49.4), ten methylene sp^3 (δ_C 41.0, 38.4, 34.0, 32.9, 27.1, 26.1, 23.7, 21.3, 20.6 and 18.0) and eight methyl (δ_C 30.8, 29.0, 28.2, 16.8, 16.4, 16.0, 15.9 and 15.7) carbons.

The ^{1}H NMR spectrum (Table 6), in combination with HSQC spectrum, exhibited a doublet of one hydroxyl proton at δ_H 4.30 (J = 5.2 Hz), one singlet of another hydroxyl proton at δ_H 3.83, a double double doublet (*ddd*) of one oxymethine proton at δ_H 2.97 (J =10.3, 5.7, 5.7 Hz; δ_C 76.8), another *ddd* of one methine sp^3 proton at δ_H 2.10 (J = 9.8, 9.8, 8.8 Hz; δ_C 50.4), eight methyl singlets at δ_H 1.07 (δ_C 30.8), 1.03 (δ_C 29.0), 0.92 (δ_C 16.4), 0.90 (δ_C 16.8), 0.88 (δ_C 28.2), 0.76 (δ_C 15.7), 0.71 (δ_C 16.0) and 0.66 (δ_C 15.9) and several overlapped multiplets at δ_H 0.6-1.7.

The HMBC spectrum (Table 6) displayed correlations from the hydroxyl proton at δ_H 4.30 (J = 5.2 Hz/OH-3) to the oxymethine sp^3 carbon at δ_C 78.6 (C-3), the quaternary sp^3 carbon at δ_C 38.5 (C-4) and the methylene sp^3 carbon at δ_C 27.2 (C-2), the methyl singlet at δ_H 0.88 (δ_C 28.2, Me-23) to C-3, the carbons at δ_C 38.5 (C-4) and δ_C 54.7 (C-5), from the methyl singlet at δ_H 0.66 (δ_C 15.9, Me-24) to C-3, C-4, C-5, from the methyl singlet at δ_H 0.76 (δ_C 15.7, Me-25) to the carbon δ_C 54.7 (C-5), the quaternary sp^3 carbon at δ_C 36.6 (C-10), the methine sp^3 carbon at δ_C 49.8 (C-9), the methylene sp^3 carbon at δ_C 38.4 (C-1), and from the methyl singlet at δ_H 0.92 (δ_C 16.4, Me-26) to C-9, the quaternary sp^3 carbons at δ_C 41.2 (C-8) and 41.4 (C-14) and the methylene sp^3 carbon at δ_C 32.9 (C-7). The number of methyl singlets, the coupling

constants of the oxymethine proton (H-3) and the HMBC correlations suggested the presence of a 2*β*-hydroxy-4,4,8,10-tetramethyltetradecahydrophenanthrene moiety as a partial structure in the molecule (Figure 79):

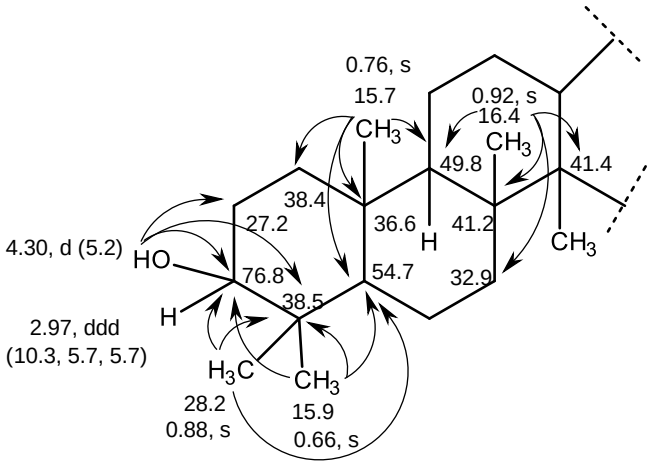

Figure 79. Key HMBC (⟶) correlations of 2β-hydroxy-4,4,8,10-tetramethyltetradecahydrophenanthrene moiety in **NT 4**

Moreover, the methyl singlet at δ_H 0.90 (δ_C 16.8, Me-27) also showed HMBC correlations to C-8, C-14, the methine sp^3 carbon at δ_C 49.4 (C-13) and the methylene sp^3 carbon at δ_C 34.0 (C-15), while the methyl singlet at δ_H 0.71 (δ_C 16.0, Me-28) exhibited HMBC cross peaks to C-13, the quaternary sp^3 carbon at δ_C 43.7 (C-18), the methine sp^3 carbon at δ_C 53.8 (C-17) and the methylene sp^3 carbon at δ_C 41.0 (C-19). Therefore, the 1,3-dimethylcyclohexane ring was fused with 2*β*-hydroxy- 4,4,8,10-tetramethyltetradecahydrophenanthrene at C-13 and C-14, extending the partial structure to the structure shown in figure 80:

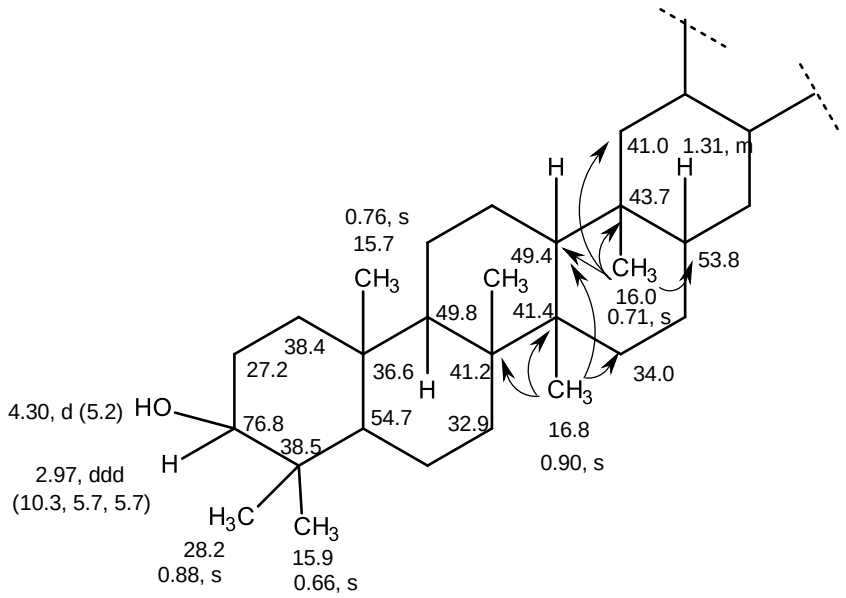

Figure 80. Key HMBC (⟶) correlations of the partial structure in **NT 4**

On the other hand, the methyl singlets at δ_H 1.07 (δ_C 30.8, Me-29) and δ_H 1.03 (δ_C 29.0, Me-30) showed HMBC correlations to the oxyquaternary sp^3 carbon at δ_C 71.6 (C-22) and the methine sp^3 carbon at δ_C 50.4 (C-21). Since the singlet at δ_H 3.83 (OH-22) also showed HMBC correlations to the carbons at δ_C 30.8 (C-29), δ_C 29.0 (C-30), C-21 and C-22, the presence of the 2-hydroxypropan-2-yl substituent was linked to C-21. The HMBC spectrum also displayed correlations from a multiplet at δ_H 1.31 (H-17/δ_C 53.8 49.4, C-13), to C-19, C-22 and C-22 (Figure 81).

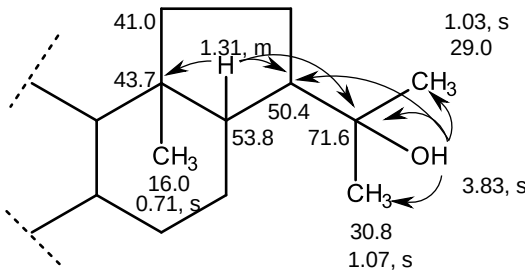

Figure 81. Key HMBC (⟶) correlations in the partial structure of **NT 4**

Table 6. ^{1}H and ^{13}C NMR (500 MHz and 125 MHz, $CDCl_3$) and HMBC assignment for **NT 4**

Position	δ_C, type	δ_H, (*J* in Hz)	COSY	HMBC
1α	38.4 CH_2	1.58, *m*	-	-
β		0.83, *m*	-	-
2	27.1 CH_2	1.44, *m*	-	-
3	78.6 CH	2.99, *ddd* (10.3, 5.7, 5.7)	-	-
4	38.5 C	-	-	-
5	54.7 CH	0.62, *d* (11.5)	H-6β	C-4, 24
6α	18.0 CH_2	1.45, *m*	-	C-8
β		1.32, *m*	-	-
7α	32.9 CH_2	1.40, *m*	-	-
β		1.15, *m*	H-6α, 7α	C-5
8	41.2 C	-	-	-
9	49.8 CH	1.18, *m*	-	-
10	36.6 C	-	-	-
11α	20.6 CH_2	1.40, *m*	-	-
β		1.27, *m*	H-9	-
12α	23.7 CH_2	1.58, *m*	-	-
β		0.83, *m*	H-11α	-
13	49.4 CH	1.31, *m*	-	C-18
14	41.4 C		-	
15α	34.0 CH_2	1.30, *m*	H-16α, β	C-8
β		1.14, *m*		
16α	21.3 CH_2	1.91, *d* (12.5)	-	-
β		1.53, *m*		
17	53.8 CH	1.32, *m*	-	C-18, 21, 22
18	43.7 C	-	-	
19α	41.0 CH_2	1.43, *m*	-	C-17, 21
β		0.86, *m*		
20	26.1 CH_2	1.61, *m*	-	-
21	50.4 CH	2.10, *ddd* (9.8, 9.8, 8.8)	-	-
22	71.6 C		-	-
23	28.2 CH_3	0.88, *s*	-	C-3, 4, 5
24	15.9 CH_3	0.66, *s*	-	C- 3,4, 5
25	15.7 CH_3	0.76, *s*	-	C-1, 5, 9, 10
26	16.4 CH_3	0.92, *s*	-	C-8, 9, 14
27	16.8 CH_3	0.90, *s*	-	C-8, 14
28	16.0 CH_3	0.71, *s*	-	C-13, 17, 18
29	30.8 CH_3	1.07, *s*		C-21, 22, 30
30	29.0 CH_3	1.03, *s*		C-21, 22, 29
	OH-3	4.3, *d* (5.2)		C-2, 3, 4
	OH-22	3.83, *s*		C-21, 22, 29, 30

The number of carbon atoms and HMBC correlations confirmed that **NT 4** is a hopane triterpene with the hydroxyl groups on C-3 and C-22. Therefore, the planar structure of **NT 4** is established as shown in figure 82.

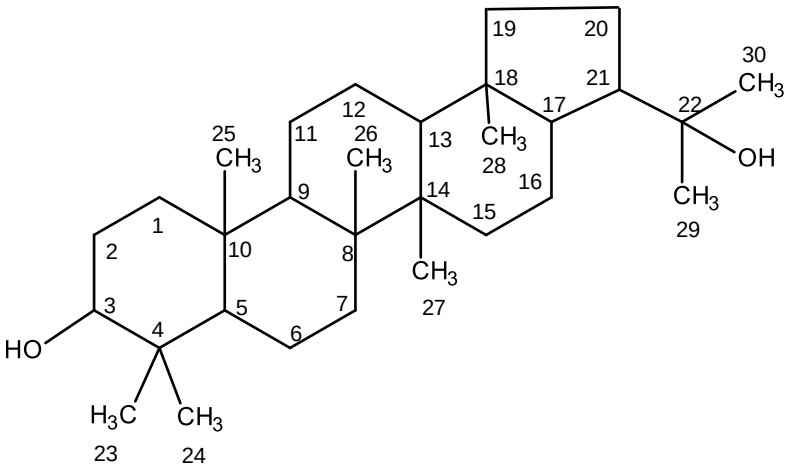

Figure 82. The planar structure of **NT 4**

In order to confirm the stereochemistry of **NT 4**, X-ray analysis was performed and the ORTEP view is shown in figure 83.

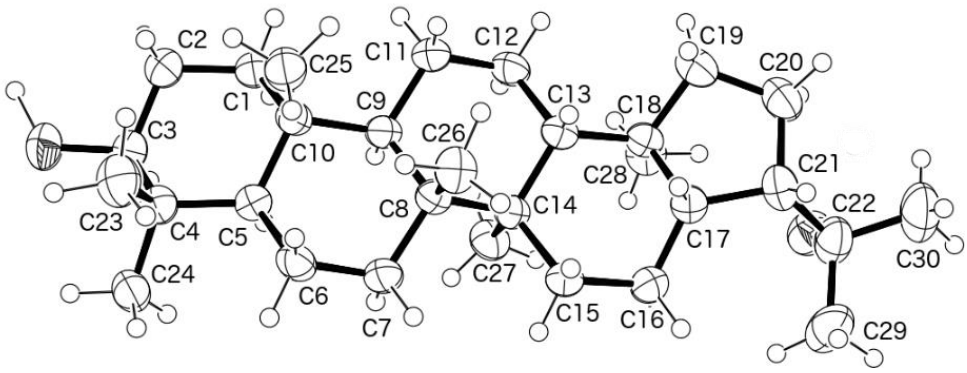

Figure 83. ORTEP view of **NT 4**

Therefore, the structure of **NT 4** was established as hopan-3*β*, 22-diol (Figure 84).

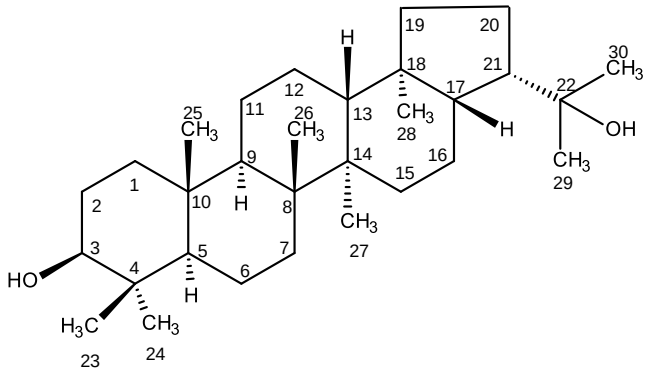

Figure 84. Structure of hopan-3*β*, 22-diol (**NT 4**)

Literature search revealed that hopan-3*β*, 22-diol has been previously reported from the bacterium *Acetobacter pasteuriunum* (Rohmer *et al*., 1980) and also from the stem bark of *Abies veitchii* (Tanaka and Matsunaga, 1992). Later on, the same group has described the same compound from the bark of *Abies mariesii* (Tanaka *et al*., 1994).

3.1.1.5. Chevalone C (NT 5)

Compound **NT 5** was isolated as a white solid (mp 198-201 °C). The ^{13}C NMR spectrum showed 28 carbon signals which, in combination with DEPT and HSQC spectra (Table 7), can be categorized as one conjugated ketone carbonyl (δ_C 180.7), one ester carbonyl (δ_C 171.0), three non-ptotonated sp^2 (δ_C 162.8, 160.8 and 98.5), one methine sp^2 (δ_C 111.8), four methine sp^3 (δ_C 80.6, 60.2, 55.4 and 52.2), four quaternary sp^3 (δ_C 84.4, 37.8, 37.3 and 37.0), seven methylene sp^3 (δ_C 40.9, 40.0, 38.0, 23.5, 18.7, 17.8 and 15.4) and seven methyl (δ_C 27.9, 21.3, 20.5, 19.3, 16.5, 16.4 and 16.1) carbons.

The ^{1}H NMR spectrum, in conjunction with the HSQC spectrum (Table 7), exhibited the signals of one olefinic proton at δ_H 6.03, *s* (δ_C 111.8), one oxymethine proton at δ_H 4.47, *dd* (*J* = 11.1, 5.0 Hz, δ_C 80.6), three methine protons at δ_H 1.52, *dd* (*J* = 12.5, 4.9 Hz, δ_C 52.2), 0.95, *d* (*J* = 11.9 Hz, δ_C 60.2) and 0.88, *d* (*J* = 9.9 Hz, δ_C 55.4), seven methylene groups at δ_H 2.55, *dd*, *J* = 16.3, 4.9 Hz and 2.12, *dd*, *J* = 16.2,

3.7 (δ_C 15.4); 2.11, *dd*, *J* = 8.2, 3.9 Hz and 1.68, *m* (δ_C 40.0); 1.90, *ddd*, *J* = 12.8, 3.0, 3.0 Hz and 1.04, *m* (δ_C 40.9); 1.73, *dd*, *J* = 15.5, 3.2 Hz and 1.35, *dd*, *J* = 12.0, 3.0 Hz (δ_C 18.7); 1.72, *m* and 1.08, *m* (δ_C 38.0); 1.65, *m* and 1.61,*m* (δ_C 23.5) and 1.59, *m* and 1.47, *m* (δ_C 17.8) and six methyl singlets at δ_H 2.21 (δ_C 19.3), 2.05 (δ_C 21.3), 1.29 (δ_C 20.5), 0.89 (δ_C 16.1), 0.87 (δ_C 16.4) and 0.86 (6H, δ_C 27.9 and 16.5).

The COSY spectrum (Table 7) exhibited cross peaks from the oxymethine proton signal at δ_H 4.47, *dd* (*J* = 11.1, 5.0 Hz, H-3/δ_C 80.6) to the signal of the methylene protons at δ_H 1.65, *m* (H_2-2/δ_C 23.5), while the HMBC spectrum (Table 7) displayed correlations from H-3 to the carbons at δ_C 171.0 (CO; OAc-3), 38.0 (C-1), 23.5 (C-2), 27.9 (C-23) and 16.5 (C-22), from the methyl protons at δ_H 2.05, *s* (Me-OAc/δ_C 21.3) to the carbonyl carbon at δ_C 171.0 (CO-3), from the methylene protons at δ_H 1.72, *m* (H_2-1/δ_C 38.0) to C-3, C-5 and the carbon at δ_C 37.0 (C-10), as well as from the methyl protons at δ_H 0.86, *s* (Me-22/ δ_C 16.5) to C-3, C-4 and C-5. Furthermore, the HMBC spectrum also showed correlations from the methyl protons at δ_H 0.87, *s* (Me-24/δ_C 16.4) to C-5, C-10 and the carbon at δ_C 60.2 (C-9), the methylene proton at δ_H 1.90, *ddd*, (*J* = 12.8, 3.0, 3.0 Hz, H-7/δ_C 40.9) to C-5, C-9 and the carbon at δ_C 37.3 (C-8), and the methyl protons at δ_H 0.89, *s* (Me-25/δ_C 16.1) C-7, C-8 and C-9. Taking together the COSY and HMBC correlations, it was clear that **NT 5** had the 1,1,4a,6-tetramethyldecahydronaphthalen-2-yl acetate (Figure 85) as a partial structure.

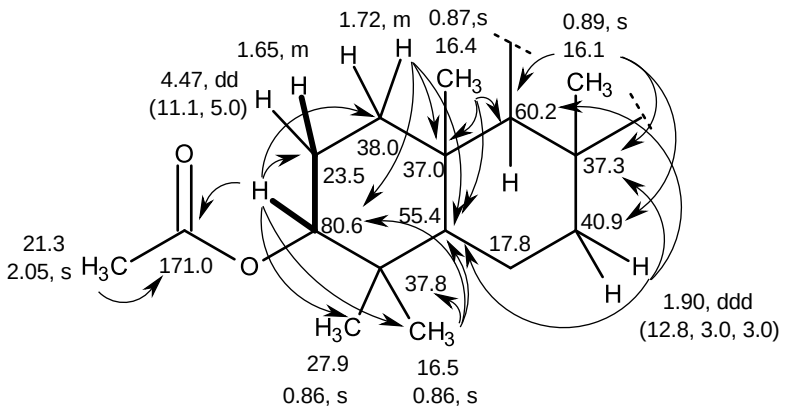

Figure 85. COSY (▬) and HMBC (⟶) correlations of the 1,1,4a,6-tetramethyldecahydronaphthalen-2-yl acetate moiety of **NT 5**

Moreover, the COSY spectrum (Table 7) also showed correlations from the methylene proton at δ_H 1.35, *dd* (*J* = 12.0, 3.0 Hz, H-11b/δ_C 18.7) to the methine proton at δ_H 0.95, *d* (*J* = 11.9 Hz, H-9/δ_C 60.2), the proton at δ_H 2.11, *dd*, (*J* = 8.2, 3.9 Hz, H-12a/δ_C 40.0) to another methylene proton at δ_H 1.73, *dd* (*J* = 15.5, 3.2 Hz, H-11a/δ_C 18.7). The HMBC spectrum (Table 7) also showed correlations from the methine proton at δ_H 1.52, *dd* (*J* = 12.5, 4.9 Hz, H-14/δ_C 52.2) to C-8 and the carbons at δ_C 84.4 (C-13) and δ_C 20.5 (C-26), the methyl protons at δ_H 1.29, *s* (Me-26/δ_C 20.5) to C-13 and the carbons at δ_C 40.2 (C-12) and δ_C 52.2 (C-14) and the methyl protons at δ_H 0.89, *s* (Me-25/δ_C 16.1) to C-14.

In addition, the singlet of the olefinic proton at δ_H 6.03 (H-18/δ_C 111.8) also showed HMBC correlations to the carbons at δ_C 19.3 (C-20), 98.5 (C-16) and 160.6 (C-19), from the methyl protons at δ_H 2.21 (Me-20/δ_C 19.3, C-20) to the carbons at δ_C 111.8 (C-18) and C-19, as well as from the methylene proton at δ_H 2.55, *dd* (*J* = 16.3, 4.9 Hz, H-15a/ δ_C 15.4 to C-12, C-14, C-16 and the carbons at 162.8 (C-21) and δ_C 180.7 (C-17), and from another methylene proton at δ_H 2.12, *dd* (*J* = 16.2, 3.7 Hz, H-15b/δ_C 15.4) to C-14, C-16 and C-21. These COSY and HMBC correlations, therefore, suggested the presence of the 2,6,9a-trimethyl-5a,6,7,8,9,9a-hexahydro-4*H*,5*H*-pyrano[2,3-*b*] chromen-4-one moiety (Figure 86) as another partial structure of **NT 5**.

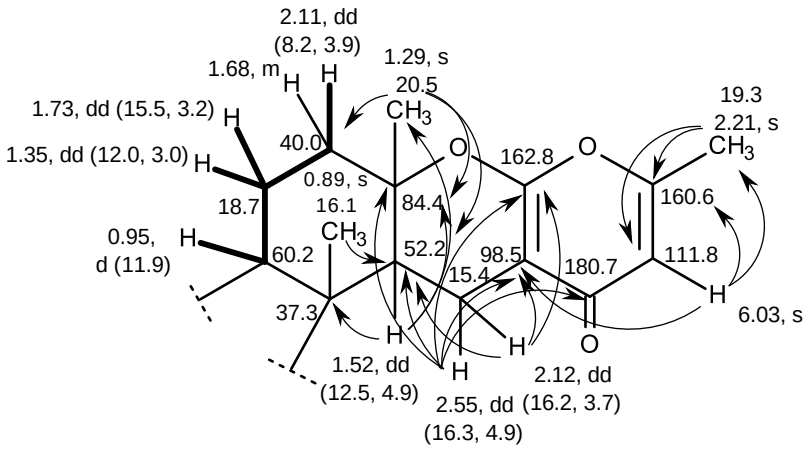

Figure 86. COSY (▬) and HMBC (⟶) correlations in the 2,6,9a-trimethyl-5a,6,7,8,9,9a-hexahydro-4*H*,5*H*-pyrano[2,3-*b*]chromen-4-one moiety of **NT 5**

That the 1,1,4a,6-tetramethyldecahydronaphthalen-2-yl acetate moiety was linked to the 2,6,9a-trimethyl-5a,6,7,8,9,9a-hexahydro-4*H*,5*H*-pyrano[2,3-*b*]chromen-4-one moiety was supported by the HMBC correlations from the proton at δ_H 0.95, *d* (*J* = 11.9 Hz,H-9/ δ_C 60.2) to C-8, C-10, C-14 and the carbons at δ_C 16.1 (C-25) and δ_C 16.4 (C-24), thus confirming the connectivity between the two moieties. Taking together the ^{1}H and ^{13}C chemical shift values, the COSY and HMBC correlations, the planar structure of **NT 5** was elucidated as shown in figure 87.

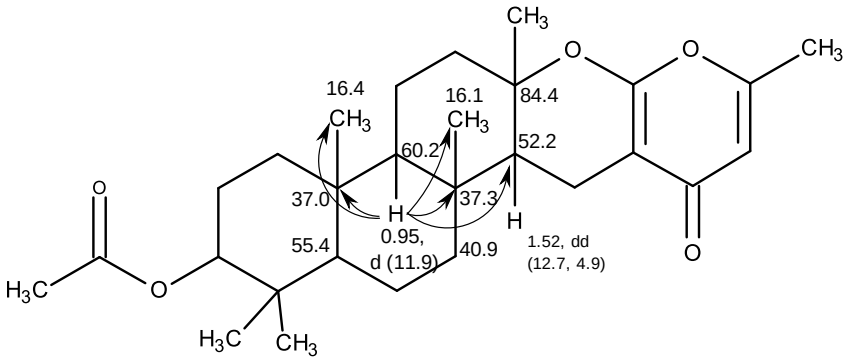

Figure 87. Key HMBC (⟶) correlations in **NT 5**

The ^{1}H, ^{13}C NMR chemical shift values and other physical data, including the signal of the optical rotation, of **NT 5** were in agreement with those reported for chevalone C, a meroditerpenoid isolated from several fungal species from our laboratory, including *Neosartoyra tsunodae* (Eamvijarn *et al*., 2013), *N. siamensis* (Gomes *et al*., 2014) and *Aspergillus similanensis* KUFA 0013 (Prompanya C., 2018).

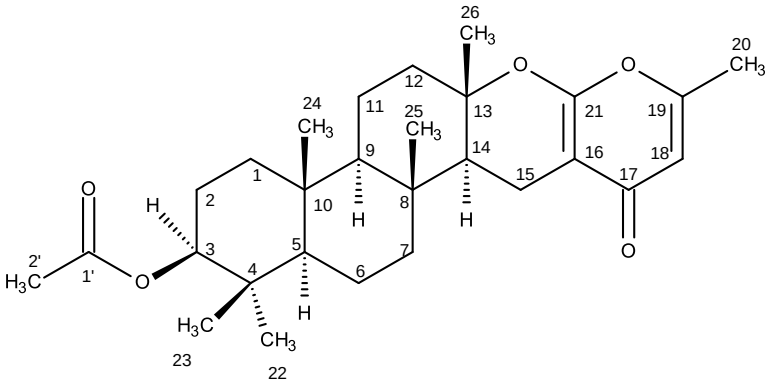

Figure 88. Structure of chevalone C (**NT 5**)

Table 7. ^{1}H and ^{13}C NMR (300 MHz and 75 MHz, DMSO-d_6) and HMBC assignment for **NT 5**

Position	δ_C, type	δ_H, (*J* in Hz)	COSY	HMBC
1a	38.0 CH_2	1.72, *m*	-	C-3, 5, 10
b		1.08, *m*	-	-
2a	23.5 CH_2	1.65, *m*	-	-
b		1.61, m		
3	80.6 CH	4.47, *dd* (11.1, 5.0)	H-2a	C-1, 2, 22, 23, 1’
4	37.8 C	-	-	-
5	55.4 CH	0.88, *d* (9.9)	-	C-1, 3, 7, 9, 22, 23, 24
6a	17.8 CH_2	1.59, *m*	-	-
b		1.47, *m*	-	-
7a	40.9 CH_2	1.90, *ddd* (12.8, 3.0, 3.0)	-	C-5, 8, 9
b		1.04, *m*	-	C-25
8	37.3 C	-	-	-
9	60.2 CH	0.95, *d* (11.9)	-	C-8, 10, 14, 24, 25
10	37.0 C	-	-	-
11a	18.7 CH_2	1.73, *dd* (15.5, 3.2)	-	-
b		1.35, *dd* (12.0, 3.0)	H-9	-
12a	40.0 CH_2	2.11, *dd* (8.2, 3.9)	H-11	-
b		1.68, *m*	-	-
13	84.4 C	-	-	-
14	52.2 CH	1.52, *dd* (12.5, 4.9)	-	C-8, 13, 26
15a	15.4 CH_2	2.55, *dd* (16.3, 4.9)	H-14	C-13, 14, 16, 17, 21
b		2.12, *dd* (16.2, 3.7)	-	C-14, 16, 21
16	98.5 C	-	-	-
17	180.7 C	-	-	-
18	111.8 CH	6.03, *s*	H-20	C16, 19, 20
19	160.6 C	-	-	-
20	19.3 CH_3	2.21, *s*	-	C-18, 19
21	162.8 C	-	-	-
22	16.5 CH_3	0.86, *s*	-	C-3, 4, 5
23	27.9 CH_3	0.86, *s*	-	C-3, 4, 5
24	16.4 CH_3	0.87, *s*	-	C- 5, 9, 10
25	16.1 CH_3	0.89, *s*	-	C-7, 8, 9, 14
26	20.5 CH_3	1.29, *s*	-	C-12, 13, 14
1’	171.0 C	-	-	-
2’	21.3 CH_3	2.05, *s*	-	C-1’

Chevalone C was also reported from other fungi such as *Eurotium chevalieri* (Kanokmedhakul *et al*., 2011), *N. spinosa* KKU-1NK1 (Rajachan *et al*., 2016) and also from two members of the genus *Xylaria*, i. e. *Xylaria* cf. *cubensis* PK108 (Sawadsitang *et al*., 2015) and *Xylaria humosa* (Sodngam *et al*., 2013).

3.1.1.6. Sartorypyrone B (NT 6)

Compound **NT 6** was isolated as yellow viscous mass, and its molecular formula $C_{30}H_{42}O_7$ was established on the basis of the (+)-HRESIMS *m/z* 515.3018, (calculated 515.3009 for $C_{30}H_{43}O_7$), indicating ten degrees of unsaturation. The ^{13}C NMR spectrum (Table 8) displayed 30 carbon signals which can be identified, in combination with DEPT and HSQC spectra (Table 8), as one carbonyl of a conjugated ketone (δ_C 180.7), two ester carbonyls (δ_C 170.7 and δ_C 170.2), three non-protonated sp^2 (δ_C 162.7, 160.7, 98.4), one methine sp^2 (δ_C 111.8), one oxyquaternary sp^3 (δ_C 84.2), three quaternary sp^3 (δ_C 37.4, 37.3, 36.9), two oxymethine sp^3 (δ_C 77.7, 69.4), three methine sp^3 (δ_C 60.8, 55.3, 52.3), six methylene sp^3 (δ_C 41.7, 40.8, 40.0, 18.8, 17.6, 15.3) and eight methyl (δ_C 28.9, 21.3, 20.9, 20.5, 19.2, 17.4, 17.0, 16.3) carbons.

The ^1H NMR spectrum (Table 8), together with the HSQC spectrum, exhibited a singlet of an olefinic proton at δ_H 6.01 (δ_C 111.8), two double doublets of methine protons at δ_H 5.33 (*J* =7.2, 3.7 Hz; δ_C 69.4) and 1.49, (*J* = 12.7, 5.0 Hz; δ_C 52.3), a doublet of the methine proton at δ_H 4.58 (*J* = 3.9 Hz; δ_C 77.7), two multiplets of methine protons at δ_H 0.99 (δ_C 55.3) and δ_H 0.91 (δ_C 60.8), five double doublets of methylene protons at δ_H 2.52, (*J* = 16.4, 4.9 Hz; δ_C 15.3), δ_H 2.12, (*J* = 16.4, 11.4 Hz; δ_C 15.3), δ_H 2.05, (*J* = 14.7, 3.6 Hz; δ_C 41.7), δ_H 1.59, (*J* = 11.1, 2.8 Hz; δ_C 17.6) and δ_H 1.33, (*J* = 14.7, 3.6 Hz; δ_C 41.7), a doublet of methylene proton δ_H 1.90, (*J* = 12.9 Hz; δ_C 40.8), five multiplets of methylene protons at δ_H 2.11 (δ_C 40.0), δ_H 1.69 (δ_C 18.8), 1.65 (δ_C 40.0), δ_H 1.38 (δ_C 18.8) and δ_H 1.06 (δ_C 40.8) and eight methyl singlets at δ_H 2.19 (δ_C 19.2), δ_H 2.03 (δ_C 21.3), δ_H 2.00 (δ_C 20.9), δ_H 1.27 (δ_C 20.5), δ_H 1.10 (δ_C 17.0), δ_H 1.03 (δ_C 17.4), δ_H 0.89 (δ_C 16.3) and δ_H 0.87 (δ_C 28.9).

The COSY spectrum (Table 8) exhibited correlations from the double doublet of the methylene proton at δ_H 2.05, (*J* = 14.7, 3.6 Hz, H-1β/ δ_C 41.7) and the doublet of the methine proton at δ_H 4.58, (*J* = 3.9 Hz, H-3/δ_C 77.7) to the double doublet of the methine proton at δ_H 5.33, (*J* =7.2, 3.7 Hz, H-2/ δ_C 69.4). The HMBC spectrum (Table 8) showed correlations from H-2 to the ester carbonyl at δ_C 170.2 (C-1''), the quaternary sp^3 carbon at δ_C 37.4 (C-4), the methine sp^3 carbon at δ_C 77.7 (C-3), and the methylene sp^3 carbon at δ_C 41.7 (C-1), from H-3 to the carbonyl carbon at δ_C 170.7 (C-1'), the carbons at δ_C 69.4 (C-2) and C-4, the two methyl carbons at δ_C 28.9 (C-22) and 17.4 (C-23), whereas the two methyl singlets at δ_H 1.03 (Me-23/δ_C 17.4) and δ_H 0.87 (Me-22/δ_C 28.9) displayed cross peaks to C-3, C-4, and the carbon at δ_C 55.3 (C-5), from the methyl singlets at δ_H 2.03 (OAc, δ_C 21.3) and 2.00 (OAc, δ_C 20.9) to C-1" and C-1', respectively. Moreover, the COSY spectrum also revealed the coupling of the double doublets of the methylene proton at δ_H 1.59, (*J* = 11.1, 2.8 Hz/H-6, δ_C 17.6) to the doublet at δ_H 1.90 (*J* = 12.9 Hz/H-7α, δ_C 40.8), a multiplet at δ_H 1.06 (H-7β/δ_C 40.8) and a multiplet at δ_H 0.99 (H-5/δ_C 55.3). These correlations suggested the presence of the 1,1,4a,6-tetramethyldecahydronaphthalene-2,3-diyl diacetate moiety (Figure 89).

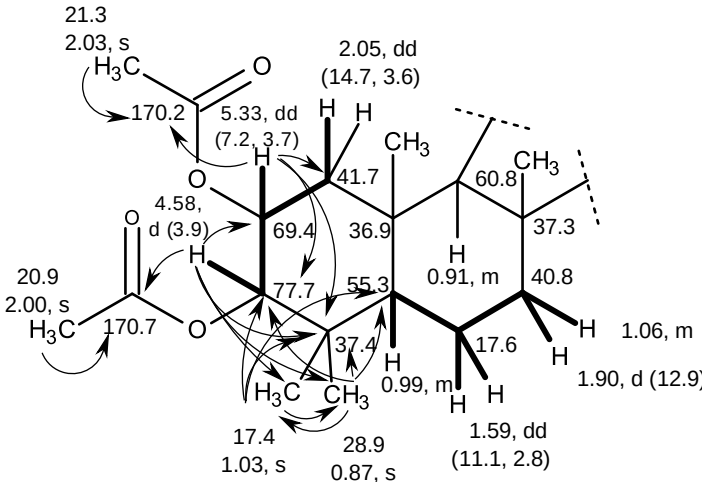

Figure 89. Key COSY (▬) and HMBC (⟶) correlations in the 1,1,4a,6-tetramethyldecahydronaphthalene-2,3-diyl diacetate portion of **NT 6**

Additionally, the COSY spectrum also exhibited correlations from the multiplet at δ_H 1.69 (H-11, δ_C 18.8) to the multiplet at δ_H 0.91 (H-9/δ_C 60.8) and the multiplet at δ_H 2.11 (H-12, δ_C 40.0), from the double doublet at δ_H 1.49, (*J* = 12.7, 5.0 Hz/H-14, δ_C 52.3) to the double doublets at δ_H 2.52 (*J* = 16.4, 4.9 Hz/H-15α, δ_C 15.3) and δ_H 2.12, (*J* = 16.4, 11.4 Hz/H-15β, δ_C 15.3), as well as from a singlet of the olefinic proton at δ_H 6.01 (H-18/δ_C 111.8) to the methyl singlet at δ_H 2.19 (H-20/δ_C 19.2). Moreover, the HMBC spectrum also exhibited correlations from H-18 to the carbons at δ_C 160.7 (C-19), 98.4 (C-16) and 19.2 (C-20), from H-15α to C-16 and the carbons at δ_C 180.7 (C-17), 162.7 (C-21), 84.2 (C -13) and 52.3 (C-14), from of methine proton at δ_H 1.49, *dd* (*J* = 12.7, 5.0 Hz/H-14, δ_C 52.3) to C-13 and the carbons at δ_C 37.3 (C-8) and 20.5 (C-26). The HMBC spectrum also showed cross peaks from the methyl singlet at δ_H 1.27 (Me-26/δ_C 20.5) to C-13, C-14 and the carbons at δ_C 40.0 (C-12), suggesting the presence of the 2,6,9a-trimethyl-5a,6,7,8,9,9a-hexahydro-4*H*,5*H*-pyrano[2,3-*b*]chromen-4-one moiety (Figure 90).

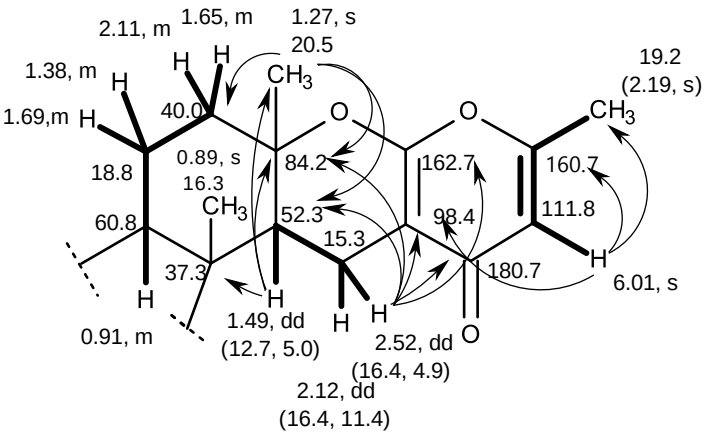

Figure 90. Key COSY (▬) and HMBC (⟶) correlations in the 2,6,9a-trimethyl-5a,6,7,8,9,9a-hexahydro-4*H*,5*H*-pyrano[2,3-*b*]chromen-4-one portion of **NT 6**

That the 1,1,4a,6-tetramethyldecahydronaphthalene-2,3-diyl diacetate moiety linked to the 2,6,9a-trimethyl-5a,6,7,8,9,9a-hexahydro-4*H*,5*H*-pyrano[2,3-*b*]chromen-4-one moiety was supported by the HMBC correlations from the methyl singlet at δ_H 0.89 (Me-25/δ_C 16.3) to C-8 and the carbons at δ_C 60.8 (C-9) and δ_C 40.8 (C-7), as well as from H-11 (δ_H 1.38*, m,* δ_C 18.8) to the quaternary sp^3 carbon at δ_C 36.9 (C-10) (Figure 91).

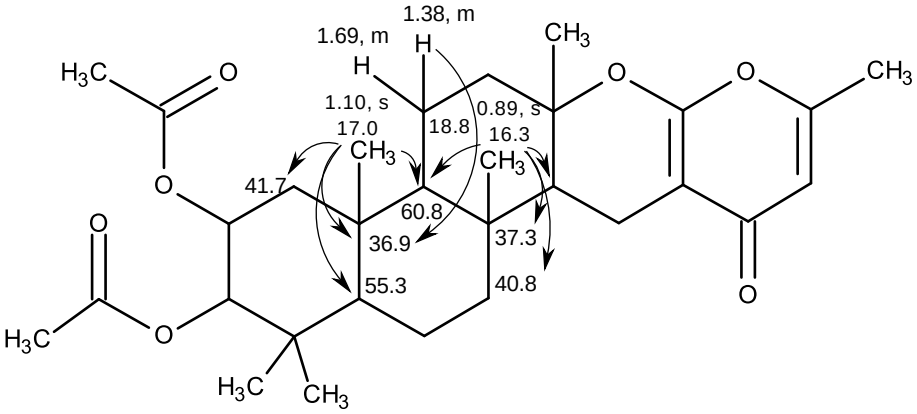

Figure 91. Key HMBC (⟶) correlations in **NT 6**

The ^{1}H and ^{13}C NMR data, together with the COSY and HMBC correlations, allowed the formulation of the structure of **NT 6** as sartorypyrone B (Figure 92). The identity of **NT 6** was confirmed by comparison of its NMR and other physical data with those of sartorypyrone B from the literature (Eamvijarn *et al*., 2013) as well as by co-elution with the authentic sample on TLC.

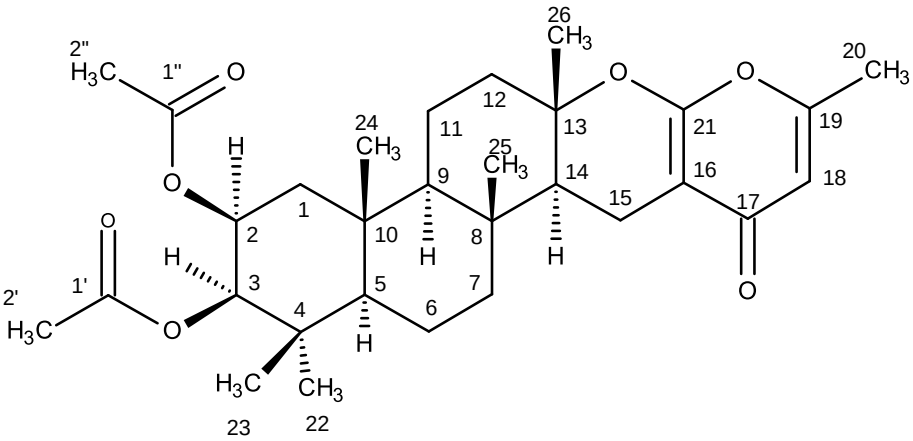

Figure 92. Structure of sartorypyrone B (**NT 6**)

Table 8. ^{1}H and ^{13}C NMR (300 MHz and 75 MHz, $CDCl_3$) and HMBC assignment for **NT 6**

Position	δ_C, type	δ_H, (*J* in Hz)	COSY	HMBC
1α	41.7 CH_2	1.33, *dd* (14.7, 3.6)	H-2	
β		2.05, *dd* (14.7, 3.6)	H-2	
2	69.4 CH	5.33, *dd* (7.2, 3.7)	H-1α, 3	C-1, 3, 4, 1''
3	77.7 CH	4.58, *d* (3.9)	H-2	C-1, 2, 4, 22, 23
4	37.4 C			
5	55.3 CH	0.99, *m*		C-23
6	17.6 CH_2	1.59, *dd* (11.1, 2.8)	H-5	
7α	40.8 CH_2	1.90, *d* (12.9)	H-6, 7β	
β		1.06, *m*		
8	37.3 C			
9	60.8 CH	0.91, *m*		
10	36.9 C			
11a	18.8 CH_2	1.38, *m*	H-9	C-10
b		1.69, *m*	H-9, 12b	
12a	40.0 CH_2	1.65, m	H-11b, 12b	C-13
b		2.11, m	H-12a	
13	84.2 C			
14	52.3 CH	1.49, *dd* (12.7, 5.0)	H-15α ,β	C-8, 13, 26
15α	15.3 CH_2	2.52, *dd* (16.4, 4.9)	H-14, 15β	C-13,14, 16, 17, 21
β		2.12, *dd* (16.4, 11.4)	H-14	C-14, 16
16	98.4 C			
17	180.7 C			
18	111.8 CH	6.01, *s*	H-20	C-16, 19, 20
19	160.7 C			
20	19.2 CH_3	2.19, *s*		C-18, 19
21	162.7 C			
22	28.9 CH_3	0.87, *s*		C-3, 4, 5, 23
23	17.4 CH_3	1.03, *s*		C-3, 4, 5, 22
24	17.0 CH_3	1.10, *s*		C-1, 5, 9, 10
25	16.3 CH_3	0.89, *s*		C-7, 8, 9, 14
26	20.5 CH_3	1.27, *s*		C-12, 13, 14
1'	170.7 C			
2'	20.9 CH_3	2.00, *s*		C-1'
1''	170.2 C			
2''	21.3 CH_3	2.03, *s*		C-1''

Sartorypyrone B (**NT 6**) is an analogue of chevalone C (**NT 5**), which was also isolated from the extract of this fungus. Sartorypyrone B was first reported from the ethyl acetate extract of the culture of *N. tsunodae* KUFC 9213. This compound exhibited strong growth inhibitory activity against three human cancer cell lines, i. e. MCF-7 (breast adenocarcinoma), NCI-H460 (non-small cell lung cancer) and A375-C5 (melanoma) (Eamvijarn *et al*., 2013).

3.1.1.7. Helvolic acid (NT 7)

Compound **NT 7** was isolated as a white solid (mp, 209-210 ^{o}C). The ^{13}C NMR spectrum (Table 9) showed 31 carbon signals which can be categorized, through a combination with DEPTs and HSQC spectra, as two ketone carbonyls (δ_C 208.8 and 201.4), one carboxyl carbonyl (δ_C 173.8), two ester carbonyls (δ_C 170.0 and 168.9), three methine sp^2 (δ_C 157.3, 127.8 and 122.8), six methine sp^3 (δ_C 73.8, 73.5, 49.5, 47.2, 41.7 and 40.4), three quaternary sp^3 (δ_C 52.7, 46.6 and 38.2), five methylene sp^3 (δ_C 40.7, 28.6, 28.4, 25.9, 23.9) and eight methyl (δ_C 27.5, 25.8, 20.7, 20.6, 18.3, 17.9, 17.8 and 13.1) carbons.

The ^{1}H NMR spectrum, in conjunctions with the HSQC spectrum (Table 9), showed signals of a pair of *cis*-coupled olefinic protons at δ_H 7.31, *d* (*J* = 10.0 Hz) and δ_H 5.87, *d* (*J* = 10.0 Hz), a double doublet of an olefinic proton at δ_H 5.11 (*J* = 7.7, 6.6 Hz), a multiplet of a methine proton at δ_H 5.90, two doublets of methine protons at 5.23 (*J* = 0.5 Hz) and 2.58 (*J* = 11.0 Hz), one double quartet of a methine proton at δ_H 2.78 (*J* = 6.7 Hz), two double doublets of methine protons at δ_H 2.62 (*J* = 11.7 ,2.4 Hz) and δ_H 2.27 (*J* = 11.9, 0.9 Hz), seven multiplets of methylene protons at δ_H 2.48, 2.42, 2.23, 2.12, 1.97, 1.92 and 1.56, as well as seven methyl singlets at δ_H 2.12, 1.95, 1.69, 1.45, 1.18, 1.16, 0.93, and one methyl doublet at δ_H 1.28 (*J* = 6.8 Hz).

The COSY spectrum (Table 9) displayed correlations from the olefinic proton at δ_H 7.31, *d* (*J* = 10.0 Hz, H-1/ δ_C 157.3) to another olefinic proton at δ_H 5.87,*d* (*J* = 10.0 Hz, H-2/ δ_C 127.8), from the methine double doublet at δ_H 2.27 (*J* = 11.9, 0.9 Hz, H-5/ δ_C 47.2) to the double quartet of the methine proton at δ_H 2.78 (*J* = 6.7 Hz, H-4/

δ_C 40.4) and the methine doublet at δ_H 5.23 (*J* = 0.9 Hz, H-6/ δ_C 73.8), from H-4 to the methyl doublet at δ_H 1.28 (*J* = 6.8 Hz, Me-28/ δ_C 13.1).

The HMBC spectrum (Table 9) exhibited cross peaks from H-2 to the carbon at δ_C 40.4 (C-4), from H-1 to the ketone carbonyl carbon at δ_C 201.4 (C-3), the carbons at δ_C 47.2 (C-5) and δ_C 38.2 (C-10), from H-4 to C-3 and the methyl carbon at δ_C 13.1 (C-28), from H-5 to C-4, C-10 and the carbons at δ_C 157.3 (C-1), from H-6 to C-4, C-5, C-10, the ketone carbonyl at δ_C 208.8 (C-7) and the ester carbonyl at δ_C 168.9 (C-1'), from the methyl singlet at δ_H 1.45 (Me-18/δ_C 27.5) to C-1, C-5 and the carbon at δ_C-41.7 (C-9), as well as from the methyl singlet at δ_H 1.18 (Me-19/δ_C 18.3) to C-7, C-9 and the carbon at δ_C 52.7 (C-8), from Me-28 to C-3, C-4 and C-5. Moreover, the methyl singlet at δ_H 2.12 (Me-2'/δ_C 20.7) also gave cross peak to C-1'. These correlations suggested the presence of the 3,4a,8-trimethyl-2,7-dioxo-1,2,3,4,4a,7,8,8a-octahydronaphthalen-1-yl acetate portion (Figure 93).

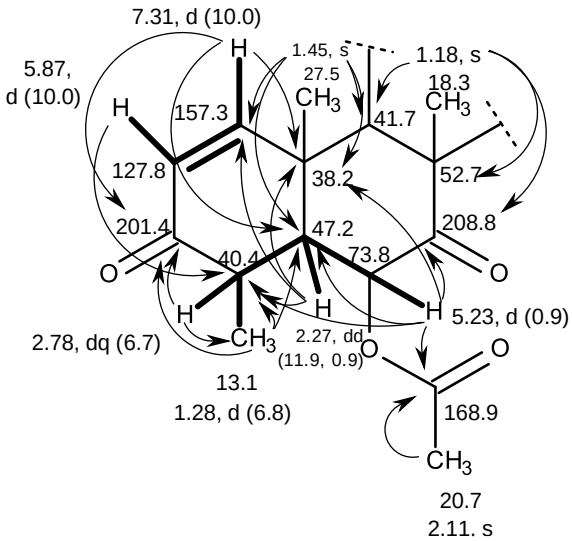

Figure 93. Key COSY (▬) and HMBC (⟶) correlations in the 3,4a,8-trimethyl-2,7-dioxo-1,2,3,4,4a,7,8,8a-octahydronaphthalen-1-yl acetate portion of **NT 7**

The COSY spectrum also exhibited correlations from the double doublet of the methine proton at δ_H 2.62 (*J* = 11.7, 2.4 Hz, H-9/ δ_C 41.7) and the multiplet of the methylene proton at δ_H 2.42 (H-12/δ_C 25.9) to the multiplet of the methylene proton at

δ_H 1.97 (H-11α/δ_C 23.9), as well as from the multiplet of the methine proton at δ_H 5.90 (H-16/ δ_C 73.5) to the multiplet of the methylene proton at δ_H 1.92 (H-15α/ δ_C 40.7). Furthermore, the HMBC spectrum also showed correlations from the methyl singlet at δ_H 0.93 (Me-29/δ_C 17.9) to C-8, the carbons at δ_C 49.5 (C-13), 46.6 (C-14) and 40.7 (C-15), while H-15α exhibited correlations to C-13 and the carbon at δ_C 147.8 (C-17). Moreover, the methyl singlet at δ_H 1.95 (δ_C 20.6) also gave cross peak to the ester carbonyl at δ_C 170.0 (C-1''). These correlations suggested the presence of a 3a,4-dimethyl-1-methylideneoctahydro-1*H*-inden-2-yl acetate portion (Figure 94).

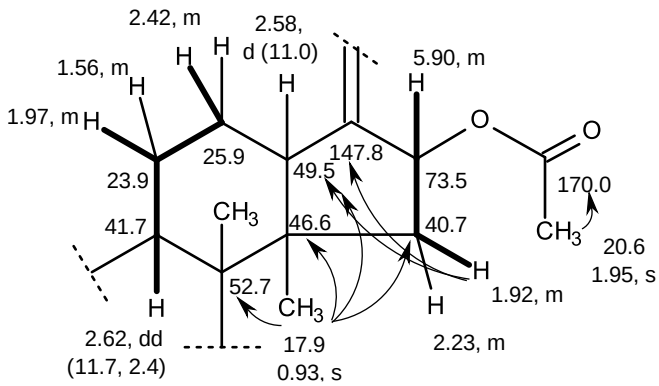

Figure 94. Key COSY (▬) and HMBC (⟶) correlations in the 3a,4-dimethyl-1-methylideneoctahydro-1*H*-inden-2-yl acetate portion of **NT 7**

The COSY spectrum (Table 9) also displayed the correlations from the double doublet of the olefinic proton at δ_H 5.11 (*J* = 7.7, 6.6 Hz, H-24/ δ_C 122.8) to the methyl singlet at δ_H 1.69 (Me-26/δ_C 25.8), from the multiplet at δ_H 2.48 (H_2-22/ δ_C 28.6) to the multiplet at δ_H 2.12 (H_2-23/δ_C 28.4), while the HMBC spectrum (Table 9) showed cross peaks from Me-26 to the carbons at δ_C 132.9 (C-25), 122.8 (C-24) and 17.8 (C-27), from the methyl singlet at δ_H 1.16 (Me-27/δ_C 17.8) to C-24, C-25 and the carbon at δ_C 25.8 (C-26). These correlations suggested the presence of the 6-methyl-2-methylidenehept-5-enoic acid side chain (Figure 95).

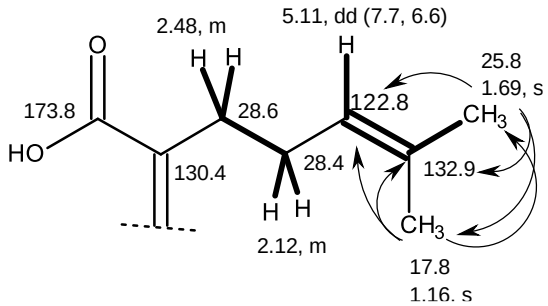

Figure 95. Key COSY (▬) and HMBC (⟶) correlations in the 6-methyl-2 methylidenehept-5-enoic acid side chain of **NT 7**

That the 3,4a,8-trimethyl-2,7-dioxo-1,2,3,4,4a,7,8,8a-octahydronaphthalen-1-yl acetate portion was linked to the 3a,4-dimethyl-1-methylideneoctahydro-1*H*-inden-2-yl acetate portion was supported by the HMBC correlations from the methyl singlet at δ_H 1.18 (Me-19/δ_C 18.3) to C-14. In turn, the 6-methyl-2-methylidenehept-5-enoic acid moiety was linked to the 3a,4-dimethyl-1-methylideneoctahydro-1*H*-inden-2-yl acetate portion through the double bond between C-17 (δ_C 147.8) and C-20 (δ_C 130.4) was supported by the HMBC correlations from H-16 and a triplet at δ_H 2.58 (J = 11.0 Hz, H-13/ δ_C 49.5) to C-20. Therefore, the planar structure of **NT 7** was elucidated as shown in figure 96.

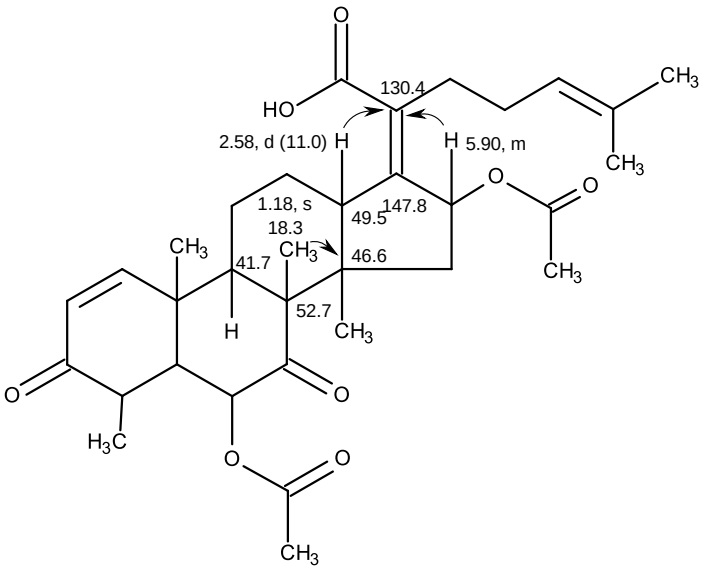

Figure 96. Planar structure of **NT 7**

Table 9. ^{1}H and ^{13}C NMR (300 MHz and 75 MHz, $CDCl_3$) and HMBC assignment for **NT 7**

Position	δ_C, type	δ_H, (*J* in Hz)	COSY	HMBC
1	157.3, CH	7.31, *d* (10.0)	H-2	C-3, 5, 10
2	127.8, CH	5.87, *d* (10.0)	-	C-4
3	201.4, C		-	
4	40.4, CH	2.78, *dq* (6.7)	H-28	C-3, 28
5	47.2, CH	2.27, *dd* (11.9, 0.9)	-	C-1, 4, 10, 18
6	73.8, CH	5.23, *d* (0.9)	H-5	C-1', 4, 5, 7, 10
7	208.8, C	-	-	-
8	52.7, C	-	-	-
9	41.7, CH	2.62, *dd* (11.7, 2.4)	H-11α	-
10	38.2, C	-	-	-
11α	23.9, CH_2	1.56, *m*	-	-
β		1.97, *m*	H-11α	-
12	25.9, CH_2	2.42, *m*	-	-
13	49.5, CH	2.58, *d* (11.0)	-	C-20
14	46.6, C	-	-	-
15α	40.7, CH_2	1.92, *m*	-	C-13, 17
β		2.23, *m*	-	-
16	73.5, CH	5.90, *m*	H-15	C-20
17	147.8, C	-	-	-
18	27.5, CH_3	1.45, *s*	-	C-1, 5, 9, 10
19	18.3, CH_3	1.18, *s*	-	C-7, 8, 9, 14
20	130.4, C	-	-	-
21	173.8, C	-	-	-
22	28.6, CH_2	2.48, *m*	H-23	-
23	28.4, CH_2	2.12, *m*	-	-
24	122.8, CH	5.11, *dd* (7.7, 6.6)	H-26	-
25	132.9, C	-	-	-
26	25.8 CH_3	1.69, *s*	-	C-24, 25, 27
27	17.8, CH_3	1.16, *s*	-	C-24, 25, 26
28	13.1, CH_3	1.28, *d* (6.8)	-	C-3, 4, 5
29	17.9, CH_3	0.93, *s*	-	C-8, 13, 14, 15
1'	168.9, C	-	-	-
2'	20.7, CH_3	2.12, *s*	-	C-1'
1''	170.0, C	-	-	-
2''	20.6, CH_3	1.95, *s*	-	C-1'', 16

Literature search revealed that the structure of **NT 7** corresponded to that of helvoric acid (Figure 97). The identity of **NT 7** was confirmed by comparison of their ^{1}H and ^{13}C NMR data with those reported for helvoric acid (Fujimoto *et al*., 1996; Zin *et al*., 2016) and also by co-elution on TLC with the authentic sample.

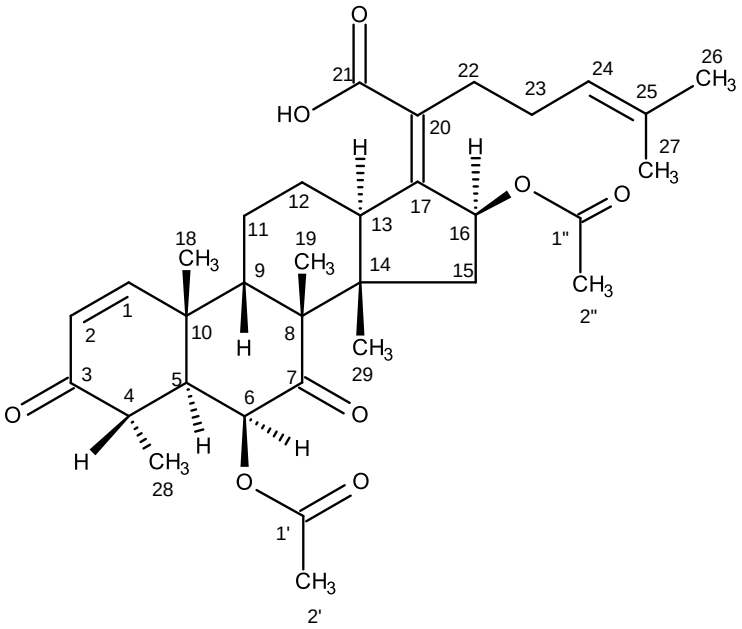

Figure 97. Structure of helvolic acid (**NT 7**)

Helvolic acid is a nordammarane triterpenoid, which was first isolated from the fungus *Corynascus setosus* (Fujimoto *et al*., 1996), and later from other fungi such as marine sponge-associated fungi *Aspergillus sydowi* (Zhang *et al*., 2008), *Emericellopsis minima* (Pinheiro *et al*., 2012), *Neosartorya glabra* KUFA 0702 (Zin *et al*., 2016) and *N. fennelliae* KUFA 0811 (Aung, 2017), entomopathogenic fungus *Metarhizium anisopliae* (Lee *et al*., 2008), the rice fungal pathogen *Sarocladium oryzae* (Sakthivel *et al*., 2002), endophytic fungus *Aspergillus* sp. CY725 isolated from *Cynodon dactylon* (Li *et al.,* 2005), *Alternaria* sp. FL25 isolated from *Ficus carica* (Feng and Ma 2010) and *Pichia guilliermondii* (Zhao *et al*., 2010), as well as from soil fungus *N. spinosa* KKU-1NK1 (Sanmanoch *et al*., 2016).

3.1.1.8. Lumichrome (NT 8)

Compound **NT 8** was isolated as a yellow amorphous powder, and its molecular formula $C_{12}H_{10}N_4O_2$ was determined based on the (+)-HRESIMS *m/z* 243.0888 $[M+H]^+$ (calculated 243.0882 for $C_{12}H_{11}N_4O_2$), indicating ten degrees of unsaturation. The ^{13}C NMR spectrum (Table 10) displayed twelve carbon signals which, in combination with DEPTs and HSQC, can be categorized as eight non-protonated–sp^2 (δ_C160.4, 149.8, 146.3, 144.5, 141.5, 138.7, 138.3 and 129.9), two protonated sp^2 (δ_C 128.6; δ_H 7.91 and δ_C 125.7; δ_H 7.70) and two methyl (δ_C 20.0; δ_H 2.50 and δ_C19.4; δ_H 2.47) carbons. The ^1H NMR spectrum (Table 10) exhibited, besides two aromatic proton singlets at δ_H 7.91 and δ_H 7.70, and two methyl singlets at δ_H 2.50 and δ_H 2.47, a broad signal of two protons at δ_H 11.64, characteristic of the NH or OH protons. The COSY spectrum (Table 10) showed correlations from the singlet of the aromatic proton at δ_H7.91 (H-9) to the methyl singlet at δ_H 2.47 (Me-12) as well as from another singlet of the aromatic proton at δ_H 7.70 (H-6) to the methyl singlet at δ_H 2.50 (Me-11). This pattern of correlations supported the existence of a 1,3,4,6-tetrasubsituted benzene ring where the two methyl substituents are on the vicinal carbons (Figure 98).

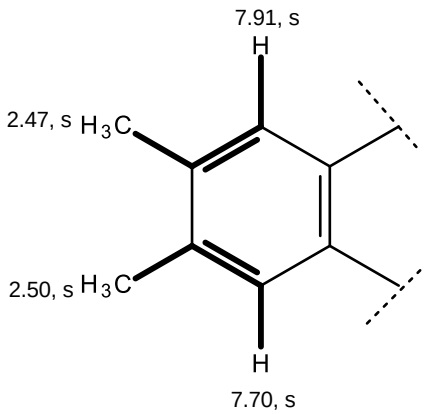

Figure 98. COSY correlations (▬) of the 3,4-dimethyl-1,3,4,6-tetrasubsituted benzene ring of **NT 8**

This partial structure was supported by HMBC correlations from H-9 to the non-protonated sp^2 carbons at δ_C 141.5 (C-5a) and 144.5 (C-7) and the methyl carbon at

δ_C 19.4 (CH_3-12), H-6 to the quaternary non-protonated sp^2 carbons at δ_C 138.3 (C-9a) and 138.7 (C-8), the methyl singlet at δ_H 2.47 (Me-12), the protonated sp^2 carbons at δ_C 128.6 (C-9) and C-7, and from the methyl singlet at δ_H 2.50 (Me-11) to the protonated sp^2 carbons at δ_C 125.7 (C-6) and C-8 (Figure 99).

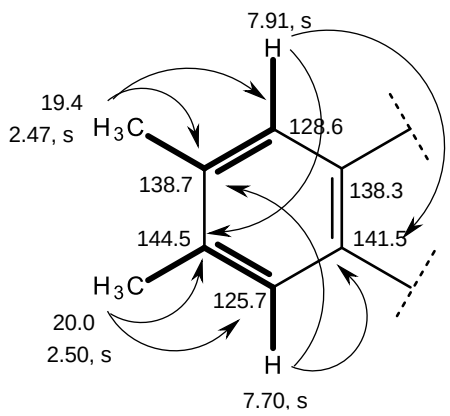

Figure 99. COSY (▬) and HMBC (⟶) correlations of the 3,4-dimethyl-1,3,4,6-tetrasubsituted benzene ring of **NT 8**

As this partial structure corresponds to C_8H_8, another part of the molecule must have $C_4H_2N_4O_2$, corresponding to four protonated sp^2 quaternary carbons (δ_C 160.4, 149.8, 146.3 and 129.9), four nitrogen, two oxygen and two hydrogen atoms. Taking together the number of the carbon, hydrogen, nitrogen and oxygen atoms and the ^{13}C chemical shift values, this moiety should have two amide carbonyl groups, two secondary amines (NH) and two imine (C=N) groups. The chemical shift values of the non-protonated sp^2 carbon at δ_C 160.4 and δ_C 149.8 resemble those of the carbonyl carbons whereas the carbons at δ_C146.3 and 129.9 could be attributed to the imine carbons of the pteridine-2,4 [1*H*, 3*H*]-dione (Figure 100).

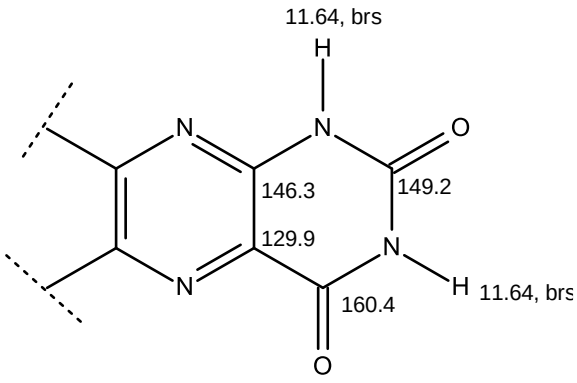

Figure 100. ^{1}H and ^{13}C chemical shift values of pteridine-2,4 [1*H*, 3*H*]-dione ring system

Table 10. ^{1}H and ^{13}C NMR (300 MHz and 75 MHz, DMSO-d_6) and HMBC assignment for **NT 8**

Position	δ_C, type	δ_H, (*J* in Hz)	COSY	HMBC
1	NH	11.64, *brs*	-	-
2	149.8, C	-	-	-
3	NH	11.64, *brs*	-	-
4	160.4, C	-	-	-
4a	129.9, C	-	-	-
5	N	-	-	-
5a	141.5, C	-	-	-
6	125.7, CH	7.70, *s*	H-11	C-8, 9a, 11
7	144.5, C	-	-	-
8	138.7, C	-	-	-
9	128.6, CH	7.91, *s*	H-12	C-5a, 7, 12
9a	138.3, C	-	-	-
10	N	-	-	-
10a	146.3, C	-	-	-
11	20.0, CH_3	2.47, *s*	-	C-7, 9
12	19.4, CH_3	2.50, *s*	-	C-6, 8

Combination of the two partial structures, the complete structure of **NT 8** was established as:

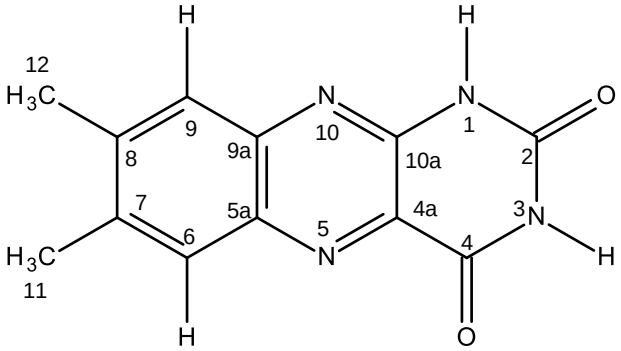

Figure 101. Structure of lumichrome (**NT 8**)

Literature search revealed that the structure of **NT 8** corresponds to lumichrome (Figure 101), a natural product previously reported from the culture filtrate of *Aspergillus oniki* 1784 by Sasaki *et al.*, in 1974. Later on, Silva *et al.,* (2013) reported isolation of lumichrome from the marine alga *Gelidium microdon,* collected from the Azores Archipelago. Lumichrome was also found to be a product of photoconversion of riboflavin (vitamin B 2) in plant tissue (George *et al*., 1972).

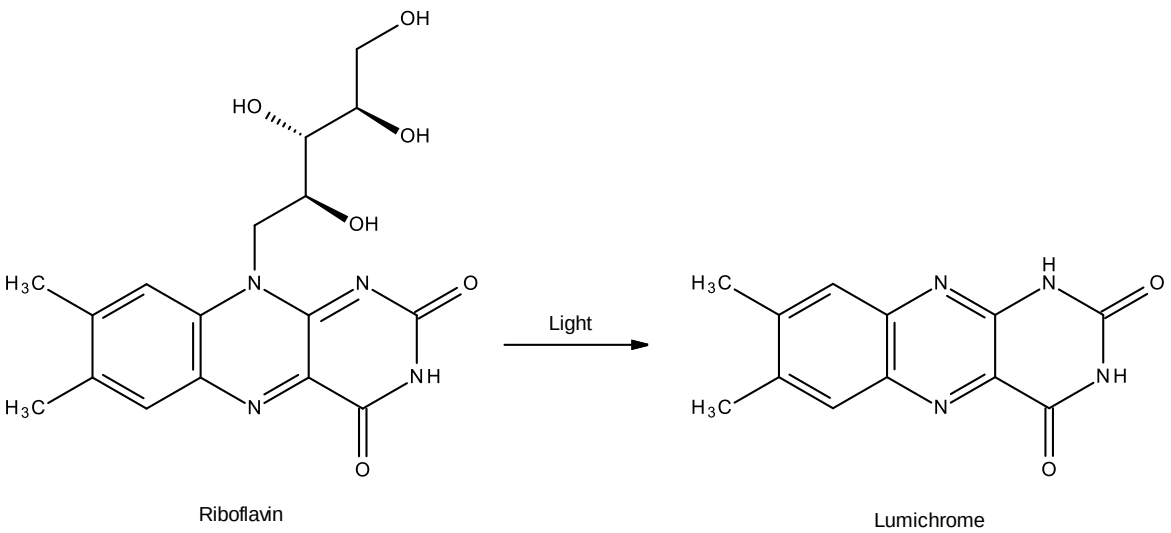

Interestingly, lumichrome isolated from the culture filtrates of the alga *Chlamydomonas* was capable of stimulating the *Pseudomonas aeruginosa* LasR quorum sensing (QS) receptor (Rajamani *et al*., 2008). LasR normally recognizes the *N*-acyl homoserine lactone (AHL) signal, *N*-3-oxo-dodecanoyl homoserine lactone. Interestingly, bacteria, plants, and algae commonly secrete riboflavin or lumichrome, raising the possibility that these compounds could serve as either QS signals or as interkingdom signal mimics capable of manipulating QS in bacteria with a LasR-like receptor.

Due to interesting biological activity, many attempts to produce large amount of lumichrome have been undertaken. In this perspective, Kazunori and Asano have cultivated a soil bacterium *Microbacterium* sp. Strain TPU 3598, in the presence of riboflavin, to efficiently produce lumichrome (Yamamoto and Asano, 2015).

3.1.1.9. Harmane (NT 9)

Compound **NT 9** was isolated as an amorphous powder, and its (+)-HRESIMS spectrum displayed the $(M+H)^+$ signal at *m/z* 183.0922 (calculated 183.0922 for $C_{12}H_{11}N_2$), indicating the molecular formula $C_{12}H_{10}N_2$ and nine degrees of unsaturation. The ^{13}C NMR spectrum (Table 11), together with DEPT and HSQC spectra, exhibited five non-protonated sp^2 (δ_C 142.1, 140.4, 135.5, 126.8, 121.0), six protonated sp^2 (δ_C 137.5, 127.8, 121.7, 119.2, 112.6, and 112.0) and one methyl (δ_C 20.5) carbons, respectively. The ^1H NMR spectrum (Table 11), in conjunction with the HSQC spectrum, exhibited six aromatic proton signals at δ_H 8.21, *d* (*J* = 5.3 Hz; δ_C 137.5), 8.20, *dd* (*J* = 8.2, 2.6 Hz; δ_C 121.7), 7.93, *d* (*J* = 5.3 Hz; δ_C 112.6), 7.60, *dt* (*J* = 8.0, 0.9 Hz; δ_C 112.0), 7.53, *ddd* (*J* = 8.0, 7.0, 1.0 Hz; δ_C 127.8), 7.23, *ddd* (*J* = 8.0, 7.0, 1.0 Hz; δ_C 119.2), one methyl singlet at δ_H 2.77 (δ_C 20.5), in addition to a broad singlet, characteristic of the NH proton, at δ_H 11.69. That part of the molecule contained 1, 2-disubstituted benzene ring was evidenced by the COSY correlations from the proton signals at δ_H 8.20, *dd* (*J* = 8.2, 2.6 Hz, H-5)/ 7.23, *ddd* (*J* = 8.0, 7.0, 1.0 Hz, H-6)/ 7.53, *ddd* (*J* = 8.0, 7.0, 1.0 Hz, H-7)/ 7.60, *dt* (*J* = 8.0, 0.9 Hz, H-8). This was corroborated by HMBC correlations from H-5 to the carbons at δ_C 126.8 (C-8a) and 127.8 (C-7), H-6 to the carbons at δ_C 121.0 (C-4a) and 112.0 (C-8), H-7 to the

carbon at δ_C 121.5 (C-5) and C-8a, H-8 to the carbons at δ_C 121.0 (C-4b) and 119.2 (C-6) respectively. Since the *brs* at δ_H 11.69 showed HMBC correlations to the carbon at δ_C 134.5 (C-9a), C-8a and C-4b, the presence of the indole moiety was confirmed:

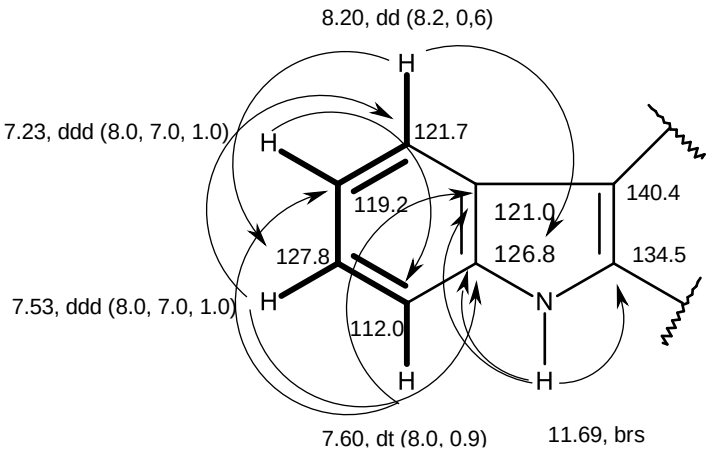

Figure 102. COSY correlations (▬) and key HMBC correlations (⟶) in the indole moiety

That another portion of the molecule was 2-methyl-3,4-disubstituted pyridine was evidenced by the COSY correlation from the doublet at δ_H 7.93 (*J* = 5.3 Hz, H-4) to another doublet at δ_H 8.21 (*J* = 5.3 Hz, H-3), as well as HMBC correlations from H-3 to the carbons at δ_C 141.1 (C-1) and 112.6 (C-4), from H-4 to the carbons at δ_C 137.5 (C-3) and 112.6 (C-4), as well as from the methyl singlet at δ_H 2.77 to C-1.

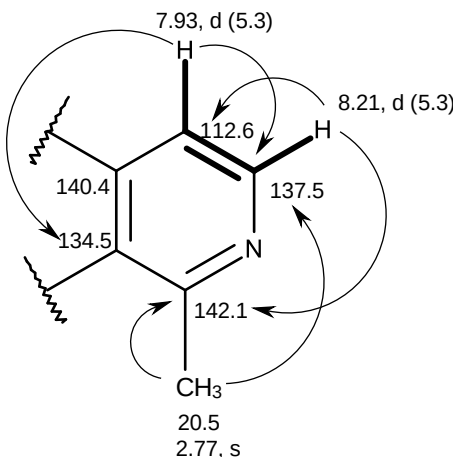

Figure 103. COSY correlations (▬) and key HMBC correlations (⟶) in the 2-methyl-3,4-disubstituted pyridine moiety

That the indole portion was fused with the 2-methyl-3,4-disubstituted pyridine moiety, through C-4a and C-9a, was supported by the HMBC correlation from Me-10 to C-9a as well as from H-4 to C-9a and C-4b. Taking together the 1D and 2D NMR data and the molecular formula, the structure of **NT 9** was established as harmane (Figure 104).

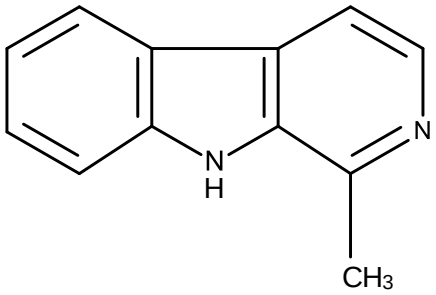

Figure 104. Structure of Harmane (**NT 9**)

Harmane has been previously reported from several plant species, including from bark of *Hippophaë rhamnoides* L., *Elaeagnus angustifolia* L., *E. orientalis* L., *E. umbellate* Thunb., *E. multiflora* Thunb. and *E. argentea*. It was also produced by cigarette smoke (Tolkachev *et al*., 2008). Concerning its isolation from fungi, Wrońska *et al*. have reported its detection by GC-MS analysis of cell-free filtrates of the entomopathogenic fungus *Conidiobolus coronatus* (Entomopthorales). Harman and norharman, metabolites of entomopathogenic fungus *Conidiobolus coronatus*, disorganize development of *Galleria mellonella* (Lepidoptera) and affect serotonin-regulating enzymes (Wrońska *et al*., 2018).

Table 11. ^{1}H and ^{13}C NMR (500 MHz and 125 MHz, DMSO-d_6) and HMBC assignment for **NT 9**

Position	δ_C, type	δ_H, (*J* in Hz)	COSY	HMBC
1.	142.1 C	-	-	-
2.	-N	-	-	-
3.	137.5 CH	8.21, *d* (5.3)	H-4	C-1, 4, 4a
4.	112.6 CH	7.93, *d* (5.3)	H-6	C-3, 4b, 9a
4a	140.4 C	-	-	-
4b	121.0 C	-	-	-
5.	121.7 CH	8.20, *dd* (8.2, 0.6)	-	C-7, 8a
6.	119.2 CH	7.23, *ddd* (8.0, 7.0, 1.0)	-	C-4a, 8
7.	127.8 CH	7.53, *ddd* (8.0, 7.0, 1.0)	H-6	C-5, 8a
8.	112.0 CH	7.60, *dt* (8.2, 0.9)	H-7	C-4b, 6
8a.	126.8 C	-	-	-
9.	-NH	11.69, *brs*	-	C-4b, 8a, 9a
9a	134.5 C	-	-	-
10.	20.5 CH_3	2.77, *s*	-	C-1, 9a

3.1.2. Secondary Metabolites Isolated from the Marine-Derived *Penicillium erubescens* KUFA 0220

Chromatographic fractionation, followed by several purification procedures, of the crude ethyl acetate of the culture of the marine- derived fungus *Penicillium erubescens* KUFA 0220 furnished six previously unreported metabolites, including 1-hydroxy-12-methoxycitromycin (**PE 5**), penialidin G (**PE 10**), erubescensoic acid (**PE 13**), erubescenschromone A (**PE 14**), 7-hydroxy-6-methoxy-4-oxo-3-[(1*E*)-3-oxobut-1-en-1-yl]-4H-chromene-5-carboxylic acid (**PE 15**) and erubescenschromone B (**PE 16**), together with fourteen known metabolites: *β*-sitostenone (**PE 1**), ergosterol 5,8-endoperoxide (**PE 2**), citromycin (**PE 3**), 12-methoxycitromycin (**PE 4**), myxotrichin D (**PE 6**), 12-methoxycitromycetin (**PE 7**), anhydrofulvic acid (**PE 8**), myxotrichin C (**PE 9**), penialidin D (**PE 11**), penialidin F (**PE 12**), SPF-3059-30 (**PE 17**), SPF-3059-26 (**PE 18**), GKK1032B (**PE 19**) and secalonic acid A (**PE 20**) (Figure 105).

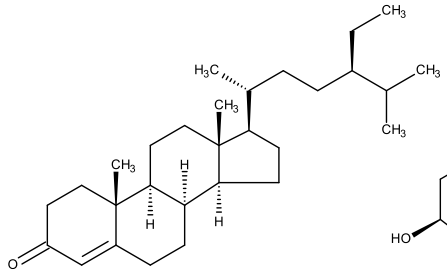

PE 1

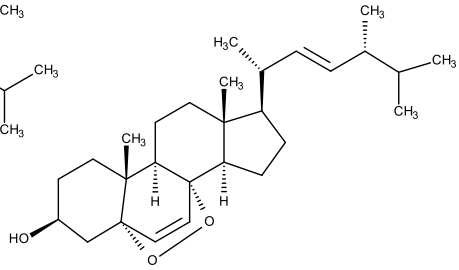

PE 2

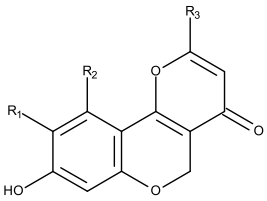

PE 3: R_1= OH, R_2= H, R_3= Me
PE 4: R_1= OMe, R_2= H, R_3= Me
PE 5: R_1= OMe, R_2= H, R_3= CH_2OH
PE 6: R_1= H, R_2= COOH, R_3= Me
PE 7: R_1= OMe, R_2= COOH, R_3= Me

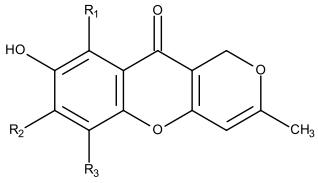

PE 8: R_1= COOH, R_2= OH, R_3= H
PE 9: R_1= H, R_2= OH, R_3= H
PE 11: R_1= H, R_2= OMe, R_3= COOH

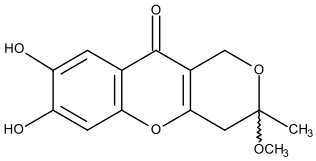

PE 10

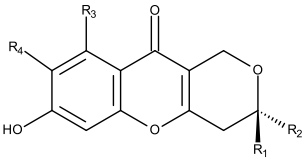

PE 12: R_1= OH, R_2= Me, R_3= H, R_4= OH
PE 13: R_1= Me, R_2= H, R_3= COOH, H_4= OH

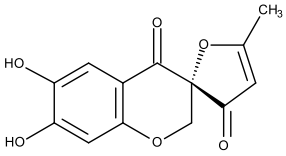

PE 14

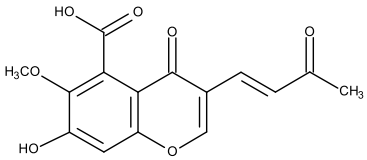

PE 15

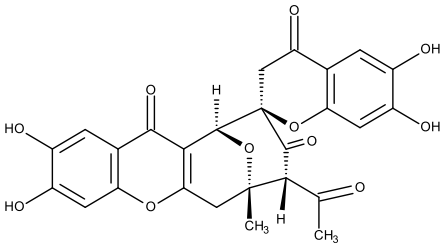

PE 16

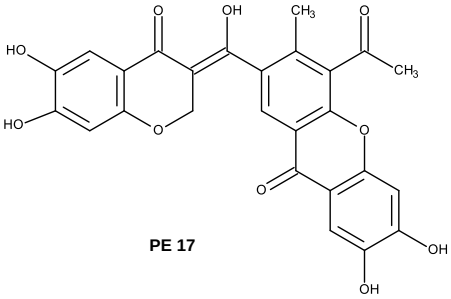

PE 17

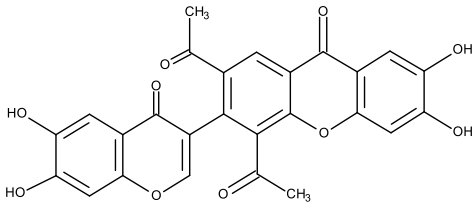

PE 18

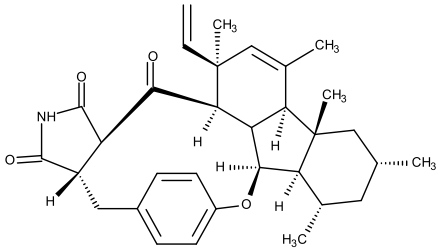

PE 19

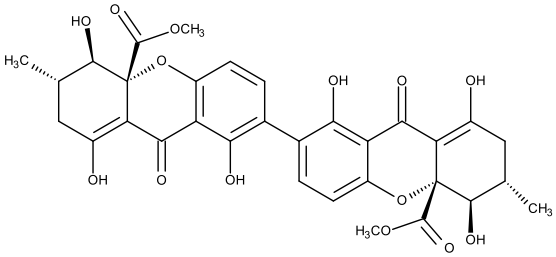

PE 20

Figure 105. Secondary metabolites isolated from the culture of *Penicillium erubescens* KUFA 0220

3.1.2.1. Sitostenone (PE 1)

Compound **PE 1** was isolated as white solid (mp, 92-95 ^{o}C) and its molecular formula $C_{29}H_{48}O$, was established on the basis of the (+)-HRESIMS *m/z* 413.3778 $[M+H]^+$ (calculated 413.3783 for $C_{29}H_{49}O$), indicating six degrees of unsaturation. The ^{13}C NMR spectrum showed 29 carbon signals which were categorized, by DEPTs and HSQC spectra (Table 12), as one conjugated ketone carbonyl (δ_C 199.8), one non-protonated sp^2 (δ_C 171.8), two quaternary sp^3 (δ_C 42.4 and 38.6), one methine sp^2 (δ_C 123.7), seven methine sp^3 (δ_C 56.0, 55.9, 53.8, 45.8, 36.1, 35.6 and 29.1), eleven methylene sp^3 (δ_C 39.6, 35.7, 34.0, 33.9, 33.0, 32.1, 28.2, 26.0, 24.2, 23.1 and 21.0), and six methyl (δ_C 19.8, 19.0, 18.7, 17.4, 12.0 and 11.9) carbons.

The ^{1}H NMR spectrum (Table 12), together with the HSQC spectrum, exhibited a singlet of one olefinic proton at δ_H 5.72 (δ_C 123.7), seven methine multiplets at δ_H 2.01 (δ_C 35.6), δ_H 1.65 (δ_C 29.1), δ_H 1.34 (δ_C 36.1), δ_H 1.11 (δ_C 56.0), δ_H 1.03 (δ_C 55.9), δ_H 0.93 (δ_C 45.8) and δ_H 0.91 (δ_C 53.8), and several multiplets of the methylene protons at δ_H 2.42 and 2.34 (δ_C33.9), δ_H 2.36 and 2.26 (δ_C 33.0), δ_H 2.02 and 1.17 (δ_C 39.6),1.86 and 1.29 (δ_C 28.2), δ_H 1.83 and 1.01 (δ_C 32.1), δ_H 1.69 and 1.52 (δ_C 35.7), δ_H 1.59 and 1.00 (δ_C 24.2), δ_H 1.51 and 1.43 (δ_C 21.0), δ_H 1.31 and 1.02, (δ_C 34.0), δ_H 1.26 (δ_C 23.1) and δ_H 1.16 (δ_C 26.0), two methyl singlets at δ_H 1.18 (δ_C 17.4) and 0.71 (δ_C 12.0), three methyl doublets at δ_H 0.92 (*J* = 6.5 Hz / δ_C 18.7), δ_H 0.84 (*J* = 6.4 Hz/ δ_C 19.8), δ_H 0.81 (*J* = 6.7 Hz/ δ_C 19.0) and a methyl triplet at δ_H 0.85 (*J* =7.0 Hz/ δ_C 11.9).

The COSY spectrum (Table 12) showed correlations from the methylene protons at δ_H 2.42, *m* (H-2/δ_C 33.9) to the methylene protons at δ_H 1.69, *m* (H-1/δ_C 35.7), as well as from methylene protons at δ_H 1.51 (H-11/δ_C 21.0) to the methylene protons at δ_H 2.02, *m* (H-12/δ_C 39.6) and δ_H 1.43, *m* (H-11/δ_C 21.0) to δ_H 0.91, *m* (H-9/δ_C 53.8), and also from the proton at δ_H 2.36, *m* (H-6/δ_C 33.0) to δ_H 1.83, *m* (H-7/δ_C 32.1).

That **PE 1** consisted of a 4a,7- dimethyl- 4,4a,4b,5,6,7,8,8a,9,10-decahydrophenanthren-2(3*H*)-one moiety (Figure 106) with the ketone carbonyl on C-3 (δ_C 199.8) and one conjugated double bond on C-4 (δ_C 123.7) /C-5 (δ_C 171.8) was

supported by the HMBC correlations from the olefinic proton at δ_H 5.72, *s*, (H-4/δ_C 123.7) to the quaternary sp^3 carbon at δ_C 38.6 (C-10) and methylene sp^3 carbon at δ_C 33.0 (C-6), the multiplets at δ_H 2.42 and 2.34 (H_2-2/δ_C 33.9) to C-3 and C-5, the multiplet at δ_H 1.69 (H-1/δ_C 35.7) to C-10 and the carbons at δ_C 53.8 (C-9) and 17.4 (C-19), the multiplet at δ_H 2.26 (H-6a/δ_C 33.0) to C-4 and the carbons at δ_C 35.6 (C-8) and 32.1 (C-7), the multiplet at δ_H 2.36 (H-6b/δ_C 33.0) to C-3. C-5 and C-8, as well as from the methyl singlet at δ_H1.18 (Me-19/δ_C 17.4) to C-5, C-9 and the carbon at δ_C 35.7 (C-1).

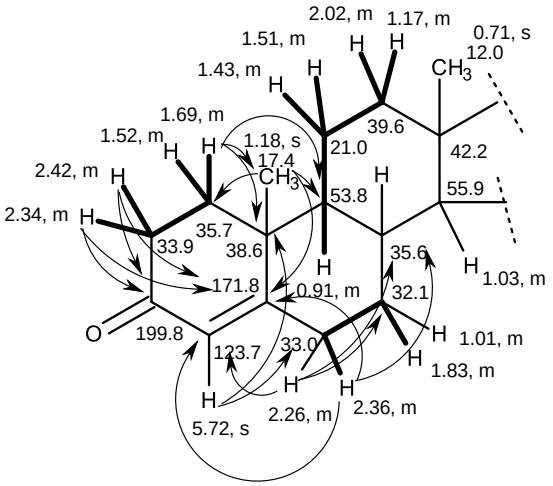

Figure 106. COSY (▬) and HMBC (⟶) correlations of the 4a,7- dimethyl-4,4a,4b,5,6,7,8,8a,9,10-decahydrophenanthren-2(3*H*)-one moiety in **PE1**

That this dimethyldecahydrophenanthrene moiety was fused with the cyclopentane ring through C-7 and C-8 was supported by HMBC cross peaks from the methyl singlet at δ_H 0.71 (Me-18/δ_C 12.0) to the quaternary sp^3 carbon at δ_C 42.4 (C-13), methine sp^3 carbons at δ_C 55.9 (C-14) and δ_C 56.0 (C-17) and to the methylene sp^3 carbon at δ_C 39.6 (C-12) (Figure 107).

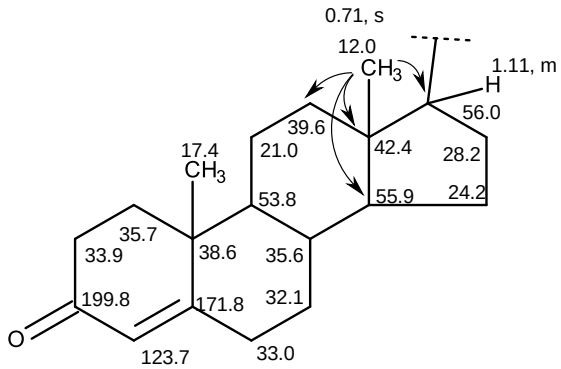

Figure 107. Key HMBC (⟶) correlations of the cyclopentyl dimethyl decahydrophenanthrene moiety in **PE 1**

Consequently, another portion of the molecule contained ten carbons, which was established as 5-ethyl-6-methylheptan-2-yl moiety, was evidenced by the COSY correlations from the methyl doublet at δ_H 0.92, *J* = 6.5 (Me-21/δ_C 18.7) to the multiplet at δ_H 1.34 (H-20/δ_C 36.1) and the multiplets at δ_H 1.02 and 1.31 (H_2-22/ δ_C 34.0), from the multiplet at δ_H 1.26 (H_2-28/δ_C 23.1) to the methyl triplet at δ_H 0.85, *J* = 7.0 Hz (Me-29/δ_C 11.9) and the multiplet at δ_H 0.93 (H-24/δ_C 45.8), and from the multiplet at δ_H 1.65 (H-25/δ_C 29.1) to methyl doublets at δ_H 0.84, *J* = 6.4 Hz (Me-26/δ_C 19.8) and 0.81, *J* = 6.7 Hz (Me-27/ δ_C 19.0). The proposed structure was also supported by HMBC cross peaks from H-20 to the methyl carbon at δ_C 18.7 (C-21), from Me-21 to the carbons at δ_C 36.1 (C-20) and δ_C 34.0 (C-22), from H_2-28 to the carbons at δ_C 11.9 (C-29), δ_C 45.8 (C-24) and δ_C 29.1 (C-25), from Me-29 to methylene carbon at δ_C 23.1 (C-28), from Me-27 to C-24 and C-25, as well as from Me-26 to C-25 (Figure 108).

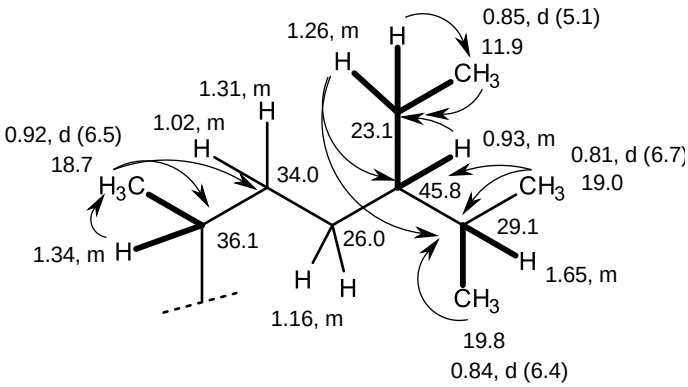

Figure 108. COSY (▬) and HMBC (⟶) correlations in the 5-ethyl-6-methylheptan-2-yl moiety

That the 5-ethyl-6-methylheptan-2-yl moiety (Figure 109) was connected to the cyclopentanoperhydrophenanthrene ring system, through C-20 of the former and C-17 of the latter, was supported by the HMBC correlations from Me-21 and the multiplet at δ_H 1.02 (H-22b/δ_C 34.0) to C-17 (Figure 109).

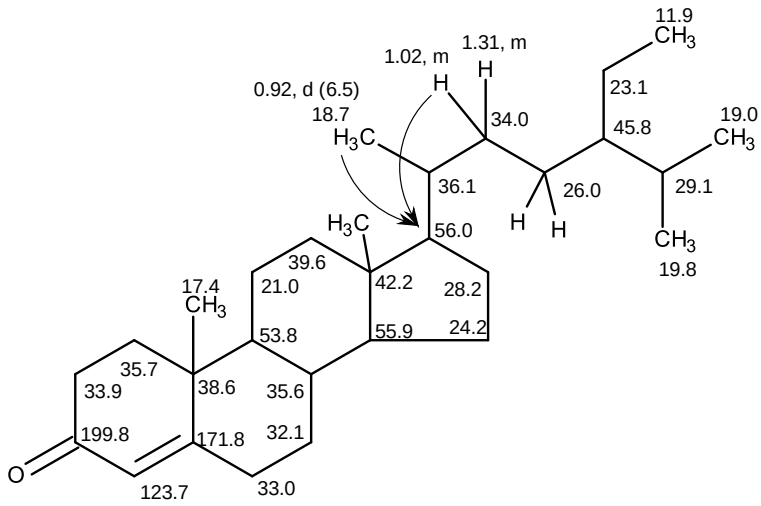

Figure 109. Key HMBC (⟶) correlations in the cyclopentanoperhydrophenanthrene moiety of **PE 1**

Taking together the ^{1}H and ^{13}C chemical shift values and the COSY and HMBC correlations, the structure of **PE 1** was proposed as sitostenone (Figure 110).

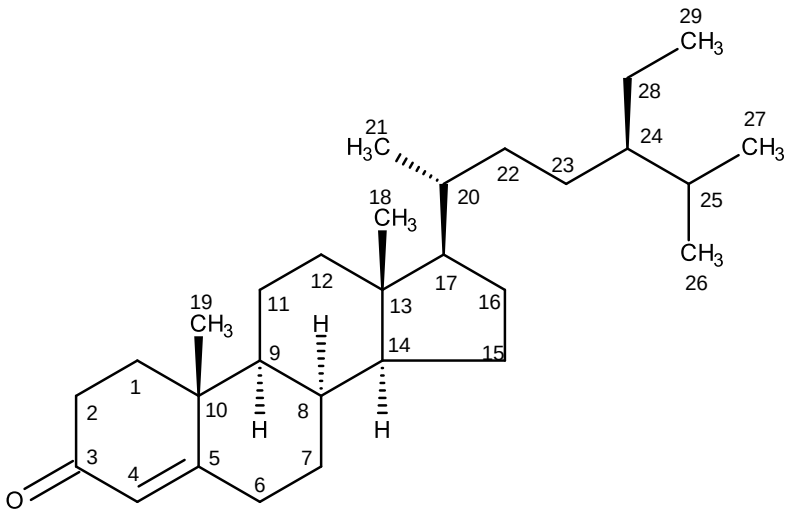

Figure 110. The structure of sitostenone (**PE 1**)

Literature search revealed that **PE 1** is a sterone, named sitostenone which was previously isolated from several plant species, including *Typha latifolia* (Della *et al*., 1990), *Leonurus heterophyllus* (Hotta *et al*., 2003), *Cryptomeria japonica* (Li *et al*., 2008), *Punica granatum* (Pongpuntaruk, 2010), *Annona muricata* Linn. (Ragasa *et al*., 2013), *Michelia compressa var. lanyuensis* (Chu *et al*., 2015), *Commiphora myrrha* (Ge and Jun Zhang, 2018). Sitostenone, isolated from *Zanthoxylum pistaciiflorum*, exhibited effective cytotoxicity against human colon carcinoma (HT-29) and leukaemia (P-388) cell lines with ED_{50} values higher than 50 µg/mL (Chen *et al*., 2004). This compound was also isolated from the traditional medicinal plant, *Spilanthes acmella* Murr., and was found to exhibit significant hypoglycemic, antiarrhythmic and antitubercular actions (Prachayasittikul, 2009). Moreover, sitostenone was also isolated from fungi such as the marine sponge-associated fungus *Neosartorya fennelliae* KUFA 0811 (Aung, 2017), the endophytic fungus, *Chaetomium* sp. YMF432 (Li *et al*., 2018) and the deep-sea-derived fungus, *Sarocladium kiliense* (Fan *et al*., 2019).

Table 12. ^{1}H and ^{13}C NMR (500 MHz and 125 MHz, $CDCl_3$,) and HMBC assignment for **EP 1**

Position	δ_C, type	δ_H, (*J* in Hz)	COSY	HMBC
1a.	35.7 CH_2	1.69, *m*	-	C-9, 10, 19
b		1.52, *m*	-	-
2a	33.9 CH_2	2.34, *m*	-	C-3, 5
b		2.42, *m*	H-1α	C-3, 5
3.	199.8 C	-	-	-
4.	123.7 CH	5.72, *s*	-	C-6, 10
5.	171.8 C	-	-	-
6a	33.0 CH_2	2.26, *m*	-	C-4, 7, 8
b		2.36, *m*	H-7α	C-4, 5, 8
7a	32.1 CH_2	1.83, *m*	-	-
b		1.01, *m*	-	-
8.	35.6 CH	2.01 *m*	-	-
9.	53.8 CH	0.91, *m*	H-11β	C-11
10.	38.6 C	-	-	-
11a	21.0 CH_2	1.51, *m*	H-12 α	-
b		1.43, *m*	-	-
12a	39.6 CH_2	2.02, *m*	-	-
b		1.17, *m*	-	-
13.	42.4 C	-	-	-
14.	55.9 CH	1.03, *m*	-	-
15a	24.2 CH_2	1.59, *m*	-	-
b		1.00, *m*	-	-
16a	28.2 CH_2	1.86, *m*	-	-
b		1.29, *m*	-	-
17.	56.0 CH	1.11, *m*	-	C-13, 14, 18
18.	12.0 CH_3	0.71, *s*	-	C-12, 13, 14, 17
19.	17.4 CH_3	1.18, *s*	-	C-1, 5, 9
20.	36.1 CH	1.34, *m*	-	C-21
21.	18.7 CH_3	0.92, *d* (6.5)	H-20, 21	C-17, 20, 22
22a	34.0 CH_2	1.31, *m*	-	-
b		1.02, *m*	-	C-17
23.	26.0 CH_2	1.16, *m*	-	-
24.	45.8 CH	0.93, *m*	H-28	C-28
25.	29.1 CH	1.65, *m*	H-26	-
26.	19.8 CH_3	0.84, *d* (6.4)	-	C-25
27.	19.0 CH_3	0.81, *d* (6.7)	-	C-24, 25
28.	23.1 CH_2	1.26, *m*	-	C-24, 25, 29
29.	11.9 CH_3	0.85, *t* (7.5)	H-28	C-28

3.1.2.2. Ergosterol-5,8-endoperoxide (PE 2)

Compound **PE 2** was isolated as white crystals (180-182 ºC). The ^{13}C NMR spectrum (Table 13) of **PE 2** displayed 28 carbon signals which can be categorized, through DEPT and HSQC spectra, as four methine sp^2 (δ_C 135.5, 135.2, 132.3, 130.7), two oxyquaternary sp^3 (δ_C 82.2, 79. 4), two quaternary sp^3 (δ_C 44.6, 37.0), one oxymethine sp^3 (δ_C 64.4), six methine sp^3 (δ_C 56.2, 51.7, 51.1, 42.8, 39.7, 33.1), seven methylene sp^3 (δ_C 39.3, 36. 9, 34.7, 33.1, 28.7, 23.4, 20.6) and six methyl (δ_C 20. 9, 20.0, 19.7, 18.2, 17.6, 12.9) carbons.

The ^{1}H NMR spectrum, together with the HSQC spectrum (Table 13), displayed the signals of two olefinic protons of a *cis* double bond at δ_H 6.50, *d* (*J* = 8.5 Hz) and δ_H 6.24, *d* (*J* =8.5 Hz), two olefinic protons of a *trans* double bond at δ_H 5.23, *dd* (*J* = 15.2, 7.1 Hz/ δ_C 132.2 CH) and δ_H 5.14, *dd* (*J* =15.2, 7.8 Hz/ δ_C 135.2 CH), a multiplet of an oxymethine proton at δ_H 3.97, a double double doublet of a methylene proton at δ_H 2.11 (*J* = 13.8, 5.1, 1.8 Hz), six multiplets of methine protons at δ_H 2.02, 1.84, 1.56, 1.50, 1.47 and 1.24, twelve multiplets of methylene protons at δ_H 1.95, 1.93, 1.90, 1.85, 1.74, 1.69, 1.58, 1.53, 1.50, 1.40, 1.38 and 1.23 and four doublets of methyl protons at δ_H 1.00 (*J* = 6.6 Hz), δ_H 0.91 (*J* = 6.8 Hz), δ_H 0.83 (*J* = 6.8 Hz) and δ_H 0.82 (*J* = 6.8 Hz).

The COSY spectrum (Table 13) showed correlations from the methine protons at δ_H 2.02, *m* (H-20) to the methyl protons at δ_H 1.00, *d* (*J* = 6.6 Hz/ Me-21) and the olefinic proton at δ_H 5.14, *dd* (*J* =15.2, 7.8 Hz/ H-22), from the olefinic proton δ_H 5.23, *dd* (*J* =15. 2, 7. 1 Hz/ H-23) to another olefinic proton at δ_H 5. 14, *dd* (*J* =15. 2, 7. 8 Hz/ H-22) and the methine proton at δ_H 1.84, *m* (H-24), from H-24 to H-23, the methine proton at δ_H 1.47, *m* (H-25) and the methyl protons at δ_H 0.83, *d* (*J* = 6.8 Hz/ Me-26), as well as from H-25 to H-24, the methyl protons at δ_H 0.91, *d* (*J* = 6.8 Hz/ Me-28) and δ_H 0.82, *d* (*J* = 6.8 Hz/ Me-27). This connectivity was confirmed by the HMBC correlations from H-23 to the methine sp^3 carbon at δ_C 39.7 (C-20), from Me-28 to C-23 (δ_C 132.3), C-24 (δ_C 42.8) and C-25 (δ_C 31.1), from Me-27 to C-23, C-24, from H-24 to C-22 (δ_C 135.2), C-23, C-25 and C-26 (δ_C 17.6), from Me-26 to C-23, indicating also the presence the (3*E*)-5,6-dimethylhept-3-en-2-yl moiety.

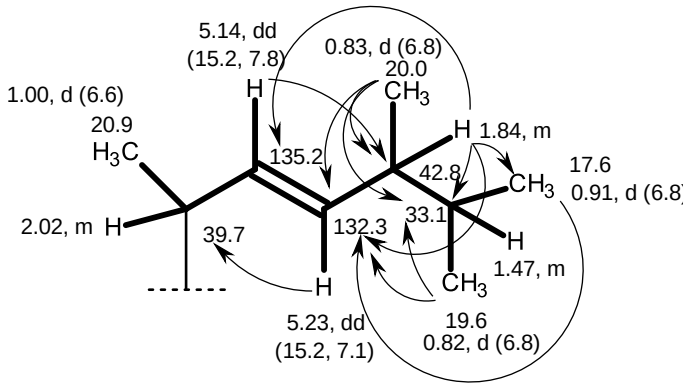

Figure 111. COSY (▬) and HMBC (⟶) correlations in the)3*E*(-5,6-dimethylhept-3-en-2-yl moiety

The COSY spectrum (Table 13) also showed correlation from the olefic proton at δ_H 6.50 *d*, *J* = 8.5 Hz (H-7/ (δ_C 130.7) to another olefinic proton at δ_H 6.24 *d*, *J* = 8.5 Hz(H-6/ δ_C 135.4) of the *cis* double bond, from the multiplet of the oxymethine proton at δ_H 3.97 (H-3) to the methylene protons at δ_H 1.85, *m* (H-2) and δ_H 2.11 *ddd* (*J* = 13.8, 5.1, 1.8 Hz/ H-4). On the other hand, the multiplet of the methylene proton at δ_H 1.58 (H-11) showed cross peaks to multiplets at δ_H 1.95 (H-12) and δ_H 1.50 (H-9), indicating the presence of a *cis* double bond-containing perhydrocyclopentanophenanthrene moiety.

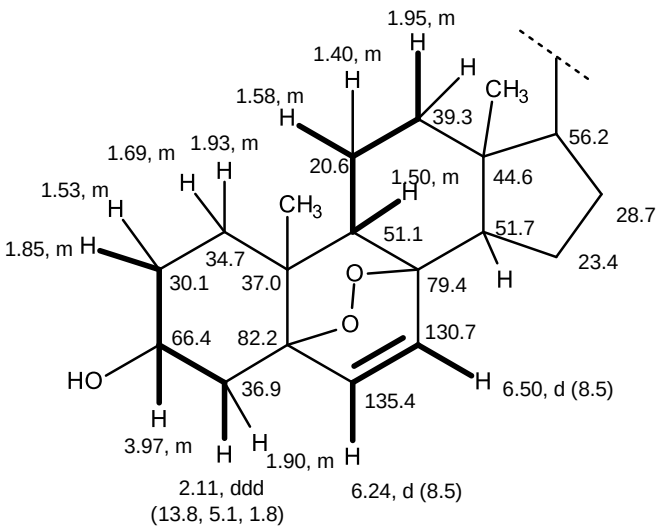

Figure 112. Key COSY (▬) correlations in the perhydrocyclopentanophenanthrene moiety

The HMBC spectrum (Table 13) showed correlations from H-4 to C-2 (δ_C 30.1), C-3 (δ_C 66.4) and C-10 (δ_C 37.0), from the methyl singlet at δ_H 0.88 (Me-18/δ_C 18.2) to C-1 (δ_C 34.7), C-5 (δ_C 82.2), C-9 (δ_C 51.1) and C-10 (δ_C 37.0), from the methyl singlet at δ_H 0.82 (Me-19/δ_C 12.9) to the carbons at δ_C 39.3 (C-12), 44.6 (C-13), C-14 (δ_C 51.7) and δ_C 56.2 (C-17). Furthermore, the position of the peroxide bond was confirmed by HMBC correlations from the olefinic proton H-6 to C-4, C-5, C-7 (δ_C 130.7), C-8 (δ_C 79.4) and C-10 (δ_C 37.0), as well as from H-7 to C-4, C-5, C-8 and C-9 (δ_C 51.1).

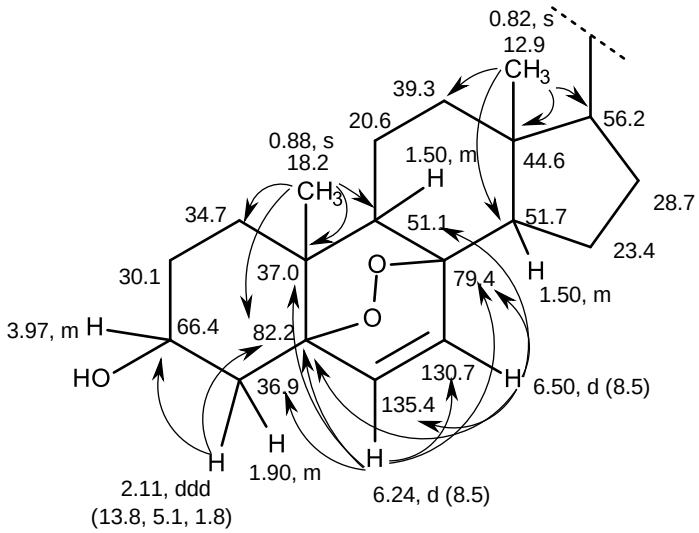

Figure 113. Key HMBC (⟶) correlations in the perhydrocyclopentanophenanthrene moiety

That the perhydrocyclopentanophenanthrene moiety (Figures 112 and 113) was connected to the (3*E*)-5,6-dimethylhept-3-en-2-yl side chain (Figure 111), through the carbon at δ_C 56.2 (C-17) of the former and the carbon at δ_C 39.7 (C-20) of the latter, was supported by the HMBC cross peaks from Me-18 to C-20, and from Me-21 to C-17. In turn, the COSY spectrum also showed a correlation from the multiplet at δ_H 1.24 (H-17) to H-20. Therefore, the planar structure of **PE 2** was elucidated as:

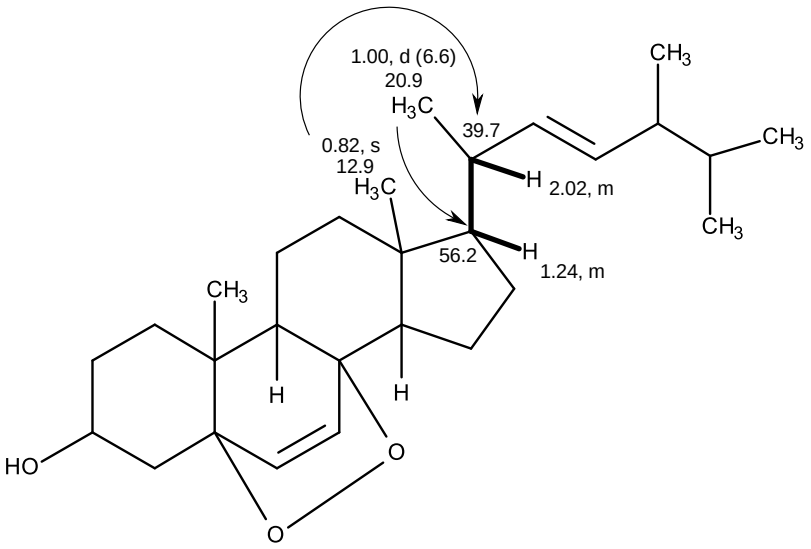

Figure 114. COSY (▬) and HMBC (⟶) correlations in the **PE 2**

Taking together the ^{1}H and ^{13}C chemical shifts and the COSY and HMBC correlations, and other physical data, the structure of **PE 2** was identified as ergosterol-5,8-endoperoxide (Figure 115). The identity of **PE 2** was also confirmed by the co-elution of the sample of **PE 2** with the authentic sample of ergosterol-5,8-endoperoxide, isolated previously by our group.

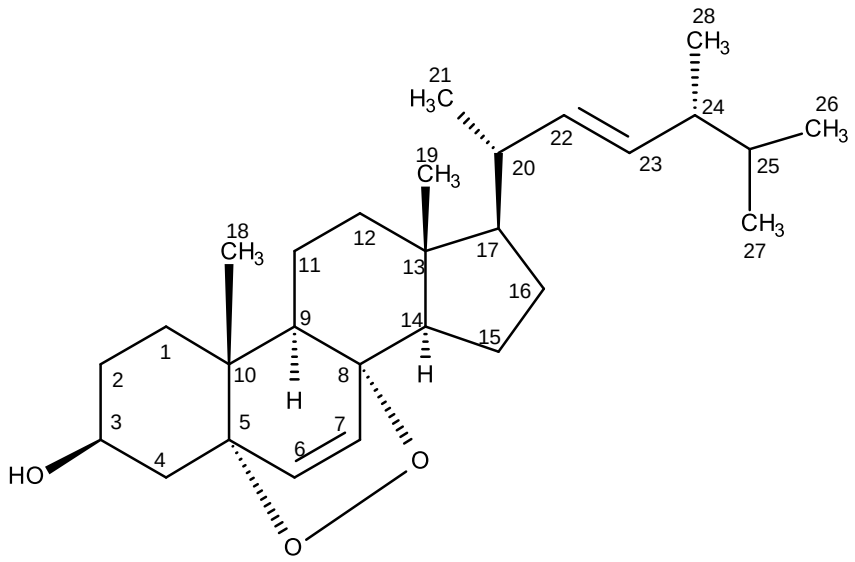

Figure 115. Structure of ergosterral-5,8-endoperoxide (**PE 2**)

Table 13. ^{1}H and ^{13}C NMR (300 MHz and 75 MHz, $CDCl_3$) and HMBC assignment for **PE 2**

Position	δ_C, type	δ_H, (*J* in Hz)	COSY	HMBC
1α	34.7, CH_2	1.93, *m*	-	C-3
β		1.69, *m*	-	-
2α	30.1, CH_2	1.85, *m*	H- 3	-
β		1.53, *m*	-	-
3	66.4, CH	3.97, *m*	H-2β, 4 α	-
4α	36.9, CH_2	2.11, *ddd* (13.8, 5.1, 1.8)	H-3	C-2, 3, 10
β		1.90, *m*	-	-
5	82.2, C	-	-	-
6	135.4, CH	6.24, *d* (8.5)	H-7	C-4, 5, 7, 8, 10
7	130.7, CH	6.50, *d* (8.5)	H-6	C-5, 6, 8, 9
8	79.4, C	-	-	-
9	51.1, CH	1.50, *m*	H-11	C-5, 10
10	37.0, C	-	-	-
11α	20.6, CH_2	1.58, *m*	H-9	-
β		1.40, *m*	-	-
12α	39.3, CH_2	1.95, *m*	H-11	C-8, 10
β		1.23, *m*	-	-
13	44.6, C	-	-	-
14	51.7, CH	1.56, *m*	-	-
15α	23.4, CH_2	1.50, *m*	-	-
β		1.23, *m*	-	-
16α	28.7, CH_2	1.74, *m*	-	-
β		1.38, *m*	-	-
17	56.2, CH	1.24, *m*	H-20	-
18	12.9, CH_3	0.82, *s*	-	C-13, 14, 17, 20
19	18.2, CH_3	0.88, *s*	-	C-1, 5, 9,10
20	39.7, CH	2.02, *m*	H-17, 21, 22	-
21	20.9, CH_3	1.00, *d* (6.6)	-	C-17
22	135.2, CH	5.14, *dd* (15.2, 7.8)	H-20, 23	C-24
23	132.3, CH	5.23, *dd* (15.2, 7.1)	H- 22, 24	C-20
24	42.8, CH	1.84, *m*	H-23, 25, 28	C-22, 23, 25, 26
25	33.1, CH	1.47, *m*	H-24, 26, 27	-
26	17.6, CH_3	0.91, *d* (6.8)	H-25	C-23
27	19.6, CH_3	0.82, *d* (6.8)	H-25	C-24, 25
28	20.0, CH_3	0.83, *d* (6.8)	H-24	C-23, 24, 25

Literature search revealed that ergosterol-5,8-endoperoxide (**PE 2**) has been previously reported from different sources such as from the aerial parts of *Ajuga remota* Benth.(Cantrell *et al*., 1999), from the pathogenic fungus *Sporothrix schenckii* (Sgarbi *et al*., 1997), from the fungus *Lactarium volemus* (Yue *et al*., 2001), from the endophytic fungus *Verticillium* sp., which was isolated from *Rehmannia glutinosa* (You *et al*., 2009) and *Eurotium chevalieri* KUFA0006, which was isolated from the leaf of the mangrove *Rhizophora mucronata* Poir (May Zim *et al*., 2017), as well as from the marine sponge-associated fungi *Talaromyces trachyspermus* (KUFA 0021) (Kumla *et al*., 2014), *Sporidesmium circinophorum* KUFA 0043 (Buttachon *et al*., 2016), *T. stipitatus* KUFA 0207 (Noinart *et al.,* 2017), *Phoma* sp. (Wu *et al.,* 2018) and *Acremonium persicinum* KUFA 1007 (Alves *et al*., 2019).

3.1.2.3. Citromycin (PE 3)

Compound **PE 3** was isolated as a viscous liquid. The ^{13}C NMR spectrum (Table 14) displayed 13 carbon signals which, in combination with DEPT and HSQC spectra, can be categorized as one conjugated ketone carbonyl (δ_C 174.9), seven non-protonated sp^2 (δ_C 164.5, 155.4, 150.7, 150.4, 140.9, 110.3, 106.2), three methine sp^2 (δ_C 113.3, 108.7, 103.9), one oxymethylene sp^2 (δ_C 62.3) and one methyl (δ_C 19.2) carbons. The ^{1}H NMR spectrum (Table 14), in combination with the HSQC spectrum, showed two broad singlets of two phenolic hydroxyl protons at δ_H 9.96 and 9.07, two singlets of aromatic protons at δ_H 7.00 (δ_C 108.7) and 6.39 (δ_C 103.9) and one doublet of the olefinic proton at δ_H 6.15 (J = 0.8 Hz; δ_C 108.7), one singlet (2H) of the oxymethylene protons at δ_H 4.97 (δ_C 62.3) and one methyl doublet at δ_H 2.32 (J = 0.8 Hz; δ_C 19.2).

That **PE 3** contains 2*H*-chromene-6,8-diol core was supported by the HMBC correlations from the proton singlet at δ_H 7.00 (H-13) to the carbon signals at δ_C 140.9 (C-12), 150.4 (C-11), 150.7 (C-9) and 155.4 (C-7), the proton singlet at δ_H 6.39 (H-10) to the carbon signals at δ_C 106.2 (C-8), C-12 and C-11, as well as from the oxymethylene singlet at δ_H 4.97 (H_2-6) to the carbon signals at δ_C 110.3 (C-5), C-9 and C-7.

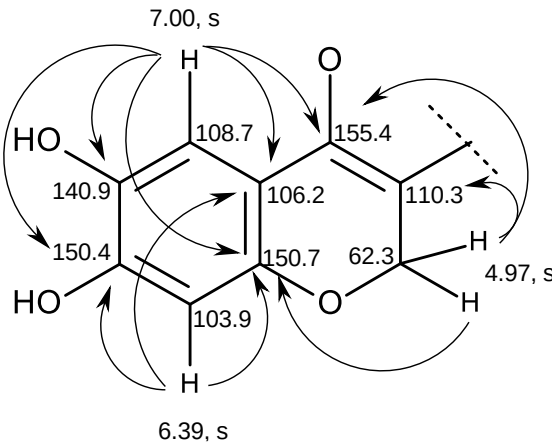

Another moiety of **PE 3** consists of 5,6-disubstituted 2-methyl-4-pyran-4-one, which was substantiated by the COSY correlation from H-3 at δ_H 6.15 *d*, *J* = 0.8 Hz (δ_C 113.3) to the methyl doublet at δ_H 2.32, *J* = 0.8 Hz (δ_C 19.2) as well as by the HMBC correlations from H-3 to the carbons at δ_C 164.5 (C-2) and C-5, from the methyl doublet at δ_H 2.32 to C-2 and C-3.

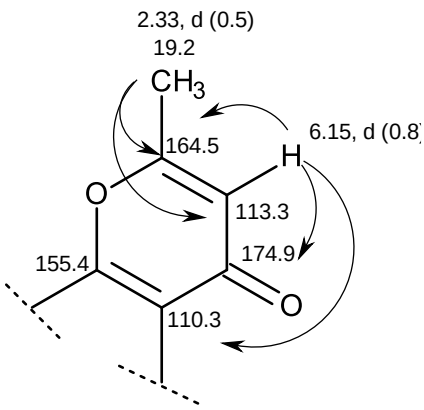

That the 5,6-disubstituted 2-methyl-4-pyran-4-one was fused to the 2*H*-chromene-6,8-diol through C-5 and C-7 was supported by the HMBC correlations from H-6 to C-5, C-7 and the carbonyl carbon at δ_C 174.9 (C-4), and from H-13 to C-7.

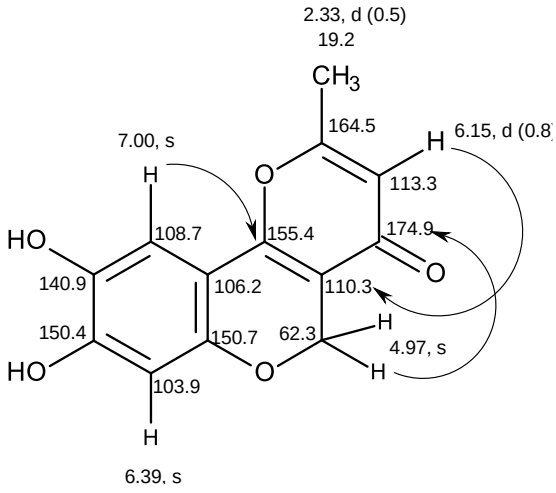

Table 14. ^{1}H and ^{13}C NMR (300 MHz and 75 MHz, DMSO-d_6) and HMBC assignment for **PE 3**

Position	δ_C, type	δ_H, (*J* in Hz)	COSY	HMBC
1	19.2, CH_3	2.32, *d* (0.8)		C-2, 3
2	164.5, C			
3	113.3, CH	6.15, *d* (0.8)		C-2, 5
4	174.9, C			
5	110.3, C			
6	62.3, CH_2	4.97, *s*		C-4, 5, 7, 9
7	155.4, C			
8	106.2, C			
9	150.7, C			
10	103.9, CH	6.39, s		C-9, 11, 12
11	150.4, C			
12	140.9, C			
13	108.7, CH_3	7.00, *s*		C-9, 11

Therefore, the complete structure of **PE 3** was elucidated as 8,9-dihydroxy-2-methyl-4*H*,5*H*-pyrano[3,2-*c*]chromen-4-one (Figure 116).

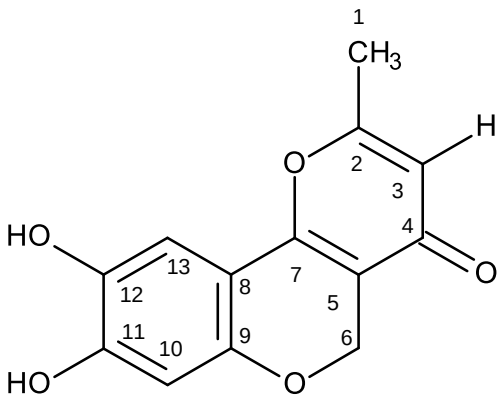

Figure 116. Structure of citromycin (**PE 3**)

Literature search revealed that the NMR data of **PE 3** are compatible with those of citromycin, a fungal metabolite previously reported from several fungal strains including *Citromyces* sp. (Hetherington and Raistrick, 1931), *Penicillium* spp. (Capon *et al*., 2007), as well as from the culture of *Streptomyces* strain IN-1483 (Kusakabe *et al*., 1968).

3.1.2.4. 12-Methylcitromycin (PE 4)

Compound **PE 4** was isolated as a yellow oil, and its molecular formula $C_{14}H_{12}O_5$ was established based on the (+)-HRESIMs *m/z* 283.0599 $(M+Na)^+$ (calculated 283.0582 for $C_{14}H_{12}O_5Na$), which is 14 amu more than that of citromycin (**PE 3**). Therefore, **PE 4** has nine degrees of unsaturation. The ^1H and ^{13}C NMR spectra (Table 15) of **PE 4** resembled those of citromycin (**PE 3**), except for an additional methoxyl group, implying that **PE 4** also has the same 2-methyl-4*H*,5*H*-pyrano[3,2-*c*]chromen-4-one scaffold. The ^{13}C NMR spectrum (Table 15) exhibited 14 carbon signals and, in combination with DEPT and HSQC spectra, can be identified as one conjugated ester carbonyl (δ_C 174.8), seven non-protonated sp^2 (δ_C 164.6, 155.2,

151.9, 151.7, 143.5, 110.3 and 106.0), three methine sp^2 (δ_C 113.4, 106.2, 104.1), one oxymethylene sp^3 (δ_C 62.5), one methoxy (δ_C 56.4) and one methyl (δ_C 19.2) carbons. Similar to the ^{1}H NMR spectrum of citromycin (**PE 3**), the ^{1}H NMR spectrum of **PE 4** (Table 15) displayed a broad signal of the hydrogen-bonded hydroxyl group at δ_H 10.12, two aromatic proton singlets at δ_H 7.09 and 6.63, one olefinic methine at δ_H 6.16, *d* (*J* = 0.8 Hz), a singlet of two oxymethylene protons at δ_H 5.00, a methoxyl singlet at δ_H 3.79, and a methyl doublet at δ_H 2.34 (*J* = 0.8 Hz). That the hydroxyl group on C-12 of citromycin (**PE 3**) was replaced by a methoxyl group was substantiated by not only the COSY correlation from H-13 (δ_H 7.09) to the methoxyl proton signal at δ_H 3.79 but also by the HMBC correlations from the methoxyl proton signal at δ_H 3.79 (δ_C 56.4) to C-12 (δ_C 143.5), H-10 (δ_H 6.34 *s* / δ_H 104.1) to C-12, C-8 (δ_C 106.0), C-11 (δ_C 151.7) and C-9 (δ_C 151.9). The rest of the HMBC correlations were the same as those observed in citromycin (**PE 3**) (Table 15).

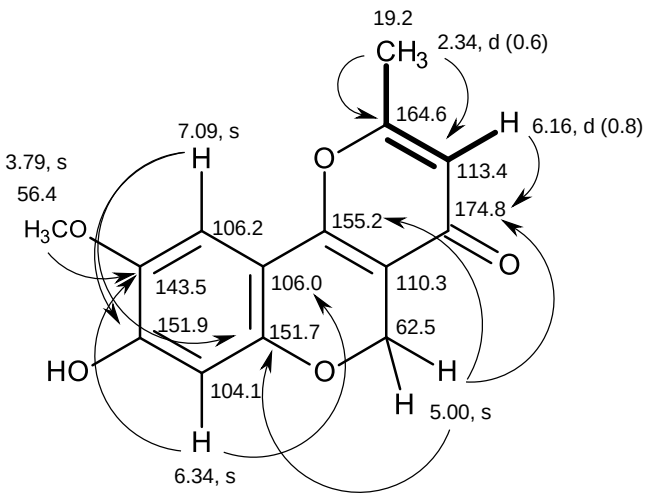

Figure 117. COSY (▬) and HMBC (⟶) correlations of **PE 4**

Table 15. ^{1}H and ^{13}C NMR (300 MHz and 75 MHz, DMSO-d_6) and HMBC assignment for **PE 4**

Position	δ_C, type	δ_H, (*J* in Hz)	COSY	HMBC
1	19.2, CH_3	2.34, *d* (0.8)		C-2, 3
2	164.6, C			
3	113.4, CH	6.16, *d* (0.8)	H-1	C-4
4	174.8, C			
5	110.3, C			
6	62.5, CH_2	5.00, *s*		C-4, 7, 9
7	155.2, C			
8	106.0, C			
9	151.7, C			
10	104.1, CH	6.43, s		C-8, 12
11	151.9, C			
12	143.5, C			
13	106.2, CH_3	7.09, *s*		C-9, 11
14	56.4, CH_3	3.79, *s*		C-12

Therefore, **PE 4** was identified as 12-methylcitromycin (Figure 118).

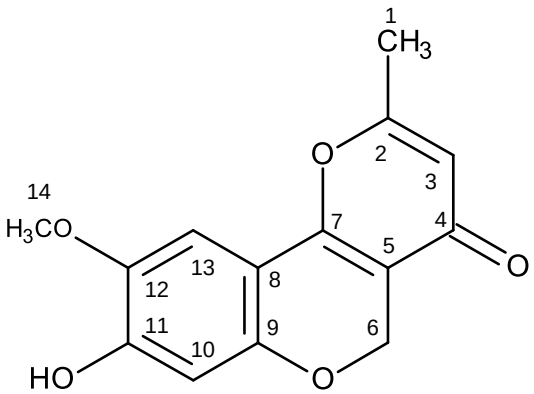

Figure 118. Structure of 12-methylcitromycin (**PE 4**)

Literature search revealed that 12-methylcitromycin (**PE 4**) was previously reported from the marine-derived fungus *Penicillium bilaii*, which was isolated from a boat ramp on the Huon estuary, Port Huon, Tasmania, Australia (Capon *et al*., 2007).

3.1.2.5. 1-Hydroxy-12-methoxycitromycin (PE 5)

Compound **PE 5** was isolated as a white solid (mp 232-233 °C), and its molecular formula $C_{14}H_{12}O_6$ was established based on its (+)-HRESIMS *m/z* 277.0715 $[M+H]^+$, (calculated 277.0712 for $C_{14}H_{13}O_6$), indicating nine degrees of unsaturation. The IR spectrum showed absorption bands for the hydroxyl (3420 cm^{-1}), conjugated ketone carbonyl (1662 cm^{-1}), aromatic (1627, 1555 cm^{-1}), and ether (1270 cm^{-1}) groups.

The ^{13}C NMR spectrum of **PE 5** (Table 16) displayed 14 carbon signals which, according to DEPT and HSQC spectra (Table 16), can be classified as one conjugated ketone carbonyl (δ_C 174.8), seven non-protonated sp^2 (δ_C 167.3, 155.2, 152.2, 151.9, 143.6, 111.2, 105.9), three methine sp^2 (δ_C 110.7, 106.5, 104.1), two oxymethylene sp^3 (δ_C 62.5 and 59.5) and one methoxyl (δ_C 56.4) carbons.

The ^1H NMR spectrum (Table 16) showed two singlets of aromatic protons at δ_H 7.15 (H-12) and 6.44 (H-10), another singlet of one olefinic proton at δ_H 6.25 (H-3), two singlets of oxymethylene protons at δ_H 5.02 (H_2-6) and 4.41 (H_2-1), and a singlet of methoxyl protons at δ_H 3.80 (Me-14). The general features of the ^1H and ^{13}C NMR spectra of **PE 5** resembled those of 12-methoxycitromycin (**PE 4**), which was previously isolated from the Australian marine-derived and terrestrial *Penicillium* spp. (Capon *et al*., 2007), and also isolated in this work. The only difference between the two compounds is the methyl group in **PE 4** (δ_H 2.34, *d*, *J* = 0.6 Hz; δ_C 19.2) is replaced by a hydroxymethyl group (δ_H 4.41; δ_C 59.5) in **PE 5**. The position of the methoxyl group was also confirmed by the NOESY correlation from the methoxyl protons (δ_H 3.80, *s*) to H-13 (δ_H 7.15, *s*).

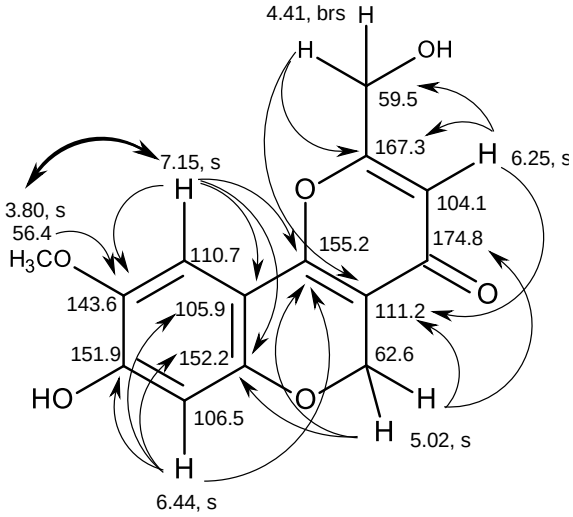

Figure 119. Key HMBC (⟶) and NOESY (⟷) correlations in **PE 5**

Table 16. ^{1}H and ^{13}C NMR (500 MHz and 125 MHz, DMSO-*d*$_6$) and HMBC assignment for **PE 5**

Position	δ_C, Type	δ_H, (*J* in Hz)	HMBC	NOESY
1	59.5, CH_2	4.41, *brs*	C-2, 5	-
2	167.3, C	-	-	-
3	104.1, CH	6.25, *s*	C-1, 2, 5	-
4	174.8, CO	-	-	-
5	111.2, C	-	-	-
6	62.6, CH_2	5.02, *s*	C-4, 5, 7, 9	-
7	155.2, C	-	-	-
8	105.9, C	-	-	-
9	152.2, C		-	-
10	106.5, CH	6.44, *s*	C-7, 8, 9, 11, 12	-
11	151.9, C	-	-	-
12	143.6, C	-	-	-
13	110.7, CH	7.15, *s*	C-7, 8, 9, 11, 12	-
14	56.4, CH_3	3.80, *s*	C-12	H-13

Therefore, **PE 5** is 1-hydroxy-12-methoxycitromycin (Figure 120). The literature search revealed that **PE 5** has never been previously reported.

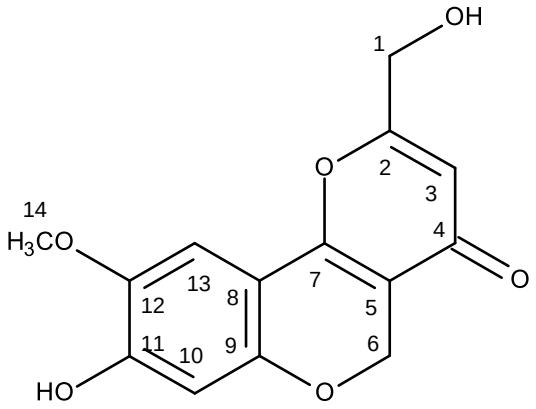

Figure 120. Structure of 1-hydroxy-12-methoxycitromycin (**PE 5**)

3.1.2.6. Myxotrichin D (PE 6)

Compound **PE 6** was isolated as a pale yellow viscous oil, and showed its (+)-HRESIMS *m/z* 275.0561 $(M+H)^+$ (calculated 275.0556 for $C_{14}H_{11}O_6$), establishing its molecular formula as $C_{14}H_{10}O_6$, and thus ten degrees of unsaturation. Surprisingly, its ^{13}C NMR spectrum (Table 17) showed only 13 carbon signals, one carbon less than those indicated by the (+)-HRESIMS data. By combination with DEPT and HSQC spectra, these carbons are categorized as two conjugated ester carbonyl (δ_C 175.0), seven non-protonated sp^2 (δ_C 164.8, 162.2, 161.5, 158.3, 156.7, 110.5), three methine sp^2 (δ_C 112.7, 109.0, 101.3), one oxymethylene sp^2 (δ_C 61.9) and one methyl (δ_C 18.9) carbons. The ^1H NMR spectrum (Table 17) showed a broad signal at δ_H 8.45 (1H), a broad singlet at δ_H 6.47 (1H), two singlets at δ_H 6.23 (1H) and 6.08 (1H), a singlet at δ_H 4.89 (2H) and a broad singlet of a methyl group at δ_H 2.21.

The existence of a 2-methyl-4*H*,5*H*-pyrano[3,2-*c*]chromen-4-one skeleton, similar to that of citromycin (**PE 3**) was supported by HMBC correlations from H-3 (δ_H 6.08) to C-2 (δ_C 164.8), C-5 (δ_C 110.4), from H_2-6 (δ_H 4.89, *s*) to C-5, C-7 (δ_C 156.7), C-4 (δ_C175.0) and C-9 (δ_C 158.3), from H-10 (δ_H 6.23, *s*) to C-8 (δ_C 103.5), C-9, C-11 (δ_C 161.5). However, HMBC correlations were not observed for H-12 (δ_H 6.47, *brs*)

and CH_3-1 (δ_H 2.21). Therefore, there is one carbon that was not accounted for, i. e. at δ_C 162.2, and one carbon was missing. This suggested that C-13 must be substituted by a carboxyl group, which normally showed very week intensity or undetectable signal in the ^{13}C NMR spectrum.

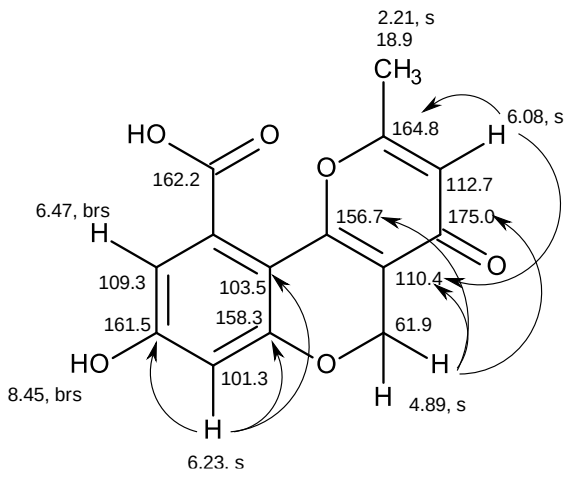

Figure 121. Key HMBC (⟶) correlations in **PE 6**

Table 17. ^1H and ^{13}C NMR (500 MHz and 125 MHz, DMSO-d_6) and HMBC assignment for **PE 6**

Position	δ_C, type	δ_H, (*J* in Hz)	COSY	HMBC
1	18.9, CH_3	2.21, *brs*		
2	164.8, C			
3	112.7, CH	6.08, *s*		C-1, 2, 5
4	175.0, C			
5	110.4, C			
6	61.9, CH_2	4.89, *s*		C-4, 5, 7, 9
7	156.7, C			
8	103.5, C			
9	158.3, C			
10	101.3, CH	6.23, *s*		C-8, 9, 11
11	161.5, C			
12	109.0, CH	6.47, *brs*		
13	n			
14.	162.2 C			

**n = not observed

Therefore, the structure of **PE 6** was proposed as 8-hydroxy-2-methyl-4-oxo-4*H*,5*H*-pyrano[3,2-*c*]chromene-10-carboxylic acid or commonly known as myxotrichin D (Figure 122).

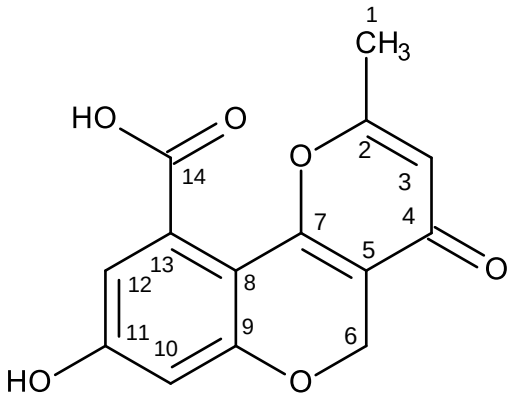

Figure 122. Structure of myxotrichin D (**PE 6**)

Literature search revealed that myxotrichin D (**PE 6**) has been previously reported from the cutures of the endolichenic fungus *Myxotrichum* sp., isolated from the lichen *Cetraria islandica*, which was collected from Laojun Mountain, Yunnan Province, People's Republic of China (Yuan *et al*., 2013). Although there is some discrepancy in the value of C-14, the chemical shift values of the rest of the carbons and protons were compatible with those reported in the literature.

3.1.2.7. 12-Methoxycitromycetin (PE 7)

Compound **PE 7** was isolated as a pale yellow oil, and its molecular formula $C_{15}H_{12}O_7$ was established on the basis of the (+)-HRESIMS *m/z* 305.0668 $(M+H)^+$ (calculated 305.0661 for $C_{15}H_{13}O_7$), indicating ten degree of unsaturation. The ^1H and ^{13}C NMR spectra of **PE 7** resembled those of **PE 4**. The ^{13}C NMR spectrum (Table 18) displayed only 13 carbon signals which is one carbon less than those indicated by (+)-HRESIMS. These carbons are categorized, according to DEPTs and HSQC spectra,

as one conjugated ketone (δ_C 175.4), one conjugated carboxyl carbonyl (δ_C 167.2), seven non-protonated sp^2 (δ_C 164.5, 155.0, 154.1, 153.6, 139.5, 111.4, 103.8), two methine sp^2 (δ_C 113.4, 104.9), one oxymethylene sp^3 (δ_C 62.2), one methoxyl (δ_C 61.1) and one methyl (δ_C 18.6) carbons. The ^{1}H NMR spectrum (Table 18) exhibited a broad signal of the hydroxyl group of a carboxylic acid at δ_H 10.80, one singlet at δ_H 6.53 (1H), one doublet at δ_H 6.19 (*J* = 0.8 Hz), one singlet at δ_H 5.00 (2H), one methoxyl singlet at δ_H 3.71 (3H), and a methyl singlet at δ_H 2.09. The existence of the 8-hydroxy-9-methoxy-2-methyl-4*H*,5*H*-pyrano[3,2-*c*]chromen-4-one skeleton was supported by the COSY correlations from H-3 (δ_H 6.19, *d*, *J* = 0.8 Hz) to Me-1 (δ_H 2.09, *s*) as well as by the HMBC correlations from Me-1 to C-2 (δ_C 164.5) and C-3 (δ_C 113.4), H-3 to Me-1 (δ_C 18.6), C-5 (δ_C 111.4), C-4 (δ_C 174.7), H_2-5 (δ_H 5.00, *s*) to C-5, C-9 (δ_C 154.1), C-7 (δ_C 155.0), C-4, H-10 (δ_H 6.53, *s*) to C-8 (δ_C 103.0), C-12 (δ_C 139.5) and C-9, and from OMe (δ_H 3.71/ δ_C 61.0) to C-12).

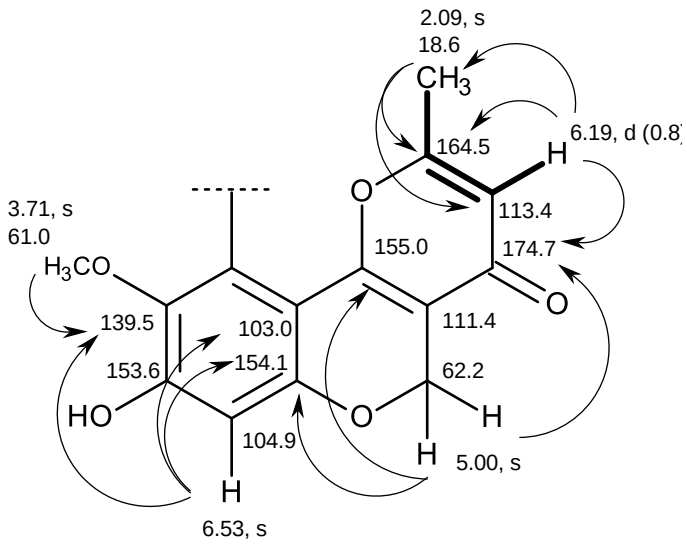

Figure 123. COSY (▬) and key HMBC (⟶) correlations in **PE 7**

Table 18. ^{1}H and ^{13}C NMR (300 MHz and 75 MHz, DMSO-d_6) and HMBC assignment for **PE 7**

Position	δ_C, type	δ_H, (*J* in Hz)	COSY	HMBC
1	18.6, CH_3	2.09, *s*	-	-
2	164.5, C	-	-	-
3	113.4, CH	6.19, *d* (0.8)	-	C-1, 2, 5
4	174.7, C	-	-	-
5	111.4, C	-	-	-
6	62.2, CH_2	5.00, *s*	-	C-4, 5, 7, 9
7	155.0, C	-	-	-
8	103.0, C	-	-	-
9	154.1, C	-	-	-
10	104.9, CH	6.53, *s*	-	C-8, 9, 11
11	153.6, C	-	-	-
12	139.5, C	-	-	-
13	n	-	-	-
14.	167.2 C	-	-	-

**n = not observed

This partial structure constitutes $C_{14}H_{11}O_5$, short of CO_2H from the molecular formula ($C_{15}H_{12}O_7$). Therefore, the carboxyl group was placed on C-13, giving rise to 8-hydroxy-9-methoxy-2-methyl-4-oxo-4*H*,5*H*-pyrano[3,2-*c*]chromene-10-carboxylic acid.

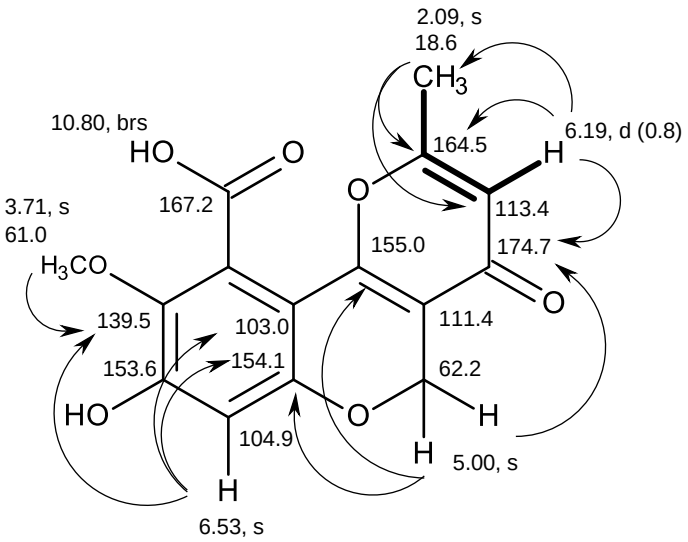

It is noteworthy observing that, like in myxotrichin D (**PE 6**), the signal of C-13 in **PE 7** was not observed in the ^{13}C NMR spectrum.

Literature search revealed that **PE 7** corresponded to 12-methoxycitromycetin (Figure 124), which was previously isolated from the culture of the marine-derived fungus *Penicillium bilaii* (Capon *et al*., 2007).

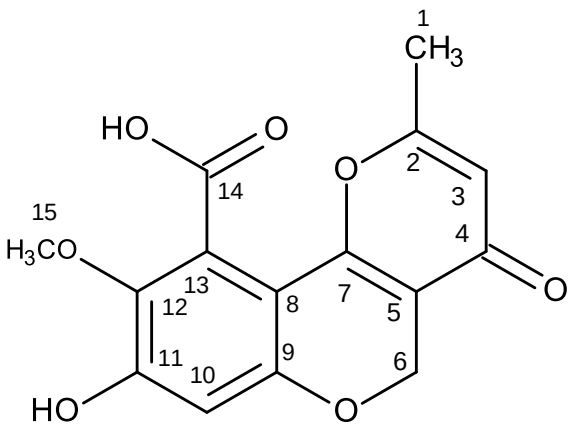

Figure 124. Structure of 12-methoxycitromycetin (**PE 7**)

3.1.2.8. Anhydrofulvic acid (PE 8)

Compound **PE 8** was isolated as white crystals (mp, 235-237 ºC) and its molecular formula $C_{14}H_{10}O_7$ was established on the basis of the (+)-HRESIMS *m/z*

313.0359 $(M+Na)^+$ (calculated 313.0324 for $C_{14}H_{10}O_7Na$), indicating ten degrees of unsaturation. The ^{13}C NMR spectrum displayed 14 carbon signals (Table 19) which, according to DEPT and HSQC spectra, can be categorized as two conjugated carbonyl (δ_C 170.1 and 168.9), eight non-protonated sp^2 (δ_C 167.4, 158.5, 151.9, 149.7, 143.4, 117.8, 112.8 and 110.2), two methine sp^2 (δ_C 103.2 and 94.3), one oxymethylene sp^3 (δ_C 64.1) and one methyl (δ_C 19.9) carbons. The ^1H NMR spectrum (Table 19) displayed one singlet of aromatic proton at δ_H 6.90, one doublet of an olefinic proton at δ_H 5.68 (J = 0.8 Hz), one singlet of oxymethylene protons at δ_H 5.14, and a methyl doublet at δ_H 1.99 (J = 0.8 Hz). That the structure of **PE 8** consists of 7,8-dihydroxy-3-methyl-4a,10a-dihydro-1*H*,10*H*-pyrano[4,3-*b*]chromen-10-one skeleton was substantiated by COSY correlations from H-4 (δ_H 5.68, *d*, J = 0.8 Hz) to the methyl doublet at δ_H 1.99, J = 0.8 Hz (Me-11), as well as HMBC correlations from H-4 to Me-11, C-4a (δ_C 158.5), C-3 (δ_C 167.4), from H_2-1 (δ_H 5.14, *s*) to C-10a (δ_C 101.2), C-4a, C-3, and C-10 (δ_C 171.1), from H-6 (δ_H 6.90, *s*) to C-5a (δ_C 151.9), C-7 (δ_C 149.7) and C-8 (δ_C 143.4).

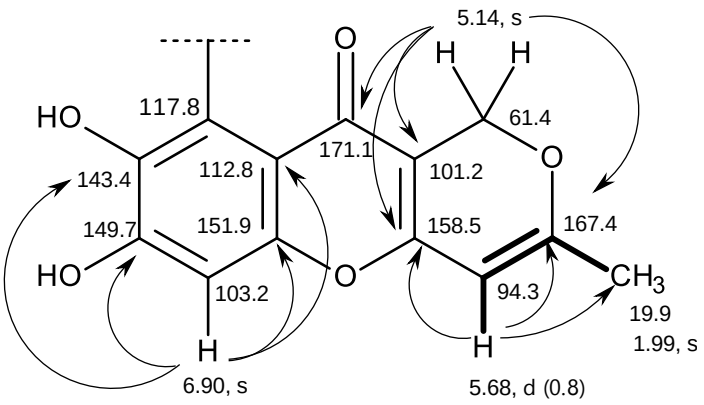

From this partial structure, there are still one conjugated carbonyl at δ_C 168.9 and one non-protonated sp^2 carbons at δ_C 117.8 that were still unaccounted for. Given the chemical shift values of these carbons and the molecular formula ($C_{14}H_{10}O_7$), the carboxyl group was placed on C-9, therefore completing the structure of **PE 8** as 7,8-dihydroxy-3-methyl-10-oxo-10,10a-dihydro-1*H*,4a*H*-pyrano[4,3-*b*]chromene-9-carboxylic acid, or commonly known as anhydrofulvic acid (Figure 125).

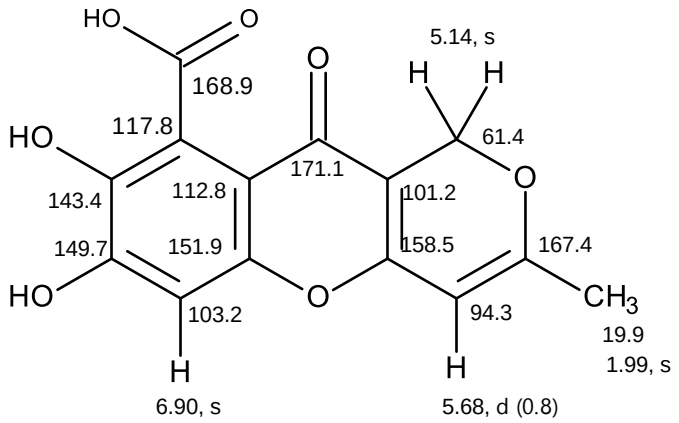

Figure 125. Structure of anhydrofulvic acid (**PE 8**), indicating ^{1}H and ^{13}C chemical shifts

Table 19. ^{1}H and ^{13}C NMR (300 MHz and 75 MHz, DMSO-d_6) and HMBC assignment for **EP 8**

Position	δ_C, type	δ_H, (*J* in Hz)	COSY	HMBC
1	64.1, CH_2	5.14, *s*	-	C-3,4a,10,10a
2		-	-	-
3	167.4, C	-	-	-
4	94.3, CH	5.68, *d* (0.8)	H-11	C-3,4a,11
4a	158.5, C	-	-	-
5a	151.9, C	-	-	-
6	103.2, CH	6.90, *s*	-	C-5a, 7, 8, 9a, 10
7	149.7, C	-	-	-
8	143.4, C	-	-	-
9	117.8, C	-	-	-
9a	112.8, C	-	-	-
10	171.10, C	-	-	-
10a	101.2, C	-	-	-
11	19.9, CH_3	1.99, *d* (0.8)	-	C-3, 4
12	168.8, C	-	-	-

Anhydrofulvic acid (**PE 8**) (Figure 126) has been previously reported as secondary metabolite isolated from the soil fungus *Penicillium afacidum* (Fujita *et al*., 1999) and also from the marine-derived fungus *Penicillium* sp .JF-55 (Lee *et al*., 2013).

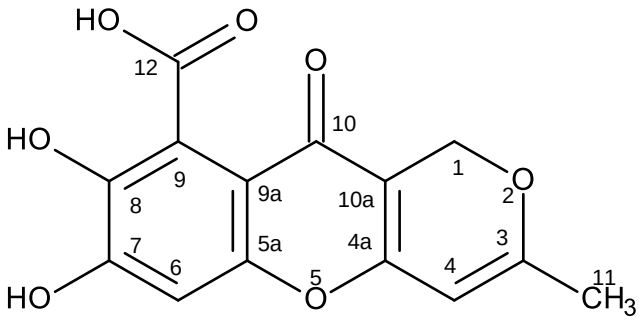

Figure 126. Structure of anhydrofulvic acid (**PE 8**)

3.1.2.9. Myxotrichin C (PE 9)

Compound **PE 9** was isolated as a mixture with another structurally similar compound (**PE 10**), as a major component (2:1) in the mixture. The (+)-HRESIMS gave the $(M+H)^+$ peak at *m/z* 247.0610 (calculated 247.0606 for $C_{13}H_{11}O_5$). Therefore, its molecular formula was determined as $C_{13}H_{10}O_5$ and possesses nine degrees of unsaturation. The ^{13}C NMR spectrum (Table 20) exhibited two set of signals, 13 of which have higher intensity which, in combination with DEPT and HSQC spectra, can be categorized as one conjugated ketone carbonyl (δ_C 171.7), seven non-protonated sp^2 (δ_C 166.3, 158.2, 151.5, 149.7, 144.2, 116.5, 101.0), three methine sp^2 (δ_C 107.9, 103.0, 94.8), one oxymethylene sp^3 (δ_C 64.1) and one methyl (δ_C 19.8) carbons. The ^1H NMR spectrum (Table 20) also showed two sets of proton signals, one of which has twice intensity of another (estimated from the integration). The higher intensity proton signals appeared as two singlets of aromatic protons at δ_H 7.25 and 6.82, one doublet of an olefnic proton at δ_H 5.64 (*J* = 0.9 Hz), a singlet of the oxymethylene protons at δ_H 5.13 (2H) and a methyl doublet at δ_H 1.98 (*J* = 0.9 Hz). The presence of a 3,4-disubstituted 6-methyl-2*H*-pyran was evidenced by the COSY correlation from H-3 (δ_H 5.64, *d*, *J* = 0.9 Hz) to Me-1 (δ_H 1.98, *d*, *J* = 0.9 Hz) as well as HMBC correlations from H-3 to Me-1 (δ_C 19.8), C-4 (δ_C 158.2), C-5 (δ_C 101.0), and C-2 (δ_C 166.3), from H_2-5 (δ_H 5.13, *s*) to C-4, C-5 and C-3, Me-1 to C-2 and C-3.

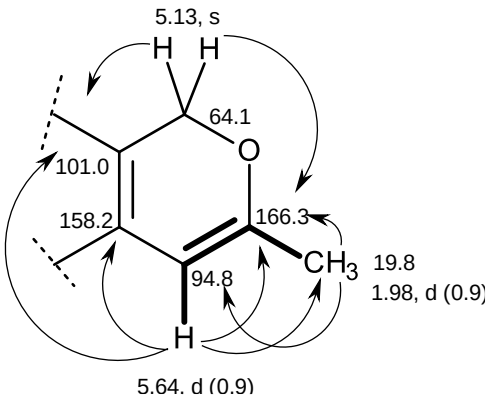

Another part of the molecule was identified as 2,4,5-trisubstituted phenone by HMBC correlations from H-10 (δ_H 6.82, *s*) to C-8 (δ_C 116.5), C-9 (δ_C 151.5), C-11 (δ_C 149.7) and C-12 (δ_C 144.2), and from H-13 (δ_H 7.25, *s*) to C-8, C-9, C-11, C-12 and the carbonyl group at δ_C 171.7 (C-7). The chemical shift values of C-9, C-11 and C-12 indicated that the substituents on C-9, C-11 and C-12 are oxygen atoms.

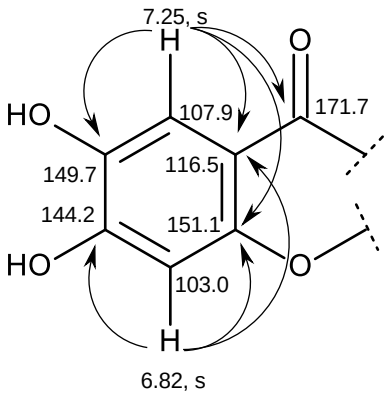

That the 2,4,5-trisubstituted phenone was fused with the 3,4-disubstituted 6-methyl-2*H*-pyran through the carbonyl (C-7) of the former and C-5 of the later, and by the ethereal bride between C-9 and C-4 was evidenced by HMBC correlation from H-6 to C-7 and by the chemical shift value of C-4.

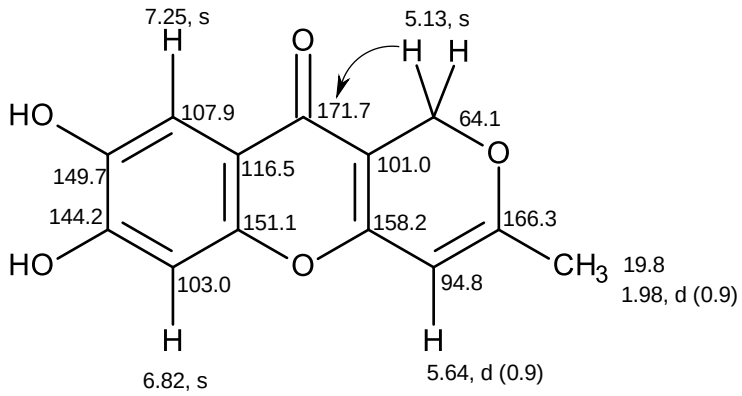

Table 20. ^{1}H and ^{13}C NMR (500 MHz and 125 MHz, DMSO-d_6) and HMBC assignment for **PE 9**

Position	**δC, type**	**δH, (*J* in Hz)**	**COSY**	**HMBC**
1	19.8, CH_3	1.98, *d* (0.9)	-	C-2, C-3
2	166.3, C	-	-	-
3	94.8, CH	5.64, *d* (0.9)	H-1	C-1, 2, 4, 5
4	158.2, C	-	-	-
5	101.0, C	-	-	-
6	64.1, CH_2	5.13, *s*	-	C-2, 5
7	171.7, C	-	-	-
8	116.5, C	-	-	-
9	151.5, C	-	-	-
10	103.0, CH	6.82, *s*	-	C-7, 8, 10
11	144.2, C	-	-	-
12	149.7, C	-	-	-
13	107.9, CH	7.25, *s*	-	C-6, 7, 8, 11,

Therefore the structure of **PE 9** was elucidated as 7,8-dihydroxy-3-methyl-1*H*,10*H*-pyrano[4,3-*b*]chromen-10-one (Figure 127).

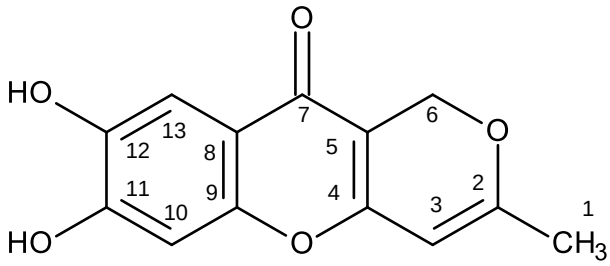

Figure 127. Structure of myxotrichin C (**PE 9**)

Literature search revealed that the structure of **PE 9** corresponds to myxotrichin C which has been previously reported from an endolichenic fungus *Myxotrichum* sp., which was isolated from the lichen *Cetraria islandica* (L.) Ach (Yuan *et al*., 2013).

3.1.2.10. Penialidin G (PE 10)

The minor compound in the mixture (**PE 10**) showed another set of proton and carbon signals, with lower intensities, which can be easily distinguished from those of myxotrichin C (**PE 9** major compound). The ^{1}H NMR spectrum, in combination with the COSY spectrum (Table 21), displayed two singlets of aromatic protons at δ_H 7.26 and 6.83, two double doublets of geminally coupled methylene protons at δ_H 2.63 (J = 17.6, 2.6 Hz) and δ_H 2.96 (J = 17.6, 2.6 Hz), a double triplet at δ_H 4.22 (J = 14.9, 0.9 Hz) and a double doublet at δ_H 4.52 (J = 14.9, 2.1 Hz) of another pair of the geminally coupled oxymethylene protons, a singlet of the methoxyl group at δ_H 3.21 and another methyl singlet at δ_H 1.44. The ^{13}C NMR spectrum (Table 21) showed 14 carbon signals which, according to DEPT and HSQC spectra, can be classified as one conjugated carbonyl ketone (δ_C 173.2), six non-protonated sp^2 (δ_C 157.9, 152.1, 150.8, 144.4, 115.4, 113.0), two protonated sp^2 (δ_C 107.4 and 102.7), one ketal (δ_C 97.7), one oxymethylene sp^3 (δ_C 57.1), one methylene sp^3 (δ_C 37.1), one methoxyl (δ_C 48.3) and one methyl (δ_C 22.4) carbons. The (+)-HRESIMS give the $(M+H)^+$ peak at *m/z* 279.0878 (calculated 279.0869 for $C_{14}H_{15}O_6$); therefore, the molecular formula of **PE 10** was established as $C_{14}H_{14}O_6$ which indicates eight degrees of unsaturation.

Comparison of the ^{1}H and ^{13}C chemical shift values of **PE 10** with those of **PE 9** revealed that they have the same 6,7-dihydroxy-4*H*-chromen-4-one scaffold. This was confirmed by the HMBC correlations from H-13 (δ_H 7.26, *s*/ δ_C 107.4) to C-9 (δ_C 152.1), C-11 (δ_C 150.8), C-2 (δ_C 144.3) and C-7 (δ_C 173.2), and from H-10 (δ_H 6.83, *s*/ δ_C 102.7) to C-8 (δ_C 115.4), C-9 and C-12.

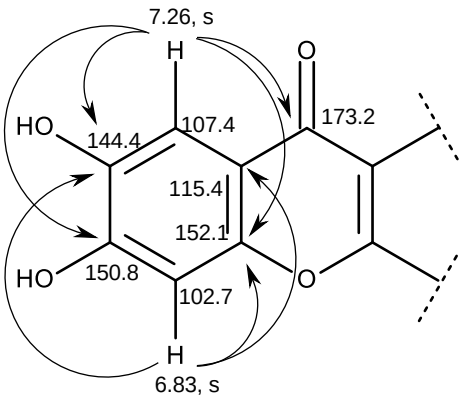

That the third ring in **PE 10** was 4, 5-disubstituted 2-methoxy-2-methyl-3,6-dihydro-2*H*-pyran instead of 3,4-disubstituted 6-methyl-2*H*-pyran in **PE 9** was substantiated by the HMBC correlations from Me-1 (δ_H 1.44, *s*) to C-2 (δ_C 97.7), C-3 (δ_C 37.1), from the methoxyl singlet at δ_H 3.21 to C-2, from H_2-3 (δ_H 2.63, *dd*, *J* = 17.6, 2.6 Hz)/δ_H 2.96, *dd*, *J* = 17.6, 2.6 Hz) to C-3 and C-4 (δ_C 157.9), from H-6 (δ_H 4.22, *dt*, *J* = 14.9, 0.9 Hz)/δ_H 4.52, *dd*, *J* = 14.9, 2.1 Hz) to C-3, C-4 and C-5 (δ_C 113.0).

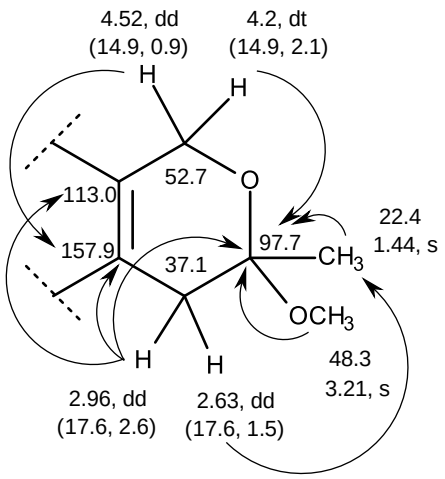

Table 21. ^{1}H and ^{13}C NMR (500 MHz and 125 MHz, DMSO-d_6) and HMBC assignment for **PE 10**

Position	δ_C, type	δ_H, (*J* in Hz)	COSY	HMBC
1	22.4, CH_3	22.4, *s*	-	C-2
2	97.7, C	-	-	-
3	37.1, CH_2	2.63, *dd* (17.6, 2.6)	-	C-1
		2.96, *dd* (17.6, 2.6)	-	C-2, 4, 5
4	157.9, C	-	-	-
5	113.0, C	-	-	-
6	52.7, CH_2	4.22, *dt* (14.9, 0.9)-	-	C-2
		4.52, *dd* (14.9, 2.1)	-	C-4
7	173.2, CO	-	-	-
8	115.4, C	-	-	-
9	152.1, C	-	-	-
10	102.7, CH	6.83, *s*	-	C-8, 9, 12
11	150.8, C	-	-	-
12	144.4, C	-	-	-
13	107.4, CH	7.26, *s*	-	C-7, 9, 11, 12
14.	48.3, CH_3	3.21, *s*	-	C-2

Therefore, the planar structure of **PE 10** was elucidated as 7,8-dihydroxy-3-methoxy-3-methyl-3,4-dihydro-1*H*,10*H*-pyrano[4,3-*b*]chromen-10-one (Figure 128).

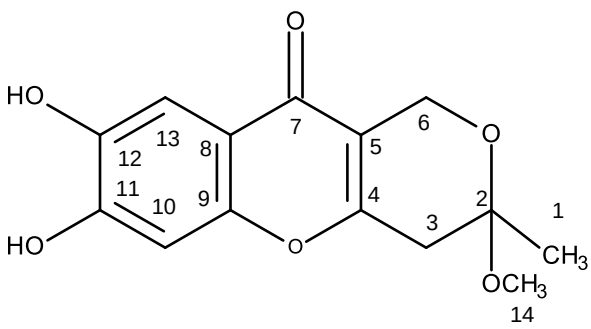

Figure 128. The planar structure of **PE 10**

As C-2 of **PE 10** is stereogenic, it is necessary to verify its absolute configuration. Since **PE 10** was isolated as a 1:2 mixture with myxotrichin C (**PE 9**) and could not be isolated as a pure compound, it was impossible to obtain its crystal for X-ray analysis. Since myxotrichin C (**PE 9**) is not chiral, it will not affect the ECD spectrum of the chiral **PE 10**. Interestingly, the ECD spectrum of the mixture did not exhibit any Cotton effects. Consequently, it was concluded that **PE 10** is a mixture of bother enantiomers. Since **PE 10** has never been previously reported, and in line with the names given to this structural type, it was named penialidin G (Figure 129).

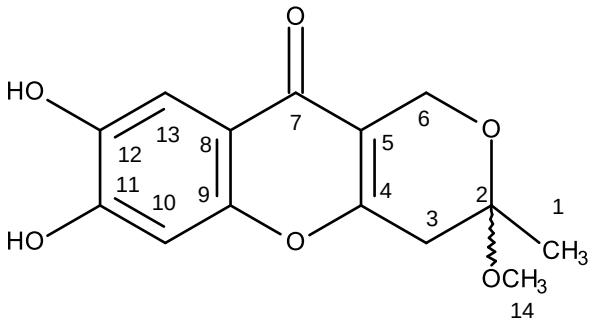

Figure 129. Structure of penialidin G (**PE 10**)

3.1.2.11. Penialidin D (PE 11)

Compound **PE 11** was isolated as a pale yellow oil, and its molecular formula $C_{15}H_{12}O_7$ was established on the basis of (+) HRESIMS *m/z* 305.0666 $(M+H)^+$ (calculated 305.0661 for $C_{15}H_{13}O_7$).The ^{1}H NMR feature of **PE 11** resembled that of myxotrichin C (**PE 9**).

The ^{13}C NMR spectrum (Table 22) displayed 15 carbon signals which, in combination with DEPT and HSQC spectra, can be classified as one conjugated ketone (δ_C 170.8), one conjugated carboxyl (δ_C 167.2), eight non-protonated sp^2 (δ_C 167.1, 158.4, 155.4, 152.1, 142.2, 127.9, 112.6, 101.5), two methine sp^2 (δ_C 104.1, 94.5), one oxymethylene sp^3 (δ_C 64.0), one methoxyl (δ_C 61.1) and one methyl (δ_C 19.8) carbons.

The ^{1}H NMR spectrum (Table 22) displayed, besides two broad signals at δ_H 11.15 and 12.89, one singlet of an aromatic proton at δ_H 6.93, one olefinic doublet at

δ_H 5.67 (*J* = 0.8 Hz), one oxymethylene singlet at δ_H 5.12, one methoxyl singlet at δ_H 3.74 and a methyl doublet at δ_H 1.10 (*J* = 0.8 Hz).

That **PE 11** has a 6-substituted 7,8-dihydroxy-3-methyl-1*H*,10*H*-pyrano[4,3-*b*]chromen-10-one scaffold was supported by the COSY correlation from H-3 (δ_H 5.67, *d*, *J* = 0.8 Hz) to Me-1 (δ_H 1.10, *d*, *J* = 0.8 Hz) as well as HMBC correlations from H-3 to C-2 (δ_C 167.1), C-4 (δ_C 158.4), C-5 (δ_C 101.2) and Me-1 (δ_C 19.8), from H-6 (δ_H 5.12, *s*) to C-2, C-4, C-5 and the carbonyl carbon at δ_C 170.8 (C-7), from H-13 (δ_H 6.93,*s*) to C-8 (δ_C 112.6), C-9 (δ_C 155.4), C-11 (δ_C 142.2), C-12 (δ_C 152.1) and C-7. That the OMe group was on C-11 was corroborated not only by the HMBC correlation from the singlet at δ_H 3.74 (OMe/δ_C 61.1) to H-12 but also by the chemical shift value of the methoxyl carbon at δ_C 61.1, indicating that this methoxyl group was flanked by oxygenated substituents.

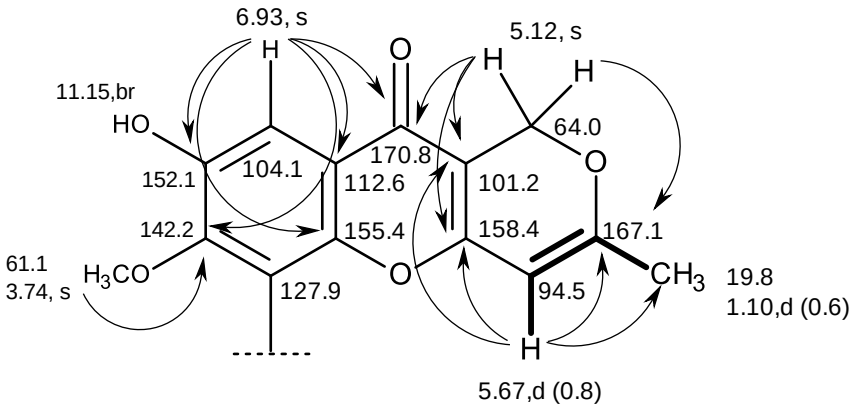

In this scaffold, there are still two carbons at δ_C 167.2 (CO) and 127.9 (C10), and the broad signal at δ_H 12.89, characteristic of the hydroxyl group of a carboxylic acid, which are unaccounted for. Therefore, the substituent on C-10 must be a carboxyl group. Thus, the structure of **PE 11** was proposed to be:

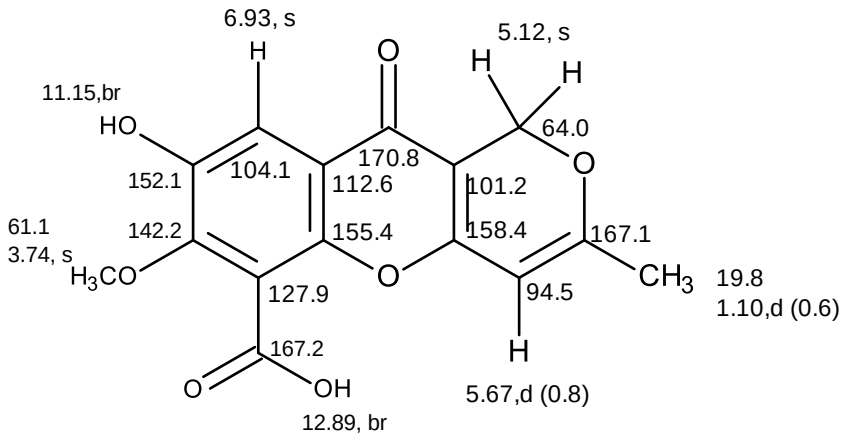

Figure 130. Structure of penialidin D (**PE 11**) indicating ^{1}H and ^{13}C chemical shifts

Table 22. ^{1}H and ^{13}C NMR (500 MHz and 125 MHz, DMSO-d_6) and HMBC assignment for **PE 11**

Position	δ_C, type	δ_H, (*J* in Hz)	COSY	HMBC
1	19.8, CH_3	1.10, *d* (0.6)	-	-
2	167.1, C	-	-	-
3	94.5, CH	5.67, *d* (0.8)	H-1	C-1, 2, 4, 5
4	158.4, C	-	-	-
5	101.2, C	-	-	-
6	64.0, CH_2	5.12, *s*	-	C-2, 4, 5, 7
7	170.8, C	-	-	-
8	112.6, C	-	-	-
9	155.4, C	-	-	-
10	127.9, C	-	-	-
11	142.2, C	-	-	-
12	152.1, C	-	-	-
13	104.1, CH	6.93, *s*	-	C- 7, 8, 9, 11, 12
14.	167.2, C	-	-	-
15.	61.1, CH_3	3.74, *s*	-	C-11
OH	-	11.15, *br*	-	-
OH	-	12.89, *br*	-	-

Therefore, the structure of **PE 11** was established as 7,8-dihydroxy-3-methyl-10-oxo-1*H*,10*H*-pyrano[4,3-*b*]chromene-6-carboxylic acid or commonly known as penialidin D (Figure 131).

Literature search revealed that penialidin D has been previously isolated from a fermentation of the sediment-derived fungus *Penicillium janthinellum* DT-F29 (Cheng *et al*., 2018).

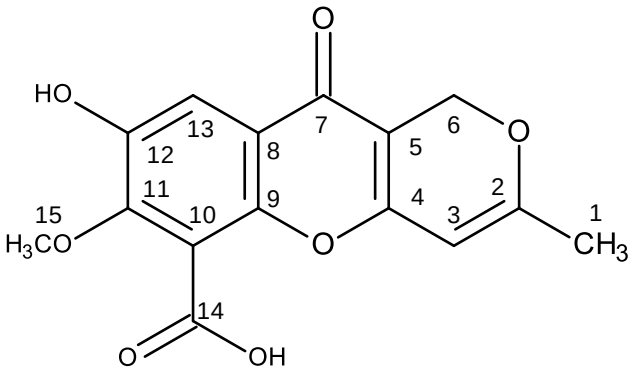

Figure 131. Structure of penialidin D (**PE 11**)

3.1.2.12. Penialidin F (PE 12)

Compound **PE 12**, a pale yellow viscous oil, displayed the (+)-HRESIMS *m/z* 265.0719 $(M+H)^+$ (calculated 265. 0712 for $C_{13}H_{13}O_6$), indicating its molecular formula $C_{13}H_{12}O_6$ and eight degrees of unsaturation. The general features of its ^1H and ^{13}C NMR spectra resembled those of penialidin G (**PE 10**) except for an absence of the methoxyl group. The ^{13}C NMR spectrum of **PE 12** (Table 23) exhibited 13 carbon signals which, according to DEPT and HSQC spectrum, can be categorized as one conjugated ketone carbonyl (δ_C 173.4), six non-protonated sp^2 (δ_C 158.5, 152.1, 150.8, 144.3, 115.4, 113.5), two methine sp^2 (δ_C 107.4, 102.8), one hemi-ketal (δ_C 94.2), one oxymethylene sp^3 (δ_C 56.3), one methylene sp^3 (δ_C 37.5) and one methyl (δ_C 28.4) carbons. The ^1H NMR spectrum (Table 23) displayed two singlets of aromatic protons at δ_H 7.26 and 6.83, a singlet of oxymethylene protons at δ_H 4.45 and a doublet of one geminally coupled methylene proton at δ_H 2.87 (J = 17.1 Hz) (another methylene proton signal at δ_H 2.55 was under the water signal and was only detected in HSQC

spectrum) and a methyl singlet at δ_H 2.09. That **PE 12** contains a 2,3-disubstituted 6,7-dihydroxy-4*H*-chromen-4-one moiety was substantiated by HMBC correlations from H-13 (δ_H 7.26, *s*) to C-7 (δ_C 173.4), C-9 (δ_C 152.1), C-11 (δ_C 150.4), C-12 (δ_C 144.3), from H-10 (δ_H 6.83, *s*) to C-8 (δ_C 115.4), C-9 and C-11.

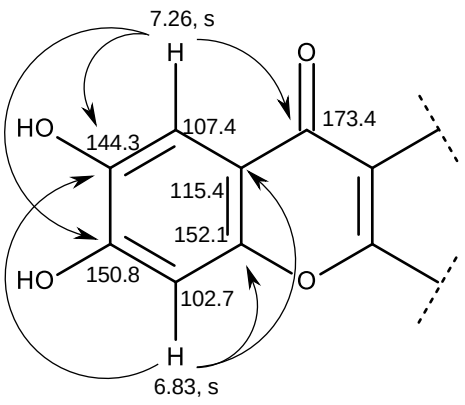

That another part of the molecule consists of 4,5-disubstituted 2-methyl-3,6-dihydro-2*H*-pyran-2-ol was supported by HMBC correlations from H_2-6 (δ_H 4.45, *s*) to C-2 (δ_C 94.2), C-4 (δ_C 158.7), C-5 (δ_C 113.5), H-3 (δ_H 2.55, *dd*, *J* = 17.5 Hz) to C-4, C-2 and Me-1 (δ_C 28.3), H_3-1 (δ_H 1.45, *s*) to C-2 and C-3 (δ_C 37.5).

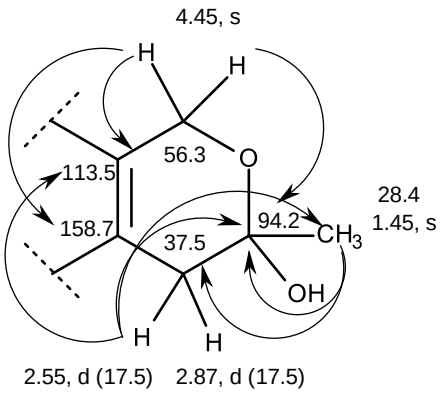

Combining the two partial structures, with a fusion through C-4 and C-5, gives the molecular formula $C_{13}H_{12}O_6$.

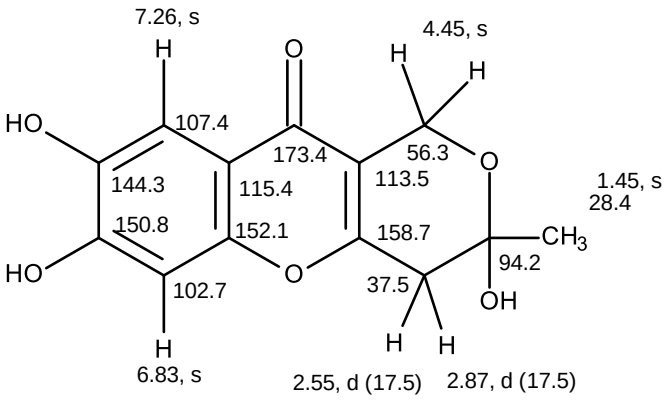

Table 23. ^{1}H and ^{13}C NMR (300 MHz and 75 MHz DMSO-d_6) and HMBC assignment for **PE 12**

Position	**δ_C, type**	**δ_H, (*J* in Hz)**	**COSY**	**HMBC**
1	28.4, CH_3	1.45, *s*	-	C-2, 3
2	994.2, C	-	-	-
3	37.5, CH_2	2.55, *d* (17.5)	-	C-1, 2, 4
		2.87, *d* (17.5)	-	-
4	158.7, C	-	-	-
5	113.5, C	-	-	-
6	56.3, CH_2	4.45, *s*	-	C-2, 4, 5
7	173.4, CO	-	-	-
8	115.4, C	-	-	-
9	152.1, C	-	-	-
10	102.7, CH	6.83, *s*	-	C-8, 9, 11
11	150.8, C	-	-	-
12	144.3, C	-	-	-
13	107.4, CH	7.26, *s*	-	C-7, 9, 11, 12

Therefore the planar structure of **PE 12** was elucidated as 3,7,8-trihydroxy-3-methyl-3,4-dihydro-1*H*,10*H*-pyrano[4,3-*b*]chromen-10-one (Figure 132).

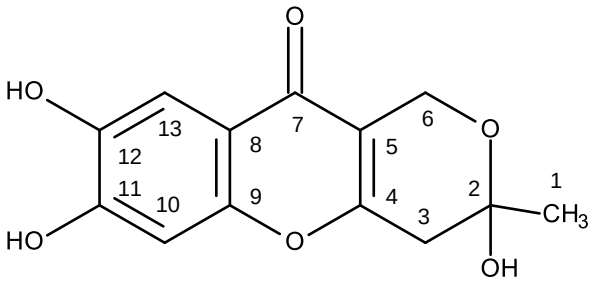

Figure 132. The planar structure of **PE 12**

Literature search revealed that the structure of **PE 12** corresponds to that of penialidinn F (Figure 135), which was previously isolated from the culture of *Penicillium janthinellum* DT-F29, collected from marine sediments (Cheng *et al*., 2018). Curiously, even though the authors reported the optical rotation of penialidin F as levorotatory ($[\alpha]_D^{25}$ −4.13, *c* = 1.0, MeOH), they did not determine the absolute configuration of its stereogenic carbon (C-2). Similarly, we have also found the optical rotation of the **PE 12** levorotatory ($[\alpha]_D^{25}$ −7.5, *c* = 0.04, MeOH). Since **PE 12** was not isolated as a suitable crystal for X-ray analysis, its calculated ECD spectrum was performed to compare with the experimental ECD spectrum (Figure 134). Therefore, the conformational analysis of **PE 12** by molecular mechanics (MM2 and MMFF95 force fields) focused on combinations of hydroxyl 120° rotations and two 3,6-dihydro-2*H*-pyran-2-ol ring conformations. A total of 30 conformations were energetically minimized and ranked using a faster DFT model (smaller basis set, APFD/6-31G). The lowest three of these, representing 99% of the model Boltzmann population, were then further energetically minimized with a larger basis set (APFD/6-311+G(2d,p)). The most stable conformation is depicted in figure 133 and represents 64% of the Boltzmann population while the other two amounts to 25% and 11%.

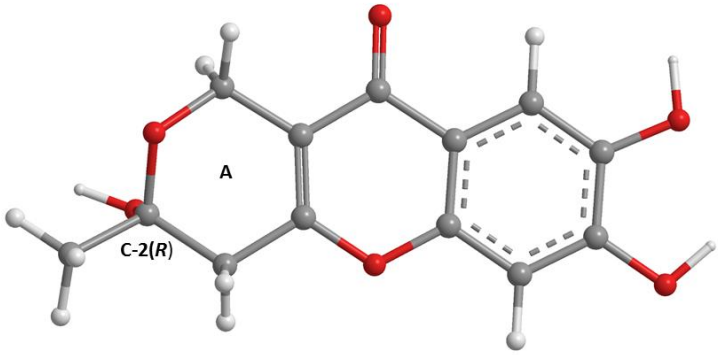

Figure 133. The most stable APFD/6-311+G(2d,p) conformation of **PE 12** (C-2*R*). The asymmetric carbon is presented with the hydroxyl group facing straight down

Interestingly, the ECD experimental signal was very weak, requiring the use of 40 accumulations, increased digital integration time and post-acquisition noise filtering (moving mean) (Figure 134).

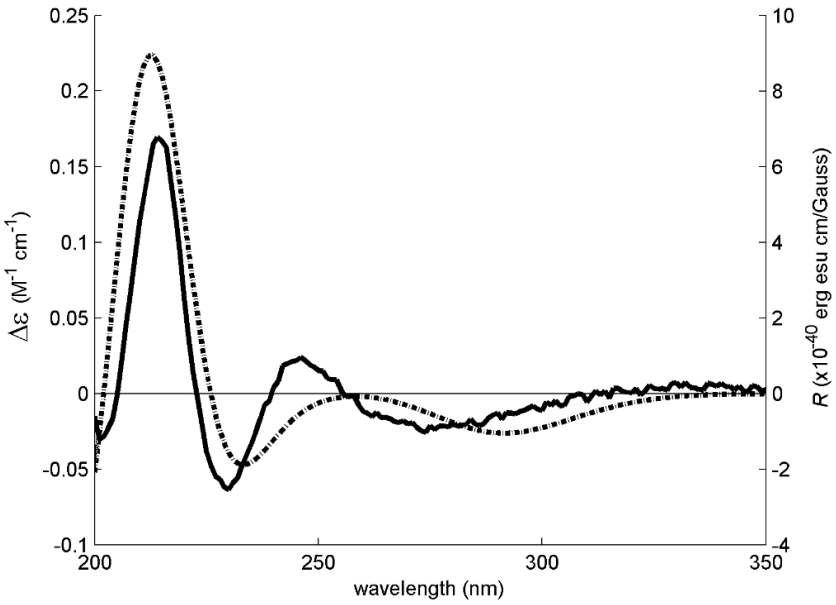

Figure 134. Experimental (solid line) and simulated (dotted line) ECD spectra of **PE 11**/C-2(*R*)

The weak experimental ECD signal of **PE 12** could indicate that this compound does not exist as a pure *R* enantiomer but as an enantiomeric mixture with an access of the *R* enantiomer (Figure 135).

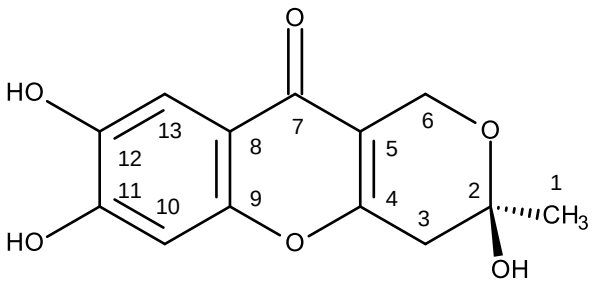

Figure 135. Structure of penialidin F (**PE 12**)

Recently, after our report on isolation of penialidinn F from *P. erubescens* (Kumla *et al*., 2018), Georgousaki *et al*., (2019) reported the isolation of penialidinn F from the fungus *Cercospora* sp. strain CF-223709.

3.1.2.13. Erubescensoic acid (PE 13)

Compound **PE 13** was isolated as white crystals (mp. 218-220ºC), and displayed its (+)-HRESIMS *m/z* at 277.0719 $[M+H]^+$, (calculated 277.0712 for $C_{14}H_{13}O_6$). Therefore, its molecular formula was established as $C_{14}H_{12}O_6$, indicating nine degrees of unsaturation. However, the ^{13}C NMR spectrum (Table 24) displayed only thirteen carbon signals which, according to DEPT and HSQC spectra, can be classified as one conjugated ketone carbonyl (δ_C 173.0), one conjugated carboxyl (δ_C 161.8), three oxyquaternary sp^2 (δ_C 160.0, 157.4, 138.2), two non-protonated sp^2 (δ_C 119.7, 115.3), two methine sp^2 (δ_C 111.8, 102.0), one oxymethylene sp^3 (δ_C 61.6), one methylene sp^3 (δ_C 33.5), one oxymethine sp^3 (δ_C 69.4) and one methyl (δ_C 20.8) carbons. That means one non-protonated sp^2 carbon signal was not observed, and this is characteristic of the carboxyl-bearing aromatic carbon.

The ^{1}H and ^{13}C NMR data of **PE 13** resembled those of anhydrofulvic acid (**PE 8**); however the benzene ring of the chromone moiety of **PE 13** has only one hydroxyl group, as evidenced by the presence of two broad singlets of the *meta*-coupled protons at δ_H 6.78 (H-6/ δ_C 102.0) and 6.27 (H-8/ δ_C 111.8), instead of two hydroxyl groups. Moreover, the double bond between C-2 and C-3 of the 3-methyl-2*H*-pyran ring was saturated, as corroborated by the presence of the methylene group (δ_C 33.5/ δ_H 2.66, *d*, *J* = 17.3 Hz/ 2.56, *dd*, *J* = 17.3, 9.8 Hz). Therefore, the planar structure of **PE 13** was elucidated as 7,8-dihydroxy-3-methyl-10-oxo-4,10-dihydro-1*H*,3*H*-pyrano[4,3-*b*]chromene-9-carboxylic acid, which was confirmed by HMBC correlations (Table 24) from the methyl protons at δ_H 1.28, *d* (*J* = 6.2 Hz, Me-11) to C-3 (δ_C 69.4) and C-4 (δ_C 33.5), from H-3 (δ_H 3.83, *m*) to C-1 (δ_C 61.6), H_2-1 (δ_H 4.56, /4.33) to C-3, C-4a (δ_C 160.0), C-10a (δ_C 115.3) as well as from H_2-4 (δ_H 2.56/2.66) to C-3, C-4a and C-10a (Figure 136).

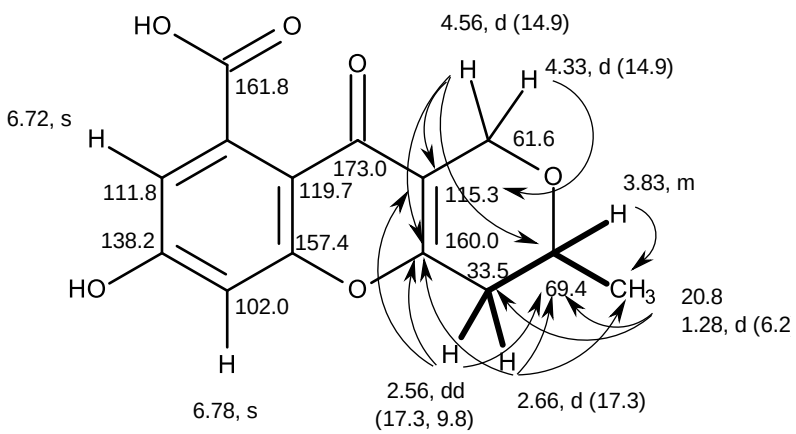

Figure 136. COSY (▬) and HMBC (⟶) correlations in **PE 13**

Table 24. ^{1}H and ^{13}C NMR (500 MHz and 125 MHz, DMSO-d_6) and HMBC assignment for **PE 13**

Position	δ_C, type	δ_C (*J* in Hz)	COSY	HMBC
1	61.6, CH_2	4.56, *d* (14.9)	-	C-3, 4a, 10a
		4.33, *d* (14.9)	-	C-10a
3	69.4, CH	3.83, *m*	-	C-1
4	33.5, CH_2	2.66, *d* (17.3)	H-3	C-3, 4a, 11
		2.56, *dd* (17.3, 9.8)	H-3	C-3, 4a, 10a
4a	160.0, C	-	-	-
5a	157.4, C	-	-	-
6	102.0, CH	6.78, *s*	-	-
7	138.2, C	-	-	-
8	111.8, CH	6.27, *s*	-	-
9	n	-	-	-
9a	119.7, C	-	-	-
10	173.0, CO	-	-	-
10a	115.3, C	-	-	-
11	20.8, CH_3	1.28, *d* (6.2)	H-3	C-3, 4
12	161.8, CO	-	-	-

**n = not observed

The saturation of the double bond between C-2 and C-3 makes C-3 stereogenic whose absolute configuration needs to be determined. Since **PE 13** was obtained as a suitable crystal, the X-ray analysis was carried out. The ORTEP diagram of **PE 13** (Figure 137) not only confirmed its structure but established the absolute configuration of C-3 as 3*S* (Figure 138). Since **PE 13** has never been previously reported, it was named erubescensoic acid.

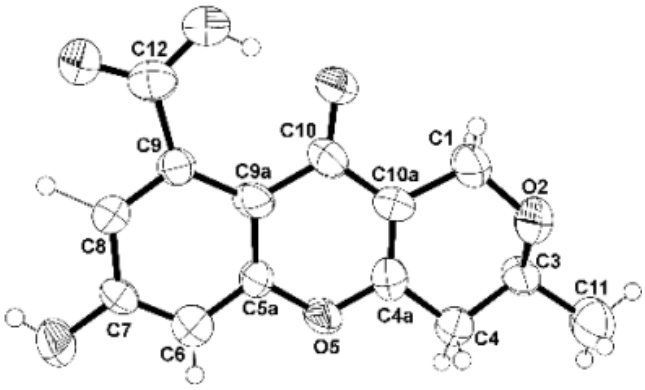

Figure 137. ORTEP view of **PE 13**

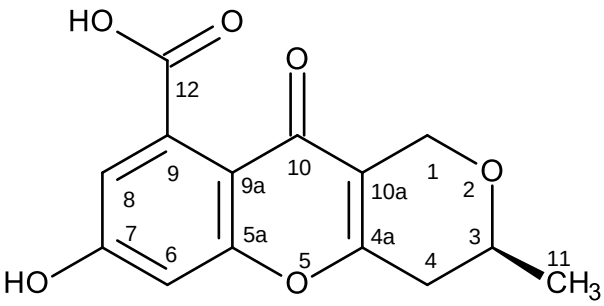

Figure 138. Structure of erubescensoic acid (**PE 13**)

3.1.2.14. Erubescenschromone A (PE 14)

Compound **PE 14** was isolated as white crystals (mp, 150–152 °C), and its molecular formula $C_{13}H_{10}O_6$ was established on the basis of the (+)-HRESIMS *m/z* 263.0569 $[M + H]^+$, (calculated 263.0556 for $C_{13}H_{11}O_6$), indicating nine degrees of unsaturation. The IR spectrum showed absorption bands for hydroxyl (3491, 3376 cm^{-1}), conjugated ketone carbonyls (1679, 1661 cm^{-1}), olefin (1648 cm^{-1}), aromatic (1587, 1523 cm^{-1}), and ether (1276 cm^{-1}) groups. The ^{13}C NMR spectrum (Table 25)

displayed 13 carbon signals which were categorized, according to the DEPTs and HSQC spectra (Table 25), as two conjugated ketone carbonyls (δ_C 198.3 and 181.6), four oxyquaternary sp^2 (δ_C 191.4, 156.9, 155.9, 141.9), one non-protonated sp^2 (δ_C 111.1), three methine sp^2 (δ_C 110.3, 103.8, 103.2), one oxyquaternary sp^3 (δ_C 86.3), one oxymethylene sp^3 (δ_C 69.8) and one methyl (δ_C 16.4) carbons. The ^{1}H NMR spectrum (Table 25) showed two singlets of aromatic protons at δ_H 7.05 and 6.41, a doublet of an olefinic proton at δ_H 5.68 (J = 0.6 Hz), a pair of doublets of the oxymethylene protons at δ_H 4.49 (J = 12.4 Hz)/4.63 (J = 12.4 Hz), and a methyl singlet at δ_H 2.31, in addition to a broad signal of the hydroxyl proton at δ_H 10.01. The presence of the 6,7-dihydroxy-2,3-dihydro-4*H*-1-benzopyran-4-one moiety was corroborated by the HMBC correlations (Table 25) from the singlet at δ_H 7.05 (H-5) to the carbons at δ_C 181.6 (C-4), 141.9 (C-6), 155.9 (C-7) and 156.9 (C-8a); from the singlet at δ_H 6.41 (H-8) to C-4, C-6, C-7, C-8a and the carbon at δ_C 111.1 (C-4a), and from the doublets at δ_H 4.49 (J = 12.4 Hz, H-2) and 4.63 (J = 12.4 Hz, H-2) to C-4 and C-8a.

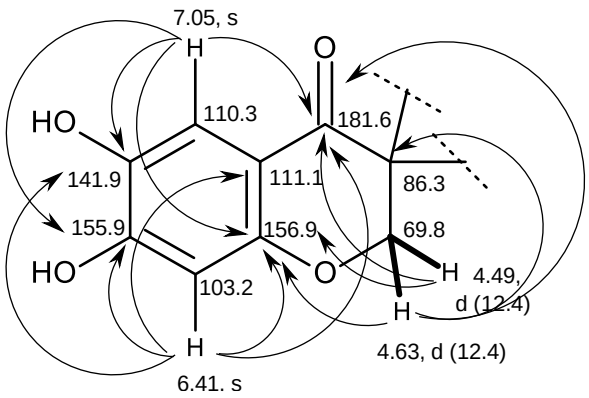

Another portion of the molecule was identified as a 5-methylfuran-3(2*H*)-one ring by the COSY correlation (Table 25) from the methyl singlet at δ_H 2.31 (Me-5') to the doublet at δ_H 5.68 (J = 0.6 Hz, H-3′), as well as by the HMBC correlations (Table 25) from H-3′ to the carbons at δ_C 86.3 (C-3), 191.4 (C-2′), δ_C 198.3(C-4′), and from Me-5' to C-2′ and the carbon at (δ_C 103.8 (C-3′).

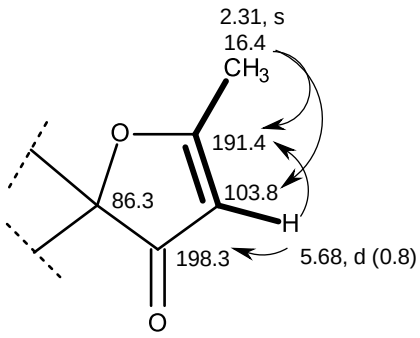

Table 25. ^{1}H and ^{13}C NMR (300 MHz and 75 MHz, DMSO-d_6) and HMBC assignment for **PE 14**

Position	δC, Type	δH, (*J* in Hz)	COSY	HMBC
2a	69.8, CH_2	4.49, *d* (12.4)	2b	C-4, 4′, 8a
b		4.63, *d* (12.4)	2a	C-3, 4, 4′, 8a-
3	86.3, C	-	-	-
4	181.6, CO	-	-	-
4a	111.1, C	-	-	-
5	110.3, CH	7.05, *s*	-	C-4, 6, 7, 8a
6	141.9, C	-	-	-
7	155.9, C	-	-	-
8	103.2, CH	6.41, *s*	-	C-4, 4a, 6, 7, 8a
8a	156.9, C	-	-	-
2′	191.4, C	-	-	-
3′	103.8, CH	5.68, *d* (0.8)	5′	C-2′, 3, 4′
4′	198.3, CO	-	-	-
5′	16.4, CH_3	2.31, *s*	3′	C-2′, 3′
OH	-	10.01, *brs*	-	-

That the 5-methylfuran-3(2*H*)-one moiety was spiro-fused with the 6,7-dihydroxy-2,3-dihydro-4*H*-1-benzopyran-4-one through C-3 was substantiated by the HMBC correlations from the doublet at δ_H 4.49 (*J* = 12.4 Hz, H-2) to C-3 and C-4′, and from H-3′ to C-3. Therefore, the planar structure of **PE 14** was elucidated as 5′-methyl-2*H*,3′*H*,4*H*-spiro [1-benzopyran-3,2′-furan]-3′,4-dione.

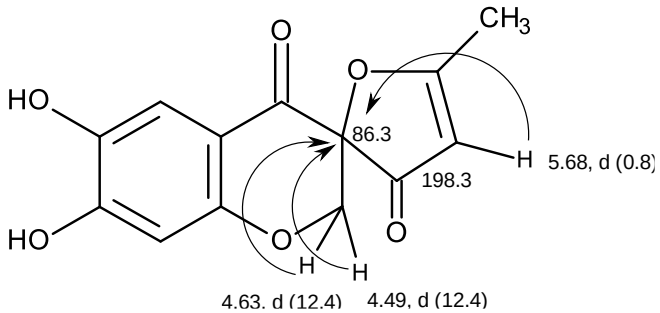

Since C-3 of **PE 14** was a stereogenic carbon, its absolute configuration needed to be established. Since **PE 14** was obtained as a suitable crystal, an X-ray analysis was carried out. The ORTEP view (Figure 139) not only confirmed the proposed structure for **PE 14** but also determined unequivocally the absolute configuration of C-3 as 3*S*.

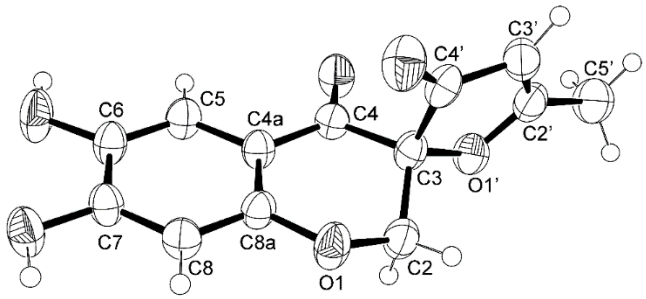

Figure 139. The ORTEP view of erubescenschromone A (**PE 14**)

Therefore, the absolute structure of **PE 14** is (3*S*)-6,7-dihydroxy-5′-methyl-3′*H*,4*H*-spiro[chromene-3,2′-furan]-3′,4-dione (Figure 140).

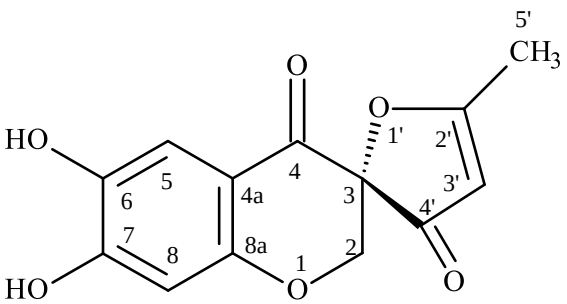

Figure 140. Structure of erubescenschromone A (**PE 14**)

Extensive literature search revealed that **PE 14** has never been previously reported. Consequently, it was named erubescenschromone A.

3.1.2.15. 7-Hydroxy-6-methoxy-4-oxo-3-[(1*E*)-3-oxobut-1-en-1-yl]-4*H*-chromene-5-carboxylic acid (PE 15)

Compound **PE 15** was isolated as a white solid (mp 276-277 °C), and displayed its (+)-HRESIMS *m/z* at 305.0667 $[M+H]^+$, (calculated 305.0661 for $C_{15}H_{13}O_7$). Therefore, its molecular formula was established as $C_{15}H_{12}O_7$, indicating ten degrees of unsaturation. The IR spectrum exhibited absorption bands for hydroxyl (3446 cm^{-1}), conjugated ketone carbonyls (1719, 1646 cm^{-1}), aromatic (1560, 1541 cm^{-1}), olefin (1618 cm^{-1}) and ether (1276 cm^{-1}) groups. However, its ^{13}C NMR spectrum (Table 26) displayed only 14 carbon signals which, in combination with DEPT and HSQC spectra, can be classified as two ketone carbonyls (δ_C 198.2 and 173.4), one conjugated carboxyl carbonyl (δ_C 167.1), three oxyquaternary sp^2 (δ_C 157.1, 152.8, 143.2), two non-protonated sp^2 (δ_C 117.4 and 112.0), one oxymethine sp^2 (δ_C 158.9), three methine sp^2 (δ_C 134.9, 128.7, 104.0), one methoxyl (δ_C 61.0) and one methyl (δ_C 27.5) carbons. The ^1H NMR spectrum (Table 26) exhibited four singlets of aromatic/olefinic protons at δ_H 8.73 (1H), 7.35 (2H), 7.03 (1H), one methoxyl singlet at δ_H 3.75 and one methyl singlet at δ_H 2.29.

That **PE 15** consists of a 7-hydroxy-6-methoxy-4-oxo-4*H*-chromene-5-carboxylic acid scaffold, with a substituent on C-3, was supported by the HMBC correlations (Table 26) from H-2 (δ_H 8.73) to C-4 (δ_C 173.4), C-8a (δ_C 152.8) and C-3 (δ_C 117.4); from H-8 (δ_H 7.03) to C-4a (δ_C 112.0), C-6 (δ_C 143.2), C-7 (δ_C 157.1), and C-8a, from OCH_3-6 (δ_H 3.75) to C-6, as well as the carbon at δ_C 61.0 (OCH_3-6), characteristic of the methoxyl group flanked by one oxygenated substituent and one carboxyl group. Like many other quaternary sp^2 carbon linked to the carboxyl substituent, the intensity of the signal of C-5 was not strong enough to be observed in the ^{13}C NMR spectrum. Moreover, since there is no proton of two or three bonds away from C-5, it was not possible to localize the C-5 signal in the HMBC spectrum.

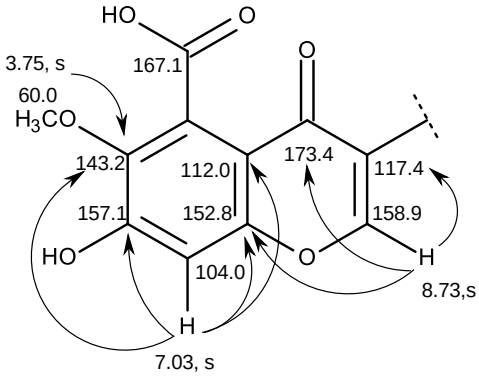

The existence of a 3-oxobut-1-en-1-yl substituent was supported by the presence of a singlet of two protons at δ_H 7.35 (H-10 and H-11) which, through the HSQC spectrum, connected to the two methine sp^2 carbons at δ_C 134.9 (C-10) and δ_C 128.7 (C-11), as well as the HMBC correlations from H-10/H-11 to the ketone carbonyl carbon at δ_C 198.2 (C-12), and from the methyl singlet at δ_H 2.29 (H_3-13) to C-12 and C-11.

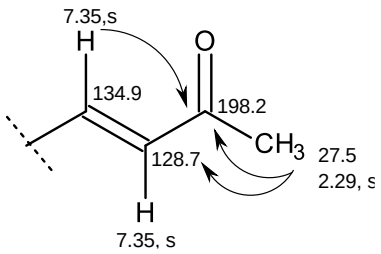

That the 3-oxobut-1-en-1-yl substituent was on C-3 was also supported by the HMBC correlations (Table 26) from H-10 to C-2 and C-4, as well as from H-2 to C-10 (Figure 141).

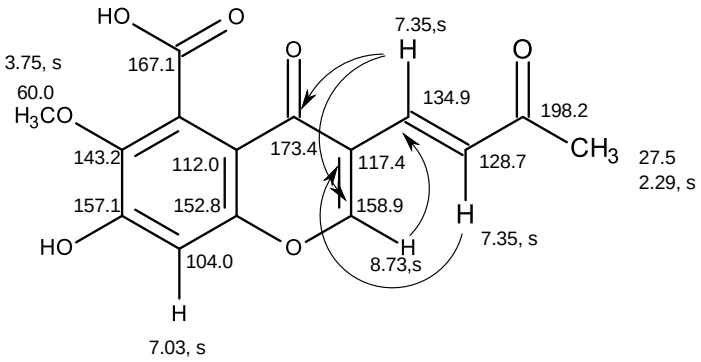

Figure 141. ^{1}H and ^{13}C chemical shift value and key HMBC correlations in **PE 15**

Table 26. ^{1}H and ^{13}C NMR (500 MHz and 125 MHz, DMSO-d_6) and HMBC assignment for **PE 15**

Position	δ_C, Type	δ_H, (*J* in Hz)	COSY	HMBC
2	158.9, CH	8.73, *s*	-	C-3, 4, 8a, 10
3	117.4, C	-	-	-
4	173.4, C	-	-	-
4a	112.0, C	-	-	-
5	n	-	-	-
6	143.2, C	-	-	-
7	157.1 C	-	-	-
8	104.0, CH	7.03, *s*	-	C-4a, 6, 7, 8a
8a	152.8, C	-	-	-
9	167.1, C	-	-	-
10	134.9, CH	7.35, *s*	-	C-2, 4, 12
11	128.7, CH	7.35, *s*	-	C-3
12	198.2, C	-	-	-
13	27.5, CH_3	2.29, *s*	-	C-11, 12
14	61.0, CH_3	3.75, *s*	-	C-6

n = not observed.

Therefore, the structure of **PE 15** was elucidated as 7-hydroxy-6-methoxy-4-oxo-3-[(1*E*)-3-oxobut-1-en-1-yl]-4*H*-chromene-5-carboxylic acid (Figure 142).

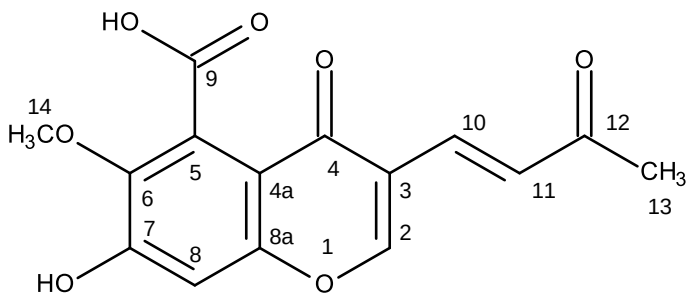

Figure 142. Structure of 7-hydroxy-6-methoxy-4-oxo-3-[(1*E*)-3-oxobut-1-en-1-yl]-4*H*-chromene-5-carboxylic acid (**PE 15**)

The literature search revealed that **PE 15** has never been previously reported; however, its structure and NMR data were very similar to those of PI-4, a fungal metabolite first isolated, by Arai *et al*., (1989) from the mycelium of *Penicillium italicum*, a phyotoxic fungus which causes the blue-mold rot of fruits, and later by Lu *et al*., (2013), from the crude extract of the fungus *Chaetomium indicum* (CBS.860.68). The only difference between PI-4 and **PE 15** is the substituent on C-6 which is a hydroxyl group in the former and a methoxyl group in the latter. Therefore, **PE 15** is identified as 7-hydroxy-6-methoxy-4-oxo-3-[(1*E*)-3-oxobut-1-en-1-yl]-4*H*-chromene-5-carboxylic acid (Figure 142).

The structure of **PE 15** and the *trans* double bond between C-10 and C-11 are confirmed by X-ray analysis, as shown in the ORTEP view in figure 143.

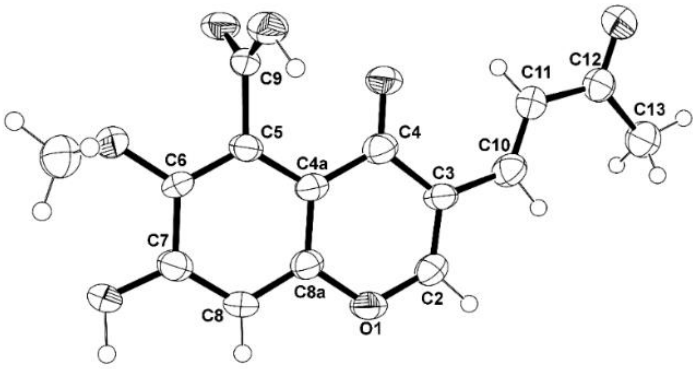

Figure 143. The ORTEP view of **PE 15**

3.1.2.16. Erubescenschromone B (PE 16)

Compound **PE 16** was isolated as a yellowish oil, and its molecular formula $C_{26}H_{20}O_{11}$ was established based on its (+)-HRESIMS *m/z* 509.1085 $[M + H]^+$, (calculated 509.1084 for $C_{26}H_{21}O_{11}$), indicating twelve degrees of unsaturation. The IR spectrum showed absorption bands for hydroxyl (3443 cm^{-1}), ketone carbonyls (1731, 1715 cm^{-1}), conjugated ketone carbonyls (1697, 1648 cm^{-1}), aromatic (1634, 1556, 1596 cm^{-1}), and ether (1261 cm^{-1}) groups.

The ^{13}C NMR spectrum (Table 27) exhibited 26 carbon signals which can be classified, according to DEPT and HSQC spectra (Table 27), as two ketone carbonyls (δ_C 204.6, 200.9), two conjugated ketone carbonyls (δ_C 185.3, 172.2), ten non-protonated sp^2 (δ_C 161.3, 156.0, 155.4, 152.5, 150.2, 144.7, 141.4, 115.1, 112.3, 109.8), four methine sp^2 (δ_C 111.1, 108.5, 102.8, 102.6), two oxyquatermary sp^3 (δ_C 61.9 and 78.2), two methine sp^3 (δ_C 71.4 and 69.8), two methylene sp^3 (δ_C 67.2 and 33.4), and two tertiary methyl (δ_C 32.7 and 29.3) carbons.

The ^1H NMR spectrum (Table 27), in combination with the HSQC spectrum, displayed four singlets of aromatic protons at δ_H 7.26, 7.17, 6.84 and 6.37, two methine singlets at δ_H 5.41 and 5.23, two doublets of the magnetically inequivalent oxymethylene protons at δ_H 4.36 (J = 12.8 Hz) and 3.59 (J = 12.8 Hz), two doublets of the magnetically inequivalent methylene protons at δ_H 3.47 (J = 19.2 Hz) and 2.89 (J = 19.2 Hz), in addition to two methyl singlets at δ_H 2.16 and 1.51.

The presence of the 7,8-dihydroxy-3-methyl-3,4-dihydro-1*H*,10*H*-pyrano[4,3-*b*]chromen-10-one moiety was substantiated by the HMBC correlations (Table 27) from H-5 (δ_H 7.26, *s*; δ_C 108.0) to C-4 (δ_C 172.2), C-8a (δ_C 152.5), C-7 (δ_C 150.2), and C-6 (144.7); from H-8 (δ_H 6.84, *s*; δ_C 102.8) to C-4, C-8a, C-7, C-6, C-4a (δ_C 115.1); from H-12 (δ_H 5.41, *s*; δ_C 71.4) to C-4, C-2 (δ_C 161.3), C-3 (δ_C 112.3), C-10 (δ_C 78.2), and from Me-13 (δ_H 1.51, *s*; δ_C 29.3) to C-2, C-10, and C-9 (δ_C 33.4) (Figure 144).

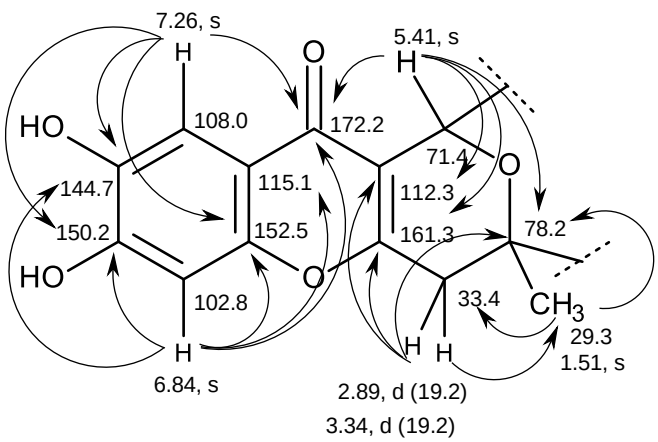

Figure 144. ^1H and ^{13}C chemical shifts and key HMBC correlations in the 7,8-dihydroxy-3-methyl-3,4-dihydro-1*H*,10*H*-pyrano[4,3-*b*]chromen-10-one moiety of **PE 16**

Another portion of the molecule was identified as 3,3-disubstituted 6,7-dihydroxy-2,3-dihydro-4*H*-1-benzopyran-4-one was based on the HMBC correlations from H-5′ (δ_H 7.17, s; δ_C 111.1) to C- 4′ (δ_C 185.3), C-8′a (δ_C 156.0), C-7′ (δ_C 155.4), C-6′ (δ_C 141.4); from H-8′ (δ_H 6.37, s; δ_C 102.6) to C-4′, C-8′a, C-6′ and C-4′a (δ_C 109.8), as well as from H_2-2′ (δ_H 4.36, *J* = 12.8 Hz/3.59, *J* = 12.8 Hz) to C-4′, C-8′a and C-3′ (δ_C 61.9) (Figure 145).

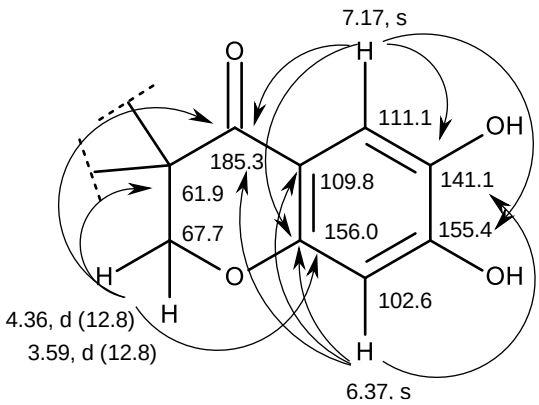

Figure 145. ^{1}H and ^{13}C chemical shifts and key HMBC correlations in the 3,3-disubstituted 6,7-dihydroxy-2,3-dihydro-4*H*-1-benzopyran-4-one moiety of **PE 16**

That the disubstituted 6,7-dihydroxy-2,3-dihydro-4*H*-1-benzopyran-4-one was connected to the 7,8-dihydroxy-3-methyl-3,4-dihydro-1*H*,10*H*-pyrano[4,3-*b*]chromen-10-one moiety, through C-3′ of the former and C-12 of the latter, was confirmed by the HMBC correlations from H-12 to C-3′, and H_2-2′ to C-12. Moreover, since the HMBC spectrum also exhibited correlations from H-12 and H_2-2′ to the ketone carbonyl carbon at δ_C 200.9 (C-14), from H-15 (δ_H 5.23, *s*; δ_C 69.8) to C-9, C-10 (δ_C 78.2), C-14, and from Me-13 to C-15, the 7,8-dihydroxy-3-methyl-3,4-dihydro-1*H*,10*H*-pyrano[4,3-*b*]chromen-10-one moiety was connected through C-10 and C-15 of the oxan-4-one ring. The presence of the acetyl group on C-15 was corroborated by the HMBC correlations from Me-17 (δ_H 2.16, *s*; δ_C 32.7) to C-15 and the carbonyl carbon at δ_C 204.6 (C-16), as well as from H-15 to C-16 (Figure 146).

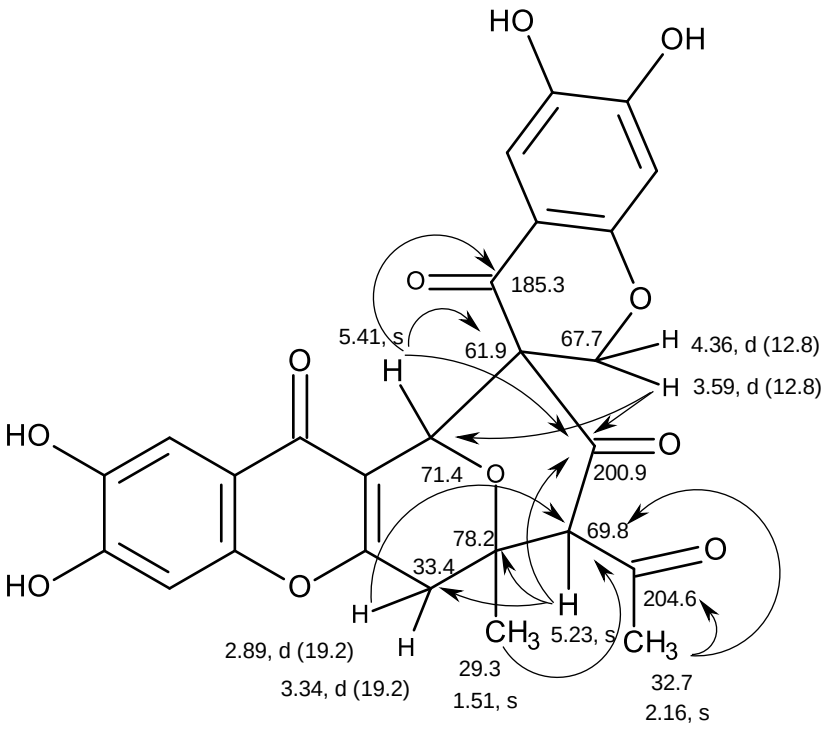

Figure 146. Key HMBC correlations in **PE 16**

Table 27. ^{1}H and ^{13}C NMR (500 MHz and 125 MHz, DMSO-d_6) and HMBC assignment for **PE 16**

Position	δ_C, Type	δ_H, (*J* in Hz)	COSY	HMBC	ROESY
2	161.3, C	-	-	-	-
3	112.3, C	-	-	-	-
4	172.2, CO	-	-	-	-
4a	115.1, C	-	-	-	-
5	108.0, CH	7.26, *s*	-	C-4, 6, 7, 8a	-
6	144.7, C	-	-	-	-
7	150.2, C	-	-	-	-
8	102.8, CH	6.84, *s*	-	C-4, 4a, 6, 7, 8a	-
8a	152.5, C		-	-	-
9α	33.4 CH_2	3.47, *d* (19.2)	H-9β	C-2, 3, 10, 13, 15	-
9β		2.89, *d* (19.2)	H-9α	C-2, 3, 10, 13, 15	-
10	78.2, C	-	-	-	-
12	71.4, CH	5.41, *s*	-	C-2, 3, 3′,4, 4′, 10, 14	H--2’
13	29.3, CH_3	1.51, *s*	-	C-2, 9, 10, 14, 15	H-9β, 15
14	200.9, CO	-	-	-	-
15	69.8, CH	5.23, *s*	H-17	C-9, 10, 13, 14, 16	H-17
16	204.6, CO	-	-	-	-
17	32.7, CH_3	2.16, *s*	H-15	C-15, 16	-
2′α	67.7, CH_2	4.36, *d* (12.8)	H-2′β	C-3′, 4, 8′a, 12, 14	-
2′β		3.59, *d* (12.8)	H-2′α, 15	C-3′, 4, 8′a, 12, 14	-
3′	61.9, C	-	-	-	-
4′	185.3, CO	-	-	-	-
4′a	109.8, C	-	-	-	-
5′	111.1, CH	7.17, *s*	-	C-4′, 6′, 7′, 8′a	-
6′	141.1, C	-	-	-	-
7′	155.4, C	-	-	-	-
8′	102.6, CH	6.37, *s*	-	C-4′, 4′a, 6′, 8′a	-
8′a	156.0, C	-	-	-	-

Taking together the molecular formula, the NMR data, and the HMBC correlations, the planar structure of **PE 16** was unambiguously established. In order to determine the relative configurations of the stereogenic carbons C-10, C-12, C-15 and

C-3′, the ROESY spectrum was obtained. The ROESY spectrum (Table 27) exhibited strong correlations from Me-13 (δ_H 1.51, *s*) to H-15 (δ_H 5.23, *s*) and the methylene proton at δ_H 2.89, *d* (*J* = 19.2 Hz), implying that these three protons are on the same face. Additionally, H-15 also shows a correlation to Me-17 (δ_H 2.16, *s*). Since the pyran ring and the oxan-4-one ring of the 9-oxabicyclo[3.3.1]nonan-3-one ring system are in a rigid half-chair conformation, Me-13 must be in a pseudoequatorial position while the methylene proton at δ_H 2.89, *d* (*J* = 19.2 Hz) and H-15 are in a pseudoaxial position. Therefore, the acetyl group on C-15 must be in a pseudoequatorial position. This was confirmed by the higher chemical shift value (δ_H 3.47, *d*, *J* = 19.2 Hz) of the pseudoequatorial H-9 as it is in the deshielding zone of the carbonyl (C-16) of the acetyl group. On the other hand, H-12 (δ_H 5.41, *s*) showed a weak correlation to one of H_2-2′ at δ_H 3.59, *d* (*J* = 12.9 Hz). Therefore, both of these protons should be in the pseudoequatorial position since the pseudoaxial H-2′ (δ_H 4.36, *d*, *J* = 12.9 Hz) is under the anisotropic effect (deshielding) of the carbonyl at C-14 of ring D. With these ROESY correlations, the relative configurations of C-10, 12, 15, and 3′ were proposed as 10*S**, 12*S**, 15*S**, and 3′*S**. However, it is necessary to determine the absolute configurations of these stereogenic carbons.

Since **PE 16** could not be obtained as a suitable crystal for an X-ray analysis, the determination of the configurations of its stereogenic carbons had to be carried out by comparison of the calculated and experimental ECD spectra. Although the ROESY correlations pointed to the relative configuration of C-10 and C-15 as 10*S*, 15*S*, it is possible that it can be 10*R*, 15*R*, thus reducing its number of possible configurations from 16 (eight pairs of diastereoisomers) to eight (four pairs of diastereoisomers). Hence, four computational models were constructed by combining the two configurations of C-3′ with the two of C-12. The conformational analysis of **PE 16** by molecular mechanics (MM2 and MMFF95 force fields) focused on combinations of hydroxyl 120° rotations and rings conformations. Most diastereoisomers did not show ring conformational freedom which limited the number of models to compute. The most stable APFD/6-31G conformation of **PE 16** whose absolute configurations of C-10, C-12, C-15, and C-3′ are 10*S*, 12*S*, 15*S*, 3′*S*, as deduced from ROESY correlations, is shown in figure 147.

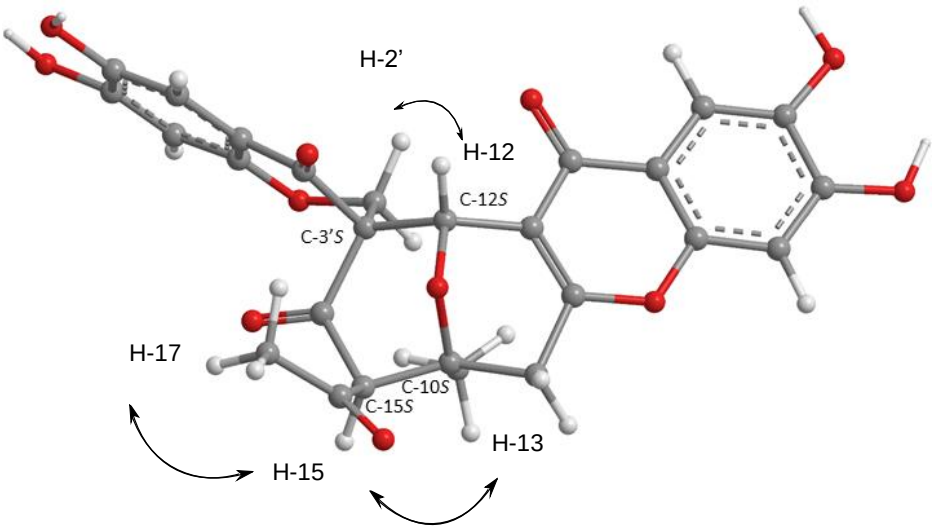

Figure 147. The most stable APFD/6-31G conformation of **PE 16**, presented with the absolute configuration found by spectrometric methods. Solid lines direct ROESY correlations of **PE 16**

All conformations were energetically minimized and ranked using a DFT model. The lowest energy ones, representing at least 95% of the model Boltzmann population, were used to calculate the expected Boltzmann-averaged ECD spectra of the four **PE 16** diastereoisomers. The fitting between the experimental and calculated spectra is presented in figure 148, showing that **PE 16** is the C-10*S*, C-12*S*, C-3′*S*, C-15*S* enantiomer.

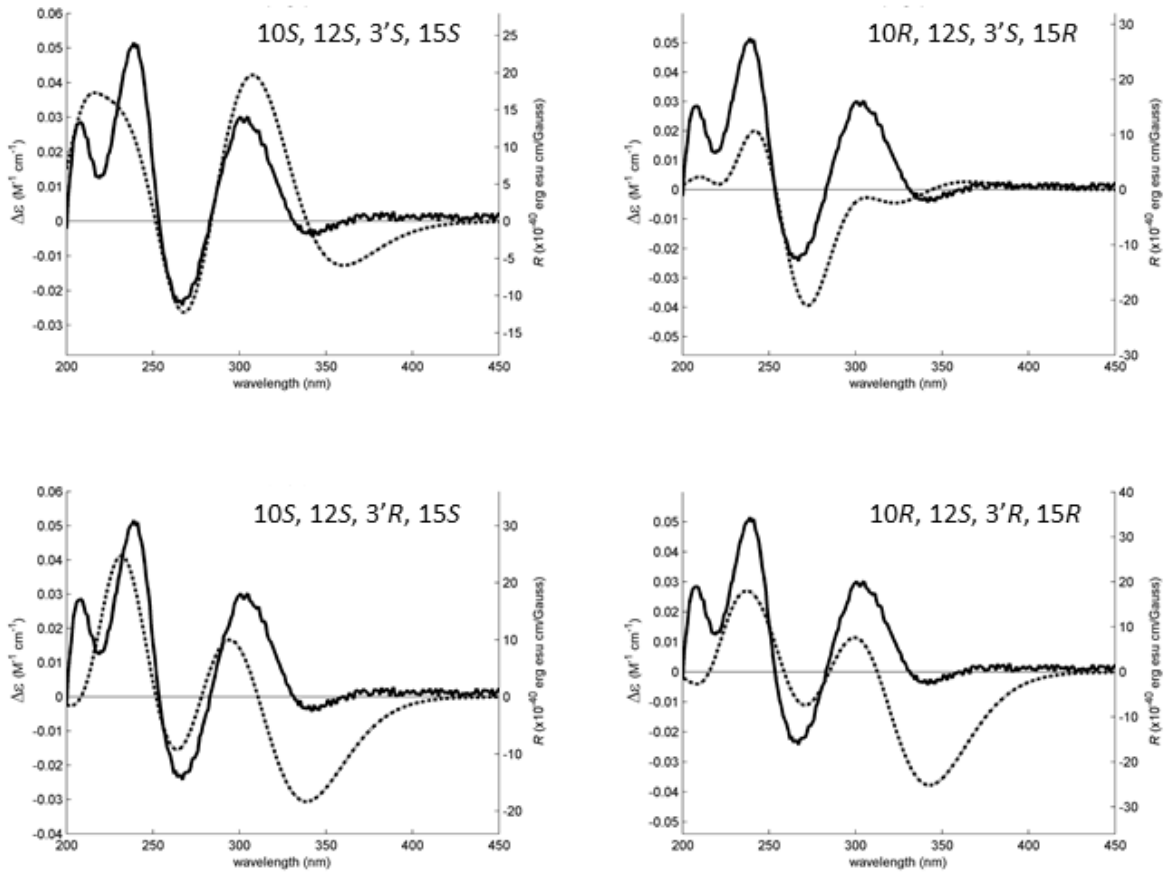

Figure 148. The experimental (solid line, left axes) and simulated (dotted line, right axes) ECD spectra of four diastereoisomers of **PE 16**. The best experimental-simulated fit belongs to the diastereoisomer with the absolute configuration 10*S*, 12*S*, 3′*S*, 15*S*. The theoretical ECD spectra of the enantiomers of the presented diastereoisomers are the exact inversions of the ones depicted here and do not fit the experimental data

The literature search revealed that **PE 16** has never been previously reported and therefore it is a new compound which was named erubescenschromone B (Figure 149).

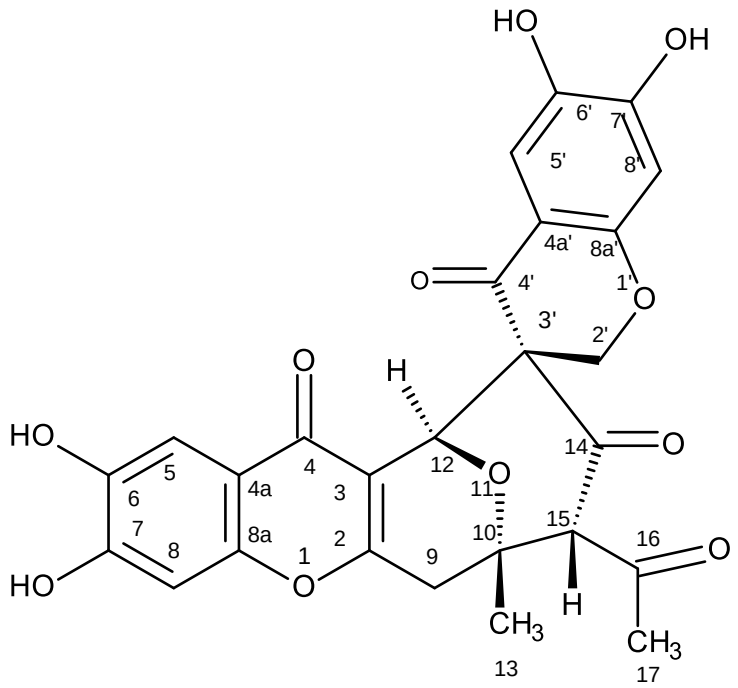

Figure 149. The structure of erubescenschromone B (**PE 16**)

3.1.2.17. SPF-3059-30 (PE 17)

Compound **PE 17** was isolated as a yellowish oil, and its molecular formula $C_{26}H_{20}O_{11}$ was established based on the (+)-HRESIMS *m/z* 509.1085 $(M+H)^+$ (calculated 509.1084 for $C_{26}H_{21}O_{11}$), indicating eighteen degrees of unsaturation. The IR spectrum showed absorption bands for hydroxyl (3491, 3376 cm^{-1}), conjugated ketone carbonyls (1679, 1661 cm^{-1}), olefin (1648 cm^{-1}), aromatic (3108, 1578, 1523 cm^{-1}), and ether (1206 cm^{-1}) groups. The ^{13}C NMR spectrum (Table 28) exhibited 26 carbon signals which, according to DEPT and HSQC spectra (Table 28), can be categorized as three carbonyls (δ_C 202.8, 183.6, 173.5), fifteen non-protonated sp^2 (δ_C 172.6, 155.9, 154.9, 154.2, 152.1, 150.7, 144.3, 141.6, 138.0, 132.4, 129.5, 118.6, 113.5, 1119, 103.9), five methine sp^2 (δ_C 125.7, 110.5, 108.7, 103.3, 103.1), one oxymethylene sp^3 (δ_C 66.2) and two methyl (δ_C 32.4 and 16.6) carbons.

The ^1H NMR spectrum (Table 28) exhibited five singlets of aromatic protons at δ_H 8.00, 7.45, 7.19, 6.93 and 6.34; a singlet of oxymethylene protons at δ_H 4.67

(2H), in addition to two methyl singlets at δ_H 2.71 and 2.32. That **PE 17** contained the 6,7-dihydroxy-2,3-dihydro-4*H*-chromen-4-one moiety was supported by the HMBC correlations (Table 28) from the aromatic proton singlet at δ_H 7.19 (H-5′/ δ_C 110.5) to the carbons at δ_C 183.6 (C-4′), 155.9 (C-6′), 154.9 (C-8′a) and 141.6 (C-7′); the aromatic proton singlet at δ_H 6.34 (H-8′/δ_C 103.3) to the carbons at δ_C 111.9 (C-4′a), C-6′, C-7′, C-8′a, and the proton singlet at δ_H 4.67 (H_2-2′/δ_C 66.2) to the carbons at δ_C 103.9 (C-3′) and δ_C 183.6 (C-4′).

Since the HMBC spectrum exhibited correlations from H_2-2′ to C-3′ (δ_C 103.9) and the enolic carbon (C-9′, δ_C 172.6), an enolic exocyclic double bond was located on C-3’.

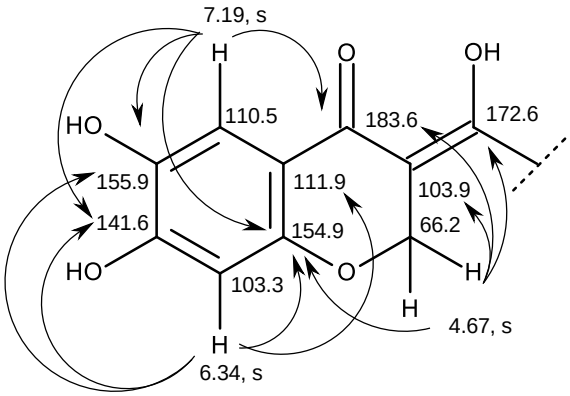

Figure 150. Key HMBC (⟶) correlations in 6,7-dihydroxy-2,3-dihydro-4*H*-chromen-4-one moiety in **PE 17**

That another portion of **PE 17** was 7-substituted 5-acetyl-2,3-dihydroxy-6-methyl-9*H*-xanthen-9-one was supported by the HMBC correlations from the proton singlet at δ_H 6.93 (H-5/δ_C 103.1) to the carbons at δ_C 143.3 (C-7), 113.5 (C-8a), 154.2 (C-10a), from the proton singlet at δ_H 7.45 (H-8/ δ_C 108.7) to C-7, C-10a, and the carbons at δ_C 150.7 (C-6), 173.5 (C-9), from the proton singlet at δ_H 8.00 (H-1/δ_C 125.7) to the carbons at δ_C 138.0 (C-3) and 152.1 (C-4a), from the methyl singlet at δ_H 2.32 (Me-13/ δ_C 16.6) to C-3 and the carbons at δ_C 129.5 (C-2), 132.2 (C-4).

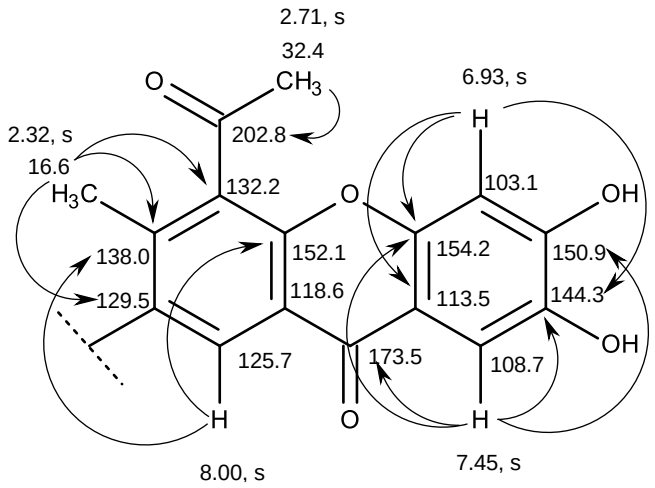

Figure 151. Key HMBC (⟶) correlations in 7-substituted 5-acetyl-2,3-dihydroxy-6-methyl-9*H*-xanthen-9-one moiety in **PE 17**

Moreover, the HMBC spectrum displayed correlation from H-1 to C-9′, suggesting that the 5-acetyl-2,3-dihydroxy-6-methyl-9*H*-xanthen-9-one and the 6,7-dihydroxy-2,3-dihydro-4*H*-chromen-4-one portions were connected through C-9′.

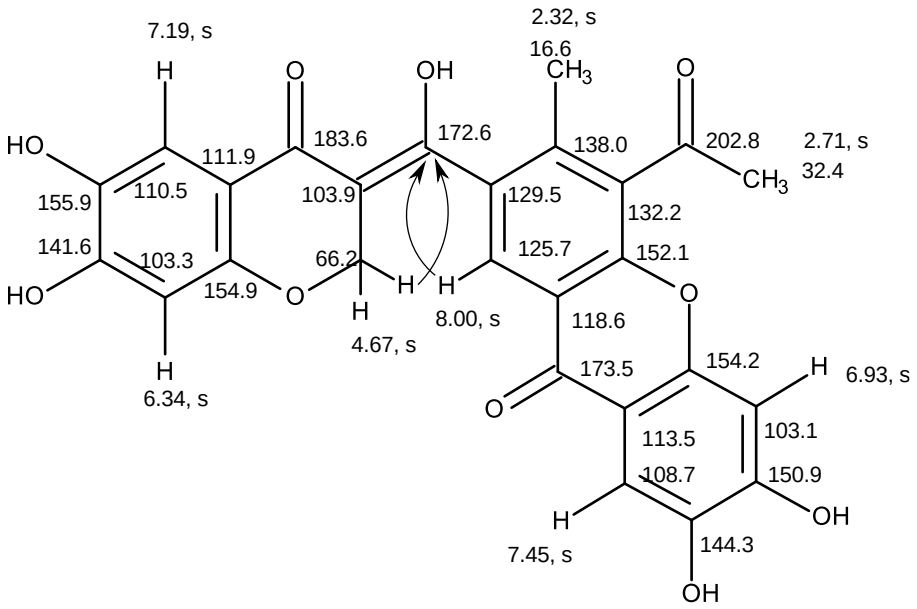

Table 28. ^{1}H and ^{13}C NMR (500 MHz and 125 MHz, DMSO-d_6) and HMBC assignment for **PE 17**

Position	δ_C, Type	δ_H, (*J* in Hz)	COSY	HMBC
1	125.7, CH	8.00, *s*	-	C-3, 4a, 9′
2	129.5, C	-	-	-
3	138.0, C	-	-	-
4	132.2, C	-	-	-
4a	152.1, C	-	-	-
5	103.1, CH	6.93, *s*	-	C-7, 8a, 10a
6	150.9, C	-	-	-
7	144.3, C	-	-	-
8	108.7, C	7.45, *s*	-	C-6, 7, 9, 10a
8a	113.5, C	-	-	-
9	173.5, CO	-	-	-
9a	118.6, C	-	-	-
10a	154.2, C	-	-	-
11	202.8, CO	-	-	-
12	32.4, CH_3	2.71, *s*	-	C-12
13	16.6, CH_3	2.32, *s*	-	C-2, 3, 4
2′	66.2, CH_2	4.67, *s*	-	C-3′, 4′, 8′a, 9′
3′	103.9, C	-	-	-
4′	183.6, CO	-	-	-
4′a	111.9, C	-	-	-
5′	110.5, CH	7.19, *s*	-	C-4′, 6′, 7′, 8′a
6′	155.9, C	-	-	-
7′	141.6, C	-	-	-
8′	103.3, CH	6.34, *s*	-	C-4′a, 6′, 7, 8′a
8′a	154.9, C	-	-	-
9′	172.6, C	-	-	-

An extensive literature search revealed that the structure of **PE 17** is the same as that of the previously reported enol tautomer of the compound, named SPF-3059-30, which was isolated from the acetone extract of the mycelium of *Penicillium* sp.

SPF-3050 (FERM BB-7663), cultured in the liquid medium (Kimura *et al*., 2007). Interestingly, the authors reported in this paper that SPF-3050-30 was isolated as a mixture of keto-enol tautomers, as supported by the duplication of the ^{1}H and ^{13}C chemical shift values (without an assignment). The authors also claimed that the ^{13}C NMR spectrum of SPF-3050-30 displayed forty one carbon signals, consisting of four signals for the methyl groups, three signals for the oxymethylene carbons, two signals for the carbonyl carbon of the acetyl group, two signals for the carbonyl of the chromone nucleus and two signals of the carbonyl of the xanthone moiety, etc., while its ^{1}H NMR spectrum exhibited two methyl signals of the methyl group on the xanthone nucleus, two methyl signals for the acetyl group and nine signals of aromatic protons. However, contrary to the ^{1}H and ^{13}C data reported by Kimura *et al*., (2007) the ^{1}H and ^{13}C NMR spectra of **PE 17** in DMSO (Table 28) showed that it was present only in an enolic form. This is supported by the fact that the enolic form is stabilized by the hydrogen bonding between OH-9′ and the carbonyl of the chromone moiety (C-4′). Therefore, the structure of **PE 17** was unambiguously elucidated as shown in figure 152.

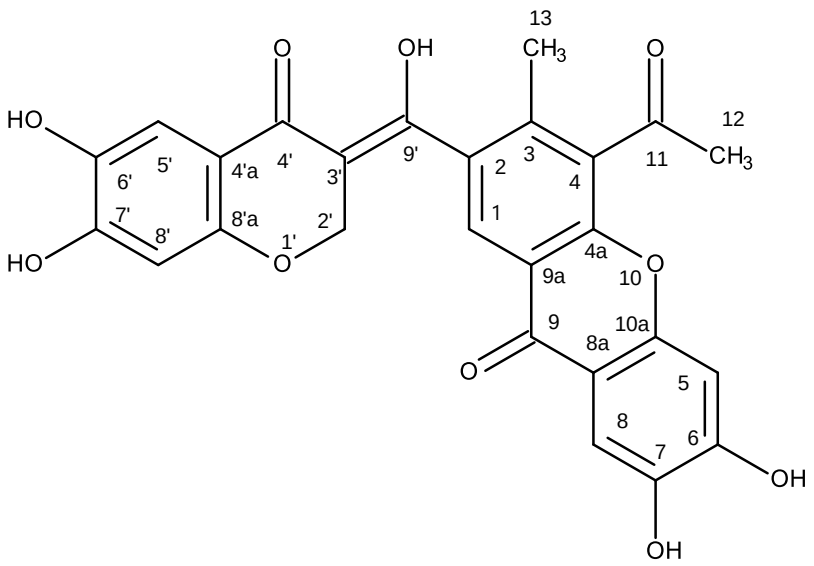

Figure 152. Structure of SPF-3059-30 (**PE 17**)

Compound **PE 17** can be considered as a decarboxylated derivative of xanthofulvin, a semaphorin inhibitor isolated from the culture broth of the fungus *Penicillium* sp. SPF-3059 (Kumagai *et al*., 2003).

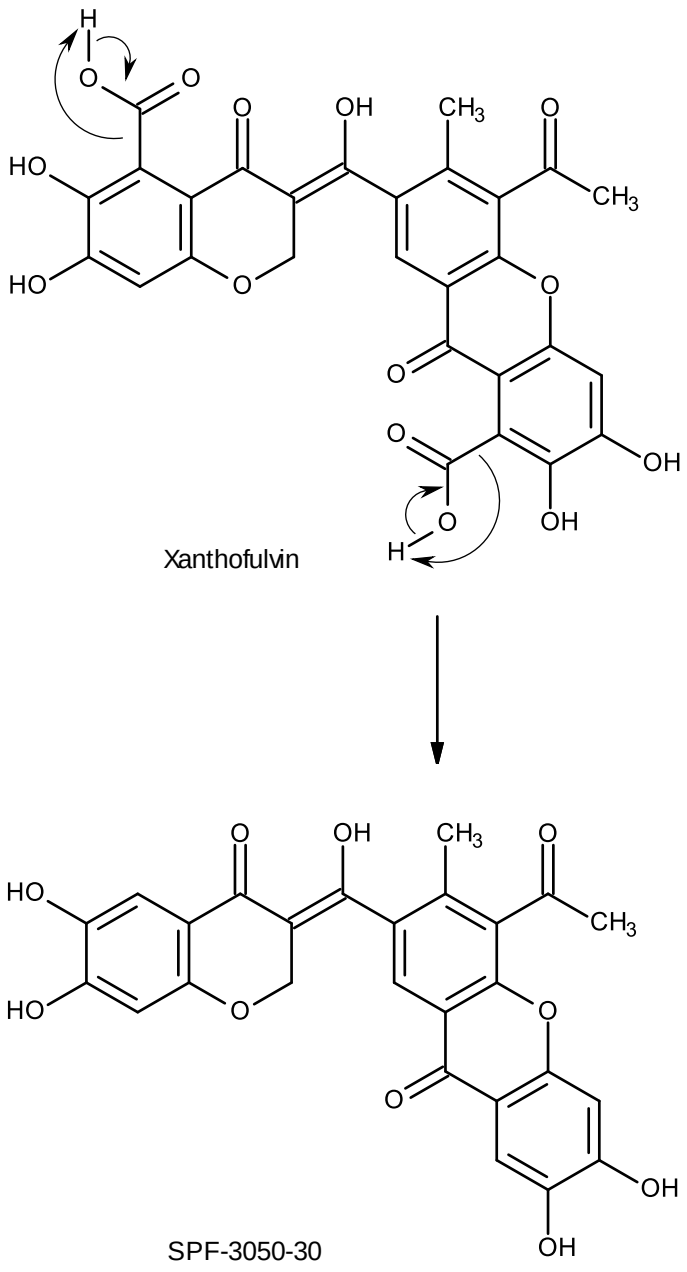

Figure 153. Formation of SPF-3050-30 by decarboxylation of xanthofulvin

3.1.2.18. SPF-3059-26 (PE 18)

Compound **PE 18** was isolated as a pale yellow viscous oil, and its molecular formula $C_{26}H_{16}O_{10}$ was established based on its (+)-HRESIMS *m/z* 489.0818 $[M+H]^+$, (calculated 489.0822 for $C_{26}H_{17}O_{10}$), indicating 19 degrees of unsaturation. The IR spectrum showed absorption bands for hydroxyl (3445 cm^{-1}), conjugated ketone (1650 cm^{-1}), olefin (1625 cm^{-1}), aromatic (1605, 1542 cm^{-1}), and ether (1262 cm^{-1}) groups. The ^{13}C NMR spectrum of **PE 18** displayed 26 carbon signals which, in combination with DEPT and HSQC spectra (Table 29), can be categorized as four conjugated ketone carbonyls (δ_C 201.3, 199.2, 173.7 and 173.4), seven oxyquaternary sp^2 (δ_C 154.5,152.8, 152.5, 151.1, 150.7, 145.0, 144.6), seven non-protonated sp^2 (δ_C 135.9, 133.5, 132.7, 120.8, 119.8, 115.7, 113.4), six methine sp^2 (δ_C 152.9, 126.4, 108.6, 107.9, 103.1, 102.9), and two methyl (δ_C 32.3 and 29.2) carbons. The ^1H and ^{13}C NMR data of **PE 18** resembled those of SPF-3059-30 **(PE 17)**, also isolated from this fungus, except for the absence of the oxymethylene sp^3 carbon at δ_C 66.2 and the appearance of the oxymethine sp^2 carbon at δ_C 152.9 in **PE 18**.

The presence of the 3-substituted 6,7-dihydroxy-4*H*-chromen-4-one portion was substantiated by HMBC correlations (Table 29) from H-5′ (δ_H 7.28, *brs*/δ_C 107.9) to C-4′ (δ_C 173.7), C-6′ (δ_C 152.8), C-7′ (δ_C 145.0) and C-8′a (δ_C 151.1), from H-8′ (δ_H 6.94, s/δ_C 103.1) to C-4′a (δ_C 113.4), C-6′, and from H-2′ (δ_H 8.13, *s* /δ_C 152.9) to C-3′ (δ_C 120.8), C-4′ and C-8′a.

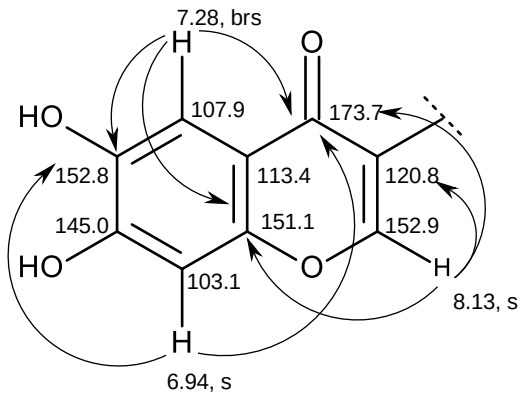

Figure 154. Key HMBC (⟶) correlations in 3-substituted 6,7-dihydroxy-4*H*-chromen-4-one in **PE 18**

That another part of the molecule was a 2,3,4-trisubstituted 6,7-dihydroxyxanthone, resembles that of SPF-3059-30 (**PE 17**), was supported by HMBC correlations (Table 29) from H-5 (δ_H 6.93, *s* /δ_C 102.9) to C-7 (δ_C 144.6), C-8a (δ_C 115.7), and from H-8 (δ_H 7.48, *s* /δ_C 108.6) to C-6 (150.5), C-9 (δ_C 173.4) and C-10a (δ_C 154.5). That the substituents on C-2 and C-4 of the benzene ring of the xanthone moiety were acetyl groups was corroborated by HMBC correlations from H-1 (δ_H 8.58, *s* /δ_C 126.4) to C-3 (δ_C 132.7), C-4a (δ_C 152.5), C-9 (δ_C 173.4), C-11 (δ_C 199.2), from Me-12 (δ_H 2.55,*s* / δ_C 29.2) to C-11 and from Me-14 (δ_H 2.53,*s* / δ_C 32.3) to C-13 (δ_C 201.3).

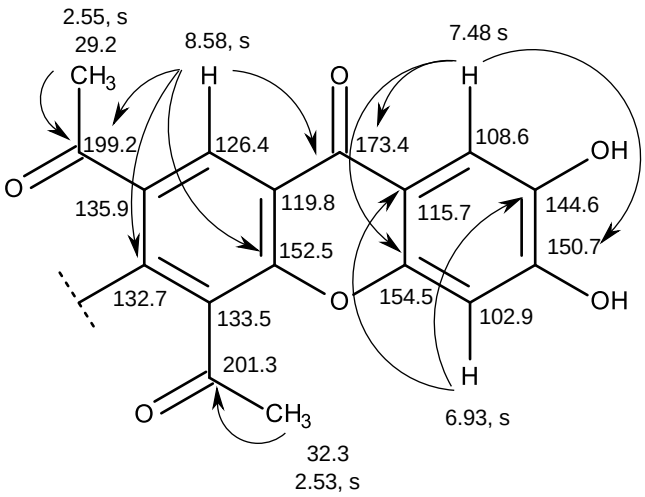

Figure 155. Key HMBC (⟶) correlations in 2,4-diacetyl-6,7-dihydroxyxanthone in **PE 18**.

Table 29. ^{1}H- and ^{13}C-NMR (500 MHz and 125 MHz, DMSO-d_6) and HMBC assignment for **PE 18**

Position	δ_C, Type	δ_H (*J* in Hz)	COSY	HMBC
1	126.4, CH	8.58, *s*	-	C-3, 4a, 9, 11
2	135.9, C	-	-	-
3	132.7, C	-	-	-
4	133.5, C	-	-	-
4a	152.5, C	-	-	-
5	102.9, CH	6.93, *s*	-	C-7, 8a, 9, 10a
6	150.7, C	-	-	-
7	144.6, C	-	-	-
8	108.6, CH	7.48, *s*	-	C-7, 8a, 9, 10a
8a	115.7, C	-	-	-
9	173.4, C	-	-	-
9a	119.8, C	-	-	-
10a	154.5, C	-	-	-
11	199.2, C	-	-	-
12	29.2, CH_3	2.55, *s*	-	C-2, 11
13	201.3, C	-	-	-
14	32.3, CH_3	2.53, *s*	-	C-4, 13
2′	152.9, CH	8.13, *s*	-	C-3′, 4’, 8’a, 9’
3′	120.8, C	-	-	-
4′	173.7, C	-	-	-
4’a	113.4, C	-	-	-
5′	107.9, CH	7.28, *brs*	-	C-4’, 6′, 7′, 8′a
6′	152.8, C	-	-	-
7′	145.0, C	-	-	-
8′	103.1, CH	6.94, *s*	-	C-4′, 6′, 7′
8′a	151.1, C	-	-	-

Finally, the 6,7-dihydroxy-4*H*-chromen-4-one and the 2,4-diacetyl-6,7-dihydroxyxanthone portions are linked through C-3′ of the former and C-3 of the latter was confirmed by HMBC correlation from H-2′ to C-3.

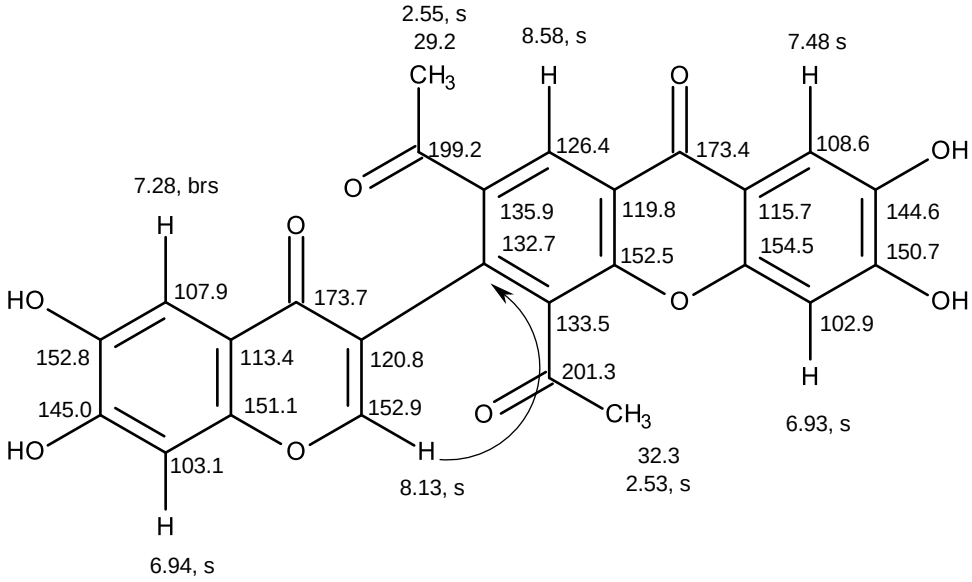

Figure 156. Key HMBC (⟶) correlations in 6,7-dihydroxy-4*H*-chromen-4-one and the 2,4-diacetyl-6,7-dihydroxyxanthone in **PE 18**

Literature search revealed that the planar structure of **PE 18** is the same as that of SPF-3059-26, another polyketide isolated from the acetone extract of the mycelium of *Penicilium* sp. SPF-3050 (FERM BB-7663), cultured in the liquid medium (Kimura *et al*., 2007). However, there were no assignments of ^{1}H and ^{13}C chemical shift values for any protons and carbons of the structure of SPF-3059-26. Analysis of the structure of **PE 18** revealed that the existence of the acetyl groups on C-2 and C-4 of the benzene ring of the xanthone moiety can impose a restriction of the rotation of the C-3 and C-3’ bond, thus creating a phenomenon of atropoisomerism. Optical rotation measurement revealed that **PE 18** is dextrorotatory, presenting $[\alpha]_D^{25}$ +266 in MeOH. Due to the interesting activity of this class of compounds, SPF-3059-26 was

later obtained, together with vinaxanthone and its derivatives, by ynone coupling reaction by Chin *et al*., (2015). Examination of the HRMS (ESI) data, ^{1}H and ^{13}C NMR spectra of SPF-3059-26, from the supporting information of the article by Chin *et al*., (2015), revealed that they are compatible with those of **PE 18**. However, neither optical rotation nor electronic circular dichroism (ECD) spectrum was mentioned in the discussion or provided in this supporting information. SPF-3059-26 (**PE 18**) can be perceived as a decarboxylated derivative of vinaxanthone, which was previously isolated from the culture of *P. vinaceum* NR6815, isolated from soil (Aoki *et al*., 1991), *P. glabrum* (Wehmer) Westling (Wrigley *et al*., 1994) and *Penicillium* sp. strain SPF-3059 (Kumagai *et al*., 2003). It is noteworthy to mention that the structure elucidation of vinaxanthone in all these articles was based on analyses of the 1D-and 2D-NMR data, nothing was mentioned about its optical rotation or ECD spectrum.

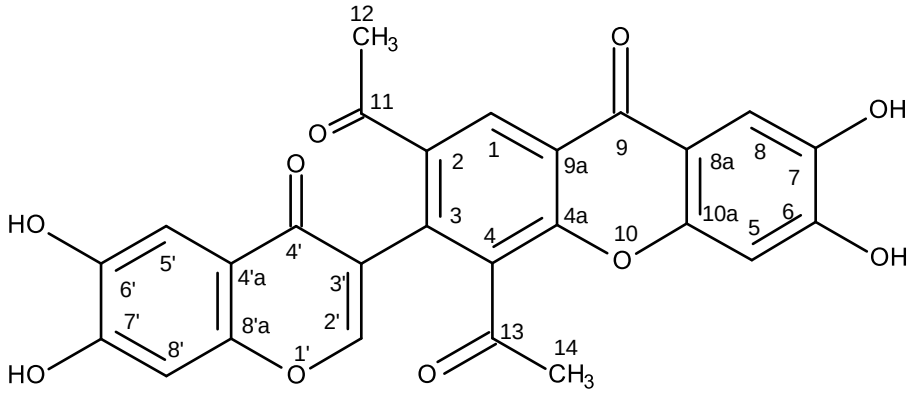

Figure 157. Structure of SPF-3059-26 (**PE 18**)

3.1.2.19. GKK1032B (PE 19)

Compound **PE 19** was isolated as white crystals (mp, 174-175 ºC), and its molecular formula was established as $C_{32}H_{39}NO_4$, based on its (+)-HRESIMS *m/z* at 502.2958 $[M+H]^+$ (calculated 502.2957 for $C_{32}H_{40}NO_4$), indicating 14 degrees of unsaturation. The ^{13}C NMR spectrum (Table 30) exhibited 32 carbon signals which, in combination with DEPT and HSQC spectra, can be classified as one ketone carbonyl

(δ_C 201.0), two amide or ester carbonyls (δ_C 177.2 and 170.5), three non-protonated sp^2 (δ_C 159.6, 138.5, 134.1), six methine sp^2 (δ_C 145.3, 133.5, 131.9, 131.8, 126.7, 120.6), one methylene sp^2 (δ_C 114.0), two quaternary sp^3 (δ_C 41.8, 41.1), one oxymethine sp^3 (δ_C 93.0), eight methine sp^3 (δ_C 61.5, 61.4, 60.4, 55.3, 53.9, 43.5, 27.9, 27.1), three methylene sp^3 (δ_C 49.2, 45.4, 45.2) and five methyl (δ_C 25.0, 22.8, 20.5, 19.7, 16.4) carbons, respectively. The ^{1}H NMR spectrum (Table 30) displayed a broad singlet of one proton at δ_H 8.31, four double doublets of aromatic protons at δ_H 7.22 (J = 8.3, 2.1 Hz), 7.04 (J = 8.4, 2.1 Hz), 6.96 (J = 8.3, 2.1 Hz) and 6.71 (J = 8.3, 2.1 Hz), one double doublet at δ_H 5.23 (J = 17.7, 10.8 Hz), a broad singlet at δ_H 5.09, two doublets at δ_H 4.75 (J = 10.9, 1.2 Hz) and 4.67 (J = 17.7, 1.2 Hz), a double doublet at δ_H 4.22 (J = 6.9, 3.4 Hz), a double double doublet at δ_{H1} 3.81 (J = 11.1, 8.2, 5.2 Hz), a double doublet at δ_H 3.67 (J = 12.9, 8.2 Hz), two doublets at δ_H 3.07 (J = 9.8 Hz) and 2.79 (J = 5.2 Hz), a double doublet at δ_H 2.41 (J = 12.9, 11.2 Hz), a multiplet at δ_H 2.19, a singlet at δ_H 1.90, a multiplet at δ_H 1.84, a singlet at δ_H 1.18 and a doublet at δ_H 1.17 (J = 6.3 Hz), a double doublet at δ_H 1.02 (J = 11.1, 6.9 Hz), a doublet at δ_H 1.02 (J = 6.3 Hz), a triplet at δ_H 0.81 (J = 12.0 Hz) and a quartet at δ_H 0.64 (J = 13.4 Hz). The presence of the 4-oxygenated benzyl moiety (fragment A) was evidenced by COSY correlations from H-2 (δ_H 6.71, *dd*, J = 8.3, 2.1 Hz/ δ_C 126.7) to H-3 (δ_H 7.22, *dd*, J = 8.3, 2.1 Hz/ δ_C 131.9), from H-5 (δ_H 6.96, *dd*, J = 8.4, 2.1 Hz/ δ_C 133.5) to H-6 (δ_H 7.04, *dd*, J = 8.4, 2.1 Hz/ δ_C 120.6) and from H-7a (δ_H 2.41, *dd*, J = 12.9, 11.2 Hz/ δ_C 37.4) to H-7b (δ_H 3.67, *dd*, J = 12.9, 8.2 Hz/ δ_C 37.4) as well as by HMBC correlations from H-2 to C-1, C-4, C-6, from H-3 to C-1, C-5, C-7, from H-5 to C-1, C-3, C-7, from H-6 to C-1, C-2, C-4 and H_2-7 to C-3, C-4, C-5.

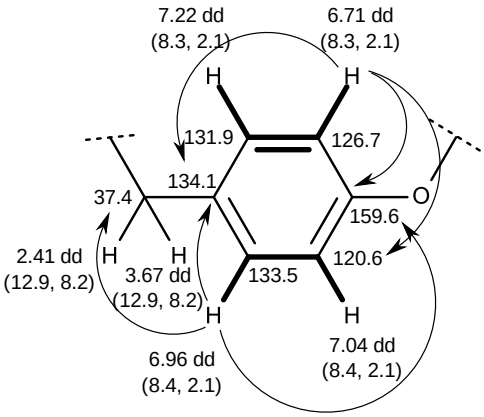

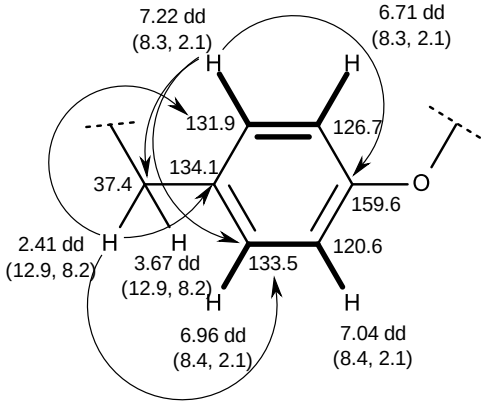

Fragment A

That the 4-oxygenated benzyl moiety (fragment A) was linked the 3,4-disubstituted pyrrolidine-2,5-dione, through the methylene group (C-7) of the former and C-3 of the latter, was corroborated by the COSY correlations from H_2-7 to H-8 at δ_H 3.81, *ddd*, (*J* = 11.1, 8.2, 5.2 Hz) and from H-8 to H-12 at δ_H 2.79, *d* (*J* = 5.2 Hz) as well as by the HMBC correlations from H-7a (δ_H 2.41 *dd*, *J* = 12.9, 11.2 Hz) to the carbons at δ_C 177.2 (CO-9), C-3, C-4, C-5 and at δ_C 43.5 (C-8), from H-7b (δ_H 3.81 *ddd*, *J* = 11.1, 8.2, 5.2 Hz) to the carbons at δ_C 60.4 (C-12), C-7 and C-9, from H-12 to C-9, C-11 (δ_C 170.5), C-7 and C-8. Moreover, both H-8 and H-12 also showed HMBC correlations to the ketone carbonyl at δ_C 201.0 (C-13) while the broad singlet at δ_H 8.31 (NH-10) showed HMBC cross peaks to C-8 and C-12. Therefore, fragment B of **PE 19** was proposed as:

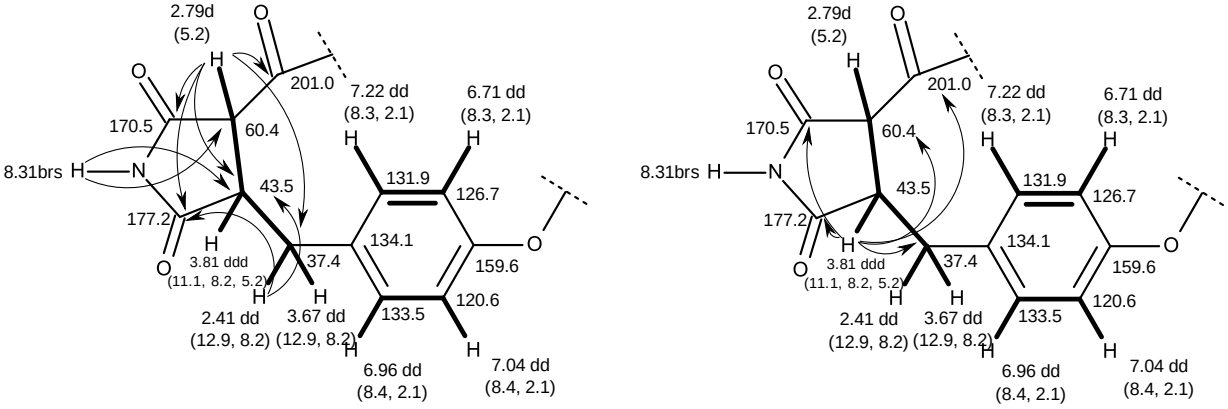

Fragment B

The existence of the 1,2,3-trisubstituted 3a, 5, 7-trimethyloctahydro-1*H*-indene moiety (fragment C) was supported by the COSY correlations from H-20 (δ_H 4.22, *dd*, *J* = 6.9, 3.4 Hz/ δ_C 93.0) to H-21 (δ_H 1.02, *dd*, *J* = 11.1, 6.9 Hz) as well as by the HMBC correlations from the methyl doublet at δ_H 1.17, *d*, *J* =6.3 Hz (Me-27) to C-26 (δ_C 27.1), C-25 (δ_C 45.2) and C-21 (δ_C 61.5), H-20 to C-21 (δ_C 64.5) and C-22 (δ_C 44.1), from Me -29 at δ_H 1.18 (*s*, δ_C 19.7) to C-18 (δ_C 53.9), C-23 (δ_C 49.4) and C-21, from Me-28 at δ_H 0.92, *d*, *J* = 6.3 Hz/ δ_C 22.8) to C-23, C-24 (δ_C 27.9) and C-25. The high frequency of the chemical shift value of C-20 (δ_C 93.0) indicated that it was an oxygenated methine sp^3 carbon.

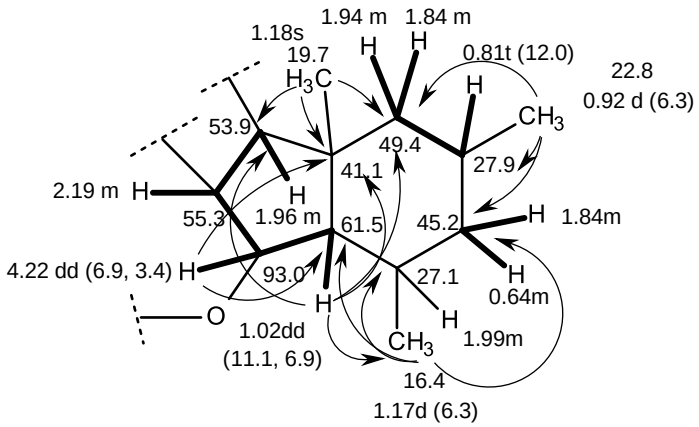

Fragment C

That the cyclopentane ring of fragment C was fused with the 1,4-dimethylcyclohexenone ring through C-18 and C-19 (fragment D) was substantiated by the COSY correlation from H-19 at δ_H 2.19 *m* (δ_C 55.3) to H-14 at δ_H 3.07, *d*, *J* = 9.8 Hz (δ_C 61.4) as well as by the HMBC correlations from H-14 to C-15 (δ_C 41.8), C-16 (δ_C 131.8), C-19 (δ_C 55.3), and Me-31 (δ_C 25.0/ δ_H 1.18), from Me-30 at δ_H 1.90 *s* (δ_C 20.5) to C-17 (δ_C 138.5), C-16, C-18, from H-16 at δ_H 5.09, *brs* (δ_C 131.8) to C-14, C-15, C-18 and Me-31. That another substituent on C-15 of the cyclohexene ring was an ethenyl group was supported by the COSY correlations from H-32 at δ_H 5.23 (*dd*, *J* = 17.7, 10.8 Hz/ δ_C 145.3) to H_2-33 at δ_H 4.67 (*dd*, *J* = 17.7, 1.2 Hz/ δ_C 145.3)/ δ_H 4.75 (*dd*, *J* = 10.9, 1.2 Hz/ δ_C 145.3), and by the HMBC correlations from H-32 to C-15, C-16 and Me-31. Therefore, the planar structure of fragment D was established as:

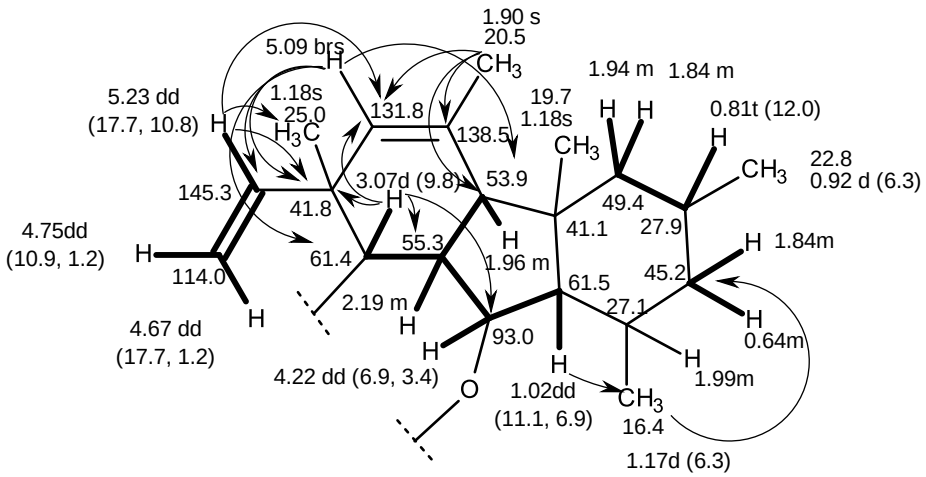

Fragment D

That C-14 of fragment D was linked to the carbonyl ketone of fragment B was supported by the HMBC correlations from H-14 and H-19 to C-13. Based on the molecular formula of **PE 19** and chemical shift values of C-1 (δ_C 159.6) and C-20 (δ_C 93), C-1 and C-20 must be linked through an ether bridge, forming a macrocyclic scaffold whose planar structure is shown below:

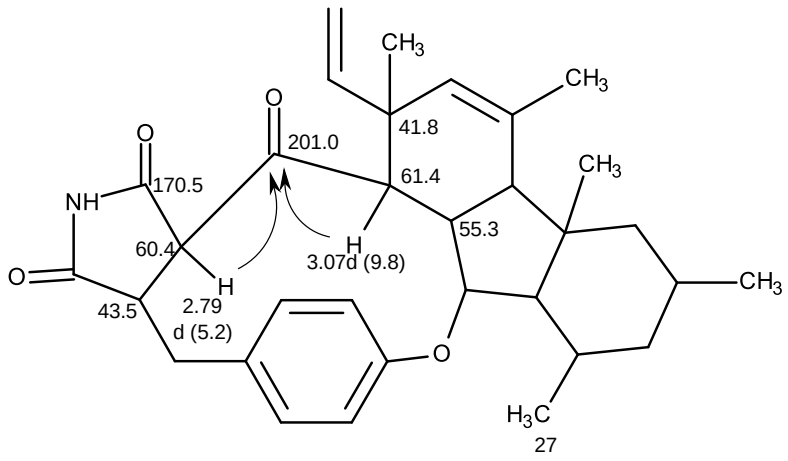

Table 30. ^{1}H and ^{13}C NMR (500 MHz and 125 MHz, $CDCl_3$) and HMBC assignments for **PE 19**

Position	δ_C, type	δ_H, (*J* in Hz)	COSY	HMBC
1	159.6, C	-	-	-
2	126.7, CH	6.71, *dd* (8.3, 2.1)	H-3	C-1, 4, 6
3	131.9, CH	7.22, *dd* (8.3, 2.1)	H-2	C-1, 5, 7
4	134.1, C	-	-	-
5	133.5, CH	6.96, *dd* (8.4, 2.1)	H-6	C-1, 3, 7
6	120.6, CH	7.04, *dd* (8.4, 2.1)	H-5	C-1, 2, 4
7α	34.7, CH_2	2.41, *dd* (12.8, 11.2)	H-7β, H-8	C-1, 3, 5, 8, 9
β		3.67, *dd* (12.8, 8.2)	H-7α, H-8	C-1, 3, 8, 12
8	43.5, CH	3.81, *ddd* (11.1, 8.2, 5.2)	H-7α, β, 12	C-7, 9, 12, 13
9	177.2, CO	-	-	-
10	-	8.31, *brs*	-	C-8, 12
11	170.5, CO	-	-	-
12	60.4, CH	2.79, *d* (5.2)	H-8	C-7, 8, 9, 13
13	201.0, CO	-	-	-
14	61.4, CH	3.07, *d* (9.8)	H-19	C-13, 16, 19, 20, 31
15	41.8, C	-	-	-
16	131.8, CH	5.09, *brs*	H-18, 30	C-14, 15, 18, 31, 32
17	138.5, C	-	-	-
18	53.9, CH	1.96, *br*	H-16, 19	C-14, 15, 17, 19
19	55.3	2.19, *m*	H-14, 18, 20	C-13, 14, 18, 20
20	93.0, CH	4.22, *dd* (6.3, 3.4)	H-19, 21	C-21, 22
21	61.5, CH	1.02, *dd* (11.1, 6.9)	H-20, 26	C-18, 22, 24, 27
22	41.1, C	-	-	C-14
23α	49.4, CH_2	1.94, *m*	H-23β, 24	C-22, 25
β		0.81, *m*	H-23 α, 24	C-18, 22, 24
24	27.9, CH	1.84, *m*	H_2-23, 25, 28	C-23
25α	45.2, CH_2	1.84, *m*	H-24, 25β, 26	C-21, 23
β		0.64, *m*	H-24, 25α, 26	C-24
26	27.1, CH	1.99, *m*	H-21, 25α, β, 27	C-22, C-27
27	16.4, CH_3	1.17, *d* (6.3)	H-26	C-21, 25, 26
28	22.8, CH_3	0.92, d (6.3)	H-24	C-23, 24, 25
29	19.7, CH_3	1.18, *s*	-	C-18, 22, 23
30	20.5, CH_3	1.90, *s*	-	C-16, 17, 18
31	25.0, CH_3	1.18, *s*	-	C-14, 15, 16, 32
32	145.3, CH	5.23, *dd* (17.6, 10.8)	H-33α, β	C-15, 16, 31
33α	114.0,CH_2	4.75, *dd* (10.9, 1.2)	H-32	C-15
β		4.67, *dd* (17.7, 1.2)	H-32	C-15, 32

Since **PE 19** furnished suitable crystal, the X-ray diffraction was carried out. The ORTEP view shown in figure 158 not only confirmed the structure of **PE 19** but also allowed to establish the absolute configuration of its stereogenic carbons.

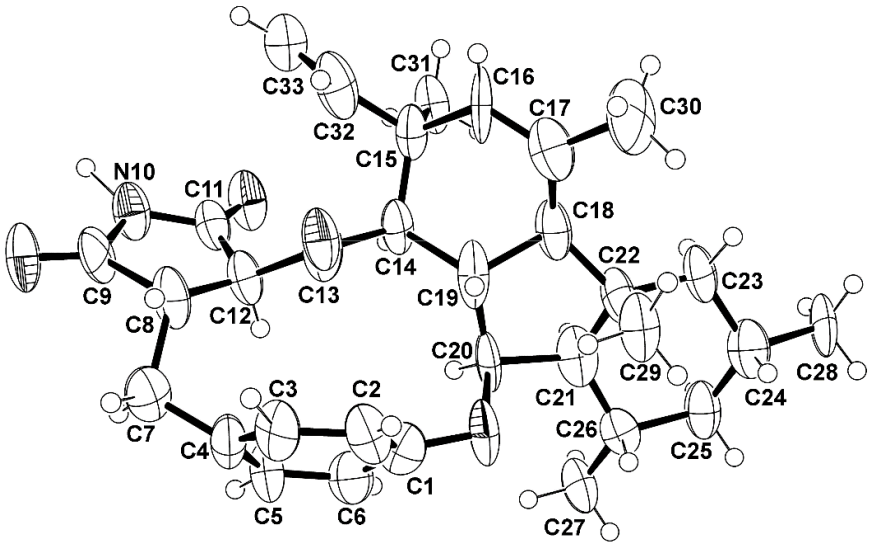

Figure 158. ORTEP view of **PE 19**

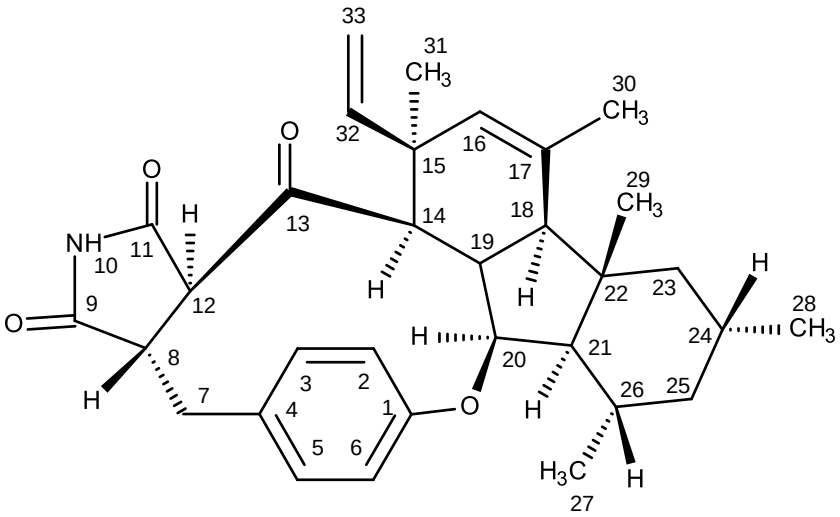

Figure 159. Structure of GKK1032B (**PE 19**)

From the literature search, the structure of **PE19** is the same as that of GKK1032B (Figure 159), a fungal metabolite which was first reported from the culture of *Penicillium* sp. GKK1032 (Hasegawa *et al*., 2001), and later from other fungal species including the seed fungus *Trichoderma* sp. BCC 7579 which was isolated from a decaying pod of *Entada* perseatha (Leguminosae) (Isaka *et al*., 2006), endophytic fungi *Penicillium* sp., isolated from *Melia azedarach and Murraya paniculate,* and *P. citrinum* which was isolated from *Garcinia mangostana* (Pastre *et al*., 2007 and Qader *et al*., 2015), as well as the marine-derived fungus *Penicillium* sp. ZZ380, which was isolated from a wild crab (*Pachygrapsus crassipes*) (Song *et al*., 2018), and from the soil fungus *Penicillium* sp. PSU-RSPG99 (Rukachaisirikul *et al*., 2014).

3.1.2.20. Secalonic acid A (PE 20)

Compound **PE 20** was isolated as yellow crystals (mp. 269-270 °C), and its molecular formula was established as $C_{32}H_{30}O_{14}$ based on of its (+)-HRESIMS *m/z* 639.1718 $[M+H]^+$, (calculated 639.1714 for $C_{32}H_{31}O_{14}$), indicating 18 degrees of unsaturation. The ^{13}C NMR spectrum (Table 31) displayed 16 carbon signals which were categorized, according to the DEPT and HSQC spectra, as one conjugated ketone carbonyl (δ_C 187.2), one ketone or enolic (δ_c 177.5), one ester carbonyl (δ_C 170.3), two oxyquaternary sp^2 (δ_C 159.4 and 158.3), three non-protonated sp^2 (118.3, 106.9 and 101.6), two methine sp^2 (δ_C 140.2 and 107.5), one oxyquaternary sp^3 (δ_C 84.8), one oxymethine sp^3 (δ_C 77.1), one methine sp^3 (δ_C 29.3), one methylene sp^3 (δ_C 36.3), one secondary methyl (δ_C 17.9) and one methoxyl (δ_C 53.1) carbons.

The ^1H NMR spectrum, in conjunction with the HSQC spectrum (Table 31), exhibited two doublets of aromatic protons at δ_H 7.46 (J = 8.5 Hz), δ_H 6.62, (J = 8.5 Hz), a multiplet of a methine proton at δ_H 2.41, a double doublet of an oxymethine proton at δ_H 3.92, (J = 11.2, 2.7 Hz), one methoxyl singlet at δ_H 3.72, and one methyl doublet at δ_H 1.17, (J = 6.5 Hz).

The presence of a 2,3,6-trisubstituted phenol moiety was corroborated by the HMBC correlations (Table 31) from the hydrogen-bonded phenolic hydroxyl proton at

δ_H 11.7 *brs* to the carbons at δ_C 159.4 (C-1), 118.3 (C- 2) and 106.9 (C-9a), from the proton at δ_H 7.46, *d* (*J* = 8.5 Hz/ H-3) to C-1, C-2, C-4a (δ_C 158.3) and from the proton at δ_H 6.62, *d* (*J* = 8.5 Hz/ H-4) to C-2, C-4a, C-9a and C-9 (δ_C 187.2).

The COSY spectrum (Table 31) exhibited cross peaks from H-4 to H-3 as shown in figure 160.

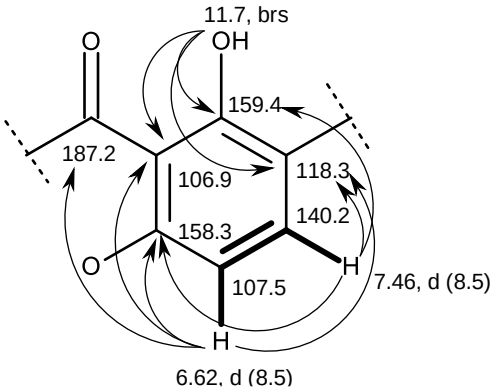

Figure 160. COSY (▬) and HMBC (⟶) correlations in the 2,3,6-trisubstituted phenol portion of **PE 20**

The COSY spectrum (Table 31) also showed correlations from the multiplet at δ_H 2.41 (H-6) to the proton at δ_H 3.92 *dd* (*J* = 11.2, 2.7 Hz, H-5) and methyl doublet at δ_H 1.17 (*J* = 6.5 Hz, Me-11), from the double doublets at 2.73 (*J* = 11.8, 2.7 Hz/ H-7a) and 2.30 (*J* = 11.5, 3.4 Hz/ H-7b) to H-6. The HMBC spectrum (Table 31) displayed correlations from H-7a and H-7b to C-5 (δ_C 71.1), C-8 (δ_C 177.5), C-8a (δ_C 101.6) and C-11 (δ_C 17.9), from H-6 to C-5 and C-11, from H-5 to C-6 (δ_C 29.3), 10a (δ_C 84.8), C-11 and C-12 (δ_C 170.3), and from Me-11 to C-5, C-6 and C-7 (δ_C 36.3). Additionally, the HMBC spectrum also displayed cross peaks from the methoxyl singlet at δ_H 3.72 (δ_C 53.1) to the ester carbonyl carbon at δ_C 170.3 (C-12), supporting the presence of the 1, 2-disubstituted methyl-3,6-dihydroxy-5-methylcyclohex-2-ene-1-carboxylate moiety. The chemical shift value of C-8a (δ_C 101.6) indicates that the substituent on C-8a was an electron withdrawing group such as a carbonyl group. This was corroborated by the presence of a singlet of the hydrogen-bonded phenolic hydroxyl

group at δ_H 13.77, which was assigned to OH-8. Therefore, the structure of the 1, 2-disubstituted methyl-3,6-dihydroxy-5-methylcyclohex-2-ene-1-carboxylate moiety can be depicted as in figure 161.

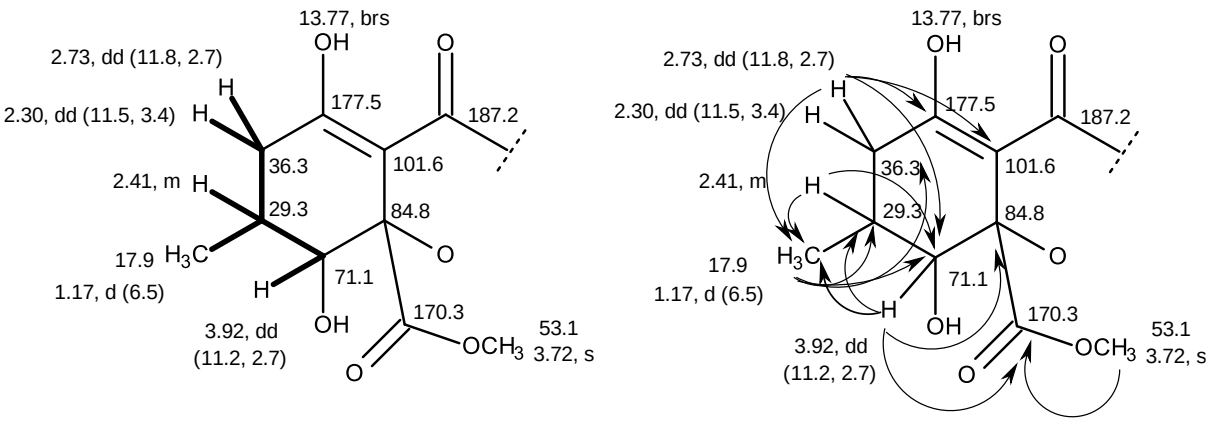

Figure 161. COSY (▬) and key HMBC (⟶) correlations in the methyl-3,6-dihydroxy-5-methylcyclohex-2-ene-1-carboxylate moiety of **PE 20**

Combining the two moieties, the structure of **PE11** was deduced as methyl 1,4-dihydroxy-3-methyl-9-oxo-2,3,4,9-tetrahydro-4a*H*-xanthene-4a-carboxylate (Figure 162).

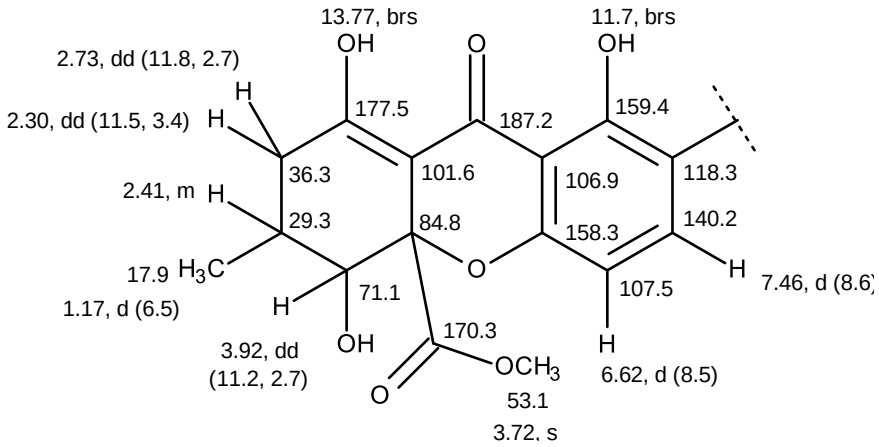

Figure 162. The partial structure of **PE 20** indicating the ^{1}H and ^{13}C chemical shift values

However, this structure not only lacks a substituent on C-2 (δ_C 118.3) but also accounts for $C_{16}H_{15}O_7$, which is only half of its molecular formula $C_{32}H_{30}O_{14}$, as determined by (+)-HRESIMS. Therefore, the structure of **PE 20** must be a dimer of the proposed structure, linked through its carbon at δ_C 118.3 (C-2). This hypothesis was confirmed by an X-ray analysis whose ORTEP view is shown in figure 163. The X-ray analysis not only confirmed the proposed structure of **PE 20** but also determined the absolute configurations of C-5/C-5′, C-6/C-6′ and C-10a/C-10′a, respectively as 5*S*/ 5′*S*, 6*R*/ 6′*R*, and 10a*S*/ 10′a *S*.

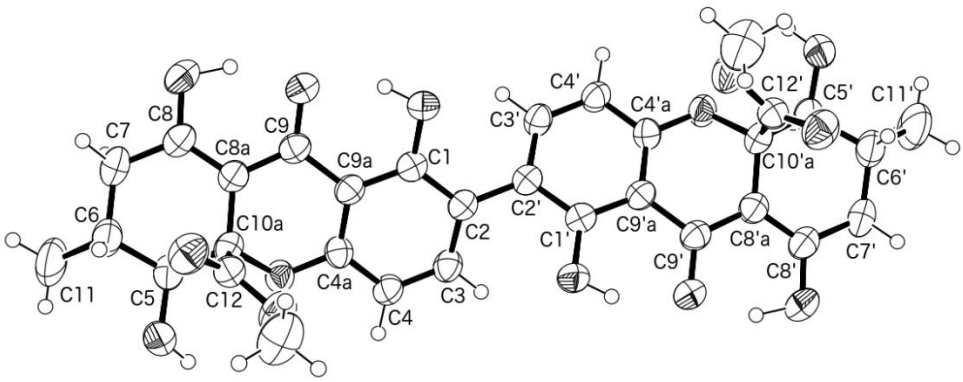

Figure 163. ORTEP view of **PE 20**

Therefore, the full structure, including its stereochemistry, of **PE 20** was elucidated as shown in figure 164.

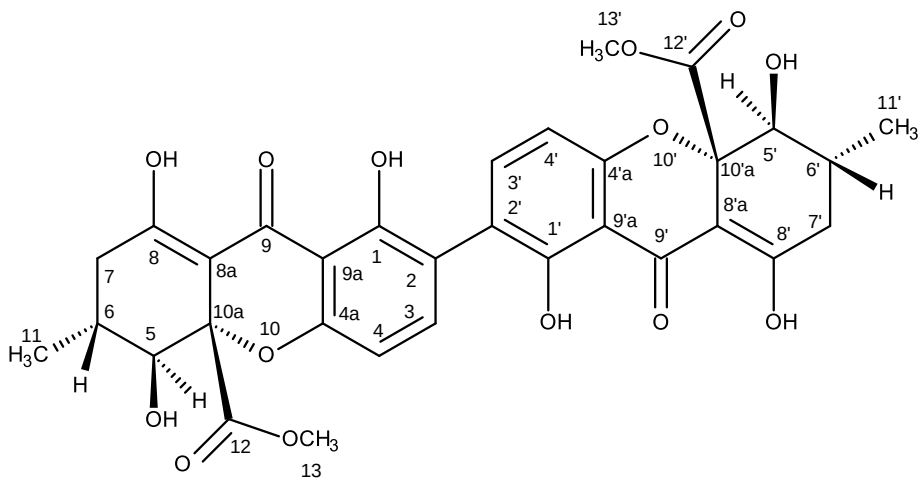

Figure 164. The structure of secalonic acid A (**PE 20**)

Literature search revealed that the structure of **PE 20** corresponded to that of secalonic acid A, a fungal metabolite which was first reported from the fungus *Aspergillus ochraceus* by Yamazaki *et al*., (1971), and later from the lichens *Pseudoparmelia sphaerospora* (Honda *et al*., 1995). This compound was also isolated from the endophytic fungus *Talaromyces* sp. ZH-154 (Liu *et al*., 2010) as well as by our group from the marine sponge-associated fungi *Talaromyces stipitatus* KUFA 0207 (Noinart *et al*., 2017) and *Neosartorya fennelliae* KUFA, 0811 (Aung, 2017).

Table 31. ^{1}H and ^{13}C NMR (500 MHz and 125 MHz, $CHCl_3$) and HMBC assignment for **PE 20**

Position	δc, type	δ_H, (*J* in Hz)	COSY	HMBC
1 (1’)	158.3, C	-	-	-
2 (2’)	118.3, C	-	-	-
3 (3’)	140.2, CH	7.46, *d* (8.6)	H-4 (4′)	C-1 (1′), 2 (2′), 4a (4’a)
4 (4’)	107.5, CH	6.62, *d* (8.5)	-	C-2 (2′), 4a (4a′), 9 (9’), 9a (9a′)
4a (4’a)	158.3, C	-	-	
5 (5’)	77.1, CH	3.92, *dd* (11.2, 2.7)	H-6, (6′)	C-6 (6’), 10a (10a′), 11 (11’), 12 (12′)
6 (6’)	29.3, CH	2.41, *m*	H-5 (5′), 11 (11′)	C-5 (5’), 11 (11’)
7a (7’a)	36.3, CH_2	2.73, *dd* (11.8, 2.7)	H-7b (7b′)	C-5 (5’), 6 (6’), 8 (8’), 8a (8’a)
b		2.30, *dd* (11.5, 3.4)	H-5, (5′), 7a (7a′)	C-6 (6′), 8 (8′), 8a (8’a), 11 (11’)
8 (8’)	177.5, C	-	-	-
8a (8’a)	101.6, C	-	-	-
9 (9’)	187.2, C	-	-	-
9a (9’a)	106.9, C	-	-	-
10a (10’a)	84.8, C	-	-	-
11 (11’)	17.9, CH_3	1.17, *d* (6.5)	H-6 (6′)	C-5 (5′), 6 (6′), 7 (7′)
12 (12’)	170.3, C	-	-	-
13 (13’)	53.1, CH_3	3.72, *s*	-	C-12 (12′)
OH-1 (1’)	-	11.7, *brs*	-	C-1 (1′), 2 (2′), 9a (9a′)
OH-8 (8’)	-	13.8, *brs*	-	-

3.2. Biological Activity Evaluation of the Isolated Secondary Metabolites from Marine-Derived Fungi

Some of the isolated metabolites from the marine sponge-associated fungi *Neosartorya tsunodae* KUFC 9213 and *Penicillium erubescens* KUFA 0220 were evaluated for their biological activities.

Antibacterial and Antibiofilm Activities Evaluation

Chromanol (**NT 1**), (3β,5α,22E)-3,5-dihydroxyergosta-7,22-dien-6-one (**NT 2**), hopan-3β,22-diol (**NT 4**), lumichrome (**NT 8**) and harmane (**NT 9**), were tested for their growth inhibitory activity against two Gram-positive (*Staphylococcus aureus* ATCC 29213 and *Enterococcus faecalis* ATCC 29212), two Gram-negative (*Escherichia coli* ATCC 25922 and *Pseudomonas aeruginosa* ATCC 27853) bacteria, a clinical isolate sensitive to the most commonly used antibiotic families, and four multidrug-resistant isolates from the environment. The results showed that none of the tested compounds exhibited antibacterial activity at the highest concentrations tested at 64 µg/mL.

Similarly, citromycin (**PE 3**), 12-methoxycitromycin (**PE 4**), 1-hydroxy-12-methoxycitromycin (**PE 5**), myxotrichin D (**PE 6**), 12-methoxycitromycetin (**PE 7**), anhydrofulvic acid (**PE 8**), Penialidin D (**PE 11**), penialidin F (**PE 12**), erubescensoic acid (**PE 13**), erubescenschromone A (**PE 14**), 7-hydroxy-6-methoxy-4-oxo-3-[(1*E*)-3-oxobut-1-en-1-yl]-4*H*-chromen-5-carboxylic acid (**PE 15**), erubescenschromone B (**PE 16**), SPF-3059-30 (**PE 17**), SPF-3059-26 (**PE 18**), GKK1032B (**PE 19**) and secalonic acid A (**PE 20**) were evaluated for their antibacterial activity against Gram-negative and Gram-positive bacteria by disc diffusion method, and the minimal inhibitory concentration (MIC) and minimal bactericidal concentration (MBC) of several reference strains and multidrug-resistant isolates from the environment were also determined. However, in the range of concentrations tested, none of the compounds were active against Gram-negative bacteria tested.

In the disc diffusion assay, a halo of growth inhibition for all Gram-positive bacteria exposed to GKK1032B (**PE 19**) (Table 32) and for methicillin-resistant

Staphylococcus aureus (MRSA) 66/1 exposed to secalonic acid A (**PE 20**) was detected. However, in the range of concentrations tested, it was only possible to determine MICs for GKK1032B (**PE 19**) (Table 32), which are 8 mg/mL for *E. faecalis* ATCC 29212 and vancomycin-resistant *E. faecalis* (VRE) B3/101, 16 mg/mL for *E. faecium* ATCC 19434, and 32 mg/mL for *E. faecium* 1/6/63 (VRE) and *S. aureus* ATCC 29213. While it was not possible to determine the MBC for the other Gram-positive strains, the MBC for *S. aureus* ATCC 29213 was 64 mg/mL (Table 32). These results suggested that GKK1032B (**PE 19**) might have a bacteriostatic effect.

Table 32. The antibacterial activity of GKK1032B (**PE 19**) against a Gram-positive reference and multidrug-resistant strains. MIC and MBC are expressed in mg/mL.

Strains	Disc diffusion	MIC	MBC
E. faecalis ATCC29212	+	8	>64
E. faecium ATCC19434	+	16	>64
S. aureus ATCC29213	+	32	64
E. faecalis B3/101 (VRE)	+	8	>64
E. faecium 1/6/63 (VRE)	+	32	>64
S. aureus 66/1 (MRSA)	+	>64	>64

MIC, minimal inhibitory concentration; MBC, minimal bactericidal concentration; VRE, vancomycin-resistant *Enterococcus*; MRSA, methicillin-resistant *Staphylococcus aureus*; (-), no inhibition halo; (+), 7–9 mm inhibition halo.

The ability of the tested compounds to prevent biofilm formation was evaluated on four reference strains by measuring the total biomass. For GKK1032B (**PE 19**), four concentrations ranging from 2 × MIC to ¼ MIC were tested against *E. faecalis* ATCC 29212, *E. faecium* ATCC 19434 and *S. aureus* ATCC 29213. For the other compounds, since it was not possible to determine their minimal inhibitory concentration (MIC) values, the highest concentration tested in the previous assays

was used. The tested compounds did not inhibit the biofilm formation of *S. aureus* ATCC 29213, *E. coli* ATCC 25922, and *P. aeruginosa* ATCC 27853. However, the biofilm forming ability of *E. faecalis* ATCC 29212, which is classified as a strong biofilm producer, was impaired by GKK1032B (**PE 19**) (8 MIC and 2 × MIC) and secalonic acid A (**PE 20**) (Table 33), while compounds penialidin D (**PE 11**), erubescensoic acid (**PE 13**), 7-hydroxy-6-methoxy-4-oxo-3-[(1*E*)-3-oxobut-1-en-1-yl]-4*H*-chromen-5-carboxylic acid (**PE 15**), erubescenschromone B (**PE 16**) and SPF-3059-26 **(PE 18)** were capable of impairing the biofilm forming ability of *E. coli* ATCC 25922, which was classified as a strong biofilm producer (Table 33). On the other hand, GKK1032B (**PE 19**) was able to increase the biofilm production of a weak biofilm producer *E. faecium* ATCC 19434.

The screening of a potential synergy between the tested compounds and clinically relevant antimicrobial drugs revealed a slight synergy, as determined by the disc diffusion assay (Table 34). 12-Methoxycitromycin (**PE 4**), in combination with cefotaxime (CTX), resulted in a small synergistic effect, as seen by a small increment in the zone of inhibition when compared to the inhibition halo of CTX alone in *E. coli* SA/2, an extended-spectrum β-lactamase producer (ESBL). A similar effect was observed for VRE *E. faecalis* B3/101 when GKK1032B (**PE 19**) was combined with vancomycin (VAN). These results were confirmed by the checkerboard method or by determination of the MIC for each antibiotic in the presence of a fixed concentration of each compound when it was not possible to determine a MIC value for the test compound. In the latter, the concentration of each compound used was the highest concentration tested in previous assays which did not inhibit the growth of the four multidrug-resistant strains under study. The effects observed using the disc diffusion assay were not replicated, however, when VRE *E. faecalis* B3/101 was exposed to myxotrichin D (**PE 6**), penialidin F (**PE 12**) and secalonic acid A (**PE 20**), there was a two-fold reduction in the MIC of VAN. On the other hand, when ESBL *E. coli* SA/2 was exposed to 1-hydroxy-12-methoxycitromycin (**PE 5**) and SPF-3059-30 (**PE 17**), there was at least a two-fold increase in the MIC of CTX. When VRE *E. faecium* 1/6/63 was exposed to secalonic acid A (**PE 20**), there was a two-fold reduction in the MIC of VAN. On the hand, when it was exposed to 12-methoxycitromycetin (**PE 7**), there was at least a two-fold increase in the MIC of VAN. Interestingly, screening of potential

synergy with antibiotics revealed that SPF-3059-26 (**PE 18**) was able to reduce the CTX MIC of *E. coli* SA/2 (ESBL) for four-fold while it increased the OXA MIC of MRSA *S. aureus* 66/1 by two-fold (Table 34).

Thus, in terms of antibacterial activity, GKK1032B (**PE 19**) is the most promising. Even though no synergy with VAN or OXA was found, this compound alone exhibited an antibiofilm activity against *E. faecalis* and antibacterial activity against the reference *S. aureus*, *E. faecalis*, and *E. faecium* strains. Notably, GKK1032B (**PE 19**) showed antibacterial activity against both vancomycin-resistant *E. faecalis* and vancomycin-resistant *E. faecium* strains, a pathogen classified by WHO as high priority for the research and development of new antibiotics (Tacconelli *et al*., 2017).

Table 33. The classification of the ability of *E. faecalis* ATCC 29212 and *E. coli* ATCC 25922 to adhere to and form biofilm after exposure to **PE 3-8** and **PE 11-20** in comparison to the untreated control.

Compound	Concentration (mg/L)	OD ± SD	Classification	
			ATCC 29212	ATCC 25922
PE 3	64	1.205 ± 0.025	strong	-
PE 4	64	1.547 ± 0.218	strong	-
PE 5	64	1.673 ± 0.308	strong	-
PE 6	64	1.522 ± 0.308	strong	-
PE 7	32	1.378 ± 0.378	strong	-
PE 8	64	1.136 ± 0.138	strong	-
PE 11	64	0.188 ± 0.012	-	moderate
PE 12	64	2.128 ± 0.248	strong	-
PE 13	64	0.195 ± 0.012	-	moderate
PE 14	64	0.867 ± 0.280	strong	-
PE 15	32	0.246 ± 0.038	-	moderate
PE 16	64	0.172 ± 0.024	-	weak
PE 17	64	1.192 ± 0.239	strong	-
PE 18	64	0.194 ± 0.013	-	moderate
PE 19	16 (2xMIC)	0.089 ± 0.002	weak	-
PE 19	8 (MIC)	0.099 ± 0.006	weak	-
PE 19	4 (1/2 MIC)	1.884 ± 0.220	strong	-
PE 19	2 (1/4MIC)	2.358 ± 0.416	strong	-
PE 20	64	0.263 ± 0.014	moderate	-
None	0	0.080 ± 0.002	strong	-

OD = optical density; SD = standard deviation; The classification used is based on criteria in (Stepanović *et al*., 2000), Average OD value for negative control was found to be 0.055 ± 0.002, therefore the optical cut-off value (ODc) is equal to 0.055 + (3 × 0.002) = 0.061; 2 × ODc = 0.122; 4 × ODc = 0.244. ATCC 29212 = *E. faecalis* ATCC 29212, ATCC 25922 = *E. coli* ATCC 25922.

Table 34. The combined effect of clinically used antibiotics with **PE 3-8**, **PE 12**, **PE 14**, **PE 17**, **PE 19** and **PE 20** against multidrug-resistant strains. MICs are expressed in mg/mL.

Compound	*E. coli* SA/2		*E. faecalis* B3/101		*E. faecium* 1/6/63		*S. aureus* 66/1	
	CTX		VAN		VAN		OXA	
	Disc Diffusion	MIC	Disc Diffusion	MIC	Disc Diffusion	MIC	Disc Diffusion	MIC
Antibiotic	+	512	-	1024	-	1024	-	64
Antibiotic + PE 3	-	512	-	1024	-	1024	-	64
Antibiotic + PE 4	+	512	-	1024	-	1024	-	64
Antibiotic + PE 5	-	>512	-	1024	-	1024	-	64
Antibiotic + PE 6	-	512	-	512	-	1024	-	64
Antibiotic + PE 7	-	512	-	1024	-	>1024	-	64
Antibiotic + PE 8	-	512	-	1024	-	1024	-	64
Antibiotic + PE 11	-	512	-	1024	-		-	64
Antibiotic + PE 12	-	512	-	512	-	1024	-	64
Antibiotic + PE 13	-	512	-	1024			-	64
Antibiotic + PE 14	-	512	-	1024	-	1024	-	64
Antibiotic + PE 15	-	512	-	1024	-		-	64
Antibiotic + PE 16	-	512	-	1024	-		-	64
Antibiotic + PE 17	-	>512	-	1024	-	1024	-	64
Antibiotic + PE 18	-	128	-	1024	-		-	128
Antibiotic + PE 19	-	512	+	*	-		-	64
Antibiotic + PE 20	-	512	-	512	-	512	-	64

MIC = minimal inhibitory concentration; (-) = no inhibition halo or no increase in the inhibition halo; (+) = halo of inhibition or increase of the inhibition halo by 2 mm; CTX = cefotaxime; VAN = vancomycin; OXA = oxacillin.* For this compound, the checkerboard assay was performed and, with FICI = 0.7 for *E. faecalis* B3/101 and FICI = 2 for *E. faecium* 1/6/63, no interaction between GKK1032B (**PE 19**) and VAN was found (0.5 < FICI ≤ 4, 'no interaction').

CHAPTER IV

MATERIALS AND METHODS

4.1. General Experimental Procedures

The melting points were determined on a Stuart Melting Point Apparatus SMP3 (Bibby Sterilin, Stone, Staffordshire, UK) and are uncorrected.

Optical rotations were measured on an ADP410 Polarimeter (Bellingham + Stanley Ltd., Tunbridge Wells, Kent, UK).

Infrared spectra were recorded in a KBr microplate in an FTIR spectrometer Nicolet iS10 from Thermo Scientific (Waltham, MA, USA) with a Smart OMNI-Transmission accessory (Software 188 OMNIC 8.3, Thermo Scientific, Waltham, MA, USA).

^{1}H and ^{13}C NMR spectra were recorded at ambient temperature on a Bruker AMC instrument (Bruker Biosciences Corporation, Billerica, MA, USA) operating at 300 or 500 and 75 or 125 MHz, respectively.

High resolution mass spectra were measured with a Waters Xevo QToF mass spectrometer (Waters Corporations, Milford, MA, USA) coupled to a Waters Aquity UPLC system.

A Merck (Darmstadt, Germany) silica gel GF_{254} was used for preparative TLC, and a Merck Si gel 60 (0.2–0.5 mm) and SephadexTM LH-20 were used for column chromatography.

The organic solvents (acetone, chloroform, ethyl acetate, methanol, petroleum ether 40-60 °C) were purchased from Merck and Fischer with analytical reagent grade. Solvents were evaporated at reduced pressure, using Büchi Heating Bath B-49, Büchi Ratavapor R-210, Büchi Vacuum Module V-801 EasyVac and Vacuum Pump V-700.

4.2. Isolation and Identification of the Biological Materials

4.2.1. *Neosartorya tsunodae* KUFC 9213

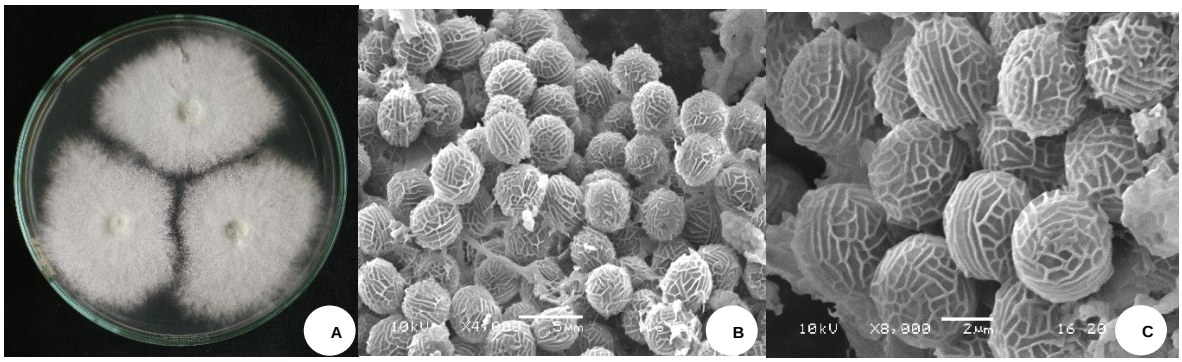

Figure 165. *Neosartorya tsunodae* KUFC 9213**,** Colony on MEA, 7 days, 28ºC (A), and SEM of ascospores (B, C)

The fungus was isolated from the marine sponge *Aka coralliphaga*, collected at the coral reef of Similan Islands, Phang Nga Provice (altitude 8º39’5.39” N 97º38’16.19” E), in April 2010. The sponge sample was washed with 0.06% sodium hypochlorite solution for 1 minute, followed by sterilized seawater three times and dried on sterile filter papers under aseptic conditions. The sponge was cut into small pieces (5 x 5 mm) and placed on Petri dish plates containing 15 mL malt extract agar (MEA) medium containing 70% seawater, and incubated at 28 ºC for 5–7 days. Hyphal tips emerged from sponge pieces were individually transferred onto MEA slant.

The fungus stain **KUFC 9213** was identified to species level, based on morphological characteristics such as colony growth rate and growth pattern on standard media, namely Czapek’s agar (CZA), Czapek yeast autolysate agar (CYA), MEA and microscopic characteristics including size, shape, ornamentation of ascospores under light and scanning electron microscopes. The fungi were further identified by molecular techniques using ITS primers. DNA was extracted from young mycelia following a modified Murray and Thompson method (Murray and Thompson,

1980). Primer pairs ITS1 and ITS4 (White *et. al*., 1990) were used for ITS gene amplification. PCR reactions were conducted on Thermal Cycler and the amplification process consisted of initial denaturation at 95 ^{o}C for 5 minute, 34 cycles at 95 ^{o}C for 1 min (denaturation), at 55 ^{o}C for 1 minute (annealing) and at 72 ^{o}C for 1.5 minute (extension), followed by final extension at 72 ^{o}C for 10 minutes. PCR products were examined by Agarose gel electrophoresis (1% agarose with 1xTBE buffer) and visualized under UV light after staining with ethidium bromide. DNA sequencing analyses were sequenced using dideoxyribonucleotide chain termination method (Sanger *et. at*., 1977) by Macrogen Inc. (Seoul, Korea). The DNA sequences were edited using FinchTV software and submitted into BLAST program for alignment and compared with that of fungal species in the NCBI database (http://www.ncbi.nlm.nih.gov/). The strain KUFC 9213 was identified as *Neosartorya tsunodae* Yaguchi, Abliz, and its ITS gene sequences was deposited in GenBank with accession numbers KT201524. The pure cultures were maintained at Department of Plant Pathology, Faculty of Agriculture, Kasetsart University, Bangkok, Thailand.

4.2.2. *Penicillium erubescens* KUFA 0220

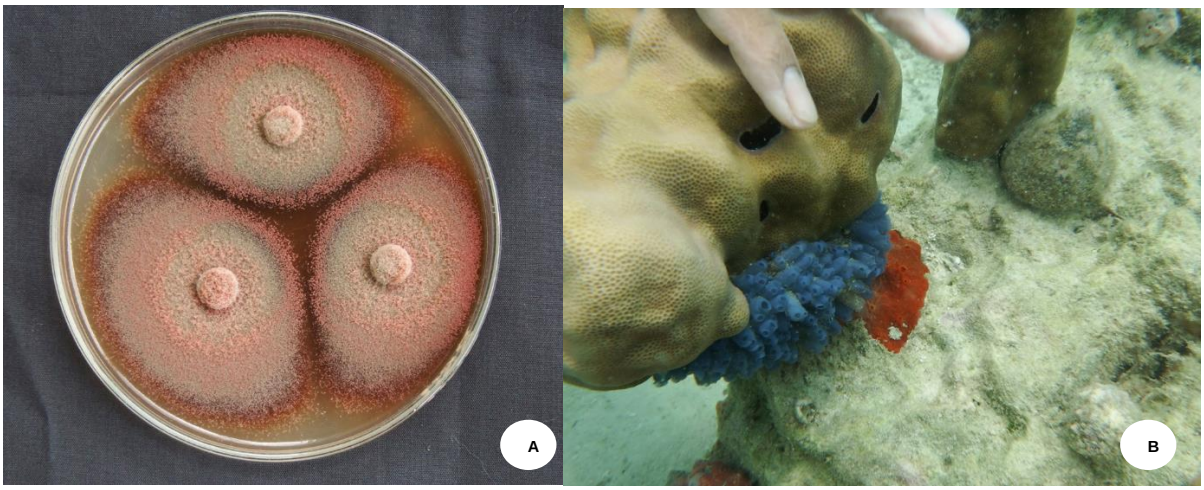

Figure 166. *Penicillium erubescens* KUFA 0220 Colony on MEA, 7 days, 28°C (A), and marine sponge *Neopetrosai* sp. (B)

The fungus was isolated from the marine sponge *Neopetrosia* sp. which was collected, by scuba diving at a depth of 5-10 m, from the coral reef at Samaesan Island (12°34′36.64″ N, 100°56′59.69″ E), Chonburi province, Thailand, in April 2014. The sponge was washed with 0.01% sodium hypochlorite solution for 1 minute, followed by sterilized seawater three times, and then dried on sterile filter paper under sterile aseptic condition. The sponge was cut into small pieces (5 mm × 5 mm) and placed on Petri dish plates containing 15 mL potato dextrose agar (PDA) medium mixed with 300 mg/L of streptomycin sulfate, and incubated at 28 °C for 7 days. The hyphal tips emerging from sponge pieces were individually transferred onto PDA slants.

The fungal strain KUFA0220 was identified as *Penicillium erubescens*, based on morphological characteristics such as colony growth rate and growth pattern on standard media, namely Czapek's agar, Czapek yeast autolysate agar, and malt extract agar. Microscopic characteristics including size, shape and ornamentation of conidiophores and spores were examined under a light microscope. This identification was confirmed by molecular techniques using ITS primers. DNA was extracted from young mycelia following a modified Murray and Thompson method (Murray and Thompson, 1980). Primer pairs ITS1 and ITS4 (White *et al*., 1990) were used for ITS gene amplification. PCR reactions were conducted on Thermal Cycler and the amplification process consisted of the initial denaturation at 95 °C for 5 minutes, 34 cycles at 95 °C for 1 minute (denaturation), at 55 °C for 1 minute (annealing) and at 72 °C for 1.5 minute (extension), followed by final extension at 72 °C for 10 min. The PCR products were examined by agarose gel electrophoresis (1% agarose with 1 × TBE buffer) and visualized under UV light after staining with ethidium bromide. DNA sequencing analyses were performed using the dideoxyribonucleotide chain termination method (Sanger *et at*., 1977) by Macrogen Inc. (Seoul, Korea). The DNA sequences were edited using the FinchTV software (version, company, city, country) and submitted into the BLAST program for alignment and compared to fungal species in the NCBI database (http://www.ncbi.nlm.nih.gov/). Its gene sequences were deposited in GenBank with accession number KY041867.

The pure cultures were maintained at Department of Plant Pathology, Faculty of Agriculture, Kasetsart University, Bangkok, Thailand.

4.3. Extraction and Isolation of Metabolites

4.3.1. *Neosartorya tsunodae* KUFC 9213

The fungus *N. tsunodae* KUFC 9213 was cultured for 7 days at 28 °C in separate Petri dish plates containing 20 mL of potato dextrose agar medium per dish. Five mycelium plugs (5 mm in diam.) of this fungus were transferred into separate Erlenmeyer flasks (500 mL) containing 200 mL of potato dextrose broth and incubated on a rotary shaker at 120 rpm for 7 days at 28 °C to prepare mycelial suspension. Fifty 1000 mL Erlenmeyer flasks containing 300 g of cooked rice, were autoclaved at 121 °C for 15 minutes, and when they were cooled to room temperature, 20 mL of mycelial suspension of a fungus were inoculated per flask, and incubated at 28 °C for 30 days. Then, 500 mL of ethyl acetate was added to each moldy flask and macerated for one week and then filtered with Whatman No. 1 filter paper. The organic solutions were combined and evaporated under reduced pressure to give 105.0 g. of the crude ethyl acetate extracts of *N. tsunodae* KUFC 9213.

The crude ethyl acetate extract of *N. tsunodae* KUFC 9213 was dissolved in 500 mL of $CHCl_3$, and then washed with H_2O (3 × 500 mL). The organic layers were combined and dried with anhydrous Na_2SO_4, filtered and evaporated under reduced pressure to give 60 g of the crude chloroform extract, which was applied on a column of silica gel (410 g), and eluted with mixtures of petrol-$CHCl_3$, $CHCl_3$-Me_2CO and $CHCl_3$-MeOH , wherein 250 mL fractions were collected as follows: Fractions 1–99 (petrol-$CHCl_3$, 1:1), 100–201 (petrol-$CHCl_3$, 3:7), 202–219 (petrol-$CHCl_3$, 1:9), 220–349 ($CHCl_3$-Me_2CO, 9:1), 350–391 ($CHCl_3$-Me_2CO, 7:3), 392–437 ($CHCl_3$-MeOH, 9:1), 438–455 ($CHCl_3$-MeOH, 7:3) and 456–459 (MeOH).

Fractions 134–196 were combined (2.0 g) and purified by TLC (Silica gel G_{254}, $CHCl_3$-petrol-HCO_2H, 14:5:1) to give 40.5 mg of byssochlamic acid (**NT 3**).

Fractions 226–234 were combined (4.0 g) and applied on a column of silica gel (33 g), and eluted with mixtures of petrol-$CHCl_3$, $CHCl_3$, and $CHCl_3$-Me_2CO, wherein 100 mL sub-fractions were collected as follows: sub-fractions 1–5 (petrol-$CHCl_3$, 7:3),

6–18 (petrol-$CHCl_3$, 3:2), 19–20 (petrol-$CHCl_3$, 1:1), 21–34 (petrol-$CHCl_3$, 3:7), 25–30 (petrol-$CHCl_3$, 9:1), 31–42 ($CHCl_3$) and 43–48 ($CHCl_3$-Me_2CO, 9:1). Sub-fractions 24–30 were combined (211 mg) and crystallized in MeOH to give 64 mg of byssochlamic acid (**NT 3**) and 35 mg of hopan-3β,22 diol (**NT 4**). Sub-fractions 31–42 were combined (174 mg) and crystallized in MeOH to give further 23.4 mg of byssochlamic acid (**NT 3**).

Fractions 235–244 were combined (1.75 g) and applied on a column of silica gel (45 g), and eluted with mixtures of petrol-$CHCl_3$ and $CHCl_3$, wherein 100 mL sub-fractions were collected as follows: sub-fractions 1–9 (petrol-$CHCl_3$, 7:3), 20–32 (petrol-$CHCl_3$, 3:2), 33–45 (petrol-$CHCl_3$, 1:1), 46–60 (petrol-$CHCl_3$, 3:7), 61–112 (petrol-$CHCl_3$, 1:9) and 113–115 ($CHCl_3$). Sub-fractions 1–5 were combined and purified by TLC (Silica gel G_{254}, $CHCl_3$-Me_2CO-HCO_2H, 97:3:0.1) to give 4.6 mg of byssochlamic acid (**NT 3**) and 12.4 mg of chevalone C (**NT 5**). Sub-fractions 6–75 were combined (91 mg) and crystalized in MeOH to give further 15 mg of byssochlamic acid (**NT 3**). Sub-fractions 76–114 were combined (863 mg) and purified by TLC (Silica gel G_{254}, $CHCl_3$-Me_2CO-HCO_2H, 97:3:0.1) to give an additional 15.7 mg of byssochlamic acid (**NT 3**), 22.4 mg of chevalone C (**NT 5**) and 39.3 mg of sartorypyrone B (**NT 6**).

Fractions 245–263 were combined (1.53 g) and applied on a column of silica gel (45 g), and eluted with mixtures of petrol-$CHCl_3$, $CHCl_3$, $CHCl_3$-Me_2CO, and Me_2CO, wherein 100 mL sub-fractions were collected as follows: sub-fractions 1–12 (petrol-$CHCl_3$, 7:3), 13–20 (petrol-$CHCl_3$, 3:2), 21–40 (petrol-$CHCl_3$, 1:1), 41–50 (petrol-$CHCl_3$, 2:3), 51–68 (petrol-$CHCl_3$, 3:7), 69–85 (petrol-$CHCl_3$, 1:4), 86–100 (petrol-$CHCl_3$, 1:9), 101–122 ($CHCl_3$), 123–148 ($CHCl_3$-Me_2CO, 9:1), 149–158 (Me_2CO). Sub-fractions 23–123 were combined (57 mg) and crystalized in MeOH to give 12 mg of byssochlamic acid (**NT 3**) and 7.1 mg of sartorypyrone B (**NT 6**).

Fractions 264–312 were combined (1.12 g) and applied on a column of silica gel (18 g), and eluted with mixtures of petrol-$CHCl_3$ and $CHCl_3$, wherein 100 mL sub-fractions were collected as follows: Sub-fractions 1–17 (petrol-$CHCl_3$, 7:3), 18–48 (petrol-$CHCl_3$, 3:2), 49–72 (petrol-$CHCl_3$, 1:1), 73–76 (petrol-$CHCl_3$, 2:3), 77–90 (petrol-$CHCl_3$, 3:7), 91–100 (petrol-$CHCl_3$, 1:9), 116 ($CHCl_3$). Sub-fractions 16–68

were combined (93 mg) and crystalized in MeOH to give 33 mg of byssochlamic acid (**NT 3**). Sub-fractions 69–115 were combined (711 mg) and purified by TLC (Silica gel G_{254}, $CHCl_3$-Me_2CO-HCO_2H, 4:1:0.01) to give 8.0 mg of helvolic acid (**NT 7**) and 14.1 mg of lumichrome (**NT 8**).

Fractions 313–352 were combined (487 mg) and applied on a Sephadex LH-20 column (10 g) and eluted with MeOH, wherein 20 mL of 42 sub-fractions were collected. Sub-fractions 15–42 were combined (104 mg) and purified by TLC (Silica gel G_{254}, $CHCl_3$-Me_2CO-HCO_2H, 4:1:0.01) to give 10 mg of byssochlamic acid (**NT 3**), 7.8 mg of helvolic acid (**NT 7**), 4.7 mg of lumichrome (**NT 8**), 10.6 mg of **(**3β,5α,22*E*)-3,5-dihydroxyergosta-7,22-dien-6-one (**NT 2**) and 21.6 mg of chromanol (**NT 1**).

Fractions 400–420 were combined (1.47 g) and applied on a Sephadex LH-20 column (20 g) and eluted with MeOH, wherein 20 mL of 42 sub-fractions were collected. Sub-fractions 23–42 were combined (306 mg) and purified by TLC (Silica gel G_{254}, $CHCl_3$-Me_2CO-HCO_2H, 9:1:0.01) to give to 25.4 mg of byssochlamic acid (**NT 3**) and 5.3 mg of harmane (**NT 9**).

Fractions 421–440 were combined (1.33 g) and applied on a Sephadex LH-20 column (20 g) and eluted with MeOH, wherein 20 mL of 33 sub-fractions were collected. Sub-fractions 18–33 were combined (126 mg) and crystalized in MeOH to give additional 42.2 mg of harmane (**NT 9**).

4.3.2. *Penicillium erubescens* KUFA 0220

The fungus was cultured for one week at 28 °C in five Petri dishes (i.d. 90 mm) containing 20 mL of potato dextrose agar per dish. The mycelial plugs (5 mm in diameter) were transferred to two 500 mL Erlenmeyer flasks containing 200 mL of potato dextrose broth, and incubated on a rotary shaker at 120 rpm at 28 °C for one week. Fifty 1000 mL Erlenmeyer flasks, each containing 300 g of cooked rice, were autoclaved at 121 °C for 15 min. After cooling to room temperature, 20 mL of a mycelial suspension of the fungus was inoculated per flask and incubated at 28 °C for 30 days, after which 500 mL of ethyl acetate was added to each flask of the moldy rice and

macerated for 7 days, and then filtered with Whatman No. 1 filter paper (GE Healthcare UK Limited, Buckinghamshire, UK). The ethyl acetate solutions were combined and concentrated under reduced pressure to yield 160 g of crude ethyl acetate extract which was dissolved in 500 mL of $CHCl_3$ and then filtered with Whatman No. 1 filter paper. The chloroform solution was then washed with H_2O (3 × 500 mL) and dried with anhydrous Na_2SO_4, filtered and evaporated under reduced pressure to give 112 g of the crude chloroform extract which was applied on a column of silica gel (450 g), and eluted with mixtures of petrol-$CHCl_3$ and $CHCl_3$-Me_2CO, wherein 250 mL fractions were collected as follow: Fractions 1–147 (petrol-$CHCl_3$, 1:1), 148–223 (petrol-$CHCl_3$, 3:7), 224–230 (petrol-$CHCl_3$, 1:9), 231–238 ($CHCl_3$), 239–452 ($CHCl_3$-Me_2CO, 9:1), 453–512 ($CHCl_3$-Me_2CO, 7:3), 512–546 (Me_2CO).

Fractions 75–117 were combined (1.18 g) and applied on a column of silica gel (35 g) and eluted with mixtures of petrol-$CHCl_3$ and $CHCl_3$-Me_2O, wherein 100 mL sub-fractions were collected as follow: sub-fractions 1–20 (petrol), 21–33 (petrol-$CHCl_3$, 9:1), 34–48 (petrol-$CHCl_3$, 7:3), 49–59 (petrol-$CHCl_3$, 1:9), 60–65 (petrol-$CHCl_3$), 66–80 ($CHCl_3$-Me_2CO, 9:1), 81–106 $CHCl_3$-Me_2CO, 7:3), 107–120 (Me_2CO). Sub-fractions 35–46 were combined (103.0 mg) and purified by TLC (Silica gel G_{254}, $CHCl_3$: Me_2CO: HCO_2H, 97:3:0.01) to give 50.2 mg of β-sitostenone (**PE 1**).

Fractions 238–245 were combined (1.75 g) and precipitated in MeOH to give 202.1 mg of GKK1032B (**PE 19**).

Fractions 246–251 were combined (2.67 g) and precipitated in MeOH to give 472.2 mg of ergosterol 5,8-endoperoxide (**PE 2**).

Fractions 252–286 were combined (493.0 mg) and crystallized in MeOH to give further 367.1 mg of ergosterol 5,8-endoperoxide (**PE 2**).

Fractions 287–299 were combined (580.4 mg) and crystallized in a mixture of $CHCl_3$-Me_2CO to give 78 mg of anhydrofulvic acid (**PE 8**), and the mother liquor was combined with sub-fractions 300–319 (837.2 mg) and precipitated in Me_2CO to give 10.0 mg of 12-methoxycitromycin (**PE 4**). The mother liquor (855 mg) was applied on a column chromatography of silica gal (30 g) and eluted with petrol-$CHCl_3$, $CHCl_3$,

$CHCl_3$-Me_2CO, and MeOH, wherein 100 mL fractions were collected as follows: Sub-fractions 1-11 (petrol-$CHCl_3$, 1:1), 12–28 (petrol-$CHCl_3$, 3:7), 29-86 (petrol-$CHCl_3$, 1:9), 87-126 ($CHCl_3$), 127-135 ($CHCl_3$-Me_2CO, 9:1), 136-138 (Me_2CO). Sub-fractions 100-126 were combined (71.3 mg) and purified by TLC (Silica gel G_{254}, $CHCl_3$: Me_2CO: HCO_2H, 9:1:0.01) to give further 10.0 mg of 12-methoxycitromycin (**PE 4**). Sub-fraction 127 (48 mg) was crystallized in a mixture of $CHCl_3$-Me_2CO to give further 30.0 mg of anhydrofulvic acid (**PE 8**).

Fractions 343–366 were combined (1.46 g) and crystallized in MeOH to give 98.3 mg of erubescenschromone A (**PE 14**), and the mother liquor was combined with fractions 367-386 (1.77 g) and recrystallized in MeOH to give further 8.0 mg of citromycin (**PE 3**). The mother liquor of the combined fractions 343-386 (1.36 g) was applied on a column chromatography of silica gel (40 g), and eluted with petrol-$CHCl_3$, $CHCl_3$, $CHCl_3$-Me_2CO and Me_2CO, wherein 100 mL fractions were collected as follows, sub-fractions 1–50 (petrol-$CHCl_3$, 1:1), 51–88 (petrol-$CHCl_3$, 3:7), 89–110 (petrol-$CHCl_3$; 1:9), 111–139 ($CHCl_3$), 140–197 ($CHCl_3$-Me_2CO, 9:1), 198–201 ($CHCl_3$-Me_2CO, 7:3), 202–215 (Me_2CO). sub-fractions 140–143 were combined (361.0 mg) and applied on a Sephadex LH-20 column (10 g), and eluted with MeOH to give 12.0 mg of citromycin (**PE 3**) and 10.1 mg of secalonic acid A (**PE 20**). Sub-fractions 147-151 were combined (221.0 mg) and applied on a Sephadex LH-20 column (10 g) and eluted with MeOH to give 10.0 mg of a mixture of myxotrichin C (**PE 9**) (major component) and penialidin G (**PE 10**). Sub-fractions 189-201 were combined (72.3 mg) and purified by TLC (Silica gel G_{254}, $CHCl_3$:MeOH:HCO_2H, 95: 5: 0.1) to give 7.1 mg of penialidin F (**PE 12**).

Fractions 387-444 were combined (2.73 g) and applied on a column of Sephadex LH-20 (20 g) and eluted with MeOH, wherein 20 mL of 30 fractions were collected. Sub-fractions 11-30 were combined (472.3 mg) and crystallized in Me_2CO to give further 19 mg of secalonic acid A (**PE 20**). The mother liquor was applied on a Sephadex LH-20 column (20 g) and eluted with a 1:1 mixture of MeOH-$CHCl_3$ to give 15 mg of SPF-3059-30 (**PE 17**).

Fractions 517-529 were combined (1.40 g) and crystallized in MeOH to give 26.6 mg of 12-methoxycitromycetin (**PE 7**), and the mother liquor was combined with

fractions 445-516 (6.90 g) and applied on a column of Sephadex LH-20 column (30 g) and eluted with MeOH, wherein 20 mL fractions were collected. Sub-fractions 21–30 were combined (106.2 mg) and purified by TLC (Silica gel G_{254}, $CHCl_3$: MeOH: HCO_2H, 9:1:0.01) to give 10 mg of penialidin F (**PE 12**) and 12 mg of erubescenschromone B (**PE 16**). Sub-fractions 31–60 were combined (5.90 g) and applied on a column chromatography of silica gal (110 g) and eluted with petrol-$CHCl_3$, $CHCl_3$, $CHCl_3$-Me_2CO and Me_2CO, wherein 100 mL fractions were collected as follows, Sub-fractions 1-26 (petrol-$CHCl_3$, 1:1), 27-56 (petrol-$CHCl_3$, 3:7), 57-98 (petrol-$CHCl_3$, 1:9), 99-200 ($CHCl_3$), 201-297 ($CHCl_3$-Me_2CO, 9:1), 298-320 ($CHCl_3$-Me_2CO, 7:3), 321-332 ($CHCl_3$-Me_2CO, 1:9), 333-358 (Me_2CO). Sub-fractions 156-184 were combined (112.0 mg) and crystallized in Me_2CO to give further 26.1 mg of secalonic acid A (**PE 20**). Sub-fractions 185-251 were combine (658 mg) and applied on a Sephadex LH-20 column (20 g) and eluted with MeOH, wherein 2 mL fractions were collected. Fractions 25-30 were combined (40.0 mg) and purified by TLC (Silica gel G_{254}, $CHCl_3$: MeOH: HCO_2H, 9:1:0.01) to give erubescensoic acid (**PE 13**) (7 mg). Sub-fractions 252–294 were combined (464.9 mg) and applied on a Sephadex LH-20 column (20 g) and eluted with MeOH to give 13.0 mg of 1-Hydroxy-12-methoxycitromycin (**PE 5**). Sub-fractions 295–344 were combined (3.0 g), applied on a Sephadex LH-20 column (20 g) and eluted with a 1:1 mixture of MeOH-$CHCl_3$, wherein 20 mL fractions were collected. Sub-fractions 1-30 were combined (217 mg) and re-applied on another Sephadex LH-20 column (20 g) and eluted with MeOH, wherein 30 sub-fractions of 2 mL were collected. Sub-fractions 8-26 were combined to give SPF-3059-26 (**PE 18**) (7.2 mg). Sub-fractions 31–72 were combined (262.9 mg) and purified by TLC (Silica gel G_{254}, $CHCl_3$:MeOH:HCO_2H, 9:1:0.01) to give 12.1 mg myxotrichin D (**PE 6**). Sub-fractions 73–96 were combined (90.6 mg) and purified by TLC (Silica gel G_{254}, $CHCl_3$:MeOH:HCO_2H, 9:1:0.01) to give 10.6 mg of penialidin D (**PE 11**). Sub-fractions 97–115 were combined (644.8 mg) and precipitated in MeOH to give 12 mg of a mixture of myxotrichin C (**PE 9**) and penialidin G (**PE 10**) and the mother liquor was dried (619.7 mg) and applied on a Sephadex LH-20 column (10 g) and eluted with a 1:1 mixture of $CHCl_3$:MeOH, wherein 70 sub-fractions (2 mL each) were collected. Sub-fractions 25–32 were combined (40.8 mg) and precipitated in MeOH to give 10 mg of 12-methoxycitromycetin (**PE 7**). Sub-fractions 33-45 were

combined (70.1 mg) and purified by TLC (Silica gel G_{254}, $CHCl_3$:MeOH:HCO_2H, 9:1:0.01) to give 6 mg of 7-hydroxy-6-methoxy-4-oxo-3-[(1E)-3-oxobut-1-en-1-yl]-4H-chromene-5-carboxylic acid (**PE 15**). Sub-fractions 46–56 were combined (65.3 mg) and precipitated in MeOH to give further 7 mg of 7-hydroxy-6-methoxy-4-oxo-3-[(1E)-3-oxobut-1-en-1-yl]-4H-chromene-5-carboxylic acid (**PE 15)**.

4.4. Physical Characteristics and Spectroscopic data

(1*R*, 8*S*, 9*R*)-1,9-Dihydroxy-8-(2-hydroxypropan-2-yl)-4-methoxy-5-methyl-1,7,8,9-tetrahydro-3*H*-furo[3,4-f]chromen-3-one (chromanol) (**NT 1**)**:** white crystal; (mp 223–224°C). $[\alpha]_D^{20}$ –80 (*c* 0.05, $CHCl_3$); IR (KBr) u_{max} 3467, 3434, 3018, 2969, 1743, 1597, 1507, 1262 cm^{-1}. For ^1H and ^{13}C spectroscopic data (300 and 75 MHz, DMSO-d_6), (see Table 3), (+)-HRESIMS *m/z* 347.1111 $[M+Na]^+$ (calculated for $C_{16}H_{20}O_7Na$, 341.1107).

(3β,5α,22*E*)-3,5-Dihydroxyergosta-7,22-dien-6-one (**NT 2**): white amorphous solid, $[\alpha]_D^{20}$ +60 (*c* 0.05, $CHCl_3$). For ^1H and ^{13}C spectroscopic data (500 and 125 MHz, $CDCl_3$,), (see Table 4), (+)-HRESIMS *m/z* 429.3388 $[M+H]^+$ (calculated for $C_{28}H_{45}O_3$, 429.3369).

Byssochlamic acid (NT 3): white solid (mp, 171-172 ^oC). For ^1H and ^{13}C spectroscopic data (300 and 75 MHz, $CDCl_3$) (see Table 5), (+)-HRESIMS *m/z* 333.1326 $[M+H]^+$ (calculated for $C_{18}H_{21}O_6$, 333.1338).

Hopan-3β,22-diol (NT 4): white crystal (mp, 176-177 ^oC). For ^1H and ^{13}C spectroscopic data (500 and 125 MHz, $CDCl_3$) (see Table 6).

Chevalone C (NT 5): white solid (mp 198-201 °C). For ^1H and ^{13}C spectroscopic data (300 and 75 MHz, DMSO-d_6) (see Table 7).

Sartorypyrone B (NT 6); yellow viscous mass, $[\alpha]_D^{20}$ -73.0 (*c* 0.05, $CHCl_3$). For ^1H and ^{13}C spectroscopic data (300 and 75 MHz, $CDCl_3$) (see Table 8), (+)-HRESIMS *m/z* 515.3018 $[M+H]^+$ (calculated for $C_{30}H_{43}O_7$, 515.3009).

Helvolic acid (NT 7); white solid (mp, 209-210 ºC). For ^{1}H and ^{13}C spectroscopic data (300 and 75 MHz, $CDCl_3$) (see Table 9).

Lumichrome (NT 8): yellow amorphous powder. For the ^{1}H and ^{13}C spectroscopic data (300 and 75 MHz, DMSO-*d*$_6$) (see Table 10), (+)-HRESIMS *m/z* 243.0888 $[M+H]^+$ (calculated for $C_{12}H_{11}N_4O_2$, 243.0882).

Harmane (NT 9): amorphous powder. For ^{1}H and ^{13}C spectroscopic data (500 and 125 MHz, DMSO-*d*$_6$) (see Table 11), (+)-HRESIMS *m/z* 183.0922 $[M+H]^+$ (calculated for $C_{12}H_{11}N_2$, 183.0922).

***β*-sitostenone (PE 1):** white solid (mp, 92-95 ºC). For ^{1}H and ^{13}C spectroscopic data (500 and 125 MHz, $CDCl_3$,) (see Table 12), (+)-HRESIMS *m/z* 413.3778 $[M+H]^+$ (calculated for $C_{29}H_{49}O$, 413.3783).

Ergosterol 5,8-endoperoxide (PE 2): white solid (180-182 ºC). For ^{1}H and ^{13}C spectroscopic data (300 and 75 MHz, $CDCl_3$) (see Table 13).

Citromycin (PE 3): viscous liquid. For ^{1}H and ^{13}C spectroscopic data (300 and 75 MHz, DMSO-*d*$_6$) (see Table 14).

12-methoxycitromycin (PE 4): yellow oil. For ^{1}H and ^{13}C spectroscopic data (300 and 75 MHz, DMSO-*d*$_6$) (see Table 15), (+)-HRESIMs *m/z* 283.0599 $[M+Na]^+$ (calculated for $C_{14}H_{12}O_5Na$, 283.0582).

1-hydroxy-12-methoxycitromycin (PE 5): white solid, (mp 232–233 °C), IR (KBr) ν_{max} 3420 (br), 2921, 1662, 1627, 1594, 1555, 1517, 1453, 1270 cm^{-1}. For ^{1}H and ^{13}C spectroscopic data (500 and 125 MHz, DMSO-*d*$_6$), (see Table 16), (+)-HRESIMS *m/z* 277.0715 $[M+H]^+$ (calculated for $C_{14}H_{13}O_6$, 277.0712).

Myxotrichin D (PE 6): pale yellow viscous oil. For ^{1}H and ^{13}C spectroscopic data (500 and 125 MHz, DMSO-*d*$_6$)**,** (see Table 17), (+)-HRESIMS *m/z* 275.0561 $[M+H]^+$ (calculated for $C_{14}H_{11}O_6$, 275.0556).

12-methoxycitromycetin (PE 7): pale yellow oil**.** For ^{1}H and ^{13}C spectroscopic data (300 and 75 MHz, DMSO-*d*$_6$) (see Table 18), (+)-HRESIMS *m/z* 305.0668 $[M+H]^+$ (calculated for $C_{15}H_{13}O_7$, 305.0661).

Anhydrofulvic acid (PE 8): white crystals (mp, 235-237 ^{o}C)**.** For ^{1}H and ^{13}C spectroscopic data (300 and 75 MHz, DMSO-*d*$_6$) (see Table 19), (+)-HRESIMS *m/z* 313.0359 $[M+Na]^+$ (calculated for $C_{14}H_{10}O_7Na$, 313.0324).

Myxotrichin C (PE 9): mixture pale yellow oil. For ^{1}H and ^{13}C spectroscopic data (500 and 125 MHz, DMSO-*d*$_6$) (seeTable 20), (+)-HRESIMS *m/z* 247.0610 $[M+H]^+$ (calculated for $C_{13}H_{11}O_5$, 247.0606).

Penialidin G (PE 10): mixture pale yellow oil. For ^{1}H and ^{13}C spectroscopic data (500 and 125 MHz, DMSO-*d*$_6$) (see Table 21), (+)-HRESIMS *m/z* 279.0878 $[M+H]^+$ (calculated for $C_{14}H_{15}O_6$, 279.0869).

Penialidin D (PE 11): pale yellow oil**.** For ^{1}H and ^{13}C spectroscopic data (500 and 125 MHz, DMSO-*d*$_6$) (see Table 22), (+) HRESIMS *m/z* 305.0666 $[M+H]^+$ (calculated for $C_{15}H_{13}O_7$, 305.0661)**.**

Penialidin F (PE 12): pale yellow viscous oil, For ^{1}H and ^{13}C spectroscopic data (300 and 75 MHz, DMSO-*d*$_6$) (see Table 23), (+)-HRESIMS *m/z* 265.0719 $[M+H]^+$ (calculated for $C_{13}H_{13}O_6$, 265. 0712)**.**

Erubescensoic acid (PE 13): white crystal (mp 218-220 ^{o}C), $[\alpha]^{25}_{D}$: -100.0 (*c* 0.04 g/mL, MeOH), IR (KBr) v_{max} 3445, 2921, 1733, 1716, 1698, 1683, 1652, 1635, 1558, 1540, 1506, 1472 cm^{-1}. For ^{1}H and ^{13}C spectroscopic data (500 and 125 MHz, DMSO-*d*$_6$) (see Table 24), (+)-HRESIMS *m/z* 277.0719 $[M+H]^+$ (calculated for $C_{14}H_{13}O_6$, 277.0712).

Erubescenschromone A (PE 14): white crystal (mp 150–152 °C), $[\alpha]^{23}_{D}$ −40.0 (*c* 0.05, $CDCl_3$); IR (KBr) v_{max} 3491, 3376, 3108, 2969, 1679, 1661, 1648, 1578, 1523, 1479, 1276 cm^{-1}. For ^{1}H and ^{13}C spectroscopic data (500 and 125 MHz, DMSO-*d*$_6$), (see Table 25), (+)-HRESIMS *m/z* 263.0596 $[M+H]^+$ (calculated for $C_{13}H_{11}O_6$, 263.0556).

7-hydroxy-6-methoxy-4-oxo-3-[(1E)-3-oxobut-1-en-1-yl]-4H-chromene-5-carboxylic acid (PE 15): white crystal (mp 276–277 °C), IR (KBr) v_{max} 3446, 2922, 1719, 1646, 1618, 1560, 1541, 1521, 1276 cm^{-1}. For ^{1}H and ^{13}C spectroscopic data (500 and 125 MHz, DMSO-*d*$_6$), (see Table 26), (+)-HRESIMS *m/z* 305.0667 $[M+H]^+$ (calculated for $C_{15}H_{13}O_7$, 305.0661).

Erubescenschromone B (PE 16): yellowish oil, $[\alpha]_D^{23}$ −150.0 (*c* 0.04, MeOH), IR (KBr) ν_{max} 3443 (br), 2922, 1731, 1715, 1697, 1648, 1634, 1556, 1540, 1506, 1261 cm^{-1}. For ^1H and ^{13}C spectroscopic data (500 and 125 MHz, DMSO-d_6), (see Table 27), (+)-HRESIMS *m/z* 509.1085 $[M+H]^+$ (calculated for $C_{26}H_{21}O_{11}$, 509.1084).

SPF-3059-30 (PE 17): yellowish oil, IR (KBr) ν_{max} 3491, 3376, 3108, 2969, 1679, 1661, 1648, 1578, 1523, 1479, 1276 cm^{-1}; For ^1H and ^{13}C spectroscopic data (500 and 125 MHz, DMSO-d_6), (see Table 28), (+)-HRESIMS *m/z* 491.0974 $[M+H]^+$ (calculated for $C_{26}H_{19}O_{10}$, 491.0978).

SPF-3059-26 (PE 18): Pale yellow viscous oil, $[\alpha]^{25}_D$ +266 (*c* 0.03 g/mL, MeOH), IR (KBr) ν_{max} 3445, 2958, 2922 1650, 1605, 1262 cm^{-1}. For ^1H and ^{13}C spectroscopic data (500 and 125 MHz, DMSO-d_6) (see Table 29), (+)-HRESIMS *m/z* 489.0818 $[M+H]^+$ (calculated for $C_{26}H_{17}O_{10}$, 489.0822).

GKK1032B (PE 19): white crystal (mp, 174-175 ºC). For ^1H and ^{13}C spectroscopic data (500 and 125 MHz, $CDCl_3$), (see Table 30), (+)-HRESIMS *m/z* 502.2958 $[M+H]^+$ (calculated for $C_{32}H_{40}NO_4$, 502.2957).

Secalonic acid A (PE 20): yellow crystal (mp. 269-270 °C). For ^1H and ^{13}C spectroscopic data (500 and 125 MHz, $CHCl_3$) (see Table 31), (+)-HRESIMS *m/z* 639.1718 $[M+H]^+$, (calculated for $C_{32}H_{31}O_{14}$, 639.1714).

4.5. X-Ray Crystallographic Analysis

4.5.1. X-ray crystal structure of (1*R*, 8*S*, 9*R*)-1,9-Dihydroxy-8-(2-hydroxypropan-2-yl)-4-methoxy-5-methyl-1,7,8,9-tetrahydro-3*H*-furo[3,4-f]chromen-3-one (NT 1)

Crystals were triclinic, space group P1, cell volume 773.78 (18) $Å^3$ and unit cell dimensions *a* = 9.1295 (12) Å, *b* = 9.2537 (14) Å and *c* = 10.4317(12) Å and angles α = 94.622 (11), β = 104.310 (11) and γ = 112.486 (13) (uncertainties in parentheses). The refinement converged to *R* (all data) = 14.12% and wR_2 (all data) = 29.88%. Diffraction data were collected at 291 K. CCDC 1579876.

4.5.2. X-Ray crystal structure of erubescensoic acid (PE 13)

A single crystal was mounted on a cryoloop using paratone. X-ray diffraction data was collected at 288 K with a Gemini PX Ultra equipped with CuK_{α} radiation (λ = 1.54184 Å). The crystal was orthorhombic, space group $P2_12_12_1$, cell volume 1413.65 (12) $Å^3$ and unit cell dimensions *a* = 6.7568 (4) Å, *b* = 13.0791 (5) Å and *c* = 15.9964 (6) Å (uncertainties in parentheses). The structure was solved by direct methods using SHELXS-97 and refined with SHELXL-97 (Sheldrick, 2008). One molecule of the compound and two water molecules were found in the asymmetric unit. Carbon and oxygen atoms were refined anisotropically. Hydrogen atoms either directly found from difference Fourier maps and were refined freely with isotropic displacement parameters or placed at their idealized positions using appropriate HFIX instructions in SHELXL and included in subsequent refinement cycles. Hydrogens of one of the water molecules were not observed in the difference Fourier maps. The refinement converged to *R* (all data) = 10.43% and *wR2* (all data) = 16.95%. Full details of the data collection and refinement and tables of atomic coordinates, bond lengths and angles, and torsion angles have been deposited with the Cambridge Crystallographic Data Centre (CCDC 1870933).

4.5.3. X-ray crystal structure of erubescenschromone A (PE 14)

A single crystal was mounted on a cryoloop using paratone. X-ray diffraction data were collected at 290 K with a Gemini PX Ultra equipped with CuK_{α} radiation (λ = 1.54184 Å). The crystal was monoclinic, space group $P2_1/n$, cell volume 1245.43 (7) $Å^3$ and unit cell dimensions *a* = 12.3445 (4) Å, *b* = 7.8088 (3) Å and *c* = 12.9397 (5) Å and angle β = 93.165 (3) (uncertainties in parentheses). There are two molecules in the asymmetric unit, one erubescenschromone A molecule and one water molecule, and the calculated crystal density is 1.495 g/cm^{-3}. The structure was solved by direct methods using SHELXS-97 and refined with SHELXL-97 (Sheldrick, 2008). Carbon and oxygen atoms were refined anisotropically. Hydrogen atoms were directly found from difference Fourier maps and were refined freely with isotropic displacement parameters. The refinement converged to *R* (all data) = 6.32% and *wR2* (all data) =

11.26%. Full details of the data collection and refinement and tables of atomic coordinates, bond lengths and angles, and torsion angles have been deposited with the Cambridge Crystallographic Data Centre (CCDC 1856735).

4.5.4. X-ray crystal structure of 7-hydroxy-6-methoxy-4-oxo-3-[(1*E*)-3-oxobut-1-en-1-yl]-4*H*-chromene-5-carboxylic acid (PE 15)

A single crystal was mounted on a cryoloop using paratone. X-ray diffraction data were collected at 290 K with a Gemini PX Ultra equipped with CuK_{α} radiation (λ = 1.54184 Å). The crystal was monoclinic, space group $P2_1/c$, cell volume 1324.77 (16) $Å^3$ and unit cell dimensions *a* = 11.6888(8) Å, *b* = 7.7695 (4) Å and *c* = 14.9560 (12) Å and angle β = 102.748 (7) (uncertainties in parentheses). The calculated crystal density was 1.525 $g \cdot cm^{-3}$. The structure was solved by direct methods using SHELXS-97 and refined with SHELXL-97 (Sheldrick, 2008). Carbon and oxygen atoms were refined anisotropically. Hydrogen atoms from one of the methyl groups were placed at their idealized positions using appropriate HFIX instructions in SHELXL and included in subsequent refinement cycles, all the others were directly found from difference Fourier maps and were refined freely with isotropic displacement parameters. The refinement converged to *R* (all data) = 12.24% and *wR2* (all data) = 14.96%. Full details of the data collection and refinement and tables of atomic coordinates, bond lengths and angles, and torsion angles have been deposited with the Cambridge Crystallographic Data Centre (CCDC 1859409).

4.6. Electronic Circular Dichroism (ECD)

4.6.1. Electronic circular dichroism (ECD) of (3*β*,5*α*,22*E*), 3,5-dihydroxyergosta-7,22-dien-6-one (NT 2)

The ECD spectrum of (3β,5α,22E), 3,5-dihydroxyergosta-7,22-dien-6-one (**NT 2**) (1.6 mM in methanol) was obtained in a Jasco J-815 CD spectropolarimeter with a

0.01 mm cuvette and eight accumulations. Dihedral driver and MMFF95 minimizations were done in Chem3D Ultra (Perkin-Elmer Inc., Waltham, MA, USA). All DFT minimizations and ECD spectral calculations (TD-DFT) were performed with Gaussian 09W (Gaussian Inc., Wallingford, CT, USA) using the APFD/6-311+G (2d, p) method/basis set (Austin *et al*., 2012) with IEFPCM solvation model of methanol. The simulated spectral lines were obtained by summation of Gaussian curves, as recommended in Stephens and Harada (Stephens and Harada, 2010). A line broadening of 0.4 eV was applied to all transitions to generate the calculated spectral lines.

4.6.2. Electronic circular dichroism (ECD) of penialidinn F (PE 12) and erubescenschromone B (PE 16)

The ECD spectra of penialidinn F (**PE 12**) and erubescenschromone B (**PE 16**) (1.5 mM in methanol) were obtained in a Jasco J-815 CD spectropolarimeter (Jasco, Mary's Court, Easton, MD, USA) with a 0.01 mm cell (40 accumulations for **PE 12**). The dihedral driver and MMFF95 minimizations were done in Chem3D Ultra (Perkin-Elmer Inc., Waltham, MA, USA). All DFT minimizations with model chemistries APFD/6-31G and APFD/6-311+G(2d,p) (Austin *et al*., 2012) as well as ECD spectral calculations (TD-APFD) were performed with Gaussian 16W (Gaussian Inc., Wallingford, CT, USA) using an IEFPCM solvation model for methanol. The simulated spectral lines for **PE 12** and **PE 16** were obtained by summation of Gaussian curves, as recommended in Reference (Stephens and Harada, 2010). A line broadening of 0.3 eV was applied to all transitions to generate the calculated line.

4.7. Antibacterial Activity Bioassays

4.7.1. Bacterial Strains and Testing Conditions

The multidrug-resistant (MDR) and reference strains were used in this study. The Gram-positive bacteria including, *Staphylococcus aureus* ATCC 29213,

Enterococcus faecalis ATCC 29212, *E. faecium* ATCC 19434, a clinical isolate *S. aureus* 40/61/24, methicillin-resistant (MRSA) *S. aureus* 66/1, isolated from public buses (Simões *et al*., 2011), three strains of vancomycin-resistant enterococci (VRE) *E. faecium* 1/6/63, *E. faecalis* A5/102 and *E. faecalis* B3/101, isolated from the river water (Bessa *et al*., 2014). Gram-negative strains included *Escherichia coli* ATCC 25922, *Pseudomonas aeruginosa* ATCC 27853 and the clinical isolate *E. coli* SA/2, an extended-spectrum β-lactamase producer (ESBL). All strains were kept in Trypto-Casein Soy agar (TSA, Biokar Diagnostics, Allone, Beauvais, France) slants, at room temperature, in the dark. Before each assay, all strains were cultured in Mueller-Hinton agar (MH, Biokar Diagnostics, Allone, Beauvais, France) and incubated overnight at 37 °C. Stock solutions of the compounds were prepared in DMSO (Alfa Aesar, Kandel, Germany) and kept at -20 °C before each assay.

4.7.2. Antimicrobial Susceptibility Testing

The antimicrobial activity of the compounds was screened using the Kirby-Bauer method, as recommended by the CLSI (CLSI, 2012): 6 mm blank paper discs (Liofilchem, Roseto degli Abruzzi TE, Italy) were impregnated with 15 µg of each compounds, and the blank paper discs impregnated with DMSO were used as negative control. MH inoculated plates were incubated for 18–20 h at 37 °C. The results were evaluated by measuring the inhibition halos. The minimal inhibitory concentration (MIC) was performed in accordance with the recommendations of the CLSI (CLSI, 2015). Two-fold serial dilutions of the compounds were prepared in cation-adjusted Mueller-Hinton broth (CAMHB-Sigma-Aldrich, St. Louis, MO, USA) within the concentration range 64-2 mg/L, except for 12-methoxycitromycetin (**PE 7**) and erubescenschromone B (**PE 16**), for which the highest concentration tested was 32 mg/L. Colony forming unit counts of the inoculum were conducted in order to determine the initial inoculum size (which should be approximately 5×10^5 CFU/mL). The 96-well U-shaped untreated polystyrene microtiter plates were incubated for 16–20 h at 37 °C and the MIC was determined as the lowest concentration of compound that prevented visible growth. The minimal bactericidal concentration (MBC) was determined by spreading 100 µL of the content of the wells with no visible growth on

the MH plates. The MBC was determined as the lowest concentration of compound that killed 99.9% of the initial inoculum after overnight incubation at 37 °C (CLSI, 1999). These assays were conducted for reference and multidrug-resistant strains.

4.7.3. Biofilm Formation Inhibition Assay

The effect of all compounds on biofilm formation was evaluated using the crystal violet method, as follows: the highest concentration of the tested compound in the MIC assay was added to bacterial suspensions of 1 × 10^6CFU/mL prepared in unsupplemented Tryptone Soy broth (TSB-Biokar Diagnostics, Allone, Beauvais, France) or TSB supplemented with 1% (*p*/*v*) glucose [D-(+)-Glucose anhydrous for molecular biology, PanReac AppliChem, Barcelona, Spain] for Gram-positive strains. When it was possible to determine a MIC, four concentrations of compound were tested, i.e., 2 × MIC, MIC, ½ MIC and ¼ MIC. A control with appropriate concentration of DMSO, as well as a negative control (TSB alone), was included. Sterile 96-well flat-bottomed untreated polystyrene microtiter plates were used. After a 24 h incubation at 37 °C, the biofilms were heat-fixed for 1 h at 60 °C and stained with 0.5% (*v*/*v*) crystal violet (Química Clínica Aplicada, Amposta, Spain) for 5 min. The stain was solubilized with 33% (*v*/*v*) acetic acid (Acetic acid 100%, AppliChem, Darmstadt, Germany) and the biofilm biomass was quantified by measuring the absorbance of each sample at 570 nm in a microplate reader (Thermo Scientific Multiskan® EX, Thermo Fisher Scientific, Waltham, MA, USA) (Stepanović *et al*., 2007 and CLSI, 2017). This assay was performed for reference strains.

4.7.4. Antibiotic Synergy Testing

The potential synergy between the compounds and clinically relevant antimicrobial drugs was screened using the Kirby-Bauer method, as previously described (Buttachon *et al*., 2018). A set of antibiotic discs (Oxoid, Basingstoke, UK) to which the isolates were resistant was selected: cefotaxime (CTX, 30 µg) for *E. coli* SA/2, vancomycin (VAN, 30 µg) for *E. faecalis* B3/101 and *E. faecium* 1/6/63, and oxacillin (OXA, 1 µg) for *S. aureus* 66/1. Antibiotic discs impregnated with 15 µg of

each compound were placed on seeded MH plates. The controls used included antibiotic discs alone, blank paper discs impregnated with 15 µg of each compound alone and blank discs impregnated with DMSO. Plates with CTX were incubated for 18–20 h and plates with VAN and OXA were incubated for 24 h at 37 °C (CLSI, 2017). The potential synergy was considered when the inhibition halo of an antibiotic disc impregnated with the compound was greater than the inhibition halo of the antibiotic or compound-impregnated blank disc alone. The combined effect of the compounds and clinical relevant antimicrobial drugs was also evaluated by determining the antibiotic MIC in the presence of each compound. Briefly, when it was not possible to determine a MIC value for the test compound, the MIC of CTX (Duchefa Biochemie, Haarlem, The Netherlands), VAN (Oxoid, Basingstoke, UK), and OXA (Sigma-Aldrich, St. Louis, MO, USA) for the respective multidrug-resistant strain was determined in the presence of the highest concentration of each compound tested in previous assays. In the case of 12-methoxycitromycetin (**PE 7**) and erubescenschromone B (**PE 16**), the concentration used was 32 mg/L while it was 64 mg/L for the other compounds. The antibiotic tested was serially diluted whereas the concentration of each compound was kept fixed. Antibiotic MICs were determined as described above. For SPF-3059-30 (**PE 17**), it was possible to determine the MIC for *E. faecalis* B3/101 and *E. faecium* 1/6/63, so the checkerboard method was used instead, as previously described (Gomes *et al*., 2014). The fractional inhibitory concentrations (FIC) were calculated as follows: FIC of compound = MIC of compound combined with antibiotic/MIC compound alone, and FIC antibiotic = MIC of antibiotic combined with a compound/MIC of antibiotic alone. The FIC index (FICI) was calculated as the sum of each FIC and interpreted as follows: FICI ≤ 0.5, ‘synergy’; 0.5 < FICI ≤ 4, ‘no interaction’; FICI > 4, ‘antagonism’ (Odds, 2003).

.

CHAPTER VI
CONCLUSIONS

CONCLUSIONS

Marine microorganisms are interesting because of the marine habitat has special characteristics for examples high salt, high pressure, oxygen deficiency and low nutrition. To survive under this environment, deep-sea-derived microorganisms have advanced specific physiological and biochemical pathways to produce secondary metabolites, while these secondary metabolites can be prevented them from predators and play an important part in the complicated signal transduction between different species. The marine environment has been a valuable source of new natural products for drug discovery and has provided many important therapeutic agents. Lead compounds with biomedical potential have been isolated from marine invertebrates, bacteria and fungi, especially marine-derived fungi. Which, marine-derived fungi have proved to be important sources of bioactive secondary metabolites, many of which exhibit cytotoxic and antibiotic activities.

This thesis studies on the secondary metabolites from the marine sponge-associated fungi, *Neosartorya tsunodae* KUFC 9213 and *Penicillium erubescens* KUFA 0220, which were collected from the coral reef of Similan Islands, Phang Nga Provice and the coral reef of Samaesan Island, Chonburi province, Thailand, respectively. The structures of the isolated compounds were established based on extensive 1D and 2D NMR and HRMS spectral analysis as well as by comparison with literature data. The isolated compounds were tested for their antibacterial activity against Gram-positive and Gram-negative reference as well as environmental multidrug-resistant (MDR) strains.

Totally twenty-nine secondary metabolites have been isolated from this study which can be identified from the fungal genera as marine sponge-associated fungus, *N. tsunodae* KUFC 9213, produced nine known compounds including, (1*R*, 8*S*, 9*R*)-1,9-dihydroxy-8-(2-hydroxypropan-2-yl)-4-methoxy-5-methyl-1,7,8,9-tetrahydro-3*H*-furo[3,4-f]chromen-3-one (chromanol) (**NT 1**), (3β,5α,22*E*), 3,5-dihydroxyergosta-7,22-dien-6-one (**NT 2**), byssochlamic acid (**NT 3**), hopan-3β,22-diol (**NT 4**), chevalone C (**NT 5**), sartorypyrone B (**NT 6**), helvolic acid (**NT 7**), lumichrome (**NT 8**) and harmane (**NT 9**).

A previously unreported chromene derivative, namely 1-hydroxy-12-methoxycitromycin (**PE 5**), a new polyketide erubescensoic acid (**PE 13**) and four previously undescribed chromone derivatives, including, penialidin G (**PE 10**), erubescenschromone A (**PE 14**), 7-hydroxy-6-methoxy-4-oxo-3-[(1E)-3-oxobut-1-en-1-yl]-4H-chromene-5-carboxylic acid (**PE 15**) and erubescenschromone B (**PE 16**), together with fourteen known metabolites: β-sitostenone (**PE 1**), ergosterol 5,8-endoperoxide (**PE 2**), citromycin (**PE 3**), 12-methoxycitromycin (**PE 4**), myxotrichin D (**PE 6**), 12-methoxycitromycetin (**PE 7**), anhydrofulvic acid (**PE 8**), myxotrichin C (**PE 9**), penialidin D (**PE 11**), penialidin F (**PE 12**), SPF-3059-30 (**PE 17**), SPF-3059-26 (**PE 18**), GKK1032B (**PE 19**) and secalonic acid A (**PE 20**) were isolated from the ethyl acetate extract of the culture of the marine sponge-associated fungus *P. erubescens* KUFA 0220.

(1*R*, 8*S*, 9*R*)-1,9-dihydroxy-8-(2-hydroxypropan-2-yl)-4-methoxy-5-methyl-1,7,8,9-tetrahydro-3H-furo[3,4-f]chromen-3-one (chromanol) (**NT 1**), (3*β*,5*α*,22*E*), 3,5-dihydroxyergosta-7,22-dien-6-one (**NT 2**), hopan-3β,22-diol (**NT 4**), lumichrome (**NT 8**) and harmane (**NT 9**) were evaluated for antibacterial activity against Gram-positive bacteria (*Staphylococcus aureus* ATCC 29213, *Enterococcus faecalis* ATCC 29212, a clinical isolate *S. aureus* 40/61/24, MRSA *S. aureus* 66/1 isolated from public buses and VRE *E. faecalis* A5/102 and VRE *E. faecalis* B3/101 isolated from river water) and Gram-negative bacteria (*Escherichia coli* ATCC 25922, *Pseudomonas aeruginosa* ATCC 27853, and a clinical isolate ESBL *E. coli* SA/2). None of the tested compounds displayed antibacterial activity at the highest concentrations tested

Furthermore, compounds citromycin (**PE 3**), 12-methoxycitromycin (**PE 4**), 1-hydroxy-12-methoxycitromycin (**PE 5**), myxotrichin D (**PE 6**), 12-methoxycitromycetin (**PE 7**), anhydrofulvic acid (**PE 8**), penialidin D (**PE 11**), penialidin F (**PE 12**), erubescensoic acid (**PE 13**), erubescenschromone A (**PE 14**), 7-hydroxy-6-methoxy-4-oxo-3-[(1E)-3-oxobut-1-en-1-yl]-4H-chromene-5-carboxylic acid (**PE 15**), erubescenschromone B (**PE 16**), SPF-3059-30 (**PE 17**), SPF-3059-26 (**PE 18**), GKK1032B (**PE 19**) and secalonic acid A (**PE 20**) were tested for their antibacterial activity against Gram-negative and Gram-positive bacteria. Only GKK1032B (**PE 19**) exhibited an *in vitro* growth inhibition of Gram-positive bacteria, *E. faecalis* ATCC

29212, vancomycin-resistant *E. faecalis* (VRE) B3/101, *E. faecium* ATCC 19434, *E. faecium* 1/6/63 (VRE) and *S. aureus* ATCC 29213 with minimal inhibitory concentration (MIC) values of 8, 8, 16, 32 and 32 mg/mL, respectively. While, secalonic acid A (**PE 20**) exhibited growth inhibition of methicillin-resistant *Staphyllococus aureus* (MRSA) with minimal inhibitory concentration (MIC) value >64 mg/mL.

Interestingly, screening of potential synergy with antibiotics revealed that SPF-3059-26 (**PE 18**), was able to reduce the CTX MIC of *E. coli* SA/2 (ESBL) for four-fold while it increased the OXA MIC of MRSA *S. aureus* 66/1 by two-fold. Given the capacity of the neuronal regenerative effects of some of these compounds isolated from this fungus, it is desirable to test the extract of this fungus and its constituents for this effect.

Thus, in terms of antibacterial activity, GKK1032B (**PE 19**) is the most promising. Even though no synergy with VAN or OXA was found, this compound alone exhibited an antibiofilm activity against *E. faecalis* and antibacterial activity against the reference *S. aureus*, *E. faecalis*, and *E. faecium* strains. Most importantly, GKK1032B (**PE 19**) showed antibacterial activity against both vancomycin-resistant *E. faecalis* and vancomycin-resistant *E. faecium* strains, a pathogen classified by WHO as high priority for the research and development of new antibiotics (Tacconelli *et al*., 2017).

REFERENCES

Abad, M. J., Bedoya, L.M. and Bermejo, P. (**2011**) Marine Compounds and their Antimicrobial Activities. Science against Microbial Pathogens:Communicating Current. *Research and Technological Advances*, 1293-1306.

Abastabar, M., Mirhendi, H., Hedayati, M.T., Shokohi, T., Matehkolaei, A.R., Mohammadi, R., Badali, H., Moazeni, M., Ghojoghi, A. and Akhtari, J. (**2016**). Genetic and Morphological Diversity of the Genus *Penicillium* From Mazandaran and Tehran Provinces, Iran. *Jundishapur Journal of Microbiology 9* (1), e28280.

Achenbach, H., Mülhlenfeld, A. and Brillinger, G.U. (**1985**). Stiffwechselprodukte von mikroorganismen, XXX. Phthalideund chromanole aus *Aspergillus duricaulis*. *Justus Liebigs Annalen der Chemie*, 1596-1628.

Achenbach, H., Mülhlenfeld, A., Weber, B. and Brillinger, G.U. (**1982**). Highly substituted chromanols from culture of *Aspergillus duricaulis*. *Tetrahedron Letters 45*, 4659-4660.

Afiyatullov, S.S., Leshchenko, E.V., Berdyshev, D.V., Sobolevskaya, M.P., Antonov, A.S., Denisenko, V.A., Popov, R.S., Pivkin, M.V., Udovenko, A.A., Pislyagin, E.A., Amsberg, G. and Dyshlovoy, S.A. (**2017**). Zosteropenillines: Polyketides from the Marine-Derived Fungus *Penicillium thomii*. *Marine Drugs 15*, 46.

Afiyatullov, S.S., Leshchenko, E.V., Sobolevskaya, M.P., Denisenko, V.A., Kirichuk, N. N., Khudyakova, Y.V., Hoai, T.P.T., Dmitrenok, P.S., Menchinskaya, E.S., Pislyagin, E.A. and Berdyshev, D.V. (**2015**). New eudesmane sesquiterpenes from the marine-derived fungus *Penicillium thomii*. *Phytochemistry Letters 14*, 209-214.

Aiello, A., Fattorusso, E., Magno, S., Menna, M. (**1991**). Isolation of five new 5α-hydroxy-6-keto-Δ^7sterols from the marine sponge *Oscarella lobularis*. *Steroids 56*, 337-340.

Alves, A.J.S., Pereira, J.A., Dethoup, T., Cravo, S., Mistry, S., Silva, A.M.S. Pinto, M.M.M. and Kijjoa, A. (**2019**). A New Meroterpene, A New Benzofuran Derivative and Other Constituents from Cultures of the Marine Sponge-

Associated Fungus *Acremonium persicinum* KUFA 1007 and Their Anticholinesterase Activities. *Marine Drugs 17* (6), 379.

An, C.Y., Li, X.M., Li, C.S., Xu, G.M. and Wang, B.G. (**2014**). Prenylated indolediketopiperazine peroxides and related homologues from the marine sediment-derived fungus *Penicillium brefeldianum* SD-273. *Marine Drugs 12*, 746-756.

Aoki, M., Itezono, Y., Shirai, H., Nakayama, N., Sakai, A., Tanaka, Y., Yamaguchi, A., Shimma, N. and Yokose, K. (**1991**). Structure of a novel phospholipase C inhibitor, vinaxanthone (Ro 09-1450), produced by *Penicillium vinaceum. Tetrahedron Letters 32,* 4737-4740.

Arai, M., Niikawa, H. and Kobayashi, M. (**2013**). Marine-derived fungal sesterterpenes, ophiobolins, inhibit biofilm formation of *Mycobacterium* species. *Journal of Natural Medicines 67* (2), 271-275.

Arai, K., Miyajima, H., Mushiroda, T. and Yamamoto, Y. (**1989**). Metabolites of *Penicillium italicum* Wehmer. Isolation and structures of new metabolites including naturally occurring 4-ylidene-acyltetronic acids, italicinic acid and italicic acid. *Chemical and Pharmaceutical Bulletin 37*, 3229-3235.

Arasu, M.V., Duraipandiyan, V. and Ignacimuthu, S. (**2013**). Antibacterial and antifungal activities of polyketide metabolite from marine *Streptomyces* sp. AP-123 and its cytotoxic effect. *Chemosphere 90* (2), 479-487.

Asiri, I.A.M., Badr, J.M. and Youssef, D.T.A. (**2015**). Penicillivinacine, antimigratory diketopiperazine alkaloid from the marine-derived fungus *Penicillium vinaceum*. *Phytochemistry Letters 13*, 53-58.

Aung, T.S. (**2017**). Bioactive Secondary Metabolites from the Culture of the Marine Sponge-Associated Fungus *Neosartorya fennelliae* KUFA 0811. (Master's thesis) institute of Biomedical Sciences Abel Salazar of the University of Porto, Portugal, 158p.

Austin, A., Petersson, G.A., Frisch, M.J., Dobek, F.J., Scalmani, G. and Throssel, K. (**2012**). A density functional with Spherical atom dispersion terms. *Journal of Chemical Theory and Computation 8*, 4989-5007.

Bai, M., Huang, G.L., Mei, R.Q., Wang, B., Luo, Y.P., Nong, X.H., Chen, G.Y. and Zheng, C.J. (**2019**). Bioactive Lactones from the Mangrove-Derived Fungus *Penicillium* sp. TGM112. *Marine Drugs 17* (8).

Bang, S., Song, J.H., Lee, D., Lee, C., Kim, S., Kang, K.S., Lee, J.H. and Shim, S.H. (**2019**). Neuroprotective Secondary Metabolite Produced by an Endophytic Fungus, *Neosartorya fischeri* JS0553, Isolated from *Glehnia littoralis*. *Journal of Agricultural and Food Chemistry 67*, 1831-1838.

Banskota, A.H. (**2002**). Antiproliferative activity of Vietnamese medicinal plants. *Biological Pharmaceutical Bulletin 25* (6), 753-760.

Bao, J., Luo, J.F., Qin, X.C., Xu, X.Y., Zhang, X.Y., Tu, Z.C. and Qi, S.H. (**2014**). Dihydrothiophene-condensed chromones from a marine-derived fungus *Penicillium oxalicum* and their structure-bioactivity relationship. *Bioorganic and Medicinal Chemistry Letters 24* (11), 2433-2436.

Bao, J., Sun, Y.L., Zhang, X.Y., Han, Z., Gao, H.C., He, F., Qian, P.Y. and Qi, S.H. (**2013**) Antifouling and antibacterial polyketides from marine gorgonian coral-associated fungus *Penicillium* sp. SCSGAF 0023. *The Journal of Antibiotics 66*, 219-223.

Bentley, R. (**2000**). Mycophenolic acid: a one-hundred year odyssey from antibiotic to immunosuppressant. *Chemical Reviews*. 100, 3801-3825.

Benyhe, S. (**1994**). Morphine: New aspects in the study of an ancient compound. *Life Sciences 55* (13), 969-979.

Berdai, M.A., Labib, S., Chetouani, K. and Harandou, M. (**2012**). *Atropa belladonna* intoxication: a case report. *Pan African Medical Journal 11*, 72.

Bergmann, W. and Feeney, R.J. (**1950**). The isolation of a new thymine pentoside from sponges 1. *Journal of the American Chemical Society 72*, 2809-2810.

Bessa, L.J., Barbosa, V.A., Mendes, A., Vaz, P.P. and Martins de Costa, P. (**2014**). High prevalence of multidrug-resistant *Escherichia coli* and *Enterococcus* spp. in river water, upstream and downstream of a wastewater treatment plant. *Journal of Water and Health 12*, 426-435.

Bugni, T.S. and Ireland, C.M. (**2004**). Marine-derived fungi: A chemically and biologically diverse group of microorganisms. *Natural Product Reports 21*, 143-163.

Buss, A.D. and Waigh, R.D. (**1995**). Natural products as leads for new pharmaceuticals. In: Wolff, ME., editor.Burger's medicinal chemistry and drug discovery. Principles and practice. Vol. 1. John Wiley and Sons, Inc; New York, NY: p. 983-1033.

Butler, M.S. (**2004**). The role of natural product in chemistry in drug discovery. *Journal of Natural Products 67*, 2141–2153.

Buttachon, S., Zin, W.W.M., Dethoup, T., Gales, L., Pereira, J.A., Silva, A.M.S. and Kijjoa, A. (**2016**). Secondary Metabolites from the Culture of the Marine Sponge-Associated Fungi *Talaromyces tratensis* and *Sporidesmium circinophorum*. *Planta Medica 82* (9), 888-896.

Buttachon, S., Chandrapatya, A., Manoch, L., Silva, A., Gales, L., Bruyère, C., Kiss, R. and Kijjoa, A. (**2012**). Sartorymensin, a new indole alkaloid, and new analogues of tryptoquivaline and fiscalins produced by *Neosartorya siamensis* (KUFC 6349). *Tetrahedron 68*, 3253-3262.

Buttachon, S., Ramos, A.A., Inácio, Â., Dethoup, T., Gales, L., Lee, M., Costa, P.M., Silva, A.M.S., Sekeroglu, N. and Rocha, E. (**2018**). Bis-indolyl benzenoids, hydroxypyrrolidine derivatives and other constituents from cultures of the marine sponge-associated fungus *Aspergillus candidus* KUFA0062. *Marine Drugs 16*, 1-22.

Cantrell, C.L., Rajab, M.S., Franzblau, S.G., Fronczek, F.R. and Fischer, N.H. (**1999**). Antimycobacterial ergosterol-5,8-endoperoxide from *Ajuga remota. Planta Medica 65*, 732-734.

Capon, R.J., Stewart, M., Ratnayake, R., Lacey, E. and Gill, J.H. (**2007**). Citromycetins and Bilains A-C: New aromatic polyketides and diketopiperazines from Australian Marine-Derived and Terrestrial *Penicillium* spp. *Journal of Natural Products 70*, 1746-1752.

Cegelski, L., Marshall, G.R., Eldridge, G.R. and Hultgren, S.J. (**2008**). The biology and future prospects of of antivirulence therapies. *Nature Reviews Microbiology* 6, 17-27.

Chai, Y.J., Cui, C.B., Li, C.W., Wu, C.J., Tian, C.K. and Hua, W. (**2012**). Activation of the dormant secondary metabolite production by introducing gentamicin-resistance in a marine-derived *Penicillium purpurogenum* G59. *Marine Drugs 10* (3), 559-582.

Chauhan, R., Ruby, K.M. and Jaya, D. (**2012**). *Bergenia Ciliata* Mine of Medicinal properties: A Reviews. *International Journal of Pharmaceutical Sciences Review and Research 15* (2), 20-23.

Chen, H., Aktas, N., Konuklugil, B., Mándi, A., Daletos, G., Lin, W., Dai, H., Kurtán, T. and Proksch, P. (**2015**). A new fusarielin analogue from *Penicillium* sp. isolated from the Mediterranean sponge *Ircinia oros*. *Tetrahedron Letters 56*, 5317-5320.

Chen, J.J., Huanga, H.Y., Duhb, C.Y. and Chenc, I.S. (**2004**). Cytotoxic Constituents from the Stem Bark of *Zanthoxylum pistaciiflorum*. *Journal of the Chinese Chemical Society 51*, 659-663.

Chen, L., Fang, Y., Zhu, T., Gu, Q. and Zhu, W. (**2008**). Gentisyl Alcohol Derivatives from the Marine-Derived Fungus *Penicillium terrestre*. *Journal of Natural Products 71* (1), 66-70.

Chen, B.Y., Wang, Z., Ying, Y.M., Jiang, L.X., Zhan, Z.J., Wang, J.L. and Zhang, W. (**2014**). Neofipiperzine D, a new prenylated indole alkaloid metabolite of the fungus *Neosartorya fischeri*. *Journal of Chemical Research 38*, 539-541.

Cheng, X., Yu, L., Wang, Q., Ding, W., Chen, Z. and Ma, Z. (**2018**). New brefeldins and penialidins from marine fungus *Penicillium janthinellum* DT –F29. *Natural Products Research 32* (3), 282-286.

Chin, M.R., Zlotkowski, C., Han, M., Patel, S., Eliasen, A.M., Axelrod, A. and Siegel, D. (2015). Expedited access to vinaxanthone and chemically edited derivatives possessing neuronal tegenerative effects through ynone coupling reactions. *ACS Chemical Neuroscience 6*, 542–550.

Chooi, Y.H., Fang, J., Liu, H., Filler, S.G., Wang, P. and Tang, Y. (**2013**). Genome Mining of a Prenylated and Immunosuppressive Polyketide from Pathogenic Fungi. *Organic Letters 15*, 780-783

Chu, C.W., Liu, C.M., Chung, M.I. and Chen, C.Y. (**2015**). Biofunctional Constituents from *Michelia compressa var. lanyuensis* with Anti-Melanogenic Properties. *Molecules 20*, 12166-12174.

Clinical and Laboratory Standards Institute (CLSI). (**1999**). Methods for Determining Bactericidal Activity of Antimicrobial Agents; Approved Guideline; Clinical and Laboratory Standards Institute: Wayne, PA, USA.

Clinical and Laboratory Standards Institute (CLSI). (**2012**). Performance Standards for Antimicrobial Disk Susceptibility Tests; Approved Standard-11th ed., CLSI Document M02-A11; Clinical and Laboratory Standards Institute: Wayne, PA, USA.

Clinical and Laboratory Standards Institute (CLSI). (**2015**). Methods for Dilution Antimicrobial Susceptibility Tests for Bacteria That Grow Aerobically; Approved Standard-10th ed., CLSI Document M07-A10; Clinical and Laboratory Standards Institute: Wayne, PA, USA.

Clinical and Laboratory Standards Institute (CLSI). (**2017**). Performance Standards for Antimicrobial Susceptibility Testing, 27th ed.; CLSI Supplement M100; Clinical and Laboratory Standards Institute: Wayne, PA, USA.

Cutignano, A., Bifulco, G., Bruno, I., Casapullo, A., Gomez, P.L. and Riccio, R. (**2000**). Dragmacidin F: A New Antiviral Bromoindole Alkaloid from the Mediterranean Sponge *Halicortex* sp. *Tetrahedron 56*, 3743-3748.

Daly, J.W., Spande, T.F. and Garrafo, H.M. (**2005**). Alkaloids from amphibian skins. A tabulation of over eight hundred compounds. *Journal of Natural Products 68*, 1556-1575.

Deleu, D., Hanssens, Y. and Northway, M.G. (**2004**). Subcutaneous apomorphine:an evidence-based review of its use in Parkinson' s disease. *Drugs and Aging 21*, 687-709.

Della, M.G., Monaco, P. and Previtera, L. (**1990**). Stigmasterols from *Typha latifolia*, *Journal of Natural Products 53* (6), 1430-1435.

Demain, A.L. and Sanchez, S. (**2009**). Microbial drug discovery: 80 years of progress, *The Journal of antibiotics 62*, 5-16.

Devarajan, P.T., Suryanarayanan, T.S. and Geetha, V. (**2002**). Endophytic fungi associated with the tropical seagrass *Halophila ovalis* (Hydrocharitaceae). *Indian Journal of Geo-Marine Sciences 31*, 73-74.

Dewick, P.M. Medicinal Natural Products: A Biosynthentic Approach, 2nd ed.; John Wiley and Son: West Sussex, UK, 2002; p. 520.

Du, F.Y., Li, X., Li, X.M., Zhu, L.W. and Wang, B.G. (**2017**). Indolediketopiperazine Alkaloids from *Eurotium cristatum* EN-220, an Endophytic Fungus Isolated from the Marine Alga *Sargassum thunbergii*. *Marine Drugs 25*,15(2).

Duggar, B.M. (**1948**). Aureomycin: a product of the continuing search for new antibiotics. *Annals of the New York Academy of Sciences 51*, 177-181.

Eamvijarn, A., Gomes, N.M., Dethoup, T., Buaruang, J., Manoch, L., Silva, A., Pedro, M., Marini, I., Roussis, V. and Kijjoa, A. (**2013**). Bioactive meroditerpenes and indole alkaloids from the soil fungus *Neosartorya fischeri* (KUFC 6344), and the marine-derived fungi *Neosartorya laciniosa* (KUFC 7896) and *Neosartorya tsunodae* (KUFC 9213). *Tetrahedron 69*, 8583-8591.

Eamvijarn, A., Kijjoa, A., Bruyére, C., Mathieu, V., Manoch, L., Lefranc, F., Silva, A., Kiss, R., Herz, W. (**2012**). Secondary metabolites from a culture of the fungus *Neosartorya pseudofischeri* and their *in vitro* cytostatic activity in human cancer cells. *Planta Medica 78*, 1767-1776.

El-Beih, A.A., Kawabata, T., Koimaru, K., Ohta, T. and Tsukamoto, S. (**2007**). Monodictyquinone A: A new antimicrobial anthraquinone from a sea urchin-derived fungus *Monodictys* sp. *Chemical and Pharmaceutical Bulletin 55*, 1097-1098.

Elsebai, M.F., Kehraus, S., Gütschow, M. and König, G.M. (**2010**). Spartinoxide, a new enantiomer of A82775C with inhibitory activity toward HLE from the marine-derived Fungus *Phaeosphaeria spartinae*. *Natural Product Communications 5* (7), 1071-1076.

Fan, S.Q., Xie, C.L., Xia, J.M., Xing, C.P., Luo, Z.H., Shao, Z. and Yang, X. (**2019**). Sarocladione, a unique 5,10:8,9-diseco-steroid from the deep-sea-derived fungus *Sarocladium kiliense*. *Organic and Biomolecular Chemistry 17*, 5925-5928.

Fan, Y.Q., Li, P.H., Chao, Y.X., Chen, H., Du, N., He, Q.X. and Liu, K.C. (**2015**). Alkaloids with Cardiovascular Effects from the Marine-Derived Fungus *Penicillium expansum* Y32. *Marine Drugs 13* (10), 6489-6504.

Fang, S.M., Cui, C.B., Li, C.W., Wu, C.J., Zhang, Z.J., Li, L., Huang, X.J. and Ye, W.C. (**2012**). Purpurogemutantin and purpurogemutantidin, new drimenyl cyclohexenone derivatives produced by a mutant obtained by diethyl sulfate mutagenesis of a marine-derived *Penicillium purpurogenum* G59. *Marine Drugs 10* (6), 1266-1287.

Fangkrathok, N., Sripanidkulchai, B., Umehara, K., Noguchi, H. (**2013**). Bioactive ergostanoids and a new polyhydroxyoctane from *Lentinus polychrous* mycelia and their inhibitory effects on E2-enhanced cell proliferation of T47D cells. *Natural Product Research 27*, 1611-1619.

Feling, R.H., Buchanan, G.O., Mincer, T.J., Kauffman, C.A., Jensen, P.R. and Fenical, W. (**2003**). Salinosporamide A: A highly cytotoxic proteasome inhibitor from a novel microbial source, a marine bacterium of the new genus *salinospora*. *Angewandte Chemie International Edition 42*, 355-357.

Feng, C. and Ma, Y. (**2010**). Isolation and anti-phytopathogenic activity of secondary metabolites from *Alternaria*sp. FL25, an endophytic fungus in *Ficus carica*. Chin. *Journal of Applied Environmental and Biological Sciences 16*, 76-78.

Fleming, A. (**1929**). On the antibacterial action of cultures of a *penicillium*, with special reference to their use in the isolation of B. Influenzae. *British journal of experimental pathology 10*, 226.

Ford, P.W., Gustafson, K.R., McKee, T.C., Shigematsu, N., Maurizi, L.K., Pannell, L.K., Williams, D.E., Silva, E.D., Lassota, P., Alien, T.M., Van, S.R., Andersen, R.J. and Boyd, M.R. (**1999**). Papuamides A–D, HIV-inhibitory and cytotoxic depsipeptides from the sponges *Theonella mirabilis* and *Theonella swinhoei* collected in Papua New Guinea. *Journal of the American Chemical Society* 121, 5899-5909.

Fouillaud, M., Mekala, V., Emmanuelle, G.V., Yanis, C. and Laurent, D. (**2016**). Anthraquinones and Derivatives from Marine-Derived Fungi: Structural Diversity and Selected Biological Activities. *Marine Drugs 14* (64), 1-64.

Fujimoto, H., Negishi, E., Yamaguchi, K., Nishi, N. and Yamazaki, M. (**1996**). Isolation of new tremorgenic metabolites from an Ascomycete, *Corynascus setosus*. *Chemical and Pharmaceutical Bulletin 44*, 1843-1848.

Fujita, K.I., Nagamine, Y., Ping, X. and Taniguchi, K. (**1999**). Mode of Action of anhydrofulvic acid against *Candida utilis* ATCC 42402 under acid condition. *The Journal of Antibiotics 52*, 628-634.

Füllbeck, M., Michalsky, E., Dunkel, M. and Preissner, R. (**2006**). Natural products: sources and databases. *Natural Product Reports 23* (3), 347-356.

Gao, H., Zhou, L., Li, D., Gu, Q. and Zhu, T.J. (**2013**). New Cytotoxic Metabolites from the Marine-Derived Fungus *Penicillium* sp. ZLN29. *Helvetica Chimica Acta* 96, 514-519.

Gao, S.S., Li, X.M., Zhang, Y., Li, C.S., Cui, C.M. and Wang, B.G. (**2011**). Comazaphilones A-F, azaphilone derivatives from the marine sediment-derived fungus *Penicillium commune* QSD-17. *Journal of Natural Products* 25; *74* (2), 256-261.

Ge, C.Y. and Zhang, J.L. (**2018**). Bioactive sesquiterpenoids and steroids from the resinous exudates of *Commiphora myrrha*. *Natural Product Research,* 309-315.

George, E. Treadwell, J.R. and David, E. M. (**1972**). Photoconversion of Riboflavin to Lumichrome in Plant Tissues. *Plant Physiology 49*, 991-993.

Georgousaki, K., Tsafantakis, N., Gumeni, S., Menéndez, V.G., Pedro, N., Tormo, J.R., Almeida, C., Lambert, C., Genillou, O., Trougakos, L.P. and Fokialakis, N. (**2019**). *Cercospora* sp. as a source of anti-aging polyketides targeting 26S proteasome and scale-up production in submerged bioreactor. *Journal of Biotechnology 301*, 88-96.

Ghanbari, M.A.T., Mohammadkhani, H.S. and Babaeizad, V. (**2014**). Identification of some secondary metabolites produced by four *Penicillium* species. *Mycologia Iranica 1* (2), 107-113.

Givern, J.G. (**2007**). Ziconotide: a review of its pharmacology and use in the treatment of pain. *Neuropsychiatric Disease and Treatment 3* (1), 69-85.

Glaser, K.B. and Mayer, A.M.S. (**2009**). A renaissance in marine pharmacology: From preclinical curiosity to clinical reality. *Biochemical Pharmacology 78* (5), 440-448.

Gomes, N.M., Bessa, L.J., Buttachon, S., Costa, P.M., Bauruang, J., Dethoup, T., Silva, A.M.S. and Kijjoa, A. (**2014**). Antibacterial and antibiofilm activities of tryptoquivalines and meroditerpenes isolated from the marine-derived fungi *Neosartorya paulistensis, N. laciniosa, N. tsunodae,* and the soil fungi *N. fischeri* and *N. siamensis. Marine Drugs 12*, 822-839.

Gordon, M.C. and David, J.N. (**2013**). Natural products: A continuing source of novel drug leads. *Biochimica et Biophysica Acta* 1830, 3670-3695.

Gulder, T.A. and Moore, B.S. (**2009**). Chasing the treasures of the sea - bacterial marine natural products. *Current opinion in microbiology 12* (3), 252-260.

Hasegawa, A., Koizumi, F., Takahashi, Y., Ando, K., Ogawa, T., Hara, M.and Yoshida, M. (**2001**). Symposium on the Chemistry of Natural Products, symposium papers., 43, 467-472.

He, J., Lion, U., Sattler, I., Gollmick, F.A., Grabley, S., Cai, J., Meiners, M., Schünke, H., Schaumann, K., Dechert, U. and Krohn, M. (**2005**). Diastereomeric Quinolinone Alkaloids from the Marine-Derived Fungus *Penicillium janczewskii*. *Journal of Natural Products 68* (9), 1397-1399.

Hetherington, A. C. and Raistrick, H. (**1931**). On Citromycetin, a New Yellow Colouring Matter Produced from Glucose by Species of Citromyces. *Philosophical Transactions of the Royal Society B: Biological Sciences* 220 (468-473), 209-244.

Hiramatsu, K., Hanaki, H., Ino, T., Yabuta, K., Oguri, T. and Tenover, F.C. (**1997**). Methicillin-resistant Staphylococcus aureus clinical strain with reduced vancomycin susceptibility. *Journal of Antimicrobial Chemotherapy 40*, 135-136.

Honda, N.K., Devincenzi, I.A. and Xavier, F.L. (**1995**). Secalonic Acid A from *Pseudoparmelia sphaerospora* (Nyl.) Hale and *Pseudoparmelia. hypomilta* (Fée) Hale (Parmeliaceae). *Tropical Bryology 10*, 201-204.

Hotta, K., Noguchi, Y., Matsunaga, M., Nishibe, K., Uchida, K., Shimizu, K., Kono, T. and Sumio, K. (**2003**). *Leonurus heterophyllus* extracts and *β*-sitostenone as antiarrhythmics. *Journal PLOS Pathogens 138,* 107-113.

Hu, Y., Chen, J., Hu, G., Yu, J., Zhu, X., Lin, Y., Chen, S. and Yuan, J. (**2015**). Statistical Research on the Bioactivity of New Marine Natural Products Discovered during the 28 Years from 1985 to 2012. *Marine Drugs 13* (1), 202-221.

Huang, C.H., Pan, J.H., Chen, B., Yu, M., Huang, H.B., Zhu, X., Lu, Y.J., She, Z.G. and Lin, Y.C. (**2011**). Three bianthraquinone derivatives from the mangrove endophytic fungus *Alternaria* sp. ZJ9–6B from the South China Sea. *Marine Drugs 9*, 832-843.

Huang, G.L., Zhou, X.M., Bai, M., Liu, Y.X., Zhao, Y.L., Luo, Y.P., Niu, Y.Y., Zheng, C.J. and Chen, G.Y. (**2016**). Dihydroisocoumarins from the Mangrove-Derived Fungus *Penicillium citrinum*. *Marine Drugs 10*, 14 (10).

Huang, H., Wang, F., Luo, M., Chen, Y., Song, Y., Zhang, W., Zhang, S. and Ju, J. (**2012**). Halogenated anthraquinones from the marine-derived fungus *Aspergillus* sp. SCSIO F063. *Journal of Natural Products 75*, 1346-1352.

Imhoff, J.F. (**2016**). Natural Products from Marine Fungi-still an Underrepesented Resource. *Marine Drugs 14* (19), 1-19.

Isaka, M., Prathumpai, W., Wongsa, P. and Tanticharoen, M. (**2006**). Hirsutellone F, a Dimer of Antitubercular Alkaloids from the Seed Fungus *Trichoderma* Species BCC 7579. *Organic Letters 8* (13), 2815-2817.

Ishizuka, T., Yaoita, Y. and Kikuchi, M. (**1997**). Sterol constituents from the fruit bodies of *Grifola frondosa* (Fr.) S.F. Gray. *Chemical and Pharmaceutical Bulletin 45*, 1756-1760.

Jang, K.H., Chung, S.C., Shin, J., Lee, S.H., Kim, T.I., Lee, H.S. and Oh, K.B. (**2007**). Aaptamines as sortase A inhibitors from the tropical sponge *Aaptos aaptos*. *Bioorganic and Medicinal Chemistry Letters 17*, 5366-5369.

Jayasuriya, H., Zink, D., Basilio, A., Vicente, F., Collado, J., Bills, G., Goldman, M.L., Motyl, M., Huber, J. and Dezeny, G. (**2009**). Discovery and antibacterial activity of glabramycin A-C from *Neosartorya glabra* by an antisense strategy. *The Journal of Antibiotics 62*, 265-269.

Jia, Q., Du, Y., Wang, C., Wang, Y., Zhu, T. and Zhu, W. (**2019**). Azaphilones from the Marine Sponge- Derived Fungus *Penicillium sclerotiorum* OUCMDZ- 3839. *Marine Drugs 17* (5).

Jin, L., Quan, C., Hou, X. and Fan, S. (**2016**). Potential Pharmacological Resources: Natural Bioactive Compounds from Marine-derived Fungi. *Marine Drugs 14* (76), 1-25.

Jyoti, S. and Singh, D.P. (**2016**). Production of Secondary Metabolites from Two *Penicillium* Strains Adapted to Different Temperature Conditions: A Study on Differential Response of Fungal Strains to Temperature Stress. *Molecular and Cellular Biology 62*, 3.

Kaifuchi, S., Mori, M., Nonaka, K., Masuma, R., Omura, S. and Shiomi, K. (**2015**). Sartorypyrone D: a new NADH-fumarate reductase inhibitor produced by *Neosartorya fischeri* FO-5897. *Journal of Antibiotics 68*, 403-405.

Kanokmedhakul, K., Kanokmedhakul, S., Suwannatrai, R., Soytong, K., Prabpai, S. and Kongsaeree, P. (**2011**). Bioactive meroterpenoids and alkaloids from the fungus *Eurotium chevalieri*, *Tetrahedron 67*, 5461-5468.

Katzenschlager, R., Evans, A. and Manson, A. (**2004**). *Mucuna pruriens* in Parkinson's disease: a double blind clinical and pharmacological study. *Journal of Neurology, Neurosurgery and Psychiatry 75*, 1672-1677.

Kem, W., Soti, F., Wildeboer, K., Francois, S., Dougall, K., Wei, D.Q., Chou, K.C. and Arias, H.R. (**2006**). The Nemertine Toxin Anabaseine and Its Derivative DMXBA (GTS-21): Chemical and Pharmacological Properties. *Marine Drugs 4* (3), 255-273.

Kijjoa, A., Santos, S., Dethoup, T., Manoch, L., Almeida, A. P., Vasconcelos, M. H., Silva, A., Gales, L. and Herz, W. (**2011**). Sartoryglabrins, analogs of ardeemins, from *Neosartorya glabra*. *Natural Product Communications 6*, 807-812.

Kimura, T., Kikuchi, K., Kumagai, K., Hosotani, N. and Kishino, A. Nerve regeneration promoters containing semaphorin inhibitor as the active ingredient. European Patent EP 1 306 093 B1. Date of Publication and mention of the grant of the patent 03.10.2007. Bulletin 2007/40- https://data.epo.org/publication-server/rest/v1.0/publicationdates/20071003/patents/EP1306093NWB1/document.html-access on 07 July 2018.

Klayman, D. (**1985**). Qinghaosu (artemisinin): an antimalarial drug from China. *Science*, 228 (4703), 1049-1055.

Koch, K.F. and Rhoades, J.A. (**1970**). Structure of nebramycin factor 6, a new aminoglycosidic antibiotic. *Antimicrob Agents Chemother (Bethesda) 10*, 309-313.

Koparde, A.A., Doijad, R.C. and Magdum, C.S. (**2019**). Natural Products in Drug Discovery. Intech Open world's leading publisher of Open Access books Built by scientists. DOI: 10.5772/intechopen.82860

Kremsner, P.G., Winkler, S., Brandts, C., Neifer, S., Bienzle, U. and Graninger, W. (**1994**). Clindamycin in combination with chloroquine or quinine is an effective therapy for uncomplicated *Plasmodium falciparum* Malaria in children from Gabon. *Journal Infectious Diseases* 169, 467-470.

Krishnamurti, C. and Rao, S.C. (**2016**). The isolation of morphine by Serturner. *Indian Journal Anaesthesis 60* (11), 861-862.

Kumagai, K., Hosotani, N., Kikuchi, K., Kimura, T. and Saji, I. (**2003**). Xanthofulvin, a novel semaphoring inhibitor produced by a strain of *Penicillium*. *The Journal of Antibiotics 56*, 610–616.

Kumla, D., Aung, T.S., Buttachon, S., Dethhoup, T., Gales, L., Pereira, J., Inácio, Â., Costa, P.M, Lee, M., Sekeroglu, N., Silva, A.M.S., Pinto, M.M.M. and Kijjoa, A. (**2017**). A New Dihydrochromone Dimer and Other Secondary Metabolites from the Cultures of the Marine Sponge-Associated Fungi *Neosartorya fennelliae* KUFA 0811 and *Neosartorya tsunodae* KUFC 9213. *Marine Drugs, 15* (12), 375; 1-17.

Kumla, D., Pereira, J.A., Dethoup, T., Gales, L., Silva, J.F., Costa, P.M., Lee, M., Silva, A.M.S., Sekeroglu, N., Pinto, M.M.M. and Kijjoa, A. (**2018**). Chromone Derivatives and Other Constituents from Cultures of the Marine Sponge-Associated Fungus *Penicillium erubescens* KUFA0220 and Their Antibacterial Activity. *Marine Drugs 16* (8), 289.

Kumla, D., Dethoup, T., Buttachon, S., Singburaudom, N., Silva, A.M.S. and Kijjoa, A. (**2014**). Spiculisporic acid E, a new spiculisporic acid derivative and ergosterol derivatives from the marine-sponge associated fungus *Talaromyces trachyspermus* (KUFA 0021). *Natural Product Communications 9* (8), 1147-1150.

Kunze, B., Reichenbach, H., Augustiniak, H. and Höfle, G. (**1982**). Isolation and identification of althiomycin from *cystobacter fuscus* (myxobacterales). *The Journal of Antibiotics 35*, 635-636.

Kurobane, I., Vining, L.C. and Mcinnes, A.G. (**1979**). Biosynthetic relationships among the secalonic acids. *The Journal of antibiotics 32*, 1256-1266.

Kusakabe, Y., Yamauchi, Y., Nagatsu, C., Abe, H., Akasaki, K. And Shirato, S. (**1968**). Citromycin, A New Antibiotic. I. Isolation and Characterization. *The Journal of Antibiotics 22* (3), 112-118.

Kwon, H.C., Kauffman, C.A., Jensen, P.R. and Fenical, W. (**2006**). Marinomycins A-D, antitumor-antibiotics of a new structure class from a marine actinomycete of the recently discovered genus "*Marinispora*". *Journal of the American Chemical Society* 128, 1622-1632.

Lan, W., Fu, S., Xu, M., Liang, W., Lam, C., Zhong, G., Xu, J., Yang, D. and Li, H. (**2016**). Five new cytotoxic metabolites from the marine fungus *Neosartorya pseudofischeri. Marine Drugs 14*, 18-30.

Le, T., Wolbers, M., Chi, N.H., Quang, V.M., Chinh, N.T., Huong, N.P., Lam, P.S., Kozal, M.J., Shikuma, C.M., Day, J.N. and Farrar, J. (**2011**). Epidemiology, Seasonality, and Predictors of Outcome of AIDS-Associated *Penicillium marneffei* Infection in Ho Chi Minh City, Viet Nam. *Clinical Infectious Diseases 52* (7), 945–952.

Lee, D.S., Jang, J.H., Ko, W., Kim, K.S., Sohn, J.H., Kang, M.S., Ahn ,J.S., Kim, Y.C. and On, H. (**2013**). PTP1B inhibitory and anti-inflamatory effects of secondary metabolites isolated from the marine-derived fungus *Penicillium* sp. JF-55. *Marine Drugs 11*, 1409-1429.

Lee, S.Y., Kinoshita, H., Ihara, F., Igarashi, Y. and Nihira, T. (**2008**). Identification of novel derivative of helvolic acid from *Metarhizium anisopliae* grown in medium with insect component. *Journal of Bioscience and Bioengineering* 105, 476-480.

Li, C., Yang, R., Lin, Y. and Zhou, S. (**2006**). Isolation and crystal structure of (−)-byssochlamic acid from mangrove fungus (strain no. k38). *Chemistry of Natural Compounds 4* (3), 290-293.

Li, C.S., An, C.Y., Li, X.M., Gao, S.S., Cui, C.M., Sun, H.F., Wang, B.G. (**2011**). Triazole and dihydroimidazole alkaloids from the marine sediment-derived fungus *Penicillium paneum* SD-44. *Journal of Natural Products 74* (5), 1331-1334.

Li, C.S., Li, X.M., An, C.Y. and Wang, B.G. (**2014**). Prenylated Indole Alkaloid Derivatives from Marine Sediment-Derived Fungus *Penicillium paneum* SD-44. *Helvetica Chimica Acta 97*, 1440-1444.

Li, C.S., Li,X.M., Gao, S.S., Lu, Y.H. and Wang, B.G. (**2013**). Cytotoxic anthranilic acid derivatives from deep sea sediment-derived fungus *Penicillium paneum* SD-44. *Marine Drugs 11* (8), 3068-3076.

Li D., Chen L., Zhu T.J., Kurtán T., Mándi A., Zhao Z., Li J. and Gu Q., (**2011**). Chloctanspirones A and B, novel chlorinated polyketides with an unprecedented skeleton, from marine sediment derived fungus *Penicillium terrestre*. *Tetrahedron 67*, 7913-7918.

Li, G., Kusari, S. and Spiteller, M. (**2014**). Natural products containing “decalin” motif in microorganisms*. Natural Product Reports 31* (9),1175-1201.

Li H., Huang H., Shao C., Huang H., Jiang J., Zhu X., Liu Y., Liu L., Lu Y., Li M., Lin Y. and She Z. (**2011**). Cytotoxic norsesquiterpene peroxides from the endophytic fungus *Talaromyces flavus* isolated from the mangrove plant *Sonneratia apetala*. *Journal of Natural Products 74* (5), 1230-1235.

Li, W.H., Chang, S.T., Chang, S.C. and Chang, H.T. (**2008**). Isolation of antibacterial diterpenoids from *Cryptomeria japonica* bark. *Natural Product Research 22* (12), 1085-1093.

Li, X., Li, X.M., Zhang, P. and Wang, B.G. (**2015**). A new phenolic enamide and a new meroterpenoid from marine alga-derived endophytic fungus *Penicillium oxalicum* EN-290, *Journal of Asian Natural Products Research 17* (12), 1204-1212.

Li, Y., Song, Y.C., Liu, J.Y., Ma, Y.M. and Tan, R.X. (**2005**). Anti-*Helicobacter pylori* substances from endophytic fungal cultures. *World Journal of Microbiology and Biotechnology 21*, 553-558.

Li, Z., Ma, N. and Zhao, P.J. (**2018**). Acetylcholinesterase inhibitory active metabolites from the endophytic fungus *Colletotrichum* sp*. YMF432. Natural Product Research 33* (12), 1794-1797.

Liang, W.L., Le, X., Li, H.J., Yang, X.L., Chen, J.X., Xu, J., Liu, H.L., Wang, L.Y., Wang, K.T., Hu, K.C., Yang, D.P. and Lan, W.J. (**2014**). Exploring the chemodiversity and biological activities of the secondary metabolites from the marine fungus *Neosartorya pseudofischeri. Marine Drugs 12*, 5657-5676.

Liu, F., Cai, X.L., Yang, H., Xia, X.K., Guo, Z.Y., Yuan, J., Li, M.F., She, Z.G. and Lin, Y.C. (**2010**). The bioactive metabolites of the mangrove endophytic fungus *Talaromyces* sp. ZH-154 isolated from *Kandelia candel* (L.) Druce. *Planta Medica 76*, 185-189.

Liu, H., Chen, S., Liu, W., Liu, Y., Huang, X. and She, Z. (**2016**). Polyketides with Immunosuppressive Activities from Mangrove Endophytic Fungus *Penicillium* sp. ZJ-SY2. *Marine Drugs 14* (12), 217.

Liu, Q.Y., Zhou, T., Zhao, Y.Y., Chen, L., Gong, M.W., Xia, Q.W., Ying, M.G.2, Zheng, Q.H. and Zhang, Q.Q. (**2015**). Antitumor Effects and Related Mechanisms of Penicitrinine A, a Novel Alkaloid with a Unique Spiro Skeleton from the Marine Fungus *Penicillium citrinum*. *Marine Drugs 13* (8), 4733-4753.

Liu, T., Zhang, S., Li, Z., Wang, Y., Chen, Z., Bai, J., Tian, L., Pei, Y. and Hua, H. (**2016**). A new polyketide, penicillolide from the marinederived fungus *Penicillium sacculum*. *Natural Product Research 30* (9), 1025-1029.

Liu, W., Gu, Q., Zhu, W., Cui, C. and Fan, G. (**2005a**). Two new benzoquinone derivatives and two new bisorbicillinoids were isolated from a marine-derived fungus *Penicillium terrestre*. *Journal of Antibiotics* (Tokyo) *58* (7), 441-446.

Liu, W., Gu Q., Zhu, W., Cui, C.B. Fan, G., Zhu T., Liu, H. and Fang, Y. (**2005b**). Penicillones A and B, Two Novel Polyketides with Tricyclo [5.3.1.0^{3,8}]undecane Skeleton, from a Marine-Derived Fungus *Penicillium terrestre*. *Tetrahedron Letters 46* (30), 4993-4996.

Liu, W., Gu, Q., Zhu, W., Cui, C. and Fan, G. (**2005c**). Dihydrotrichodimerol and tetrahydrotrichodimerol, two new bisorbicillinoids, from a marine-derived *Penicillium terrestre*. *Journal of Antibiotics* (Tokyo) *58* (10), 621-624.

Liu, Y., Li, X.M., Meng, L.H., Jiang, W.L., Xu, G.M., Huang, C.G. and Wang, B.G. (**2015**). Bisthiodiketopiperazines and Acorane Sesquiterpenes Produced by the Marine-Derived Fungus *Penicillium adametzioides* AS-53 on Different Culture Media. *Journal of Natural Products 78*, 1294-1299.

Liu, W.H., Zhao, H., Li, R.Q., Zheng, H.B. and Yu, Q. (**2015**). Polyketides and Meroterpenoids from *Neosartorya glabra*. *Helvetica Chimica Acta 98*, 515-519.

Lu, Z., Zhu, H., Fu, P., Wang, Y., Zhang, Z., Lin, H., Liu, P., Zhuang, Y., Hong, K. and Zhu, W. (**2010**). Cytotoxic polyphenols from the marine-derived fungus *Penicillium expansum. Journal of Natural Products 73*, 911-914

Lu, K., Zhang, Y., Li, L., Wang, X. and Ding, G. (**2013**). Chaetochromones A and B, two new polyketides from the fungus *Chaetomium indicum* (CBS.860.68). *Molecules 18*, 10944-10952.

Ma, L.Y., Liu, D.S., Li, D.G., Huang, Y.L., Kang, H.H., Wang, C.H. and Liu, W.Z. (**2016**). Pyran Rings Containing Polyketides from *Penicillium raistrickii*. *Marine Drugs 15* (1).

Ma, Y., Li, J., Huang, M., Liu, L., Wang, J., and Lin, Y. (**2015**). Six New Polyketide Decalin Compounds from Mangrove Endophytic Fungus *Penicillium aurantiogriseum* 328#. *Marine Drugs 13*, 6306-6318.

Manimegalai, K., Devi, N.K.A. and Padmavathy, S. (**2013**). Marine fungi as a source of secondary metabolites of antibiotics. *Biotechnology and Bioengineering Research 4* (3), 275-282.

Maridass, M. and Britto, A.J. (**2008**). Origins of Plant Derived Medicines. *Ethnobotanical Leaflets 12*, 373-387.

Masi, M., Bndolft, A., Mathieu, V., Boari, A., Cimmino, A., Banuls, L.M.Y., Vurro, M., Kornienko, A., Kiss, R. and Evidente, A. (**2013**). Fischerindoline, a pyrroloindole sesquiterpenoid isolated from *Neosartorya pseudofischeri* with *in vitro* growth inhibitory activity in human cancer cell lines. *Tetrahedon 69*, 7466-7470.

Matsunaga, S., Fusetani, N. and Konosu, S. (**1985**). Bioactive marine metabolites, VII: structures of discodermins B, C, and D, antimicrobial peptides from the marine sponge *Discodermia kiiensis*. *Tetrahedron Letters 26*, 855-856.

May Zin, W.W., Buttachon, S., Dethoup, T., Pereira, J.A., Gales, L., Inácio, A., Costa, P.M., Lee, M., Sekeroglu, N., Silva, A.M.S., Pinto, M.M.M. and Kijjoa, A. (**2017**). Antibacterial and antibiofilm activities of the metabolites isolated from the culture of the mangrove-derived endophytic fungus *Eurotium chevalieri* KUFA0006. *Phytochemistry* 141, 86-97.

Mayer, A.M., Glaser, K.B., Cuevas, C., Jacobs, R.S., Kem, W., Little, R.D., McIntosh, J.M., Newman, D.J., Potts, B.C. and Shuster, D.E. (**2010**). The odyssey of marine pharmaceuticals: a current pipeline perspective. *Trends in pharmacological sciences 31* (6), 255-265.

Mayer A.M.S. and Gustafson K.R. **(2006)**. Marine pharmacology in 2003–2004: Anti-tumour and cytotoxic compounds. *European Journal of Cancer 42* (14), 2241-2270.

Mayer A.M.S. and Gustafson K.R. **(2008)**. Marine pharmacology in 2005-2006: antitumour and cytotoxic compounds. *European Journal of Cancer 44* (16), 2357-2387.

McGuire, J.M., Bunch, R.L., Anderson, R.C., Boaz, H.E., Flynn, E.H., Powell, H.M. and Smith, J.W. (**1952**). Ilotycin, a new antibiotic. *Antibiot Chemother (Northfield)* 2, 281.

Meng, L.H., Li, X.M., Lv, C.T., Huang, C.G. and Wang, B.G. (**2014**). Brocazines A–F, Cytotoxic Bisthiodiketopiperazine Derivatives from *Penicillium brocae* MA-231, an Endophytic Fungus Derived from the Marine Mangrove Plant *Avicennia marina*. *Journal of Natural Products 77* (8), 1921-1927.

Meng, L.H., Wang, C.Y., Mándi, A., Li, X.M., Hu, X.Y., Kassack, M.U., Kurtán, T. and Wang, B.G. (**2016**). Three Diketopiperazine Alkaloids with Spirocyclic Skeletons and One Bisthiodiketopiperazine Derivative from the Mangrove-Derived Endophytic Fungus *Penicillium brocae* MA-231. *Organic Letters* 21, *18* (20), 5304-5307.

Meng, L.H., Zhang, P., Li, X.M. and Wang, B.G. (**2015**). Penicibrocazines A–E, Five New Sulfide Diketopiperazines from the Marine-Derived Endophytic Fungus *Penicillium brocae*. *Marine Drugs 13* (1), 276–287.

Mildred, C.R., Harry, M.C., John, C. and Quentin, R.B. (**1949**). Chloramphenicol (Chloromycetin).1 IV.1a Chemical Studies. *Journal of the American Chemical Society 71* (7), 2458-2462.

Miquel, S., Lagrafeuille, R., Souweine, B. and Forestier, C. (**2016**). Anti-biofilm activity as a health issue. *Frontiers in Microbiology 7*, 1-14.

Mitchell, G., Bartlett, D.W., Fraser, T.E.M., Hawkes, T.R., Holt, D.C., Townson, J.K. and Wichert, R.A. (**2001**). Mesotrione: a new selective herbicide for use in maize*. Pest Management Science 57*, 120-128.

Montaser, R. and Luesch, H. **(2011)**. Marine natural products: a new wave of drugs? *Future medicinal chemistry 3* (12), 1475-1489.

Murray, M.G. and Thompson, W.F. (**1980**). Rapid isolation of high molecular weight plant DNA. *Nucleic Acids Research 8*, 4321-4325.

Newman, D.J. and Cragg, G.M. **(2007)**. Natural products as sources of new drugs over the last 25 years. *Journal of Natural Products 70*, 461–477.

Newman D.J. and Cragg G.M. **(2016)**. Natural products as sources of new drugs from 1981 to 2014. *Journal of Natural Products 79* (3), 629–661.

Noinart, J., Buttachon, S., Dethoup, T., Gales, L., Pereira, J.A., Urbatzka, R., Freitas, S., Lee, M., Silva, A.M.S., Pinto, M.M.M., Vasconcelos, V. and Kijjoa, A. (**2017**). A New Ergosterol Analog, a New *Bis*-Anthraquinone and Anti-Obesity Activity of Anthraquinones from the Marine Sponge-Associated Fungus *Talaromyces stipitatus* KUFA 0207. *Marine Drugs 15* (5), 139.

Odds, F.C. (**2003**). Synergy antagonism and what the chequerboard puts between them. *Journal of Antimicrobial Chemotherapy 52* (1):1.

Ozoe, Y., Kuriyama, T., Tachibana, Y., Harimaya, K., Takahashi, N., Yaguchi, T., Suzuki, E., Imamura, K.I. and Oyama, K. **(2004)**. Isocoumarin derivative as a novel GABA receptor ligand from *Neosartorya quadricincta*. *Journal of Pesticide Science 29*, 328-331.

Pang, X., Cai, G., Lin, X., Salendra, L., Zhou, X., Yang, B., Wang, J., Xu, S. and Liu, Y. (**2019**). New Alkaloids and Polyketides from the Marine Sponge-Derived Fungus *Penicillium* sp. SCSIO41015. *Marine Drugs 17*, 398.

Park, S.C., Julanti, E., Ahn, S., Kim, D., Lee, S.K., Noh, M., Oh, D.C., Oh, K.B. and Shin, S.K. (**2019**). Phenalenones from a Marine-Derived Fungus *Penicillium* sp. *Marine Drugs 17*, 176.

Pastre, R., Marino, A.M.R., Rodrigues-Son, E., Souza, A.Q.L. and Pereira, J.O. (**2007**). Diversity of polyketides produced by *Penicillium* species isolated from Melia azedarach and *Murraya paniculata*. *Química Nova 30*, 1867-1871.

Patridge, E., Gareiss, P., Kinch, M.S. and Hoye, D. (**2016**). An analysis of FDA-approved drugs: natural products and their derivatives. *Drug Discovery Today 21* (2), 204-207.

Pinheiro, Â., Dethoup, T., Bessa, J., Silva, A.M.S. and Kijjoa, A. (**2012**). A new bicyclic sesquiterpene from the marine sponge associated fungus *Emericellopsis minima*. *Phytochemistry Letters 5* (1), 68-70.

Plaza, A., Gustchina, E., Baker, H.L., Kelly, M. and Bewley, C.A. (**2007**). Mirabamides A–D, depsipeptides from the sponge Siliquari-aspongia mirabilis that inhibit HIV-1 fusion. *Journal of Natural Products 70*, 1753-1760.

Pongpuntaruk, J. (**2010**). *Chemical constituents from the stem of punica granatum and the root of mechelia alba*, (Master dissertation). Prince of Songkla University, Thailand, 138p.

Prachayasittikul, S., Suphapong, S, Worachartcheewan, A, Lawung, R., Ruchirawat, S. and Prachayasittikul, V. (**2009**). Bioactive Metabolites from *Spilanthes acmella* Murr. *Molecules 14* (2), 850–867.

Prata-Sena, M., Ramos, A.A., Buttachon ,S., Castro-Carvalho, B., Marques, P., Dethoup, T., Kijjoa, A. and Rocha, E. (**2016**). Cytotoxic activity of Secondary Metabolites from Marine-derived Fungus *Neosartorya siamensis* in Human Cancer Cells. *Phytotherapy Research 30* (11), 1862-1871.

Proksa, B., Uhrín, D., Liptaj, T. and Sturdíková, M. (**1998**). Neosartorin, and ergochrome biosynthesized by *Neosartorya fischri. Phytochemistry 48*, 1161-1164.

Prompanya C., (**2018**). Study of bioactive secondary metabolites from the marine sponges and marine sponge - associated fungi. Thesis, institute of Biomedical Sciences Abel Salazar of the University of Porto.

Prompanya, C., Dethoup, T., Gales, L., Lee, M., Pereira, J. A., Silva, A., Pinto, M. M., and Kijjoa, A. (**2016**). New polyketides and new benzoic acid derivatives from the marine sponge-associated fungus *Neosartorya quadricincta* KUFA 0081. *Marine Drugs 14*, 134.

Qader, M.M., Kumar, N.S., Jayasinghe, L. and Fujimoto, Y. (**2015**). Production of Antitumor Antibiotic GKK1032B by *Penicillium citrinum*, an Endophytic Fungus Isolated from *Garcinia mangostana* Fruits. *Medicinal and Aromatic Plants 5* (1), 255-261.

Qureshi, A. and Faulkner, D.J. (**1999**). Haplosamates A and B: new steroidal sulfamate esters from two haplosclerid sponges. *Tetrahedron 55*, 8323-8330.

Ragasa, C.Y., Torres, O. B. and Soriano, G. (**2013**). Sterols and Triterpenes From the Fruit of *Annona muricata* Linn. *Silliman Journal 54* (1), 107-112.

Raistrick, H. and Smith, G. (**1933**). Studies in the biochemistry of micro-organisms*. Biochemical Journal, 27* (6), 1814–1819.

Rajachan, O., Kanokmedhakul, K., Sanmanoch, W., Boonlue, S., Hannongbua, S., Saparpakorn, P. and Kanokmedhakul, S. (**2016**). Chevalone C analogues and globoscinic acid derivatives from the fungus *Neosartorya spinosa* KKU-1NK1. *Phytochemistry 132*, 68-75.

Rajamani, S., Bauer, W.D., Robinson, J.B., Farrow, J.M.III, Pesci, E.C., Teplitski, M., Gao, M., Sayre, R.T. and Phillips, D.A. (**2008**). The Vitamin Riboflavin and Its Derivative Lumichrome Activate the LasR Bacterial Quorum-Sensing Receptor. *Molecular Plant-Microbe Interactions 21*, 1184-1192.

Rateb, M. E. and Ebel, R. (**2011**). Secondary metabolites of fungi from marine habitats. *Natural Product Reports 28* (2), 290-344.

Rates, S.M.K. (**2001**). Plants as source of drugs. *Toxicon 39*, 603-613.

Rohmer, M., Anding, C. and Ourisson, G. (**1980)**. Non-specific biosynthesis of hopane triterpenes by a cell-free system from *Acetobacter pasteurianum*. *European Journal of Biochemistry 112* (3), 541-547.

Rowley, D.C., Kelly, S., Kauffman, C.A., Jensen, P.R. and Fenical, W. (**2003**). Halovirs A–E, new antiviral agents from a marine-derived fungus of the genus Scytalidium. *Bioorganic and Medicinal Chemistry Letters 11*, 4263-4274.

Rukachaisirikul, V., Satpradit, S., Klaiklay, S., Phongpaichit, S., Borwornwiriyapan, K. and Sakayaroj, J. *(***2014**). Polyketide anthraquinone, diphenyl ether, and xanthone derivatives from the soil fungus *Penicillium* sp. PSU- RSPG99. *Tetrahedron 70*, 5148-5152.

Sakthivel, N., Amudha, R. and Muthukrishnan, S**.** (**2002**). Production of phytotoxic metabolites by *Sarocladium oryzae*. *Mycological Research* 106, 609-614.

Salehi, B., Sestito, S., Rapposelli, S., Peron, G., Calina, D., Rad, M.S., Sharopov, F., Martins, N. and Rad, J.S. (**2019**). Epibatidine: A Promising Natural Alkaloid in Health. *Biomolecules 9* (1), 6.

Samson R.A., Hong S., Peterson S.W., Frisvad J.C. and Varga J. (**2007**). Polyphasic taxonomy of *Aspergillus* section *Fumigati* and its teleomorph *Neosartorya*. *Studies in Mycology 59*, 147-203.

Sanger, F., Nicklen, S. and Coulson, A.R. (**1977**). DNA sequencing with chain-terminating inhibitors. *Proceedings of the National Academy of Sciences of the United States of America* 72, 5463-5467.

Sanmanoch, W., Mongkolthanaruk, W., Kanokmedhakul, S., Aimi, T. and Boonlue, S. (**2016**). Helvolic Acid, A Secondary Metabolite Produced by *Neosartorya spinosa* KKU-1NK1 and Its Biological Activities. *Chiang Mai Journal of Science 43* (43), 1-11.

Sasaki, M., Tsuda, M., Sekiguchi, M., Mikami, Y. and Kobayashi, J. (**2005**). Perinadine A, a Novel Tetracyclic Alkaloid from Marine-Derived Fungus *Penicillium citrinum*. *Organic letters 7* (19), 4261-4264.

Sasaki, M., Takamatsu, H., Oshita, K., Yukio, Kaneko, Y. and Yokotsuka, T. (**1974**). Isolation of lumichrome from the culture filtrate of *Aspergillus oniki* 1784. *Nippon Nōgeikagaku Kaishi 48*, 569–571.

Sawadsitang, S., Mongkolthanaruk, W., Suwannasai, N. and Sodngam, S. (**2015**). Antimalarial and cytotoxic constituents of *Xylaria* cf. *cubensis* PK108*. Natural Product Research 29* (21), 2033-2036.

Schlesinger, N., Schumacher, R., Catton, M. and Maxwell, L. (**2006**). Colchicine for acute gout. Cochrane Database Syst Rev. 2006;4:CD006190.

Schmitz, R. (**1985**). Friedrich Wilhelm Sertürner and the discovery of morphine. *Pharmacy in History 27*, 61-74.

Sgarbi, D.B., Silva, A.J., Carlos, I.Z., Silva, C.L., Angluster, J. and Alviano, C.S. (**1997**). Isolation of ergosterol peroxide and its reversion to ergosterol in the pathogenic fungus *Sporothrix schenckii*. *Mycopathologia 139* (1), 9-14.

Shah, N.C. **(2010)**. My Experience with the Herbal plants & Drugs as I Know Part xvi: *Dioscorea* and *Costus*. Herbal tech Industry, pp21:30.

Shan, W., Wang, S., Ying, Y., Ma, L. and Zhan, Z. (**2014**). Indole-benzodiazepine-2, 5-dione derivatives from *Neosartorya fischeri*. *Journal of Chemical Research 38*, 692-694.

Shao, C.L., Wang, C.Y., Zheng, C.J., She, Z.G., Gu, Y.C. and Lin, Y.C. (**2010**). A new anthraquinone derivative from the marine endophytic fungus *Fusarium* sp. (No. b77). *Natural Product Research 24*, 81-85.

Sheldrick, G.M. (**2008**). A short story of SHELX. *Acta Crystallographica 64*, 112–122.

Shen, S., Li, W. and Wang, J. (**2013**). A novel and other bioactive secondary metabolites from a marine fungus *P. oxalicum* 0312F1. *Natural Product Research 27* (24), 2286-2291.

Shen, S., Li, W., Ouyang, M.A., Wu, Z.J., Lin, Q.Y. and Xie, L.H. (**2009**). Identification of two marine fungi and evaluation of their antivirus and antitumor activities. *Acta Microbiologica Sinica 49*, 1240-1246.

Shin, H.J., Pil, G.B., Heo, S.J., Lee, H.S., Lee, J.S., Lee, Y.J., Lee, J. and Won, H.S. (**2016**). Anti-Inflammatory Activity of Tanzawaic Acid Derivatives from a Marine-Derived Fungus *Penicillium steckii* 108YD142. *Marine Drugs 14* (1), 14.

Silva, M., Vieira, L.M.M., Almeida, A.P., Silva, A.M.S., Seca, A.M.l., Barreto, M.C, Neto, A.I., Pedro, M., Pinto, E. and Kijjoa, A. (**2013**). Chemical Study and Biological Activity Evaluation of Two Azorean Macroalgae. *Ulva rigida* and *Gelidium microdon*. *Journal of Oceanography and Marine Research* 1, 102.

Simões, R.R., Aires-de-Sousa, M., Conceicao, T., Antunes, F., da Costa, P.M. and Lencastre, H. (**2011**). High prevalence of EMRSA-15 in Portuguese public buses: A worrisome finding. *PLoS ONE*, 6, e17630.

Sodngam S., Sawadsitang, S., Suwannasai, N. and Mongkolthanaruk, W. (**2013**). Chemical constituents, and their cytotoxicity, of the rare wood decaying fungus *Xylaria humosa*. *Natural product communications 9* (2), 157-158.

Song, F., Ren, B., Yu, K., Chen, C., Guo, H., Yang, N., Gao, H., Liu, X., Liu, M., Tong, Y., Dai, H., Bai, H., Wang, J. and Zhang, L. (**2012**). Quinazolin-4-one Coupled with Pyrrolidin-2-iminium Alkaloids from Marine-Derived Fungus *Penicillium aurantiogriseum*. *Marine Drugs 10*, 1297-1306.

Song, T., Chen, M., Chai, W., Zhang, Z., and Lian, X.Y. (**2018**). New bioactive pyrrospirones C−I from a marine-derived fungus *Penicillium* sp. ZZ380. *Tetrahedron 74* (8), 884-891.

Song, T., Tang, M., Ge, H., Chen, M., Lian, X. and Zhang. (**2019**). Novel Bioactive Penicipyrroether A and Pyrrospirone J from the Marine-Derived *Penicillium* sp. ZZ380. *Marine Drugs 17*, 292

Stepanović, S., Vuković, D., Dakic, I., Savić, B. and Švabic-Vlahović, M. (**2000**). A modified -plate test for quantification of staphylococcal biofilm formation. *Journal of Microbiological Methods 40*, 175-179.

Stepanović, S., Vuković, D., Hola, V., Di Bonaventura, G., Djukić, S., Ćirković, I. and Ruzicka, F. (**2007**). Quantification of biofilm in microtiter plates: Overview of testing conditions and practical recommendations for assessment of biofilm production by staphylococci. *APMIS* 115, 891-899.

Stephens, P.J. and Harada, N. (**2010**). ECD Cotton effect approximated by the Gaussian curve and other methods. *Chirality 22*, 229-233.

Sun, F-Y., Chen, G., Bai, J., Li, W. and Pei, Y.H. (**2012**). Two new alkaloids from a marine-derived fungus *Neosartorya* sp.HN-M-3. *Journal of Asian Natural Products Research* 14 (12), 1109-1115.

Sun, Y.L., He, F., Liu, K.S., Zhang, X.Y., Wang, Y.F., Nong, X.H., Xu, X.Y. and Qi, S.H. (**2012**). Cytotoxic Dihydrothiophene-Condensed Chromones from Marine-Derived Fungus *Penicillium oxalicum. Planta Medica 78* (18) 1957-1961.

Tacconelli, E., Carrara, E., Savoldi, A., Harbarth, S., Mendelson, M., Monnet, D.L., Pulcini, C., Kahlmeter, G., Kluytmans, J. and Carmeli, Y. (**2017**). Discovery, research, and development of new antibiotics: The WHO priority list of antibiotic-resistant bacteria and tuberculosis. *Lancet Infectious Diseases.18*, 318-327.

Tan, Q., Ouyang, M., Shen, S. and Li, W. (**2012**). Bioactive metabolites from a marine-derived strain of the fungus *Neosartorya fischeri. Natrual Product Research 26*, 1402-1407.

Tanaka, R., Mizota, T. and Matsunaga, S. (**1994**). Saturated Gammaceranes from the Stem Bark of *Abies mariesii*. *Journal of Natural Products 57* (6), 761-766.

Tanaka, R. and Matsunaga, S. (**1992**). Saturated hopane and gammacerane triterpene-duils from the stem bark of *Abies veitchii*. *Phytochemisty 31*, 3535–3539.

Tolkachev, O.N., Abizov, E.A., Abizova, E.V. and Mal'tsev, S.D. (**2008**). Phytochemical study of the bark of some plants of the Elaeagnaceae family as a natural source of β-carboline indole alkaloids*. Pharmaceutical Chemistry Journal 42* (11), 630–632.

Torre, B.G. and Albericio, F. (**2019**). The Pharmaceutical Industry in 2018. An Analysis of FDA Drug Approvals from the Perspective of Molecules. *Molecules 24* (4), 809.

Torres, Y.R., Berlink, R.G., Nascimento, G.G., Fortier, S.C., Pessoa, C. and Moraes, M.O. (**2002**). Antibacterial activity against resistant bacteria and cytotoxicity of four alkaloid toxins isolated from the marine sponge *Arenosclera brasiliensis*. *Toxicon 40*, 885-891.

Tsuda, M., Sasaki, M., Mugishima, T., Komatsu, K., Sone, T., Tanaka, M., Mikami, Y. and Kobayashi, J. (**2005**). Scalusamides A-C, New Pyrrolidine Alkaloids from the Marine-Derived Fungus *Penicillium citrinum*. *Journal of Natural Products 68*, 273-276.

Urban, S., Almeida, L.P., Carroll, A.R., Fechner, G.A., Smith, J., Hooper, J.N. and Quinn, R.J. (**1999**). Axinellamines A–D, novel imidazo-azolo-imidazole alkaloids from the australian marine sponge *Axinella* sp. *The Journal of Organic Chemistry 64*, 731-735.

Verpoorte, R. (**1998**). Exploration of nature's chemodiversity: the role of secondary metabolites as leads in drug development. *Drug DiscoveryToday* 3, 232-238.

Wakana, D., Hosoe, T., Itabashi, T., Nozawa, K., Okadaa, K., Takaki, G.M.C., Yaaguchi, T., Fukushima, K. and Kawai, K. (**2006**). Isolation of isoterrein from *Neosartorya fischeri. Mycotoxins 56* (1), 3-6.

Wang, H., Wang, Y., Wang, W., Fu, P., Liu, P. and Zhu, W. (**2011**). Anti-influenza Virus Polyketides from the Acid-Tolerant Fungus *Penicillium purpurogenum* JS03-21. *Journal of Natural Products 74* (9), 2014-2018.

Wang, M.H., Li, X.M., Li, C.S., Ji, N.Y. and Wang, B.G. (**2013**). Secondary Metabolites from *Penicillium pinophilum* SD-272, a Marine Sediment-Derived Fungus. *Marine Drugs 11* (6), 2230-2238.

Wang, W., Liao, Y., Zhang, B., Gao, M., Ke, W., Li, F. and Shao, Z. (**2019**). Citrinin Monomer and Dimer Derivatives with Antibacterial and Cytotoxic Activities Isolated from the Deep Sea-Derived Fungus *Penicillium citrinum* NLG-S01-P1. *Marine Drugs 17* (46).

Wang, R., Guo, Z.K., Li, X.M., Chen, F.X., Zhan, X.F. and Shen, M.H. (**2015**). Spiculisporic acid analogues of the marine-derived fungi, *Aspergillus candidas* strain HDf2, and their antibactial activity. *Antonie van Leeuwhoek* 108, 215-219.

White, T.J., Bruns, T., Lee, S. and Taylor, J. (**1990**). Amplification and direct sequencing of fungal ribosomal RNA genes for phylogenetics. In *PCR Protocols: A Guide to Methods and Applications*; Innis, M.A., Gelfand, D.H., Sninsky, J.J., White, T.J., Eds.; Academic Press: New York, NY, USA, pp. 315-322.

Williams, P.G., Asolkar, R.N., Kondratyuk, T., Pezzuto, J.M., Jensen, P.R. and Fenical, W. (**2007**). Saliniketals A and B, bicyclic polyketides from the marine actinomycete *Salinispora arenicola*. *Journal of Natural Products 1*, 83-88.

Wong, S., Musza, L.L., Kydd, G.C., Kullnig, R., Gillum, A.M. and Cooper, R. (**1993**). Fiscalins: new substance P inhibitors produced by the fungus *Neosartorya fischeri. The Journal of Antibiotics 46*, 545-553.

Wrigley, S.K., Latif, M.A., Gibson, T.M., Chicarelli-Robinson, M.I. and Williams, D.H. (**1994**). Structure elucidation of xanthone derivatives with CD4-binding activity from *Penicillium glabrum* (Wehmer) Westling. *Pure and Applied Chemistry 66*, 2383-2386.

Wrońska, A.K., Boguś, M.I., Kaczmarek, A. and Kazek, M. (**2018**). Harman and norharman, metabolites of entomopathogenic fungus *Conidiobolus coronatus* (Entomopthorales), disorganize development of *Galleria mellonella* (Lepidoptera) and affect serotonin-regulating enzymes*. PLOS ONE 13* (10).

Wu, B., Chen, G., Liu, Z. and Pei, Y. (**2015**). Two New Alkaloids from a Marine-derived Fungus *Neosartorya fischeri*. *Records of Natural Products 9* (3), 271-275.

Wu, B., Oesker, V., Wiese, J., Schmaljohann, R. and Imhoff, J.F. (**2014**). Two new antibiotic pyridones produced by a marine fungus, *Trichoderma* sp. strain MF106. *Marine Drugs 12* (3), 1208-1219.

Wu C.J., Yi L., Cui C.B., Li C.W., Wang N. and Han X. (**2015**). Activation of the silent secondary metabolite production by introducing neomycin-resistance in a marine-derived *Penicillium purpurogenum* G59. *Marine Drugs 13*, 2465-2487.

Wu, H.Y., Yang, F.L., Li, L.H., Rao, Y.K., Ju, T.C., Wong, W.T., Hsieh, C.Y., Pivkin, M.V., Hua, K.F. and Wu, S.H. (**2018**). Ergosterol peroxide from marine fungus *Phoma* sp. induces ROS-dependent apoptosis and autophagy in human lung adenocarcinoma cells. *Scientific Reports 8*, 17956.

Xia, M.W., Cui, C.B., Li, C.W., Wu, C.J., Peng, J.X. and Li, D.H. (**2015**). Rare Chromones from a Fungal Mutant of the Marine-Derived *Penicillium purpurogenum* G59. *Marine Drugs 13*, 5219-5236.

Xie, C.L., Zhang, D., Xia, J.M., Hu, C.C., Lin, T., Lin, Y.K., Wang, G.H., Tian, W.J., Li, Z.P., Zhang, X.K., Yang, X.W. and Chen, H.F. (**2019**). Steroids from the Deep-Sea-Derived Fungus *Penicillium granulatum* MCCC 3 A0 0 4 7 5 Induced Apoptosis via Retinoid X Receptor (*RXR*) α Pathway. *Marine Drugs 19*, 17 (3).

Xin, Z.H., Tian, L., Zhu, T.J., Wang, W.L., Du, L., Fang, Y.C., Gu, Q.Q. and Zhu, W.M. (**2007**). Isocoumarin Derivatives from the Sea Squirt-derived Fungus *Penicillium stoloniferum* QY2-10 and the Halotolerant Fungus *Penicillium notatum* B-52. *Archives of Pharmacal Research 30* (7), 816-819.

Xu, X. Zhang, X., Nong, X., Wang, J. and Qi, S. (**2017**). Brevianamides and Mycophenolic Acid Derivatives from the Deep-Sea-Derived Fungus *Penicillium brevicompactum* DFFSCS025. *Marine Drugs 15* (2), 43.

Yamaguchi, H., Nakayama, Y., Takeda, K., Tawara, K., Maeda, K., Takeuchi, T., Umezawa, H. (**1957**). A new antibiotic, althiomycin. *The Journal of Antibiotics* (Tokyo) *10*, 195-200.

Yamamoto, K. and Asano, Y. (**2015**). Efficient Production of Lumichrome by *Microbacterium* sp. Strain TPU 3598. *Applied and Environmental Microbiology 81*, 7360-7367.

Yan, H.J., Gao, S.S., Li, C.S., Li, X.M. and Wang, B.G. (**2010**). Chemical constituents of a marine-derived endophytic fungus *Penicillium commune* G2M. *Molecules* 15 (5), 3270-3275.

Yang, B., Sun, W., Wang, J., Lin, S., Li, X.N., Zhu, H., Luo, Z., Xue, Y., Hu, Z. and Zhang, Y. (**2018**). A New Breviane Spiroditerpenoid from the Marine-Derived Fungus *Penicillium* sp. TJ403-1. *Marine Drugs 16* (4).

Yim, T., Kanokmedhakul, K., Kanokmedhakul, S., Sanmanoch, W. and Boonlue, S. (**2014**). A new meroterpenoid tatenoic acid from the fungus *Neosartorya tatenoi* KKU-2NK23. *Natural Product Research 28* (21), 1847-1852.

Ying, Y.M., Huang, L., Tian, T., Li, C.Y., Wang, S.L., Ma, L.F. and Zhan, Z.J. (**2018**). Studies on the Chemical Diversities of Secondary Metabolites Produced by *Neosartorya fischeri* via the OSMAC Method. *Molecules 23* (11), 2772.

You, F., Han, T., Wu, J.-z., Huang, B.-k., and Qin, L.-p. (**2009**). Antifungal secondary metabolites from endophytic *Verticillium* sp. *Biochemical Systematics and Ecology 37*, 162-165.

Youssef, D.T.A. and Alahdal, A.M. (**2018**). Cytotoxic and Antimicrobial Compounds from the Marine-Derived Fungus, *Penicillium* Species. *Molecules 23* (2).

Yu, G., Wang, S., Wang, L., Che, Q4. Zhu, T., Zhang, G., Gu, Q., Guo, P. and Li, D. (**2018**). Lipid-Lowering Polyketides from the Fungus *Penicillium Steckii* HDN13-279. *Marine Drugs 12*, 16 (1).

Yu, G., Zhou, G., Zhu, M., Wang, W., Zhu, T., Gu, Q. and Li, D. **(2016**). Neosartoryadins A and B, Fumiquinazoline Alkaloids from a Mangrove-Derived Fungus *Neosartorya udagawae* HDN13-313. *Organic Letters 18* (2), 244-247.

Yu, J., Han, H., Zhang, X., Ma, C., Sun, C., Che, Q., Gu, Q., Zhu, T., Zhang, G. and Li, D. (**2019**). Discovery of Two New Sorbicillinoids by Overexpression of the Global Regulator LaeA in a Marine-Derived Fungus *Penicillium dipodomyis* YJ-11. *Marine Drugs 17* (8).

Yu, K., Ren, B., Wei, J., Chen, C., Sun, J., Song, F., Dai, H. and Zhang, L. (**2010**). Verrucisidinol and Verrucosidinol Acetate, Two Pyrone-Type Polyketides Isolated from a Marine Derived Fungus, *Penicillium aurantiogriseum*. *Marine Drugs 8*, 2744-2754.

Yuan, C., Wang, H.Y., Wu, C.S., Jiao, Y. Li, M. Wang, Y.Y. Wang, S.Q. Zhao, Z.T. and Lou, H.X. (**2013**). Austdiol, fulvic acid and citromycetin derivative from an endolichenic fungus, *Myxotrichum* sp. *Phytochemistry Letters 6*, 662-666.

Yue, J.M., Chen, S.N., Lin, Z.W. and Sun, H.D. (**2001**). Sterols from the fungus *Lactarium volemus*. *Phytochemistry 56*, 801-806.

Zeng, Y., Wang, H., Kamdem, R.S.T., Orfali, R.S., Dai, H., Makhloufi, G., Janiak, C., Liu, Z. and Proksch, P. (**2016**). A new cyclohexapeptide, penitropeptide and a new polyketide, penitropone from the endophytic fungus *Penicillium tropicum*. *Tetrahedron Letters 57*, 2998-3001.

Zhang, H.M., Ju, C.X., Li, G., Sun, Y., Peng, Y., Li, Y.X., Peng, X.P. and Lou, H.X. (**2019**). Dimeric 1,4-benzoquinone Derivatives with Cytotoxic Activities from the Marine-Derived Fungus *Penicillium* sp. L129. *Marine Drugs 17* (7).

Zhang, M., Wang, W.L., Fang, Y.C., Zhu, T.J., Gu, Q.Q. and Zhu, W.M. (**2008**). Cytotoxic alkaloids and antibiotic nordammarane triterpenoids from the marine-derived fungus Aspergillus sydowi. *Journal of Natural Products 71*, 985-989.

Zhang, P., Li, X.M., Liu, H., Li, X. and Wang, B.G. (**2015**). Two new alkaloids from *Penicillium oxalicum* EN-201, an endophytic fungus derived from the marine mangrove plant *Rhizophora stylosa*. *Phytochemistry Letters 13*, 160-164.

Zhang, P., Meng, L.H., Mándi, A., Kurtán, T., Li, X.M., Liu, Y. and Wang, B.G. (**2014**). Brocaeloids A-C, 4-oxoquinoline and indole alkaloids with C-2 reversed prenylation from the mangrove-derived endophytic fungus *Penicillium brocae*. *European Journal of Organic Chemistry* (19), 4029-4036.

Zhao, D.L., Shao, C.L., Zhang, Q., Wang, K.L., Guan, F.F., Shi, T. and Wang, C.Y. (**2015**). Azaphilone and Diphenyl Ether Derivatives from a Gorgonian-Derived Strain of the Fungus *Penicillium pinophilum*. *Journal of Natural Products 78* (9), 2310-2314.

Zhao, J., Mou, Y., Shan, T., Li, Y., Zhou, L., Wang, M. and Wang, J. (**2010**). Antimicrobial Metabolites from the Endophytic Fungus *Pichia guilliermondii* Isolated from *Paris polyphylla* var. *yunnanensis. Molecules 15*, 7961-7970.

Zheng, C.J., Huang, G.L., Xu, Y., Song, X.M., Yao, J., Liu, H., Wang, R.P. and Sun, X.P. (**2016**). A new benzopyrans derivatives from a mangrove-derived fungus *Penicillium citrinum* from the South China Sea, *Natural Product Research 30* (7), 821-825.

Zheng, Y.Y., Liang, Z.Y., Shen, N.X., Liu, W.L., Zhou, X.J., Fu, X.M., Chen, M. and Wang, C.Y. (**2019**). New Naphtho-γ-Pyrones Isolated from Marine-Derived Fungus *Penicillium* sp. HK1-22 and Their Antimicrobial Activities. *Marine Drugs 17*, 322.

Zheng, Z.Z., Shan, W.G., Wang, S.L., Ying, Y.M., Ma, L.F. and Zhan, Z.J. (**2014**). Three new prenylated diketopiperazines from *Neosartorya fischeri*. *Helvetica Chimica Acta 97*, 1020-1026.

Zhu, H., Hua, X.X., Gong, T., Pang, J., Hou, Q. and Zhu, P. (**2013**). Hypocreaterpenes A and B, cadinane-type sesquiterpenes from a marine-derived fungus, *Hypocreales* sp. *Phytochemistry Letters 6*, 392-396.

Zhuravleva, O.I., Sobolevskaya, M.P., Leshchenko, E.V., Kirichuk, N.N., Denisenko, V.A., Dmitrenok, P.S., Dyshlovoy, S.A., Zakharenko, A.M., Kim, N.Y. and Shamil, S. (**2014a**). Afiyatullov. Meroterpenoids from the Alga-Derived Fungi *Penicillium thomii* Maire and *Penicillium lividum* Westling. *Journal of Natural Products 77*, 1390-1395.

Zhuravleva, O.I., Sobolevskaya, M.P., Afiyatullov, S.S., Kirichuk, N.N., Denisenko, V.A., Dmitrenok, P.S., Yurchenko, E.A. and Dyshlovoy, S.A. **(2014b)**. Sargassopenillines A–G, 6,6-Spiroketals from the Alga-Derived Fungi *Penicillium thomii* and *Penicillium lividum*. *Marine Drugs 12* (12), 5930-5943.

Zin, W.W.M., Buttachon, S., Buaruang, J., Gales, L, Pereira, J.A., Pinto, M.M.M., Silva, A.M.S. and Kijjoa, A. (**2015**). A New Meroditerpene and a New Tryptoquivaline Analog from the Algicolous Fungus *Neosartorya takakii* KUFC 7898. *Marine Drugs 13*, 3776-3790.

Zin, W.W.M., Buttachon, S., Dethoup, T., Fernandes, C., Cravo, S., Pinto, M.M.M., Gales, L., Pereira, J.A., Silva, A.M.S., Sekeroglu, N. and Kijjoa, A. (**2016**). New Cyclotetrapeptides and a New Diketopiperzine Derivative from the Marine Sponge-Associated Fungus *Neosartorya glabra* KUFA 0702. *Marine Drugs 14* (7), 136-150.

APPENDICES

APPENDIX I

Kumla, D., Aung T.S., Buttachon S., Dethoup T., Gales L., Pereira J.A., Inácio A., Costa P.M., Lee M., Sekeroglu N., Silva A.M.S, Pinto M.M.M. and Kijjoa A. **2017**. A New Dihydrochromone Dimer and Other Secondary Metabolites from Cultures of the Marine Sponge-Associated Fungi *Neosartorya fennelliae* KUFA 0811 and *Neosartorya tsunodae* KUFC 9213. *Mar. Drugs 15* (12), 375.

marine drugs

MDPI

Article

A New Dihydrochromone Dimer and Other Secondary Metabolites from Cultures of the Marine Sponge-Associated Fungi *Neosartorya fennelliae* KUFA 0811 and *Neosartorya tsunodae* KUFC 9213

Decha Kumla [1,2,†], Tin Shine Aung [1,2,†], Suradet Buttachon [1,2], Tida Dethoup [3], Luís Gales [1,4], José A. Pereira [1,2], Ângela Inácio [2], Paulo M. Costa [1,2], Michael Lee [5], Nazim Sekeroglu [6], Artur M. S. Silva [7], Madalena M. M. Pinto [2,8] and Anake Kijjoa [1,2,*]

1 ICBAS-Instituto de Ciências Biomédicas Abel Salazar, Rua de Jorge Viterbo Ferreira, 228, 4050-313 Porto, Portugal; decha1987@hotmail.com (D.K.); tinshineaung@gmail.com (T.S.A.); nokrari_209@hotmail.com (S.B.); lgales@ibmc.up.pt (L.G.); jpereira@icbas.up.pt (J.A.P.); pmcosta@icbas.up.pt (P.M.C.)

2 Interdisciplinary Centre of Marine and Environmental Research (CIIMAR), Terminal de Cruzeiros do Porto de Lexões, Av. General Norton de Matos s/n, 4450-208 Matosinhos, Portugal; angelainacio@gmail.com (A.I.); madalena@ff.up.pt (M.M.M.P.)

3 Department of Plant Pathology, Faculty of Agriculture, Kasetsart University, Bangkok 10240, Thailand; tdethoup@yahoo.com

4 Instituto de Biologia Molecular e Celular (i3S-IBMC), Universidade do Porto, Rua de Jorge Viterbo Ferreira, 228, 4050-313 Porto, Portugal

5 Department of Chemistry, University of Leicester, University Road, Leicester LE1 7RH, UK; ml34@leicester.ac.uk

6 Medicinal and Aromatic Plant Programme, Plant and Animal Sciences Department, Vocational School, Kilis 7 Aralık University, Kilis 79000, Turkey; nsekeroglu@gmail.com

7 Departamento de Química & QOPNA, Universidade de Aveiro, 3810-193 Aveiro, Portugal; artur.silva@ua.pt

8 Laboratório de Química Orgânica, Departamento de Ciências Químicas, Faculdade de Farmácia, Universidade do Porto, Rua de Jorge Viterbo Ferreira, 228, 4050-313 Porto, Portugal

* Correspondence: ankijjoa@icbas.up.pt; Tel.: +351-22-0428331; Fax: +351-22-2062232

† These authors contributed equally to this work.

Received: 4 November 2017; Accepted: 24 November 2017; Published: 1 December 2017

Abstract: A previously unreported dihydrochromone dimer, paecilin E (**1**), was isolated, together with eleven known compounds: β-sitostenone, ergosta-4,6,8 (14), 22-tetraen-3-one, cyathisterone, byssochlamic acid, dehydromevalonic acid lactone, chevalone B, aszonalenin, dankasterone A (**2**), helvolic acid, secalonic acid A and fellutanine A, from the culture filtrate extract of the marine sponge-associated fungus *Neosartorya fennelliae* KUFA 0811. Nine previously reported metabolites, including a chromanol derivative (**3**), (3β, 5α, 22*E*), 3,5-dihydroxyergosta-7,22-dien-6-one (**4**), byssochlamic acid, hopan-3β,22-diol, chevalone C, sartorypyrone B, helvolic acid, lumichrome and the alkaloid harmane were isolated from the culture of the marine-sponge associated fungus *Neosartorya tsunodae* KUFC 9213. Paecilin E (**1**), dankasterone A (**2**), a chromanol derivative (**3**), (3β, 5α, 22*E*)-3,5-dihydroxyergosta-7,22-dien-6-one (**4**), hopan-3β,22-diol (**5**), lumichrome (**6**), and harmane (**7**) were tested for their antibacterial activity against Gram-positive and Gram-negative reference and multidrug-resistant strains isolated from the environment. While paecilin E (**1**) was active against *S. aureus* ATCC 29213 and *E. faecalis* ATCC 29212, dankastetrone A (**2**) was only effective against *E. faecalis* ATCC 29212 and the multidrug-resistant VRE *E. faecalis* A5/102. Both compounds neither inhibit biofilm mass production in any of the strains at the concentrations tested nor exhibit synergistic association with antibiotics.

Keywords: *Neosartorya fennelliae*; *Neosartorya tsunodae*; Trichocomaceae; dihydrochromone dimer; paecilin E; dankasterone A; chromanol derivative; marine sponge-associated fungi; antibacterial activity

1. Introduction

In the past decade, marine-derived fungi have increasingly become an important source of bioactive marine natural products, since many consider them among the world's greatest resources for unprecedented biodiversity and chemodiversity. Moreover, with established methods of cultivation, they can produce quantity of compounds with potential for medicinal chemistry development, clinical trials and marketing [1]. The fungi belonging to the genus *Neosartorya* (Trichocomaceae) have been revealed to be an important source of interesting bioactive metabolites such as polyketides, isocoumarins, ergosterol analogs, meroditerpenes, pyripyropenes, benzoic acid derivatives, prenylated indole derivatives, tryptoquivalines, fiscalins, phenylalanine-derived alkaloids and cyclopeptides [2]. Marine-derived fungi are also known to produce a myriad of structurally unique metabolites not produced by their terrestrial counterparts [3]. Our group has recently isolated and identified meroditerpene analogs and the indole alkaloids, from some marine-derived fungi from the genus *Neosartorya*, with interesting antibacterial activity against Gram-positive bacteria (*S. aureus* and *B. subtillis*) and multidrug-resistant isolates from the environment (MRSA and VRE). Some of these compounds also had synergistic effects with antibiotics to which the bacteria are resistant. Some of these compounds also inhibit biofilm formation at MIC [4].

In our ongoing search for new natural antibiotics from marine-derived fungi, we have investigated secondary metabolites from the culture of *Neosartorya fennelliae* KUFA 0811, isolated from the marine sponge *Clathria reinwardtii*, collected from Samaesan Island in the Gulf of Thailand. Previously, we only isolated two compounds from the marine sponge-associated *N. tsunodae* KUFC 9213 [5], therefore we have cultured this fungus to reexamine its secondary metabolites.

Chromatographic fractionation and further purification of the ethyl acetate extract of *N. fennelliae* KUFA 0811, yielded a previously undescribed 2,3-dihydro-4*H*-chromen-4-one dimer which we have named paecilin E (**1**), in addition to the previously described dehydromevalonic acid lactone [6], byssochlamic acid [7], β-sitostenone [8], ergosta-4,6,8 (14), 22-tetraen-3-one [9], cyathisterone [10], dankasterone A (**2**) [11], chevalone B [12], helvolic acid [5], aszonalenin [13], secalonic acid A [14] and fellutanine A [13]. The ethyl acetate extract of *N. tsunodae* KUFC 9213 furnished, besides sartorypyrone B and helvolic acid which were previous isolated in our first study [5], byssochlamic acid [7], hopan-3β,22-diol (**5**) [15], chevalone C [16], a chromanol derivative (**3**) [17,18], (3β,5α,22*E*)-3,5-dihydroxyergosta-7,22-dien-6-one (**4**) [19], the alkaloid harmane (**7**) [20], and lumichrome (**6**) [21].

Paecilin E (**1**), dankasterone A (**2**), a chromanol derivative (**3**), (3β,5α,22E)-3,5-dihydroxyergosta-7,22-dien-6-one (**4**), hopan-3β,22-diol (**5**), lumichrome (**6**) and harmane (**7**), (Figure 1) were tested for their growth inhibitory activity against two Gram-positive (*Staphylococcus aureus* ATCC 29213 and *Enterococcus faecalis* ATCC 29212), two Gram-negative (*Escherichia coli* ATCC 25922 and *Pseudomonas aeruginosa* ATCC 27853) bacteria, a clinical isolate sensitive to the most commonly used antibiotic families, and four multidrug-resistant isolates from the environment. Paecilin E (**1**) and dankasterone A (**2**) were also investigated for their capacity to inhibit biofilm formation in the four reference strains. The potential synergism between these two compounds and the clinically used antibiotics was also investigated against multidrug-resistant isolates from the environment.

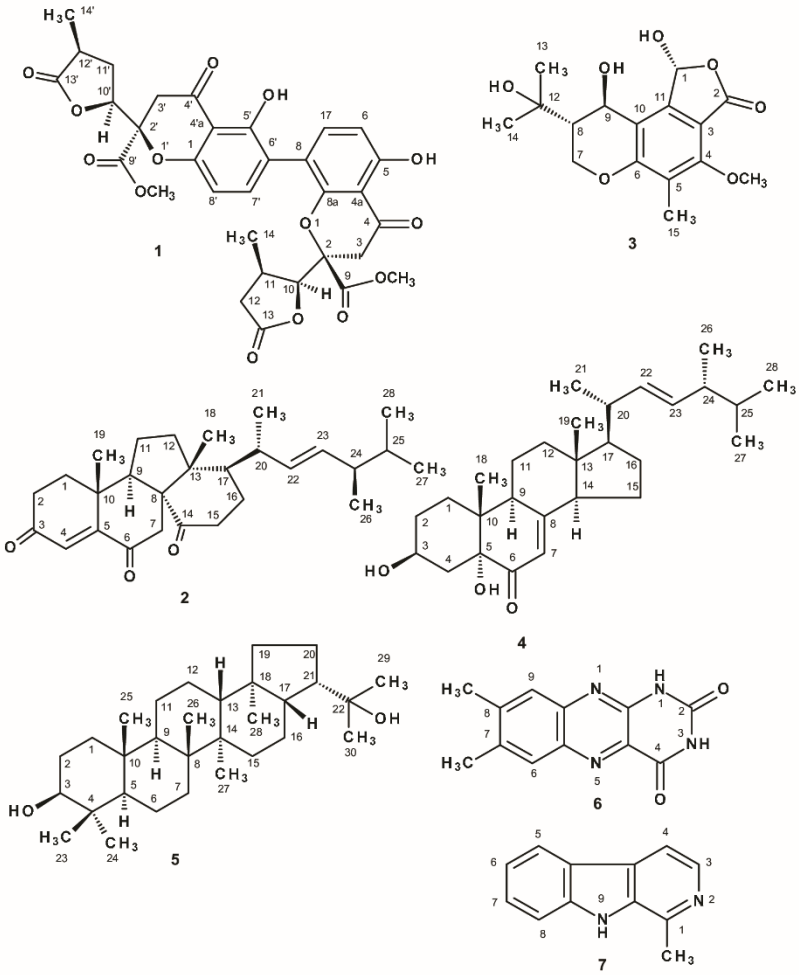

Figure 1. Structures of paecilin E (**1**) and dankasterone A (**2**), a chromanol derivative (**3**), (3β,5α,22*E*), 3,5-dihydroxyergosta-7,22-dien-6-one (**4**), hopan-3β,22-diol (**5**), lumichrome (**6**), harmane (**7**).

2. Results and Discussion

The structures of byssochlamic acid [7], hopan-3β,22-diol (**5**) [15], chevalone B [12], chevalone C [16], sartorypyrone B [5], helvolic acid [5], lumichrome (**6**) [21], harmane (**7**) [20], β-sitostenone [8], ergosta-4,6,8 [14] 22-tetraen-3-one [19], cyathisterone [10], dehydromevalonic acid lactone [6], aszonalenin [13], secalonic acid A [14] and fellutanine A [13] (Figure 1 and Supplementary Materials, Figure S1) were elucidated by analysis of their ^{1}H, ^{13}C NMR spectra and HRMS data, as well as by comparison of their spectral data to those reported in the literature (Supplementary Materials, Figures S2–S31).

The molecular formula of **1**, a white crystal (mp 203–205 °C), was established as $C_{32}H_{30}O_{14}$ on the basis of its (+)-HRESIMS *m*/*z* 639.1718 $[M + H]^+$, (calculated 639.1712 for $C_{32}H_{31}O_{14}$), which indicated

eighteen degrees of unsaturation. The IR spectrum showed absorption bands for hydroxyl (3443 cm^{-1}), conjugated ketone carbonyl (1645 cm^{-1}), ester carbonyl (1790 cm^{-1}), lactone carbonyl (1738 cm^{-1}), and aromatic (1470 cm^{-1}) groups. The ^{13}C NMR spectrum (Table 1, Supplementary Materials, Figure S33) displayed thirty two carbon signals which, based on DEPT and HSQC spectrum (Supplementary Materials, Figure S35), can be classified as two conjugated ketone carbonyl (δ_C 195.3 and 194.9), four ester carbonyl (δ_C 175.5, 174.9, 169.3 and 168.9), eight quaternary sp^2 (δ_C 160.4, 158.2, 158.1, 156.1, 116.6, 114.8, 107.5 and 107.0), four methine sp^2 (δ_C 140.9, 140.6, 109.2 and 107.4), two oxyquaternary sp^3 (δ_C 85.4 and 83.9), two oxymethine sp^3 (δ_C 81.9 and 81.7), two methoxyl (δ_C 53.3 and 53.3), two methine sp^3 (δ_C 32.9 and 32.5), four methylene sp^3 (δ_C 39.2, 39,2, 36.9, 35.3) and two methyl (δ_C 14.6 and 14.1) groups. Based on the type and values of their chemical shifts, these carbons were suspected to arise from two structurally similar moieties within compound **1**.

Table 1. ^1H and ^{13}C Nuclear magnetic resonance (NMR) (DMSO, 500 and 125 MHz) and Heteronuclear Multiple Bond Correlation (HMBC) assignment for **1**.

Position	δ_C, Type	δ_H, (*J* in Hz)	COSY	HMBC
2	85.4, C	-		
3α	32.9, CH_2	3.58, d (17.4)	H-3β	C-2, 4, 9, 10
β		3.05, d (17.4)	H-3α	C-4, 4a
4	194.9, CO	-		
5	107.5, C	-		
6	109.2, CH	6.61, d (8.6)	H-7	C-4a, 8
7	140.9, CH	7.50, d (8.6)	H-6	C-5, 8a
8	114.6, C	-		
9	168.9, CO (Ac)	-		
OMe-9	53.3, CH_3	3.70, s		C-9
10	81.7, CH	4.85, d (7.3)	H-11	C-2, 3, 12, 13, 14
11	32.9, CH	2.85, m	H-10, H_2-12, Me-14	C-2, 13, 14
12α	35.3, CH_2	1.75, dd (17.0, 9.9)	H-11, 12β	C-10, 13, 14
β		2.41, dd (17.0, 8.4)	H-11, 12 α	C-10, 13, 14
13	174.9, CO	-		
14	14.1, CH_3	1.06, d (7.1)	H-11	C-10, 11, 12
2′	83.9, C	-		
3′α	39.2, CH_2	3.57, d (17.4)	H-3′β	C-2′, 4′, 9′, 10′
β		3.09, d (17.4)	H-3′α	C-4′, 4′a
4′	195.3, CO	-		
4′a	107.0, C	-		
5′	158.1, C	-		
6′	116.6, C	-		
7′	140.6, CH	7.61, d (8.6)	H-8′	C-5′, 8′a, 8
8′	107.4, CH	6.60, d (8.6)	H-7′	C-6′, 8′a
8′a	158.2, C	-		
9′	169.3, CO (Ac)	-		
OMe-9′	53.3, CH_3	3.69, s		C-9′
10′	81.9, CH	4.97, d (6.7)	H-11′	C-3′, 11′, 13′, 14′
11′	32.5, CH	2.97, m	H-10′, 11′, 12′a, 12′β	C-2′, 13′, 14′
12′α	36.9, CH_2	2.33, dd (17.0, 5.4)	H-11′, 12′β	C-10′, 13′, 14′
β		2.86, dd (17.0, 8.1)	H-11′, 12′α	C-10′, 13′, 14′
13′	175.5, CO	-		
14′	14.6, CH_3	1.17, d (7.1)	H-11′	C-10′, 11′, 12′
OH-5	-	11.56, s		C-4a, 5, 6
OH-5′	-	11.83, s		C-4′a, 5′, 6′

The ^1H NMR and COSY spectra (Table 1, Supplementary Materials, Figures S32 and S34) exhibited two singlets of the hydrogen-bonded phenolic hydroxyl groups at δ_H 11.56 and 11.83, two pairs of *ortho*-coupled aromatic protons at δ_H 7.50, d (*J* = 8.6 Hz)/6.61, d (*J* = 8.6 Hz) and 7.61, d (*J* = 8.6 Hz)/6.60,

d (J = 8.6 Hz), a pair of doublets at δ_H 4.85, d (J = 7.3 Hz) and δ_H 4.97, d (J = 6.7 Hz), two pairs of mutually coupled methylene protons at δ_H 3.58, d (J = 17.4 Hz)/3.05, d (J = 17.4 Hz); δ_H 3.57, d (J = 17.4 Hz)/3.09, d (J = 17.4 Hz) and δ_H 2.41, dd (J = 17.0, 8.4 Hz)/1.75 dd (J = 17.0, 9.9 Hz); δ_H 2.86, dd (J = 17.0, 8.1 Hz)/2.33, dd (J = 17.0, 5.4 Hz), two methyl singlets at δ_H 1.06, d (J = 7.1 Hz) and δ_H 1.17, d (J = 7.1 Hz) and two methoxyl singlets at δ_H 3.70 and 3.69.

The existence of a 2,2,8-trisubstituted 5-hydroxy-2,3-dihydro-4*H*-chromen-4-one moiety was substantiated by COSY correlations from H-6 (δ_H 6.61, d, J = 8.6 Hz; δ_C 109.2) to H-7 (δ_H 7.50, d, J = 8.6 Hz; δ_C 140.9), and HMBC correlations (Supplementary Materials, Figure S36) from H-6 to C-4a (δ_C 107.5) and C-8 (δ_C 114.6), H-7 to C-5 (δ_C 160.4) and C-8a (δ_C 156.1), OH-5 (δ_H 11.56, s) to C-4a, C-5, C-6 (δ_C 109.2), H-3α (δ_H 3.58, d, J = 17.4 Hz; δ_C 39.2) to C-2 (δ_C 85.4) and C-4 (δ_C 194.9), H-3β (δ_H 3.05, d, J = 17.4 Hz; δ_C 39.2) to C-4 and C-4a. One of the substituents on C-2 was deduced as a methyl formate since both H-3α and the methoxyl singlet (δ_H 3.70) exhibited HMBC cross peaks to the ester carbonyl at δ_C 168.9 (C-9). Another substituent was 4-methyldihydrofuran-2-(3*H*)-one, which linked through C-10, was substantiated by COSY correlations from H-10 (δ_H 4.85, d, J = 7.3 Hz)/H-11 (δ_H 2.85, m)/H_2-12 (δ_H 1.75, dd, J = 17.0, 9.9 Hz and 2.41, dd, J = 17.0, 8.4 Hz), and from H-11 to Me-14 (δ_H 1.06, d, J = 7.1 Hz) as well as by HMBC correlations from H-10 to C-3, C-11 (δ_C 32.9), C-12 (δ_C 35.3) and C-13 (δ_C 174.9), H_2-12 to C-10 (δ_C 81.7), C-13, and Me-14 (δ_C 14.1) as well as from H-3α to C-10. However, this first monomer constituted only half of the molecular formula, i.e., $C_{16}H_{15}O_7$ and still lacked the substituent on C-8.

The second monomer also consisted of a 5-hydroxy-2,3-dihydro-4*H*-chromen-4-one core, but it was 2,2,6-trisubstituted as can be corroborated by COSY correlations from H-7′ (δ_H 7.61, d, J = 8.6 Hz; δ_C 140.6) to H-8′ (δ_H 6.60, d, J = 8.6 Hz; δ_C 107.4) as well as by HMBC correlations from H-7′ to C-5′ (δ_C 158.1), C-8′a (δ_C 158.2), H-8′ to C-6′ (δ_C 116.6) and C-4′a (δ_C 107.0), OH-5′ (δ_H 11.83, s) to C-5′, C-4′a and C-6′, H-3′β (δ_H 3.09, d, J = 17.4 Hz, δ_C 39.2) to C-4′ (δ_C195.3) and C-4′a, and H-3′α (δ_H 3.57, dd, J = 17.4 Hz; δ_C 39.2) to C-4′ and C-2′(δ_C 83.9). Similarly, the substituents on C-2′ were methyl formate and 4-methyldihydrofuran-2-(3*H*)-one, through C-10′, which were based on HMBC correlations from H-3′α to C-9′ (δ_C 169.3), C-10′ (δ_C 81.9), H-10′ (δ_H 4.97, d, J = 6.4 Hz) to C-2′, C-3′, C-11′ (δ_C 32.5), C-13′ (δ_C 175.5) and Me-14′ (δ_C 14.6) as well as the coupling system, as observed in the COSY spectrum, from H-10′, through H-11′ (δ_H 2.97, m) and H_2-12′ (δ_H 2.33, dd, J = 17.0, 5.4 Hz and 2.86, dd, J = 17.0, 8.1 Hz), and from H-11′ to Me-14′. Like the first monomer, the second monomer also had $C_{16}H_{15}O_7$, and still also lacked the substituent on C-6′. That the two monomers were connected through C-8 and C-6′ was supported by HMBC correlations from H-7 to C-6′ as well as from H-7′ to C-8.

A literature search revealed that both monomers and dimers of 5-hydroxy-2,3-dihydro-4*H*-chromen-4-one with the methyl formate and γ-lactone substituents on C-2 have been previously reported. Guo et al. [22] reported the isolation of a 8-8′ dimer (paecilin A) and its monomer (paecilin B) of 5-hydroxy-2,3-dihydro-4*H*-chromen-4-one with the methyl formate and γ-lactone substituents on C-2 from the crude extract of mycelium of the endophytic fungus *Paeciliomyces* sp. (tree 1–7), which was isolated from mangrove bark from Xiamen, China. However, the authors did not determine the stereochemistry of both compounds. Bao et al. [23] reported the isolation, among others, of another 8-8′dimer whose ^{1}H and ^{13}C NMR chemical shift values of the 4-methyldihydrofuran-2-(3*H*)-one moiety were slightly different from those of paecilin A. Through the NOESY correlations, they postulated that the compound might be an epimer of paecilin A, and thus named it paecilin C. However, only the relative configurations of the stereogenic carbons of the methyl γ-lactone rings were established. El-Elimat et al. [24] mentioned the isolation of paecilin D using a bioactivity-guided fractionation of the organic extract of an unidentified fungus (MSX 45109). However, the structure of paecilin D was published later with the name 11-deoxyblennolide D [25], another monomer of 5-hydroxy-2,3-dihydro-4*H*-chromen-4-one with the methyl formate and γ-lactone substituents on C-2.

Since **1** was obtained as a suitable crystal, its X-ray analysis was carried out. The ORTEP view, shown in Figure 2, not only confirmed the proposed structure of **1** as a 6-8 dimer of 5-hydroxy-2,3-dihydro-4*H*-chromen-4-one with the methyl formate and γ-lactone substituents on C-2,

but also determined unequivocally the absolute configurations of C-2, C-2′, C-10, C-10′, C-11, C-11′ as 2*R*, 2′*R*, 10*S*, 10′*S*, 11*R* and 11′*R*. Literature search revealed that **1** has never been previously reported and therefore named paecilin E. It is worth mentioning that this is the first dimer of 5-hydroxy-2,3-dihydro-4*H*-chromen-4-one with the methyl formate and γ-lactone substituents on C-2 with complete assignment of the absolute configurations of the stereogenic carbons of both 2,3-dihydropyrone and hydroxyl-γ-lactone rings.

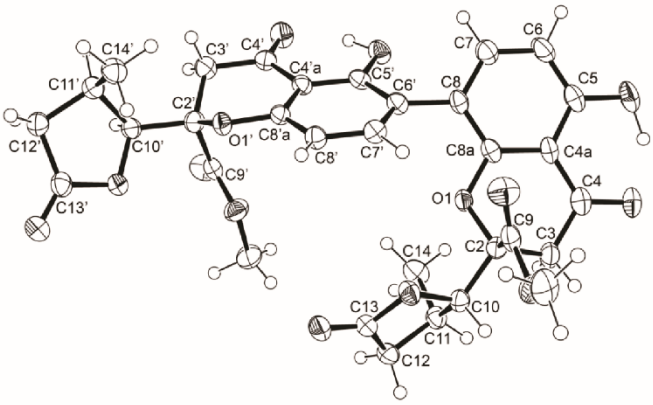

Figure 2. Ortep view of paecilin E (**1**).

Analysis of the (+)-HRESIMS, ^{1}H, ^{13}C NMR, COSY, HSQC and HMBC and X-ray crystallographic data of compound **2** (Supplementary Materials, Table S2, Figures S37–S40 and S49) revealed that it was dankasterone A. This compound was first reported as dankasterone, a cytotoxic steroid, isolated from a marine-derived fungus *Gymnascella dankaliensis* (Castellani) Currah OUPS-N 134, by Amagata et al. [26]. However, the stereochemistry of C-24 was incorrectly assigned. Later on, Amagata and coworkers [11] published the structure of dankasterone, together with other analogs, but inverted the stereochemistry of C-24 and renamed it dankasterone A.

Analysis of the ^{1}H, ^{13}C NMR, COSY, HSQC, HMBC, NOESY (Table 2, Supplementary Materials, Figures S41–S46) and (+)-HRESIMS data of **3**, revealed that it has the same planar structure as that of one of the highly substituted chromanols, isolated from cultures of *Aspergillus duricaulis* [17]. However, there were no details of the ^{1}H and ^{13}C NMR data of the isolated compounds. The authors have proposed that the compound was a mixture of two diastereoisomers, differing in the absolute configurations at C-1, due to a ring-chain tautomerism of the hydroxyphthalide. Moreover, the authors have found that this compound did not show any optical rotation or a Cotton effect [17] and there was no indication of the determination of the absolute configurations of any stereogenic carbons of the isolated chromanol derivatives.

Later on, the same group [18] described the same compound as colorless oil which contained a mixture of the epimers and reported two sets of ^{1}H and ^{13}C NMR data (in deuterated acetone) for both epimers in the mixture but without assignment of the stereochemistry of C-1. On the contrary, compound **3** is optically active (levorotatory), with $[[\alpha]_{D}^{25}$ −80 (*c* 0.05, $CHCl_3$), and exhibited only one set of the ^{1}H and ^{13}C NMR data (Table 2). Therefore, we concluded that **3** was a pure compound and not a mixture of the epimers as described by Archenbach et al. [17,18]. This prompted us to investigate the absolute configurations of the stereogenic carbons in **3**. Since **3** could be obtained in a suitable crystal (mp 223–224 °C), its X-ray analysis was carried out and the ORTEP view is shown in Figure 3. Therefore, **3** was identified as (1*R*, 8*S*, 9*R*)-1,9-dihydroxy-8-(2-hydroxypropan-2-yl)-4-methoxy-5-methyl-1,7,8,9-tetrahydro-3*H*-furo[3,4-f]chromen-3-one.

Table 2. ^{1}H and ^{13}C NMR ($CDCl_3$, 300 MHz and 75 MHz) and HMBC assignment for **3**.

Position	δ_C, Type	δ_H, (*J* in Hz)	COSY	HMBC	NOESY
1	95.6, CH	6.64, s	-	C-3	OH-1, H-9
3	166.1, CO	-			
3a	109.4, C	-			
4	155.9, C	-			
5	120.0, C	-			
5a	158.4, C				
7α	63.9, CH_2	4.29, dd (12.0, 10.6)	H-7β, 8	C-5a, 8, 9	H-7β
β		4.53, dd (11.6, 2.4)	H-7α	C-5a, 8, 9	
8	46.6, CH	1.79, dt (11.9, 2.8)	H-7α	C-2′, 7	H-8, Me-1′, 3′
9	57.8, CH	5.16, br	-		
9a	146.8, C	-			
9b	117.4, C	-			
10	8.6, CH_3	2.05, s	-	C-3a, 4, 5, 5a, 9a	OMe-4
1′	28.4, CH_3	1.27, s	-	C-2′, 3′, 8	H-8, OH-2′, Me-3′
2′	69.9, C	-			
3′	27.7, CH_3	1.24, s		C-1′, 2′, 8	H-8, OH-2′, Me-1′

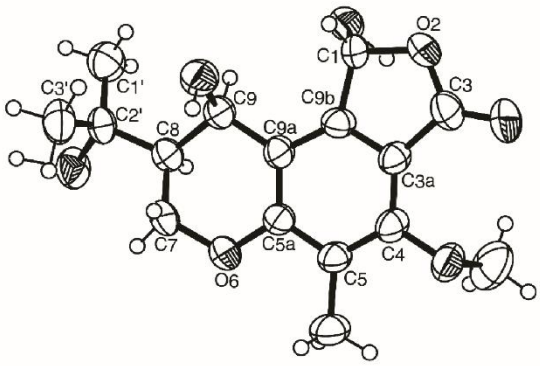

Figure 3. Ortep view of **3**.

Analysis of the (+)-HRESIMS, ^{1}H, ^{13}C NMR, COSY, HSQC and HMBC data of **4** revealed that it was (3β,22*E*)-3,5-dihydroxyergosta-7,22-dien-6-one (Supplementary Materials, Table S2, Figures S47 and S48). However, from a survey of the literature, the stereochemistry of C-5 remained elusive. Aiello et al. [27] first described the isolation of 24-methylcholesta-7,22*E*-dien-3β,5α-diol-6-one and suggested that, due to the low field chemical shift of H-3 (δ_H 4.03, m), the hydroxyl group on C-5 was in the α position. However, no optical rotation of this compound was reported. Later on, Ishizuka et al. [28] reported the isolation of 3β,5α-dihydroxy (22*E*, 24*R*)-ergosta-7,22-dien-6-one from the fruit bodies of an edible mushroom *Grifola frondosa* (Fr.) S.F. Gray (Polyporaceae). Interestingly, the optical rotation of this compound was reported as dextrorotatory, $[\alpha]_D^{25}$ +9.1 ($CHCl_3$, 0.1). Finally, the authors confirmed the structure of this compound by chemical transformation of ergosterol acetate by treatment with $Na_2Cr_2O_7$, followed by deprotection of 3-acetoxy group. Recently, Fangkratok et al. [19] reported the isolation of (3β,5α22*E*)-3,5-dihydroxyergosta-7,22-dien-6-one from the extract of the mycelia of *Lentinus polychrous*, a Thai local edible mushroom. The ^{1}H and ^{13}C NMR data of this compound were very similar to those of **4** except for the chemical shift value of C-10. Furthermore, the sign of the optical rotation reported by Fangkratok et al. was levorotatory, $[\alpha]_D^{20}$ −4.37 (EtOH, 0.01), which is opposite to that of **4**, i.e., $[\alpha]_D^{20}$ +60 ($CHCl_3$, 0.05).

In order to clarify the controversy and to determine unequivocally the position of the hydroxyl group on C-5 of **4**, the absolute configuration of C-5 was determined by comparison of the experimental electronic circular dichroism (ECD) spectrum with the calculated ECD spectra. Conformational

analysis of the C-5*S* and C-5*R* diastereoisomers of **4** by molecular mechanics (MMFF95 force field) resulted in similar lowest energy conformations for both compounds, with rings A and C with chair conformation (Figure 4).

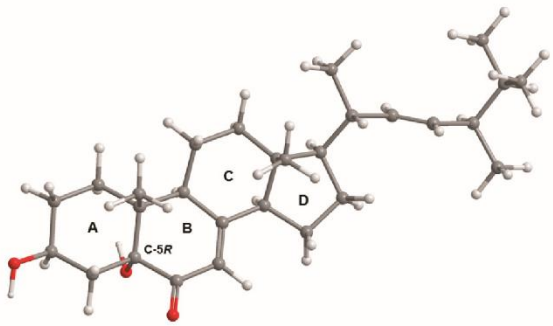

Figure 4. Most stable conformation of **4** (C-5*R*). Rings A and C have chair conformation.

However, both model's conformational energies were further minimized by a DFT (density functional theory) method starting with ring A in chair conformation and also in boat conformation. This was considered necessary because rings A and B house the main low energy UV and ECD chromophore groups, which may engage in intramolecular hydrogen bonds, depending on the particular conformation of ring A. The DFT minimization showed that the amount of energy released by the formation of intramolecular hydrogen bonds is not enough to stabilize the boat conformations. The chair conformations are more stable than its boat counterparts in excess of 2 kcal/mol (Gibbs energy in methanol), making it overwhelmingly predominant. As such, ECD spectra were calculated for the A-chair C-5*S* and C-5*R* diastereoisomers of **4**, using a TD-DFT method. Figure 5 compares these spectra and shows how the calculated spectrum for the C-5*R* isomer fits the experimental data much better, providing enough evidence to conclude that compound **4** is the C-5*R* diastereoisomer, rather than the C-5*S*.

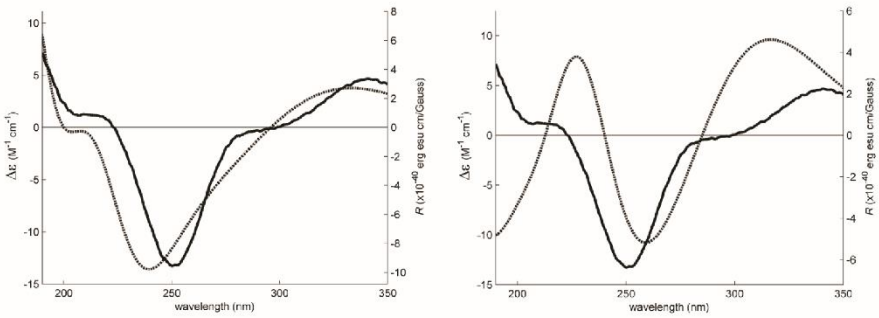

Figure 5. Experimental Electronic Circular Dichroism (ECD) spectrum (solid lines, **left axes**) of **4** in methanol (equal on both sides). Simulated ECD spectra (dotted lines, **right axes**) for both configurations.

Paecilin E (**1**), dankasterone A (**2**), a chromanol derivative (**3**), (3β,5α,22*E*)-3,5-dihydroxyergosta-7,22-dien-6-one (**4**), hopan-3β,22-diol (**5**), lumichrome (**6**) and harmane (**7**) (Figure 1) were tested for their antibacterial activity against Gram-positive and Gram-negative bacteria, including four

reference strains, a clinical isolate sensitive to the most commonly used antibiotic families, and four multidrug-resistant isolates from the environment. In the range of concentrations tested, none of the compounds were active against Gram-negative bacteria. Paecilin E (**1**) exhibited an inhibitory effect on both *Staphylococcus aureus* ATCC 29213 and *Enterococcus faecalis* ATCC 29212 (Table 3), with MIC values of 32 μg/mL and 16 μg/mL, respectively. However, when tested in a vancomycin-resistant (VRE) strain that was sensitive to ampicillin (*E. faecalis* A5/102), the MIC obtained was higher than that of the reference strain (64 μg/mL as opposed to 16 μg/mL). In the range of concentration tested, paecilin E (**1**) was ineffective against a VRE strain which was also resistant to ampicillin (*E. faecalis* B3/101). In the case of *S. aureus* strains isolated from the environment, paecilin E (**1**) was incapable of inhibiting the growth of the bacterial strain sensitive to the most commonly used antibiotic families (*S. aureus* 40/61/24) as well as of MRSA *S. aureus* 66/1. However, dankasterone A (**2**) was only effective against *E. faecalis* ATCC 29212 and VRE *E. faecalis* A5/102, with MIC of 32 μg/mL and 64 μg/mL, respectively.

Table 3. Antibacterial activity of paecilin E (**1**) and dankasterone A (**2**). MIC and MBC are expressed in μg/mL.

	Paecilin E (1)		**Dankasterone A (2)**	
Bacterial strain	MIC	MBC	MIC	MBC
E.coli ATCC 25922	>64	>64	>64	>64
E.coli SA/2 (ESBL)	>64	>64	>64	>64
P. aeruginosa ATCC 27853	>64	>64	>64	>64
E. faecalis ATCC29212	16	>64	32	>64
E. faecalis A5/102 (VRE)	64	>64	64	>64
E. faecalis B3/101 (VRE)	>64	>64	>64	>64
S. aureus ATCC 29213	32	>64	>64	>64
S. aureus 40/61/24	>64	>64	>64	>64
S. aureus 66/1 (MRSA)	>64	>64	>64	>64

MIC = mininmum inhibitory concentration; MBC = minimum batericidal concentration.

The effect of paecilin E (**1**) and dankasterone A (**2**) on biofilm formation was also assessed in four reference strains and neither of them revealed an inhibitory effect on biomass production in any of the strains at the concentration tested. Regarding the screening for potential synergies between the test compounds and clinical relevant antibiotics, none of the compounds revealed a synergistic association with antibiotics, as determined by the different methodologies used.

3. Experimental Section

3.1. General Experimental Procedures

Melting points were determined on a Bock monoscope and are uncorrected. Optical rotations were measured on an ADP410 Polarimeter (Bellingham + Stanley Ltd., Tunbridge Wells, Kent, UK). Infrared spectra were recorded in a KBr microplate in a FTIR spectrometer Nicolet iS10 from Thermo Scientific (Waltham, MA, USA) with Smart OMNI-Transmission accessory (Software 188 OMNIC 8.3). ^{1}H and ^{13}C NMR spectra were recorded at ambient temperature on a Bruker AMC instrument (Bruker Biosciences Corporation, Billerica, MA, USA) operating at 300 or 500 and 75 or 125 MHz, respectively. High resolution mass spectra were measured with a Waters Xevo QToF mass spectrometer (Waters Corporations, Milford, MA, USA) coupled to a Waters Aquity UPLC system. A Merck (Darmstadt, Germany) silica gel GF_{254} was used for preparative TLC, and a Merck Si gel 60 (0.2–0.5 mm) was used for column chromatography.

3.2. Fungal Material

The fungal strains, KUFC 9213 and KUFA 0811, were isolated from the marine sponges *Aka coralliphaga*, collected at the coral reef of Similan Islands, Phang Nga Provice (altitude 8°39′5.39″ N

97°38′16.19″ E), in April 2010 and *Clathria reinwardtii*, collected from Samaesan Island, Amphur Sattahip, Chonburi Province, Thailand (altitude 12°34′30.61″ N 100°57′5.56″ E) in February 2015, respectively. The sponge samples were washed with 0.06% sodium hypochlorite solution for 1 min, followed by sterilized seawater three times and dried on sterile filter papers under aseptic conditions. The sponges were cut into small pieces (5 × 5 mm) and placed on Petri dish plates containing 15 mL malt extract agar (MEA) medium containing 70% seawater, and incubated at 28 °C for 5–7 days. Hyphal tips emerged from sponge pieces were individually transferred onto MEA slant for further identification.

The fungi were identified to species level, based on morphological characteristics such as colony growth rate and growth pattern on standard media, namely Czapek's agar (CZA), Czapek yeast autolysate agar (CYA), MEA and microscopic characteristics including size, shape, ornamentation of ascospores under light and scanning electron microscopes. The fungi were further identified by molecular techniques using ITS primers. DNA was extracted from young mycelia following a modified Murray and Thompson method [29]. Primer pairs ITS1 and ITS4 [30] were used for ITS gene amplification. PCR reactions were conducted on Thermal Cycler and the amplification process consisted of initial denaturation at 95 °C for 5 min, 34 cycles at 95 °C for 1 min (denaturation), at 55 °C for 1 min (annealing) and at 72 °C for 1.5 min (extension), followed by final extension at 72 °C for 10 min. PCR products were examined by Agarose gel electrophoresis (1% agarose with 1× TBE buffer) and visualized under UV light after staining with ethidium bromide. DNA sequencing analyses were sequenced using dideoxyribonucleotide chain termination method [31] by Macrogen Inc. (Seoul, Korea).

The DNA sequences were edited using FinchTV software and submitted into BLAST program for alignment and compared with that of fungal species in the NCBI database (http://www.ncbi.nlm.nih.gov/). The strain KUFC 9213 and KUFA 0811 were identified as *Neosartorya tsunodae* Yaguchi, Abliz and Y. Horie and *N. fennelliae* Kwon-Chung and S.J. Kim, respectively, and their ITS gene sequences were deposited in GenBank with accession numbers KT201524 for KUFC 9213 and KU955859 for KUFA 0811. The pure cultures were maintained at Department of Plant Pathology, Faculty of Agriculture, Kasetsart University, Bangkok, Thailand.

3.3. Extraction and Isolation

Each fungus was cultured for one week at 28 °C in separate Petri dish plates containing 20 mL of potato dextrose agar medium per dish. Five mycelium plugs (5 mm in diam.) of each fungus were transferred into separate 500 mL Erlenmeyer flasks containing 200 mL of potato dextrose broth and incubated on a rotary shaker at 120 rpm for one week at 28 °C to prepare mycelial suspension. Fifty 1000 mL Erlenmeyer flasks (for each fungus), each containing 300 g of cooked rice, were autoclaved at 121 °C for 15 min, and when they were cooled to room temperature, 20 mL of mycelial suspension of a fungus were inoculated per flask, and incubated at 28 °C for 30 days. Then, 500 mL of ethyl acetate was added to each moldy flask and macerated for 7 days and then filtered with Whatman No. 1 filter paper. The organic solutions were combined and evaporated under reduced pressure to furnish the crude ethyl acetate extracts of *N. tsunodae* KUFC 9213 (105 g) and *N. fennelliae* KUFA 0811 (135 g).

The crude ethyl acetate of *N. fennelliae* KUFA 0811 (135 g) was washed with H_2O and extracted with $CHCl_3$ in the same manner. The crude chloroform extract (85 g) was applied on a column of silica gel (420 g), and eluted with mixtures of petrol-$CHCl_3$, $CHCl_3$-Me_2CO and $CHCl_3$-MeOH, wherein 250 mL fractions were collected as follows: Frs 1–30 (petrol-$CHCl_3$, 1:1), 31–86 (petrol-$CHCl_3$, 3:7), 87–202 (petrol-$CHCl_3$, 1:9), 203–436 ($CHCl_3$), 437–579 ($CHCl_3$-Me_2CO, 9:1), 580–690 ($CHCl_3$-Me_2CO, 7:3). Frs 31–60 were combined (6.12 g) and purified by TLC (Silica gel G_{254}, Petrol-$CHCl_3$-EtOAc-HCO_2H, 1:8:1:0.01) to give 16.4 mg of β-sitostenone [8] and 10.5 mg of ergosta-4,6,8 (14), 22-tetraen-3-one [9]. Frs 106–135 were combined (254 g) and purified by TLC (Silica gel G_{254}, Petrol-$CHCl_3$-Petrol-HCO_2H, 9:1:0.01) to give 93 mg of yellow viscous liquid which was applied on a Sephadex LH-20 column (10 g) and eluted with MeOH and a 1:1 mixture of MeOH:CH_2Cl_2 wherein 1 mL 30 sfrs were collected.

Sfrs 16–30 were combined and crystallized in a mixture of CHCl3 and MeOH to give 12.5 mg of dehydromevalonic acid lactone [6]. Frs 211–255 were combined (201 mg) and crystalized in a mixture of $CHCl_3$ and petrol to give 12.3 mg of byssochlamic acid. The mother liquor was combined with the combined frs 136–165 (546 mg) and the combined frs 226–255 (700 mg), and applied on a a column of silica gel (35 g), and eluted with mixtures of petrol-$CHCl_3$, wherein 250 mL sfrs were collected as follows: Sfrs 1–77 (petrol-$CHCl_3$, 1:1), 78–142 (petrol-$CHCl_3$, 3:7), 143–220 (petrol-$CHCl_3$, 1:9), 221–255 ($CHCl_3$). Sfrs 51–63 were combined (50 mg) and crystalized in a mixture of $CHCl_3$ and petrol to give 26 mg of byssochlamic acid. Sfrs 125–220 were combined (160 mg) and crystalized in a mixture of $CHCl_3$ and petrol to give 120 mg of cyathisterone [10]. Frs 361–420 were combined (312 mg) and purified by TLC (Silica gel G_{254}, petrol-$CHCl_3$-EtOAc-HCO_2H, 1:8:1:0.01) to give 9 mg of byssochlamic acid and 20.3 mg of dankasterone A (**2**) [11]. The combined frs 256–360 (1.33 g) and 421–443 (4.9 g) were joined together and applied on a column of silica gel (65 g), and eluted with mixtures of petrol-$CHCl_3$ and $CHCl_3$-Me_2CO, wherein 250 mL sfrs were collected as follows: Sfrs 1–250 (petrol-$CHCl_3$, 1:1), 251–386 (petrol-$CHCl_3$, 3:7), 387–605 (petrol-$CHCl_3$, 1:9), 606–858 ($CHCl_3$), 859–915 ($CHCl_3$-Me_2CO, 9:1). Sfrs 316–365 were combined (35 mg) and purified by TLC (Silica gel G_{254}, petrol-$CHCl_3$-EtOAc-HCO_2H, 1:8:1:0.01) to give 10.5 mg of chevalone B [12] and 4 mg of dankasterone A (**2**). Sfrs 418–480 were combined (11.3 mg) and crystallized in MeOH to give 7 mg of aszonalenin [13] Fr 449 (736 mg) was crystallized in MeOH to give 138 mg of secalonic acid A [14]. Frs 450–452 were combined (1.7 g) and applied on a column of silica gel (100 g), and eluted with mixtures of petrol-$CHCl_3$ and$CHCl_3$-Me_2CO, wherein 250 mL sfrs were collected as follows: Sfrs 1–23 (petrol-$CHCl_3$, 1:1), 24–58 (petrol-$CHCl_3$, 3:7), 59–150 (petrol-$CHCl_3$, 1:9), 151–594 ($CHCl_3$), 595–649 ($CHCl_3$-Me_2CO, 19:1), 650–735 ($CHCl_3$-Me_2CO, 9:1), 736–955 ($CHCl_3$-Me_2CO, 9:1). Sfrs 601–602 were combined and crystalized in MeOH to give 10.5 mg of paecilin E (**1**). Frs 453–457 were combined (1.49 g) and crystalized in MeOH to give 118 mg of secalonic acid A. The mother liquor was applied on a column of Sephadex LH-20 (10 g) and eluted with a 1:1 mixture of MeOH-CH_2Cl_2, wherein 20 sfrs of 10 mL were collected. Sfrs 10–12 were combined (10.6 mg) and crystalized in MeOH to give another 8.7 mg of helvoloic acid. Frs 617–623 were combined (39 mg) and applied on a column of Sephadex LH-20 (10 g) and eluted with a 1:1 mixture of MeOH: CH_2Cl_2, wherein 30 sfrs of 3 mL were collected. Sfrs 17–30 were combined and crystalized in MeOH to give 4.5 mg of fellutanine A [13]. Frs 631–675 were combined (3.61 g) and crystallized in MeOH to give further 68.3 mg of secalonic acid A.

The crude ethyl acetate extract of *N. tsunodae* KUFC 9213 was dissolved in 500 mL of $CHCl_3$, and then washed with H_2O (3 × 500 mL). The organic layers were combined and dried with anhydrous Na_2SO_4, filtered and evaporated under reduced pressure to give 60 g of the crude chloroform extract, which was applied on a column of silica gel (410 g), and eluted with mixtures of petrol-$CHCl_3$, $CHCl_3$-Me_2CO and $CHCl_3$-MeOH , wherein 250 mL fractions were collected as follows: Frs 1–99 (petrol-$CHCl_3$, 1:1), 100–201 (petrol-$CHCl_3$, 3:7), 202–219 (petrol-$CHCl_3$, 1:9), 220–349 ($CHCl_3$-Me_2CO, 9:1), 350–391 ($CHCl_3$-Me_2CO, 7:3), 392–437 ($CHCl_3$-MeOH, 9:1), 438–455 ($CHCl_3$-MeOH, 7:3) and 456–459 (MeOH). Frs 134–196 were combined (2.0 g) and purified by TLC (Silica gel G_{254}, $CHCl_3$-petrol-HCO_2H, 14:5:1) to give 40.5 mg of byssochlamic acid [7]. Frs 226–234 were combined (4.0 g) and applied on a column of silica gel (33 g), and eluted with mixtures of petrol-$CHCl_3$, $CHCl_3$, and $CHCl_3$-Me_2CO, wherein 100 mL subfractions (sfrs) were collected as follows: Sfrs 1–5 (petrol-$CHCl_3$, 7:3), 6–18 (petrol-$CHCl_3$, 3:2), 19–20 (petrol-$CHCl_3$, 1:1), 21–34 (petrol-$CHCl_3$, 3:7), 25–30 (petrol-$CHCl_3$, 9:1), 31–42 ($CHCl_3$) and 43–48 ($CHCl_3$-Me_2CO, 9:1). Sfrs 24–30 were combined (211 mg) and crystallized in MeOH to give 64 mg of byssochlamic acid and 35 mg of hopan-3β,22 diol [15]. Sfrs 31–42 were combined (174 mg) and crystallized in MeOH to give further 23.4 mg of byssochlamic acid. Frs 235–244 were combined (1.75 g) and applied on a column of silica gel (45 g), and eluted with mixtures of petrol-$CHCl_3$ and $CHCl_3$, wherein 100 mL sfrs were collected as follows: Sfrs 1–9 (petrol-$CHCl_3$, 7:3), 20–32 (petrol-$CHCl_3$, 3:2), 33–45 (petrol-$CHCl_3$, 1:1), 46–60 (petrol-$CHCl_3$, 3:7), 61–112 (petrol-$CHCl_3$, 1:9) and 113–115 ($CHCl_3$). Sfrs 1–5 were combined and purified by TLC (Silica gel G_{254}, $CHCl_3$-Me_2CO-HCO_2H, 97:3:0.1) to give 4.6 mg of byssochlamic acid

and 12.4 mg of chevalone C [16]. Sfrs 6–75 were combined (91 mg) and crystalized in MeOH to give further 15 mg of byssochlamic acid. Sfrs 76–114 were combined (863 mg) and purified by TLC (Silica gel G_{254}, $CHCl_3$-Me_2CO-HCO_2H, 97:3:0.1) to give an additional 15.7 mg of byssochlamic acid, 22.4 mg of chevalone C and 39.3 mg of sartorypyrone B [5]. Frs 245–263 were combined (1.53 g) and applied on a column of silica gel (45 g), and eluted with mixtures of petrol-$CHCl_3$, $CHCl_3$, $CHCl_3$-Me_2CO, and Me_2CO, wherein 100 mL sfrs were collected as follows: Sfrs 1–12 (petrol-$CHCl_3$, 7:3), 13–20 (petrol-$CHCl_3$, 3:2), 21–40 (petrol-$CHCl_3$, 1:1), 41–50 (petrol-$CHCl_3$, 2:3), 51–68 (petrol-$CHCl_3$, 3:7), 69–85 (petrol-$CHCl_3$, 1:4), 86–100 (petrol-$CHCl_3$, 1:9), 101–122 ($CHCl_3$), 123–148 ($CHCl_3$-Me_2CO, 9:1), 149–158 (Me_2CO). Sfrs 23–123 were combined (57 mg) and crystalized in MeOH to give 12 mg of byssochlamic acid and 7.1 mg of sartorypyrone B. Frs 264–312 were combined (1.12 g) and applied on a column of silica gel (18 g), and eluted with mixtures of petrol-$CHCl_3$ and $CHCl_3$, wherein 100 mL sfrs were collected as follows: Sfrs 1–17 (petrol-$CHCl_3$, 7:3), 18–48 (petrol-$CHCl_3$, 3:2), 49–72 (petrol-$CHCl_3$, 1:1), 73–76 (petrol-$CHCl_3$, 2:3), 77–90 (petrol-$CHCl_3$, 3:7), 91–100 (petrol-$CHCl_3$, 1:9), 116 ($CHCl_3$). Sfrs 16–68 were combined (93 mg) and crystalized in MeOH to give 33 mg of byssochlamic acid. Sfrs 69–115 were combined (711 mg) and purified by TLC (Silica gel G_{254}, $CHCl_3$-Me_2CO-HCO_2H, 4:1:0.01) to give to 14.1 mg of lumichrome [21] and 8.0 mg of helvolic acid [5]. Frs. 313–352 were combined (487 mg) and applied on a Sephadex LH-20 column (10 g) and eluted with MeOH, wherein 20 mL of 42 sfrs were collected. Sfrs 15–42 were combined (104 mg) and purified by TLC (Silica gel G_{254}, $CHCl_3$-Me_2CO-HCO_2H, 4:1:0.01) to give 10 mg of byssochlamic acid, 7.8 mg of helvolic acid, 4.7 mg of lumichrome, 10.6 mg of (3β,5α,22*E*)-3,5-dihydroxyergosta-7,22-dien-6-one (**4**) [28] and 21.6 mg of chromanol (**3**). Fractions 400–420 were combined (1.47 g) and applied on a Sephadex LH-20 column (20 g) and eluted with MeOH, wherein 20 mL of 42 sfrs were collected. Sfr 23–42 were combined (306 mg) and purified by TLC (Silica gel G_{254}, $CHCl_3$-Me_2CO-HCO_2H, 9:1:0.01) to give to 25.4 mg of byssochlamic acid and 5.3 mg of harmane [20]. Frs 421–440 were combined (1.33 g) and applied on a Sephadex LH-20 column (20 g) and eluted with MeOH, wherein 20 mL of 33 sfrs were collected. Sfrs 18–33 were combined (126 mg) and crystalized in MeOH to give additional 42.2 mg of harmane.

3.3.1. Paecilin E (**1**)

White crystal; mp 203–204 °C. $[\alpha]_D^{20}$ +154 (*c* 0.03, MeOH); IR (KBr) υ_{max} 3444, 2959, 2920, 1790, 1738, 1645, 1470, 1261cm^{-1}. For ^{1}H and ^{13}C spectroscopic data (DMSO, 500 and 125 MHz), see Table 2; (+)-HRESIMS *m*/*z* 639.1718 (M + H)$^+$ (calcd. for $C_{32}H_{31}O_{14}$, 639.1714).

3.3.2. Dankasterone (**2**)

White crystal; mp 135–137 °C. $[\alpha]_D^{20}$ +166 (*c* 0.04, $CHCl_3$); IR (KBr) υ_{max} 2959, 2924, 1727, 1710, 1536, 1462 cm^{-1}. For ^{1}H and ^{13}C spectroscopic data ($CDCl_3$, 500.13 and 125.8 MHz), see Table S1; (+)-HRESIMS *m*/*z* 347.1111 (M + Na)$^+$ (calcd. for $C_{16}H_{20}O_7$ Na, 341.1107). (+)-HRESIMS *m*/*z* 425.3054 (M + H)$^+$ (calcd. for $C_{28}H_{41}O_3$, 425.3056).

3.3.3. (1*R*, 8*S*, 9*R*)-1,9-Dihydroxy-8-(2-hydroxypropan-2-yl)-4-methoxy-5-methyl-1,7,8,9-tetrahydro-3*H*-furo[3,4-f]chromen-3-one (**3**)

White crystal; mp 223–224 °C. $[\alpha]_D^{20}$ –80 (*c* 0.05, $CHCl_3$); IR (KBr) υ_{max} 3467, 3434, 3018, 2969, 1743, 1597, 1507, 1262 cm^{-1}. For ^{1}H and ^{13}C spectroscopic data (DMSO, 300.13 and 75.4 MHz), see Table 2; (+)-HRESIMS *m*/*z* 347.1111 (M + Na)$^+$ (calcd. for $C_{16}H_{20}O_7$ Na, 341.1107).

3.3.4. (3β,5α,22*E*)-3,5-Dihydroxyergosta-7,22-dien-6-one (**4**)

White amorphous solid; $[\alpha]_D^{20}$ +60 (*c* 0.05, $CHCl_3$); For ^{1}H and ^{13}C spectroscopic data ($CDCl_3$, 500.13 and 125.8 MHz), see Table S2. (+)-HRESIMS *m*/*z* 429.3388 (M + H)$^+$ (calcd. for $C_{28}H_{45}O_3$, 429.3369).

3.4. Electronic Circular Dichroism (ECD)

The ECD spectrum of **4** (1.6 mM in methanol) was obtained in a Jasco J-815 CD spectropolarimeter with a 0.01 mm cuvette and eight accumulations. Dihedral driver and MMFF95 minimizations were done in Chem3D Ultra (Perkin-Elmer Inc., Waltham, MA, USA). All DFT minimizations and ECD spectral calculations (TD-DFT) were performed with Gaussian 09W (Gaussian Inc., Wallingford, CT, USA) using the APFD/6-311+G (2d, p) method/basis set [32] with IEFPCM solvation model of methanol. The simulated spectral lines (Figure 4) were obtained by summation of Gaussian curves, as recommended in Stephens and Harada [33]. A line broadening of 0.4 eV was applied to all transitions to generate the calculated spectral lines.

3.5. X-ray Crystal Structure of **1** *and* **3**

Diffraction data were collected with a Gemini PX Ultra equipped with CuK_{α} radiation (λ = 1.54184 Å). The structures were solved by direct methods using SHELXS-97 and refined with SHELXL-97 [34]. Carbon, oxygen and sulfur atoms were refined anisotropically. Hydrogen atoms were either placed at their idealized positions using appropriate HFIX instructions in SHELXL, and included in subsequent refinement cycles, or were directly found from difference Fourier maps and were refined freely with isotropic displacement parameters. Full details of the data collection and refinement and tables of atomic coordinates, bond lengths and angles, and torsion angles have been deposited with the Cambridge Crystallographic Data Centre.

Paecilin E (**1**). Crystals were monoclinic, space group $P2_1$, cell volume 1487.9(2) $Å^3$ and unit cell dimensions a = 13.5112(7) Å, b = 8.1824(11) Å and c = 14.7531(9) Å and β = 114.179(7)° (uncertainties in parentheses). The refinement converged to R (all data) = 5.27% and wR_2 (all data) = 10.31%. The absolute structure was established with confidence (flack x parameter 0.0(2)). Diffraction data were collected at 148 K. CCDC 1579859.

(1R, 8S, 9R)-1,9-Dihydroxy-8-(2-hydroxypropan-2-yl)-4-methoxy-5-methyl-1,7,8,9-tetrahydro-3H-furo[3,4-f]chromen-3-one (**3**). Crystals were triclinic, space group P1, cell volume 773.78(18) $Å^3$ and unit cell dimensions a = 9.1295(12) Å, b = 9.2537(14) Å and c = 10.4317(12) Å and angles α = 94.622(11)°, β = 104.310(11)° and γ = 112.486(13)° (uncertainties in parentheses). The refinement converged to R (all data) = 14.12% and wR_2 (all data) = 29.88%. Diffraction data were collected at 291 K. CCDC 1579876.

3.6. Antibacterial Activity Bioassays

3.6.1. Bacterial Strains and Growth Conditions

For reference, a clinical isolate sensitive to the most commonly used antibiotic families, and four multidrug-resistant bacterial strains were used in this study. The Gram-positive bacteria comprised *Staphylococcus aureus* ATCC 29213, *Enterococcus faecalis* ATCC 29212, a clinical isolate *S. aureus* 40/61/24, MRSA *S. aureus* 66/1 isolated from public buses [35], and VRE *E. faecalis* A5/102 and VRE *E. faecalis* B3/101 isolated from river water [36]. The Gram-negative bacteria used were *Escherichia coli* ATCC 25922, *Pseudomonas aeruginosa* ATCC 27853, and a clinical isolate ESBL *E. coli* SA/2. Frozen stocks of all strains were grown in Mueller-Hinton agar (MH-BioKar diagnostics, Allone, France) at 37 °C. All bacterial strains were sub-cultured in MH agar and incubated overnight at 37 °C before each assay.

3.6.2. Antimicrobial Susceptibility Testing

The minimum inhibitory concentration (MIC), which was used for determining the antibacterial activity of each compound, was determined according to the method described previously by May Zin et al. [37].

3.6.3. Biofilm Formation Inhibition Assay

The effect of the compounds on biofilm formation was assessed using crystal violet staining as previously described by May Zin et al. [37].

3.6.4. Antibiotic Synergy Testing

Evaluation of the combined effect of the compounds and clinical relevant antimicrobial drugs was performed according to the method previously described by May Zin et al. [37].

4. Conclusions

Chemical investigation of the culture of the marine-derived fungus *Neosartorya fennelliae* KUFA 0811, isolated from the marine sponge *Clathria reinwardtii*, resulted in the isolation of the previously undescribed 6-8 dimer of substituted 3,5-dihydrochromone which we have named paecilin E (**1**), and the previously reported metabolites including β-sitostenone, ergosta-4,6,8 (14), 22-tetraen-3-one, cyathisterone, byssochlamic acid, dehydromevalonic acid lactone, chevalone B, aszonalenin, dankasterone A (**2**), helvolic acid, secalonic acid A and fellutanine A. Re-examination of the culture of *N. tsunodae* KUFC 9213, led to the isolation of the chromanol derivative (**3**), in addition to sartorypyrone B and helvolic which were previously isolated from this fungus, and other known compounds including byssochlamic acid, hopan-3β,22-diol (**5**), chevalone C, (3β,5α,22*E*)-3,5-dihydroxyergosta-7,22-dien-6-one (**4**), the alkaloid harmane (**7**) and lumichrome (**6**). The absolute configurations of the stereogenic carbons of the previously undescribed paecilin E (**1**) and the chromanol derivative (**3**) were unambiguously established by X-ray analysis. Although (3β,5α,22*E*)-3,5-dihydroxyergosta-7,22-dien-6-one (**4**) has been reported from several sources, the absolute configuration of its C-5 had never been determined unambiguously by any modern techniques. By comparison of the experimental and calculated ECD spectra, we determined conclusively the absolute configuration of C-5 as 5*R*. Paecilin E (**1**), dankasterone A (**2**), the chromanol derivative (**3**) and some of the isolated compounds which have not been previously tested for antibacterial activity, i.e., (3β,5α,22*E*)-3,5-dihydroxyergosta-7,22-dien-6-one (**4**), hopan-3β,22-diol (**5**), lumichrome (**6**) and harmane (**7**) were tested for their antibacterial activity against Gram-positive and Gram-negative bacteria of four reference strains, a clinical isolate sensitive to the most commonly used antibiotic families, and four multidrug-resistant isolates from the environment. Only paecilin E (**1**) and dankasterone A (**2**) were able to inhibit growth of Gram-positive bacteria. While paecilin E (**1**) exhibited an inhibitory effect on both *S. aureus* ATCC 29213 and *E. faecalis* ATCC 29212 with MIC values of 32 μg/mL and 16 μg/mL, respectively, dankasterone (**2**) was only effective against *E. faecalis* ATCC 29212 and VRE *E. faecalis* A5/102, with MIC of 32 μg/mL and 64 μg/mL, respectively. Despite a great structural diversity of the secondary metabolites produced by these two marine-derived species of *Neosartorya*, a majority of them did not possess the antibacterial activity. Nevertheless, it does not mean that they do not have other interesting biological activities. Therefore, more biological assays will be performed in the future.

Supplementary Materials: The following are available online at www.mdpi.com/1660-3397/15/12/375/s1, Figure S1: Structures of metabolites isolated from *Neosartorya tsunodae* KUFC 9231 and *N. fennelliae* KUFA 0811, Figures S2–S48: 1D and 2D NMR spectra of isolated compounds, Figure S49: Ortep view of dankasterone A (**2**), Table S1: ^{1}H and ^{13}C NMR ($CDCl_3$, 500 MHz and 125 MHz) and HMBC assignment for **2,** Table S2: ^{1}H and ^{13}C NMR ($CDCl_3$, 500 MHz and 125 MHz) of **4**.

Acknowledgments: This work was partially supported through national funds provided by FCT/MCTES—Foundation for Science and Technology from the Minister of Science, Technology and Higher Education (PIDDAC) and European Regional Development Fund (ERDF) through the COMPETE—Programa Operacional Factores de Competitividade (POFC) programme, under the project PTDC/MAR-BIO/4694/2014 (reference POCI-01-0145-FEDER-016790; Project 3599—Promover a Produção Científica e Desenvolvimento Tecnológico e a Constituição de Redes Temáticas (3599-PPCDT)) in the framework of the programme PT2020 as well as by the project INNOVMAR—Innovation and Sustainability in the Management and Exploitation of Marine Resources (reference NORTE-01-0145-FEDER-000035, within Research Line NOVELMAR), supported by North Portugal Regional Operational Programme (NORTE 2020), under the PORTUGAL 2020 Partnership Agreement, through the European Regional Development Fund (ERDF). Decha Kumla and Tin Shine Aung thank the Alfabet and

Lotus Unlimited Projects of the Erasmus Mundus for scholarships. We thank Júlia Bessa and Sara Cravo for technical support.

Author Contributions: Anake Kijjoa and Madalena M. M. Pinto conceived, designed the experimental and elaborated the manuscript; Decha Kumla and Tin Shine Aung performed isolation and purification of the compounds; Suradet Buttachon assisted in purification and determination of physical data of the compounds; Tida Dethoup collected, isolated, identified and culture the fungi; Luís Gales performed X-ray analysis; José A. Pereira performed calculations and measurement of ECD spectra. Paulo M. Costa and Ângela Inácio performed and interpreted the results of antibacterial assays; Nazim Sekeroglu assisted elaboration of the manuscript; Michael Lee provided HRMS; Artur M. S. Silva provided NMR spectra.

Conflicts of Interest: The authors declare no conflict of interest.

References

1. Prompanya, C.; Fernandes, C.; Cravo, S.; Pinto, M.M.M.; Dethoup, T.; Silva, A.M.S.; Kijjoa, A. A new cyclic hexapeptide and a new isocoumarin derivative from the marine sponge-associated fungus *Aspergillus similanensis* KUFA 0013. *Mar. Drugs* **2015**, *13*, 1432–1450. [CrossRef] [PubMed]
2. Zin, W.W.; Prompanya, C.; Buttachon, S.; Kijjoa, A. Bioactive secondary metabolites from a Thai collection of soil and marine-derived fungi of the genera *Neosartorya* and *Aspergillus*. *Curr. Drug Deliv.* **2016**, *13*, 378–388. [PubMed]
3. Bugni, T.S.; Ireland, C.M. Marine-derived fungi: A chemically and biologically diverse group of microorganisms. *Nat. Prod. Rep.* **2004**, *21*, 143–163. [CrossRef] [PubMed]
4. Gomes, N.M.; Bessa, L.J.; Buttachon, B.; Costa, P.M.; Buaruang, J.; Dethoup, T.; Silva, A.M.S.; Kijjoa, A. Antibacterial and antibiofilm activity of tryptoquivalines and meroditerpenes from marine-derived fungi *Neosartorya paulistensis*, *N. laciniosa*, *N. tsunodae*, and the soil fungi *N. fischeri* and *N. siamensis*. *Mar. Drugs* **2014**, *12*, 822–839. [CrossRef] [PubMed]
5. Eamvijarn, A.; Gomes, N.M.; Dethoup, T.; Buaruang, J.; Manoch, L.; Silva, A.; Pedro, M.; Marini, I.; Roussis, V.; Kijjoa, A. Bioactive meroditerpenes and indole alkaloids from the soil fungus *Neosartorya fischeri* (KUFC 6344), and the marine-derived fungi *Neosartorya laciniosa* (KUFC 7896) and *Neosartorya tsunodae* (KUFC 9213). *Tetrahedron* **2013**, *69*, 8583–8591. [CrossRef]
6. Krings, U.; Zelena, K.; Wu, S.; Berger, R.G. Thin-layer high-vacuum distillation to isolate volatile flavour compounds of cocoa powder. *Eur. Food Res. Technol.* **2006**, *223*, 675–681. [CrossRef]
7. Szwalbe, A.J.; Williams, K.; O'Flynn, D.E.; Bailey, A.M.; Mulholland, N.P.; Vincent, J.L.; Willis, C.L.; Cox, R.J.; Simpson, T.J. Novel nonadride, heptadride and maleic acid metabolites from the byssochlamic acid producer *Byssochlamys fulva* IMI 40021—An insight into the biosynthesis of maleidrides. *Chem. Commun.* **2015**, *51*, 17088–17091. [CrossRef] [PubMed]
8. Prachayasittikul, S.; Suphapong, S.; Worachartcheewan, A.; Lawung, R.; Ruchirawat, S.; Prachayasittikul, V. Bioactive metabolites from *Spilanthes acmella* Murr. *Molecules* **2009**, *14*, 850–867. [CrossRef] [PubMed]
9. Kobayashi, M.; Krishna, M.M.; Ishida, K.; Anjaneyulu, V. Marine sterols. XXII. Occurrence of 3-oxo-4,6,8(14)-triunsaturated steroids in the sponge *Dysidea herbacea*. *Chem. Pharm. Bull.* **1992**, *40*, 72–74. [CrossRef]
10. Kawahara, K.; Sekita, S.; Satake, M. Steroids from *Calvatia cyathiformis*. *Phytochemistry* **1994**, *37*, 213–215. [CrossRef]
11. Amagata, T.; Tanaka, M.; Yamada, T.; Doi, M.; Minoura, K.; Ohishi, H.; Yamori, T.; Numata, A. Variation in cytostatic constituents of a sponge-derived *Gymnascella dankaliensis* by manipulating the carbon source. *J. Nat. Prod.* **2007**, *70*, 1731–1740. [CrossRef] [PubMed]
12. Zin, W.W.; Buttachon, S.; Buaruang, J.; Gales, L.; Pereira, J.A.; Pinto, M.M.M.; Silva, A.M.S.; Kijjoa, A. A new meroditerpene and a new tryptoquivaline from the algicolous fungus *Neosartorya takakii* KUFC 7898. *Mar. Drugs* **2015**, *13*, 3776–3790. [CrossRef] [PubMed]
13. Zin, W.W.; Buttachon, S.; Dethoup, T.; Fernandes, C.; Cravo, S.; Pinto, M.M.M.; Gales, L.; Pereira, J.A.; Silva, A.M.S.; Sekeroglu, N.; et al. New cyclotetrapeptides and a new diketopiperzine derivative from the marine sponge-associated fungus *Neosartorya glabra* KUFA 0702. *Mar. Drugs* **2016**, *14*, 136. [CrossRef] [PubMed]

14. Noinart, J.; Buttachon, S.; Dethoup, T.; Gales, L.; Pereira, J.A.; Urbatzka, R.; Freitas, S.; Lee, M.; Silva, A.M.S.; Pinto, M.M.M.; et al. A new ergosterol analog, a new bis-anthraquinone and anti-obesity activity of anthraquinones from the marine sponge-associated fungus *Talaromyces stipitatus* KUFA 0207. *Mar. Drugs* **2017**, *15*, 139. [CrossRef] [PubMed]
15. Tanaka, R.; Matsunaga, S. Saturated hopane and gammacerane triterpene-duils from the stem bark of *Abies veitchii*. *Phytochemisty* **1992**, *31*, 3535–3539. [CrossRef]
16. Prata-Sena, M.; Ramos, A.A.; Buttachon, S.; Castro-Carvalho, B.; Marques, P.; Dethoup, T.; Kijjoa, A.; Rocha, E. Cytotoxic activity of secondary metabolites from marine-derived fungus *Neosartorya siamensis* in human cancer cells. *Phytother. Res.* **2016**, *30*, 1862–1971. [CrossRef] [PubMed]
17. Achenbach, H.; Mülhlenfeld, A.; Weber, B.; Brillinger, G.U. Highly substituted chromanols from culture of *Aspergillus duricaulis*. *Tetrahedron Lett.* **1982**, *45*, 4659–4660. [CrossRef]
18. Achenbach, H.; Mülhlenfeld, A.; Brillinger, G.U. Stiffwechselprodukte von mikroorganismen, XXX. Phthalide und chromanole aus *Aspergillus duricaulis*. *Liebigs Ann. Chem.* **1985**, *1985*, 1596–1628. [CrossRef]
19. Fangkrathok, N.; Sripanidkulchai, B.; Umehara, K.; Noguchi, H. Bioactive ergostanoids and a new polyhydroxyoctane from *Lentinus polychrous* mycelia and their inhibitory effects on E2-enhanced cell proliferation of T47D cells. *Nat. Prod. Res.* **2013**, *27*, 1611–1619. [CrossRef] [PubMed]
20. Kodani, S.; Imoto, A.; Mitsutani, A.; Murakami, M. Isolation and identification of the antialgal compound, harmane (1-methyl-β-carboline), produced by the algicidal bacterium, *Pseudomonas* sp. K44-1. *J. Appl. Phycol.* **2002**, *14*, 109–114. [CrossRef]
21. Sasaki, M.; Takamatsu, H.; Oshita, K.; Yukio Kaneko, Y.; Yokotsuka, T. Isolation of lumichrome from the culture filtrate of *Aspergillus oniki* 1784. *Nippon Nōgeikagaku Kaishi* **1974**, *48*, 569–571. [CrossRef]
22. Guo, Z.; She, Z.; Shao, C.; Wen, L.; Liu, F.; Zheng, Z.; Lin, Y. ^{1}H and ^{13}C NMR signal assignments of paecilin A and B, two new chromone derivatives from mangrove endophytic fungus *Paeciliomyces* sp. (tree 1–7). *Magn. Reson. Chem.* **2007**, *45*, 777–780. [CrossRef] [PubMed]
23. Bao, J.; Sun, Y.-L.; Zhang, X.-Y.; Han, Z.; Gao, H.-C.; He, F.; Qian, P.Y.; Qi, S.-H. Antifouling and antibacterial polyketides from marine gorgonian coral-associated fungus *Penicillium* sp. SCSDAF 0023. *J. Antibiot.* **2013**, *66*, 219–223. [CrossRef] [PubMed]
24. El-Elimat, T.; Figueroa, M.; Adcock, A.F.; Kroll, D.J.; Swanson, S.M.; Wani, M.C.; Pearce, C.J.; Oberlies, N.H. Cytotoxic polyketides from an unidentified fungus (MSX 45109). *Planta Med.* **2013**, *79-PL13*. [CrossRef]
25. El-Elimat, T.; Figueroa, M.; Raja, H.A.; Graf, T.N.; Swanson, S.M.; Falkinham, J.O., III; Wani, M.; Pearce, C.J.; Oberlies, N.H. Biosythetically distinct cytotoxic polyketides from *Setophoma terrestris*. *Eur. J. Org. Chem.* **2015**, *2015*, 109–121. [CrossRef] [PubMed]
26. Amagata, T.; Doi, M.; Tohgo, M.; Minoura, K.; Numanta, A. Dankasterone, a new class of cytotoxic steroid produced by *Gymnascella* species from a marine sponge. *Chem. Commun.* **1999**, *30*, 1321–1322. [CrossRef]
27. Aiello, A.; Fattorusso, E.; Magno, S.; Menna, M. Isolation of five new 5α-hydroxy-6-keto-Δ^{7}sterols from the marine sponge *Oscarella lobularis*. *Steroids* **1991**, *56*, 337–340. [CrossRef]
28. Ishizuka, T.; Yaoita, Y.; Kikuchi, M. Sterol constituents from the fruit bodies of *Grifola frondosa* (Fr.) S.F. Gray. *Chem. Pharm. Bull.* **1997**, *45*, 1756–1760. [CrossRef]
29. Murray, M.G.; Thompson, W.F. Rapid isolation of high molecular weight plant DNA. *Nucleic Acids Res.* **1980**, *8*, 4321–4325. [CrossRef] [PubMed]
30. White, T.J.; Bruns, T.; Lee, S.; Taylor, J. Amplification and direct sequencing of fungal ribosomal RNA genes for phylogenetics. In *PCR Protocols: A Guide to Methods and Applications*; Innis, M.A., Gelfand, D.H., Sninsky, J.J., White, T.J., Eds.; Academic Press: New York, NY, USA, 1990; pp. 315–322.
31. Sanger, F.; Nicklen, S.; Coulson, A.R. DNA sequencing with chain-terminating inhibitors. *Proc. Natl. Acad. Sci. USA* **1977**, *72*, 5463–5467. [CrossRef]
32. Austin, A.; Petersson, G.A.; Frixch, M.J.; Dobek, F.J.; Scalmani, G.; Throssel, K. A density functional with spherical atom dispersion terms. *J. Chem. Theory Comput.* **2012**, *8*, 4989–5007. [CrossRef] [PubMed]
33. Stephens, P.J.; Harada, N. ECD Cotton effect approximated by the Gaussian curve and other methods. *Chirality* **2010**, *22*, 229–233. [CrossRef] [PubMed]
34. Sheldrick, G.M. A short story of SHELX. *Acta Crystallogr. A* **2008**, *64*, 112–122. [CrossRef] [PubMed]
35. Simões, R.R.; Aires-de-Sousa, M.; Conceicao, T.; Antunes, F.; da Costa, P.M.; de Lencastre, H. High prevalence of EMRSA-15 in Portuguese public buses: A worrisome finding. *PLoS ONE* **2011**, *6*, e17630. [CrossRef] [PubMed]

36. Bessa, L.J.; Barbosa-Vasconcelos, A.; Mendes, A.; Vaz-Pires, P.; Martins da Costa, P. High prevalence of multidrug-resistant *Escherichia coli* and *Enterococcus* spp. in river water, upstream and downstream of a wastewater treatment plant. *J. Water Health* **2014**, *12*, 426–435. [CrossRef] [PubMed]
37. Zin, W.W.; Buttachon, S.; Dethoup, T.; Pereira, J.A.; Gales, L.; Inácio, A.; Costa, P.M.; Lee, M.; Sekeroglu, N.; Silva, A.M.S.; et al. Antibacterial and antibiofilm activities of the metabolites isolated from the culture of the mangrove-derived endophytic fungus *Eurotium chevalieri* KUFA 0006. *Phytochemistry* **2017**, *141*, 86–97. [CrossRef] [PubMed]

APPENDIX II

Kumla D., Pereira J.A., Dethoup T., Gales L., Silva J.F., Lee M., Costa P.M., Silva A.M.S., Sekeroglu N., Pinto M.M.M. and Kijjoa A., 2018. Chromone Derivatives and Other Constituents from Cultures of the Marine Sponge-Associated Fungus *Penicillium erubescens* KUFA0220 and Their Antibacterial Activity. *Mar. Drugs 16* (8), 289.

marine drugs

MDPI

Article

Chromone Derivatives and Other Constituents from Cultures of the Marine Sponge-Associated Fungus *Penicillium erubescens* KUFA0220 and Their Antibacterial Activity

Decha Kumla [1,2], José A. Pereira [1,2], Tida Dethoup [3], Luis Gales [1,4], Joana Freitas-Silva [1,2], Paulo M. Costa [1,2], Michael Lee [5], Artur M. S. Silva [6], Nazim Sekeroglu [7], Madalena M. M. Pinto [2,8,*] and Anake Kijjoa [1,2,*]

1 *ICBAS*—Instituto de Ciências Biomédicas Abel Salazar, Universidade do Porto, Rua de Jorge Viterbo Ferreira, 228, 4050-313 Porto, Portugal; Decha1987@hotmail.com (D.K.); jpereira@icbas.up.pt (J.A.P.); lgales@ibmc.up.pt (L.G.); joanafreitasdasilva@gmail.com (J.F.-S.); pmcosta@icbas.up.pt (P.M.C.)
2 Interdisciplinary Centre of Marine and Environmental Research (CIIMAR), Universidade do Porto, Terminal de Cruzeiros do Porto de Lexões, Av. General Norton de Matos s/n, 4450-208 Matosinhos, Portugal
3 Department of Plant Pathology, Faculty of Agriculture, Kasetsart University, Bangkok 10240, Thailand; tdethoup@yahoo.com
4 Instituto de Biologia Molecular e Celular (i3S-IBMC), Universidade do Porto, Rua de Jorge Viterbo Ferreira, 228, 4050-313 Porto, Portugal
5 Department of Chemistry, University of Leicester, University Road, Leicester LE 7 RH, UK; ml34@leicester.ac.uk
6 Departamento de Química & QOPNA, Universidade de Aveiro, 3810-193 Aveiro, Portugal; artur.silva@ua.pt
7 Department of Food Engineering, Faculty of Engineering and Architecture, Kilis 7 Aralık University, 79000 Kilis, Turkey; nsekeroglu@gmail.com
8 Laboratório de Química Orgânica, Departamento de Ciências Químicas, Faculdade de Farmácia, Universidade do Porto, Rua de Jorge Viterbo Ferreira, 228, 4050-313 Porto, Portugal
* Correspondence: madalena@ff.up.pt (M.M.M.P.); ankijjoa@icbas.up.pt (A.K.); Tel.: +351-22-042-8331 (M.M.M.P. & A.K.); Fax: +351-22-206-2232 (M.M.M.P. & A.K.)

Received: 2 August 2018; Accepted: 18 August 2018; Published: 20 August 2018

check for updates

Abstract: A previously unreported chromene derivative, 1-hydroxy-12-methoxycitromycin (**1c**), and four previously undescribed chromone derivatives, including pyanochromone (**3b**), spirofuranochromone (**4**), 7-hydroxy-6-methoxy-4-oxo-3-[(1*E*)-3-oxobut-1-en-1-yl]-4*H*-chromene-5-carboxylic acid (**5**), a pyranochromone dimer (**6**) were isolated, together with thirteen known compounds: β-sitostenone, ergosterol 5,8-endoperoxide, citromycin (**1a**), 12-methoxycitromycin (**1b**), myxotrichin D (**1d**), 12-methoxycitromycetin (**1e**), anhydrofulvic acid (**2a**), myxotrichin C (**2b**), penialidin D (**2c**), penialidin F (**3a**), SPF-3059-30 (**7**), GKK1032B (**8**) and secalonic acid A (**9**), from cultures of the marine sponge- associated fungus *Penicillium erubescens* KUFA0220. Compounds **1a–e**, **2a**, **3a**, **4**, **7–9**, were tested for their antibacterial activity against Gram-positive and Gram-negative reference and multidrug-resistant strains isolated from the environment. Only **8** exhibited an in vitro growth inhibition of all Gram-positive bacteria whereas **9** showed growth inhibition of methicillin-resistant *Staphyllococus aureus* (MRSA). None of the compounds were active against Gram-negative bacteria tested.

Keywords: *Penicillium erubescens*; Aspergillaceae; marine sponge-associated fungus; *Neopetrosia* sp.; chromone derivatives; GKK 1032B; pyranochromone; spirofuranochromone; antibacterial activity

1. Introduction

The fungi of the genus *Penicillium* (Family Aspergillaceae) are the most common fungi occurring in a diverse range of habitats from soil to vegetation to various food products, air, indoor environments, and marine environments. They have a worldwide distribution and a large economic impact on human life [1]. The marine-derived *Penicillium* species can be found to be associated with a variety of marine invertebrates such as marine sponges, corals, and tunicates, as well as with fish, marine algae, mangroves and also from the sediments; although sediments and sponges are their main sources or hosts for producing new marine natural products. Interestingly, marine-derived *Penicillium* species produce diverse structural classes of secondary metabolites such as polyketides, sterols, terpenoids, alkaloids, among others, and more than half of these metabolites exhibited bioactivities [2].

Thus, in our ongoing search for antibiotics from marine-derived fungi from the tropical sea, we investigated secondary metabolites from cultures of *Penicillium erubescens* KUFA 0220, which was isolated from the marine sponge *Neopetrosia* sp., collected from the coral reef at Samaesan Island, Chonburi province, in the Gulf of Thailand.

Chromatographic fractionation and the further purification of the crude ethyl acetate extract of the cultures of *P. erubescens* KUFA 0220, furnished an unreported chromene derivative, 1-hydroxy-12-methoxycitromycin (**1c**), and four previously undescribed chromone derivatives, including a pyanochromone (**3b**), a spirofuranochromone (**4**), 7-hydroxy-6-methoxy-4-oxo-3-[(1*E*)-3-oxobut-1-en-1-yl]-4*H*-chromene-5-carboxylic acid (**5**), and a pyranochromone dimer (**6**) (Figure 1), in addition to thirteen known compounds: β-sitostenone [3,4], citromycin (**1a**) [5], 12-methoxycitromycin (**1b**) [5], myxotrichin D (**1d**) [6], 12-methoxycitromycetin (**1e**) [5], anhydrofulvic acid (**2a**) [7,8], myxotrichin C (**2b**) [6], penialidin D (**2c**) [9], penialidin F (**3a**) [9,10], SPF-3059-30 (**7**) [11], GKK1032B (**8**) [12–14] and secalonic acid A (**9**) [3] (Figure 1). The structures of the previously undescribed compounds were established based on extensive analyses of their 1D and 2D NMR as well as HRMS data while the identity of the known compounds was elucidated by comparison of their ^{1}H and ^{13}C NMR data with those reported in the literature. The absolute configuration of the stereogenic carbon of the previously unreported **4** was established by an X-ray analysis whereas those of the previously undescribed **6** and penialidin F (**3a**) were determined by comparison of their calculated and experimental ECD spectra.

Compounds **1a**–**e**, **2a**, **3a**, **4**, **7**–**9** were tested for their antibacterial activity against five reference bacterial strains consisting of three Gram-positive (*Staphylococcus aureus* ATCC 29213, *Enterococcus faecium* ATCC 19434 and *Enterococcus faecalis* ATCC 29212) and two Gram-negative bacteria (*Escherichia coli* ATCC 25922 and *Pseudomonas aeruginosa* ATCC 27853), three multidrug-resistant isolates from the environment (MRSA *S. aureus* 66/1, VRE *E. faecium* 1/6/63 and *E. faecalis* B3/101) and a clinical isolate ESBL *E. coli* SA/2. Some of the isolated compounds were also investigated for their capacity to inhibit biofilm formation in the four reference strains as well as for their potential synergism with the clinically used antibiotics against multidrug-resistant isolates from the environment.

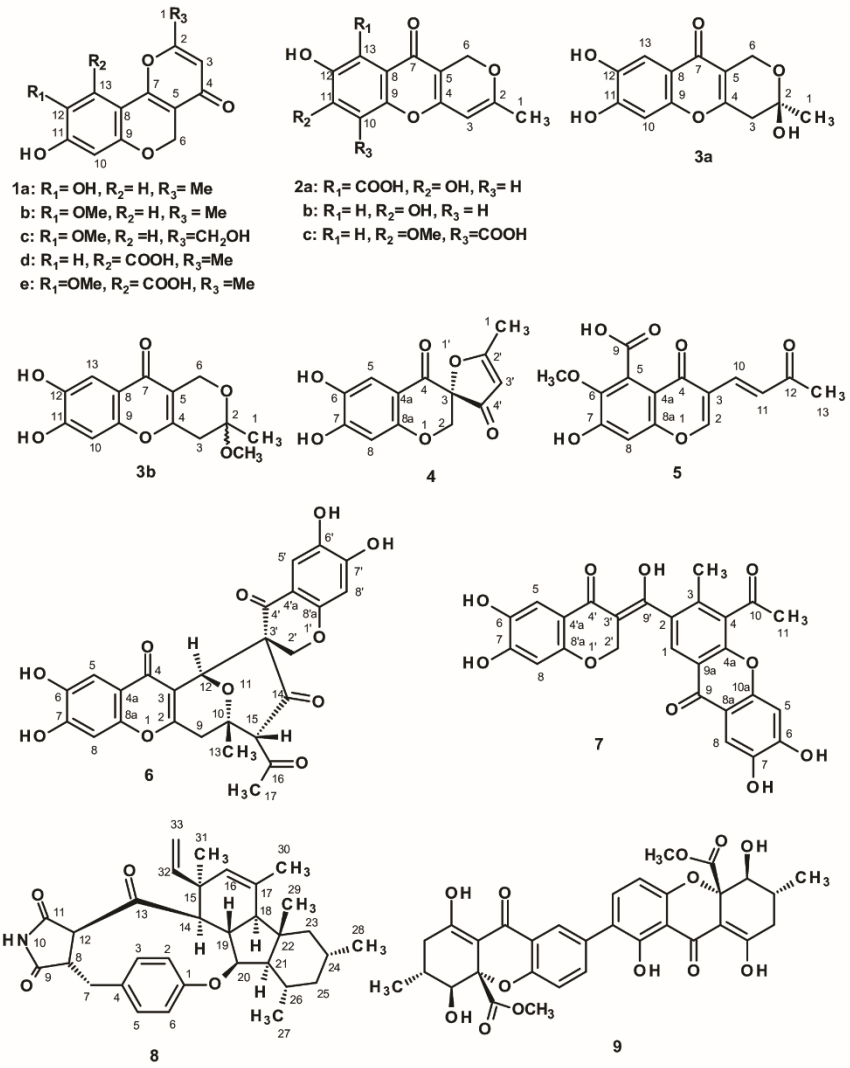

Figure 1. The structures of some secondary metabolites, isolated from cultures of the marine sponge-associated fungus *P. erubescens* KUFA 0220.

2. Results and Discussion

The structure of β-sitostenone [3], ergosterol 5,8-endoperoxide [4] (Figure S1), citromycin (**1a**) [5], 12-methoxycitromycin (**1b**) [5], myxotrichin D (**1d**) [6], 12-methoxycitromycetin (**1e**) [5], anhydrofulvic acid (**2a**) [7,8], myxotrichin C (**2b**) [6], penialidin D (**2c**) [9], penialidin F (**3a**) [9,10], SPF-3059-30 (**7**) [11], GKK1032B (**8**) [12–14], and secalonic acid A (**9**) [3,15] (Figure 1) were elucidated by analysis of their 1D and 2D NMR spectra as well as HRMS data, and also by comparison of their spectral data (Figures S2–S11, S15–S29, S45–S50, S52 and S53) to those reported in the literature. In the case of

GKK1032B (**8**), the X-ray analysis was also performed to confirm the absolute configurations of all the stereogenic centers (Figure S51).

Compound **1c** was isolated as a white solid (mp 232–233 °C), and its molecular formula $C_{14}H_{12}O_6$ was established based on its (+)-HRESIMS *m/z* 277.0715 $[M + H]^+$, (calculated 277.0712 for $C_{14}H_{13}O_6$), indicating nine degrees of unsaturation. The IR spectrum showed absorption bands for the hydroxyl (3420 cm^{-1}), conjugated ketone carbonyl (1662 cm^{-1}), aromatic (1627, 1555 cm^{-1}), and ether (1270 cm^{-1}) groups. The ^{13}C NMR spectrum of **1c** (Table 1, Figure S11) displayed fourteen carbon signals which, according to DEPTs and HSQC spectra (Table 1, Figure S12), can be classified as one conjugated ketone carbonyl (δ_C 174.8), seven quaternary sp^2 (δ_C 167.3, 155.2, 152.2, 151.9, 143.6, 111.2, 105.9), three methine sp^2 (δ_C 110.7, 106.5, 104.1), two oxymethylene sp^3 (δ_C 62.5 and 59.5), and one methoxyl (δ_C 56.4) carbon. The ^1H NMR spectrum (Table 1, Figure S10) showed two aromatic singlets at δ_H 7.15 and 6.44, another singlet of one olefinic proton at δ_H 6.25, two singlets of oxymethylene protons at δ_H 5.02 (2H) and 4.41 (2H), and a singlet of methoxyl protons at δ_H 3.80 (3H). The general features of the ^1H and ^{13}C NMR spectra of **1c** resembled those of 12-methoxycitromycin (**1b**), which was previously isolated from the Australian marine-derived and terrestrial *Penicillium* spp. [5], and also isolated in this work. The only difference between the two compounds is the methyl group in **1b** (δ_H 2.34, d, J = 0.6 Hz; δ_C 19.2) is replaced by a hydroxymethyl group (δ_H 4.41; δ_C 59.5) in **1c**. The position of the methoxyl group was also confirmed by the NOESY correlation from the methoxyl protons to H-13 (δ_H 7.15, s) (Figure S14). Therefore, **1c** is 1-hydroxy-12-methoxycitromycin. The literature search revealed that **1c** has never been previously reported.

Table 1. The ^1H and ^{13}C NMR (DMSO-d_6, 500.13 and 125.4 MHz) and HMBC assignment for **1c**.

Position	δ_C, Type	δ_H, (J in Hz)	HMBC
1	59.5, CH_2	4.41, brs	C-2, 5
2	167.3, C	-	-
3	104.1, CH	6.25, s	C-1, 2, 5
4	174.8, CO	-	-
5	111.2, C	-	-
6	62.6, CH_2	5.02, s	C-4, 5, 7, 9
7	155.2, C	-	-
8	105.9, C	-	-
9	152.2, C		-
10	106.5, CH	6.44, s	C-7, 8, 9, 11, 12
11	151.9, C	-	-
12	143.6, C	-	-
13	110.7, CH	7.15, s	C-7, 8, 9, 11, 12
OCH_3-12	56.4, CH_3	3.80	C-12

The analysis of the ^1H, ^{13}C NMR (Table 2, Figures S28 and S29) and the (+)-HRESIMS spectra of **3a** revealed that its planar structure was the same as that of penialidin F, previously isolated from the culture of *Penicillium janthinellum* DT-F29, collected from marine sediments [9]. Curiously, even though the authors reported the optical rotation of penialidin F as levorotatory ($[\alpha]_D^{25}$ −4.13, c = 1.0, MeOH), they did not determine the absolute configuration of its stereogenic carbon (C-2). Similarly, we have also found the optical rotation of the **3a** levorotatory, ($[\alpha]_D^{25}$ −7.5, c = 0.04, MeOH). Since **3a** was not isolated as a suitable crystal for X-ray analysis, its calculated ECD spectrum was performed to compare with the experimental ECD spectrum. Therefore, the conformational analysis of **3a** by molecular mechanics (MM2 and MMFF95 force fields) focused on combinations of hydroxyl 120° rotations and two 3,6-dihydro-2*H*-pyran-2-ol ring conformations. A total of 30 conformations were energetically minimized and ranked using a faster DFT model (smaller basis set, APFD/6-31G). The lowest three of these, representing 99% of the model Boltzmann population, were then further energetically minimized with a larger basis set (APFD/6-311+G(2d,p)). The most stable conformation is depicted in Figure 2 and represents 64% of the Boltzmann population while the other two amount to 25% and 11%.

Table 2. The ^{1}H and ^{13}C NMR of **3a** (DMSO-d_6, 300.13 and 75.4 MHz) and **3b** (DMSO, 500.13 and 125.4 MHz).

	3a		3b	
Position	**δ_C, Type**	**δ_H, (*J* in Hz)**	**δ_C, Type**	**δ_H, (*J* in Hz)**
1	28.4, CH_3	1.45, s	22.4, CH_3	1.44, s
2	94.2, C	-	97.7, C	-
3	37.5, CH_2	2.55, d (17.5) 2.87, d (17.5)	37.1, CH_2	2.63, dd (17.6, 2.6) 2.96, dd (17.6, 2.6)
4	158.7, C	-	157.9, C	-
5	113.5, C	-	113.0, C	-
6	56.3, CH_2	4.45, s -	52.7, CH_2	4.22, dt (14.9, 0.9) 4.52, dd (14.9, 2.1)
7	173.4, CO	-	173.2, CO	-
8	115.4, C	-	115.4, C	-
9	152.1, C	-	152.1, C	-
10	102.7, CH	6.83, s	102.7, CH	6.83, s
11	150.8, C	-	150.8, C	-
12	144.3, C	-	144.4, C	-
13	107.4, CH	7.26, s	107.4, CH	7.26, s
OCH_3	-	-	48.3, CH_3	3.21, s

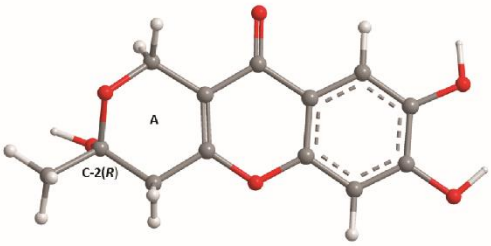

Figure 2. The most stable APFD/6-311+G(2d,p) conformation of **3a** (C-2*R*). The asymmetric carbon is presented with the hydroxyl group facing straight down.

These three models were then used to calculate the expected Boltzmann-averaged ECD spectrum of **3a**'s *R* enantiomer. The good fit between the calculated and experimental ECD spectra shown in Figure 3 is enough evidence to conclude that **3a** is the *R* enantiomer. However, the weak experimental ECD signal of **3a** could indicate that this compound does not exist as a pure *R* enantiomer but as an enantiomeric mixture with an excess of the *R* enantiomer.

Compound **3b** was isolated as a 1:2 mixture (estimated from the integration of the proton signals in the ^{1}H NMR spectrum) with myxotrichin C (**2b**). Based on the (+)-HRESIMS *m/z* 279.0878 $[M + H]^+$, (calculated 277.0869 for $C_{14}H_{15}O_6$), the molecular formula $C_{14}H_{14}O_6$ was attributed to **3b**. The ^{1}H and ^{13}C NMR spectra of **3b** (a minor compound) resembled those of penialidin F (**3a**) (Table 2). The ^{13}C NMR spectrum of **3b** (Table 2, Figure S22) exhibited fourteen carbon signals which, in combination with DEPTs and HSQC spectra (Figure S24), can be categorized as one conjugated ketone carbonyl (δ_C 173.2), six quaternary sp^2 (δ_C 157.9, 152.1, 150.8, 144.4, 115.4, 113.0), two methine sp^2 (δ_C 107.4 and 102.7), one ketal (δ_C 97.7), one oxymethylene sp^3 (δ_C 57.1), one methylene sp^3 (δ_C 37.1), one methyl (δ_C 22.4), and one methoxyl (δ_C 48.3) carbon. The ^{1}H NMR spectrum (Figure S21) displayed two aromatic singlets at δ_H 7.26 (H-13) and 6.83 (H-10), two pairs of geminally coupled methylene protons at δ_H 4.52, dd (*J* = 14.9, 0.9 Hz)/4.22, dt, (*J* = 4.9, 2.1 Hz) and 2.63, dd (*J* = 17.6, 1.5 Hz)/2.96, dd (*J* = 1.76, 2.6 Hz), a methyl singlet at δ_H 1.44 and a methoxyl singlet at δ_H 3.21. Comparison of the ^{1}H and ^{13}C data of **3b** with those of **3a** (Table 2) led to the conclusion that **3b** is a methyl ketal of **3a**. This hypothesis is confirmed not only by the molecular formula of **3b**, which is 14 *amu* more than that of **3a**, but also by the HMBC correlation (Figure S25) of the singlet of the methoxyl protons to the ketal carbon at δ_C 97.7. Therefore, **3b** was named penialidin G.

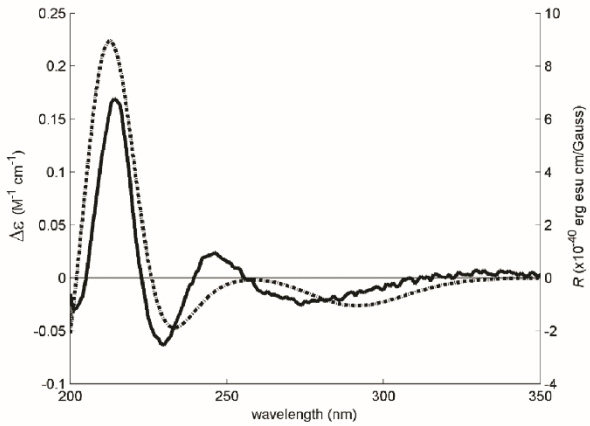

Figure 3. The experimental (solid line, left axis) and simulated (dotted line, right axis) ECD spectra of 3a/C-2(*R*). The ECD experimental signal was very weak, requiring the use of 40 accumulations, increased digital integration time and post-acquisition noise filtering (moving mean).

Surprisingly, the ECD spectrum of the mixture of myxotrichin C (**2b**) and **3b** did not exhibit any Cotton effects. Consequently, we concluded that **3b** is a mixture of both enantiomers.

The biogenesis of **2b**, **3a**, and **3b** can be hypothesized as originated from the hexaketide intermediate (i) (Figure 4). Enzyme-catalyzed nucleophilic addition of the primary hydroxyl group to the ketone carbonyl led to a cyclization to form a 2-methyl-3,6-dihydro-2*H*-pyran-2-ol ring, through an intermediate (ii), in **3a** (2*R*). Dehydration of the hemiketal in **3a** furnished myxotrichin C (**2b**), which underwent a nucleophilic addition of methanol (chromatographic solvent) at C-2 to form an enantiomeric mixture of **3b**. Therefore, **3b** can be an artifact and not a natural product. The co-occurrence of **2b** and **3b** can be a concrete proof of this hypothesis.

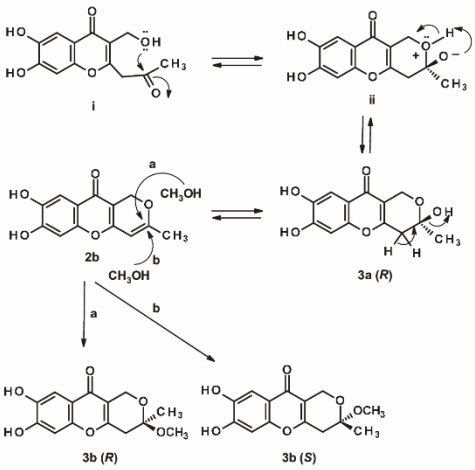

Figure 4. The formation of **3a**, **2b** and a pair of enantiomers of **3b** by nucleophilic addition of methanol to **2b**.

Compound **4** was isolated as white crystals (mp 150–152 °C), and its molecular formula was established as $C_{13}H_{10}O_6$ on the basis of its (+)-HRESIMS *m/z* 263.0569 $[M + H]^+$, (calculated 263.0556 for $C_{13}H_{11}O_6$), indicating nine degrees of unsaturation. The IR spectrum showed absorption bands for hydroxyl (3491, 3376 cm^{-1}), conjugated ketone carbonyls (1679, 1661 cm^{-1}), olefin (1648 cm^{-1}), aromatic (1587, 1523 cm^{-1}), and ether (1276 cm^{-1}) groups. The ^{13}C NMR spectrum (Table 3, Figure S31) displayed thirteen carbon signals which were categorized, according to the DEPTs and HSQC spectra (Figure S33), as two conjugated ketone carbonyls (δ_C 198.3 and 181.6), four oxyquaternary sp^2 (δ_C 191.4, 156.9, 155.9, 141.9), one quaternary sp^2 (δ_C 111.1), three methine sp^2 (δ_C 110.3, 103.8, 103.2), one quaternary sp^3 (δ_C 86.3), one oxymethylene sp^3 (δ_C 69.8) and one methyl (δ_C 16.4) carbons. The ^1H NMR spectrum (Table 3, Figure S31) showed two aromatic singlets at δ_H 7.05 and 6.41, a doublet of an olefinic proton at δ_H 5.68 (J = 0.6 Hz), a pair of doublets of the oxymethylene protons at δ_H 4.49 (J = 12.4 Hz)/4.63 (J = 12.4 Hz), and a methyl singlet at δ_H 2.31, in addition to a broad signal of the hydroxyl protons at δ_H 10.01. The presence of the 6,7-dihydroxy-2,3-dihydro-4*H*-1-benzopyran-4-one moiety was corroborated by the HMBC correlations (Table 3, Figure S34) from H-5 (δ_H 7.05, s) to C-4 (δ_C 181.6), C-6 (δ_C 141.9), C-7 (δ_C 155.9) and C-8a (δ_C 156.9); H-8 (δ_H 6.41, s) to C-4, C-4a (δ_C 111.1), C-6, C-7 and C-8a, and from H_2-2 (δ_H 4.49, d, J = 12.4 Hz/4.63, d, 12.4 Hz) to C-4 and C-8a. That another portion of the molecule was a 5-methylfuran-3(2*H*)-one ring was substantiated by the COSY correlation (Table 3, Figure S32) from the methyl singlet at δ_H 2.31 to H-3′ (δ_H 5.68, d, J = 0.6 Hz), as well as the HMBC correlations (Table 3, Figure S34) from H-3′ to C-3 (δ_C 86.3), C-2′ (δ_C 191.4), C-4′ (δ_C 198.3), and from the methyl singlet at δ_H 2.31 to C-2′ and C-3′ (δ_C 103.8). Finally, the 5-methylfuran-3(2*H*)-one moiety and the 6,7-dihydroxy-2,3-dihydro-4*H*-1-benzopyran-4-one were connected through C-3 since the HMBC spectrum exhibited correlations from H-2 (δ_H 4.49, d, J = 12.4 Hz) to C-3 and C-4′, and from H-3′ to C-3. Therefore, the planar structure of **4** corresponds to 5′-methyl-2*H*,3′*H*,4*H*-spiro [1-benzopyran-3,2′-furan]-3′,4-dione. Since **4** was obtained as a suitable crystal, an X-ray analysis was carried out to determine the absolute configuration of the stereogenic carbon (C-3).

Table 3. The ^1H and ^{13}C NMR (DMSO-d_6, 300.13 and 75.4 MHz) and HMBC assignment for **4**.

Position	Δ_c, Type	δ_H, (J in Hz)	COSY	HMBC
2a	69.8, CH_2	4.49, d (12.4)	2b	C-4, 4′, 8a
2b		4.63, d (12.4)	2a	C-3, 4, 4′, 8a-
3	86.3, C	-	-	-
4	181.6, CO	-	-	-
4a	111.1, C	-	-	-
5	110.3, CH	7.05, s	-	C-4, 6, 7, 8a
6	141.9, C	-	-	-
7	155.9, C	-	-	-
8	103.2, CH	6.41, s	-	C-4, 4a, 6, 7, 8a
8a	156.9, C	-	-	-
2′	191.4, C	-	-	-
3′	103.8, CH	5.68, d (0.8)	5′	C-2′, 3, 4′
4′	198.3, CO	-	-	-
5′	16.4, CH_3	2.31, s	3′	C-2′, 3′
OH	-	10.01, brs	-	-

The ORTEP view, shown in Figure 5, not only confirmed the proposed structure for **4** but also determined unequivocally the absolute configuration of C-3 as 3*S*. Therefore, the absolute structure of **4** is (3*S*)-6,7-dihydroxy-5′-methyl-3′*H*,4*H*-spiro[chromene-3,2′-furan]-3′,4-dione, which was named erubescenschromone A.

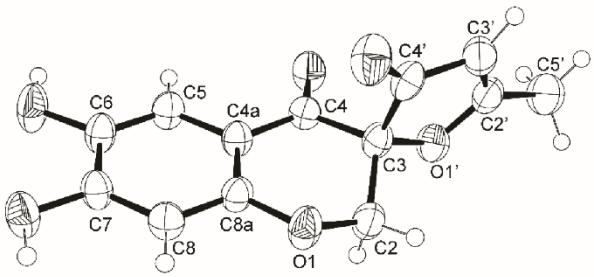

Figure 5. The Ortep view of **4**.

Compound **5** was isolated as a white solid (mp 276–277 °C), and displayed its (+)-HRESIMS *m*/*z* at 305.0667 $[M + H]^+$, (calculated 305.0661 for $C_{15}H_{13}O_7$). Therefore, its molecular formula was established as $C_{15}H_{12}O_7$, indicating ten degrees of unsaturation. The IR spectrum exhibited absorption bands for hydroxyl (3446 cm^{-1}), conjugated ketone carbonyls (1719, 1646 cm^{-1}), aromatic (1560, 1541 cm^{-1}), olefin (1618 cm^{-1}) and ether (1276 cm^{-1}) groups. However, its ^{13}C NMR spectrum (Table 4, Figure S36) displayed only fourteen carbon signals which, in combination with DEPTs and HSQC spectra (Figure S37), can be classified as two ketone carbonyls (δ_C 198.2 and 173.4), one conjugated carboxyl carbonyl (δ_C 167.1), three oxyquaternary sp^2 (δ_C 157.1, 152.8, 143.2), two quaternary sp^2 (δ_C 117.4 and 112.0), one oxymethine sp^2 (δ_C 158.9), three methine sp^2 (δ_C 134.9, 128.7, 104.0), one methoxyl (δ_C 61.0) and one methyl (δ_C 27.5) carbons. The ^1H NMR spectrum (Table 4, Figure S35) exhibited four singlets of aromatic/olefinic protons at δ_H 8.73 (1H), 7.35 (2H), 7.03 (1H), one methoxyl singlet at δ_H 3.75 and one methyl singlet at δ_H 2.29. That **5** consists of a 7-hydroxy-6-methoxy-4-oxo-4*H*-chromene-5-carboxylic acid nucleus, with a substituent on C-3, was supported by the HMBC correlations (Table 4, Figure S38) from H-2 (δ_H 8.73) to C-4 (δ_C 173.4), C-8a (δ_C 152.8) and C-3 (δ_C 117.4); H-8 (δ_H 7.03) to C-4a (δ_C 112.0), C-6 (δ_C 143.2), C-7 (δ_C 157.1), and C-8a, from OCH_3-6 (δ_H 3.75) to C-6, as well as the carbon chemical shift value of OCH_3-6 (δ_C 61.0), characteristic of the methoxyl group flanked by one oxygenated substituent and one carboxyl group. Like many other quaternary sp^2 carbon linked to the carboxyl substituent, the intensity of the signal of C-5 was not strong enough to be observed in the ^{13}C NMR spectrum. Moreover, since there is no proton two or three bonds away from C-5, it was not possible to localize the C-5 signal in the HMBC spectrum. The existence of a 3-oxobut-1-en-1-yl substituent was supported by the presence of a singlet of two protons at δ_H 7.35 (H-10 and H-11) which, through the HSQC spectrum, connected to the two methine sp^2 carbons at δ_C 134.9 (C-10) and δ_C 128.7 (C-11), as well as the HMBC correlations from H-10/H-11 to the ketone carbonyl carbon at δ_C 198.2 (C-12), and from the methyl singlet at δ_H 2.29 (H_3-13) to C-12 and C-11. That the 3-oxobut-1-en-1-yl substituent was on C-3 was also supported by the HMBC correlations (Table 4, Figure S38) from H-10 to C-2 and C-4 as well as from H-2 to C-10. Therefore, the structure of **5** was elucidated as 7-hydroxy-6-methoxy-4-oxo-3-[3-oxobut-1-en-1-yl]-4*H*-chromene-5-carboxylic acid. The literature search revealed that **5** has never been previously reported; however its structure and NMR data were very similar to those of PI-4, a fungal metabolite first isolated by Arai et al. [16] from the mycelium of *Penicillium italicum*, a phyotoxic fungus which causes the blue-mold rot of fruits, and later by Lu et al. [17] from the crude extract of the fungus *Chaetomium indicum* (CBS.860.68). The only difference between PI-4 and **5** is the substituent on C-6 which is a hydroxyl group in the former and a methoxyl group in the latter. Therefore, **5** is identified as 7-hydroxy-6-methoxy-4-oxo-3-[(1*E*)-3-oxobut-1-en-1-yl]-4*H*-chromene-5-carboxylic acid.

Table 4. The ^{1}H and ^{13}C NMR (DMSO-d_6, 500.13 and 125.4 MHz) and HMBC assignment for **5**.

Position	δ_C, Type	δ_H, (*J* in Hz)	HMBC
2	158.9, CH	8.73, s	C-3, 4, 8a, 10
3	117.4, C	-	-
4	173.4, CO	-	-
4a	112.0, C	-	-
5	*	-	-
6	143.2, C	-	-
7	157.1	-	-
8	104.0, CH	7.03, s	-
8a	152.8, C	-	-
9	167.1, CO	-	-
10	134.9, CH	7.35, s	2, 4, 12
11	128.7, CH	7.35, s	3
12	198.2, CO	-	-
13	17.5, CH_3	2.29, s	11, 12
OCH_3-6	61.0, CH_3	3.75, s	6

* not observed.

The structure of **5** and the *trans* double bond between C-10 and C-11 are confirmed by X-ray analysis, as shown in the ORTEP view in Figure 6.

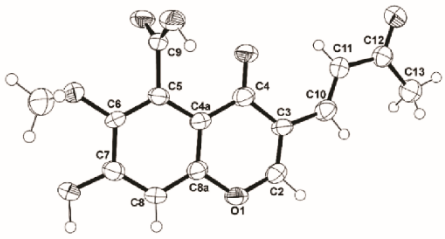

Figure 6. The Ortep view of **5**.

Compound **6** was isolated as a pale yellow viscous oil, and its molecular formula $C_{26}H_{20}O_{11}$ was established based on its (+)-HRESIMS *m/z* 509.1085 $[M + H]^+$, (calculated 509.1084 for $C_{26}H_{21}O_{11}$), indicating twelve degrees of unsaturation. The IR spectrum showed absorption bands for hydroxyl (3443 cm^{-1}), ketone carbonyls (1731, 1715 cm^{-1}), conjugated ketone carbonyls (1697, 1648 cm^{-1}), aromatic (1634, 1556, 1596 cm^{-1}), and ether (1261 cm^{-1}) groups. The ^{13}C NMR spectrum (Table 5, Figure S40) exhibited twenty six carbon signals which can be classified, according to the DEPTs and HSQC spectra (Table 5, Figure S42) as two ketone carbonyls (δ_C 204.6, 200.9), two conjugated ketone carbonyls (δ_C 185.3, 172.2), ten quaternary sp^2 (δ_C 161.3, 156.0, 155.4, 152.5, 150.2, 144.7, 141.4, 115.1, 112.3, 109.8), four methine sp^2 (δ_C 111.1, 108.5, 102.8, 102.6), two oxyquatermary sp^3 (δ_C 61.9 and 78.2), two methine sp^3 (δ_C 71.4 and 69.8), two methylene sp^3 (δ_C 67.2 and 33.4), and two tertiary methyl (δ_C 32.7 and 29.3) carbons. The ^{1}H NMR spectrum (Table 5, Figure S39), in combination with the HSQC spectrum, displayed four singlets of aromatic protons at δ_H 7.26, 7.17, 6.84 and 6.37, two methine singlets at δ_H 5.41 and 5.23, two doublets of the magnetically inequivalent oxymethylene protons at δ_H 4.36 (*J* = 12.8 Hz) and 3.59 (*J* = 12.8 Hz), two doublets of the magnetically inequivalent methylene protons at δ_H 3.47 (*J* = 19.2 Hz) and 2.89 (*J* = 19.2 Hz), in addition to two methyl singlets at δ_H 2.16 and 1.51. The presence of the 7,8-dihydroxy-3-methyl-3,4-dihydro-1*H*,10*H*-pyrano[4,3-*b*]chromen-10-one moiety was substantiated by the HMBC correlations (Table 5, Figure S43) from H-5 (δ_H 7.26, s; δ_C 108.0) to C-4 (δ_C 172.2), C-8a (δ_C 152.5), C-7 (δ_C 150.2), and C-6 (144.7); H-8 (δ_H 6.84, s; δ_C 102.8) to C-4,

C-8a, C-7, C-6, C-4a (δ_C 115.1); H-12 (δ_H 5.41, s; δ_C 71.4) to C-4, C-2 (δ_C 161.3), C-3 (δ_C 112.3), C-10 (δ_C 78.2), and from Me-13 (δ_H 1.51, s; δ_C 29.3) to C-2, C-10, and C-9 (δ_C 33.4). Another portion of the molecule was identified as 3,3-disubstituted 6,7-dihydroxy-2,3-dihydro-4*H*-1-benzopyran-4-one, based on the HMBC correlations from H-5′ (δ_H 7.17, s; δ_C 111.1) to C- 4′ (δ_C 185.3), C-8′a (δ_C 156.0), C-7′ (δ_C 155.4), C-6′ (δ_C 141.4); H-8′ (δ_H 6.37, s; δ_C 102.6) to C-4′, C-8′a, C-6′ and C-4′a (δ_C 109.8), as well as from H_2-2′ (δ_H 4.36, *J* = 12.8 Hz/3.59, *J* = 12.8 Hz) to C-4′, C-8′a and C-3′ (δ_C 61.9). That the disubstituted 6,7-dihydroxy-2,3-dihydro-4*H*-1-benzopyran-4-one was connected to the 7,8-dihydroxy-3-methyl-3,4-dihydro-1*H*,10*H*-pyrano[4,3-*b*]chromen-10-one moiety, through C-3′ of the former and C-12 of the latter, was confirmed by the HMBC correlations from H-12 to C-3′ and H_2-2′ to C-12. Moreover, since the HMBC spectrum also exhibited correlations from H-12 and H_2-2′ to the ketone carbonyl carbon at δ_C 200.9 (C-14), from H-15 (δ_H 5.23, s; δ_C 69.8) to C-9, C-10 (δ_C 78.2), C-14, and from Me-13 to C-15, the 7,8-dihydroxy-3-methyl-3,4-dihydro-1*H*,10*H*-pyrano[4,3-*b*]chromen-10-one moiety was connected through C-10 and C-15 of the oxan-4-one ring. The acetyl group on C-15 was corroborated by the HMBC correlations from Me-17 (δ_H 2.16, s; δ_C 32.7) to C-15 and the carbonyl carbon at δ_C 204.6 (C-16), as well as from H-15 to C-16. Taking together the molecular formula, the NMR data, and the HMBC correlations, the planar structure of **6** was unambiguously established. In order to determine the relative configurations of the stereogenic carbons C-10, C-12, C-15 and C-3′, the ROESY spectrum was obtained. The ROESY spectrum (Figure S44) exhibited strong correlations from Me-13 (δ_H 1.51, s) to H-15 (δ_H 5.23, s) and the methylene proton at δ_H 2.89, d (*J* = 19.2 Hz), implying that these three protons are on the same face. Additionally, H-15 also shows a correlation with Me-17 (δ_H 2.16, s). Since the pyran ring and the oxan-4-one ring of the 9-oxabicyclo[3.3.1]nonan-3-one ring system are in a rigid half-chair conformation, Me-13 must be in a pseudoequatorial position while the methylene proton at δ_H 2.89, d (*J* = 19.2 Hz) and H-15 are in a pseudoaxial position. Therefore, the acetyl group on C-15 must be in a pseudoequatorial position. This was confirmed by the higher chemical shift value (δ_H 3.47, d, *J* = 19.2 Hz) of the pseudoequatorial H-9 as it is in the deshielding zone of the carbonyl (C-16) of the acetyl group. On the other hand, H-12 (δ_H 5.41, s) showed a weak correlation to one of H-2′ at δ_H 3.59, d (*J* = 12.9 Hz). Therefore both of these protons should be in the pseudoequatorial position since the pseudoaxial H-2′ (δ_H 4.36, d, *J* = 12.9 Hz) is under the anisotropic effect (deshielding) of the carbonyl at C-14 of ring D. With these ROESY correlations, the relative configurations of C-10, 12, 15, and 3′ were proposed as 10*S**, 12*S**, 15*S**, and 3′*S**. However, it is necessary to determine the absolute configurations of these stereogenic carbons.

Since **6** could not be obtained as a suitable crystal for an X-ray analysis, the determination of its stereogenic carbons had to be carried out by comparison of the calculated and experimental ECD spectra. Although the ROESY correlations pointed to the relative configuration of C-10 and C-15 as 10*S*, 15*S*, it is possible that it can be 10*R*, 15*R*, thus reducing its number of possible configurations from 16 (eight pairs of diastereoisomers) to eight (four pairs of diastereoisomers). Hence, four computational models were constructed by combining the two configurations of C-3′ with the two of C-12. The conformational analysis of **6** by molecular mechanics (MM2 and MMFF95 force fields) focused on combinations of hydroxyl 120° rotations and rings conformations. Most diastereoisomers did not show ring conformational freedom which limited the number of models to compute. The most stable APFD/6-31G conformation of **6** whose absolute configurations of C-10, C-12, C-15, and C-3′ are 10*S*, 12*S*, 15*S*, 3′*S*, as deduced from ROESY correlations, is shown in Figure 7.

Table 5. The ^{1}H and ^{13}C NMR (DMSO-d_6, 500.13 and 125.4 MHz) and HMBC assignment for **6**.

Position	δ_C, Type	δ_H, (*J* in Hz)	COSY	HMBC
2	161.3, C	-	-	-
3	112.3, C	-	-	-
4	172.2, CO	-	-	-
4a	115.1, C	-	-	-
5	108.0, CH	7.26, s	-	C-4, 6, 7, 8a
6	144.7, C	-	-	-
7	150.2, C	-	-	-
8	102.8, CH	6.84, s	-	C-4, 4a, 6, 7, 8a
8a	152.5, C		-	-
9α	33.4 CH_2	3.47, d (19.2)	H-9β	C-2, 3, 10, 13, 15
9β		2.98, d (19.2)	H-9α	C-2, 3, 10, 13, 15
10	78.2, C	-	-	-
12	71.4, CH	5.41, s	-	C-2, 3, 3′,4, 4′, 10, 14
13	29.3, CH_3	1.51, s	-	C-2, 9, 10, 14, 15
14	200.9, CO	-	-	-
15	69.8, CH	5.23, s	H-17	C-9, 10, 13, 14, 16
16	204.6, CO	-	-	-
17	32.7, CH_3	2.16, s	H-15	C-15, 16
2′α	67.7, CH_2	4.36, d (12.8)	H-2′β	C-3′, 4, 8′a, 12, 14
2′β		3.59, d (12.8)	H-2′α, 15	C-3′, 4, 8′a, 12, 14
3′	61.9, C	-	-	-
4′	185.3, CO	-	-	-
4′a	109.8, C	-	-	-
5′	111.1, CH	7.17, s	-	C-4′, 6′, 7′, 8′a
6′	141.1, C	-	-	-
7′	155.4, C	-	-	-
8′	102.6, CH	6.37, s	-	C-4′, 4′a, 6′, 8′a
8′a	156.0, C	-	-	-

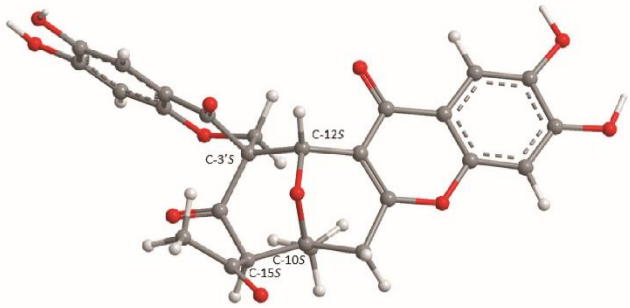

Figure 7. The most stable APFD/6-31G conformation of **6**, presented with the absolute configuration found by spectrometric methods.

All conformations were energetically minimized and ranked using a DFT model. The lowest energy ones, representing at least 95% of the model Boltzmann population, were used to calculate the expected Boltzmann-averaged ECD spectra of the four **6** diastereoisomers. The fitting between the experimental and calculated spectra is presented in Figure 8, showing that the **6** is the C-10*S*, C-12*S*, C-3′*S*, C-15*S* enantiomer.

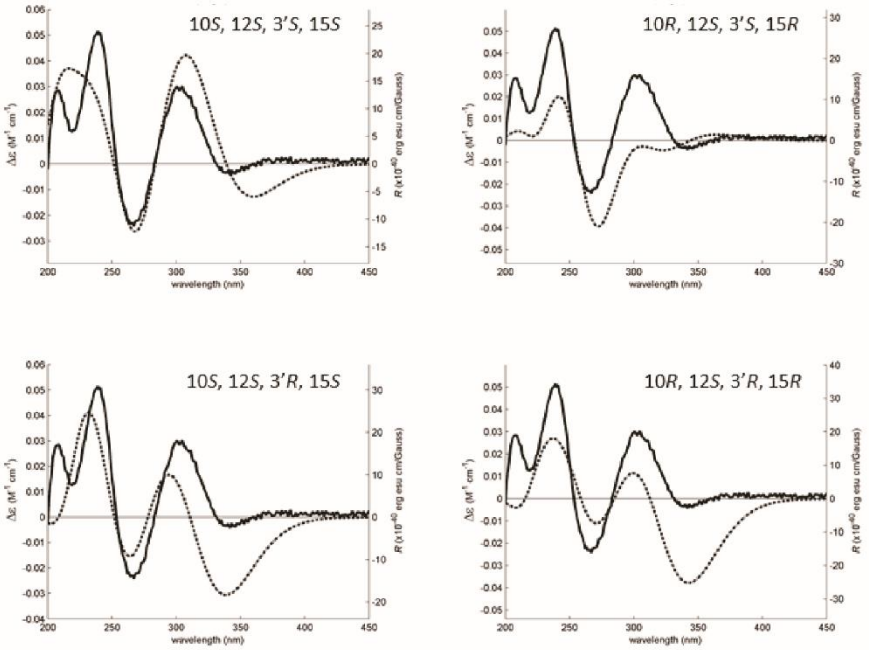

Figure 8. The experimental (solid line, left axes) and simulated (dotted line, right axes) ECD spectra of four diastereoisomers of **6**. The best experimental-simulated fit belongs to the diastereoisomer with the absolute configuration 10*S*, 12*S*, 3′*S*, 15*S*. The theoretical ECD spectra of the enantiomers of the presented diastereoisomers are the exact inversions of the ones depicted here and do not fit the experimental data.

The literature search revealed that **6** has never been previously reported and therefore it is a new compound which was named erubescenschromone B.

Compound **7** was isolated as a pale yellow oil and the (+)-HRESIMS showed the $[M + H]^+$ peak at m/z 509.1085 (calculated 509.1084 for $C_{26}H_{21}O_{11}$). Therefore, its molecular formula is $C_{26}H_{20}O_{11}$, indicating eighteen degrees of unsaturation. The IR spectrum showed absorption bands for hydroxyl (3491, 3376 cm^{-1}), conjugated ketone carbonyls (1679, 1661 cm^{-1}), olefin (1648 cm^{-1}), aromatic (3108, 1578, 1523 cm^{-1}), and ether (1206 cm^{-1}) groups. The ^{13}C NMR spectrum (Table 6, Figure S46) exhibited twenty six carbon signals which, in combination with DEPTs and HSQC spectra (Table 6, Figure S47), can be classified as three carbonyls (δ_C 202.8, 183.6, 173.5), fifteen quaternary sp^2 (δ_C 172.6, 155.9, 154.9, 154.2, 152.1, 150.7, 144.3, 141.6, 138.0, 132.4, 129.5, 118.6, 113.5, 1119, 103.9), five methine sp^2 (δ_C 125.7, 110.5, 108.7, 103.3, 103.1), one methylene sp^3 (δ_C 66.2) and two methyl (δ_C 32.4 and 16.6) carbons. The ^1H NMR spectrum (Table 6, Figure S45) exhibited five singlets of aromatic protons at δ_H 8.00, 7.45, 7.19, 6.93, and 6.34; a singlet of oxymethylene protons at δ_H 4.67 (2H) and two methyl singlets at δ_H 2.71 and 2.32. The presence of the 6,7-dihydroxy-2,3-dihydro-4*H*-chromen-4-one moiety was corroborated by the HMBC correlations (Table 6, Figure S48) from H-5′ (δ_H 7.19, s; δ_C 110.5) to C-4′ (δ_C 183.6), C-6′(δ_C 155.9), C-8′a (δ_C 154.9) and C-7′ (δ_C 141.6); H-8′ (δ_H 6.34, s; δ_C 103.3) to C-4′a (δ_C 111.9), C-6′, C-7′, C-8′a, and H_2-2′ (δ_H 4.67, s; δ_C 66.2) to C-3′ (δ_C 103.9) and C-4′ (δ_C 183.6). That the substituent on C-3′ was an enolic exocyclic double bond was substantiated by the HMBC correlations from H_2-2′ to C-3′ (δ_C 103.9) and the enolic carbon (C-9′, δ_C 172.6). Another moiety was established as 7-substituted 5-acetyl-2,3-dihydroxy-6-methyl-9*H*-xanthen-9-one since the HMBC spectrum showed correlations

from H-5 (δ_H 6.93, s; δ_C 103.1) to C-7 (δ_C 143.3), C-8a (δ_C 113.5), C-10a (δ_C 154.2); H-8 (δ_H 7.45, s; δ_C 108.7) to C-6 (δ_C 150.7), C-7, C-9 (δ_C 173.5), C-10a; H-1 (δ_H 8.00, s; δ_C 125.7) to C-3 (δ_C 138.0) and C-4a (δ_C 152.1); Me-11 (δ_H 2.32, s; δ_C 16.6) to C-2 (δ_C 129.5), C-3, C-4 (δ_C 132.2). Since H-1 also showed the HMBC correlation to C-9′, the 5-acetyl-2,3-dihydroxy-6-methyl-9*H*-xanthen-9-one was linked to the 6,7-dihydroxy-2,3-dihydro-4*H*-chromen-4-one moiety through C-9′. An extensive literature search revealed that the structure of **7** is the same as that of the enol tautomer of the compound, named SPF-3059-30, isolated from the acetone extract of the mycelium of *Penicillium* sp. SPF-3050 (FERM BB-7663), cultured in the liquid medium [11]. However, the authors claimed that SPF-3050-30 was isolated as a mixture of keto-enol tautomers, as supported by the duplication of the ^{1}H and ^{13}C chemical shift values but without an assignment. The ^{13}C NMR data of SPF-3050-30 displayed forty one carbon signals, e.g., four signals for the methyl groups, three signals for the oxymethylene carbons, two signals for the carbonyl carbon of the acetyl group, two signals for the carbonyl of the chromone nucleus and two signals of the carbonyl of the xanthone moiety, etc., while its ^{1}H NMR data presented two methyl signals of the methyl group on the xanthone nucleus, two methyl signals for the acetyl group and nine signals of aromatic protons. On the contrary, the ^{1}H and ^{13}C NMR spectra of **7** in DMSO (Table 6, Figures S45 and S46) showed that it was present only in an enolic form. This is supported by the fact that the enolic form is stabilized by the hydrogen bonding between OH-9′ and the carbonyl of the chromone moiety (C-4′).

Table 6. The ^{1}H and ^{13}C NMR (DMSO-d_6, 500.13 and 125.4 MHz) and HMBC assignment for **7**.

Position	δ_C, Type	δ_H, (*J* in Hz)	HMBC
1	125.7, CH	8.00, s	C-3, 4a, 9′
2	129.5, C	-	-
3	138.0, C	-	-
4	132.2, C	-	-
4a	152.1, C	-	-
5	103.1, CH	6.93, s	C-7, 8a, 10a
6	150.9, C	-	-
7	144.3, C	-	-
8	108.7, C	7.45, s	C-6, 7, 9, 10a
8a	113.5, C	-	-
9	173.5, CO	-	-
9a	118.6, C	-	-
10a	154.2, C	-	-
11	16.6, CH_3	2.32, s	C-2, 3, 4
12	202.8, CO	-	-
13	32.4, CH_3	2.71, s	C-12
2′	66.2, CH_2	4.67, s	C-3′, 4′, 8′a, 9′
3′	103.9, C	-	-
4′	183.6, CO	-	-
4′a	111.9, C	-	-
5′	110.5, CH	7.19, s	C-4′, 6′, 7′, 8′a
6′	155.9, C	-	-
7′	141.6, C	-	-
8′	103.3, CH	6.34, s	C-4′a, 6′, 7, 8′a
8′a	154.9, C	-	-
9′	172.6, C	-	-

Compound **7** can be considered as a decarboxylated derivative of xanthofulvin, a semaphorin inhibitor isolated from the culture broth of the fungus *Penicillium* sp. SPF-3059 [18].

Compounds **1a–e**, **2a**, **3a**, **4**, **7–9** were evaluated for their antibacterial activity against Gram-negative and Gram-positive bacteria by disc diffusion method, and the MIC and MBC of several reference strains and multidrug-resistant isolates from the environment were also determined. In the disc diffusion assay, a halo of growth inhibition for all Gram-positive bacteria exposed to **8**

(Table 7) and for methicillin-resistant *Staphylococcus aureus* (MRSA) 66/1 exposed to **9** was detected. However, in the range of concentrations tested, it was only possible to determine MICs for **8** (Table 7), with MIC values of 8 mg/mL for *E. faecalis* ATCC 29212 and vancomycin-resistant *E. faecalis* (VRE) B3/101, 16 mg/mL for *E. faecium* ATCC 19434, and 32 mg/mL for *E. faecium* 1/6/63 (VRE) and *S. aureus* ATCC 29213. While it was not possible to determine the MBC for the other Gram-positive strains, the MBC for *S. aureus* ATCC 29213 was 64 mg/mL (Table 7). These results suggested that **8** might have a bacteriostatic effect.

Table 7. The antibacterial activity of **8** against a Gram-positive reference and multidrug-resistant strains. MIC and MBC are expressed in mg/mL.

Strains	*E. faecalis* ATCC29212	*E. faecium* ATCC19434	*S. aureus* ATCC29213	*E. faecalis* B3/101 (VRE)	*E. faecium* 1/6/63 (VRE)	*S. aureus* 66/1 (MRSA)
Disc diffusion	+	+	+	+	+	+
MIC	8	16	32	8	32	>64
MBC	>64	>64	64	>64	>64	>64

MIC, minimal inhibitory concentration; MBC, minimal bactericidal concentration; VRE, vancomycin-resistant *Enterococcus*; MRSA, methicillin-resistant *Staphylococcus aureus*; (-), no inhibition halo; (+), 7–9 mm inhibition halo.

The ability of the tested compounds to prevent biofilm formation was evaluated on four reference strains by measuring the total biomass. For **8**, four concentrations ranging from 2 × MIC to $\frac{1}{4}$ MIC were tested against *E. faecalis* ATCC 29212, *E. faecium* ATCC 19434 and *S. aureus* ATCC 29213. For the other compounds, since it was not possible to determine their MIC values, the highest concentration tested in the previous assays was used. The results were interpreted using a comparative classification that divides adherence capability of tested strains into four categories: (i) non-adherent, (ii) weakly adherent, (iii) moderately adherent, and (iv) strongly adherent [19]. OThe optical density cut-off value (ODc) for each microtiter plate was defined as three standard deviations above the mean OD of the negative control. The use of this classification, which uses the negative control as the starting point instead of using the positive control as a reference, reduces the risk of inconsistencies due to external factors that influence biofilm production [20]. The tested compounds did not inhibit the biofilm formation of *S. aureus* ATCC 29213, *E. coli* ATCC 25922, and *P. aeruginosa* ATCC 27853. However, the biofilm forming ability of *E. faecalis* ATCC 29212, which is classified as a strong biofilm producer, was impaired by **8** (MIC and 2 × MIC) and **9** (Table 8). On the other hand, **8** was able to increase the biofilm production of a weak biofilm producer *E. faecium* ATCC 19434.

Table 8. The classification of the ability of *E. faecalis* ATCC 29212 to adhere to and form biofilm after exposure to **1a–e**, **2a**, **3a**, **4**, **7–9**, in comparison to the untreated control.

Compound	Concentration (mg/L)	OD ± SD	Classification
1a	64	1.205 ± 0.025	strong
1b	64	1.547 ± 0.218	strong
1c	64	1.673 ± 0.308	strong
1d	64	1.522 ± 0.308	strong
1e	32	1.378 ± 0.378	strong
2a	64	1.136 ± 0.138	strong
3a	64	2.128 ± 0.248	strong
4	64	0.867 ± 0.280	strong
7	64	1.192 ± 0.239	strong
8	16 (2 × MIC)	0.089 ± 0.002	weak
8	8 (MIC)	0.099 ± 0.006	weak
8	4 (1/2 MIC)	1.884 ± 0.220	strong
8	2 (1/4MIC)	2.358 ± 0.416	strong
9	64	0.263 ± 0.014	moderate
None	0	0.080 ± 0.002	strong

OD = optical density; SD = standard deviation; The classification used is based on criteria in [19], Average OD value for negative control was found to be 0.055 ± 0.002, therefore the optical cut-off value (ODc) is equal to 0.055 + (3 × 0.002) = 0.061; 2 × ODc = 0.122; 4 × ODc = 0.244.

The screening of a potential synergy between the tested compounds and clinically relevant antimicrobial drugs revealed a slight synergy, as determined by the disc diffusion assay (Table 9). Compound **1b**, in combination with cefotaxime (CTX), resulted in a small synergistic effect, as seen by a small increment in the zone of inhibition when compared to the inhibition halo of CTX alone in *E. coli* SA/2, an extended-spectrum β-lactamase producer (ESBL). A similar effect was observed for VRE *E. faecalis* B3/101 when **8** was combined with VAN. These results were confirmed by the checkerboard method or by determining the MIC for each antibiotic in the presence of a fixed concentration of each compound when it was not possible to determine a MIC value for the test compound. In the latter, the concentration of each compound used was the highest concentration tested in previous assays which did not inhibit the growth of the four multidrug-resistant strains under study. The effects observed using the disc diffusion assay were not replicated, however, when VRE *E. faecalis* B3/101 was exposed to **1d**, **3a** and **9**, there was a two-fold reduction in the MIC of VAN. On the other hand, when ESBL *E. coli* SA/2 was exposed to **1c** and **7**, there was at least a two-fold increase in the MIC of CTX. When VRE *E. faecium* 1/6/63 was exposed to **9**, there was a two-fold reduction in the MIC of VAN. On the contrary, when it was exposed to **1e**, there was at least a two-fold increase in the MIC of VAN (Table 9). The differences in the results obtained using both techniques may be explained by different diffusion rates of each compound in the agar plates.

Thus, in terms of antibacterial activity, **8** is the most promising. Even though no synergy with VAN or OXA was found, this compound alone exhibited an antibiofilm activity against *E. faecalis* and antibacterial activity against the reference *S. aureus*, *E. faecalis*, and *E. faecium* strains. Most importantly, **8** showed antibacterial activity against both vancomycin-resistant *E. faecalis* and vancomycin-resistant *E. faecium* strains, a pathogen classified by WHO as high priority for the research and development of new antibiotics [21]. These results call for a more in-depth study of this compound.

Table 9. The combined effect of clinically used antibiotics with **1a–e**, **2a**, **3a**, **4**, **7–9** against multidrug-resistant strains. MICs are expressed in mg/mL.

Compound	*E. coli* SA/2		*E. faecalis* B3/101		*E. faecium* 1/6/63		*S. aureus* 66/1	
	CTX		VAN		VAN		OXA	
	Disc Diffusion	MIC	Disc Diffusion	MIC	Disc Diffusion	MIC	Disc Diffusion	MIC
Antibiotic	+	512	-	1024	-	1024	-	64
Antibiotic + **1a**	-	512	-	1024	-	1024	-	64
Antibiotic + **1b**	+	512	-	1024	-	1024	-	64
Antibiotic + **1c**	-	>512	-	1024	-	1024	-	64
Antibiotic + **1d**	-	512	-	512	-	1024	-	64
Antibiotic + **1e**	-	512	-	1024	-	>1024	-	64
Antibiotic + **2a**	-	512	-	1024	-	1024	-	64
Antibiotic + **3a**	-	512	-	512	-	1024	-	64
Antibiotic + **4**	-	512	-	1024	-	1024	-	64
Antibiotic + **7**	-	>512	-	1024	-	1024	-	64
Antibiotic + **8**	-	512	+	*	-	*	-	64
Antibiotic + **9**	-	512	-	512	-	512	-	64

MIC = minimal inhibitory concentration; (-) = no inhibition halo or no increase in the inhibition halo; (+) = halo of inhibition or increase of the inhibition halo by 2 mm; CTX = cefotaxime; VAN = vancomycin; OXA = oxacillin. * For this compound, the checkerboard assay was performed and, with FICI = 0.7 for *E. faecalis* B3/101 and FICI = 2 for *E. faecium* 1/6/63, no interaction between **8** and VAN was found ($0.5 < \text{FICI} \leq 4$, 'no interaction').

3. Experimental Section

3.1. General Experimental Procedures

The melting points were determined on a Stuart Melting Point Apparatus SMP3 (Bibby Sterilin, Stone, Staffordshire, UK) and are uncorrected. Optical rotations were measured on an ADP410 Polarimeter (Bellingham + Stanley Ltd., Tunbridge Wells, Kent, UK). Infrared spectra were recorded in a KBr microplate in an FTIR spectrometer Nicolet iS10 from Thermo Scientific (Waltham, MA, USA) with a Smart OMNI-Transmission accessory (Software 188 OMNIC 8.3, Thermo Scientific, Waltham, MA, USA). ^{1}H and ^{13}C NMR spectra were recorded at ambient temperature on a Bruker

AMC instrument (Bruker Biosciences Corporation, Billerica, MA, USA) operating at f300 or 500 and 75 or 125 MHz, respectively. High resolution mass spectra were measured with a Waters Xevo QToF mass spectrometer (Waters Corporations, Milford, MA, USA) coupled to a Waters Aquity UPLC system. A Merck (Darmstadt, Germany) silica gel GF_{254} was used for preparative TLC, and a Merck Si gel 60 (0.2–0.5 mm) was used for column chromatography.

3.2. Fungal Material

The fungus was isolated from the marine sponge *Neopetrosia* sp. which was collected, by scuba diving at a depth of 5–10 m, from the coral reef at Samaesan Island (12°34′36.64″ N, 100°56′59.69″ E), Chonburi province, Thailand, in April 2014. The sponge was washed with 0.01% sodium hypochlorite solution for 1 min, followed by sterilized seawater three times, and then dried on sterile filter paper under sterile aseptic condition. The sponge was cut into small pieces (5 mm × 5 mm) and placed on Petri dish plates containing 15 mL potato dextrose agar (PDA) medium mixed with 300 mg/L of streptomycin sulfate, and incubated at 28 °C for 7 days. The hyphal tips emerging from sponge pieces were individually transferred onto PDA slants and maintained as pure cultures at Kasetsart University Fungal Collection, Department of Plant Pathology, Faculty of Agriculture, Kasetsart University, Bangkok, Thailand, for further identification. The fungal strain KUFA0220 was identified as *Penicillium erubescens*, based on morphological characteristics such as colony growth rate and growth pattern on standard media, namely Czapek's agar, Czapek yeast autolysate agar, and malt extract agar. Microscopic characteristics including size, shape and ornamentation of conidiophores and spores were examined under a light microscope. This identification was confirmed by molecular techniques using Internal Transcribed Spacer (ITS) primers. DNA was extracted from young mycelia following a modified Murray and Thompson method [22]. Primer pairs ITS1 and ITS4 [23] were used for ITS gene amplification. PCR reactions were conducted on Thermal Cycler and the amplification process consisted of the initial denaturation at 95 °C for 5 min, 34 cycles at 95 °C for 1 min (denaturation), at 55 °C for 1 min (annealing) and at 72 °C for 1.5 min (extension), followed by final extension at 72 °C for 10 min. The PCR products were examined by agarose gel electrophoresis (1% agarose with 1 × TBE buffer) and visualized under UV light after staining with ethidium bromide. DNA sequencing analyses were performed using the dideoxyribonucleotide chain termination method [24] by Macrogen Inc. (Seoul, Korea). The DNA sequences were edited using the FinchTV software (version 1.4, Geospiza Inc, Seattle, WA, USA) and submitted into the BLAST program for alignment and compared to fungal species in the NCBI database (http://www.ncbi.nlm.nih.gov/). Its gene sequences were deposited in GenBank with accession number KY041867.

3.3. Extraction and Isolation

The fungus was cultured for one week at 28 °C in five Petri dishes (i.d. 90 mm) containing 20 mL of potato dextrose agar per dish. The mycelial plugs (5 mm in diameter) were transferred to two 500 mL Erlenmeyer flasks containing 200 mL of potato dextrose broth, and incubated on a rotary shaker at 120 rpm at 28 °C for one week. Fifty 1000 mL Erlenmeyer flasks, each containing 300 g of cooked rice, were autoclaved at 121 °C for 15 min. After cooling to room temperature, 20 mL of a mycelial suspension of the fungus was inoculated per flask and incubated at 28 °C for 30 days, after which 500 mL of ethyl acetate was added to each flask of the moldy rice and macerated for 7 days, and then filtered with Whatman No. 1 filter paper (GE Healthcare UK Limited, Buckinghamshire, UK). The ethyl acetate solutions were combined and concentrated under reduced pressure to yield 160 g of crude ethyl acetate extract which was dissolved in 500 mL of $CHCl_3$ and then filtered with Whatman No. 1 filter paper. The chloroform solution was then washed with H_2O (3 × 500 mL) and dried with anhydrous Na_2SO_4, filtered and evaporated under reduced pressure to give 112 g of the crude chloroform extract which was applied on a column of silica gel (450 g), and eluted with mixtures of petrol-$CHCl_3$ and $CHCl_3$-Me_2CO, wherein 250 mL fractions were collected as follow: Frs 1–147 (petrol-$CHCl_3$, 1:1), 148–223 (petrol-$CHCl_3$, 3:7), 224–230 (petrol-$CHCl_3$, 1:9), 231–238 ($CHCl_3$), 239–452 ($CHCl_3$-Me_2CO,

9:1), 453–512 ($CHCl_3$-Me_2CO, 7:3), 512–546 (Me_2CO, 7:3). Frs 75–117 were combined (1.18 g) and applied on a column of silica gel (35 g) and eluted with mixtures of petrol-$CHCl_3$ and $CHCl_3$-Me_2O, wherein 100 mL sfrs were collected as follow: Sfrs 1–20 (petrol), 21–33 (petrol-$CHCl_3$, 9:1), 34–48 (petrol-$CHCl_3$, 7:3), 49–59 (petrol-$CHCl_3$, 1:9), 60–65 (petrol-$CHCl_3$), 66–80 ($CHCl_3$-Me_2CO, 9:1), 81–106 $CHCl_3$-Me_2CO, 7:3), 107–120 (Me_2CO). Sfrs 35–46 were combined (103.0 mg) and purified by TLC (Silica gel G_{254}, $CHCl_3$:Me_2CO:HCO_2H, 97:3:0.01) to give 50.2 mg of β-sitostenone [3]. Frs 238–245 were combined (1.75 g) and precipitated in MeOH to give 202.1 mg of **8** [12–14]. Frs 246–251 were combined (2.67 g) and precipitated in MeOH to give 472.2 mg of ergosterol 5,8-endoperoxide [4]. Frs 252–286 were combined (493.0 mg) and crystallized in MeOH to give further 367.1 mg of ergosterol 5,8-endoperoxide. Frs 287–299 were combined (580.4 mg) and crystallized in a mixture of $CHCl_3$-Me_2CO to give 78 mg of **2a** [7,8], and the mother liquor was combined with frs 300–319 (837.2 mg) and precipitated in Me_2CO to give 10.0 mg of **1b** [5]. The mother liquor (855 mg) was applied on a column chromatography of silica gal (30 g) and eluted with petrol-$CHCl_3$, $CHCl_3$, $CHCl_3$-Me_2CO, and MeOH, wherein 100 mL fractions were collected as follows: Sfrs 1–11 (petrol-$CHCl_3$, 1:1), 12–28 (petrol-$CHCl_3$, 3:7), 29–86 (petrol-$CHCl_3$, 1:9), 87–126 ($CHCl_3$), 127–135 ($CHCl_3$-Me_2CO, 9:1), 136–138 (Me_2CO). Sfrs 100–126 were combined (71.3 mg) and purified by TLC (Silica gel G_{254}, $CHCl_3$:Me_2CO:HCO_2H, 9:1:0.01) to give further 10.0 mg of **1b**. Sfrs 127 (48 mg) was crystallized in a mixture of $CHCl_3$-Me_2CO to give further 30.0 mg of **2a**. Frs 343–366 were combined (1.46 g) and crystallized in MeOH to give 98.3 mg of **4**, and the mother liquor was combined with frs 367–386 (1.77 g) and recrystallized in MeOH to give further 8.0 mg of **1a** [5]. The mother liquor of the combined frs 343–386 (1.36 g) was applied on a column chromatography of silica gel (40 g), and eluted with petrol-$CHCl_3$, $CHCl_3$, $CHCl_3$-Me_2CO and Me_2CO, wherein 100 mL fractions were collected as follows, Sfrs 1–50 (petrol-$CHCl_3$, 1:1), 51–88 (petrol-$CHCl_3$, 3:7), 89–110 (petrol-$CHCl_3$; 1:9), 111–139 ($CHCl_3$), 140–197 ($CHCl_3$-Me_2CO, 9:1), 198–201 ($CHCl_3$-Me_2CO, 7:3), 202–215 (Me_2CO). Sfrs 140–143 were combined (361.0 mg) and applied on a Sephadex LH-20 column (10 g), and eluted with MeOH to give 12.0 mg of **1a** and 10.1 mg of **9** [3]. Sfrs 147–151 were combined (221.0 mg) and applied on a Sephadex LH-20 column (10 g) and eluted with MeOH to give 10.0 mg of a mixture of **2b** (major component) [6] and **3b**. Sfrs 189–201 were combined (72.3 mg) and purified by TLC (Silica gel G_{254}, $CHCl_3$:MeOH:HCO_2H, 95: 5: 0.1) to give 7.1 mg of **3a** [9]. Frs 387–444 were combined (2.73 g) and applied on a column of Sephadex LH-20 (20 g) and eluted with MeOH, wherein 20 mL of 30 fractions were collected. Sfrs 11–30 were combined (472.3 mg) and crystallized in Me_2CO to give further 19 mg of **9**. The mother liquor was applied on a Sephadex LH-20 column (20 g) and eluted with a 1:1 mixture of MeOH-$CHCl_3$ to give 15 mg of **7** [11]. Frs 517–529 were combined (1.40 g) and crystallized in MeOH to give 26.6 mg of **1e** [5], and the mother liquor was combined with frs 445–516 (6.90 g) and applied on a column of Sephadex LH-20 column (30 g) and eluted with MeOH, wherein 20 mL fractions were collected. Sfrs 21–30 were combined (106.2 mg) and purified by TLC (Silica gel G_{254}, $CHCl_3$:MeOH:HCO_2H, 9:1:0.01) to give 10 mg of **3a** [9,10] and 12 mg of **6**. Sfrs 31–60 were combined (5.90 g) and applied on a column chromatography of silica gal (110 g) and eluted with petrol-$CHCl_3$, $CHCl_3$, $CHCl_3$-Me_2CO and Me_2CO, wherein 100 mL fractions were collected as follows, Sfrs 1–26 (petrol-$CHCl_3$, 1:1), 27–56 (petrol-$CHCl_3$, 3:7), 57–98 (petrol-$CHCl_3$, 1:9), 99–200 ($CHCl_3$), 201–297 ($CHCl_3$-Me_2CO, 9:1), 298–320 ($CHCl_3$-Me_2CO, 7:3), 321–332 ($CHCl_3$-Me_2CO, 1:9), 333–358 (Me_2CO). Sfrs 156–184 were combined (112.0 mg) and crystallized in Me_2CO to give further 26.1 mg of **9**. Sfrs 252–294 were combined (464.9 mg) and applied on a Sephadex LH-20 column (20 g) and eluted with MeOH to give 23.0 mg of **1c**. Sfrs 295–344 were combined (3.0 g), applied on a Sephadex LH-20 column (20 g) and eluted with a 1:1 mixture of MeOH-$CHCl_3$, wherein 20 mL fractions were collected. Sfrs 31–72 were combined (262.9 mg) and purified by TLC (Silica gel G_{254}, $CHCl_3$:MeOH:HCO_2H, 9:1:0.01) to give 12.1 mg **1d** [6]. Sfrs 73–96 were combined (90.6 mg) and purified by TLC (Silica gel G_{254}, $CHCl_3$:MeOH:HCO_2H, 9:1:0.01) to give 10.6 mg of **2c** [9]. Sfrs 97–115 were combined (644.8 mg) and precipitated in MeOH to give 12 mg of a mixture of **2b** and **3b**, and the mother liquor was dried (619.7 mg) and applied on a Sephadex LH-20 column (10 g) and eluted with a 1:1 mixture of $CHCl_3$:MeOH, wherein 70 sub-fractions (2 mL each) were collected. Sfrs 25–32 were

combined (40.8 mg) and precipitated in MeOH to give 10 mg of **1e** [5]. Sfrs 33–45 were combined (70.1 mg) and purified by TLC (Silica gel G_{254}, $CHCl_3$:MeOH:HCO_2H, 9:1:0.01) to give 6 mg of **5**. Sfrs 46–56 were combined (65.3 mg) and precipitated in MeOH to give further 7 mg of **5**.

3.3.1. 1-Hydroxy-12-methoxycitromycin (**1c**)

White solid, mp 232–233 °C ($CHCl_3$/MeOH); IR (KBr) ν_{max} 3420 (br), 2921, 1662, 1627, 1594, 1555, 1517, 1453, 1270 cm^{-1}; For ^1H and ^{13}C spectroscopic data (DMSO-d_6, 500.13 and 125.4 MHz), see Table 1; (+)-HRESIMS m/z 277.0715 $[M + H]^+$ (calculated for $C_{14}H_{13}O_6$, 277.0712).

3.3.2. Erubescenschromone A [(3*S*)-6,7-Dihydroxy-5′-methyl-3′*H*,4*H*-spiro[chromene-3,2′-furan]-3′, 4-dione (**4**)]

White crystal, mp 150–152 °C ($CHCl_3$/MeOH); $[\alpha]_D^{23}$ −40.0 (*c* 0.05, $CDCl_3$); IR (KBr) ν_{max} 3491, 3376, 3108, 2969, 1679, 1661, 1648, 1578, 1523, 1479, 1276 cm^{-1}; For ^1H and ^{13}C spectroscopic data (DMSO-d_6, 500.13 and 125.4 MHz), see Table 3; (+)-HRESIMS m/z 263.0596 $[M + H]^+$ (calculated for $C_{13}H_{11}O_6$, 263.0556).

3.3.3. 7-Hydroxy-6-methoxy-4-oxo-3-[(1*E*)-3-oxobut-1-en-1-yl]-4*H*-chromene-5-carboxylic Acid (**5**)

White crystal, mp 276–277 °C ($CHCl_3$/MeOH); IR (KBr) ν_{max} 3446, 2922, 1719, 1646, 1618, 1560, 1541, 1521, 1276 cm^{-1}; For ^1H and ^{13}C spectroscopic data (DMSO, 500.13 and 125.4 MHz), see Table 4; (+)-HRESIMS m/z 305.0667 $[M + H]^+$ (calculated for $C_{15}H_{13}O_7$, 305.0661).

3.3.4. Erubescenschromone B (**6**)

Yellowish oil; $[\alpha]_D^{23}$ −150.0 (*c* 0.04, MeOH); IR (KBr) ν_{max} 3443 (br), 2922, 1731, 1715, 1697, 1648, 1634, 1556, 1540, 1506, 1261 cm^{-1}; For ^1H and ^{13}C spectroscopic data (DMSO-d_6, 500.13 and 125.4 MHz), see Table 5; (+)-HRESIMS m/z 509.1085 $[M + H]^+$ (calculated for $C_{26}H_{21}O_{11}$, 509.1084).

3.3.5. SPF-3059-30 (**7**)

Yellowish oil; IR (KBr) ν_{max} 3491, 3376, 3108, 2969, 1679, 1661, 1648, 1578, 1523, 1479, 1276 cm^{-1}; For ^1H and ^{13}C spectroscopic data (DMSO-d_6, 500.13 and 125.4 MHz), see Table 6; (+)-HRESIMS m/z 491.0974 $[M + H]^+$ (calculated for $C_{26}H_{19}O_{10}$, 491.0978).

3.4. Electronic Circular Dichroism (ECD)

Electronic Circular Dichroism (ECD) of **3a** and **6**

The ECD spectra of **3a** and **6** (1.5 mM in methanol) were obtained in a Jasco J-815 CD spectropolarimeter (Jasco, Mary's Court, Easton, MD, USA) with a 0.01 mm cell (40 accumulations for **3a**). The dihedral driver and MMFF95 minimizations were done in Chem3D Ultra (Perkin-Elmer Inc., Waltham, MA, USA). All DFT minimizations with model chemistries APFD/6-31G and APFD/6-311+G(2d,p) [25] as well as ECD spectral calculations (TD-APFD) were performed with Gaussian 16W (Gaussian Inc., Wallingford, CT, USA) using an IEFPCM solvation model for methanol. The simulated spectral lines for **3a** (Figure 3) and **6** (Figure 8) were obtained by summation of Gaussian curves, as recommended in Reference [26]. A line broadening of 0.3 eV was applied to all transitions to generate the calculated line.

3.5. X-ray Crystal Structures

3.5.1. X-ray Crystal Structure of **4**

A single crystal of **4** was mounted on a cryoloop using paratone. X-ray diffraction data were collected at 290 K with a Gemini PX Ultra equipped with CuK_α radiation (λ = 1.54184 Å). The crystal was monoclinic, space group $P2_1/n$, cell volume 1245.43(7) $Å^3$ and unit cell dimensions a = 12.3445(4)

Å, b = 7.8088(3) Å and c = 12.9397(5) Å and angle β = 93.165(3)° (uncertainties in parentheses). There are two molecules in the asymmetric unit, one Erubescenschromone A molecule and one water molecule, and the calculated crystal density is 1.495 g/cm^{-3}. The structure was solved by direct methods using SHELXS-97 and refined with SHELXL-97 [27]. Carbon and oxygen atoms were refined anisotropically. Hydrogen atoms were directly found from difference Fourier maps and were refined freely with isotropic displacement parameters. The refinement converged to R (all data) = 6.32% and wR2 (all data) = 11.26%.

Full details of the data collection and refinement and tables of atomic coordinates, bond lengths and angles, and torsion angles have been deposited with the Cambridge Crystallographic Data Centre (CCDC 1856735).

3.5.2. X-ray Crystal Structure of **5**

A single crystal of **5** was mounted on a cryoloop using paratone. X-ray diffraction data were collected at 290 K with a Gemini PX Ultra equipped with CuK$_\alpha$ radiation (λ = 1.54184 Å). The crystal was monoclinic, space group $P2_1/c$, cell volume 1324.77(16) Å^3 and unit cell dimensions a = 11.6888(8) Å, b = 7.7695(4) Å and c = 14.9560(12) Å and angle β = 102.748(7)° (uncertainties in parentheses). The calculated crystal density was 1.525 g·cm^{-3}. The structure was solved by direct methods using SHELXS-97 and refined with SHELXL-97 [27]. Carbon and oxygen atoms were refined anisotropically. Hydrogen atoms from one of the methyl groups were placed at their idealized positions using appropriate HFIX instructions in SHELXL and included in subsequent refinement cycles, all the others were directly found from difference Fourier maps and were refined freely with isotropic displacement parameters. The refinement converged to R (all data) = 12.24% and wR2 (all data) = 14.96%.

Full details of the data collection and refinement and tables of atomic coordinates, bond lengths and angles, and torsion angles have been deposited with the Cambridge Crystallographic Data Centre (CCDC 1859409).

3.6. Antibacterial Activity Bioassays

3.6.1. Bacterial Strains and Growth Conditions

Gram-positive bacteria included *Staphylococcus aureus* ATCC 29213, *Enterococcus faecium* ATCC 19434, *Enterococcus faecalis* ATCC 29212, methicillin-resistant *Staphylococcus aureus* (MRSA) 66/1 isolated from public buses [28], and vancomycin-resistant enterococci (VRE) *Enterococcus faecium* 1/6/63 and *Enterococcus faecalis* B3/101 isolated from river water [29]. Gram-negative strains comprised *Escherichia coli* ATCC 25922, *Pseudomonas aeruginosa* ATCC 27853 and the clinical isolate SA/2, an extended-spectrum β-lactamase producer (ESBL). All strains were kept in Trypto-Casein Soy agar (TSA—Biokar Diagnostics, Allone, Beauvais, France) slants, at room temperature, in the dark. Before each assay, all strains were cultured in Mueller-Hinton agar (MH-Biokar Diagnostics, Allone, Beauvais, France) and incubated overnight at 37 °C. Stock solutions of the compounds were prepared in dimethyl sulfoxide (DMSO—Alfa Aesar, Kandel, Germany) and kept at −20 °C. With the exception of **1e**, 10 mg/mL stock solutions were prepared. Compound **1e** was less soluble in DMSO than other compounds, so a 2 mg/mL stock solution was prepared. In the experiments, the final concentration of DMSO in the medium was below 1%, as recommended by the Clinical and Laboratory Standards Institute [30].

3.6.2. Antimicrobial Susceptibility Testing

The antimicrobial activity of the compounds was screened using the Kirby-Bauer method, as recommended by the CLSI [31]: 6 mm blank paper discs (Liofilchem, Roseto degli Abruzzi TE, Italy) were impregnated with 15 μg of each compound, and the blank paper discs impregnated with DMSO were used as negative control. MH inoculated plates were incubated for 18–20 h at 37 °C. The results were evaluated by measuring the inhibition halos. The minimal inhibitory concentration (MIC) was performed in accordance with the recommendations of the CLSI [32]. Two-fold serial dilutions of

the compounds were prepared in cation-adjusted Mueller-Hinton broth (CAMHB—Sigma-Aldrich, St. Louis, MO, USA) within the concentration range 64–0.063 mg/L, except for **1e**, for which the highest concentration tested was 32 mg/L. Colony forming unit counts of the inoculum were conducted in order to determine the initial inoculum size (which should be approximately 5×10^5 CFU/mL). The 96-well U-shaped untreated polystyrene microtiter plates were incubated for 16–20 h at 37 °C and the MIC was determined as the lowest concentration of compound that prevented visible growth. The minimal bactericidal concentration (MBC) was determined by spreading 100 µL of the content of the wells with no visible growth on the MH plates. The MBC was determined as the lowest concentration of compound that killed 99.9% of the initial inoculum after overnight incubation at 37 °C [33]. These assays were conducted for reference and multidrug-resistant strains.

3.6.3. Biofilm Formation Inhibition Assay

The effect of all compounds on biofilm formation was evaluated using the crystal violet method, as follows: the highest concentration of the tested compound in the MIC assay was added to bacterial suspensions of 1×10^6 CFU/mL prepared in unsupplemented Tryptone Soy broth (TSB—Biokar Diagnostics, Allone, Beauvais, France) or TSB supplemented with 1% (p/v) glucose [D-(+)-Glucose anhydrous for molecular biology, PanReac AppliChem, Barcelona, Spain] for Gram-positive strains. When it was possible to determine a MIC, four concentrations of compound were tested, i.e., 2 × MIC, MIC, $\frac{1}{2}$ MIC and $\frac{1}{4}$ MIC. A control with appropriate concentration of DMSO, as well as a negative control (TSB alone), was included. Sterile 96-well flat-bottomed untreated polystyrene microtiter plates were used. After a 24 h incubation at 37 °C, the biofilms were heat-fixed for 1 h at 60 °C and stained with 0.5% (v/v) crystal violet (Química Clínica Aplicada, Amposta, Spain) for 5 min. The stain was solubilized with 33% (v/v) acetic acid (Acetic acid 100%, AppliChem, Darmstadt, Germany) and the biofilm biomass was quantified by measuring the absorbance of each sample at 570 nm in a microplate reader (Thermo Scientific Multiskan® EX, Thermo Fisher Scientific, Waltham, MA, USA) [20,34]. This assay was performed for reference strains.

3.6.4. Antibiotic Synergy Testing

The potential synergy between the compounds and clinically relevant antimicrobial drugs was screened using the Kirby-Bauer method, as previously described [35]. A set of antibiotic discs (Oxoid, Basingstoke, UK) to which the isolates were resistant was selected: cefotaxime (CTX, 30 µg) for *E. coli* SA/2, vancomycin (VAN, 30 µg) for *E. faecalis* B3/101 and *E. faecium* 1/6/63, and oxacillin (OXA, 1 µg) for *S. aureus* 66/1. Antibiotic discs impregnated with 15 µg of each compound were placed on seeded MH plates. The controls used included antibiotic discs alone, blank paper discs impregnated with 15 µg of each compound alone and blank discs impregnated with DMSO. Plates with CTX were incubated for 18–20 h and plates with VAN and OXA were incubated for 24 h at 37 °C [30]. The potential synergy was considered when the inhibition halo of an antibiotic disc impregnated with the compound was greater than the inhibition halo of the antibiotic or compound-impregnated blank disc alone. The combined effect of the compounds and clinical relevant antimicrobial drugs was also evaluated by determining the antibiotic MIC in the presence of each compound. Briefly, when it was not possible to determine a MIC value for the test compound, the MIC of CTX (Duchefa Biochemie, Haarlem, The Netherlands), VAN (Oxoid, Basingstoke, UK), and OXA (Sigma-Aldrich, St. Louis, MO, USA) for the respective multidrug-resistant strain was determined in the presence of the highest concentration of each compound tested in previous assays. In the case of **1e**, the concentration used was 32 mg/L while it was 64 mg/L for the other compounds. The antibiotic tested was serially diluted whereas the concentration of each compound was kept fixed. Antibiotic MICs were determined as described above. For **7**, it was possible to determine the MIC for *E. faecalis* B3/101 and *E. faecium* 1/6/63, so the checkerboard method was used instead, as previously described [34]. The fractional inhibitory concentrations (FIC) were calculated as follows: FIC of compound = MIC of compound combined with antibiotic/MIC compound alone, and FIC antibiotic = MIC of antibiotic combined with

a compound/MIC of antibiotic alone. The FIC index (FICI) was calculated as the sum of each FIC and interpreted as follows: FICI $\leq$ 0.5, 'synergy'; 0.5 < FICI $\leq$ 4, 'no interaction'; FICI > 4, 'antagonism' [36].

4. Conclusions

Marine-derived fungi have proved to be important sources of bioactive secondary metabolites, many of which exhibit cytotoxic and antibiotic activities. One of the most studied marine-derived fungi is of the genus *Penicillium*. In the past ten years, the *Penicillium* species from the marine environment received more attention than other fungal genera since compounds isolated from members of the *Penicillium* genus accounted for more than 25% of compounds of marine fungal origin. Although polyketides are the major secondary metabolites isolated from marine-derived *Penicillium* species, other structural classes of secondary metabolites such as alkaloids, terpenoids, and sterols are also isolated. In this work, we have described isolation and structure elucidation of two common fungal sterol derivatives: β-sitostenone and ergosterol 5,8-endoperoxide, fifteen polyketides, five of which have not been previously described, and a macrocyclic ether containing 1,4-disubstituted phenyl and succinamide moiety called GKK1032B, from the culture of the fungus *P. erubescens* strain KUFA 0220, which was isolated from the marine sponge *Neopetrosia* sp., collected from the Gulf of Thailand. From the compounds evaluated for their antibacterial activity against Gram-positive and Gram-negative bacteria of reference strains and multidrug-resistant isolates, their capacity to inhibit biofilm formation and synergistic effect, only GKK1032B displayed significant activities in all assays. Although the rest of the compounds, including those which have not been previously described, did not show significant antibacterial activity, it does not mean that they are void of bioactivities. Therefore, it is necessary to test these compounds in other bioassay platforms to explore their potential. Finally, it is worth mentioning that this is the first report of the chemical study of the marine-derived *P. erubescens*.

Supplementary Materials: The following are available online at http://www.mdpi.com/1660-3397/16/8/289/s1, Figure S1: Structures of β-sitosteanone and ergosterol-5,8-endoperoxide, isolated from the marine sponge-associated fungus Penicillium reubescens KUFA0220, Figures S2–S50 and S52–S53: 1D and 2D NMR spectra of isolated compounds, Figure S51: Ortep view of GKK1032B (**8**).

Author Contributions: A.K., M.M.M.P. and J.A.P. conceived, designed the experimental and elaborated the manuscript; D.K. performed isolation, purification and structure elucidation of the compounds; T.D. collected, isolated, identified and cultured the fungus; L.G. performed X-ray analysis; J.A.P. performed calculations and measurement of ECD spectra. P.M.C. and J.F.S. performed and interpreted the results of antibacterial assays; N.S. assisted elaboration of the manuscript; M.L. provided HRMS; A.M.S.S. provided NMR spectra.

Funding: This research was funded by Fundação para a Ciências e Tecnologia (FCT) (grant number POCI-01-0145-FEDER-016790) and North Portugal Regional Operational Programme (NORTE 2020)(grant number NORTE-01-0145-FEDER-000035).

Acknowledgments: This work was partially supported through national funds provided by FCT/MCTES-Foundation for Science and Technology from the Minister of Science, Technology and Higher Education (PIDDAC) and European Regional Development Fund (ERDF) through the COMPETE—Programa Operacional Factores de Competitividade (POFC) programme, under the project PTDC/MAR-BIO/4694/2014 (reference POCI-01-0145-FEDER-016790; Project 3599-Promover a Produção Científica e Desenvolvimento Tecnológico e a Constituição de Redes Temáticas (3599-PPCDT)) in the framework of the programme PT2020 as well as by the project INNOVMAR-Innovation and Sustainability in the Management and Exploitation of Marine Resources (reference NORTE-01-0145-FEDER-000035, within Research Line NOVELMAR), supported by North Portugal Regional Operational Programme (NORTE 2020), under the PORTUGAL 2020 Partnership Agreement, through the European Regional Development Fund (ERDF). Decha Kumla thanks the Alfabet Project of the Erasmus Mundus for a PhD's scholarship. We thank Júlia Bessa and Sara Cravo for technical support.

Conflicts of Interest: The authors declare no conflict of interest.

References

1. Visagle, C.M.; Houbraken, J.; Frisvad, J.C.; Hong, S.B.; Klaassen, C.H.W.; Perrone, G.; Seifert, K.A.; Vatga, J.; Yaguchi, T.; Samson, R.A. Identification and nomenclature of the genus Penicillium. *Sud. Mycol.* **2014**, *78*, 343–371. [CrossRef] [PubMed]

2. Ma, H.-G.; Liu, Q.; Zhu, G.-L.; Liu, H.-S.; Zhu, W.-M. Marine Natural Products sources from marine-derived *Penicillium* fungi. *J. Asian Nat. Prod. Res.* **2016**, *18*, 92–115. [CrossRef] [PubMed]
3. Kumla, D.; Aung, T.S.; Buttachon, S.; Dethoup, T.; Gales, L.; Pereira, J.A.; Inácio, A.; Costa, P.M.; Lee, M.; Sekeroglu, N.; et al. A New Dihydrochromone Dimer and Other Secondary Metabolites from Cultures of the Marine Sponge-Associated Fungi Neosartorya fennelliae KUFA 0811 and Neosartorya tsunodae KUFC 9213. *Mar. Drugs* **2017**, *15*, 375. [CrossRef] [PubMed]
4. May Zin, W.W.; Buttachon, S.; Dethoup, T.; Pereira, J.A.; Gales, L.; Inácio, A.; Costa, P.M.; Lee, M.; Sekeroglu, N.; Silva, A.M.S.; et al. Antibacterial and antibiofilm activities of the metabolites isolated from the culture of the mangrove-derived endophytic fungus Eurotium chevalieri KUFA0006. *Phytochemistry* **2017**, *141*, 86–97. [CrossRef] [PubMed]
5. Capon, R.J.; Stewart, M.; Ratnayake, R.; Lacey, E.; Gill, J.H. Citromycetins and Bilains A–C: Newaromatic polyketides and diketopiperazines from Australian Marine-Derived and Terrestrial Penicillium spp. *J. Nat Prod.* **2007**, *70*, 1746–1752. [CrossRef] [PubMed]
6. Yuan, C.; Wang, H.-Y.; Wu, C.-S.; Jiao, Y.; Li, M.; Wang, Y.-Y.; Wang, S.-Q.; Zhao, Z.-T.; Lou, H.-X. Austdiol, fulvic acid and citromycetin derivative from an endolichenic fungus, Myxotrichum sp. *Phytochem. Lett.* **2013**, *6*, 662–666. [CrossRef]
7. Fujita, K.-I.; Nagamine, Y.; Ping, X.; Taniguchi, M. Mode of Action of anhydrofulvic acid against Candida utilis ATCC 42402 under acid condition. *J. Antibiot.* **1999**, *52*, 628–634. [CrossRef] [PubMed]
8. Lee, D.-S.; Jang, J.-H.; Ko, W.; Kim, K.-S.; Sohn, J.H.; Kang, M.-S.; Ahn, J.S.; Kim, Y.-C.; On, H. PTP1B inhibitory and anti-inflamatory effects of secondary metabolites isolated from the marine-derived fungus Penicillium sp. JF-55. *Mar. Drugs* **2013**, *11*, 1409–1429. [CrossRef] [PubMed]
9. Cheng, X.; Yu, L.; Wang, Q.; Ding, W.; Chen, Z.; Ma, Z. New brefeldins and penialidins from marine fungus Penicillium janthinellum DT-F29. *Nat. Prod. Res.* **2018**, *32*, 282–286. [CrossRef] [PubMed]
10. Jouda, J.B.; Kusari, S.; Lamshoft, M.; Moufo Taontsi, F.; Douala Meli, C.; Wandji, J.; Spitteller, M. Penialidins A–C with strong bacterial acivity from Penicillium sp., an endophytic fungus harboring leaves of Garcinia nobilis. *Fitoterapia* **2014**, *98*, 209–214. [CrossRef] [PubMed]
11. Kimura, T.; Kikuchi, K.; Kumagai, K.; Hosotani, N.; Kishino, A. Nerve Regeneration Promoters Containing Semaphorin Inhibitor as the Active Ingredient. European Patent EP 1 306 093 B1. Date of Publication and Mention of the Grant of the Patent 03.10. 2007. Bulletin 2007/40. Available online: https://data.epo.org/publication-server/rest/v1.0/publication-dates/20071003/patents/EP1306093NWB1/document.html (accessed on 7 July 2018).
12. Song, T.; Chen, M.; Chai, W.; Zhang, Z.; Lian, X.-Y. New bioactive pyrrospirones C-I from a marine-derived fungus Penicillium sp. ZZ380. *Tetrahedron* **2018**, *74*, 884–891. [CrossRef]
13. Rukachaisirikul, V.; Satpradit, S.; Klaiklay, S.; Phongpaichit, S.; Borwornwiriyapan, K.; Sakayaroj, J. Polyketide anthraquinone, diphenyl ether, and xanthone derivatives from the soil fungus Penicillium sp. PSU-RSPG99. *Tetrahedron* **2014**, *70*, 5148–5152. [CrossRef]
14. Pastre, R.; Marinho, A.M.R.; Rodrigues-Filho, E.; Souza, A.Q.L.; Pereira, J.O. Diversity of polyketides produced by Penicillium species isolated from Melia azedarach and Murraya paniculata. *Quim. Nova* **2007**, *30*, 1867–1871. [CrossRef]
15. Noinart, J.; Buttachon, S.; Dethoup, T.; Gales, L.; Pereira, J.A.; Urbatzka, R.; Freitas, S.; Lee, M.; Silva, A.M.S.; Pinto, M.M.M.; et al. A new ergosterol analog, a new bis-anthraquinone and anti-obesity activity of anthraquinones from the marine sponge-associated fungus Talaromyces stipitatus KUFA 0207. *Mar. Drugs* **2017**, *15*, 139. [CrossRef] [PubMed]
16. Arai, K.; Miyajima, H.; Mushiroda, T.; Yamamoto, Y. Metabolites of Penicillium italicum Wehmer. Isolation and structures of new metabolites including naturally occurring 4-ylidene-acyltetronic acids, italicinic acid and italicic acid. *Chem. Pharm. Bull.* **1989**, *37*, 3229–3235. [CrossRef]
17. Lu, K.; Zhang, Y.; Li, L.; Wang, X.; Ding, G. Chaetochromones A and B, two new polyketides from the fungus Chaetomium indicum (CBS.860.68). *Molecules* **2013**, *18*, 10944–10952. [CrossRef] [PubMed]
18. Kumagai, K.; Hosotani, N.; Kikuchi, K.; Kimuran, T.; Saji, I. Xanthofulvin, a novel semaphorin inhibitor produced by a strain of Penicillium. *J. Antibiot.* **2003**, *56*, 610–616. [CrossRef] [PubMed]
19. Stepanović, S.; Vuković, D.; Dakic, I.; Savić, B.; Švabic-Vlahović, M. A modified -plate test for quantification of staphylococcal biofilm formation. *J. Microbiol. Methods* **2000**, *40*, 175–179. [CrossRef]

20. Stepanović, S.; Vuković, D.; Hola, V.; Di Bonaventura, G.; Djukić, S.; Ćirković, I.; Ruzicka, F. Quantification of biofilm in microtiter plates: Overview of testing conditions and practical recommendations for assessment of biofilm production by staphylococci. *Apmis* **2007**, *115*, 891–899. [CrossRef] [PubMed]
21. Tacconelli, E.; Carrara, E.; Savoldi, A.; Harbarth, S.; Mendelson, M.; Monnet, D.L.; Pulcini, C.; Kahlmeter, G.; Kluytmans, J.; Carmeli, Y.; et al. Discovery, research, and development of new antibiotics: The WHO priority list of antibiotic-resistant bacteria and tuberculosis. *Lancet Infect. Dis.* **2017**, *18*, 318–327. [CrossRef]
22. Murray, M.G.; Thompson, W.F. Rapid isolation of high molecular weight plant DNA. *Nucleic Acids Res.* **1980**, *8*, 4321–4325. [CrossRef] [PubMed]
23. White, T.J.; Bruns, T.; Lee, S.; Taylor, J. Amplification and direct sequencing of fungal ribosomal RNA genes for phylogenetics. In *PCR Protocols: A Guide to Methods and Applications*; Innis, M.A., Gelfand, D.H., Sninsky, J.J., White, T.J., Eds.; Academic Press: New York, NY, USA, 1990; pp. 315–322.
24. Sanger, F.; Nicklen, S.; Coulson, A.R. DNA sequencing with chain-terminating inhibitors. *Proc. Natl. Acad. Sci. USA* **1977**, *72*, 5463–5467. [CrossRef]
25. Austin, A.; Petersson, G.A.; Frisch, M.J.; Dobek, F.J.; Scalmani, G.; Throssel, K. A density functional with Spherical atom dispersion terms. *J. Chem. Theory Comput.* **2012**, *8*, 4989–5007. [CrossRef] [PubMed]
26. Stephens, P.J.; Harada, N. ECD Cotton effect approximated by the Gaussian curve and other methods. *Chirality* **2010**, *22*, 229–233. [CrossRef] [PubMed]
27. Sheldrick, G.M. A short story of SHELX. *Acta Cryst.* **2008**, *A64*, 112–122. [CrossRef] [PubMed]
28. Simões, R.R.; Aires-de-Sousa, M.; Conceicao, T.; Antunes, F.; da Costa, P.M.; de Lencastre, H. High prevalence of EMRSA-15 in Portuguese public buses: A worrisome finding. *PLoS ONE* **2011**, *6*, e17630. [CrossRef] [PubMed]
29. Bessa, L.J.; Barbosa-Vasconcelos, A.; Mendes, A.; Vaz-Pires, P.; Martins da Costa, P. High prevalence of multidrug-resistant *Escherichia coli* and *Enterococcus* spp. in river water, upstream and downstream of a wastewater treatment plant. *J. Water Health* **2014**, *12*, 426–435. [CrossRef] [PubMed]
30. Clinical and Laboratory Standards Institute (CLSI). *Performance Standards for Antimicrobial Susceptibility Testing*, 27th ed.; CLSI Supplement M100; Clinical and Laboratory Standards Institute: Wayne, PA, USA, 2017.
31. Clinical and Laboratory Standards Institute (CLSI). *Performance Standards for Antimicrobial Disk Susceptibility Tests*; Approved Standard-11th ed., CLSI Document M02-A11; Clinical and Laboratory Standards Institute: Wayne, PA, USA, 2012.
32. Clinical and Laboratory Standards Institute (CLSI). *Methods for Dilution Antimicrobial Susceptibility Tests for Bacteria That Grow Aerobically*; Approved Standard-10th ed., CLSI Document M07-A10; Clinical and Laboratory Standards Institute: Wayne, PA, USA, 2015.
33. Clinical and Laboratory Standards Institute (CLSI). *Methods for Determining Bactericidal Activity of Antimicrobial Agents*; Approved Guideline; Clinical and Laboratory Standards Institute: Wayne, PA, USA, 1999.
34. Gomes, N.M.; Bessa, L.J.; Buttachon, S.; Costa, P.M.; Buaruang, J.; Dethoup, T.; Silva, A.M.S.; Kijjoa, A. Antibacterial and antibiofilm activities of tryptoquivalines and meroditerpenes isolated from the marine-derived fungi Neosartorya paulistensis, N. laciniosa, N. tsunodae, and the soil fungi N. fischeri and N. siamensis. *Mar. Drugs* **2014**, *12*, 822–839. [CrossRef] [PubMed]
35. Buttachon, S.; Ramos, A.A.; Inácio, Â.; Dethoup, T.; Gales, L.; Lee, M.; Costa, P.M.; Silva, A.M.S.; Sekeroglu, N.; Rocha, E.; et al. Bis-indolyl benzenoids, hydroxypyrrolidine derivatives and other constituents from cultures of the marine sponge-associated fungus Aspergillus candidus KUFA0062. *Mar. Drugs* **2018**, *16*, 119. [CrossRef] [PubMed]
36. Odds, F.C. Synergy, antagonism, and what the chequerboard puts between them. *J. Antimicrob. Chemother.* **2003**, *52*. [CrossRef] [PubMed]

APPENDIX III

Kumla D., Dethoup T., Gales L., Pereira J.A., Silva J.F., Costa P.M., Silva A.M.S., Pinto M.M.M. and Kijjoa A., 2019. Erubescensoic Acid, a New Polyketide and a Xanthonopyrone SPF-3059-26 from the Culture of the Marine Sponge-Associated Fungus *Penicillium erubescens* KUFA 0220 and Antibacterial Activity Evaluation of Some of Its Constituents. *Molecules 24* (1), 208.

molecules

MDPI

Article

Erubescensoic Acid, a New Polyketide and a Xanthonopyrone SPF-3059-26 from the Culture of the Marine Sponge-Associated Fungus *Penicillium erubescens* KUFA 0220 and Antibacterial Activity Evaluation of Some of Its Constituents

Decha Kumla [1,2], Tida Dethoup [3], Luís Gales [1,4], José A. Pereira [1,2], Joana Freitas-Silva [1,2], Paulo M. Costa [1,2], Artur M. S. Silva [5], Madalena M. M. Pinto [2,6,*] and Anake Kijjoa [1,2,*]

1 ICBAS-Instituto de Ciências Biomédicas Abel Salazar, Universidade do Porto, Rua de Jorge Viterbo Ferreira, 228, 4050-313 Porto, Portugal; Decha1987@hotmail.com (D.K.); lgales@ibmc.up.pt (L.G.); jpereira@icbas.up.pt (J.A.P.); joanafreitasdasilva@gmail.com (J.F.-S.); pmcosta@icbas.up.pt (P.M.C.)
2 Interdisciplinary Centre of Marine and Environmental Research (CIIMAR), Terminal de Cruzeiros do Porto de Lexões, Av. General Norton de Matos s/n, 4450-208 Matosinhos, Portugal
3 Department of Plant Pathology, Faculty of Agriculture, Kasetsart University, Bangkok 10240, Thailand; tdethoup@yahoo.com
4 Instituto de Biologia Molecular e Celular (i3S-IBMC), Universidade do Porto, Rua de Jorge Viterbo Ferreira, 228, 4050-313 Porto, Portugal
5 Departamento de Química & QOPNA, Universidade de Aveiro, 3810-193 Aveiro, Portugal; artur.silva@ua.pt
6 Laboratório de Química Orgânica, Departamento de Ciências Químicas, Faculdade de Farmácia, Universidade do Porto, Rua de Jorge Viterbo Ferreira, 228, 4050-313 Porto, Portugal
* Correspondence: madalena@ff.up.pt (M.M.M.P.); ankijjoa@icbas.up.pt (A.K.); Tel.: +351-220428331 (A.K.)

Academic Editor: Isabel C.F.R. Ferreira
Received: 4 December 2018; Accepted: 3 January 2019; Published: 8 January 2019

check for updates

Abstract: A new polyketide erubescensoic acid (**1**), and the previously reported xanthonopyrone, SPF-3059-26 (**2**), were isolated from the uninvestigated fractions of the ethyl acetate crude extract of the marine sponge-associated fungus *Penicillium erubescens* KUFA0220. The structures of the new compound, erubescensoic acid (**1**), and the previously reported SPF-3059-26 (**2**), were elucidated by extensive analysis of 1D and 2D-NMR spectra as well as HRMS. The absolute configuration of the stereogenic carbon of erubescensoic acid (**1**) was determined by X-ray analysis. Erubescensoic acid (**1**) and SPF-3059-26 (**2**), together with erubescenschromone B (**3**), penialidin D (**4**), and 7-hydroxy-6-methoxy-4-oxo-3-[(1*E*)-3-oxobut-1-en-1-yl]-4*H*-chromen-5-carboxylic acid (**5**), recently isolated from this fungus, were assayed for their antibacterial activity against gram-positive and gram-negative reference strains and the multidrug-resistant (MDR) strains from the environment. The capacity of these compounds to interfere with the bacterial biofilm formation and their potential synergism with clinically relevant antibiotics for the MDR strains were also investigated.

Keywords: *Penicillium erubescens*; marine sponge-associated fungus; polyketides; erubescensoic acid; SPF-3059-267; antibacterial activity; antibiofilm activity; antibiotic synergy

1. Introduction

Penicillium (Family Aspergillaceae) is a diverse genus with more than 300 known species today, which are widely present throughout the world. Its species play important roles as decomposers of organic materials and cause destructive rots in the food industry where they produce a wide range of mycotoxins. Other species are considered enzyme factories or are common indoor allergens [1].

The biggest impact and claim to fame is the production of penicillin, which revolutionized the pharmaceutical industry and saved millions of lives around the world. Moreover, compactin, the first member of the anticholestolemic drug "statins", was first isolated from *P. citrinum* [2]. Species of *Penicillium* are found in both terrestrial and marine environments. The marine-derived *Penicillium* species, normally associated with a variety of marine invertebrates, mangroves, and sediments, are a source of structurally diverse classes of secondary metabolites such as polyketides, sterols, terpenoids, and alkaloids, most of which exhibit a myriad of biological activities [3]. Although members of the genus *Penicillium* from terrestrial environments have been extensively investigated for their secondary metabolites, their marine counterparts are still underexplored.

During our search for antibiotics from marine-derived fungi from the Gulf of Thailand and the Andaman Sea, we have reported isolation of several previously undescribed chromone and chromene derivatives as well as a chromone dimer, from the culture of *Penicillium erubescens* strain KUFA 0220, isolated from the marine sponge *Neopetrosia* sp., which was collected from the coral reef at Samaesan Island in the Gulf of Thailand [4]. Reexamination of the column fractions of *P. erubescens*, which have not been investigated in the previous study led us to further isolate one previously unreported polyketide which we have named erubescensoic acid (**1**) and the xanthonopyrone, SPF-3059-26 (**2**), which was previously reported from the culture of *Penicillium* sp. SPF-3059 [5] (Figure 1). Compounds **1** and **2**, were tested for their antibacterial activity against different strains of gram-positive and gram-negative bacteria, including reference strains and environmental multidrug-resistant isolates, together with erubescenschromone B (**3**), penialidin D (**4**), and 7-hydroxy-6-methoxy-4-oxo-3-[(1*E*)-3-oxobut-1-en-1-yl]-4*H*-chromen-5-carboxylic acid (**5**), which were isolated in our previous study [4] but were not tested for antibacterial activity. Compounds **1**–**5** were also evaluated for their capacity to prevent biofilm formation of the four reference strains as well as for their potential synergy between the compounds and clinically relevant drugs against the multidrug-resistant isolates.

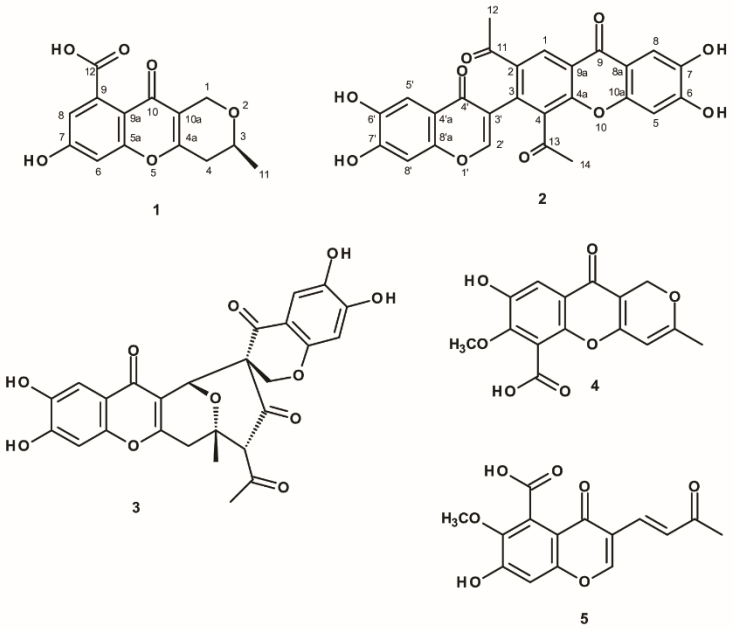

Figure 1. Structures of erubescensoic acid (**1**), SPF-3059-26 (**2**), erubescenschromone B (**3**), penialidin D (**4**), and 7-hydroxy-6-methoxy-4-oxo-3-[(1*E*)-3-oxobut-1-en-1-yl]-4*H*-chromen-5-carboxylic acid (**5**).

2. Results and Discussion

Compound **1** was isolated as a white crystal (mp. 218–220 °C), and displayed its (+)-HRESIMS *m/z* at 277.0719 $[M + H]^+$, (calculated 277.0712 for $C_{14}H_{13}O_6$). Therefore, its molecular formula was established as $C_{14}H_{12}O_6$, indicating nine degrees of unsaturation. However, the ^{13}C-NMR spectrum (Table 1, see Supplementary materials, Figure S2) displayed only thirteen carbon signals which, according to DEPTs and HSQC (Supplementary materials, Figure S2), can be classified as one conjugated ketone carbonyl (δ_C 173.0), one conjugated carboxyl (δ_C 161.8), three oxyquaternary sp^2 (δ_C 160.0, 157.4, 138.2), two quaternary sp^2 (δ_C 119.7, 115.3), two methine sp^2 (δ_C 111.8, 102.0), one oxymethylene sp^3 (δ_C 61.6), one methylene sp^3 (δ_C 33.5), one oxymethine sp^3 (δ_C 69.4), and one methyl (δ_C 20.8) carbons. That means one quaternary sp^2 carbon signal was not observed, and this is characteristic of the carboxyl-bearing aromatic carbon. The ^{1}H- and ^{13}C-NMR data of **1** resembled those of anhydrofulvic acid [6]; however the benzene ring of the chromone moiety of **1** has only one hydroxyl group, as evidenced by the presence of two broad singlets of the meta-coupled protons at δ_H 6.78 (H-6/δ_C 102.0) and 6.27 (H-8/δ_C 111.8), instead of two hydroxyl groups. Moreover, the double bond between C-2 and C-3 of the 3-methyl-2*H*-pyran ring was saturated as corroborated by the presence of the methylene group (δ_C 33.5/δ_H 2.66, d, *J* = 17.3 Hz/2.56, dd, *J* = 17.3, 9.8 Hz). Therefore, the planar structure of **1** was elucidated as 7,8-dihydroxy-3-methyl-10-oxo-4,10-dihydro-1*H*,3*H*-pyrano[4,3-*b*]chromene-9-carboxylic acid. This was confirmed by HMBC correlations (Table 1, Supplementary materials, Figure S4) from the methyl protons at δ_H 1.28, d (*J* = 6.2 Hz, Me-11) to C-3 (δ_C 69.4) and C-4 (δ_C 33.5), H-3 (δ_H 3.83, m) to C-1 (δ_C 61.6), H_2-1 (δ_H 4.56/4.33) to C-3, C-4a (δ_C 160.0), C-10a (δ_C 115.3) as well as H_2-4 (δ_H 2.56/2.66) to C-3, C-4a and C-10a. The saturation of the double bond between C-2 and C-3 makes C-3 stereogenic, whose absolute configuration needs to be determined.

Table 1. The ^{1}H- and ^{13}C-NMR (DMSO-d_6, 500 and 125 MHz) and HMBC assignment for **1**.

Position	δ_C, Type	δ_C (*J* in Hz)	HMBC
1	61.6, CH_2	4.56, d (14.9)	C-3, 4a, 10a
		4.33, d (14.9)	C-10a
3	69.4, CH	3.83, m	C-1
4	33.5, CH_2	2.66, d (17.3)	C-3, 4a, 11
		2.56, dd (17.3, 9.8)	C-3, 4a, 10a
4a	160.0, C	-	
5a	157.4, C	-	
6	102.0, CH	6.78, s	4
7	138.2, C	-	
8	111.8, CH	6.27, s	
9	-	-	
9a	119.7, C	-	
10	173.0, CO	-	
10a	115.3, C	-	
11	20.8, CH_3	1.28, d (6.2)	C-3, 4
12	161.8, CO	-	

Since **1** was obtained as a suitable crystal, the X-ray analysis was carried out. The Ortep diagram of **1** (Figure 2) not only confirms its structure but establishes the absolute configuration of C-3 as 3*S*. Since **1** has never been previously reported, it was named erubescensoic acid.

Compound **2** was isolated as a pale yellow viscous oil, and its molecular formula $C_{26}H_{16}O_{10}$ was established based on its (+)-HRESIMS *m/z* 489.0818 $[M + H]^+$, (calculated 489.0822 for $C_{26}H_{17}O_{10}$), indicating nineteen degrees of unsaturation. The infrared (IR) spectrum showed absorption bands for the hydroxyl (3445 cm^{-1}), conjugated ketone (1650 cm^{-1}), olefin (1625 cm^{-1}), aromatic (1605, 1542 cm^{-1}), and ether (1262 cm^{-1}). The ^{13}C-NMR spectrum of **2** (Table 2, Supplementary materials, Figure S7) displayed twenty six carbon signals which, in combination with DEPTs and HSQC spectra (Supplementary materials, Figures S8–S10), can be categorized as four conjugated ketone carbonyls

(δ_C 201.3, 199.2, 173.7 and 173.4), seven oxyquaternary sp^2 (δ_C 154.5,152.8, 152.5, 151.1, 150.7, 145.0, 144.6), seven quaternary sp^2 (δ_C 135.9, 133.5, 132.7, 120.8, 119.8, 115.7, 113.4), six methine sp^2 (δ_C 152.9, 126.4, 108.6, 107.9, 103.1, 102.9), and two methyl (δ_C 32.3 and 29.2) carbons. The ^{1}H- and ^{13}C-NMR data of **2** resemble those of SPF-3059-30, also isolated from this fungus [4], except for the absence of the oxymethylene sp^3 carbon at δ_C 66.2 and the appearance of the oxymethine sp^2 carbon at δ_C 152.9 in **2**. The presence of the 3-substituted 6,7-dihydroxy-4*H*-chromen-4-one was substantiated by HMBC correlations (Supplementary materials, Figures S11 and S12) from H-5′ (δ_H 7.28, brs/δ_C 107.9) to C-4′ (δ_C 173.7), C-6′ (δ_C 152.8), C-7′ (δ_C 145.0) and C-8′a (δ_C 151.1), H-8′ (δ_H 6.94, s/δ_C 103.1) to C-4′a (δ_C 113.4), C-6′, and from H-2′ (δ_H 8.13, s/ δ_C 152.9) to C-3′ (δ_C 120.7), C-4′ and C-8′a. That another part of the molecule was a 2,3,4-trisubstituted 6,7-dihydroxyxanthone, resembles that of SPF-3059-30 [5] was supported by HMBC correlations (Supplementary materials, Figures S11 and S12) from H-5 (δ_H 6.93, s/δ_C 102.9) to C-7 (δ_C 144.6), C-8a (δ_C 115.7), and from H-8 (δ_H 7.48, s/δ_C 108.6) to C-6 (150.5), C-9 (δ_C 173.4) and C-10a (δ_C 154.5). That the substituents on C-2 and C-4 of the benzene ring of the xanthone moiety were acetyl groups was corroborated by HMBC correlations (Supplementary materials, Figures S11 and S12) from H-1 (δ_H 8.58, s/δ_C 126.4) to C-3 (δ_C 132.7), C-4a (δ_C 152.5), C-9 (δ_C 173.4), C-11 (δ_C 199.2), from Me-12 (δ_H 2.55,s/δ_C 29.2) to C-11) and Me-14 (δ_H 2.53,s/δ_C 32.3) to C-13 (δ_C 201.3). Finally, the 6,7-dihydroxy-4*H*-chromen-4-one and the 2,4-diacetyl-6,7-dihydroxyxanthone are linked through C-3′ of the former and C-3 of the latter was confirmed by HMBC correlation from H-2′ to C-3. iterature search revealed that the planar structure of **2** is the same as that of SPF-3059-26, another polyketide isolated from the acetone extract of the mycelium of *Penicilium* sp. SPF-3050 (FERM BB-7663), cultured in the liquid medium [5]. However, there were no assignments of ^{1}H and ^{13}C chemical shift values for any protons and carbons of the structure of SPF-3059-26. Analysis of the structure of **2** revealed that the existence of the acetyl groups on C-2 and C-4 of the benzene ring of the xanthone moiety can impose a restriction of the rotation of the C-3 and C-3′ bond, thus creating a phenomenon of atropoisomerism. Optical rotation measurement revealed that **2** is dextrorotatory, presenting $[\alpha]^{25}_D$ +266 in MeOH. Due to the interesting activity of this class of compounds, SPF-3059-26 was later obtained, together with vinaxanthone and its derivatives, by ynone coupling reaction by Chin et al. [7]. Examination of the HRMS (ESI) data, ^{1}H- and ^{13}C-NMR spectra of SPF-3059-26 (compound **29** in Ref. 7) from the supporting information of the article by Chin et al. [7] revealed that they are compatible with those of **2**. However, neither optical rotation nor electronic circular dichroism (ECD) spectrum was mentioned in the discussion or provided in this supporting information. SPF-3059-26 (**2**) can be perceived as a decarboxylated derivative of vinaxanthone, which was previously isolated from the culture of *P. vinaceum* NR6815, isolated from soil [8], *P. glabrum* (Wehmer) Westling [9] and *Penicillium* sp. strain SPF-3059 [10]. It is noteworthy to mention that the structure elucidation of vinaxanthone in all these articles was based on analyses of the 1D-and 2D-NMR data, nothing was mentioned about its optical rotation or ECD spectrum.

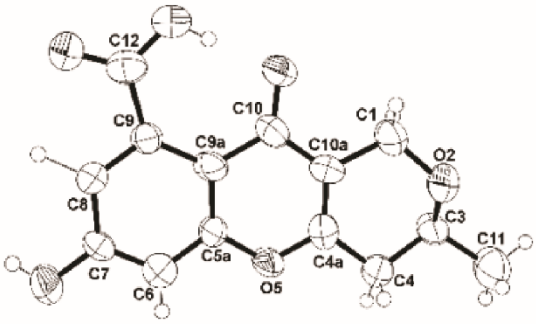

Figure 2. Ortep view of **1**.

Table 2. The ^{1}H- and ^{13}C-NMR (DMSO-d_6, 500 and 125 MHz) and HMBC assignment for **2**.

Position	δ_C, Type	δ_C (*J* in Hz)	HMBC
1	126.4, CH	8.58, s	C-3, 4a, 9, 11
2	135.9, C	-	
3	132.7, C	-	
4	133.5, C	-	
4a	152.5, C	-	
5	102.9, CH	6.93, s	C-7, 8a, 9, 10a
6	150.7, C	-	
7	144.6, C	-	
8	108.6, CH	7.48, s	C-7, 8a, 9, 10a
8a	115.7, C	-	
9	173.4, CO	-	
9a	119.8, C		
10a	154.5, C		
11	199.2, CO		
12	29.2, CH_3	2.55, s	C-2, 11
13	201.3, CO	-	
14	32.3, CH_3	2.53, s	C-4, 13
2′	152.9, CH	8.13, s	C-3′, 4′, 8′a, 9′
3′	120.8, C	-	
4′	173.7, CO	-	
4′a	113.4, C	-	
5′	107.9, CH	7.28, brs	C-4′, 6′, 7′, 8′a
6′	152.8, C	-	
7′	145.0, C	-	
8′	103.1, CH	6.94, s	C-4′, 6′, 7′
8′a	151.1, C		

Compounds **1** and **2**, were evaluated, together with erubescenschromone B (**3**), penialidin D (**4**), and 7-hydroxy-6-methoxy-4-oxo-3-[(1*E*)-3-oxobut-1-en-1-yl]-4*H*-chromen-5-carboxylic acid (**5**) (Figure 1), for their antibacterial activity against different strains of gram-positive and gram-negative bacteria, including reference strains and multidrug-resistant environmental isolates. However, in the range of concentrations tested, none of the compounds were active. The ability of **1**–**5** to prevent biofilm formation was also evaluated on four reference strains by measuring the total biomass. Since it was not possible to determine MIC (minimal inhibitory concentration) values of these compounds, the highest concentration tested in previous assays was used (64 mg/L or 32 mg/L for **3**). The results were interpreted using a comparative classification that divides adherence capabilities of tested strains into four categories: Non-adherent, weakly adherent, moderately adherent and strongly adherent [11]. The use of this classification, which uses the negative control as a starting point, instead of using the positive control as a reference, reduces the risk of inconsistencies due to external factors that influence biofilm production [12]. None of the compounds inhibited biofilm formation of *Pseudomonas aeruginosa* ATCC 27853, *Staphyllococus aureus* ATCC 29213, or *Enterococcus faecalis* ATCC 29212. Nonetheless, all the compounds tested were capable of impairing the biofilm forming ability of *Escherichia coli* ATCC 25922, which was classified as a strong biofilm producer (Table 3). These results suggest that the mechanism for impairing biofilm formation might be other than bactericidal activity. Other mechanisms for anti-biofilm activity have been described, such as inhibition of bacterial surface attachment, interference with quorum sensing signaling or even inhibition of biosynthesis of matrix components [13,14].

Potential synergy between the tested compounds and clinically relevant antimicrobial drugs were also screened using different methodologies. No associations were found with the disc diffusion assay. These results were obtained by determination of the MIC for each antibiotic in the presence of a fixed concentration of each compound, as it was not possible to determine MIC values for the test compounds. The concentration of each compound used was the highest concentration tested in previous assays (64 mg/L or 32 mg/L for **3**), which did not inhibit the growth of the three multidrug-resistant strains

under study. This method allows to determine that **2** causes a four-fold reduction in the cefotaxime (CTX) MIC of this strain (Table 4). However, this compound increased the oxacillin (OXA) MIC of methicillin-resistant *Staphylococcus aureus* (MRSA) *S. aureus* 66/1 by two-fold.

Table 3. Classification of the ability of *E. coli* ATCC 25922 to adhere to and form a biofilm after an exposure to **1–5**.

Compound	Concentration (mg/L)	OD ± SD	Classification
None	0	0.361 ± 0.159	strong
1	64	0.188 ± 0.012	moderate
2	64	0.195 ± 0.012	moderate
3	32	0.246 ± 0.038	moderate
4	64	0.172 ± 0.024	weak
5	64	0.194 ± 0.013	moderate

OD, optical density; SD, standard deviation; ODc, optical density cut-off value. Average OD value for negative control was found to be 0.065 ± 0.007, therefore ODc equals 0.065 + (3 × 0.007) = 0.086; 2 × ODc = 0.172; 4 × ODc = 0.344.

Table 4. Combined effect of clinically used antibiotics with **1–5** against multidrug-resistant strains. Minimal inhibitory concentration (MICs) are expressed in mg/L.

	E. coli SA/2 (ESBL)		*E. faecalis* B3/101 (VRE)		*S. aureus* 66/1 (MRSA)	
	CTX		VAN		OXA	
Compound	Distribution	MIC	Distribution	MIC	Distribution	MIC
Antibiotic	-	512	-	1024	-	64
Antibiotic +**1**	-	512	-	1024	-	64
Antibiotic +**2**	-	128	-	1024	-	128
Antibiotic +**3**	-	512	-	1024	-	64
Antibiotic +**4**	-	512	-	1024	-	64
Antibiotic +**5**	-	512	-	1024	-	64

MIC, minimal inhibitory concentration; (-), no inhibition halo or no increase in the inhibition halo; CTX, cefotaxime; VAN, vancomycin; OXA, oxacillin; ESBL, extended-spectrum β-lactamase producer; VRE, vancomycin-resistant *Enterococcus*; MRSA, methicillin-resistant *Staphylococcus aureus*.

3. Experimental Section

3.1. General Experimental Procedures

Melting points were determined on a Stuart Melting Point Apparatus SMP3 (Bibby Sterilin, Stone, Staffordshire, UK) and are uncorrected. Optical rotations were measured on an ADP410 Polarimeter (Bellingham + Stanley Ltd., Tunbridge Wells, Kent, UK). ^{1}H- and ^{13}C-NMR spectra were recorded at ambient temperature on a Bruker AMC instrument (Bruker Biosciences Corporation, Billerica, MA, USA), operating at 300 or 500 and 75 or 125 MHz, respectively. High resolution mass spectra were measured with a Waters Xevo QToF mass spectrometer (Waters Corporations, Milford, MA, USA) coupled to a Waters Aquity UPLC system. A Merck (Darmstadt, Germany) silica gel GF_{254} was used for preparative TLC, and a Merck Si gel 60 (0.2–0.5 mm) was used for column chromatography.

3.2. Fungal Material

Isolation, identification and cultivation of the fungus as well as preparation of the crude fungal extract were previously described by us [4].

3.3. Extraction and Isolation

Chromatographic isolation of the compounds from the crude EtOAc extract of *P. erubescens* KUFA 0220 was recently described by us [4]. For isolation of **1** and **2**, sub-fractions 185–251 from the silica

gel column frs 445–529 were combine (658 mg) and applied on a Sephadex LH-20 column (20 g) and eluted with MeOH, wherein 2 mL fractions were collected. Frs 25–30 were combined (40.0 mg) and purified by TLC (Silica gel G_{254}, $CHCl_3$:MeOH:HCO_2H, 9:1:0.01) to give **1** (7 mg). Sfrs 295–344 were combined (3.0 g) and applied on a Sephadex LH-20 column (20 g) and eluted with a 1:1 mixture of $CHCl_3$:MeOH, wherein 20 mL fractions were collected. Frs 1–30 were combined (217 mg) and re-applied on another Sephadex LH-20 column (20 g) and eluted with MeOH, wherein 30 sfrs of 2 mL were collected. Sfrs 8–26 were combined to give **2** (7.2 mg).

3.3.1. Erubescensoic Acid (**1**)

White crystal. Mp 218–220 °C; $[\alpha]^{25}_{D}$: −100.0 (MeOH, *c* 0.04 g/mL); IR (KBr) ν_{max} 3445, 2921, 1733, 1716, 1698, 1683, 1652, 1635, 1558, 1540, 1506, 1472 cm^{-1}.For ^{1}H- and ^{13}C-NMR data, see Table 1; (+)-HRESIMS *m/z* 277.0719 $[M + H]^+$ (calculated for $C_{14}H_{13}O_6$, 277.0712).

3.3.2. SPF-3059-26 (**2**)

Pale yellow viscous oil; $[\alpha]^{25}_{D}$ +266 (MeOH, *c* = 0.03 g/mL), IR (KBr) ν_{max} 3445, 2958, 2922 1650, 1605, 1262 cm^{-1}; For ^{1}H- and ^{13}C-NMR data, see Table 2; (+)-HRESIMS *m/z* 489.0818 $[M + H]^+$ (calculated for $C_{26}H_{17}O_{10}$, 489.0822).

3.4. X-Ray Crystal Structure of **1**

A single crystal was mounted on a cryoloop using paratone. X-ray diffraction data was collected at 288 K with a Gemini PX Ultra equipped with CuK_α radiation (λ = 1.54184 Å). The crystal was orthorhombic, space group $P2_12_12_1$, cell volume 1413.65(12) $Å^3$ and unit cell dimensions *a* = 6.7568(4) Å, *b* = 13.0791(5) Å and *c* = 15.9964(6) Å (uncertainties in parentheses). The structure was solved by direct methods using SHELXS-97 and refined with SHELXL-97 [15]. One molecule of the compound and two water molecules were found in the asymmetric unit. Carbon and oxygen atoms were refined anisotropically. Hydrogen atoms either directly found from difference Fourier maps and were refined freely with isotropic displacement parameters or placed at their idealized positions using appropriate HFIX instructions in SHELXL and included in subsequent refinement cycles. Hydrogens of one of the water molecules were not observed in the difference Fourier maps. The refinement converged to R (all data) = 10.43% and wR2 (all data) = 16.95%. Full details of the data collection and refinement and tables of atomic coordinates, bond lengths and angles, and torsion angles have been deposited with the Cambridge Crystallographic Data Centre (CCDC 1870933).

3.5. Antibacterial Activity Bioassays

3.5.1. Bacterial Strains and Testing Conditions

Four reference strains and three multidrug-resistant (MDR) strains were used in this study. Gram-negative strains included *Escherichia coli* ATCC 25922, *Pseudomonas aeruginosa* ATCC 27853 and the clinical isolate SA/2, an extended-spectrum β-lactamase producer (ESBL). Gram-positive bacteria comprised *Staphylococcus aureus* ATCC 29213, *Enterococcus faecalis* ATCC 29212, methicillin-resistant *Staphylococcus aureus* (MRSA) 66/1, isolated from public buses [16] and vancomycin-resistant *Enterococcus faecalis* (VRE) B3/101, isolated from river water [17]. All strains were kept in Trypto-Casein Soy agar (TSA, Biokar Diagnostics, Allone, Beauvais, France) slants, at room temperature, in the dark. Before each assay, all strains were cultured in Mueller-Hinton agar (MH, Biokar Diagnostics, Allone, Beauvais, France) and incubated overnight at 37 °C. Stock solutions of the compounds were prepared in DMSO (Alfa Aesar, Kandel, Germany) and kept at −20 °C. With the exception of compound **3**, 10 mg/mL stock solutions were prepared. Compound **3** was less soluble in DMSO than other compounds, so a 2 mg/mL stock solution was prepared. In all experiments, the final in-test concentration of DMSO was maintained below 1%, as recommended by the Clinical and Laboratory Standards Institute [18].

3.5.2. Antimicrobial Susceptibility Testing

The antimicrobial activity of the compounds was screened using the Kirby-Bauer method, as recommended by the CLSI [19]. Briefly, 6 mm blank paper discs (Liofilchem, Roseto degli Abruzzi, Teramo, Italy) were impregnated with 15 μg of each compound, and blank paper discs impregnated with DMSO were used as negative control. MH inoculated plates were incubated for 18–20 h at 37 °C. The results were evaluated by measuring the inhibition halos. Minimal inhibitory concentrations (MIC) for each compound were accessed in accordance with the CLSI standard [20]. Two-fold serial dilutions of the compounds were prepared in cation-adjusted Mueller-Hinton broth (CAMHB, Sigma-Aldrich, St. Louis, MO, USA) within the concentration range 64–2 mg/L, except for **3**, for which the highest concentration tested was 32 mg/L. The initial inoculum size (which should be approximately 5×10^5 CFU/mL) was determined by colony forming unit counts. The 96-well U-shaped untreated polystyrene plates were incubated for 16–20 h at 37 °C and the MIC was defined as the lowest concentration of compound that prevented visible growth. These assays were conducted for reference and MDR strains.

3.5.3. Biofilm Formation Inhibition Assay

The effect of **1**–**5** on biofilm formation was evaluated using the crystal violet method, as previously described [4]. Briefly, the highest concentration of compound tested in the MIC assay was added to bacterial suspensions of 1×10^6 CFU/mL prepared in unsupplemented Tryptone Soy broth (TSB, Biokar Diagnostics, Allone, Beauvais, France) or TSB supplemented with 1% (*p*/*v*) glucose [D(+)-Glucose anhydrous for molecular biology PanReac AppliChem, Barcelona, Spain] for Gram-positive strains. A control with appropriate concentration of DMSO, as well as a negative control (TSB alone) were included. Sterile 96-well flat-bottomed untreated polystyrene plates were used. After a 24 h incubation at 37 °C, the biofilms were stained and their biomass was quantified by measuring the absorbance of each sample at 570 nm in a microplate reader (Thermo Scientific Multiskan® EX, Thermo Fisher Scientific, Waltham, MA, USA). This assay was performed for reference strains.

3.5.4. Antibiotic Synergy Testing

In order to screen for potential synergy between the compounds and clinically relevant antimicrobial drugs, the Kirby-Bauer method was used, as previously described [21]. A set of antibiotic discs (Oxoid, Basingstoke, England) to which the isolates were resistant was selected: cefotaxime (CTX, 30 μg) for *E. coli* SA/2, vancomycin (VAN, 30 μg) for *E. faecalis* B3/101, and oxacillin (OXA, 1 μg) for *S. aureus* 66/1. Antibiotic discs impregnated with 15 μg of each compound were placed on seeded MH plates. The controls used included antibiotic discs alone, blank paper discs impregnated with 15 μg of each compound alone and blank discs impregnated with DMSO. Plates with CTX were incubated for 18–20 h and plates with VAN and OXA were incubated for 24 h at 37 °C [18]. Potential synergy was considered when the inhibition halo of an antibiotic disc impregnated with compound was greater than the inhibition halo of the antibiotic or compound-impregnated blank disc alone. The combined effect of the compounds and clinical relevant antimicrobial drugs was also evaluated by determining the antibiotic MIC in the presence of each compound. Briefly, when it was not possible to determine a MIC value for the test compound, the MIC of CTX (Duchefa Biochemie, Haarlem, The Netherlands), VAN (Oxoid, Basingstoke, England), and OXA (Sigma-Aldrich, St. Louis, MO, USA) for the respective multidrug-resistant strain was determined in the presence of the highest concentration of each compound tested in previous assays. For **3** the concentration used was 32 mg/L, while it was 64 mg/L for the other compounds. The antibiotic tested was serially diluted whereas the concentration of each compound was kept fixed. Antibiotic MICs where determined as described above. Potential synergy was considered when the antibiotic MIC was lower in the presence of compound.

4. Conclusions

We have recently described the first chemical investigation and antibacterial activity assay of the constituents isolated from the culture on the solid medium (cooked rice) of the marine-derived fungus *Penicillium erubescens* strain KUFA 0220, isolated from the marine sponge *Neopetrosia* sp., which was collected from the coral reef at Samaesan Island in the Gulf of Thailand. Although nineteen compounds (five of which were reported for the first time) have been isolated, some column fractions were very complex and difficult to purify and were left over for further study. Repetition of chromatographic fractionations by silica gel and Sephadex LH-20 columns, in combination with preparative TLC of silica gel, allowed us to retrieve a previously unreported metabolite which was named erubescenoic acid (**1**) and another polyketide called SPF-3059-26 (**2**), previously reported in a European patent of the nerve regeneration promotors containing semaphoring inhibitors as active ingredient, from *Penicillium* sp. SPF-3050 (FERM BB-7663). Since we have not yet evaluated the antibacterial activity of erubescenschromone B (**3**), penialidin D (**4**) and 7-hydroxy-6-methoxy-4-oxo-3-[(1*E*)-3-oxobut-1-en-1-yl]-4*H*-chromen-5-carboxylic acid (**5**), isolated from the same extract in our previous study, we evaluated these compounds, together with the newly isolated rubescenoic acid (**1**) and SPF-3059-26 (**2**), against Gram-positive and Gram-negative reference strains and environmental multidrug-resistant (MDR) strains, as well as their capacity to interfere with the bacterial biofilm formation and their potential synergism with clinically relevant antibiotics for the MDR strains. Although all the tested compounds were neither active against the reference and multidrug-resistant strains nor able to inhibit a biofilm formation of *Pseudomonas aeruginosa* ATCC 27853, *Staphyllococus aureus* ATCC 29213 or *Enterococcus faecalis* ATCC 29212, they were capable of impairing the biofilm forming ability of a strong biofilm producer, *Escherichia coli* ATCC 25922. Interestingly, screening of potential synergy with antibiotics revealed that SPF-3059-26 (**2**) was able to reduce the CTX MIC of *E. coli* SA/2 (ESBL) for four-fold while it increased the OXA MIC of MRSA *S. aureus* 66/1 by two-fold. Given the capacity of the neuronal regenerative effects of some of these compounds isolated from this fungus, it is desirable to test the extract of this fungus and its constituents for this effect.

Supplementary Materials: The following are available online, Figures S1–S8: 1D- and 2D-NMR spectra of **1** and **2**.

Author Contributions: A.K. and M.M.M.P. conceived, designed the experiment and elaborated the manuscript. D.K. performed isolation, purification and structure elucidation of the compounds. T.D. isolated, identified and cultured the fungus and also prepared a crude fungal extract. J.F.-S. and P.M.C. performed antibacterial activity assays. L.G. obtained crystal structure. A.M.S.S provided 1D- and 2D-NMR spectra. J.A.P. assisted in structure elucidation of the compounds.

Funding: This research was partially funded the project PTDC/MAR-BIO/4694/2014 (reference POCI-01-0145-FEDER-016790); Project 3599-Promover a Produção Científica e Desenvolvimento Tecnológico e a Constituição de Redes Temáticas (3599-PPCDT).

Acknowledgments: We thank the Foundation for Science and Technology of the Ministry of Science, Technology and Higher Education (PIDDAC) and European Regional Development Fund (ERDF) through the COMPETE-Programa Operacional Factores de Competitividade (POFC) programme, under the project PTDC/MAR-BIO/4694/2014 (reference POCI-01-0145-FEDER-016790; Project 3599-Promover a Produção Científica e Desenvolvimento Tecnológico e a Constituição de Redes Temáticas (3599-PPCDT)) in the framework of the programme PT2020. Decha Kumla thanks the Alfabet Project of the Erasmus Mundus for a PhD's scholarship. We thank Michael Lee of the Department of Chemistry, University of Leicester, UK for providing HRMS spectra.

Conflicts of Interest: The authors declare no conflict of interest.

References

1. Visagle, C.M.; Houbraken, J.; Frisvad, J.C.; Hong, S.B.; Klaassen, C.H.W.; Perrone, G.; Seifert, K.A.; Vatga, J.; Yaguchi, T.; Samson, R.A. Identification and nomenclature of the genus Penicillium. *Sud. Mycol.* **2014**, *78*, 343–371. [CrossRef] [PubMed]
2. Endo, A. A historical perspective on the discovery of statins. *Proc. Jpn. Acad. Ser. B Phys. Biol. Sci.* **2010**, *86*, 484–493. [CrossRef] [PubMed]
3. Ma, H.G.; Liu, Q.; Zhu, G.L.; Liu, H.S.; Zhu, W.M. Marine natural products sources from marine-derived *Penicillium* fungi. *J. Asian Nat. Prod. Res.* **2016**, *18*, 92–115. [CrossRef] [PubMed]

4. Kumla, D.; Pereira, J.A.; Dethoup, T.; Gales, L.; Freitas-Silva, J.; Costa, P.M.; Lee, M.; Silva, A.M.S.; Sekeroglu, N.; Pinto, M.M.M.; et al. Chromone derivatives and other constituents from cultures of the marine sponge-associated fungus Penicilium erubescens KUFA 0220 and their antibacterial activity. *Mar. Drugs* **2018**, *16*, 289. [CrossRef] [PubMed]
5. Nerve Regeneration Promoters Containing Semaphorin Inhibitor as the Active Ingredient. Available online: https://data.epo.org/publication-server/rest/v1.0/publication-dates/20071003/patents/EP1306093NWB1/document.html (accessed on 7 July 2018).
6. Fujita, K.I.; Nagamine, Y.; Ping, X.; Taniguchi, M. Mode of action of anhydrofulvic acid against *Candida utilis* ATCC 42402 under acidic condition. *J. Antibiot.* **1999**, *52*, 628–634. [CrossRef] [PubMed]
7. Chin, M.R.; Zlotkowski., C.; Han, M.; Patel, S.; Eliasen, A.M.; Axelrod, A.; Siegel, D. Expedited access to vinaxanthone and chemically edited derivatives possessing neuronal tegenerative effects through ynone coupling reactions. *ACS Chem. Neurosci.* **2015**, *6*, 542–550. [CrossRef] [PubMed]
8. Aoki, M.; Itezono, Y.; Shirai, H.; Nakayama, N.; Sakai, A.; Tanaka, Y.; Yamaguchi, A.; Shimma, N.; Yokose, K. Structure of a novel phospholipase C inhibitor, vinaxanthone (Ro 09-1450), produced by *Penicillium vinaceum*. *Tetrahedron Lett.* **1991**, *32*, 4737–4740. [CrossRef]
9. Wrigley, S.K.; Latif, M.A.; Gibson, T.M.; Chicarelli-Robinson, M.I.; Williams, D.H. Structure elucidation of xanthone derivatives with CD4-binding activity from *Penicillium glabrum* (Wehmer) Westling. *Pure Appl. Chem.* **1994**, *66*, 2383–2386. [CrossRef]
10. Kumagai, K.; Hosotani, N.; Kikuchi, K.; Kimura, T.; Saji, I. Xanthofulvin, a novel semaphoring inhibitor produced by a strain of *Penicillium*. *J. Antibiot.* **2003**, *56*, 610–616. [CrossRef] [PubMed]
11. Stepanović, S.; Vuković, D.; Dakic, I.; Savić, B.; Švabic-Vlahović, M. A modified -plate test for quantification of staphylococcal biofilm formation. *J. Microbiol. Methods* **2000**, *40*, 175–179. [CrossRef]
12. Stepanović, S.; Vuković, D.; Hola, V.; Di Bonaventura, G.; Djukić, S.; Ćirković, I.; Ruzicka, F. Quantification of biofilm in microtiter plates: Overview of testing conditions and practical recommendations for assessment of biofilm production by staphylococci. *Apmis* **2007**, *115*, 891–899. [CrossRef] [PubMed]
13. Cegelski, L.; Marshall, G.R.; Eldridge, G.R.; Hultgren, S.J. The biology and future prospects of of antivirulence therapies. *Nat. Rev. Microbiol.* **2008**, *6*, 17–27. [CrossRef] [PubMed]
14. Miquel, S.; Lagrafeuille, R.; Souweine, B.; Forestier, C. Anti-biofilm activity as a health issue. *Front. Microbiol.* **2016**, *7*, 1–14. [CrossRef] [PubMed]
15. Sheldrick, G.M. A short story of SHELX. *Acta Cryst.* **2008**, *64*, 112–122. [CrossRef] [PubMed]
16. Simões, R.R.; Aires-de-Sousa, M.; Conceicao, T.; Antunes, F.; da Costa, P.M.; de Lencastre, H. High prevalence of EMRSA-15 in Portuguese public buses: A worrisome finding. *PLoS ONE* **2011**, *6*, e17630. [CrossRef] [PubMed]
17. Bessa, L.J.; Barbosa-Vasconcelos, A.; Mendes, A.; Vaz-Pires, P.; Martins da Costa, P. High prevalence of multidrug-resistant *Escherichia coli* and *Enterococcus* spp. in river water, upstream and downstream of a wastewater treatment plant. *J. Water Health* **2014**, *12*, 426–435. [CrossRef] [PubMed]
18. Clinical and Laboratory Standards Institute (CLSI). *Performance Standards for Antimicrobial Susceptibility Testing*, 27th ed.; Wayne: Wayne, PA, USA, 2017.
19. Clinical and Laboratory Standards Institute (CLSI). *Performance Standards for Antimicrobial Disk Susceptibility Tests*, 11th ed.; Wayne: Wayne, PA, USA, 2012.
20. Clinical and Laboratory Standards Institute (CLSI). *Methods for Dilution Antimicrobial Susceptibility Tests for Bacteria That Grow Aerobically*, 10th ed.; Wayne: Wayne, PA, USA, 2015.
21. Buttachon, S.; Ramos, A.A.; Inácio, Â.; Dethoup, T.; Gales, L.; Lee, M.; Costa, P.M.; Silva, A.M.S.; Sekeroglu, N.; Rocha, E.; et al. Bis-indolyl benzenoids, hydroxypyrrolidine derivatives and other constituents from cultures of the marine sponge-associated fungus Aspergillus candidus KUFA0062. *Mar. Drugs* **2018**, *16*, 119. [CrossRef] [PubMed]

Sample Availability: Not available.